

---

# **A Deep Kinematic Survey of Planetary Nebulae in the Andromeda Galaxy**

**Helen Merrett**



The University of  
**Nottingham**

Thesis submitted to the University of Nottingham  
for the degree of Doctor of Philosophy  
July 2006

---

*This is not a novel to be tossed aside lightly.  
It should be thrown with great force.*

— Dorothy Parker, 1893-1967

**Supervisor:** Prof. Michael Merrifield

**Examiners:** Dr. Omar Almaini, University of Nottingham  
Dr. Annette Ferguson, University of Edinburgh

**First Submitted:** 5<sup>th</sup> July 2006

**Examined:** 1<sup>st</sup> September 2006

**Final Version:** 27 November 2006

# Contents

<b>List of Figures</b>	<b>iv</b>
<b>List of Tables</b>	<b>viii</b>
<b>Abstract</b>	<b>ix</b>
<b>Acknowledgements</b>	<b>x</b>
<b>1 Introduction</b>	<b>1</b>
1.1 Galaxy formation and evolution . . . . .	1
1.2 Stellar kinematics . . . . .	3
1.2.1 Local measurements . . . . .	3
1.2.2 Disk galaxy kinematics . . . . .	4
1.3 Planetary nebulae as a kinematic tracer population . . . . .	4
1.4 The Andromeda Galaxy . . . . .	7
1.4.1 Properties of the Andromeda Galaxy . . . . .	8
1.4.2 Previous surveys of PNe in the Andromeda Galaxy . . . . .	10
1.5 Thesis overview . . . . .	11
<b>2 The Planetary Nebula Spectrograph</b>	<b>13</b>
2.1 Driving forces . . . . .	13
2.2 Counter-dispersed imaging and the PN.S . . . . .	14
2.3 The calibration mask . . . . .	15
2.4 Instrument specifications . . . . .	16
2.5 Photometric efficiency . . . . .	18
2.6 Advantages and disadvantages of PN.S . . . . .	19
<b>3 Surveying the Andromeda Galaxy</b>	<b>21</b>

3.1	Observations . . . . .	21
3.2	Wide Field Camera data reduction . . . . .	23
3.3	Planetary Nebula Spectrograph data reduction . . . . .	23
3.3.1	Initial pipeline . . . . .	24
3.3.2	Identification of emission-line objects . . . . .	25
3.3.3	Astrometry . . . . .	27
3.3.4	Flux calibration . . . . .	28
3.4	Comparison with other data sets . . . . .	30
3.4.1	Velocity comparison . . . . .	30
3.4.2	Astrometric comparison . . . . .	33
3.4.3	Photometric comparison . . . . .	33
3.5	Contamination and completeness . . . . .	35
3.6	The catalogue . . . . .	40
<b>4</b>	<b>Other galaxies covered in the PN.S survey</b>	<b>42</b>
4.1	M32 . . . . .	42
4.2	NGC 205 . . . . .	46
4.3	Andromeda IV . . . . .	48
4.4	2MASXi J0039374+420956 . . . . .	49
4.5	MLA93 0953 . . . . .	50
4.6	Andromeda VIII . . . . .	50
4.7	Other objects excluded from the PN.S catalogue . . . . .	52
<b>5</b>	<b>Non-kinematic properties of the Andromeda Galaxy's PN population</b>	<b>54</b>
5.1	The planetary nebula luminosity function . . . . .	54
5.2	The spatial distribution of planetary nebulae . . . . .	57
5.3	The luminosity-specific PN density . . . . .	58
<b>6</b>	<b>Kinematic properties of the Andromeda Galaxy</b>	<b>61</b>
6.1	Planetary nebula kinematics . . . . .	61
6.1.1	The rotation curve . . . . .	62
6.1.2	Velocity dispersion . . . . .	63
6.2	H II region kinematics . . . . .	66
6.3	Asymmetry in M31's disk . . . . .	68



<b>Contents</b>	<b>iii</b>
6.4 M31's warped disk . . . . .	72
6.4.1 The stellar warp . . . . .	74
6.5 Halo and velocity substructures . . . . .	78
6.5.1 The Northern Spur . . . . .	79
6.5.2 The Southern Stream . . . . .	81
6.5.3 Possible other velocity substructures . . . . .	86
<b>7 Dynamics of the Andromeda Galaxy</b>	<b>88</b>
7.1 A flaring disk model for M31's stellar disk . . . . .	88
7.2 The asymmetric drift . . . . .	90
7.3 Simple disk-bulge-halo fits to the rotation curve . . . . .	92
7.4 An analysis of the energy-angular momentum plane . . . . .	95
7.4.1 Moving groups in the Milky Way . . . . .	96
7.4.2 Searching for inhomogeneities in M31's energy-angular momentum space . . . . .	97
<b>8 Summary and future extensions</b>	<b>108</b>
8.1 Summary . . . . .	108
8.2 Future extensions . . . . .	110
8.2.1 Extensions to the data set . . . . .	110
8.2.2 Other analyses . . . . .	110
<b>Appendices</b>	<b>111</b>
<b>A The Catalogue</b>	<b>111</b>
<b>Bibliography</b>	<b>148</b>

# List of Figures

1.1	Galaxy mergers and tidal streams . . . . .	2
1.2	A schematic diagram of the post main-sequence evolution of low to intermediate mass stars. . . . .	5
1.3	Nearby planetary nebulae . . . . .	6
1.4	Multi-wavelength images of M31 . . . . .	9
2.1	Optical setup for counter-dispersed imaging . . . . .	14
2.2	Example V-band, narrow band [O III], and PN.S images . . . . .	14
2.3	A schematic representation of PN.S . . . . .	15
2.4	An example PN.S image . . . . .	16
2.5	Locations of the mask holes . . . . .	16
2.6	Detailed arc spectrum . . . . .	17
2.7	PN.S mounted on WHT . . . . .	18
3.1	Fields observed in M31 . . . . .	22
3.2	Seeing as measured for different survey fields . . . . .	23
3.3	Difference in undispersed $y$ coordinates . . . . .	26
3.4	Differences between the velocities of PNe in the field overlaps . . . . .	27
3.5	Differences between the positions of PNe in the field overlaps . . . . .	28
3.6	Magnitude variations within the PN.S data set . . . . .	30
3.7	Positions of other surveys with respect to the PN.S survey . . . . .	31
3.8	Comparison of initial PN.S velocities to H06 velocities . . . . .	31
3.9	Difference between final PN.S velocities and H06 . . . . .	32
3.10	Difference between the final PN.S and the Hurley-Keller et al. (2004) velocities . . . . .	32
3.11	Comparison between PN.S and H06 astrometry . . . . .	33
3.12	Photometric comparison between the magnitudes derived from the PN.S data and those from the M02 imaging data . . . . .	34

3.13	Comparison between PN.S magnitudes and those published in Ciarullo et al. (1989) . . . . .	35
3.14	FWHM of sources detected by the PN.S survey . . . . .	36
3.15	The flux ratio of [O III] to ( $H\alpha$ + [N II]) versus magnitude . . . . .	37
3.16	Locations in position and velocity of sources identified as probable H II regions . . . . .	38
3.17	A sample of the extended emission line objects with velocities inconsistent with membership of M31 . . . . .	39
3.18	Objects displaying two emission peaks . . . . .	39
3.19	Cumulative distribution of radii in the disk plane . . . . .	40
4.1	Positions of other galaxies contained within the PN.S survey area. An emission-line object's size and colour reflect its velocity with respect to M31's system velocity: red objects are receding and blue ones are approaching. . . . .	43
4.2	M32 . . . . .	44
4.3	M32 velocities . . . . .	45
4.4	NGC 205 . . . . .	46
4.5	NGC 205 . . . . .	47
4.6	Andromeda IV . . . . .	49
4.7	Kinematics of emission-line sources in Andromeda IV . . . . .	50
4.8	2MASXi J0039374+420956 . . . . .	51
4.9	MLA93 0953. As Figure 4.2, with M31's disk visible to the bottom left of the DSS image. . . . .	52
4.10	And VIII . . . . .	53
4.11	And VIII . . . . .	53
5.1	The PNLF of M31 . . . . .	55
5.2	The PNLF at different deprojected disk radii in M31 . . . . .	55
5.3	The PNLF on the near and far side of M31 over different radial ranges . . . . .	56
5.4	Location of an Earth based observer relative to the disk of M31 . . . . .	57
5.5	Surface brightness profile and PN number counts along the major axis . . . . .	58
5.6	Surface brightness profile and PN number counts along the minor axis . . . . .	59
5.7	Variation of $\alpha_{2.5}$ . . . . .	60
6.1	Planetary nebula velocities . . . . .	62
6.2	Position versus velocity for PNe close to the major axis . . . . .	63

6.3	PN Velocity dispersion profile . . . . .	64
6.4	Variation in velocity dispersion with apparent magnitude . . . . .	66
6.5	H II region velocities . . . . .	67
6.6	H II region circular velocities and the mean rotation curve . . . . .	68
6.7	Comparison of rotation curves from either side of M31 . . . . .	70
6.8	PN and H II region distributions . . . . .	70
6.9	PN and H II region velocities and the PN velocity dispersion profile on either side of the disk . . . . .	71
6.10	A section of Brinks & Shane (1984)'s Figure 8 showing the H I veloc- ity map for a strip of data at $Y = 0.1^\circ$ north-west of the major axis. . .	72
6.11	A compilation of Brinks & Shane (1984)'s Figure 8 . . . . .	73
6.12	A tilted ring model for M31's warped disk . . . . .	75
6.13	$X$ versus $v$ plots, equivalent to Figure 6.11 . . . . .	76
6.14	The stellar distribution in M31 . . . . .	77
6.15	Expected number density of PNe in the top 4.0 mag of the PNLf for slices parallel to the major axis . . . . .	78
6.16	The number density of RGB stars in in Andromeda's halo . . . . .	79
6.17	Velocities for M31's PN sample in the region of the Northern Spur . .	80
6.18	The Southern Stream . . . . .	82
6.19	Friendless PNe . . . . .	83
6.20	Fardal et al. (2006)'s N-body simulation of the Southern Stream . . .	85
6.21	Friendless PNe with stream objects eliminated . . . . .	87
7.1	Schematic diagram of the flaring disk of M31 . . . . .	88
7.2	Velocity dispersion profile . . . . .	89
7.3	Predicted and observed rotational motions of PNe . . . . .	91
7.4	A range of models fit to our H II rotation curve . . . . .	94
7.5	Best fit bulge-disk-halo model . . . . .	95
7.6	Projection of a selection of PNe into the energy-angular momentum plane . . . . .	99
7.7	PN tracks in the $(L, E)$ $\left(L, \sqrt{2(E - E_c)}\right)$ planes . . . . .	100
7.8	Density of PN tracks in the $\left(L, \sqrt{2(E - E_c)}\right)$ plane and the number of PN tracks crossing all the grid-boxes . . . . .	101
7.9	The density of PN tracks in the $\left(L, \sqrt{2(E - E_c)}\right)$ plane for the $5 \times 5$ (left) and a $20 \times 20$ grids (right). . . . .	102

---

7.10	Locations of the grid-points with the subsequently densest concentrations of PN tracks . . . . .	102
7.11	Physical locations of the PNe found in Figure 7.8's highest density grid-points . . . . .	103
7.12	Surface brightness profile of V-band light in M31 . . . . .	104
7.13	Number of PNe brighter than 24 mag found in rings in the disk . . . .	105
7.14	As Figure 7.6, but including error bars and the conversion to the reduced energy frame . . . . .	106
7.15	Approximations to the DF of PNe brighter than 24 mag . . . . .	107

# List of Tables

1.1	Basic observational properties of the Andromeda galaxy . . . . .	10
2.1	CCD Parameters. . . . .	18
2.2	Instrumental efficiencies . . . . .	19
3.1	Sky extinction from the Carlsberg Meridian Telescope and weather notes	29
4.1	Emission-line objects in the vicinity of And IV. <sup>a</sup> ID from Ferguson, Gallagher & Wyse (2000) Table 1. <sup>b</sup> ID from Table A.1. <sup>c</sup> RA, Dec, $m_{5007}$ and $v_{\text{helio}}$ from PN.S data, except object F1, which was not detected. <sup>d</sup> E – extended; R – below flux ratio cutoff; NP – not detected in PN.S survey; M31 – M31 like velocity; NF – not found in Ferguson, Gallagher & Wyse (2000). . . . .	48
6.1	Rotation curve and velocity dispersion profile measured from PNe close to the major axis. . . . .	64
6.2	Rotation curve measured from H II region circular velocities. . . . .	69
6.3	Parameters of the warp model fit by eye to the H I profiles of Brinks & Shane (1984), using the tilted rings template of Christodoulou, Tohline & Steiman-Cameron (1993). . . . .	74
7.1	$\chi^2$ fits of a simple bulge-disk-halo model to the H II regions rotation curve . . . . .	93
A.1	Emission line objects identified in the M31 survey. . . . .	111

# Abstract

This thesis presents a survey of compact emission-line objects in the Andromeda Galaxy (M31) performed using a novel new instrument, the Planetary Nebula Spectrograph. The final catalogue contains the positions, magnitudes and velocities for 3300 objects displaying [O III] emission at 5007 Å, of which 2615 are found likely to be planetary nebulae (PNe) associated with M31. The survey area covers some 6 square degrees, taking in the whole of M31's disk out to a projected radius of 1.5°, with extensions along the major and minor axes, and the Northern Spur and Southern Stream regions. The calibrated data have been checked for internal consistency and compared with other catalogues. With the exception of the very central, high surface brightness region of M31, this survey is complete to a magnitude limit of  $m_{5007} \sim 23.75$ , 3.5 magnitudes into the planetary nebula luminosity function.

A number of satellite and background galaxies are located within the M31 survey area and emission line objects associated with these have been identified. Analyses of the basic kinematic properties associated with each of these galaxies are presented.

The PN catalogue has been analysed for non-kinematic, kinematic and dynamical properties. We have examined the planetary nebula luminosity function across M31, the spatial distribution of PNe, and the luminosity specific PN density. These analyses indicate that apart from a small change in the luminosity specific PN density there are no other non-kinematic differences between the bulge and disk PN populations suggesting that the sample of PNe is not strongly populated by objects whose progenitors are more massive stars. There is no indication of a significant halo PN population.

Rotation curves for both the surveyed PNe and H II regions have been produced as well as the PN velocity dispersion profile. The H II rotation curve is seen to be in good agreement with those in the literature, while the PN rotation curve and velocity dispersion profile exhibit some peculiarities. However, under the approximation of an axisymmetric disk these are shown to be mutually consistent, but require the disk to flare with radius if the shape of its velocity ellipsoid remains invariant.

The kinematic properties of photometric substructures are examined and kinematic substructures are searched for. A possible kinematic extension of the Southern Stream has been discovered. A new approach is taken in order to search for dynamical streams in the disk of the galaxy, involving an examination of the energy angular momentum plane. This also provides a new way of looking at the distribution function of a tracer population in a disk galaxy.

# Acknowledgements

I would like to take this opportunity to thank all those people who have provided help and support, of one form or another, during the course of my studies. A number of people deserve special mention. My supervisor, Mike, for coming up with a great project and being a constant source of ideas and enthusiasm along the way. All the members of the PN.S consortium, in particular Nigel, Aaron, Konrad and Nicola who's help and advice has been invaluable. Our collaborators on the M31 project, particularly Dave, for his assistance at numerous observing runs, and Claire. The staff at the Isaac Newton Group of telescopes have provided great assistance during observing runs, especially Romano, the PN.S support astronomer. I'd also like to thank Aaron, Steven, Laura and my parents for proof reading sections of this thesis.

I have enjoyed my time in Nottingham immensely, thanks to the good friends I have made and I'd like to thank all of those people I've known during my time there. I must mention some people specifically: Fiona, Vicky, Leaf, Emma M and Rad who have been great housemates. Laura and Rad for the running outings, followed, of course, by many good dinners. Steven for his endless patience and help over the years, teaching me most of what I know about computers and for generally being a good friend. Also, Emma K (despite the snake sitting duties), Ian, Kyle, Michelle and all the lunch and poker gang, for making my time in Nottingham all the more interesting and enjoyable. Thanks also to Jane for distracting me and helping to keep me sane during the long months of writing up.

Many thanks go to all my family for their generous love and support, particularly my parents. And finally, James, who is always there for me.



# Chapter 1

## Introduction

The primary goal of this thesis is to produce and analyse a survey of the kinematic properties of the Andromeda Galaxy's planetary nebula population. The main motivation for this is to add to our understanding of the nature of this galaxy's stellar population, particularly within the disk of the galaxy. In order to set the scene for this thesis we will now briefly discuss some of the major topics in astronomy that affect this survey, starting with our current understanding of galaxy formation and evolution.

### 1.1 Galaxy formation and evolution

The question of how galaxies originally formed and have subsequently evolved is one of the most important topics of modern astronomy. There are two basic processes by which this may have occurred. Firstly, there is the monolithic collapse scenario, initially proposed by Eggen, Lynden-Bell & Sandage (1962). This sees massive galaxies form whole, from the rapid collapse of a proto-galactic nebula. While this 'top-down' process was able to explain some of the basic properties of the Milky Way, for example the existence of an old stellar halo and younger stellar disk, there were a number of inconsistencies. Before long 'bottom-up' processes were being incorporated into the model (e.g. Larson, 1969) in order to explain these peculiar features.

The second process involves an entirely 'bottom-up' process, wherein density fluctuations in the early universe led to the formation of small ( $10^6$ - $10^8 M_{\odot}$ ) mass fragments. These then merged together under gravitational attraction to form subsequently larger masses, while the gases within the fragments collapsed to form clusters of stars and ultimately galaxies (e.g. White & Rees, 1978). This hierarchical build up naturally produces objects with a wide range of masses, from individual globular clusters, through dwarf galaxies and up to the most massive giant elliptical galaxies.

Over the years the hierarchical model has become the standard cosmological paradigm. This model is supported by the observation of numerous galaxy mergers within the local universe, for example the Mice galaxies shown in Figure 1.1. Even in the local group of galaxies we see direct evidence of hierarchical growth, with satellite galaxies being tidally stripped of matter and seen merging into both the Milky Way and

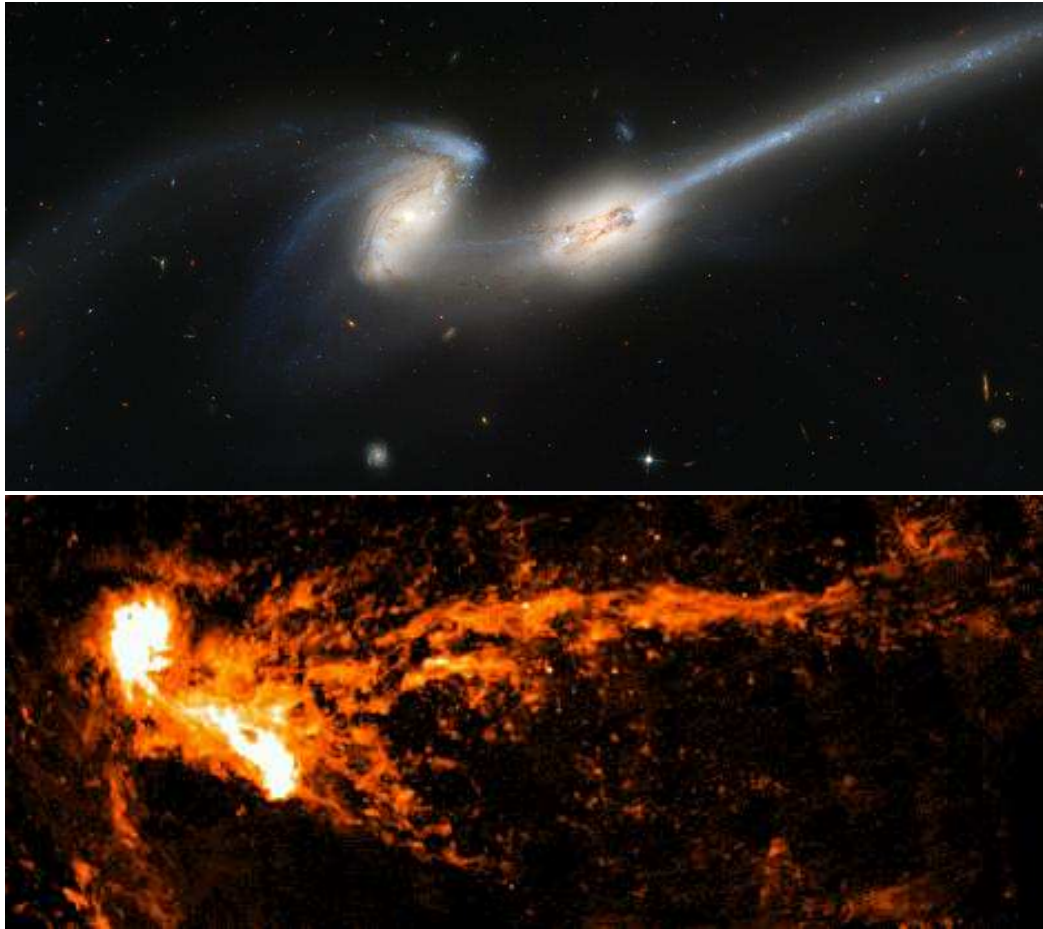


**Figure 1.1:** Galaxy mergers and tidal streams. The merging galaxies of the Mice (NGC 4676), with their prominent stellar streams are shown in the top panel. H I gas in both the Large (top left) and Small Magellanic Clouds and the tidally stripped Magellanic Stream is shown in the bottom panel. Picture credits are: NASA, H. Ford (JHU), G. Illingworth (UCSC/LO), M. Clampin (STScI), G. Hartig (STScI), the ACS Science Team, and ESA; and M.E. Putman (University of Colorado), L. Staveley-Smith (CSIRO), K.C. Freeman (Australian National University), B.K. Gibson Swinburne University) and David G. Barnes (Swinburne University), respectively.

Andromeda Galaxies [e.g. the Magellanic Stream shown in Figure 1.1, and the Andromeda Galaxy’s Southern Stream of stars (Ibata et al., 2001).]

Modern cosmological simulations, such as Springel et al. (2005)’s ‘Millennium Simulation,’ are based around this scenario. The theory, however, is not perfect. There are a number of features predicted by the simulation work that are contrary to observational evidence. One such problem is that of the ‘missing satellites.’ Simulations have shown that much of the small scale substructure would survive to the present day, yet the number of dwarf galaxies in the Local Group is small, suggesting that much of the small scale substructure has in fact been lost (e.g. Kauffmann, White & Guiderdoni, 1993). There are a number of ways of suppressing the formation of such substructures in the simulations, each displaying specific characteristics and none without their own difficulties. Distinguishing between these methods will require tighter observational constraints, particularly from dwarf spheroidal galaxies in the Local Group.

There is also some question hanging over the shape of a galaxy’s inner rotation curve.

Simulations generally produce ‘cuspy,’ centrally concentrated mass profiles (e.g. White, 1978, 1979). However, the inferred dark matter profiles of some dwarf and low-surface brightness galaxies (e.g. McGaugh & de Blok, 1998) and a number of spiral galaxies (Salucci, 2001) are ‘cored’ and not centrally concentrated.

Such inconsistencies in an otherwise fairly solid framework for galaxy formation necessitate further investigation. Both more simulations and more observational evidence will be required in order to resolve these questions. One of the best places to gather such observational evidence is in our own galaxy and within the local group of galaxies, which can be observed in great detail. This provides significant motivation for a comprehensive study of the kinematic properties of the Andromeda Galaxy’s stellar population.

## 1.2 Stellar kinematics

A star’s kinematics can be broken down into three velocity components, one parallel and two perpendicular to the line of sight. It is only possible to measure the perpendicular velocity components, commonly called the proper motion, for stars that are relatively nearby. However, the parallel component, or radial velocity, can be measured utilising Doppler shifts of emission and absorption features, for any star that is bright enough for a spectroscopic measurement to be made. Spectroscopic radial velocities can be measured both for individual stars and for the integrated light from a stellar population.

As the majority of a galaxy’s baryonic mass is locked up in its stars, with the dark matter contribution only detectable at relatively large radii, the inner part of the stellar system can be considered to be orbiting under its own self gravity. It is therefore extremely important to understand the kinematics of the stellar population. The more detail that is measured for a system’s stellar kinematics, the better we are able to understand the dynamical properties of that system, its history and evolution.

### 1.2.1 Local measurements

In the solar neighbourhood of the Milky Way, where both the proper and radial components of motion can be measured, a wealth of complex structure is seen in the distribution of velocities (Dehnen & Binney, 1998; Famaey et al., 2005). Unfortunately, such data from a single locality are difficult to interpret in terms of the global structure of the Galaxy. Although kinematic observations of more distant stars in the Milky Way have been made (see, for example, Sevenster et al., 1997), the complexity of disentangling the geometry of our own galaxy make such data difficult to interpret. We also clearly need more than one example before any general conclusions about the dynamics of disk galaxies can be drawn. Hence, we must look to the detailed stellar kinematics of other spiral systems.

### 1.2.2 Disk galaxy kinematics

The kinematic properties of external disk galaxies were a subject of study before it was even known that they were separate stellar systems that existed beyond the Milky Way. V. M. Slipher was the first person to report evidence of rotation in a spiral galaxy with his observation that absorption lines in NGC 4594, the Sombrero Galaxy, appeared to be inclined (Slipher, 1914). Slipher also noted seeing a similar effect in the Andromeda Galaxy, prompting a more detailed study by Pease (1918) who measured a change in velocity at the centre of M31 along the major axis of  $\sim 140 \text{ km s}^{-1}$  over 5 arcminutes.

Since these early measurements, technological developments have allowed spiral galaxy rotation curves to be measured at many different wavelengths, targeting different galaxy populations [a review of this topic can be found in Sofue & Rubin (2001)]. The production of red sensitive plates in the 1950s allowed the  $\text{H}\alpha$  and  $[\text{N II}]$  emission lines associated with ionised gases in  $\text{H II}$  regions to be measured. There are any number of disk galaxy kinematic tracers available to the modern day astronomer including: the 21 cm radio emission line of neutral  $\text{H I}$  gas, particularly useful due to its large spatial extent; millimetre wavelength CO emission lines from molecular gas clouds; as well as a number of stellar absorption and emission lines.

Stellar absorption lines have, until relatively recently, been detectable only in integrated light, measured using long slit spectra, from external galaxies. However, for most galaxies this is only possible in the bright central regions. At larger radii tracer populations are the best option. With the advent of 8m class telescopes and the development of technologies such as multi-object spectrographs, large surveys of individual stars in relatively nearby galaxies are becoming a realistic option.

The only individual stars that are bright enough to be observed spectroscopically in external galaxies are giant stars and the bright emission lines of planetary nebulae. Spectroscopy of red giants is only just possible with 8 m class telescopes in the nearby members of the local group of galaxies. Surveys of such stars in M31's halo have been started in recent years by Reitzel & Guhathakurta (2002) and Ibata et al. (2004). While these have proved to be an excellent tracer population for small fields at large radii, in the disk of the galaxy, these stars are packed too closely together to be individually resolved. We have therefore chosen to look instead at the considerably less abundant planetary nebula population.

## 1.3 Planetary nebulae as a kinematic tracer population

Planetary nebulae (PNe), with their bright emission lines, have long been recognised as a simple dynamical tracer of a stellar population. They are formed during a short stage of the post-main sequence evolution of low to intermediate mass stars (up to  $\sim 8M_{\odot}$ ). As stars evolve fairly rapidly (of the order a few hundred million years) but quite gently from the giant phase to the PN phase, the kinematics properties of the two populations should be essentially identical. We now summarise the major points of this stage of stellar evolution. These are also indicated in the schematic Hertzsprung-Russell diagram in Figure 1.2. A more detailed description can be found

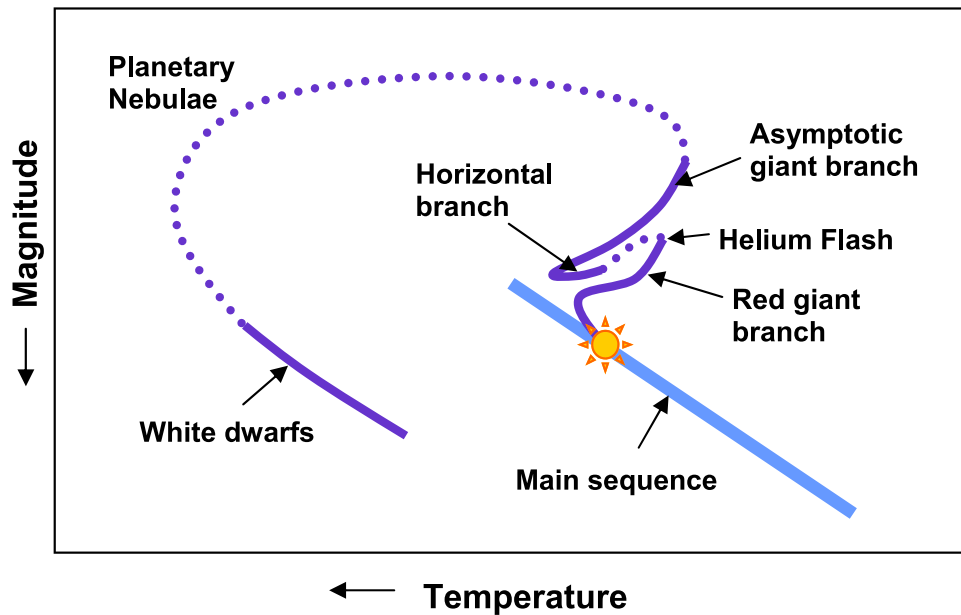


**Figure 1.2:** A schematic diagram of the post main-sequence evolution of low to intermediate mass stars.

in Section 13.2 of Carroll & Ostlie (1996).

The post-main sequence phase of stellar evolution begins when core hydrogen fusion ends. This causes an overall contraction of the star, which in turn ignites a shell of hydrogen fusion around the helium core and marks the beginning of the star's life as a subgiant. In time, the outer envelope of the star becomes convective, dredging material up from the inner layers of the star, enriching the outer layers. The increase in luminosity associated with this process moves the star onto the red giant branch. Gradually, the shell of hydrogen fusion increases the size of the helium core, which contracts and eventually collapses to the point it is supported by electron degeneracy. Eventually, suitable conditions are reached whereby quantum-mechanical tunnelling through the Coulomb barrier becomes efficient and helium in the core can undergo fusion, via the triple-alpha process, to become carbon. As the core is supported by electron degeneracy, this results in a thermonuclear runaway reaction, known as the helium flash. The star evolves rapidly until electron degeneracy is lifted, at which point the star joins the horizontal branch. It remains in this state for a significant period, fusing helium to carbon and then oxygen in the core and hydrogen to helium in a thin shell. At this point instabilities in the hydrogen fusing shell can lead to the periodic pulsations characteristic of variable stars. In much the same way as with the hydrogen fusion, the helium in the core eventually runs out and helium fusion moves to a shell around the core and a second dredge up of material occurs, further enriching the outer envelope with heavy elements. At this point the star joins the asymptotic giant branch. The shell of helium fusion is itself surrounded by a shell of hydrogen fusion, and interactions between the two shell sources lead to increasing instability and eventually the outer layers are expelled in massive stellar winds. This leaves behind a white dwarf star, which will gradually cool and fade, surrounded by a short-lived expanding cloud of hot gases: the planetary nebula.

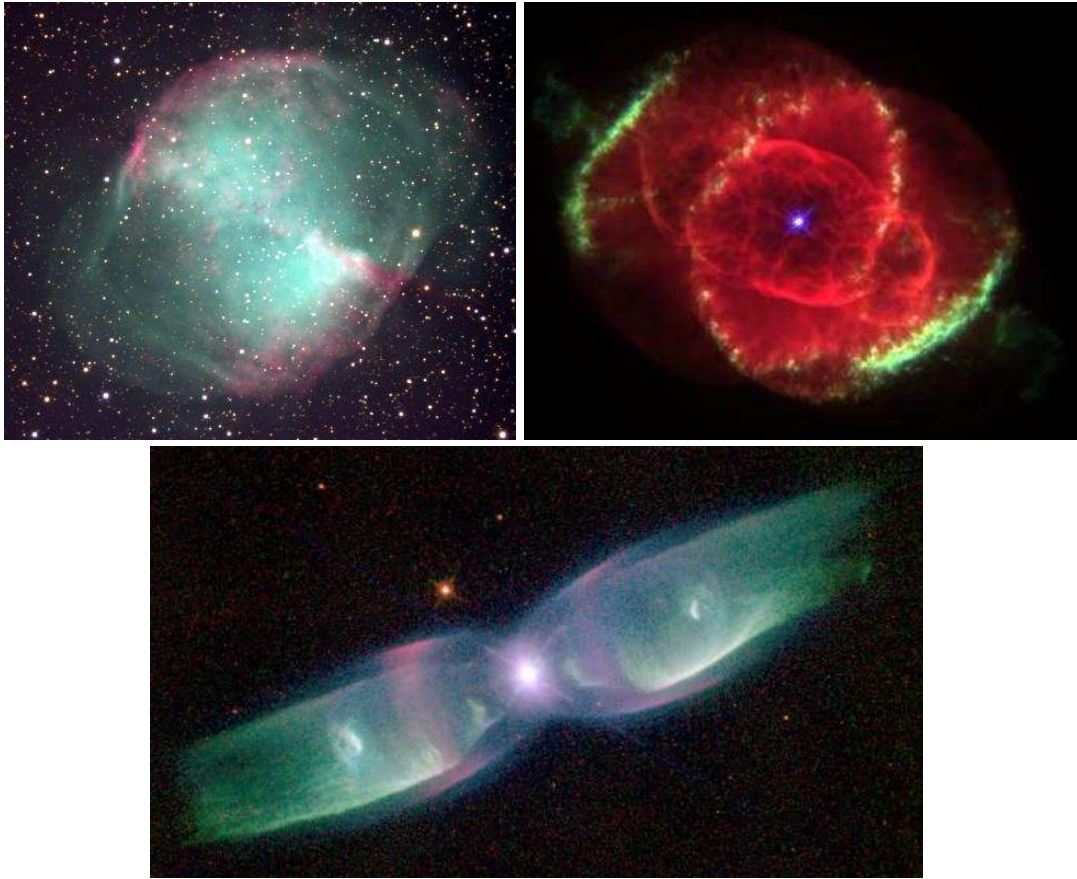


**Figure 1.3:** A selection of nearby planetary nebulae. Top left is the Dumbbell nebula (M27), top right the Cat's Eye nebula, and at the bottom M2-9. Picture credits are REU program/NOAO/AURA/NSF; J.P. Harrington and K.J. Borkowski (University of Maryland), and NASA; and Bruce Balick (University of Washington), Vincent Icke (Leiden University, The Netherlands), Garrelt Mellema (Stockholm University), and NASA, respectively.

As Figure 1.3 shows, these hot gas clouds can be highly structured and particularly beautiful when viewed at high resolution from relatively nearby. Fortunately for our purposes these structures are small, less than  $\sim 1$  pc for PNe in the Milky Way (Acker et al., 1992), and therefore, are not spatially resolved under normal ground-based observing conditions at distances beyond the Milky Way and its satellite galaxy system.

The distinctive colourings of the PNe shown in Figure 1.3 come mainly from energy emitted by a small number of bright, narrow emission lines. These are produced as the gas cloud is heated and ionised by ultra violet light from the central white dwarf. The subsequent deionisation, via emission of a photon, produces the strong, narrow emission lines that we see and that provide a simple tracer of the stars velocity. The reddish colours mostly originate from ionised hydrogen emission lines, such as  $H\alpha$  at  $6563 \text{ \AA}$ . The greenish tints are caused by light emitted from the forbidden emission lines of [O III] at  $5007 \text{ \AA}$  and  $4959 \text{ \AA}$ , through which up to  $\sim 10\%$  of the total luminosity of the PN can be emitted. The line is ‘forbidden’ as it originates from a metastable energy level, which, having a decay timescale of the order of one second, would not normally be seen in a high density gas where collision timescales are significantly shorter. It is only in diffuse astrophysical environments, where collision timescales are long enough that the transition can occur.

The presence of these strong emission lines make PNe quite easy to identify and render the measurement of their Doppler shifts fairly trivial. Recent technological developments such as wide-field multi-object and imaging spectrographs are now putting us in a position to observe large numbers of individual PNe across entire galaxies out to distances of  $\sim 25$  Mpc (Douglas et al., 2002).

One seeming disadvantage of using PNe, resulting from their very short lifetimes (only a few tens of thousands of years), is that they are quite rare objects. However, this can actually be something of an advantage as, unlike for common types of star, it is possible to observe *all* the bright PNe in a galaxy and produce a spatially complete, magnitude limited survey.

There are a number of other advantages to using PNe as our tracer population. Firstly, they are observed to have a universal luminosity function. This means a galaxy's PN population can be used as a standard candle for distance measurements [for example the eleven part series of papers beginning with Jacoby 1989], and provides us with a way to check for consistency within our sample. Secondly, the number of PNe at a given magnitude is related only to the luminosity, and hence mass, of the stellar population from which they arise (Jacoby, 1980; Buzzoni, Arnaboldi & Corradi, 2006), which also provides us with a tool that can be used to check that our survey is coherent.

At this point we must note suggestions that have been made in recent years that bright PNe may result only from relatively high mass progenitor stars (Marigo et al., 2004) and that the bright end of the luminosity function may be dependant upon the age of the stellar population. We will address this suggestion at appropriate points during the analysis of this survey.

Having chosen to perform a stellar kinematic survey of a disk galaxy using PNe as a tracer population we may now consider the target galaxy. The most logical option is the Milky Way's twin, the Andromeda Galaxy.

## 1.4 The Andromeda Galaxy

The Andromeda Galaxy is faintly visible to the naked eye and has been known of for over a millennium. The earliest record is that of Abd-al-Rahman Al-Sufi, a Persian astronomer who described it as a 'little cloud' in his Book of Fixed Stars, 964 AD. This observation was not generally known to European astronomers and the advent of the telescope led to a number of independent 'discoveries' of this object. The galaxy's best known designation 'M31' comes from its cataloguing by Charles Messier in August 1764. Since then M31's role in extra-galactic astronomy has been unparalleled. As well as being one of the first spiral galaxies to have its kinematics studied, it was Edwin Hubble's discovery of Cepheid variable stars in M31's disk and the subsequent distance estimates he made from them (Hubble, 1925) that demonstrated once and for all that the so-called spiral nebulae were in fact extra-galactic objects.

M31 is the nearest large spiral system and is similar in many ways to our own galaxy. Located at a distance of 785 kpc (McConnachie et al., 2005), its proximity has made it a prime target for modern observations aimed at understanding the nature, history



and evolution of spiral galaxies. While the very proximity of M31 allows for a great amount of detail to be seen, it causes the galaxy to subtend a very large area on the sky, making observations both difficult and time consuming. Developments in modern instrumentation have made it possible to observe this area in a relatively timely fashion and M31 has in recent years become the subject of numerous surveys at a number of wavelengths. A selection of images of M31 taken at different wavelengths are shown in Figure 1.4, including a composite of far and near ultra violet light taken by the Galaxy Evolution Explorer (GALEX, NASA), an optical image (NOAO), two infrared images, taken by the Spitzer space telescope (NASA), and a radio image taken at the Westerbork Synthesis Radio Telescope (WSRT) (Braun et al., 2002).

The UV image shows mainly young, hot, high mass stars tracing out star formation in the spiral arms and a central region containing older, cooler stars. At optical wavelengths we see the general distribution of starlight in M31; its close companion M32 is visible below and to the right of the centre. The IR images trace emission from warm dust in the spiral arms and the radio image shows the distribution of neutral hydrogen gas. Even a cursory glance at these images shows dust and star formation to be inextricably linked within the spiral arms of the galaxy. Yet the spiral arms themselves do not follow the neat patterns that are seen in some other galaxies; instead we see a mixture of spiral segments and what appears to be a large ring. This ring is visible in early measurements of the locations of emission line regions in M31 (Baade & Arp, 1964; Arp, 1964) and has been identified in a number of different emission lines (see, for example, Devereux et al., 1994; Nieten et al., 2005).

From the multi-wavelength photometric and spectroscopic studies of M31, a picture of the galaxy can be built up. Starting at the very centre, M31 has a double nucleus (Lauer et al., 1993) that houses a supermassive black hole (Kormendy & Bender, 1999). It is usually classified as an unbarred galaxy despite suggestions dating back 50 years that a misalignment between the bulge and disk in the optical photometry are indicative of a bar (Lindblad, 1956). Recent infrared imaging provides compelling evidence for a boxy bulge, characteristic of a bar as viewed in a close to edge on system (Beaton et al., 2006). The spiral arms are generally intermediately wound (normal classification is Sb) though the large inclination angle makes it difficult to trace out neat coherent spirals. The H I disk is observed to warp and flare at large radii (Brinks & Shane, 1984; Brinks & Burton, 1984; Braun, 1991). Recent studies of stellar kinematics in M31 have led to suggestions of a large, rotation dominated bulge (Hurley-Keller et al., 2004) and an extended disk of stars (Ibata et al., 2005). Beyond this the stellar halo is seen to extend a considerable distance (Guhathakurta et al., 2006a). As yet there has been little examination of the behaviour of stars in the disk of M31 and it is this that we aim to examine in this thesis.

### 1.4.1 Properties of the Andromeda Galaxy

At this point it is prudent to note that many measurements of M31's properties have been made over the years, with values continually being updated with new observations. Throughout this thesis we have used the properties summarised in Table 1.1 as being the generally accepted and most up to date values available. Distances are



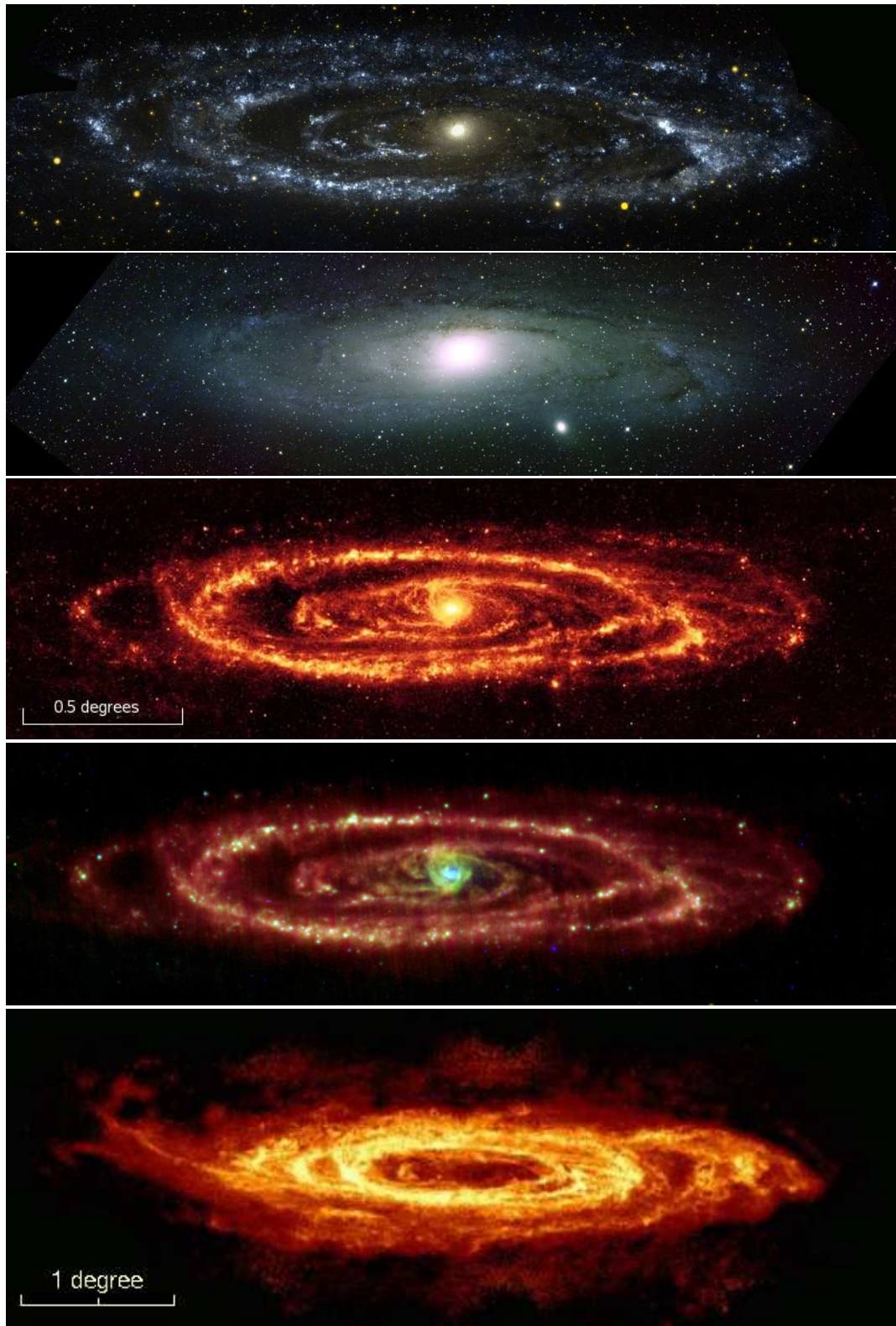


**Figure 1.4:** Multi-wavelength images of M31. From top to bottom: ultraviolet light, taken by GALEX, NASA; optical light, Bill Schoening, Vanessa Harvey/REU program/NOAO/AURA/NSF; 24  $\mu\text{m}$  infrared light; three channel infrared light at 24  $\mu\text{m}$  (blue), 70  $\mu\text{m}$  (green), and 160  $\mu\text{m}$  (red), Spitzer NASA/JPL-Caltech/K. Gordon (University of Arizona); and 21 cm radio emission, R. Braun (ASTRON). NOTE: The scale for the H I image is approximately twice that for the others.

**Table 1.1:** Basic observational properties of the Andromeda galaxy

Parameter	Value	Reference
R.A. (2000.0)	00 <sup>h</sup> 42 <sup>m</sup> 44.324 <sup>s</sup>	Crane, Dickel & Cowan (1992)
Declination (2000.0)	+41° 16′ 08.53″	Crane, Dickel & Cowan (1992)
Disk inclination	77.7°	de Vaucouleurs (1958)
Position angle of the major axis	37.7°	de Vaucouleurs (1958)
Distance	785 ± 25 kpc	McConnachie et al. (2005)
System velocity	−300 ± 4 km s <sup>−1</sup>	de Vaucouleurs et al. (1991)

generally quoted in degrees with kpc values in parentheses as this quantity has proven particularly prone to change.

For this survey, it is also useful to obtain the coordinates in an M31-based reference frame. We have therefore followed the geometric transformations of Huchra, Brodie & Kent (1991), which define right ascension and declination offsets relative to the centre of M31,  $\{\xi, \eta\}$  and coordinates aligned with the system’s major and minor axes,  $\{X, Y\}$ , via the relations

$$\xi = \sin(\text{RA} - \text{RA}_0) \cos(\text{Dec}), \quad (1.1)$$

$$\eta = \sin(\text{Dec}) \cos(\text{Dec}_0) - \cos(\text{RA} - \text{RA}_0) \cos(\text{Dec}) \sin(\text{Dec}_0), \quad (1.2)$$

$$X = -\xi \sin(\text{PA}) - \eta \cos(\text{PA}), \quad (1.3)$$

$$Y = -\xi \cos(\text{PA}) + \eta \sin(\text{PA}), \quad (1.4)$$

in which  $(\text{RA}_0, \text{Dec}_0)$  defines the centre of the system and PA the position angle. For M31 these values are taken as those given in Table 1.1. With this choice of coordinates, positive  $X$  is located southwest of the centre of M31 and positive  $Y$  lies to the northwest.

## 1.4.2 Previous surveys of PNe in the Andromeda Galaxy

PNe, with their bright [O III] emission lines, have been known to exist in the Andromeda Galaxy for many decades. In 1955, Baade detected five such objects by comparing wavelength limited images including and excluding the bright, green emission lines common to PNe. A more extensive catalogue of 315 of M31’s PNe was published by Ford & Jacoby (1978a,b) and a later paper by Ciardullo et al. (1989) presented magnitudes for 429 PNe in the central regions of the Andromeda Galaxy. Ciardullo et al. (1989) also presented pioneering work, based on their sample of M31 PNe, studying the luminosity function of the PN population and the application of its bright end cutoff as a standard candle.

Some of the earliest measurements of PN velocities in M31 were made as part of a PhD thesis by Lawrie (1978), entitled ‘*The radial velocity dispersion of planetary nebulae in the nuclear bulge of M31*’. In this, and a subsequent paper (Lawrie & Ford, 1982), 42 PNe from the central regions of M31 were identified in a series of velocity modulated photographs, with velocities being measured for 32 of these. More common spectroscopic observations were made a few years later by Nolthenius & Ford (1984),

who took measurements of a further 34 PNe at large radii. This dataset was also part of a PhD project, entitled '*The distribution and dynamics of planetary nebulae in M32 and the Andromeda Galaxy*' (Nolthenius, 1984).

The early developments in instrumentation that allowed measurements to be made of doppler shifts in extragalactic PNe, also allowed the first chemical abundance measurements to be made for such objects. One of the earliest studies was Jacoby & Ford (1986)'s measurement of abundances in three PNe and one H II region in M31.

Further developments in technology and instrumentation have led to a number of recent surveys of PNe in the Andromeda Galaxy. Measurements of chemical abundances for 15 PNe in M31 have been made by Jacoby & Ciardullo (1999) and for a number of PNe in both M31 and its satellite, M32, have been made by Richer, Stasińska & McCall (1999); Hyung et al. (2000). Two other surveys of PN kinematics have come to press whilst our survey was being conducted. The first was a survey of 135 PNe in one quadrant of M31 performed by Hurley-Keller et al. (2004). The intriguing possibility of a new and unusual satellite galaxy, Andromeda VIII, based on PN and globular cluster velocities (Morrison et al., 2003) was based on this catalogue. The second was a survey performed by a number of collaborators on this project, covering an approximately  $2^\circ \times 2^\circ$  area centred on M31, and measuring velocities for 723 PNe.

## 1.5 Thesis overview

In this thesis, Chapter 2 gives a description of the Planetary Nebula Spectrograph, the instrument we have used to perform a comprehensive survey of the Andromeda Galaxy. The survey is described in Chapter 3, along with a detailed description of the data reduction methods used for this novel instrument. Calibrations and comparisons with other data sets are also described with the aim of establishing the true quality of observations with this new instrument. We also discuss in this chapter the possibility of contamination from H II regions and background galaxies as well as the level of completeness of the survey. Also covered in the survey area are a number of satellite and background galaxies. Emission-line objects originating from these galaxies are discussed in Chapter 4.

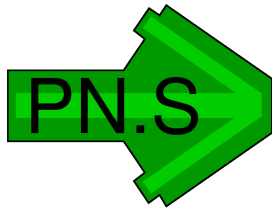
Chapter 5 presents the non-kinematic science results obtained from this survey. We aim to show the distribution of PNe across M31 and discuss the possibility of differences between the disk and bulge PN populations. In Chapter 6 we present the basic kinematic properties of the data set, producing rotation curves for both the PNe and H II regions. We also present discussions of the warp in M31's H I and stellar disks and the kinematic properties of photometrically and kinematically identified substructures in M31.

A selection of dynamical analyses of the data are presented in Chapter 7, including: a discussion of the link between the velocity dispersion profile and the stellar rotation curve via the asymmetric drift; simple fits to the rotation curve from a bulge-disk-halo model; and a novel new look at analysing discrete tracer populations in disk galaxies.

This survey and some of the basic kinematic analyses have previously been published

in Merrett et al. (2006a), *A deep kinematic survey of planetary nebulae in the Andromeda galaxy using the Planetary Nebula Spectrograph*. The existence of the velocity substructure suggested as an extension to the Southern Stream was originally presented in Merrett et al. (2003), *Tracing the star stream through M31 using planetary nebula kinematics*, and subsequently discussed in Merrett et al. (2006b), *Mapping the stellar dynamics of M31*.

## Chapter 2



# The Planetary Nebula Spectrograph

The Planetary Nebula Spectrograph (PN.S) and the principles of counter-dispersed imaging are described in this chapter. A full description of PN.S, its motivation, design and commissioning can be found in Douglas et al. 2002, *The Planetary Nebula Spectrograph: The Green Light for Galaxy Kinematics*. Other information is also available on the instrument website, [www.astro.rug.nl/~pns](http://www.astro.rug.nl/~pns).

### 2.1 Driving forces

As we have discussed in Chapter 1, understanding the kinematics of a galaxy's stellar system is critical to understanding that galaxy's mass profile, and one way stellar kinematics can be measured is by using PNe as a tracer population.

A kinematic survey of PNe using traditional techniques requires two separate observations to be made. The first, an on- off-band imaging survey to search for objects with bright emission lines. These targets are then followed up spectroscopically, usually with a multi-object spectrograph, in order to measure velocities. Surveys of this sort are well established, but require a considerable amount of telescope time.

PN.S, by contrast, was designed specifically for this task and requires only one observation to both detect and measure the velocities of all the PNe in its field of view. As a purpose-built instrument, PN.S has been optimised for this task and makes an efficient use of time, requiring a similar amount of telescope time to the imaging portion of a traditional survey.

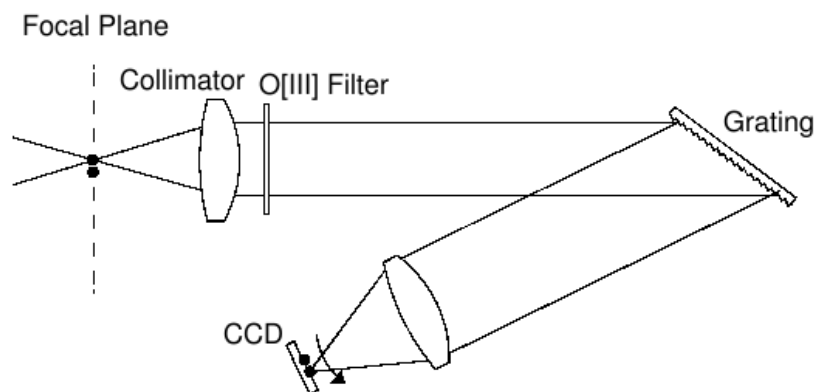


**Figure 2.1:** Optical setup for counter-dispersed imaging. Light is collimated, passed through a narrow band [O III] filter, dispersed by a grating, then focused onto a CCD.

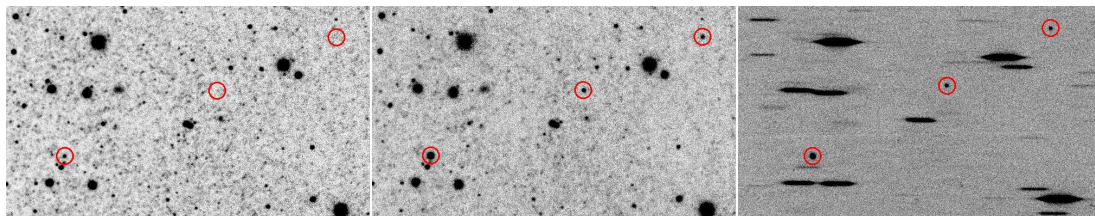


**Figure 2.2:** Example V-band, narrow band [O III], and PN.S images of the same field (left to right). Locations of the PNe are marked in the three images. In the V-band image the PNe are either not visible or very faint compared to their counterparts in the [O III] narrow band image, while in the PN.S image they are easily identified as the emission line point sources. The V-band and [O III] narrow band images are taken from Massey et al. (2002).

## 2.2 Counter-dispersed imaging and the PN.S

PN.S works using a technique called counter-dispersed imaging (CDI), a novel application of spectrographic imaging that has its roots in the work of Charles Fehrenbach in the late 1940s (Fehrenbach, 1947, 1948), but was not fully exploited until relatively recently (Douglas & Taylor, 1999). When using CDI to look for PNe, the field of interest is imaged through a narrow band [O III] filter and a slitless spectrograph, as shown in Figure 2.1. In the resulting image, stellar and ambient light is smeared out in the dispersion direction, while the [O III] emission from a PN (or any other ionised gas cloud) remains as a bright point source, as shown in Figure 2.2. PNe are shifted in the dispersion direction away from their true positions by an amount related to the observed wavelength of the emission line.

While it is extremely easy to identify emission line objects in a dispersed image, a single image is of little practical use. In order to extract useful information, a second comparison image is required. This can be a conventional [O III] image allowing comparison against the measured positions, as used by Méndez et al. (2001), but in CDI a second spectrographic image, dispersed in the opposite direction to the first, is used. In PN.S the second, counter-dispersed, image is taken simultaneously with the first by a second spectrograph rotated by  $180^\circ$  as shown in the schematic diagram of the PN.S layout in Figure 2.3. Examining the resulting two images together gives the positions and velocities of any PNe in the field, while photometry can be measured from either



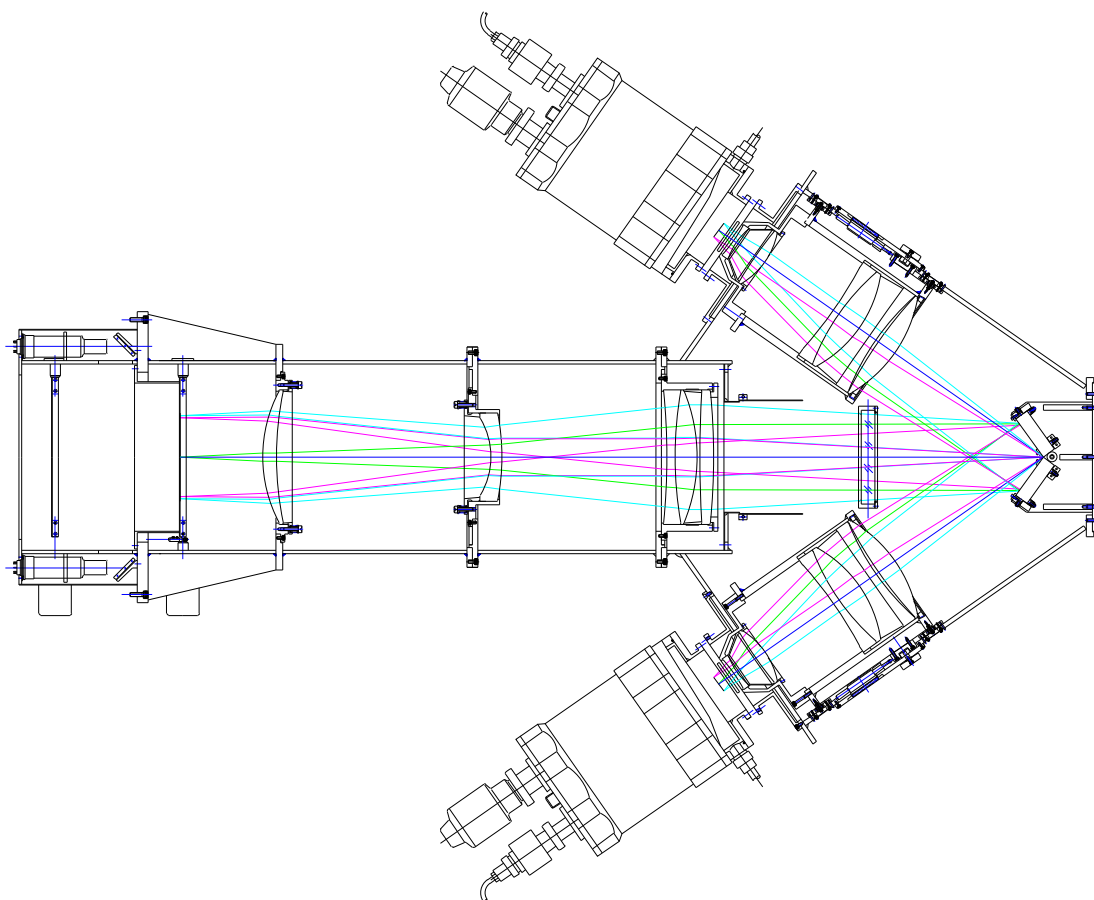


**Figure 2.3:** A schematic representation of PN.S. The instrument has a pair of gratings at its base (the right hand side of this image) allowing a pair of counter-dispersed images to be produced.

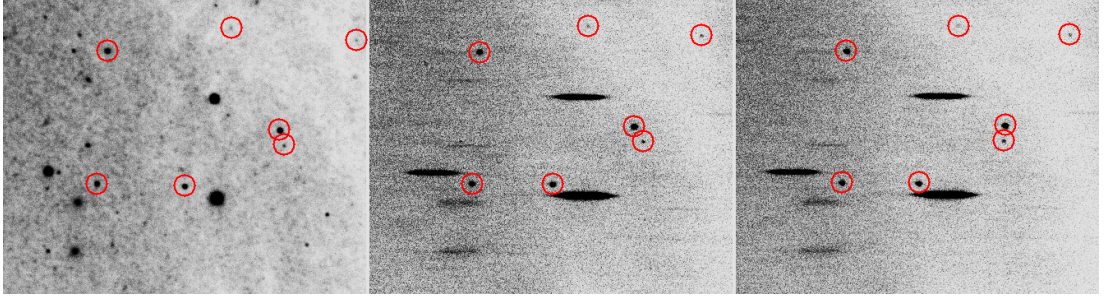
image.

Figure 2.4 shows a small section of the two PN.S images alongside an [O III] image of the same area of sky (Massey et al., 2002). It is readily apparent from the PN.S images which objects are stars and which are PNe. Whilst it is not possible to see the effect of the source velocity on dispersion when looking at individual PNe, we are fortunate in this field to find two PNe that are projected close together but have quite different velocities. These two PNe, located to the centre right of the image, are clearly displaced differently, relative to one another, in the two PN.S images.

## 2.3 The calibration mask

In practice, turning the PN.S images into useful information requires comparison against calibration images. A calibration mask was therefore built into the instrument, which can be moved into the focal plane by a motor, in between science images. The mask has 178 regularly spaced holes in it (Figure 2.5), through which the telescope's copper-neon-argon arc lamps shine 178 short filter-limited spectra (Figure 2.6).

These calibration images are used in two ways. Firstly, the locations of the brightest emission line ( $5017 \text{ \AA}$ ) are compared to an 'ideal' mask and used to map distortions and



**Figure 2.4:** An example PN.S image. The left hand image shows a section of one of Massey et al. (2002)’s [O III] images, the middle and right images are the PN.S images of that section of sky. It is readily apparent which of the sources in the [O III] imaging are PNe when compared to the PN.S images and these are highlighted in all three images.

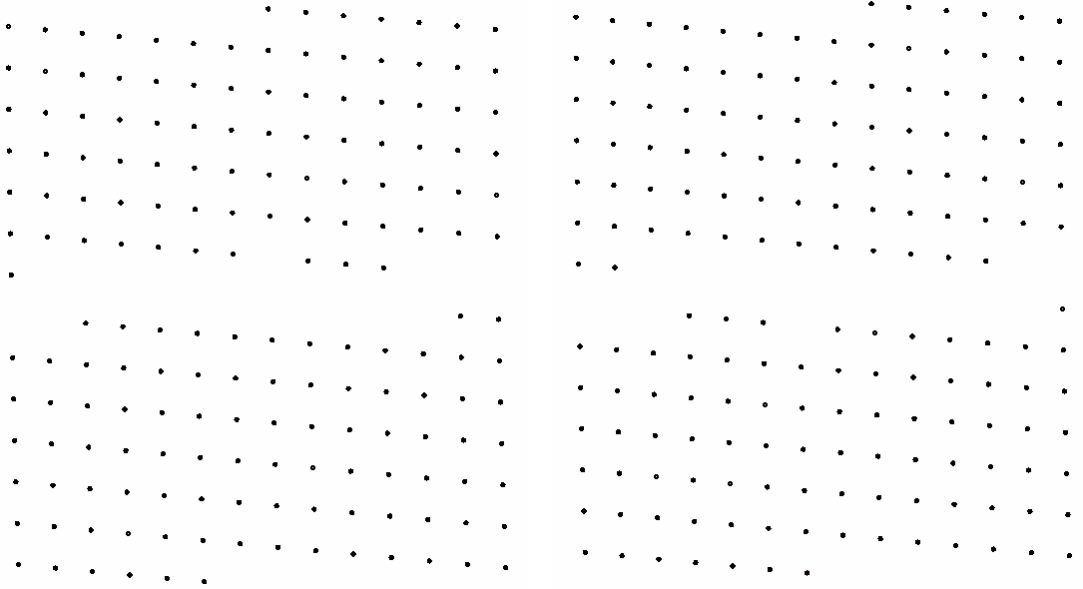


**Figure 2.5:** Locations of the mask holes as seen in the two PN.S images. For the images to line up one of these must be rotated through  $\sim 180^\circ$ .

rotations in the calibration images. The maps are then used to remove the distortions in the science images. Secondly, the spectra are used to characterise variations in the dispersion across the image in order to calibrate the PN wavelengths. Use of the calibration masks will be revisited in Chapter 3.

## 2.4 Instrument specifications

PN.S was designed with three different filters with central wavelengths of approximately 5000 Å, 5034 Å and 5058 Å, giving coverage from the Local Group out to redshift  $\sim 0.01$ . The filter mount can be tilted, tuning the filters to the systemic velocity of a target. The filters have very small bandpasses ( $\sim 35$  Å) to minimise background noise and reduce the length of stellar trails in the image which can obstruct PN detections. For this survey of the Andromeda Galaxy we use the shortest wavelength filter,



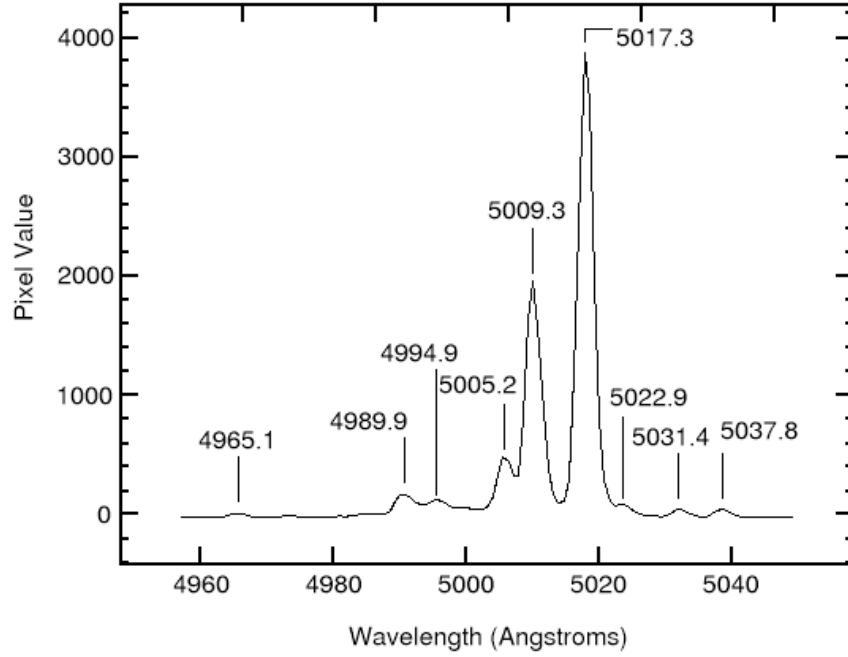


**Figure 2.6:** Detailed copper-neon-argon arc spectrum seen through filter A set at  $0^\circ$  tilt.

referred to as filter A, configured at  $0^\circ$  tilt. This has a central wavelength of  $5002.2 \text{ \AA}$  and a bandwidth of  $36.5 \text{ \AA}$ , corresponding to a velocity range for the  $[\text{O III}]$  line of  $-1380 \text{ km s}^{-1}$  to  $810 \text{ km s}^{-1}$ . This range is well matched to the velocity range of components of M31, which lie between approximately  $-600$  and  $0 \text{ km s}^{-1}$ , but also allows a significant margin for the detection of any unexpected high-velocity features.

Filter bandwidths of this size are actually rather generous for any individual galaxy, with velocity ranges of  $\sim 2000 \text{ km s}^{-1}$  catered for. Decreasing the bandwidth to around  $20 \text{ \AA}$  would still allow for a  $1200 \text{ km s}^{-1}$  velocity range, more than sufficient for most galaxies. The resulting reduction in background light, both from the galaxy and the night sky, would improve the overall system efficiency. However, more filters would be required to allow coverage of the same redshift range, and hence number of galaxies, as is allowed by the three filters listed above.

PN.S uses a pair of Spectronic 35-53  $600 \text{ g/mm}$ ,  $8.5^\circ$  blazed gratings to disperse the light. These were chosen to balance the competing needs for small and large dispersions. A small dispersion is needed: to minimise the length of star trails which obliterate a significant fraction of the field; to keep the PNe emission lines within the field of view of both the CCDs; and to minimise the confusion that a large separation between the emission line pairs creates. However, a large dispersion is needed to increase the velocity precision. In the normal setup, these gratings produce dispersions of  $1.29 \text{ pixels \AA}^{-1}$ .

Thus far PN.S has only been used at the William Herschel Telescope, part of the Isaac Newton Group of Telescopes in La Palma (Figure 2.7). We have used a pair of near-identical CCDs belonging to the ING (EEV12 and EEV13) on PN.S's two arms, the basic parameters of which are summarised in Table 2.1. When used with PN.S mounted at the  $f/10.942$  Cassegrain focus, pixel scales of  $3.32 \text{ pixels per arcsecond}$  in the disper-

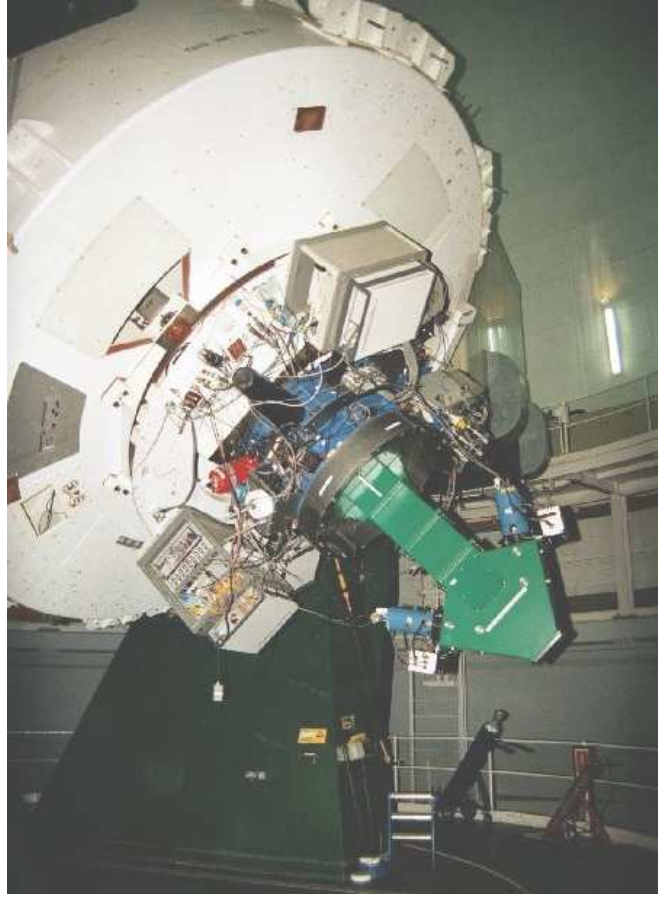


**Figure 2.7:** PN.S mounted at the Cassegrain focus of the William Herschel Telescope in La Palma.

**Table 2.1:** CCD Parameters.

	EEV12	EEV13
Pixel size (X×Y)	$13.5 \times 13.5 \mu\text{m}$	$13.5 \times 13.5 \mu\text{m}$
Size of digitised area (X×Y)	$2148 \times 4200$ pixels	$2148 \times 4200$ pixels
Bias (slow readout)	1244 ADU	1060 ADU
Gain	1.16 electrons per ADU	1.20 electrons per ADU
Noise	3.5 electrons	3.6 electrons

sion direction and 3.67 pixels per arcsecond in the spatial direction are obtained. The CCDs are windowed down to  $2150 \times 2500$  pixels, a field size of  $10.79' \times 11.35'$ . The two images PN.S produces are arbitrarily defined as the left and right hand images. For consistency EEV12 is always used on the left and EEV13 on the right.

## 2.5 Photometric efficiency

For PN.S to provide a realistic alternative to traditional spectroscopy, it had to be photometrically efficient. The design target was for a total system efficiency of  $\sim 30\%$ , about twice that of the William Herschel Telescope's Wide Field Fibre Optical Spec-

**Table 2.2:** Instrumental efficiencies calculated from spectrophotometric standard stars. References: (1) Oke (1974), (2) Oke & Gunn (1983), (3) Oke (1990)

Star	Ref.	$F_{5007}$ ( $\text{erg s}^{-1} \text{Å}^{-1}$ )	Date	Efficiency		
				Left	Right	Total
LDS 749B	1	154.759	2002-10-10	0.1424	0.1467	0.2891
BD+33 2642	2	6367.221	2002-10-10	0.1305	0.1322	0.2628
G193-74	3	63.438	2002-10-13	0.1533	0.1393	0.2926
BD+17 4708	3	18303.018	2003-09-29	0.1454	0.1435	0.2890
BD+28 4211	3	8708.624	2002-10-08	0.1365	0.1325	0.2691
BD+28 4211	3	8708.624	2002-10-10	0.1331	0.1290	0.2621
BD+28 4211	3	8708.624	2002-10-11	0.1328	0.1299	0.2626
BD+28 4211	3	8708.624	2002-10-11	0.1322	0.1312	0.2634
BD+28 4211	3	8708.624	2002-10-12	0.1331	0.1298	0.2629
BD+28 4211	3	8708.624	2003-09-29	0.1438	0.1414	0.2852
BD+28 4211	3	8708.624	2003-09-30	0.1371	0.1292	0.2662

trograph (WYFFOS).

We have estimated the total system efficiency for the observational setup described by observing spectrophotometric standard stars. These observations were short ( $\sim 30$  s), and were taken without using the shutter<sup>1</sup>. The flux per unit wavelength was measured from a narrow column through the brightest region of the stellar trail and compared with the published value for this wavelength. As Table 2.2 shows, the total system efficiency estimates are found to be surprisingly consistent, with a mean value of  $\text{Eff}_{\text{total}} = 27.3 \pm 0.4\%$ , with much of the scatter attributable to the non-photometric conditions. As only a few standard star observations were made during the run this level of consistency may be artificially low. However, since the science goals of this kinematic survey do not require high precision photometry, this uncertainty is of little significance.

## 2.6 Advantages and disadvantages of PN.S

As has been discussed, PN.S is a photometrically efficient instrument. However, it is not without some drawbacks. The maximum velocity accuracy obtainable is  $\sim 15 - 20 \text{ km s}^{-1}$ , somewhat lower than the  $\sim 2 - 10 \text{ km s}^{-1}$  that can be achieved with traditional spectroscopy (Halliday et al., 2006; Hurley-Keller et al., 2004; Ciardullo et al., 2004). Nevertheless an accuracy of  $\sim 20 \text{ km s}^{-1}$  is sufficient to study even quite subtle kinematic properties of external galaxies.

Apart from the timing efficiency of PN.S's single observation, the instrument has a number of other advantages over traditional techniques, principally, that there is relatively little loss of information. All PNe that are seen in the PN.S images can have velocities measured for them; PNe are only lost if they overlap a stellar trail. With the

<sup>1</sup>The shutter mechanism is slow, taking  $\sim 10$  s to move out and back into the focal plane making timings for short exposures inaccurate. As the CCDs were windowed down, the beginning of the readout was a fast parallel transfer of the charges, creating a fast end to the exposure and improving the accuracy of the timings.

traditional approach, preliminary imaging must be accurate to at least  $0.5''$  in order to position fibres or slits for follow up spectroscopic observations. Even then, some PNe will not be found. The on- off-band imaging in itself is not foolproof with occasional mis-identifications of continuum objects.

As a new instrument using a relatively untested observing technique, confidence in PN.S's accuracy must be established. As the Andromeda Galaxy has been the subject of a number of recent PN surveys using traditional observing techniques, this survey provides not only the largest survey of PNe in any galaxy but also a unique opportunity to thoroughly test the Planetary Nebula Spectrograph.

## Chapter 3

# Surveying the Andromeda Galaxy

In this chapter we present our PN.S and accompanying narrow band imaging surveys of the Andromeda Galaxy, including observations, data reduction and calibrations, comparisons with other data sets, and a discussion of contaminants in and completeness of the sample.

### 3.1 Observations

The PN.S observations for this survey were carried out with the instrument mounted on the William Herschel Telescope (WHT) in La Palma during two runs: 2002 October 8 – 13 and 2003 September 29 – October 5. In M31’s halo, where PNe are scarce, supplementary imaging was used to optimise the choice of fields to be observed with PN.S. This was obtained using the Wide Field Camera (WFC) on the Isaac Newton Telescope (INT), also in La Palma, on 2003 August 16 – 21. Figure 3.1 shows the locations of the fields observed with both instruments.

Single fifteen minute exposures were used for the majority of PN.S fields, although a few fields had slightly shorter exposure times and some fields were observed on multiple occasions. WFC exposures were twenty minutes long through the narrow-band [O III] filter and two minutes with the off-band  $g'$  filter. PN.S observations were made with the instrument’s ‘A’ filter at a  $0^\circ$  tilt angle as described in Chapter 2.

The adopted survey strategy was to tile the entire area of M31’s disk out to a 2 degree radius with overlapped PN.S pointings. We also mapped regions of particular interest at larger radii, such as the Northern Spur and Southern Stream (Ibata et al., 2001). However, at larger radii PNe become sufficiently scarce that most fields would be completely empty, so we used the INT narrow-band imaging to identify candidate PNe, and only made PN.S observations of fields where at least one object had been detected. In total, 226 PN.S fields were observed.

Weather conditions varied considerably during the PN.S runs with two half nights lost to cloud cover during the first run, and four full nights lost in the second. The seeing also changed significantly over the runs, with values between  $0.8''$  and  $3.1''$  recorded. To make optimum use of these varying conditions, we observed the central fields in

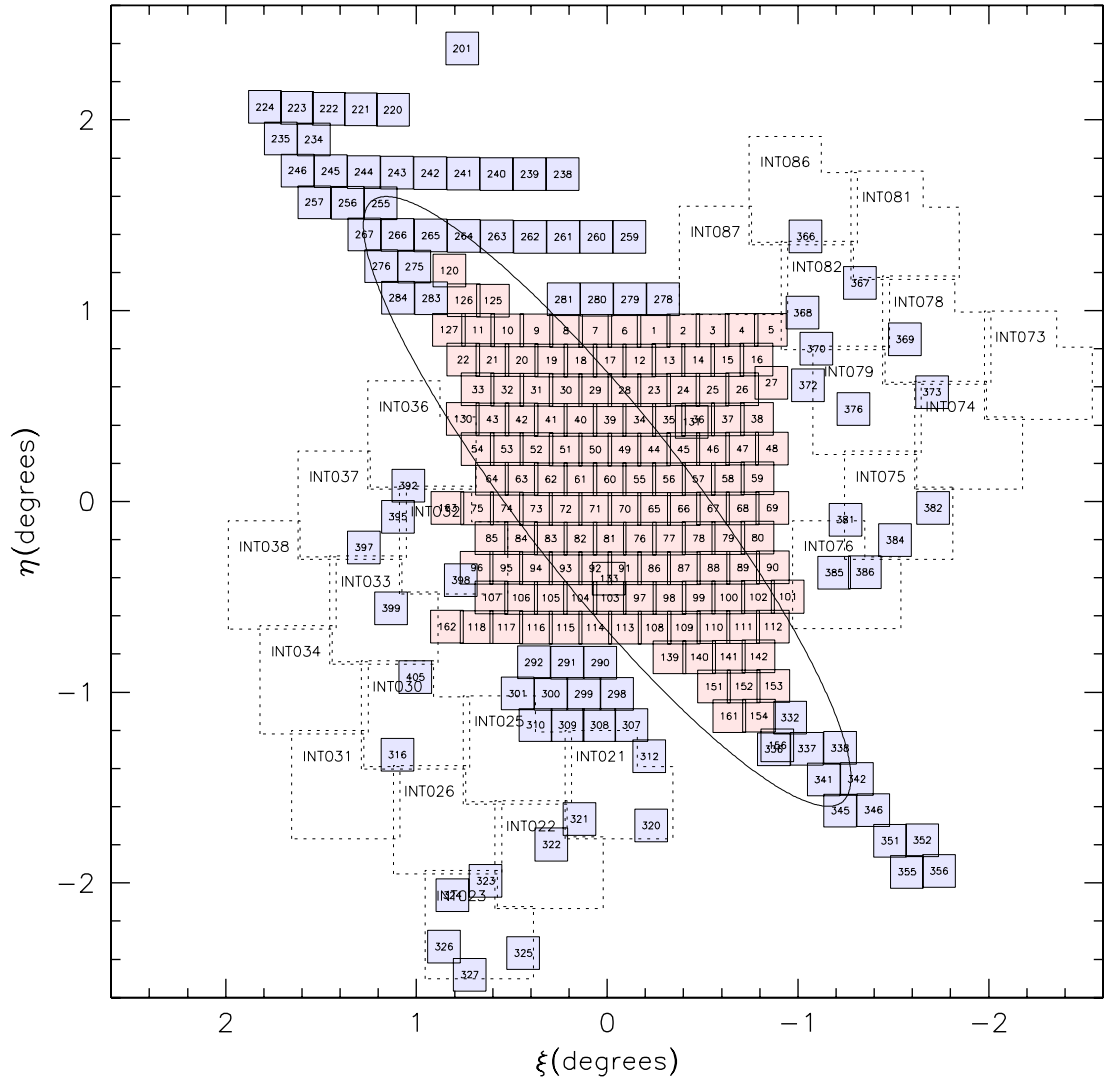


**Figure 3.1:** Fields observed in M31. The small square fields are PN.S field locations, with numbers 1-163 (shaded pink) observed on the first PN.S run, the rest (shaded pale blue) on the second; the larger fields with dotted outlines are the INT WFC fields. The ellipse marks a  $2^\circ$  (27.4 kpc) disk radius.

the worst seeing conditions (see Figure 3.2): PNe are sufficiently plentiful in these fields that we did not need to get so far down the luminosity function to obtain a useful dynamical sample, and the high continuum surface-brightness in this region meant that we would in any case not be able to achieve completeness at fainter magnitudes (see Section 3.5). Confusion with discrete objects is not a significant problem in surveys of this type as stars must be fairly bright to leave a visible trail. Even the very brightest stars at the distance of M31 leave only faint stellar trails and in the bright central regions they are not visible above the background light.

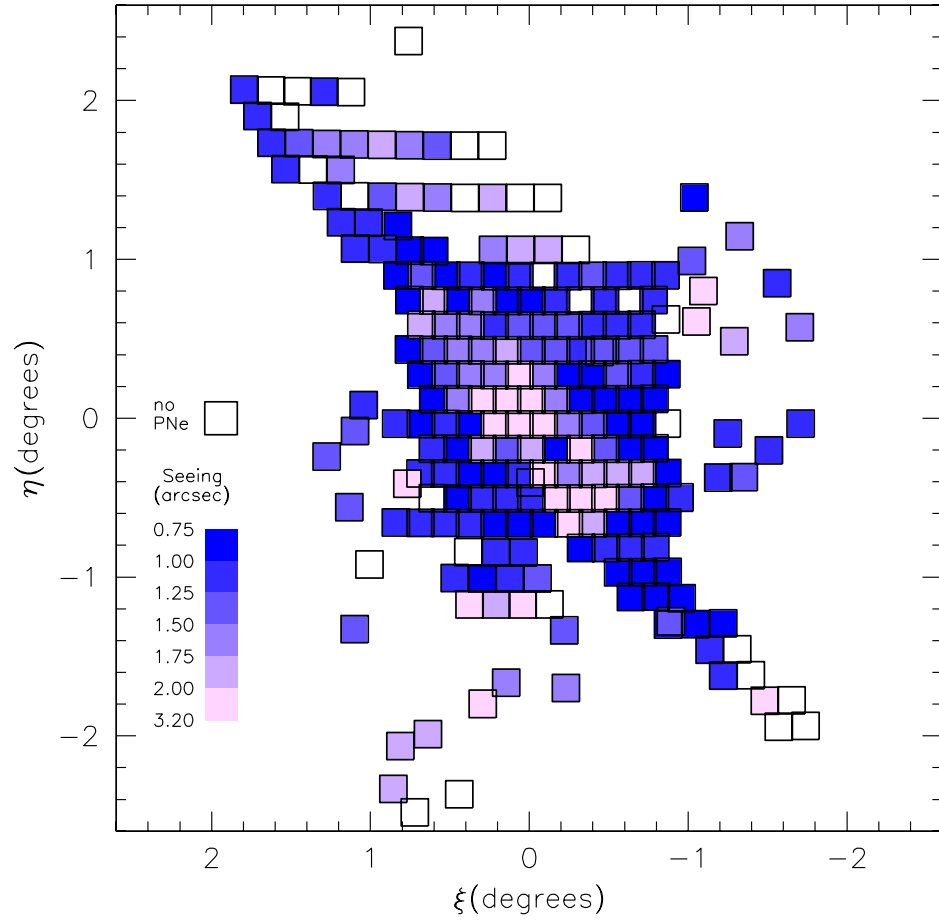


**Figure 3.2:** Seeing as measured for different survey fields. Darker squares represent better seeing, with values in arcseconds as given on the accompanying scale. Empty squares contained no detected PNe.

### 3.2 Wide Field Camera data reduction

The INT WFC data frames were debiased and flat-fielded using standard data reduction packages in *IRAF*. The  $g'$ -band images were remapped to match the coordinates of the [O III] images, and *SExtractor* (Bertin & Arnouts, 1996) was used in double-image mode to find sources in the [O III] image and simultaneously measure the flux of counterparts in the  $g'$  band. Objects with more than five times as many [O III] counts as  $g'$  counts were selected as potential PN candidates for PN.S follow-up. These candidates were then visually confirmed individually, and their approximate positions were calculated; more accurate astrometry was not required as the PN.S has a large field of view.

### 3.3 Planetary Nebula Spectrograph data reduction

Since the PN.S is such an unconventional instrument, we have had to produce a customised data reduction package to convert the raw data to a scientifically-usable form. This package has been constructed within *IRAF*, supplementing the standard tasks with

*Fortran* and *PGPLOT* extensions. Given the non-standard nature of this procedure, we now describe the reduction package and its application to the M31 observations in some detail.

### 3.3.1 Initial pipeline

Images were first debiased by subtracting a surface function fit to the pre- and over-scan regions using the *IRAF* task *imsurfit*. There was very little structure in the bias of the EEV CCDs, so the function subtracted was close to flat.

To map out and remove bad regions on the CCDs, zero-exposure bias frames were used to create a map of pixels where charge transfer problems have occurred. Skyflats were employed to locate other low-sensitivity pixels (by comparing to a median smoothed version; pixels with greater than  $9\sigma$  difference between the two were taken to be bad). These maps were then combined with a list of known bad pixel regions to make a mask which is fed to the standard *IRAF* routine *fixpix* to correct all the flats and science images.

Normalised pixel response maps were made by dividing flats by a median-filtered image (to remove spatial structures) then combining the flats using weights (to keep the noise Poissonian) and rejection (to eliminate cosmic ray events). The science and calibration images were flatfielded by dividing through by this response map.

The next step is to remove any residual cosmic rays: if they were left in through the next stages that remap pixels, then they would become smeared out, and could well mimic the point-spread function of a PN, so it is important to eliminate them at this stage. The cosmic rays were identified and removed using the Laplacian cosmic ray identification routine, *lacos\_im* (van Dokkum, 2001), with five iterations and a contrast limit between the cosmic rays and the underlying object of 1.2. This produces fairly clean images and any residual cosmic ray events are unlikely to be a problem as there would have to be a pair of residuals in the two images in locations such that they could be a PN.

The resulting cleaned science images still contain curvatures and rotations which must be eliminated in order to match up the left-right image pairs. The distortions involved are somewhat complicated for a slitless spectrograph like the PN.S, since they involve both imaging distortions and the wavelength calibration of the dispersed light. To determine the requisite mapping, we obtained frequent calibration images as described in Chapter 2. Spatial distortions mapped from the locations of the brightest emission line (5017 Å) across the field were removed from the accompanying science images using *IRAF*'s standard geometrical mapping routines, *geomap* and *geotran*. Two other lines at 4990 Å and 5009 Å were then used in conjunction with the 5017 Å line to characterise the wavelength calibration across the image by interpolating a quadratic solution between these points. A database of these solutions for the array of points on each CCD was produced; by interpolating between adjacent solutions, we can map directly from the locations of an object detected in the two arms,  $\{x_L, y_L, x_R, y_R\}$  to a true position on the sky and an emission wavelength,  $\{x_0, y_0, \lambda\}$ .

Following the spatial correction step, it is also possible to co-add images in those



cases where multiple observations of the same field have been taken. Any offsets between images were determined by measuring the positions, using *IRAF's xregister* task, of dispersed brighter stars in the field (selected from the USNO-B catalogue; Monet et al., 2003), and the necessary shifts were made. As a slight refinement, we actually performed both the image undistortion and this shift in a single transformation of the original image, so that there was only one interpolation of the data. We then combined the matched image frames using a weight determined by the quality of each image. These weights were calculated by using the *IRAF* routine *fitprofs* to fit a one-dimensional Gaussian across each star trail used in determining the shifts; the parameters of these fits were used to quantify the transparency, seeing and background level of each exposure. The appropriate weighting for each exposure was then given by

$$W = \frac{(\text{exposure time}) \times (\text{transparency})}{(\text{seeing})^2 \times (\text{background})}. \quad (3.1)$$

### 3.3.2 Identification of emission-line objects

Emission-line objects in the pipeline-processed images were identified by a semi-automated routine. The undistorted images from both the left and right arms were median-subtracted to remove unresolved continuum from M31 and a second image was produced that had been convolved with an elliptical Gaussian function elongated in the dispersion direction. *SExtractor* was then run in double image mode, detecting sources in the median subtracted image and measuring the brightness at the same position in the gaussian filtered image. Any sources originating from stellar spectra have approximately the same brightness in each image as this filtering has essentially no effect on star trails, while point sources are blurred out and are fainter in the gaussian filtered image than in the median subtracted image. This allows features in star trails incorrectly identified as point sources to be eliminated. Sources very close to the edge of each field were also eliminated as the routine tends to pick brightness peaks that are actually associated with the field edges; any genuine sources in these regions are added back in by hand at a later stage.

Sources independently identified from the two arms of the spectrograph were initially automatically matched in left–right pairs by selecting detections that have the same coordinate in the undispersed  $y$  directions to within two pixels, and whose coordinates in the dispersed  $x$  direction differ by an amount consistent with the bandpass of the filter and the wavelength calibration determined above. These candidate pairs were passed on to a custom-written *Fortran* routine which allows the two images to be examined side-by-side. Any false detections, such as bright spots within extended structures, were eliminated at this point. Further manual inspection then added back in any detections that have been missed by the automated routine, usually due to proximity to the field edge or a star. The edited list of emission-line pairs was then passed to the *IRAF phot* routine to improve the position determination and to measure the brightness of the source [using an aperture radius equal to the mean full width at half maximum (FWHM) seeing for that field to minimise sky contamination]. The FWHM of each source was determined using the Moffat parameter returned by the *IRAF imexam* task,

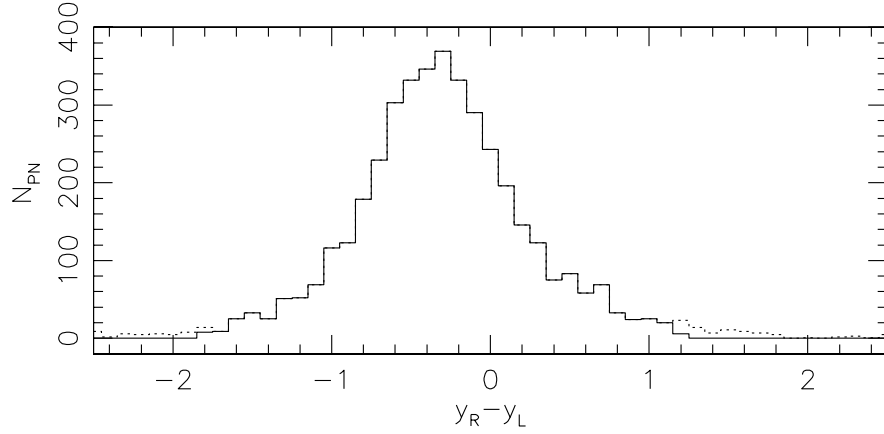


**Figure 3.3:** Difference in undispersed  $y$  coordinates of matched pairs of M31 point sources detected in the two arms of the PN.S. The dotted line shows those few pairs deemed spurious by the application of further cuts at  $y_R - y_L = -1.80$  and  $1.17$ .

as this turned out to be the most robust metric.

Once the source positions on both arms have been refined in this way, we can apply a slightly more stringent cut in matching up the spatial coordinates of sources to eliminate chance alignments: as Figure 3.3 shows, the distribution of differences in the  $y$  coordinate between the two arms is significantly tighter than the initial cut of  $\pm 2$  pixels, so we deemed the objects in tails of the distribution to be chance alignments, and eliminated them from the source list.

At this point, we have the definitive list of pairs of objects, and by applying the calibration described in Section 3.3.1 we can transform these coordinates into a spatial location and a wavelength. Identifying the emission with the  $5007 \text{ \AA}$  [O III] line, we can translate the observed wavelength into a velocity, which we correct to a heliocentric value on a field-by-field basis using *IRAF*'s *rvcorrect* routine. A measure of the internal consistency of these velocities can be obtained using the PNe that lie in the overlaps between fields for which we have multiple velocity measurements. There are 732 objects detected in more than one field (643 in two fields, 88 in three fields, 1 in four fields), so we have quite a large sample to play with. Figure 3.4 shows the distribution of velocity differences between pairs of measurements. A Gaussian fit to these data gives a dispersion of  $24 \text{ km s}^{-1}$ , implying an error on each individual measurement of  $17 \text{ km s}^{-1}$ . This value is clearly an over-simplification since the distribution appears somewhat non-Gaussian and possibly even multi-modal. This complex shape can be attributed to the complexity involved in the wavelength calibration of slitless spectroscopy. However, the repeat observations used in Fig. 3.4 all lie close to the edges of the instrument's field of view, where distortions in the wavelength solution are greatest and the amount of calibration data is smallest. The quoted error should therefore be viewed as conservative, but with some systematic residual errors on the scale of  $\sim 5\text{--}10 \text{ km s}^{-1}$  not ruled out. Nonetheless, even these pessimistic errors are entirely adequate in a study of the large-scale kinematics of a massive galaxy like M31.

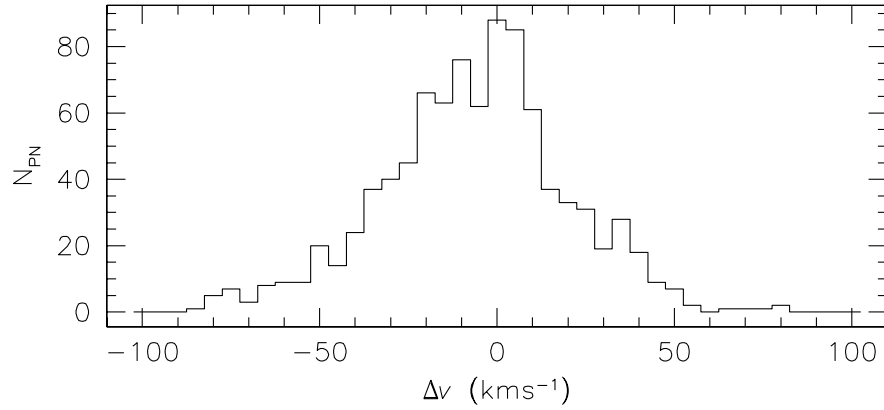


**Figure 3.4:** Differences between the velocities obtained for repeated observations of PNe in the overlaps between fields. A Gaussian fit gives a dispersion of  $24 \text{ km s}^{-1}$ , implying  $17 \text{ km s}^{-1}$  per measurement.

### 3.3.3 Astrometry

The measured coordinates must next be transformed into a standard reference frame. This process was carried out using the same basic routines as for image stacking (see Section 3.3.1). The approximate location of each field was determined from its nominal pointing, and star positions in the vicinity were read in from the USNO-B catalogue. The corresponding stars trails in the PN.S images were found and locations calculated using *IRAF's xregister* task, which cross-correlates an artificial star trail with the real one; the resulting coordinates were fed to the *ccmap* task to calculate the astrometric solution for the field. In the very central fields, the bright background means there are very few stars available. In these fields, PN positions that have already been calibrated in overlapping neighbouring fields have been added to the list of coordinates, in order to bootstrap the astrometric solution across the central region.

The PNe in the overlap regions between fields also provide an internal check on the accuracy of the astrometry, by measuring offsets between the coordinates for the same source in different fields. As with the velocity consistency check described above, this will tend to be a conservative measure of accuracy, since spatial distortions are greatest near the edges of fields where overlaps exist, so one might expect the astrometric solution to be poorest in these regions. As Figure 3.5 shows, the astrometric accuracy is somewhat better in declination than right ascension. This difference arises because right ascension corresponds to the direction in which the calibrating stars are dispersed, so centroiding their emission in this direction is fundamentally less accurate. However, the absolute positional accuracy is more than adequate for this large-scale kinematic survey of M31.

The astrometric matching of fields also allows us to make a final pass through the list of detected sources to eliminate the duplicate detections from field overlaps. Where the duplicate observations were obtained under similar seeing conditions, the positions, fluxes and velocities of the two detections were simply averaged; where the seeing conditions vary by more than  $0.5''$ , just the better-quality data were used.

As a final stage in the astrometry we have obtained coordinates in a more practical, M31 based reference frame using the transformations described in Chapter 1.

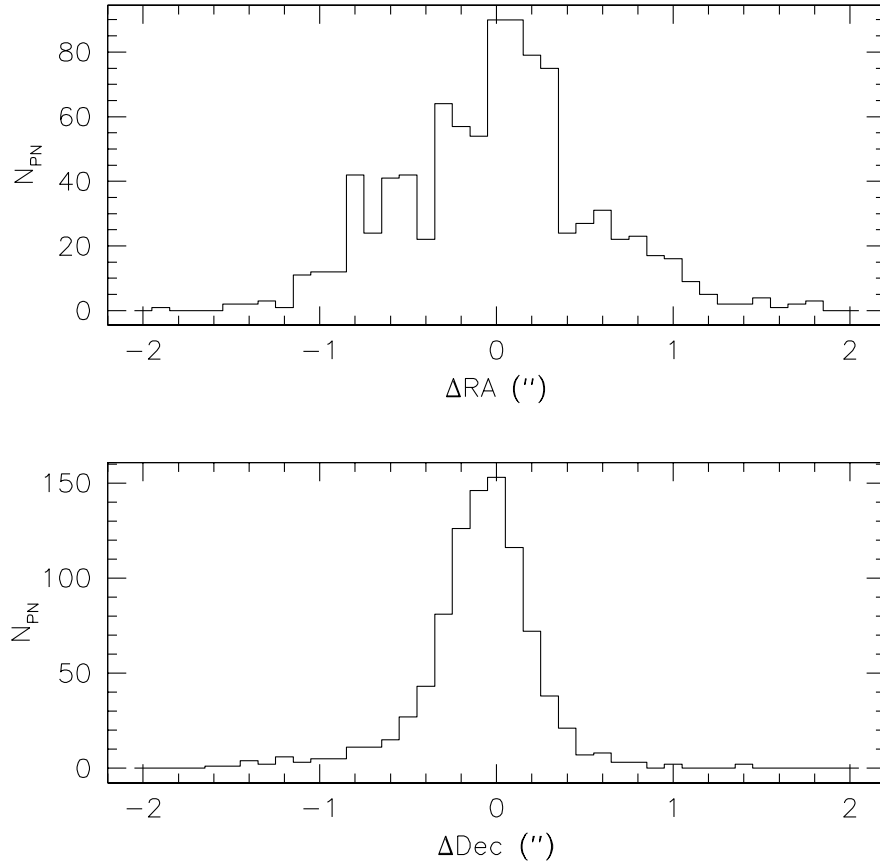


**Figure 3.5:** Differences between the positions obtained for repeated observations of PNe in the overlaps between fields. Gaussian fits to these give measurement uncertainties of  $\sigma_{RA} = 0.34''$  and  $\sigma_{Dec} = 0.16''$ .

### 3.3.4 Flux calibration

Although not primarily designed as a photometric instrument, the PN.S does provide information on the magnitudes of detected PNe through the brightness of the spots in the two arms. However, the conversion of count rates into fluxes is not entirely straightforward. The PN.S has a rather slow shutter that takes some 10 seconds to fully open and close, so the effective vignetting in short exposures is significantly different from that in long exposures. This limitation means that we could not use sky flats to determine the overall vignetting, so instead we used long exposure dome flats obtained during the day. To obtain an optimal vignetting function, dome flats obtained at many position angles were averaged to render the illumination of the field as uniform as possible. Since our science exposures are 15 minutes long, we have not applied any correction for the small variation in effective exposure time due to the slow shutter.

Fluxes of the detected sources were then calibrated using the formula

$$F_{5007} = \frac{(C_L \cdot g_L + C_R \cdot g_R) E_{5007}}{\text{Eff}_{\text{total}}} A T_{\text{exp}} 10^{\left(\frac{a_{\text{sky}} - a_{\text{Gal}}}{2.5}\right)}, \quad (3.2)$$

where  $C_L$  and  $C_R$  are the total counts from the left and right arms;  $g_L$  and  $g_R$  are the gains of the CCDs on each arm;  $E_{5007}$  is the energy of a photon at 5007 Å;  $\text{Eff}_{\text{total}}$  is the total system efficiency calculated in Chapter 2;  $A$  is the geometric collecting

**Table 3.1:** Sky extinction per unit airmass from the Carlsberg Meridian Telescope, and weather notes for the nights observed.

<sup>a</sup> The conversion to Ext(5000) is calculated from Table 2.2 in RGO/La Palma Technical Note 31 to be a factor 1.70. 5000 Å is the closest listed value to the central wavelength of our filter.

Night	Ext( $r'$ )	Error	Ext(5000 Å) <sup>a</sup>	Error	Comments
2002-10-08	0.101	0.004	0.172	0.007	Rain at end of night
2002-10-09	0.129:	0.029	0.219:	0.049	Cloudy at start of night
2002-10-10	0.106	0.006	0.180	0.010	
2002-10-11	0.107	0.005	0.182	0.009	
2002-10-12	0.106	0.005	0.180	0.009	
2002-10-13	0.112	0.009	0.190	0.015	
2003-09-29	0.234:	0.024	0.398:	0.041	
2003-09-30	0.213:	0.012	0.362:	0.020	Cloudy at start of night
2003-10-01	0.317:	0.068	0.539:	0.116	Mostly cloudy
2003-10-02	-	-	-	-	Mostly rain
2003-10-03	-	-	-	-	Rain
2003-10-04	-	-	-	-	Rain
2003-10-05	-	-	-	-	Rain

area of the telescope and is equal to 13.85 m<sup>2</sup>;  $T_{\text{exp}}$  is the exposure time;  $a_{\text{sky}}$  is the nightly sky extinction as recorded by the Carlsberg Meridian Telescope (see Table 3.1) multiplied by the airmass at which the field was observed; and  $a_{\text{Gal}}$  the Galactic extinction taken from Schlegel, Finkbeiner & Davis (1998) and corrected to our filter central wavelength using the relation from Cardelli, Clayton & Mathis (1989) giving a value of  $a_{\text{Gal}} = 0.226$ . The conversion to PN-specific magnitudes follows the Jacoby (1989) relationship,

$$m_{5007} = -2.5 \log(F_{5007}) - 13.74, \quad (3.3)$$

where the zero-point is chosen such that an emission line object has the same apparent magnitude as it would if observed through a V-band filter. To give a sense of this zero-point for objects in M31, the resulting magnitudes range from a bright H II region at 17.8 mag to the faintest PNe at  $\sim 26$  mag.

Once again, we can obtain an internal estimate of the uncertainty in magnitudes by comparing the values derived for duplicate observations in the overlaps between fields. Figure 3.6 shows the differences between magnitudes in these repeated observations; a Gaussian fit to this distribution gives a rather small measurement uncertainty of  $\sigma_{m_{5007}} = 0.07$  mag. Magnitudes for extended objects will be systematically underestimated by this technique as no allowance has been made in the choice of aperture size for objects that are larger than the field point-spread function. However, since the main focus of this survey is to determine the properties of unresolved PNe, this issue is not a major concern.

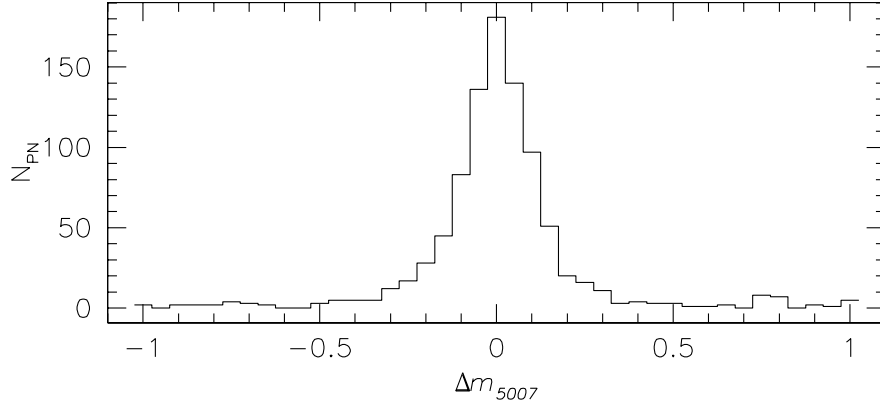


**Figure 3.6:** Magnitude variations within the PN.S data set from PNe in field overlaps. A Gaussian fit to this gives a measurement uncertainty of  $\sigma_{m_{5007}} = 0.07$  mag.

### 3.4 Comparison with other data sets

One concern with any data set from a novel instrument like the PN.S is that it may contain unpredicted systematic errors. Fortunately, a number of smaller data sets obtained using more conventional instrumentation already exist, so we can compare the new data with these subsets to check for such systematic effects. The locations of a selection of these surveys, with respect to the PN.S survey, are shown in Figure 3.7.

#### 3.4.1 Velocity comparison

The largest existing kinematic survey of PNe in M31 is that of Halliday et al. (2006, hereafter H06), which determined velocities for 723 PNe using the conventional approach of narrow-band imaging and fibre-fed spectroscopy. Of these PNe, we find 715 objects within  $4''$  of a PN.S object; the remaining 8 are likely obscured behind stellar trails in the PN.S images, but a 99% recovery rate is very respectable, and already gives a measure of the completeness for these brighter PNe.

If we plot the difference between H06 and PN.S velocities against the PN.S velocity, as in Figure 3.8, we find a small zero-point offset and a very slight linear dependence on velocity, fitted by the relation

$$v_{\text{PN.S}} - v_{\text{H06}} = 0.0151v_{\text{PN.S}} - 17.0. \quad (3.4)$$

This small systematic effect presumably arises from the limitations of the restricted range of arc lines available for PN.S wavelength calibration (see Figure 2.6). There is no large scale spatial dependence in this velocity difference, though there appears to be some small variation within the PN.S field. It makes very little difference to any of the scientific results, but for consistency we have applied the correction implicit in equation (3.4) to our complete data set and for all subsequent analysis. The residual differences in velocity between PN.S and H06 data are shown in Figure 3.9. Fitting a Gaussian to this distribution gives a dispersion of  $15.4 \text{ km s}^{-1}$ ; H06 quote an error of  $6 \text{ km s}^{-1}$  for their fibre spectroscopy, implying that the PN.S data have an uncertainty of  $14 \text{ km s}^{-1}$ . This value is somewhat smaller than the error deduced

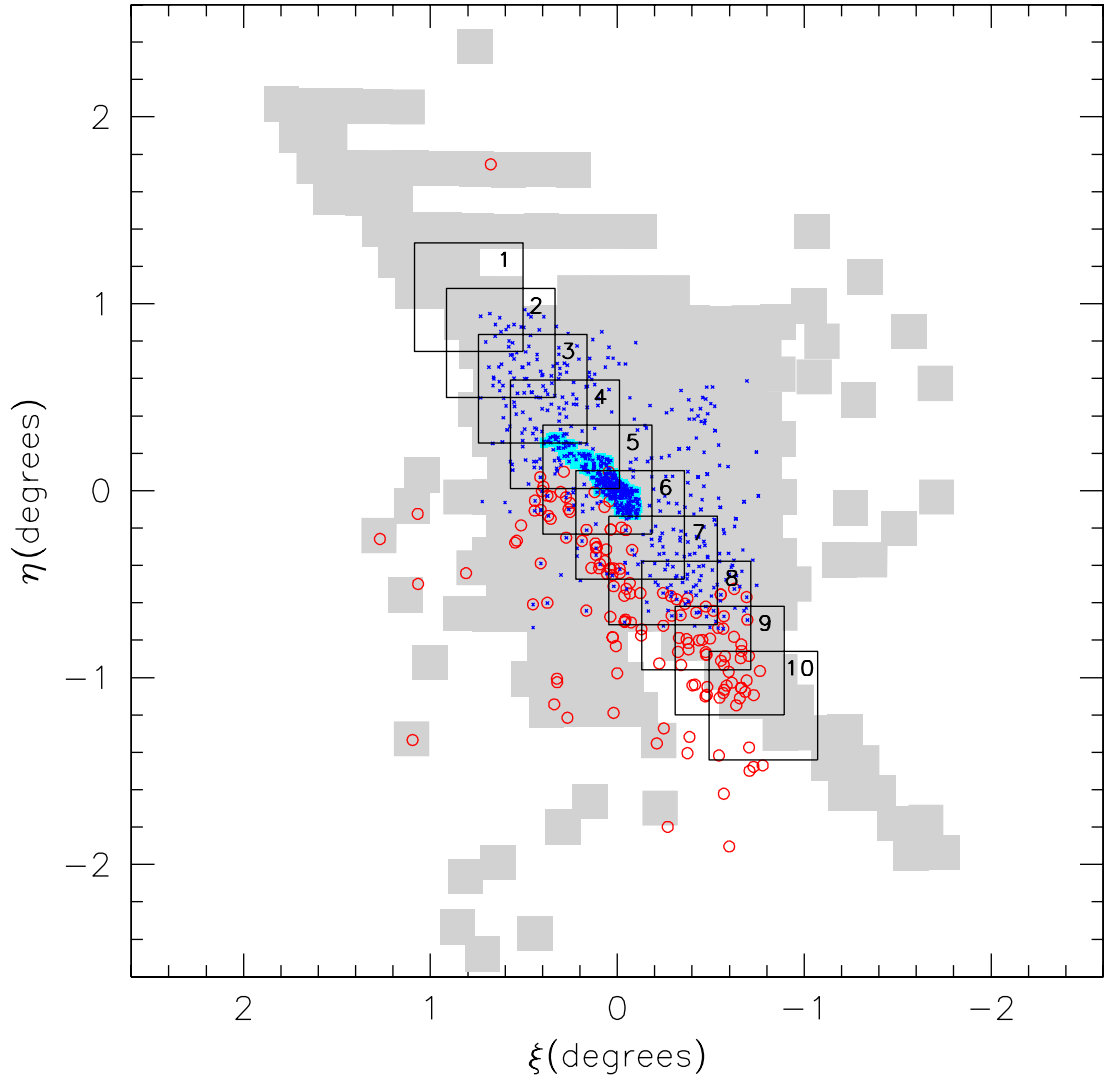


**Figure 3.7:** Positions of other surveys with respect to the PN.S survey. The PN.S survey area is shown in gray; the small, blue points are Halliday et al. (2006)’s fibre spectroscopy data; the red, open circles are the Hurley-Keller et al. (2004) data; Local Group Survey fields (Massey et al., 2002) are the large fields with solid outlines; and the Ciardullo et al. (1989) data are the solid cyan points near the centre (these have also been observed by Halliday et al.).

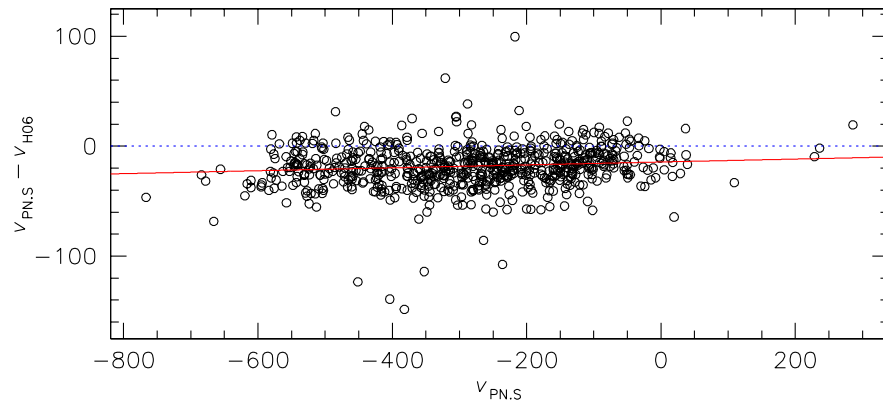


**Figure 3.8:** Comparison of initial PN.S velocities to H06 fibre-spectrograph velocities. The solid line shows the fit to the data given in equation (3.4), while the dotted line is at a difference of  $0 \text{ km s}^{-1}$ .

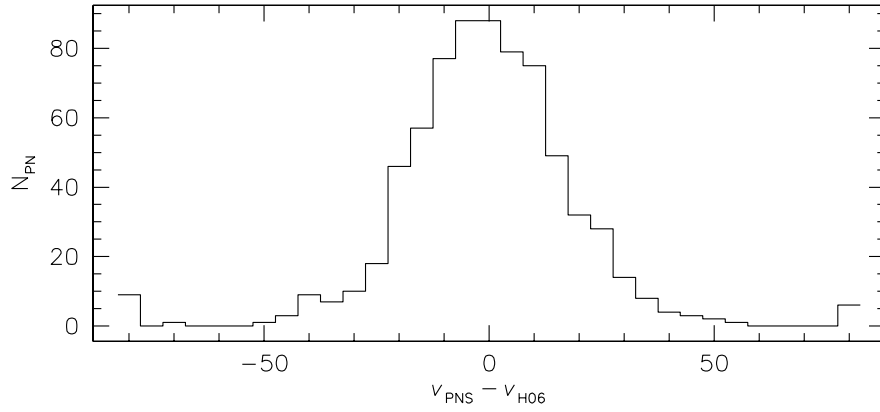


**Figure 3.9:** Plot of the difference between final PN.S velocities and H06's fibre-spectrograph velocities. A gaussian fit gives  $\overline{\Delta v} = -0.7 \pm 0.4 \text{ km s}^{-1}$  and  $\sigma = 15.4 \pm 0.4 \text{ km s}^{-1}$ .

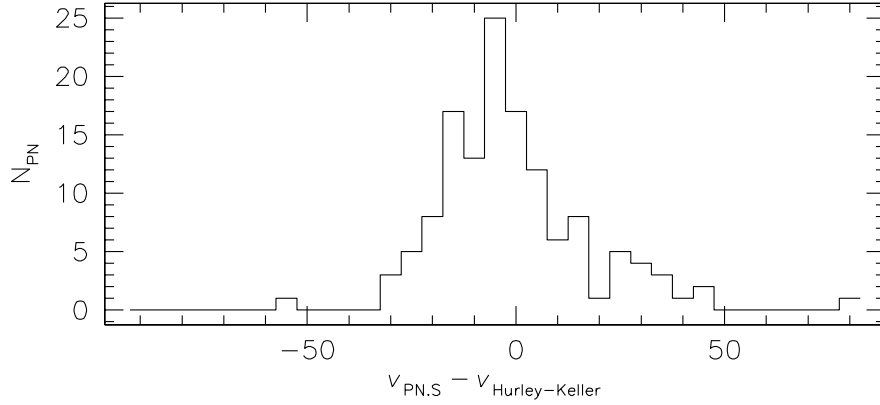


**Figure 3.10:** Plot of the difference between the final PN.S and the Hurley-Keller et al. (2004) velocities. A gaussian fit gives  $\overline{\Delta v} = -5 \pm 1 \text{ km s}^{-1}$  and  $\sigma = 12 \pm 1 \text{ km s}^{-1}$ .

from self-calibration for the reasons discussed above, and is probably a more accurate measure of the true uncertainty in the PN.S velocities.

An estimate of M31's system velocity for the PN.S data was made by averaging the mean velocities from radial bins on either side of the major axis for data within  $1^\circ$  ( $\sim 2.3$  scale lengths) of the centre so as to exclude warps and asymmetries that have been observed at large radial distances, leading to a value of  $-309 \text{ km s}^{-1}$ . This measurement is in reasonable agreement with the standard value of  $-300 \pm 4 \text{ km s}^{-1}$  (de Vaucouleurs et al., 1991) and in good agreement with H06's value of  $-310 \text{ km s}^{-1}$ .

As a test of the robustness of this conclusion, we can also compare our results with a smaller but differently located survey carried out by Hurley-Keller et al. (2004). They surveyed one quadrant of M31's halo, finding 135 PNe (see Figure 3.7). We have covered nearly their whole survey area, finding all but three of their PNe in the overlapping area. The distribution of differences in velocities is shown in Figure 3.10. A Gaussian fit to this distribution gives a mean velocity difference of  $-5 \pm 1 \text{ km s}^{-1}$  and a combined dispersion of  $12 \text{ km s}^{-1}$ , again lower than the claimed PN.S velocity error. However, the distribution of errors here is clearly non-Gaussian, so not too much weight should be given to the exact value. Nonetheless, the errors are clearly small, well below a level that would compromise this kinematic study of M31.



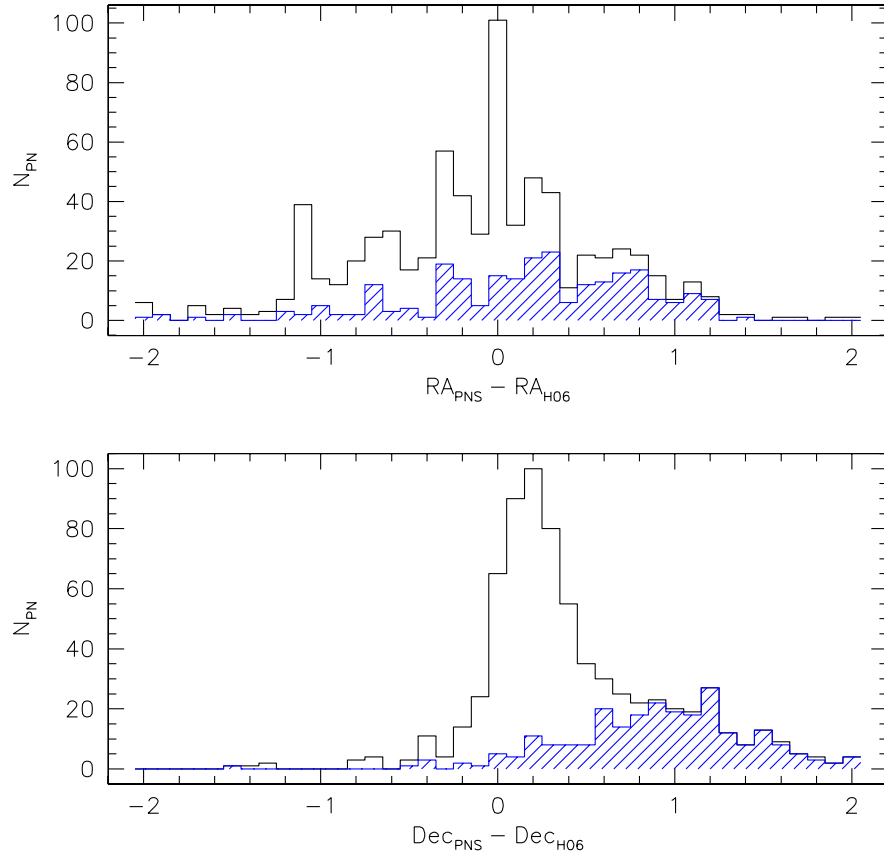


**Figure 3.11:** Comparison between PN.S and H06 astrometry, with differences measured in arcseconds. The black line represents all the PNe found in both catalogues; the blue shaded area shows those PNe in the central PN.S fields (60, 61, 70, 71)

### 3.4.2 Astrometric comparison

The PN.S astrometry can also be compared with the H06 data set. The distribution of differences in coordinates are shown in Figure 3.11. The right ascension distribution is similar to that found internally within the PN.S data, with a combined dispersion of  $\sim 0.6''$ . In declination there is a small systematic offset of  $+0.18''$ , with a long tail to positive values. As Figure 3.11 shows, the tails of the distribution are almost entirely populated by PNe from the four central PN.S fields. As discussed above, the lack of measurable stars in these fields compromises the PN.S astrometric solution somewhat, so such large errors are not surprising. Excluding these fields the combined dispersion in declination is  $\sim 0.2''$ . Given the enormous size of M31, such uncertainties are completely negligible for kinematic purposes.

### 3.4.3 Photometric comparison

Although not principally a photometric survey, we have been able to obtain quite consistent magnitudes from the PN.S data, so once again it would be useful to compare against other data to obtain an external measure of the data quality. Fortunately, M31 has been extensively imaged as part of the Local Group Survey (Massey et al., 2002, hereafter M02), which is comprised of a range of broad-band (UBVRI) and narrow-

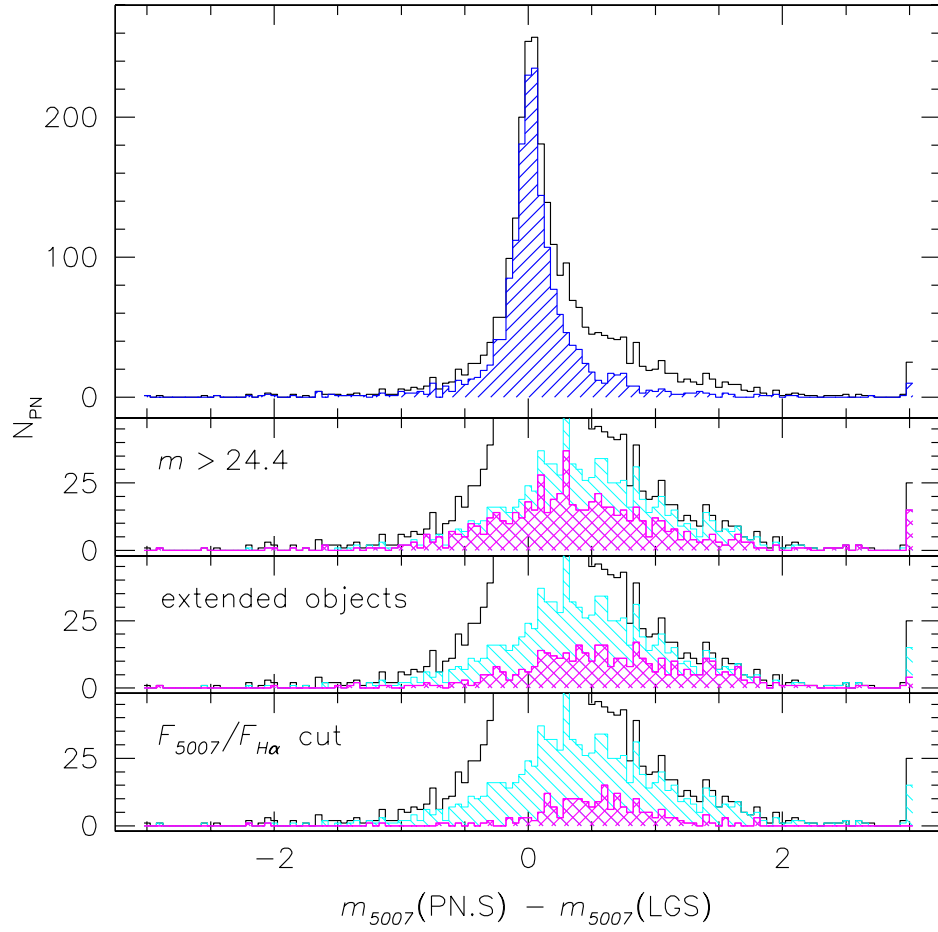


**Figure 3.12:** Photometric comparison between the magnitudes derived from the PN.S data and those from the M02 imaging data. The black outline represents all the objects that are within both surveys. In the upper panel the shaded area represents PNe remaining after a number of cuts have been applied to the data. The lower panels show the distribution of objects for the cuts indicated. The larger, cyan area is the total cut made while the smaller magenta histograms show the particular objects being excluded by each criterion.

band ( $(H\alpha + [N\ II]), [S\ II],$  and  $[O\ III])$  imaging. As Figure 3.7 shows, M02 imaged 10 fields over the majority of the disk of M31 and hence a large portion of the PN.S survey region (covering 2745 of the objects in the PN.S survey).

We therefore analysed the M02  $[O\ III]$  survey images by obtaining fluxes at the positions of PN.S sources using the *IRAF phot* task with a fixed aperture of  $2''$  – a value somewhat larger than the typical survey seeing ( $\sim 0.8'' - 1.5''$ ) to allow for positional uncertainties, but not so large as to introduce significant source confusion. The photon counts were converted to fluxes using a factor of  $3.92 \times 10^{-16}$  (Massey, private communication). A Galactic extinction correction was made using data from Schlegel, Finkbeiner & Davis (1998) and Cardelli, Clayton & Mathis (1989), as for the PN.S data, yielding an extinction of 0.225 mag.

Figure 3.12 shows the comparison between the imaging magnitudes derived in this way and the PN.S data. If we remove the faintest PNe for which photometry is rather uncertain, and probable  $H\ II$  regions for which this aperture photometry is inappropriate, there is a good overall agreement between the data sets. Fitting a Gaussian to the

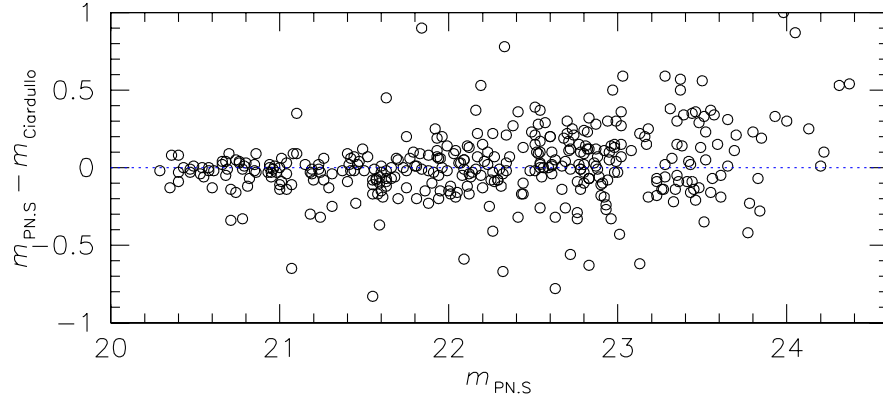


**Figure 3.13:** Comparison between PN.S magnitudes and those published in Ciardullo et al. (1989). Examining this plot by eye there appears to be a slight trend, with PN.S magnitudes being fainter than the corresponding Ciardullo et al. (1989) magnitudes for faint PNe. However, gaussian fits in half magnitude bins show this to be small ( $<0.1$  mag) and of low significance.

remaining 1769 PNe gives a negligible zero-point offset of 0.02 mag, and a combined dispersion of 0.16 mag. There is no evidence for varying offsets in different fields or for data taken on different nights.

As a further cross-check, Figure 3.13 shows the comparison between the PN.S magnitudes and the smaller data set published by Ciardullo et al. (1989). As expected, the scatter increases somewhat for the fainter PNe, but the overall agreement is very good. A Gaussian fit to the magnitude differences yields a mean of 0.00 mag with a combined dispersion of 0.13 mag, and even at the faintest magnitude the combined dispersion is less than 0.3 mag. Once again, there is no evidence of varying offsets for different fields or data taken on different nights. Since we are only going to use the photometric data to make quite crude cuts in the luminosity function of PNe, which we have measured over a range of more than three magnitudes, photometry with an error of less than 0.3 magnitudes is all that is required.

### 3.5 Contamination and completeness

The next issue to be addressed is to try to identify those emission line sources that are not PNe, and to estimate what fraction of PNe we may have missed in the survey.

With only a single emission line detected by PN.S, any object that emits [O III] may form part of the data set (or, indeed, any object along the line of sight with a redshift that places an unrelated emission line at this wavelength). The dominant contaminating objects are likely to be H II regions, which emit strongly in [O III], and exist in large numbers in disk galaxies like M31. Most of these objects will already have been excluded, since their extended nature means that they will have been cut from the data set at the source-identification stage (even the largest PNe, with diameters of up to 3 pc, will be essentially unresolved in these data). However, H II regions have a broad size distribution, and the more compact ones will be barely resolved so will still be in the sample. Figure 3.14 shows the distribution of source sizes, normalised to the seeing, of the objects remaining in the survey; there clearly remains a tail of resolved objects, so

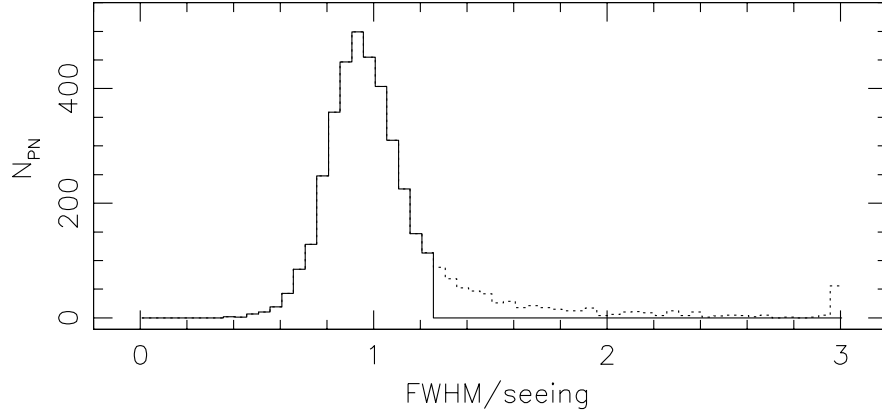


**Figure 3.14:** A plot of the FWHM of sources detected by the PN.S survey, normalised by the seeing of each observed field. Sources in the dotted long tail toward large sizes have been flagged as contaminating H II regions. The cut between extended and point sources is made at  $\text{FWHM/seeing} = 1.25$ .

we have flagged sources for which the FWHM normalised by seeing exceeds a value of 1.25 as probable H II regions in the final catalogue.

When examining the spatial distribution of the objects flagged by this process, it was found that they largely lie in a ring around M31’s centre. A further clump of 35 objects was also found in a single field close to the centre of M31. This field was the only one close to the galaxy’s centre that was observed under good seeing conditions ( $\sim 0.8''$ : see Figure 3.2). With the seeing this good, the variation in instrumental focus across the field and differences between the two PN.S images may become significant, so it is possible that these apparently extended objects are actually unresolved PNe. However, for consistency we also flag them as non-PNe; as discussed below, we in any case do not expect the survey to be complete in these crowded high surface-brightness fields.

Presumably, this cut on angular size will still miss the most compact H II regions and in the central regions where the seeing was very poor objects with diameters of up to  $\sim 15$  pc will be classified as compact by this cut. Fortunately, we do have some further information that we can use to try to identify these remaining contaminants. Specifically, M02 have produced narrow-band ( $\text{H}\alpha + [\text{N II}]$ ) images as well as  $[\text{O III}]$  images, and we have measured ( $\text{H}\alpha + [\text{N II}]$ ) fluxes for the PNe in the LGS survey area in the same way as we did for the  $[\text{O III}]$ , but with a conversion factor of  $1.79 \times 10^{-16}$  and a Galactic extinction of 0.164 mag. The ratio of these fluxes,  $R$ , is seen to differ between PNe and H II regions (Ciardullo et al., 2004). In particular, since PNe give out most of their light in the  $[\text{O III}]$  line, we would expect  $R$  to be large for these objects. Attempts have been made to quantify this criterion, leading to the suggestion that for bright PNe one should place a cut at  $R \sim 1 - 2$  (Ciardullo et al., 2002a, 2004; Magrini et al., 2000). However, it became apparent when we started investigating this quantity for the data in the PN.S survey that the appropriate value for this cut varies significantly with magnitude. As Figure 3.15 illustrates, the optimum cut in  $R$  to exclude H II regions decreases at fainter magnitudes. We have calculated this cut by estimating the location of the division between the normal PN population and the extended objects in the brighter magnitude bins (there is not clear distinction for fainter objects) and extrapolating this linearly to all magnitudes. The cut made is shown as a dashed line in

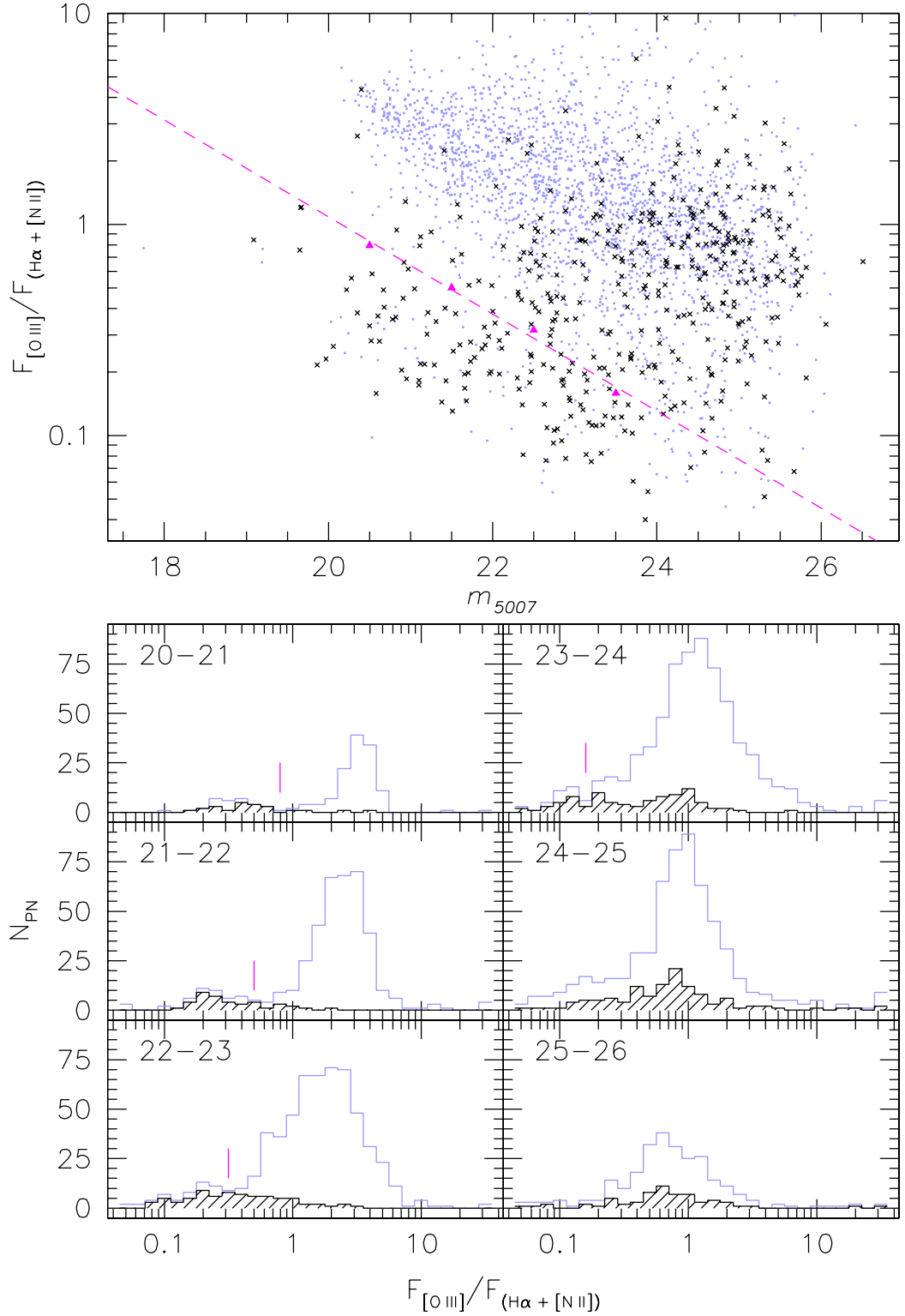


**Figure 3.15:** The flux ratio of [O III] to (H $\alpha$  + [N II]) versus magnitude. The upper panel shows all the data, with extended objects highlighted with as black crosses. The lower panel shows the same data as histograms in different magnitude bins, with the extended sources shaded. The vertical line in each histogram shows a suggested division between PNe and H II regions based on these distributions. These lines have been plotted as triangles in the upper panel, and the dashed line connects them.

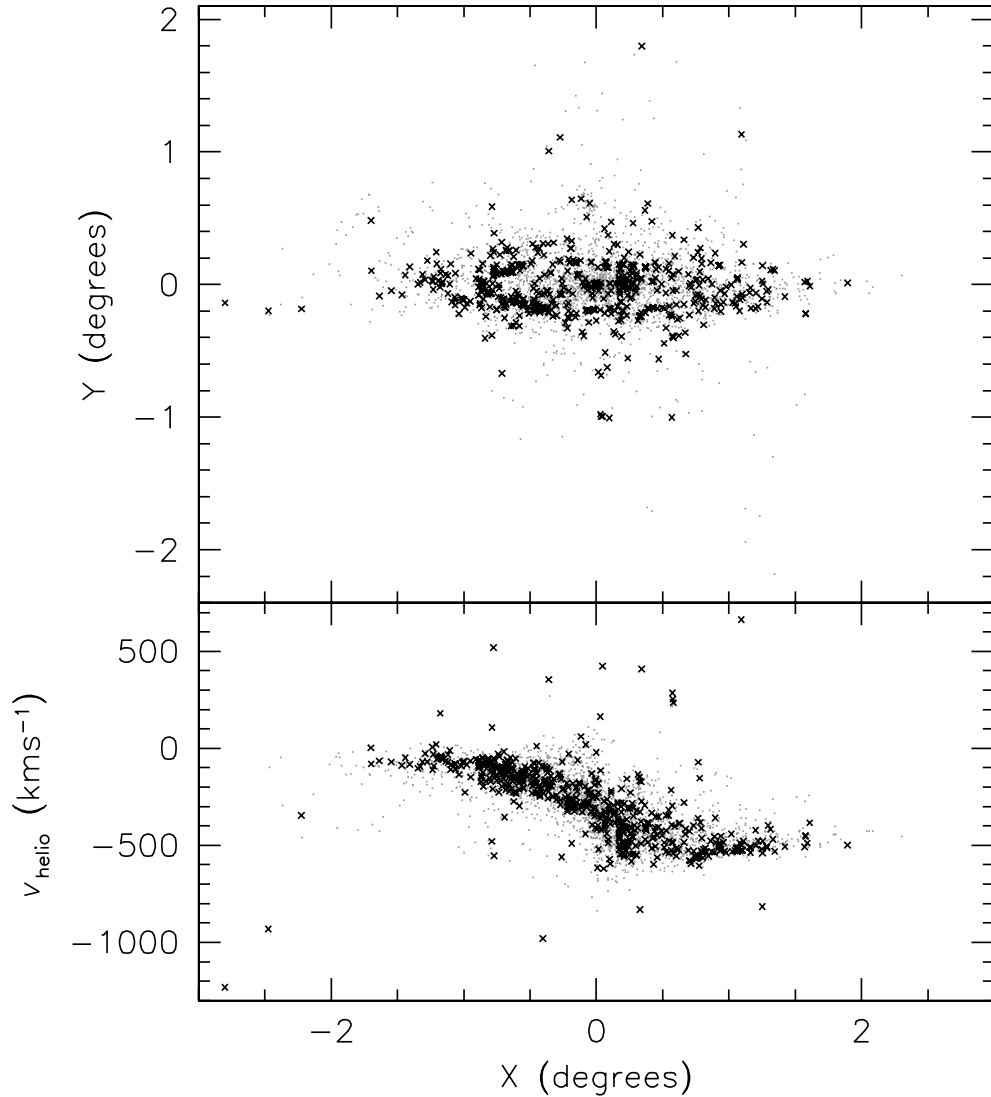


**Figure 3.16:** Locations in position and velocity of sources identified as probable H II regions. The whole sample is shown as small dots, with the probable H II regions as larger crosses.

Figure 3.15, with all sources below the line flagged as H II regions, regardless of their size. This is not especially robust at fainter magnitudes and contamination from H II regions may well remain high. This cut is also lower than the ones made by Ciardullo et al. (2002a, 2004) and Magrini et al. (2000), as we have chosen to be conservative by only selecting for exclusion the area of the plot that seems virtually devoid of PNe.

Figure 3.16 picks out the locations in the  $(X, Y)$  and  $(X, v)$  planes of the objects that these two criteria have identified as non-PNe. Although the criteria were designed to flag up probable H II regions, it is clear that they also exclude most of the objects with velocities that are inconsistent with membership of M31. A closer examination of these peculiar velocity objects show that they are nearly all slightly elongated in the dispersion direction (see Figure 3.17). The most logical sources for these objects are unresolved background galaxies with large internal rotations that are broadening the emission lines. There were also a few objects found in the survey area (but not included in the catalogue) that appeared to have double emission peaks (Figure 3.18);

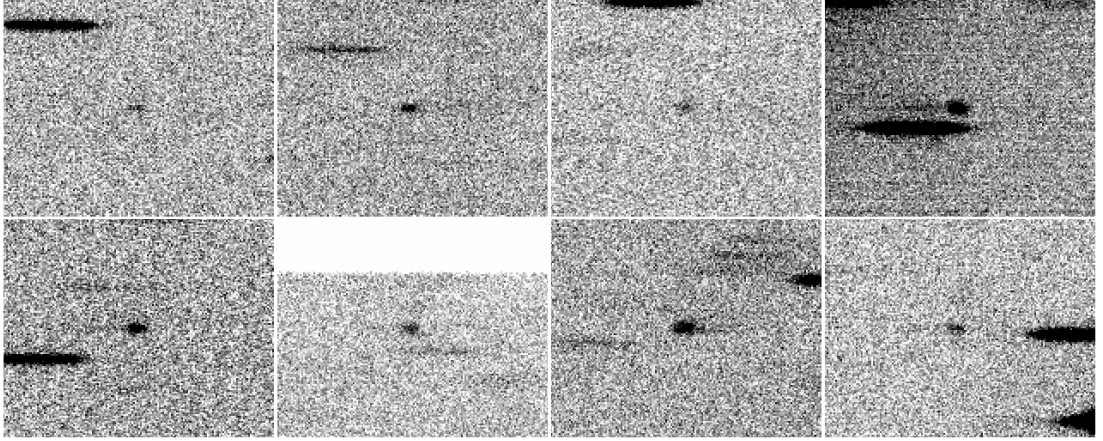


**Figure 3.17:** A sample of the extended emission line objects with velocities inconsistent with membership of M31. These objects are marginally more extended in the dispersion direction than the spatial direction.



**Figure 3.18:** Two objects that did not make the catalogue as they clearly have two emission peaks.

these can also be explained as originating from an unresolved background disk galaxy. Two types of galaxy have been identified as possible contaminants in  $5007 \text{ \AA}$  narrow band surveys: redshift  $\sim 3$  Lyman  $\alpha$  galaxies and  $3727 \text{ \AA}$  [O II] emission from redshift  $\sim 0.3$  starburst galaxies. Ciardullo et al. (2002b) have examined the contamination level from Lyman  $\alpha$  galaxies, finding them to be fairly common for monochromatic fluxes  $\lesssim 6 \times 10^{-17} \text{ ergs cm}^{-2} \text{ s}^{-1}$  ( $m_{5007} \gtrsim 26.8 \text{ mag}$ ); this is, however, significantly fainter than the limit of this survey.

Figure 3.16 also shows the structure in the distribution of H II regions associated with spiral arms as well as the ring mentioned above. At a radius of  $0.8^\circ$ , the ring coincides with the star-forming ring discussed in Chapter 1, where an excess of H II regions might be expected.

As a final check on our reliability in identifying contaminating sources, we have compared our identifications with the catalogue of 1312 emission-line objects that Meyssonnier, Lequeux & Azzopardi (1993, hereafter MLA93) detected and classified in M31 using broadband ( $4350\text{--}5300 \text{ \AA}$ ) slitless spectroscopy. We find 856 of these objects to be within  $4''$  of an object in our survey, the great majority of which are classified as PNe by both MLA93 and ourselves. Only 94 of these objects are listed by MLA93 as non-PNe, and we have successfully flagged two-thirds of these as non-PNe as well. Of the remaining 31, MLA93 identify 25 as possible Wolf–Rayet stars. Since Wolf–

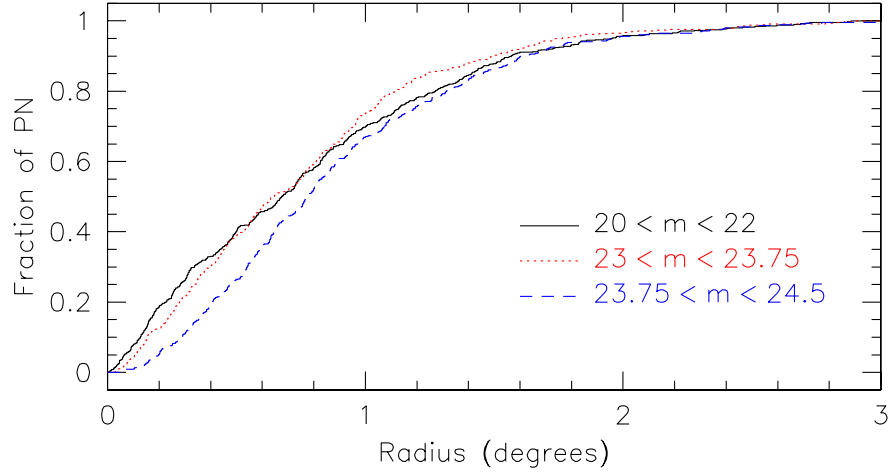


**Figure 3.19:** Cumulative distribution of radii in the disk plane for bright (solid, black line), intermediate-luminosity (dotted, red line) and faint (dashed, blue line) PNe. A Kolmogorov-Smirnov test shows the distribution of bright and intermediate-luminosity PNe to be statistically indistinguishable at the 95% confidence level. There is a dearth of faint PNe near to the centre of M31 resulting from poor seeing conditions and a high surface brightness.

Rayet stars are at a late stage in stellar evolution rather similar to PNe, and the two are sometimes even found together (Górny & Stasińska, 1995), it is not clear that they should be considered as contaminants at all. One object classified as a possible QSO or Wolf-Rayet star is discussed further in Chapter 4. The last five objects are of uncertain classification in the MLA93 catalogue and will be left in this catalogue. The 456 objects that were not found presumably do not exhibit [O III] emission.

The other side to this coin is to ask how many PNe we might have missed. A simple test of completeness can be made by comparing the distribution of PNe with radius in different magnitude bins. As Figure 3.19 shows, bright and intermediate-luminosity PNe show spatial distributions that are statistically indistinguishable, but the faint PNe display a dearth of objects at small radii. As discussed above, such incompleteness is expected given a combination of the high surface brightness of the bulge region and the poor seeing conditions during observations of the central fields. Overall, we can tentatively conclude that the sample is complete to  $m_{5007} = 23$  over the entire survey, to  $m_{5007} = 23.75$  at radii larger than  $0.2^\circ$ , and to  $m_{5007} \sim 25$  beyond  $1^\circ$ ; we will revisit this issue when we look at the PN luminosity function in Section 5.1. In terms of spatial coverage, as Figure 3.1 shows, M31 has been completely mapped out to a deprojected disk radius of  $1.5^\circ$ . Beyond that radius, the major and minor axes are somewhat unevenly sampled from one side to the other, but still with reasonable spatial coverage. Thus, although not spatially complete, useful kinematic information can be gleaned out to  $2^\circ$  (27.4 kpc).

### 3.6 The catalogue

Having calibrated the data spectroscopically, astrometrically and photometrically, both internally and against external results, we are now in a position to present the complete database from the survey. The full final version of the resulting data table of 3300



emission line objects including 2730 probable PNe is included in Appendix A, listing coordinates, magnitudes, heliocentric velocities, whether the source is a probable PN, whether it lies in M31 or originates from another galaxy (see Chapter 4), when the data were obtained, and cross-identifications with other catalogues.

## Chapter 4

# Other galaxies covered in the PN.S survey

Some of the objects in our catalogue reside in systems external to the Andromeda Galaxy, and can be identified in the database because their velocities are far from that of M31. As we have seen in Chapter 3, most such sources have already been flagged as non-PNe because of their extended nature or low  $[\text{O III}]/\text{H}\alpha$  ratio, and are probably in quite distant, faint background systems. In some cases, such as the sources in the less-distant background galaxy Andromeda IV, there may be a few genuine PNe. Of more immediate interest are the satellite galaxies around M31. In these systems, we do detect quite a number of PNe, which means we can obtain some crude measure of the internal kinematics of these systems, but we must also take some care in flagging these sources so that they do not compromise the use of this data set to model the dynamics of M31.

The locations of the known galaxies in the survey field are indicated in Figure 4.1, and we now consider them in turn, to try to identify the sources that lie within them, both on the basis of their positions and their velocities. Probable non-members of M31 identified in this way are annotated as such in the full database (see Appendix A).

### 4.1 M32

M32 (NGC 221), was discovered by Guillaume-Joseph-Hyacinthe-Jean-Baptiste Le Gentil de la Galazière on October 29th 1749 (Mateo, 1998), making it the first of Andromeda's satellite galaxies to be found. It is a compact dwarf elliptical galaxy (cE2) projected in line with the disk of M31. Its major and minor axes measure  $\sim 8.7'$  and  $6.75'$  in diameter respectively, to a B-band magnitude level of  $25.0 \text{ mag arcsec}^{-2}$  (de Vaucouleurs et al., 1991). It has a system velocity of  $-200 \pm 6 \text{ km s}^{-1}$  (Huchra, Vogele & Geller, 1999), and a velocity dispersion of  $50 \pm 10 \text{ km s}^{-1}$ , rising to  $\sim 80 \text{ km s}^{-1}$  at its centre (Simien & Prugniel, 2002). A Digitized Sky Survey (DSS) image of M32 is shown in the upper left panel of Figure 4.2, with the smaller ellipse approximately marking the  $25.0 \text{ B-mag arcsec}^{-2}$  limit.

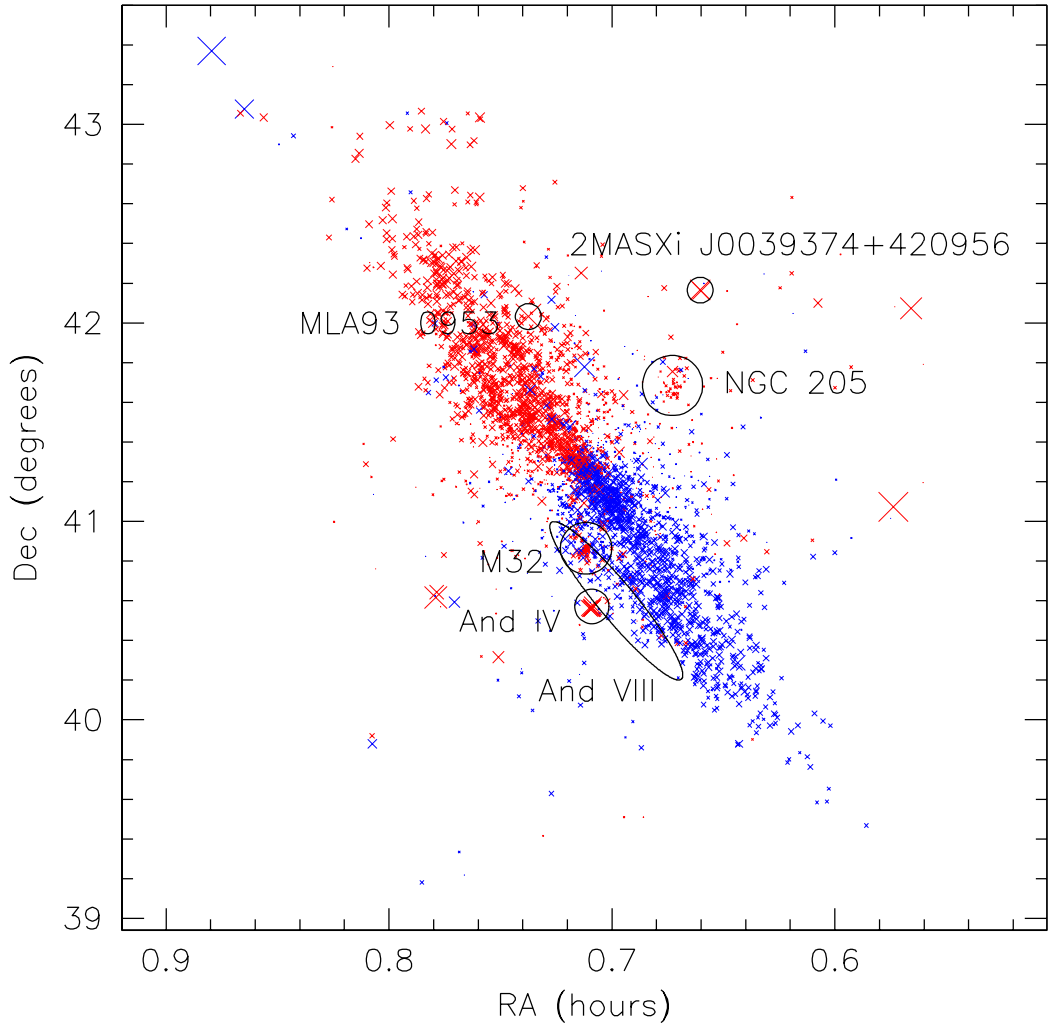


**Figure 4.1:** Positions of other galaxies contained within the PN.S survey area. An emission-line object's size and colour reflect its velocity with respect to M31's system velocity: red objects are receding and blue ones are approaching.

A number of previous studies have looked at the PN population of M32. One of the earliest is that of Nolthenius & Ford (1986) who measured radial velocities for 15 PNe in the vicinity of M32, using them to constrain the galaxy's mass. Ciardullo et al. (1989) list 30 PNe near M32, measuring magnitudes for the majority of these. More recently papers by Richer, Stasińska & McCall (1999) and Hyung et al. (2000) have presented detailed spectroscopy of a small number of PNe in the satellite galaxy, measuring line intensities and deriving temperatures where possible.

In our survey, we have detected a good number of PNe in and around M32 and the main issue we face is producing a clean separation between those objects belonging to M32 and those belonging to M31. The majority of M32's PNe will lie fairly close to its centre and in order to identify them we have designated a search area with a radius 1.5 times the mean radial extent of the 25.0 B-mag arcsec<sup>-2</sup> limit, 5.7'. This area is shown as the large circle in the two upper panels of Figure 4.2. All emission-line objects lying within this area are considered as candidate members of the satellite. Using the PNe at somewhat larger distances from M32 to characterise the kinematics of M31's disk in this region, we find that a velocity cut at  $-350 \text{ km s}^{-1}$  (three times the measured

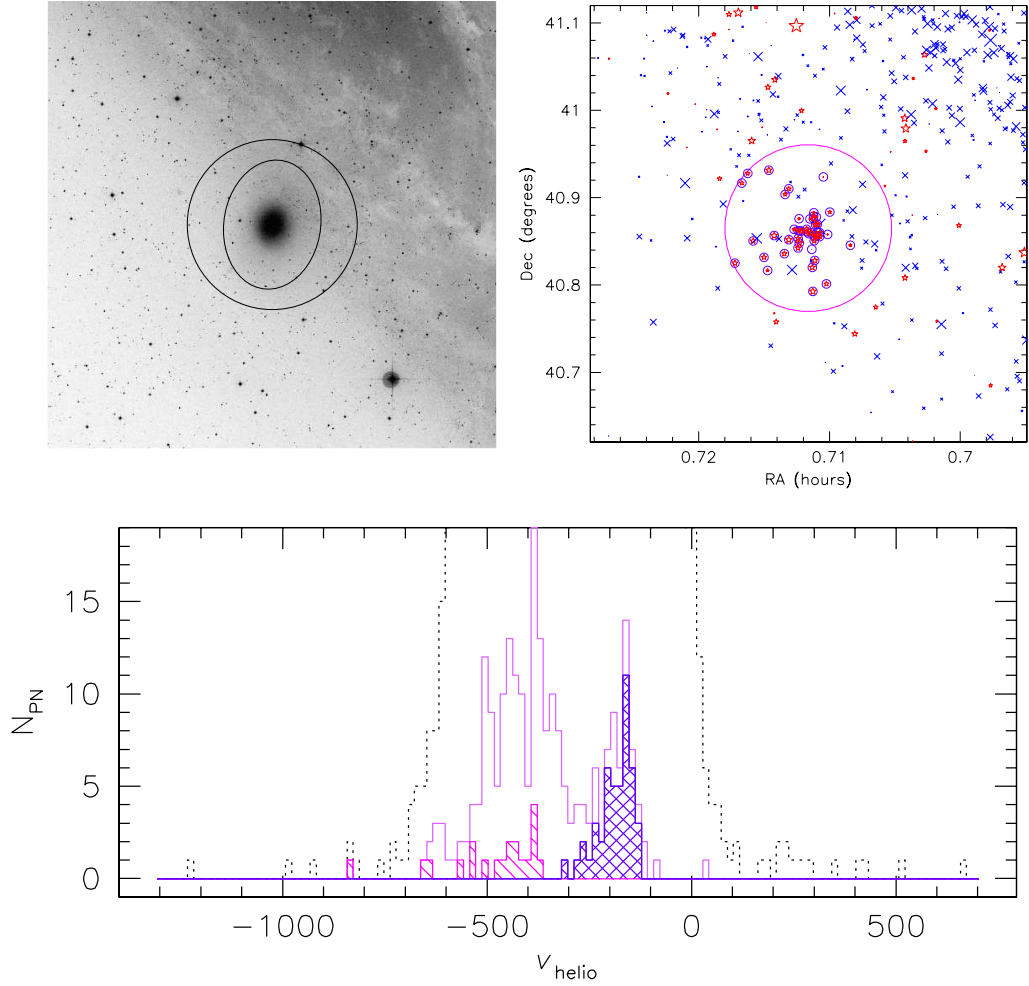


**Figure 4.2:** M32. The upper left panel is a DSS image of M32, M31’s disk is clearly visible above and to the right of its satellite. The smaller ellipse indicates M32’s 25.0 B-mag arcsec<sup>-2</sup> limit. The outer circle has a radius 1.5 times the mean of radius of the ellipse and marks the area within which we have searched for emission line objects belonging to M32. A plot of the locations of emission-line objects in the area around M32 is shown in the upper right panel. Symbol sizes are proportional to an object’s velocity with respect to M31’s system velocity; negative and positive values are indicated with blue crosses and red stars respectively. The large circle is the same as that shown in the DSS image and PNe with small circles around them have both position and velocity consistent with M32. The lower panel shows velocity histograms for emission line objects within a number of areas. The dotted line is for the whole PN.S sample; the solid line for objects in an area including M32, but extending well beyond it’s influence; the hatched histogram is for PNe within the defined search area, and the cross-hatched histogram is for PNe that agree in velocity as well as position.

dispersion from M32’s systemic velocity) yields a reasonably clean division between the two systems, as shown in the lower panel of Figure 4.2. However, it is possible that a few of the PNe on the M31 side of the cut may be objects with the most extreme velocities in M32. To warn of this possibility, objects in the catalogue are flagged as “M32” if they meet the cut in velocity as well as position, and “M32?” if they are simply coincident with M32’s location.

The sample of likely M32 PNe has 46 members, a significant improvement on previous samples, yet there is not much that we can do in terms of detailed dynamical

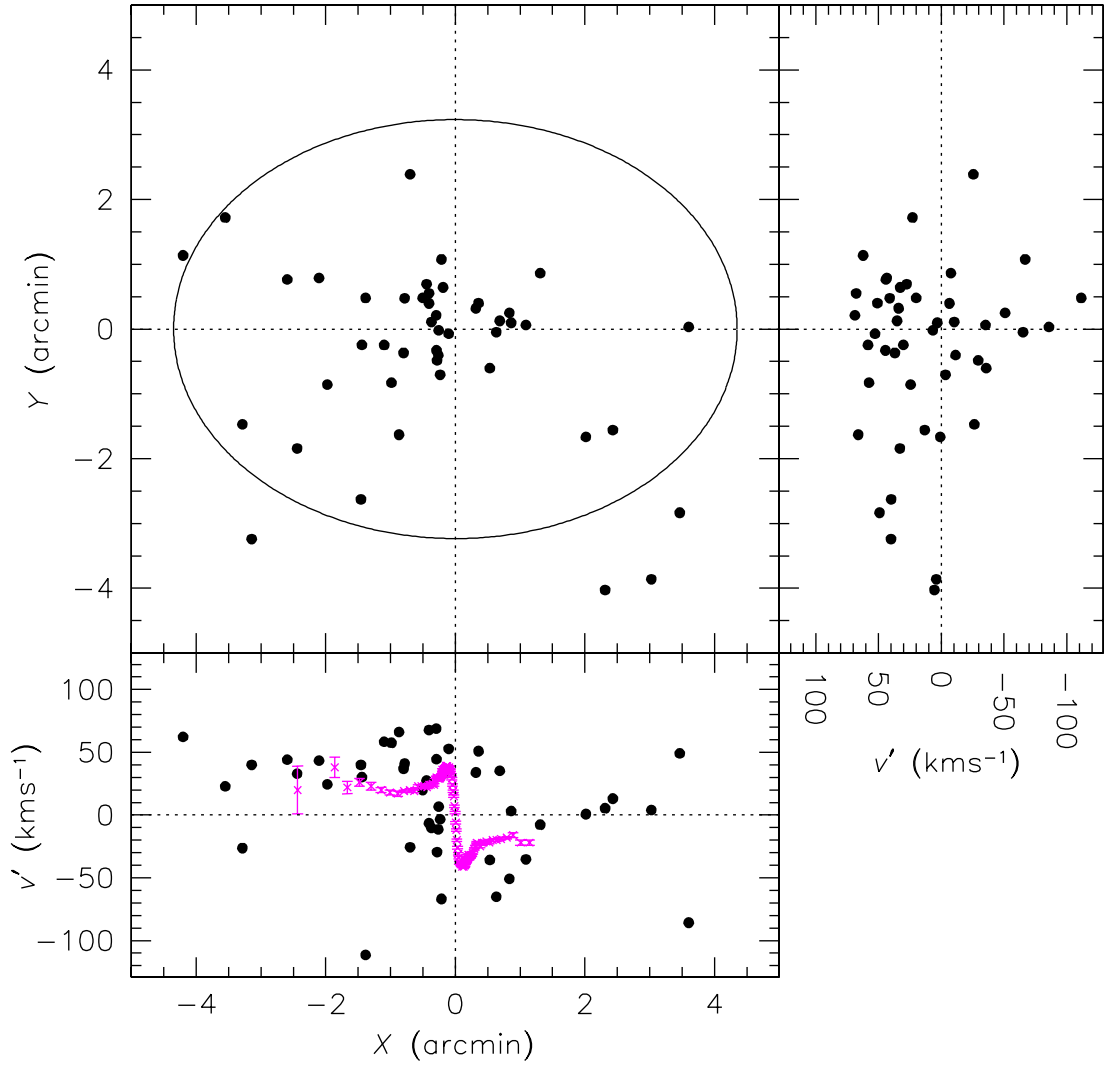


**Figure 4.3:** Velocities of M32 PNe. The main panel shows distances along M32’s major ( $X$ ) and minor ( $Y$ ) photometric axes. The ellipse is the  $25.0 \text{ B-mag arcsec}^{-2}$  limit also shown in the DSS image in Figure 4.2. The axes are indicated by the dotted lines. PN velocities with respect to M32’s accepted system velocity ( $v'$ ) are shown as a function of the  $Y$  coordinate in the right hand panel, and the  $X$  coordinate in the the lower panel. The magenta points show the rotation curve of Simien & Prugniel (2002).

modelling. A simple Gaussian fit to the velocity distribution yields a mean velocity of  $-174 \pm 6 \text{ km s}^{-1}$  and a velocity dispersion of  $36 \pm 5 \text{ km s}^{-1}$ . Neither of these is in particularly good agreement with the usually-adopted values.

Transforming the RA and Dec values for M32’s PN population to an M32 based coordinate system using equations (1.1–1.4), with  $\text{RA}_0 = 0^{\text{h}} 42^{\text{m}} 41.82^{\text{s}}$ ,  $\text{Dec}_0 = 40^\circ 51' 54.6''$ , and  $\text{PA} = 170^\circ$ , and plotting the population as shown in Figure 4.3, we are able to see a possible reason for this discrepancy: the spatial distribution of PNe in M32 is uneven, as there are more with negative values of  $X$  than positive, and there are very few PNe near the major axis on the positive side. Therefore the measured mean velocity contains an element of the system’s rotation; the somewhat low value for the velocity dispersion is also consistent with this interpretation.

Such an asymmetry could arise if different areas of the galaxy were observed under

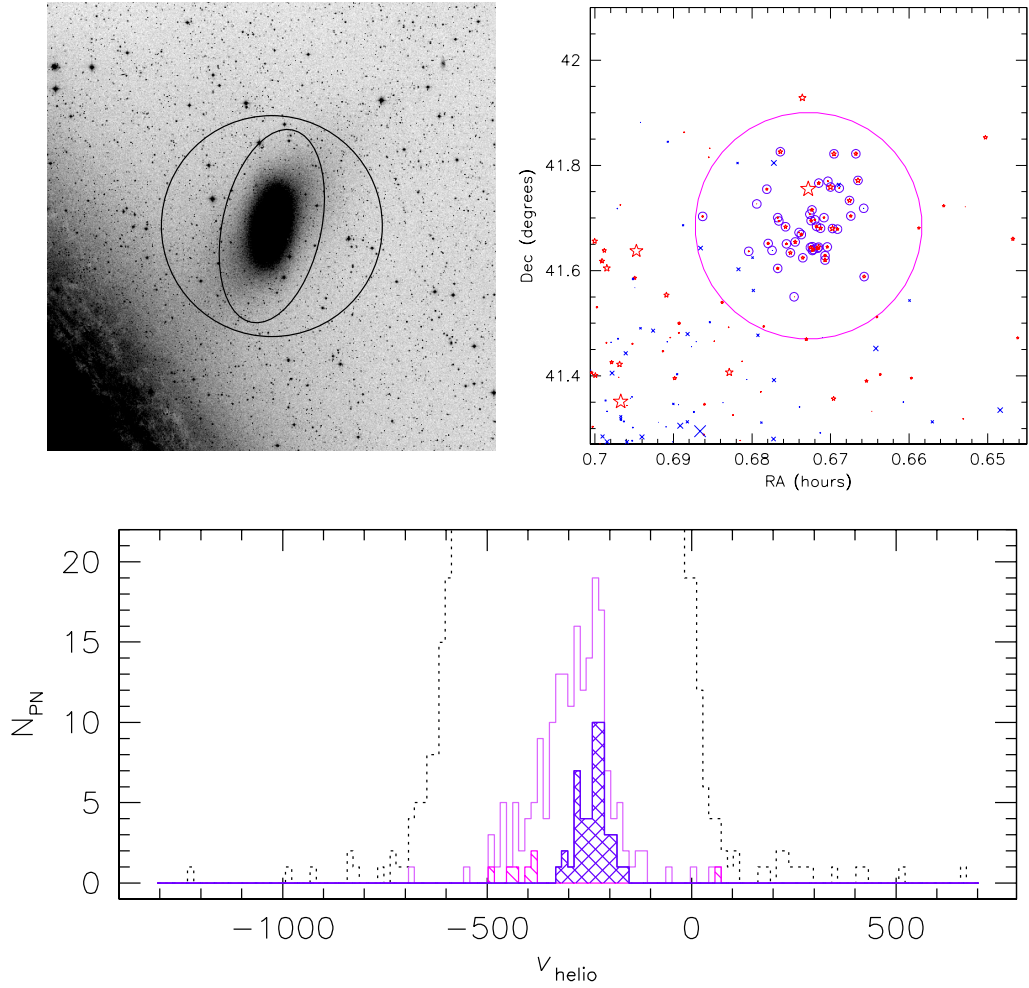


**Figure 4.4:** NGC 205. As Figure 4.2, with M31’s disk visible to the bottom left of the DSS image.

different seeing conditions. Indeed, as Figure 3.2 shows, the normal, tiled fields in this region were observed under quite different conditions. However, we also observed a field centred directly on M32 under the better of these seeing conditions. As all the PNe we associate with M32 can be found within this field, we can rule out variations in observing conditions as a source of the observed asymmetry.

## 4.2 NGC 205

NGC 205 (M 110) was discovered by Charles Messier on August 10th 1773. It is a dwarf elliptical galaxy (dE5) projected  $\sim 35'$  from the centre of M31 along the minor axis. Its major- and minor-axis diameters are  $\sim 21.9'$  and  $\sim 11.0'$  respectively at a position angle of  $170^\circ$  (de Vaucouleurs et al., 1991), as shown by the ellipse in the upper left panel of Figure 4.4. It has a mean velocity of  $-241 \pm 3 \text{ km s}^{-1}$  (Bender, Paquet & Nieto, 1991); a mean velocity dispersion of  $46 \pm 8 \text{ km s}^{-1}$ , dipping to  $\sim 20 \text{ km s}^{-1}$  at the very centre of the galaxy (Mateo, 1998; Carter & Sadler, 1990; Simien & Prugniel, 2002); and a rotation velocity of  $13 \pm 2 \text{ km s}^{-1}$  along the major axis (Geha et al.,

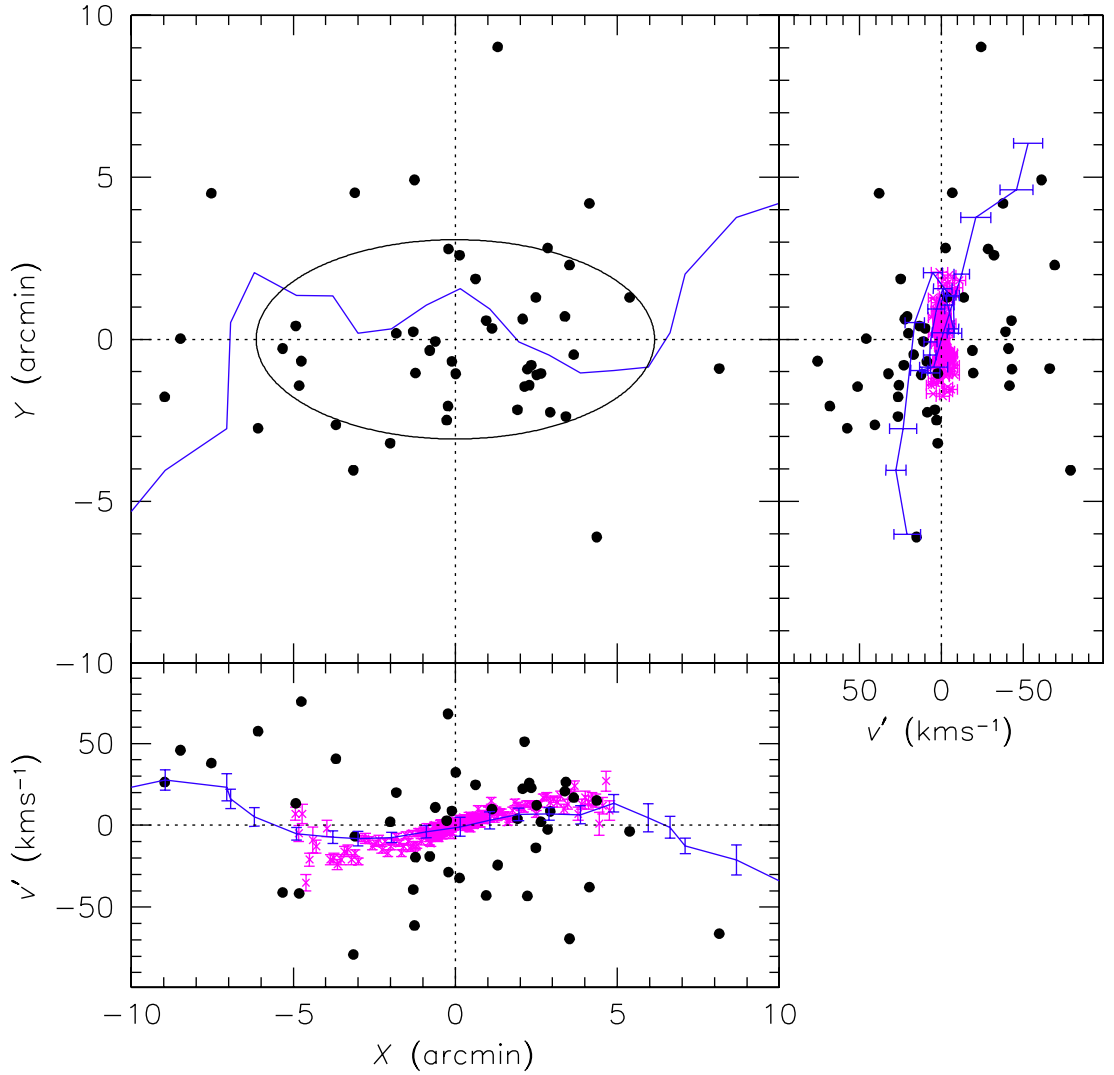


**Figure 4.5:** NGC 205. As Figure 4.3, with the magenta points showing the rotation curve from Simien & Prugniel (2002) and the blue lines representing data from Geha et al. (2006).

2006).

Previous studies of PNe in NGC 205 have identified and measured magnitudes for a number of PNe in the vicinity of NGC 205. Ciardullo et al. (1989) list 28 PNe close to the galaxy and Corradi et al. (2005) list 75 PNe in a 0.4 square degree area, 35 of which are found within 1.5 tidal radii of the centre and likely to belong to NGC 205, a significant number of those beyond this limit will belong to M31.

To identify PNe in NGC 205, we have selected the objects within 12.3' of NGC 205's centre (1.5 times the mean 25.0 B-mag arcsec<sup>-2</sup> radius, as shown by the large circles in the upper panels of Figure 4.4), and applied velocity cuts at  $-375 \text{ km s}^{-1}$  and  $-102 \text{ km s}^{-1}$  to seek to isolate the galaxy's members, as shown in Figure 4.4. These velocity selections lie at approximately  $v_{\text{NGC205}} \pm 3\sigma_{\text{NGC205}}$ , although the lower bound is placed slightly high to avoid including M31 PNe that are seen to have such velocities at slightly larger distances from NGC 205. As with M32, the possible overlap at these velocities means that there is, unavoidably, some ambiguity in the identification of satellite members, so Table A.1 annotates those objects that meet the velocity

**Table 4.1:** Emission-line objects in the vicinity of And IV. <sup>a</sup> ID from Ferguson, Gallagher & Wyse (2000) Table 1. <sup>b</sup> ID from Table A.1. <sup>c</sup> RA, Dec,  $m_{5007}$  and  $v_{\text{helio}}$  from PN.S data, except object F1, which was not detected. <sup>d</sup> E – extended; R – below flux ratio cutoff; NP – not detected in PN.S survey; M31 – M31 like velocity; NF – not found in Ferguson, Gallagher & Wyse (2000).

ID <sup>a</sup>	ID <sup>b</sup>	RA <sup>c</sup> J2000.0	Dec J2000.0	r arcsec	$m_{5007}$	$v_{\text{helio}}$ km s <sup>-1</sup>	Note <sup>d</sup>
F1		0:42:37.6	40:38:12	241			NP
F2	2114	0:42:36.6	40:34:04.8	51	23.47	213.3	
F3	2113	0:42:32.2	40:33:58.8	20	22.53	236.2	E
F4	2115	0:42:31.7	40:34:11.1	10	23.13	253.9	E
F5	2117	0:42:32.7	40:34:17.0	5	25.20	248.8	
F6	2119	0:42:30.6	40:34:47.3	35	24.43	285.7	E
F7	2110	0:42:20.3	40:32:31.8	174	25.27	-386.7	R, M31
F8	2112	0:42:21.2	40:33:50.0	130	21.74	-372.5	M31
	2111	0:42:35.3	40:33:51.0	44	24.14	219.2	NF
	2128	0:42:31.9	40:33:58.7	20	24.79	228.5	NF

constraints as “NGC205,” while those that are just spatially coincident are marked as “NGC205?”

A Gaussian fit to the velocity distribution of likely members yields a mean velocity of  $-235 \pm 6$  km s<sup>-1</sup> and a velocity dispersion of  $35 \pm 9$  km s<sup>-1</sup>, in agreement with the published values. Previous studies of NGC 205 have shown evidence for a small amount of rotation along the major axis out to  $\sim 5'$  (Simien & Prugniel, 2002), where it turns over to rotate in the opposite direction (Geha et al., 2006). These rotation curves are plotted alongside the PN.S data [which has been transformed to an NGC 205 based coordinate system according to equations (1.1–1.4) with  $\text{RA}_0 = 0^{\text{h}} 40^{\text{m}} 22.08^{\text{s}}$  and  $\text{Dec}_0 = 41^{\circ} 41' 07.1''$ ] in Figure 4.5 for comparison. The small number of PNe in NGC 205 makes such a rotation difficult to detect, although some indication of rotation along the minor axis is observed. This may be a result of NGC 205’s isophotes twisting in the outer halo, and hence actually represent the major axis rotation. Conversely the turnover in the major axis rotation curve may be a result of rotation along the minor axis, given the position of Geha et al.’s points at large radii.

### 4.3 Andromeda IV

Andromeda IV is a background dwarf irregular galaxy, lying a projected distance of  $40'$  from the centre of M31. It can be seen as the small, diffuse source near to a bright foreground star in the centre of the DSS image in the upper left panel of Figure 4.6. Ferguson, Gallagher & Wyse (2000) have previously identified a number of emission-line objects associated with this galaxy, and we list the cross-identifications in the current survey in Table 4.1. The only object that we fail to recover from the Ferguson, Gallagher & Wyse (2000) study is their “F1” source, which was originally detected in H $\alpha$ , but has no [O III] counterpart in the magnitude range of our survey. The Ferguson, Gallagher & Wyse objects F7 and F8 are located a little away from the galaxy centre,



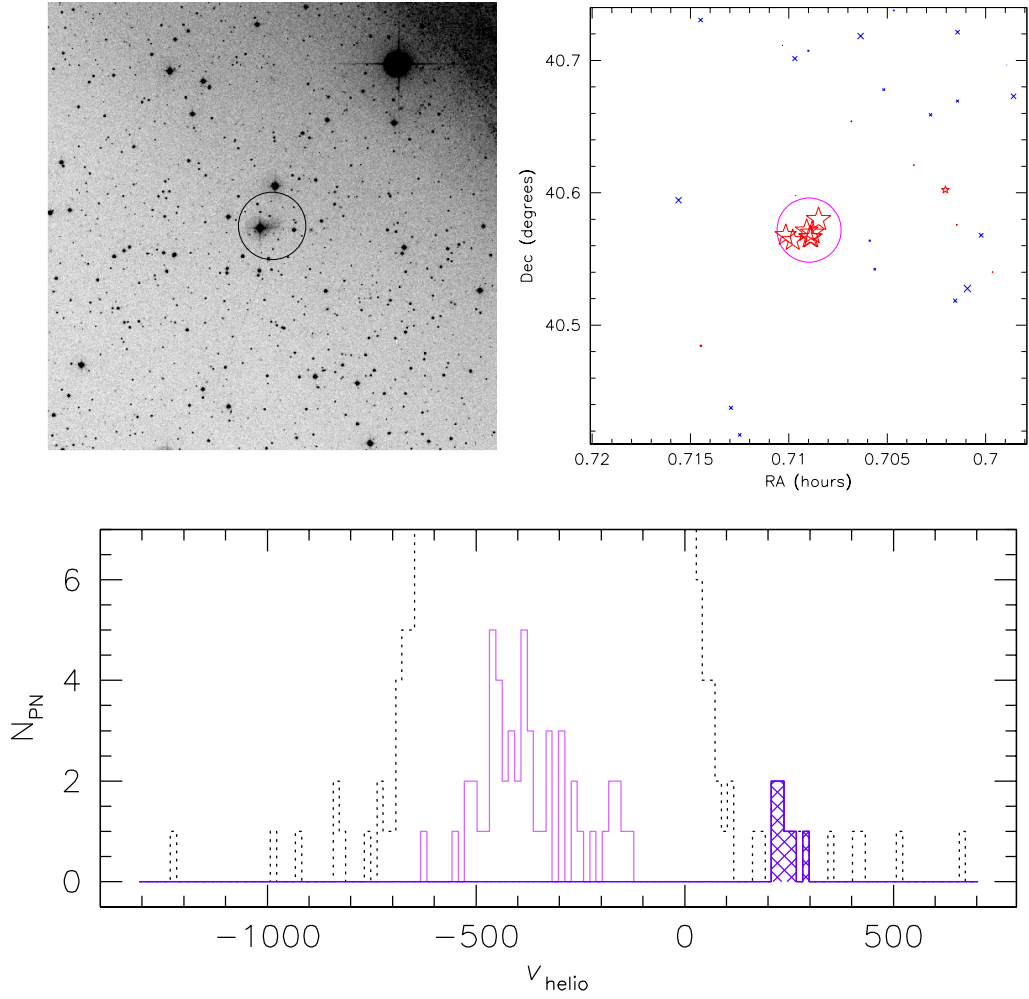


**Figure 4.6:** Andromeda IV. As Figure 4.2, with M31’s disk visible to the top right of the DSS image.

and our measurements show that their velocities are consistent with the disk of M31, so they do not appear to be members of And IV and are excluded from the remaining analysis. Table 4.1 also adds two new emission-line sources to the list of objects with positions and velocities consistent with membership of And IV.

The resulting list of seven likely And IV members are marked as such in Table A.1 and have a mean velocity of  $241 \pm 10 \text{ km s}^{-1}$ , in agreement with the published value of  $256 \pm 9 \text{ km s}^{-1}$ , as measured from spectra of only three sources (Ferguson, Gallagher & Wyse, 2000). As Figure 4.7 illustrates, the velocities do not appear to be randomly distributed through the system, but indicate a line-of-sight component of rotation of  $\sim 35 \text{ km s}^{-1}$  about a centre of  $\text{RA}_0 = 0^{\text{h}} 42^{\text{m}} 32.3^{\text{s}}$ ,  $\text{Dec}_0 = 40^{\circ} 34' 18''$ .

## 4.4 2MASXi J0039374+420956

Two PN.S emission-line objects that exhibit velocities inconsistent with M31, one of which is extended, were found in the vicinity of this extended infrared 2MASS source

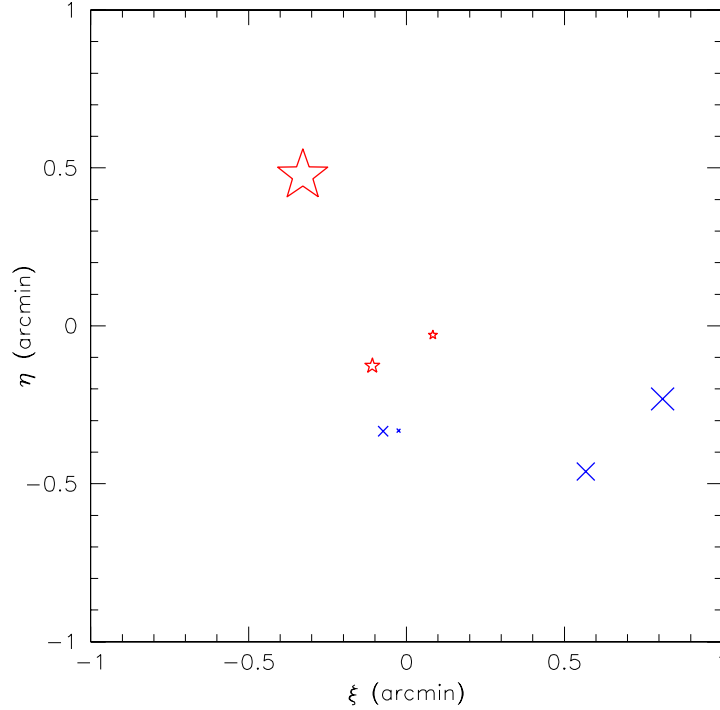


**Figure 4.7:** Kinematics of emission-line sources in Andromeda IV. The coordinates are defined relative to the centre of the satellite. Point sizes are proportional to velocity with respect to And IV, with red stars and blue crosses representing positive and negative values respectively.

shown in Figure 4.8 (marked as 2MASXi in Table A.1). The two objects lie at projected radii of  $2.8''$  and  $24.2''$  from the source centre. With only one emission line detected, we cannot unequivocally confirm its nature, but if we assume it originates from [O III], then this system would be placed at a heliocentric velocity of  $\sim 300 \text{ km s}^{-1}$ . As this velocity is similar to that derived for And IV, it is possible that both these galaxies belong to the same nearby background group. However, further observations would be required to confirm if this is the case.

## 4.5 MLA93 0953

One object with a velocity inconsistent with M31 was also listed in the Meyssonier, Lequeux & Azzopardi (1993) catalogue of M31 emission-line objects discussed in Section 3.5; this object is shown in Figure 4.9. They identified it as either a Wolf-Rayet star or a background QSO. Given our velocity measurement, it seems most likely that the object is a background QSO with an emission line that happens to lie within the [O III] bandpass. It is marked as ‘MLA93’ in Table A.1.

## 4.6 Andromeda VIII

Morrison et al. (2003) pointed out a coincidence in position and velocity of a number of globular clusters and PNe from the Hurley-Keller et al. (2004) survey. These objects

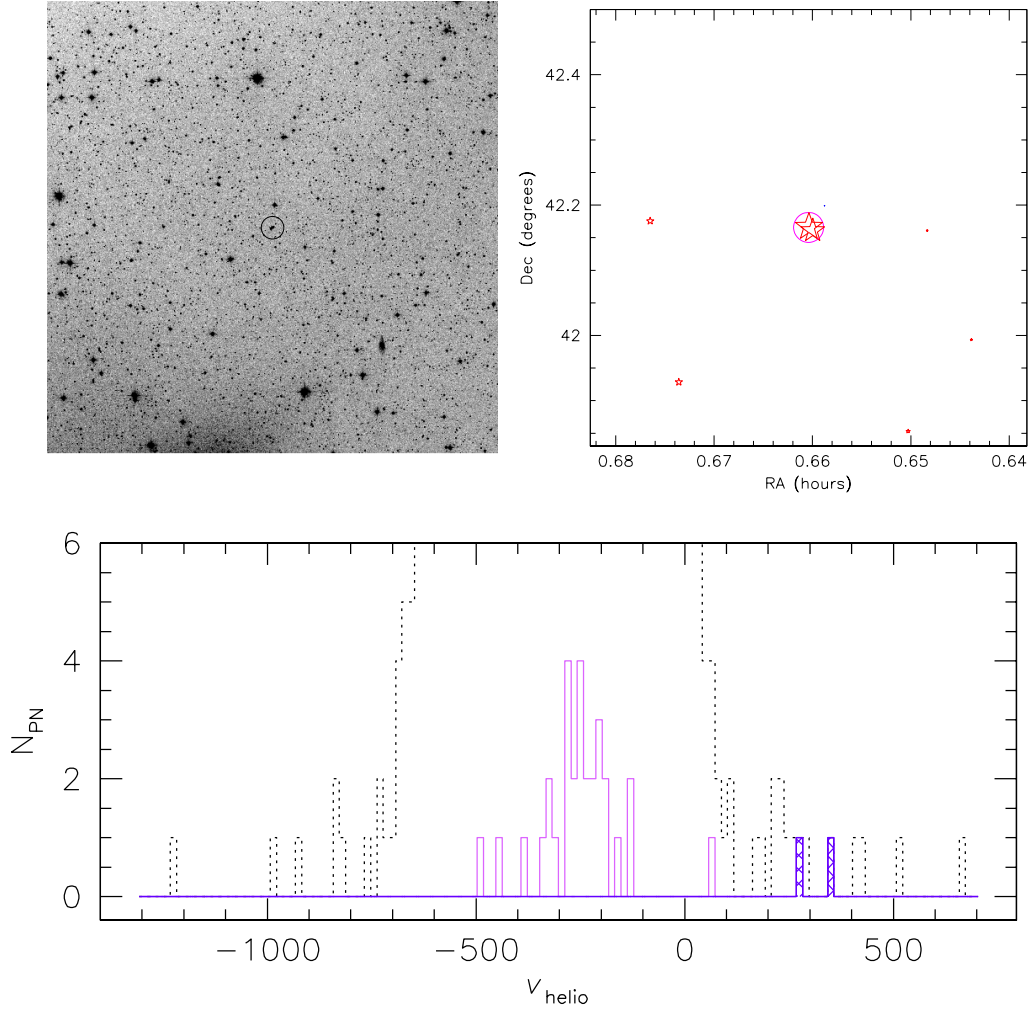


**Figure 4.8:** 2MASXi J0039374+420956. As Figure 4.2, with the edge of NGC 205 visible towards the bottom of the DSS image.

appeared to be quite well separated in velocity from both the modelled kinematics of M31’s thin disk in this region and the nearest other PNe, leading Morrison et al. to suggest that these sources might be providing the signature of a new tidally-distorted satellite galaxy in M31, Andromeda VIII.

However, as Figure 4.10 illustrates, with our larger sample of PNe the gap in velocities between the disk of M31 and And VIII is no longer devoid of PNe. The errors on the new velocities are somewhat larger than those previously published, but not sufficiently so to fill in the apparent  $\sim 50 \text{ km s}^{-1}$  gap in the original smaller data set. Perhaps more tellingly, this figure also shows that the equivalent region on the opposite side of M31 contains a very similar distribution of PNe. In fact the equivalent regions in all four quadrants of M31 are similarly populated by PNe, as shown in Figure 4.11 which plots the data from the remaining two quadrants. We therefore conclude that while these PNe do not agree with Morrison et al.’s thin disk model, they do appear constitute a normal component of the system’s PN distribution, and it is not necessary to invoke the external explanation of a tidally-distorted dwarf companion. As such these objects are marked as belonging to M31 in Table A.1.

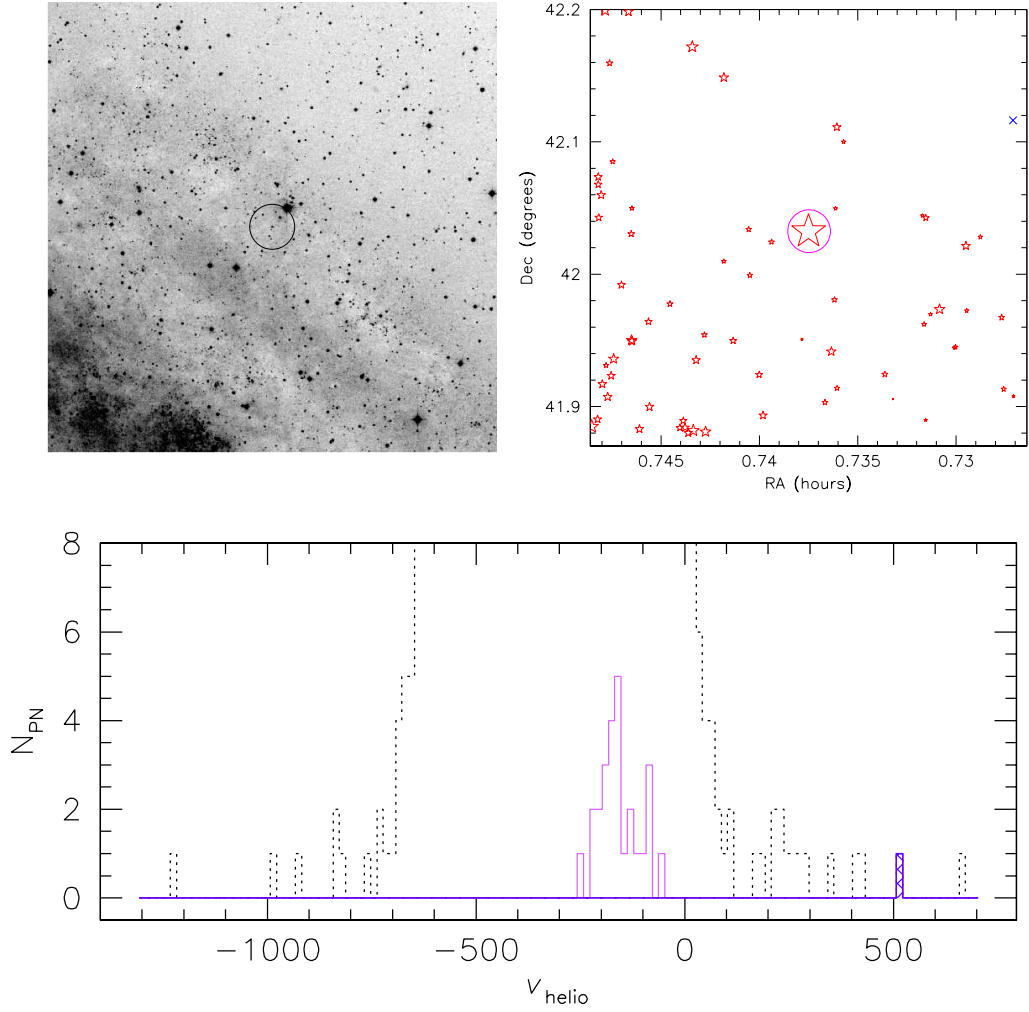


**Figure 4.9:** MLA93 0953. As Figure 4.2, with M31’s disk visible to the bottom left of the DSS image.

## 4.7 Other objects excluded from the PN.S catalogue

On the basis of the analysis in this section, all objects whose kinematics are inconsistent with M31 have either been identified with known satellites, or they have been previously flagged as non-PNe on the basis of their extended nature or line ratios (see Section 3.5). The only other source that we flag as not likely to be an M31 PN is object 2654. Although this source’s kinematics and position are consistent with membership of M31, it is nearly 0.4 magnitudes brighter than any other PN in M31. Unfortunately, it lies outside the region mapped by Massey et al.’s imaging, so we do not have the line ratio diagnostic as a further discriminant. However, given the very sharp cut-off in the PN luminosity function (see Section 5.1), it is most unlikely that this object is a PN, so we flag it in the catalogue and exclude it from the following analysis.

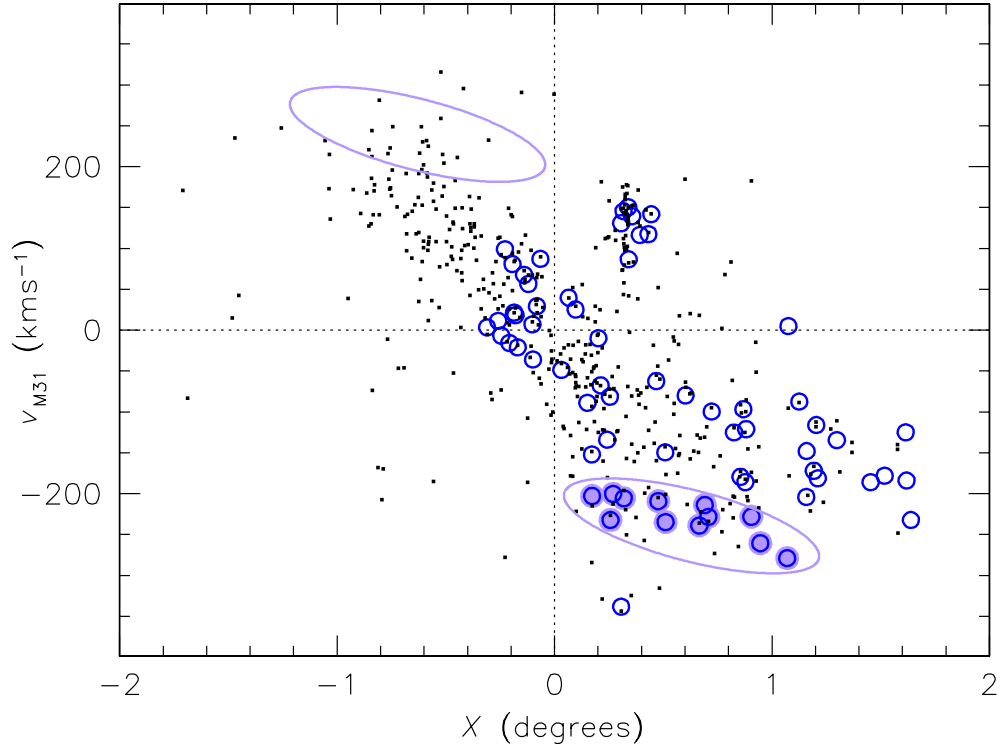


**Figure 4.10:** And VIII. The small filled squares are the PN.S data with  $Y$  values between  $-3$  and  $-6$  kpc. The large open circles are the Hurley-Keller et al. (2004) data set within the same slice in  $Y$ . The highlighted circles are the possible members of And VIII. The large ellipses indicate the approximate velocity space location of And VIII in the lower right, and the equivalent position on the opposite side of M31.

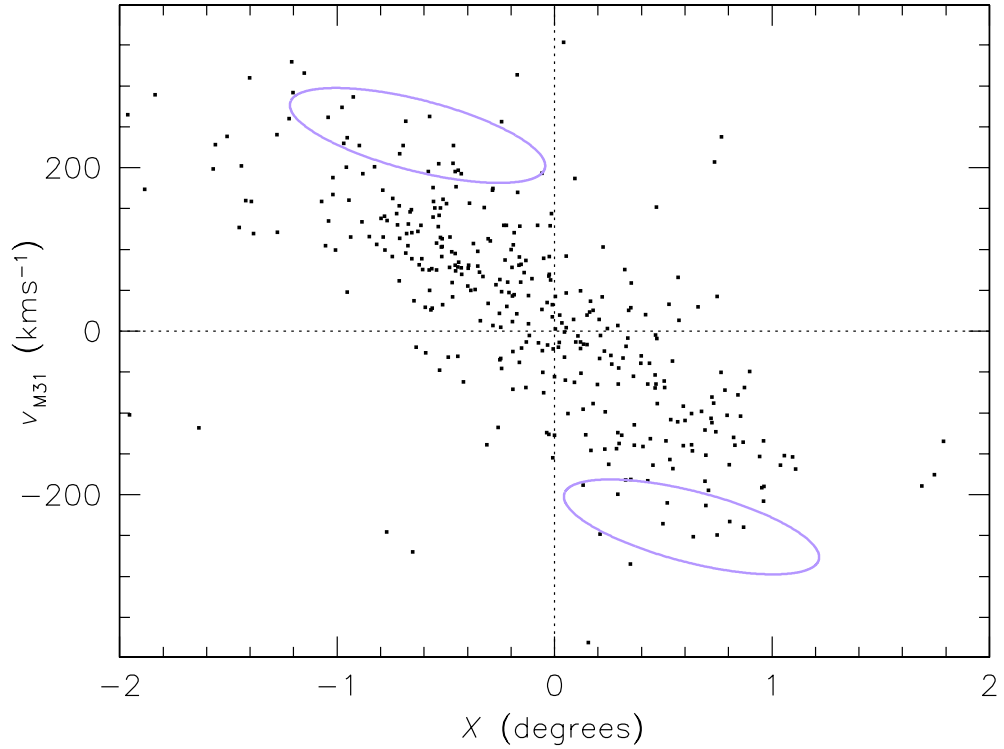


**Figure 4.11:** PN.S data with  $Y$  values between  $+3$  and  $+6$  kpc. The ellipses mark the equivalent areas of velocity space occupied by And VIII, as in Figure 4.10.

# Chapter 5

## Non-kinematic properties of the Andromeda Galaxy's PN population

While this survey was primarily carried out in order to study the kinematic properties of M31's PN population, the magnitudes and spatial distribution of the PNe also allow us to examine a number of non-kinematic properties, which we now discuss.

### 5.1 The planetary nebula luminosity function

Planetary nebulae are observed to follow a well-defined luminosity function of the form

$$N(M_{5007}) \propto e^{0.307M_{5007}} \left[ 1 - e^{3(M_{5007}^* - M_{5007})} \right] \quad (5.1)$$

(Ciardullo et al., 1989), with an equivalent formula for apparent magnitudes for any individual system. The absolute magnitude of the bright-end cutoff,  $M_{5007}^*$ , has a surprisingly universal value of  $-4.5$ , varying only weakly with the host galaxy metallicity (Ciardullo et al., 2002a). Figure 5.1 shows the PNe from this survey, with non-members of M31 removed, fitted by this function. As the figure shows, this functional form fits very well all the way to our completeness limit of  $m_{5007} = 23.75$ . The apparent magnitude of the bright end cutoff, for the sample is  $m_{5007}^* = 20.2 \pm 0.1$ . This result is in excellent agreement with the value published by Ciardullo et al. (1989) of 20.17.

The large number of PNe in our survey means we can divide up the planetary nebula luminosity function (PNLF) and examine it at different points within the galaxy to test the universality of its form. PNLFs for sections at different deprojected disk radii are shown in Figure 5.2. The positional variation in the completeness of the survey is clearly visible in this figure: as discussed above, the high surface brightness and poor seeing of the central fields mean that these data are only complete to  $m_{5007} \sim 23$ . For radii between  $0.2^\circ$  and  $1.0^\circ$ , incompleteness becomes apparent at  $m_{5007} \sim 24$ , while at the largest radii, which were observed under the best seeing conditions (see Figure 3.2), we are close to complete at  $m_{5007} \sim 25$ .

Recent observations of PNe in the Small Magellanic Cloud (Jacoby & De Marco, 2002)

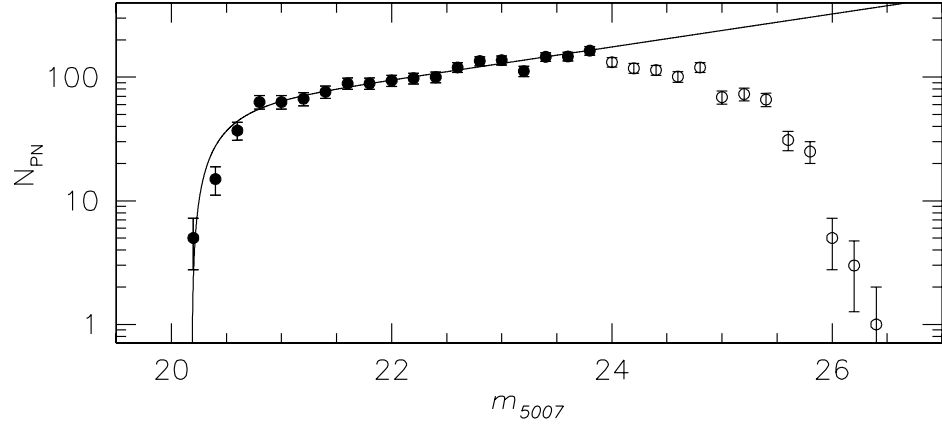


**Figure 5.1:** The planetary nebula luminosity function of M31 as derived from the current survey. Filled circles are plotted up to the magnitude completeness limit; open circles are shown beyond this point.

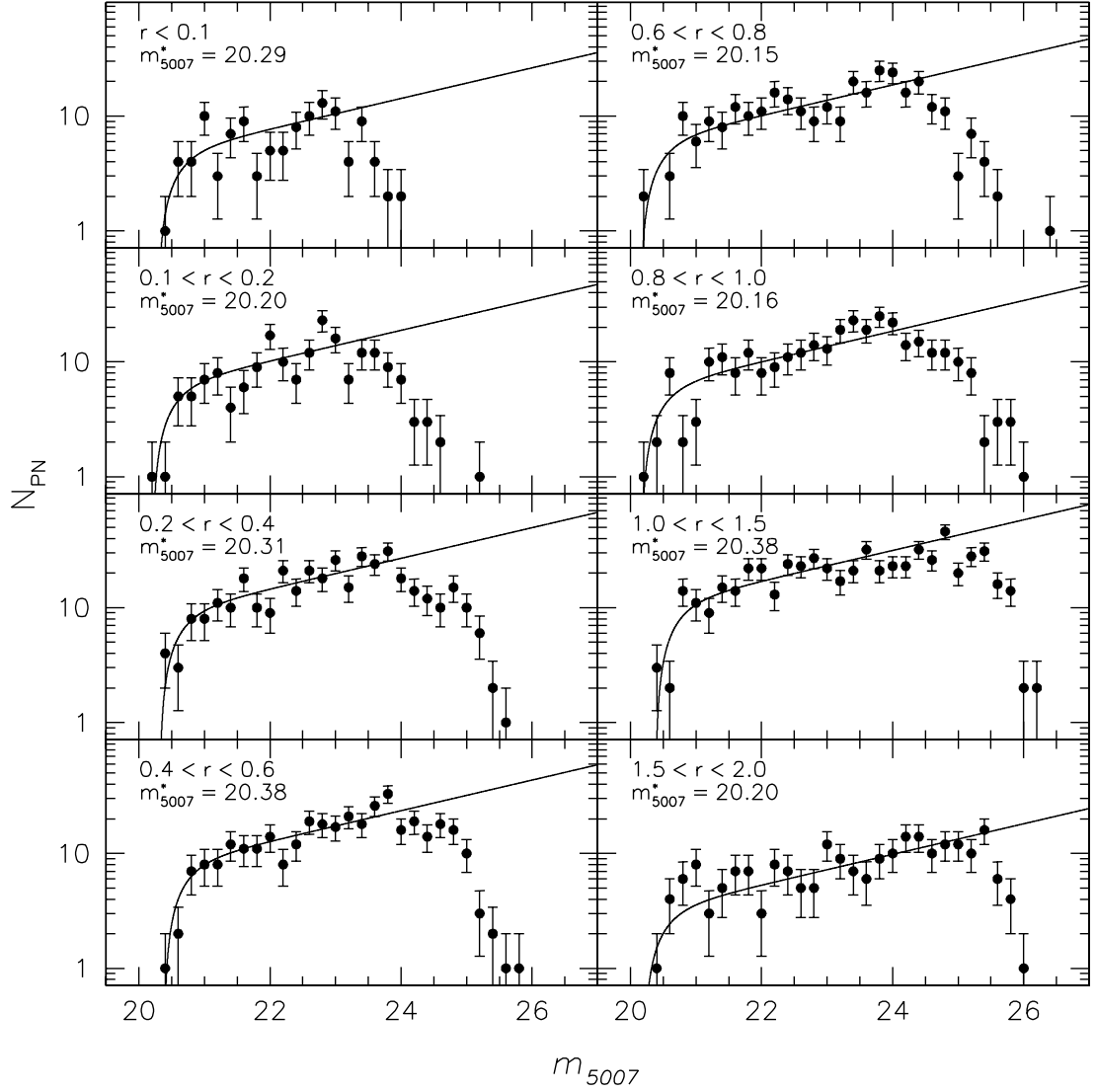


**Figure 5.2:** The planetary nebula luminosity function at different deprojected disk radii in M31.

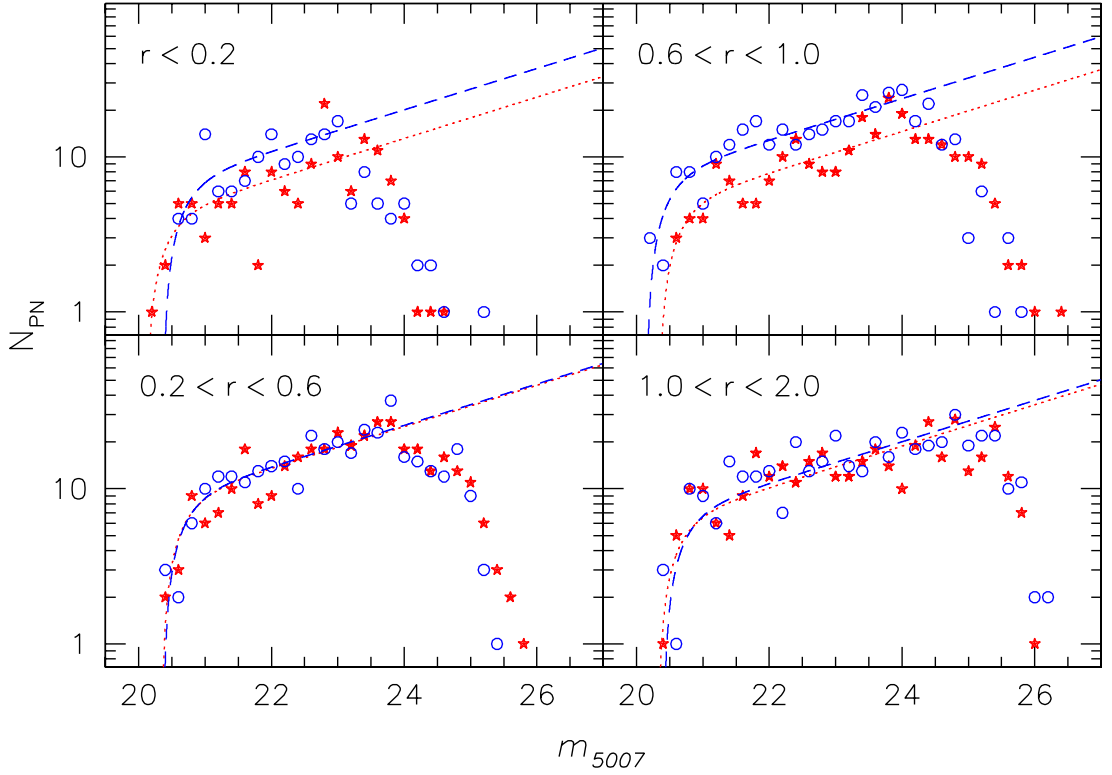


**Figure 5.3:** The planetary nebula luminosity function on the near and far side of M31 over different radial ranges. Red stars and the dotted line represent the data and fit to the near side of M31 (to the north-west), while blue circles and the dashed line show the corresponding information for the far side (to the south-east).

and M33 (Ciardullo et al., 2004) have detected deviations from the simple monotonic function of equation (5.1). In these objects, dips have been observed in the PNLf, whose origins have been proposed as resulting from a recent star formation episode. The only indication of a dip in the PN.S data set is the point at 23.2 mag in Figure 5.1 which lies  $\sim 2.5\sigma$  from the model value. It is interesting to note from Figure 5.2 that most of the signal responsible for this dip comes from the radial range  $0.6^\circ < r < 0.8^\circ$  where the data dips  $\sim 2\sigma$  below the model value at 23.2 mag. This is coincident with the star formation ring discussed in Section 3.5, where the majority of H II regions are located, suggesting that star formation may be responsible for this marginally-detected feature as well.

More radically, Marigo et al. (2004) have suggested that the brightest PNe all originate from the highest mass PN progenitors. This would make the bright end of the PNLf dependent upon the age of the stellar population and it should therefore vary significantly between spheroidal and disk populations. The absence of any significant variation in M31's PNLf with radius, as one goes from the bulge-dominated to the disk-dominated parts of the galaxy, implies that no such effect is seen in this system.

As a further test of the universality of the PNLf, and to search for the effects of obscuration, we have also divided the data according to whether it comes from the near side (positive  $Y$ ) or far side (negative  $Y$ ) of the disk. As Figure 5.3 illustrates, at most radii the PNLfs for the two sides are statistically indistinguishable. However, once again in the region of the ring at  $0.6^\circ < r < 1^\circ$ , we do see a small but significant difference,



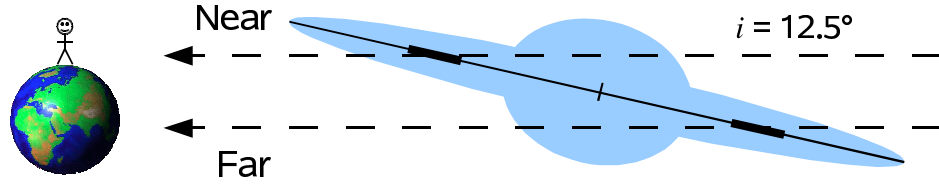


**Figure 5.4:** An illustration of the location of an Earth based observer with respect to the disk of M31. The dust lane is shown as the thick lines in the disk plane. On the near side of the disk the majority of light comes from behind the dust lane while opposite is true for the far side. Not to scale.

with the PNLF from the near side systematically fainter than that from the far side: values of the best fit for  $m_{5007}^*$  on the near and far side are 20.34 and 20.15 respectively. This rather counter-intuitive difference can be qualitatively explained if the ring of star formation also contains a modest amount of dust obscuration (Walterbos & Kennicutt, 1988; de Jong et al., 2006). As Figure 5.4 shows, on the far side of the disk, the line of sight of an observer through a highly inclined system like M31 passes through more of the galaxy in front of the dust layer than behind, while the opposite is true on the near side. Hence on the near side of the disk, most of the PNe observed are located behind the dust layer, dimming the PNLF relative to that seen on the far side. The lack of similar differences between other parts of M31 suggests that obscuration is not a major issue across most of the galaxy.

## 5.2 The spatial distribution of planetary nebulae

In order to interpret the kinematics of the PNe in this survey, we need to know what stellar population or populations these objects are tracing. It is generally assumed that PNe all originate from low-to-intermediate mass stars, so they should mainly trace the old stellar population, but, as we have discussed in Section 5.1, it has been suggested that bright PNe only originate from the high end of this mass range and hence a somewhat younger stellar population. As a further test of this possibility, we can compare the distribution of PNe with that of the red light from the galaxy, which we would expect to be dominated by relatively low-mass red giants, and hence would only be expected to follow the distribution of PNe if they originate from similar low-mass systems. To this end, we have obtained the radial distribution of the PNe with  $m_{5007} < 24$  (the completeness limit of most of the survey) along the major ( $|Y| < 0.1^\circ$ ) and minor ( $|X| < 0.1^\circ$ ) axes of M31.

Along the major axis, Figure 5.5 shows excellent agreement between the number counts of PNe and the R-band photometry of Walterbos & Kennicutt (1987). Fitting an exponential function to the distribution of PNe beyond the bulge and out to  $1.6^\circ$  yields a scale-length of  $R_d = 0.43 \pm 0.02^\circ$  ( $5.9 \pm 0.4$  kpc), also in excellent agreement with the R-band value of  $0.43 \pm 0.02^\circ$  (Walterbos & Kennicutt, 1988). There are no indications of any cut-off in the exponential disk out to the limit of the survey at  $\sim 5R_d$ .

Figure 5.6 shows a similar plot for the minor axis. Once again, there is a good match to the published R-band photometry outside the central region, including reproducing the bump at  $Y \sim 0.6^\circ$  due to NGC 205. The PNe also follow the published  $R^{1/4}$  profile fit to the photometry with a bulge effective radius of  $R_{\text{eff}} = 0.10^\circ$  (1.4 kpc) (Pritchet

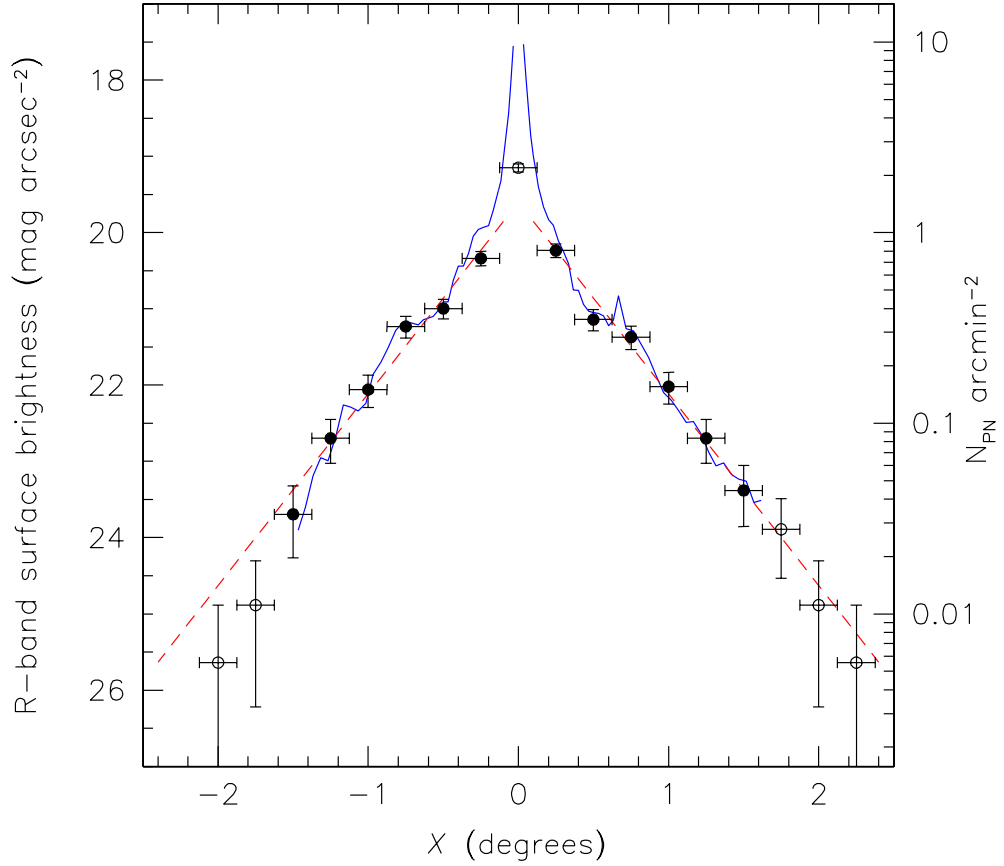


**Figure 5.5:** Surface brightness profile and PN number counts along the major axis of M31. The solid line shows the R-band surface brightness profile of Walterbos & Kennicutt (1987), and the dashed line is an exponential profile with a scale length of  $0.43^\circ$  (Walterbos & Kennicutt, 1988). The number density of PNe with  $m_{5007} < 24$  is indicated by closed circles where the survey is complete both spatially and to  $m_{5007} = 24$ ; the open circle at the centre is for an area that is complete only to  $m_{5007} \sim 23$ , while the those at the edges are for areas that are spatially incomplete.

& van den Bergh, 1994; Irwin et al., 2005). Even at  $\sim 10R_{\text{eff}}$ , there are no signs of an excess over this fit, and hence no evidence for a separate halo population even at these very faint surface brightness levels (equivalent to  $\sim 26$  mag in the R band). This is to be expected, as Irwin et al. found such flattening in RGB star counts along the major axis, to start at distances of  $\sim 1.4^\circ$ .

It thus appears that the PNe trace the same stellar population as the old stars seen in the galaxy's red light. They also seem to broadly fit a simple two-component model comprising an  $R^{1/4}$  central bulge and an exponential disk out to the very faint surface brightness levels accessible using such discrete dynamically-selected tracers.

### 5.3 The luminosity-specific PN density

Having established the proportionality between the stellar continuum emission and the distribution of PNe, we now turn to the constant of proportionality. This quantity, the luminosity-specific PN number density, is usually parametrised by the number of PNe in the top 2.5 magnitudes of the PN luminosity function per unit bolometric solar

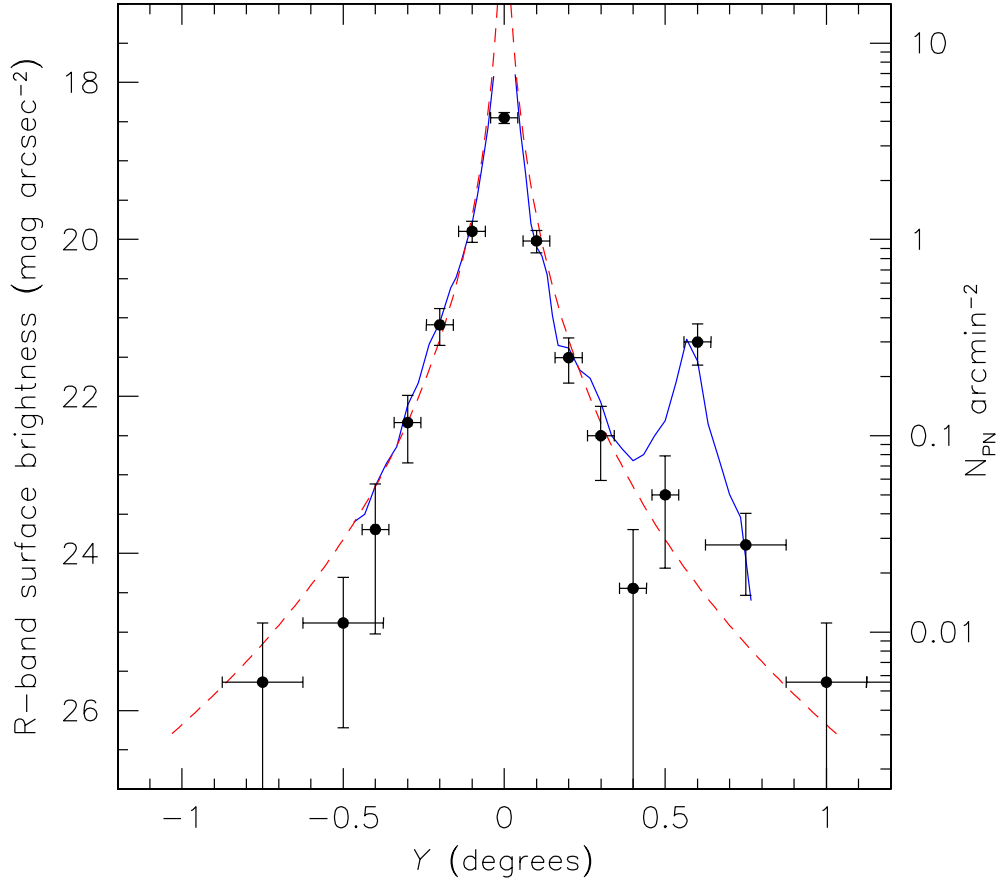


**Figure 5.6:** Surface brightness profile and PN number counts along the minor axis of M31. The solid line is the R-band surface brightness profiles of Walterbos & Kennicutt (1987), and the dashed lines is the  $R^{1/4}$  profile fit to the photometry by Irwin et al. (2005). The number density of PNe with  $m_{5007} < 24$  is indicated by the filled circles.

luminosity, and is given the symbol  $\alpha_{2.5}$ .

The bolometric luminosity of any part of M31 can be calculated via the standard relations

$$M_{bol} = M_V + BC_V \quad (5.2)$$

and

$$\frac{L_{M31,bol}}{L_{\odot,bol}} = 10^{-0.4(M_{M31,bol} - M_{\odot,bol})}, \quad (5.3)$$

where  $BC_V$  is the V-band bolometric correction which has a value of  $-0.80$  mag for M31 (Ciardullo et al., 1989). The solar absolute bolometric magnitude,  $M_{\odot,bol}$ , is taken to be  $+4.74$  mag (Cox, 2000).

The number density of PNe along the major axis and the V-band photometry of Walterbos & Kennicutt (1987) [correcting to absolute magnitudes using  $A_V = 0.206$  (Schlegel, Finkbeiner & Davis, 1998) and a distance modulus of 24.47] give an average value of  $\alpha_{2.5} = (21 \pm 1) \times (10^9 L_{\odot,bol})^{-1}$ . As the upper panel of Figure 5.7 shows, outside the very uncertain central bin there is no strong evidence for any gradient in the value of  $\alpha_{2.5}$  with position, as we would expect on the basis of the close proportionality determined in the previous section. The same calculation on the minor axis, where the light profile is dominated by the bulge, gives  $\alpha_{2.5} = (15 \pm 2) \times (10^9 L_{\odot,bol})^{-1}$ , once

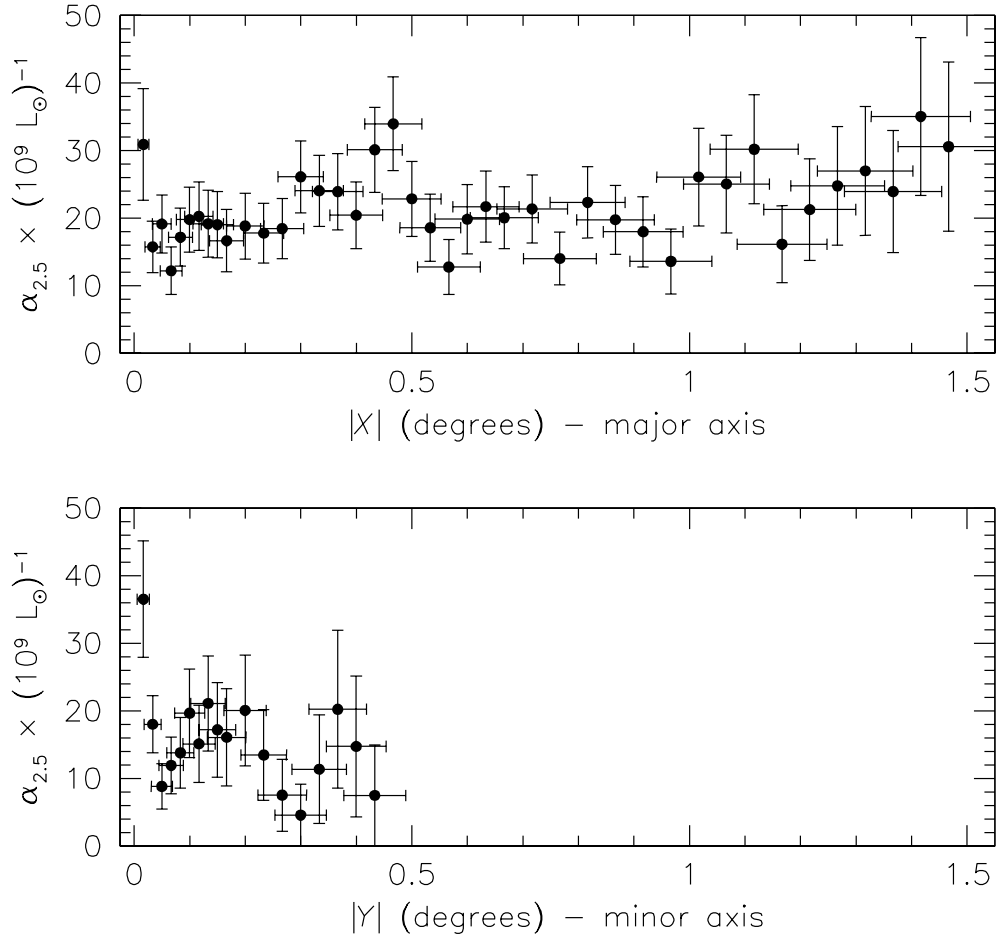


**Figure 5.7:** Variation of  $\alpha_{2.5}$  with distance along the major and minor axes.  $\alpha_{2.5}$  is estimated at positions along the two axes where Walterbos & Kennicutt (1987) list a value for the surface brightness, the number density of PNe at each location is estimated from the number of PNe in a box whose dimensions are equal to the horizontal error bar.

again with no evidence for a gradient (see the lower panel of Figure 5.7). This value agrees very well with the calculation by Ciardullo et al. (1989) for the PNe in M31's bulge, from which they derived a value of  $\alpha_{2.5} = 16.3 \times (10^9 L_{\odot, \text{bol}})^{-1}$ .

The modest difference between the mean values for the minor and major axes is consistent with the existing evidence that  $\alpha_{2.5}$  is correlated with galaxy colour, with red ellipticals being poorer in PNe per unit luminosity than blue spiral galaxies (Peimbert, 1990; Hui et al., 1993); here for the first time we are seeing evidence for such a difference between spheroidal and disk components within a single galaxy. Fortunately, such a mild deficit in the number of PNe from the bulge component relative to those from the disk will have little impact on the dynamical modelling of these data, since it merely changes the effective normalisation of the number density of tracers in these two discrete components. We can therefore proceed to study the kinematics of M31's PN system.

## Chapter 6

# Kinematic properties of the Andromeda Galaxy

Spiral galaxies are generally considered to be composed of three main constituents: a stellar bulge, usually containing a central supermassive black hole; a disk with thin and thick components containing stellar and gaseous materials; and a halo containing stellar and dark matter. The picture we have of M31 is that it is significantly more complicated than this. The centre is observed to have a central supermassive black hole (Kormendy & Bender, 1999), embedded in a double nucleus (Lauer et al., 1993); the two components being separated by  $\sim 0.5''$  (1.9 pc). M31's bulge appears to be distorted into an oval at optical wavelengths and is clearly boxy in the infrared (Beaton et al., 2006), indicative of a barred bulge (Lindblad, 1956; Stark, 1977; Athanassoula & Beaton, 2006). The H I disk is seen to be warped. The warp is extreme, folding the disk back across the line of sight (Brinks & Shane, 1984). The scale height of the H I disk is also seen to flare out (Braun, 1991). Meanwhile star counts in Andromeda's halo show that it is not smooth, but clumpy (Ferguson et al., 2002), and contains a large stellar stream (Ibata et al., 2001). These features all add up to complicate the kinematic properties of the system. We will now look at both the bulk kinematic properties of M31 and the kinematics of some of these features.

### 6.1 Planetary nebula kinematics

A quick look at a plot of the PN velocities against major axis distance (Figure 6.1) shows the system kinematics to be dominated by rotation at large radii, with a larger random component at small radii, attributable to a bulge population. This result indicates that the majority of the PNe form a relatively simple system of rotationally-supported disk and randomly-supported bulge, in agreement with the conclusion based on photometry in Section 5.2. In addition to the bulk galaxy motions, a few small features are visible in this figure, mostly PNe associated with bright satellite and background galaxies in the field. These non-M31 PNe have been examined in Chapter 4 and are excluded from the sample to be analysed here. Possible other velocity structures in this plot will be looked at in Section 6.5.

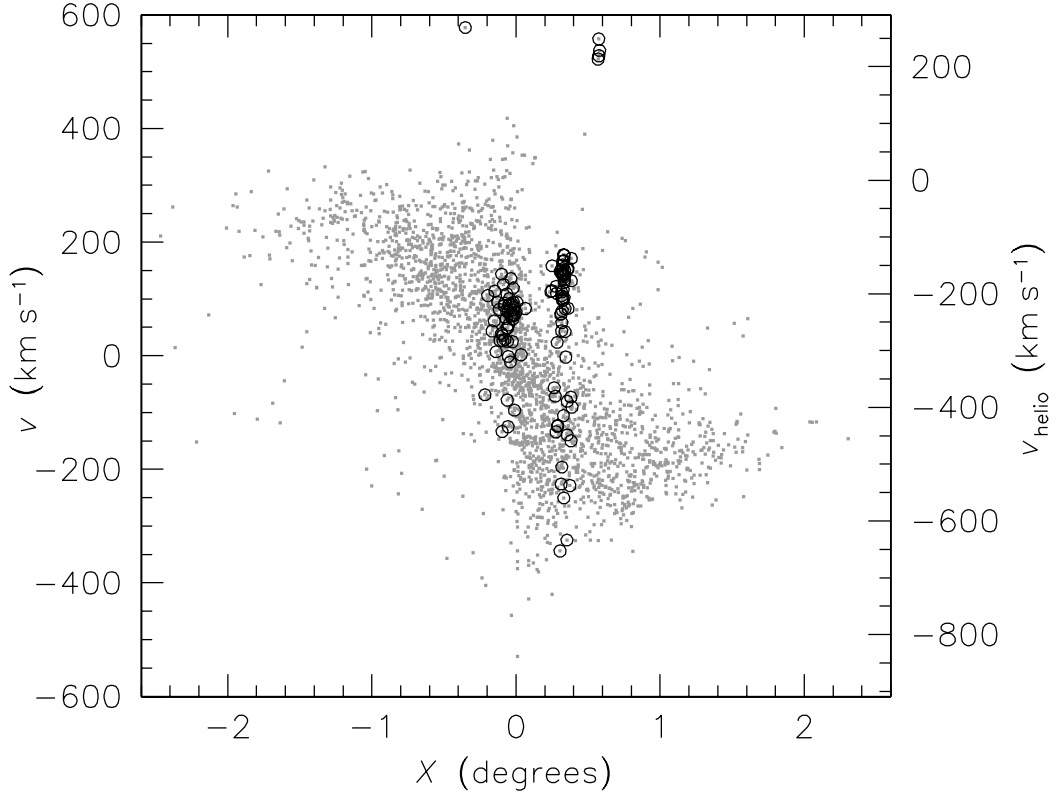


**Figure 6.1:** Planetary nebula velocities for all PNe found in the survey area. Those highlighted with black circles are PNe in the vicinity of a satellite or background galaxy, as described in Chapter 4, and are excluded from further analysis of the kinematics of M31’s PN population.

### 6.1.1 The rotation curve

A more detailed, dynamical study will be considered in Chapter 7, but first we look at the kinematics of the dataset, assuming that the galaxy is axisymmetric and considering the PNe that lie close to M31’s major axis. For a highly-inclined galaxy like M31, the observable kinematics in this region are dominated by the rotational motion, so we can essentially isolate this component of velocity. Accordingly, we have selected a sample of 690 PNe with  $|Y| < 0.04^\circ$ , close to the major axis. Figure 6.2 shows a plot of this subsample’s line-of-sight velocities versus major axis position, together with the mean velocities derived by radially binning these PNe into groups of 50 objects, the results of which are given in Table 6.1. A system velocity of  $-309 \text{ km s}^{-1}$  has been adopted as discussed previously.

The distribution of PN velocities in Figure 6.2 has an upper envelope that matches the rotation curves derived from various tracers (also shown in this figure) reasonably closely at large radii. At small radii, the PNe show a wide spread in velocities, indicative of a contribution from the bulge. It is also interesting to note the dip in the mean rotation speed of PNe at  $\sim 0.3^\circ$ . This feature, which shows up even more clearly in the CO rotation curve, has been attributed by Loinard, Allen & Lequeux (1995) to non-circular motions associated with a barred bulge. Its appearance in the PNe kinematics confirms that they are dominated by disk objects even at this fairly small radius, but also serves as a warning that large non-circular motions may complicate the observed dynamics at these radii. At larger radii, the mean velocities of the PNe trace the

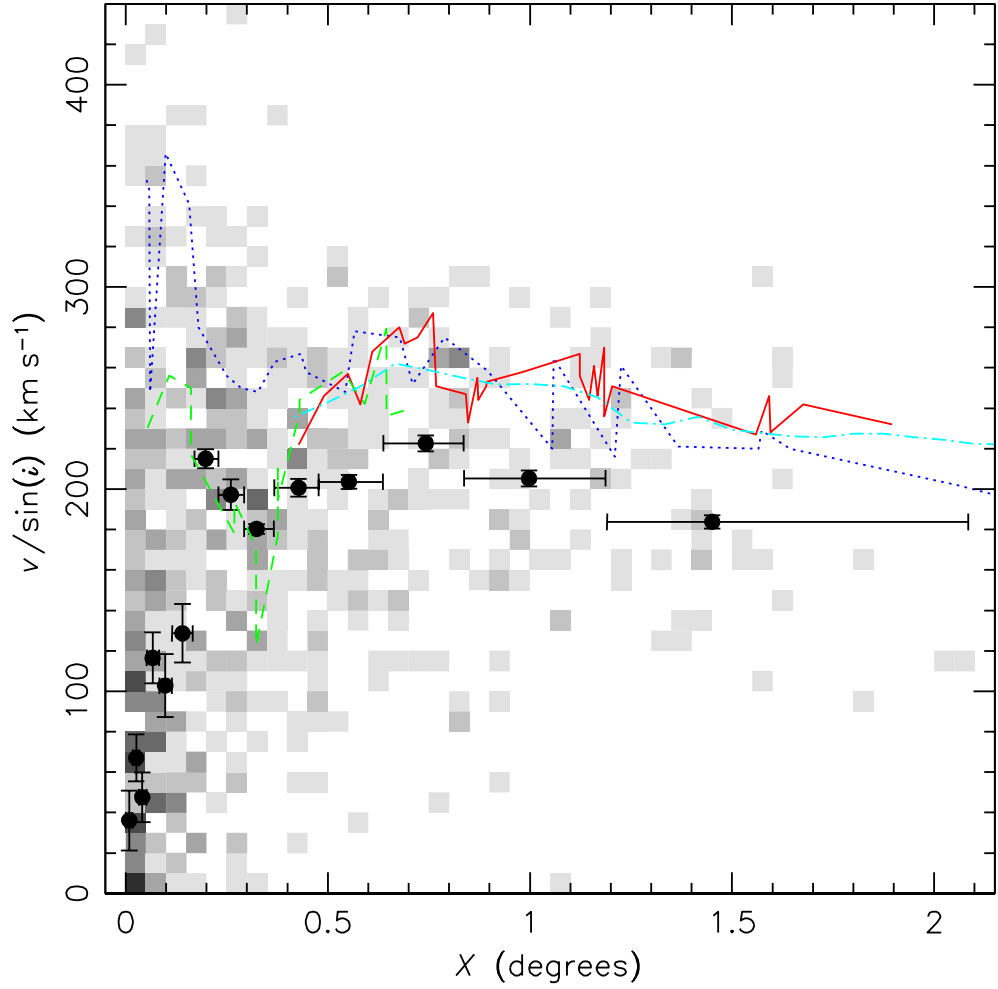


**Figure 6.2:** Plot of position versus velocity for PNe close to the major axis of M31 ( $|Y| < 0.04^\circ$ ). The data from both sides of the galaxy have been combined, and the velocities have been corrected for the galaxy's inclination. The gray-scale shows the density of PNe in this phase-space projection. The circles show the mean velocities of these data in a number of bins – the horizontal error bars show the extent of each bin, and the vertical bars the uncertainty in mean velocity. The dotted and dot-dashed lines show M31's H I rotation curve as measured by Braun (1991) and Carignan et al. (2006) respectively; the dashed line shows the rotation curve derived from CO measurements (Loinard, Allen & Lequeux, 1995); and the solid line shows a rotation curve derived from H II region velocities (Kent, 1989).

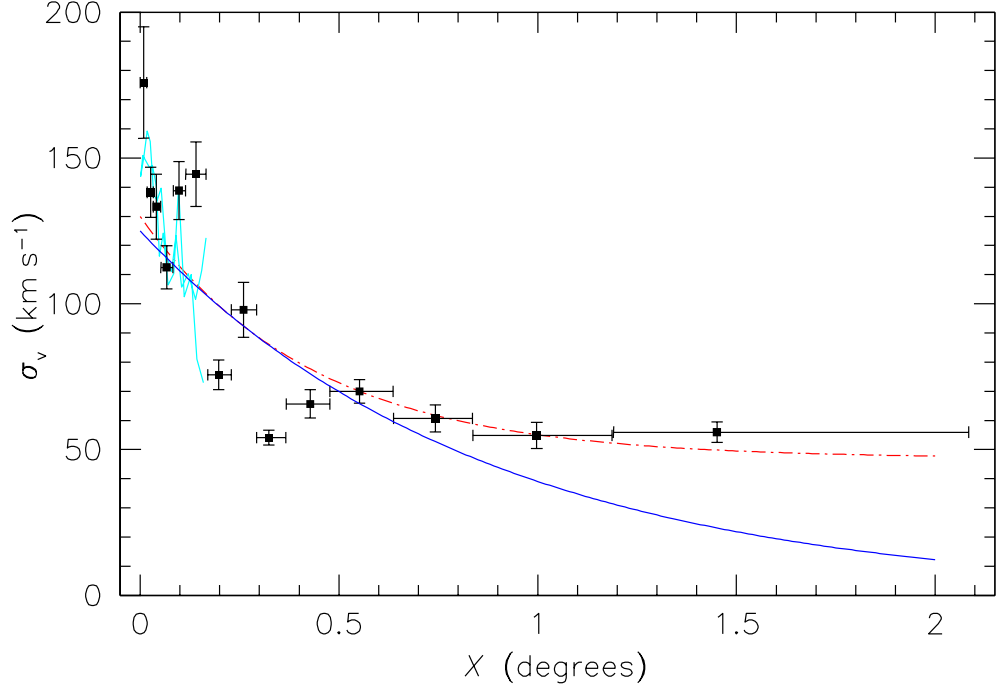
rotation curve relatively well, except that the mean velocity lies systematically below the circular speed. We will return to the origins of this asymmetric drift in the mean velocities of PNe in Section 7.2. For now we will take a look at their random motions.

### 6.1.2 Velocity dispersion

Figure 6.3 shows the observed velocity dispersion as a function of position along the major axis obtained from the PNe in Figure 6.2, binned radially into groups of 50 objects. The data are also listed in Table 6.1. Near the centre, the calculated PN velocity dispersions agree well with the declining profile derived by McElroy (1983) from stellar absorption lines (also shown in the figure), providing further confidence

**Table 6.1:** Rotation curve and velocity dispersion profile measured from PNe close to the major axis.

$\bar{X}$ (degrees)	$X_{\min}$ (degrees)	$X_{\max}$ (degrees)	$v_{\text{Rot}}$ (km s <sup>-1</sup> )	$v_{\text{err}}$ (km s <sup>-1</sup> )	$\sigma_v$ (km s <sup>-1</sup> )	$\sigma_{\text{err}}$ (km s <sup>-1</sup> )
0.01	0.00	0.02	36.1	14.8	176.7	19.1
0.03	0.02	0.03	67.1	11.6	139.3	8.6
0.04	0.03	0.05	47.6	12.3	134.4	11.1
0.07	0.05	0.08	116.5	12.6	113.8	7.4
0.10	0.08	0.11	102.8	15.6	139.8	10.0
0.14	0.11	0.17	128.6	14.5	145.5	11.1
0.20	0.17	0.23	215.0	4.7	77.6	5.1
0.26	0.23	0.29	197.2	7.5	99.4	9.5
0.32	0.29	0.37	180.3	2.4	56.7	2.5
0.43	0.37	0.48	200.7	4.3	67.8	4.9
0.55	0.48	0.64	203.6	3.5	72.0	4.0
0.74	0.64	0.84	222.7	4.0	63.1	4.6
1.00	0.84	1.19	205.3	4.0	57.4	4.5
1.45	1.19	2.08	183.8	3.2	58.5	3.5

**Figure 6.3:** Velocity dispersion profile for the major-axis PN sample shown in Figure 6.2. Points with error bars show the axisymmetrically binned PN dispersion profile, corrected in quadrature for the uncertainty in the PNe velocities. The solid cyan line is the inner stellar velocity dispersion profile of McElroy (1983). The two curves are for models fit to the PN data with a  $\chi^2$  minimisation: the red dot-dash line is the empirical fit of equation (6.1); and the solid blue line shows a standard exponential decrease.



in the PN results. However, the stellar absorption-line data only reach to  $\sim 0.2^\circ$ , while the PN profile goes out to  $\sim 2^\circ$  (27.4 kpc). It is in these previously-unexplored outer regions that the velocity dispersion starts to behave a little strangely. First, there is a dip in the observed dispersions at  $\sim 0.3^\circ$ , suggesting that the bar's influence shows up in the dispersion profile as well as the mean rotational velocity. Second, the dispersion profile seems to flatten out at larger radii to a constant value of  $\sim 55 \text{ km s}^{-1}$ . Ignoring the bar-related dip, a simple empirical fit to the large-scale profile, plotted as a red dot-dash line in Figure 6.3, is given by

$$\sigma_\phi = \sigma_A + \sigma_B \exp\left(-\frac{R}{R_d}\right). \quad (6.1)$$

with  $\sigma_A = 47 \text{ km s}^{-1}$ ,  $\sigma_B = 84 \text{ km s}^{-1}$  and  $R_d$  set to  $0.43^\circ$ , the disk scale length measured in Section 5.2. As a caveat to this, it is possible that the last point in the velocity dispersion profile is artificially enhanced by the inclusion of PNe covering a large radial range over which significant variation in the mean value of the rotation may have occurred. Indeed a decrease in the mean velocity is seen in both our PNe and in the other rotation measures at these large radii, but it is small ( $\sim 10 \text{ km s}^{-1}$ ) and while it may increase the observed velocity dispersion at this point it cannot be responsible for the bulk of the dispersion. Other recent stellar kinematic data from large radii also reveal significant dispersions: Ibata et al. (2005) find a velocity dispersion of RGB stars of  $\sim 30 \text{ km s}^{-1}$  from small fields at even larger radial distances.

These results are not consistent with the expectations of the simplest disk models. By applying the tensor virial theorem to a one-dimensional sheet approximation to the vertical distribution of stars in a disk, one can show that the vertical velocity dispersion,  $\sigma_z$ , should be given by an equation of the form

$$\sigma_z^2 = 2\pi G \Sigma z_0 \quad (6.2)$$

where  $z_0$  is the scale height and  $\Sigma$  the surface density of the disk (Binney & Merrifield, 1998, p.727). If the surface density of stars drops off exponentially with radius with a scale-length  $R_d$ , and the scale-height stays constant with radius (van der Kruit & Searle, 1982), then  $\sigma_z$  should drop exponentially to zero with a scale-length of  $2R_d$ . If the velocity ellipsoid remains roughly constant in shape, then the other components, including the observed  $\phi$  component, should decrease in the same way. The solid line in Figure 6.3 shows this decline, and it is clear that this is not what we find in M31.

We will consider possible reasons for this phenomenon in Section 7.1, but for now this flat velocity dispersion profile gives us a useful way to examine the PN sample for variations in kinematics with magnitude.

### 6.1.2.1 Variation with magnitude

It is important to search for any systematic variation in the properties of PNe with luminosity. Such a test is motivated by knowledge of the Solar neighbourhood of the Milky Way, where we know that the tangential components of the velocity dispersions of different types of star vary by more than a factor of two, with the youngest, most massive

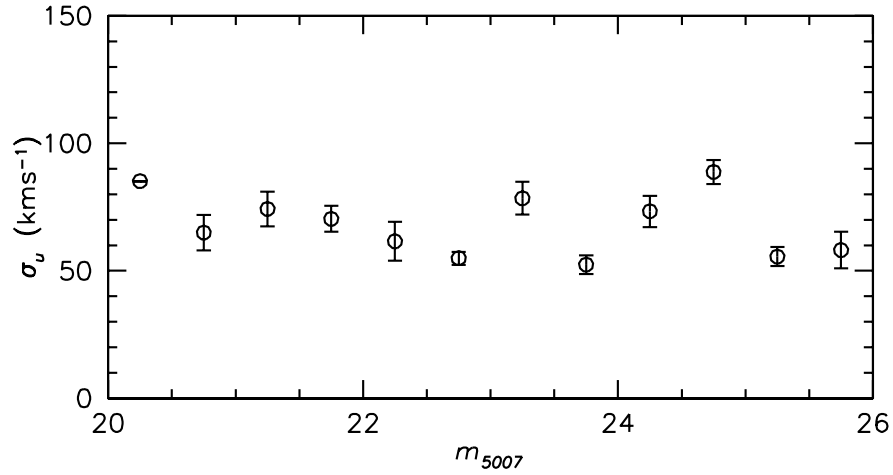


**Figure 6.4:** Variation in velocity dispersion with apparent magnitude for the major-axis data from the disk region at  $X > 0.3^\circ$ .

stars having the lowest dispersions (Binney & Merrifield, 1998). If the PNe in M31 that populate different parts of the PNLf had progenitor stars with different masses, and hence ages, then we might expect similar variations in their velocity dispersions. Not only would such a variation fit with the suggestion of Marigo et al. (2004) that the bright end of the PNLf is exclusively populated by more massive stars, but it would also resonate with the recent claim by Sambhus, Gerhard & Méndez (2006) that the PNe in NGC 4697 can be divided on the basis of their luminosities into two discrete populations with distinct kinematics.

To test for this effect, we have extracted from the major-axis subsample those objects for which  $X > 0.3^\circ$ : since the global velocity dispersion is approximately constant at these radii (see Figure 6.3), we can combine data across this range to form a meaningful average. Figure 6.4 shows the velocity dispersions determined from these data combined into half-magnitude bins. Clearly, there is no evidence for a decrease in dispersion for the brightest objects, adding further weight to the conclusion that PNe of all magnitudes stem from a relatively homogeneous population of old stars.

## 6.2 H II region kinematics

While the target of this survey was to measure and examine the Andromeda Galaxy's PN kinematics, a large number of small H II regions have also been detected and their kinematic properties may also be considered. This must be done with caution as the sample is known to include a number of background galaxies (see Figure 3.17) as well as some contamination from misclassified PNe. In order to eliminate sources that are obviously not members of M31 we have made cuts at  $v_{\text{helio}} = v_{\text{sys}} \pm 350 \text{ km s}^{-1}$ . The worst contamination from PNe is likely to come from objects in field 76 where the seeing was so good that variations in the instrument focus seem to have made some point sources appear extended (see Section 3.5); as only one of these apparently extended objects has also been selected as having an  $[\text{O III}]/(\text{H}\alpha + [\text{N II}])$  flux ratio indicative of an H II region we have chosen to exclude all sources originating from this

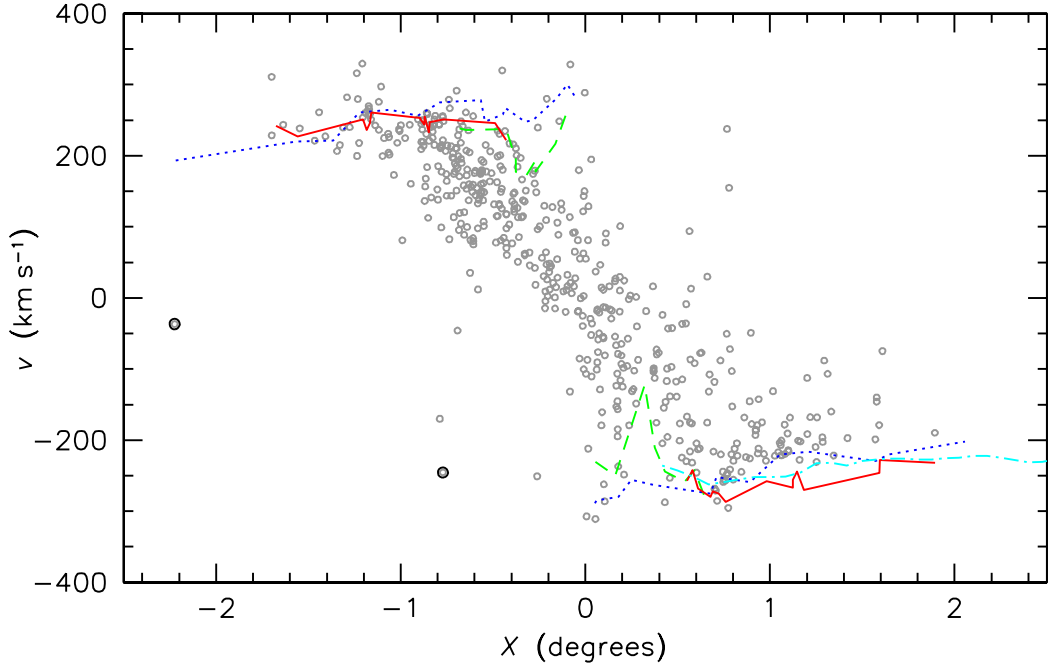


**Figure 6.5:** H II region velocities. The two sources highlighted have velocities consistent with membership of the velocity substructure identified in Section 6.5. The other rotation curves shown are those measured from H I gas (Braun 1991, dotted line; and Carignan et al. 2006, dot-dashed line); H II regions (Kent, 1989, solid line); and CO emission (Loinard, Allen & Lequeux, 1995, dashed line). The H I rotation curve of Carignan et al. (2006) has only been measured on one side of M31.

field. Sources identified as belonging to external galaxies have also been eliminated. This leaves us with a sample of 509 H II regions.

The velocities of these H II regions have been plotted against the major axis distance,  $X$ , in Figure 6.5. This shows the population to be dominated by rotation, with just a few objects with peculiar velocities remaining in the sample. A couple of these appear to be associated with the velocity substructure described in Section 6.5 and are highlighted in the plot. The rest of the peculiar velocity sources could be further background sources or sources associated with other structures in the galaxy.

Unlike PNe, H II regions should not be affected by a lag in the mean velocity of the population as seen in Section 6.1.1 (reasons for this will be discussed in Section 7.2), and it should therefore be fairly straightforward to extract a rotation curve directly from their velocities. We have calculated radii and circular velocities for the H II regions assuming that they lie on an axisymmetric, thin disk and are moving on circular orbits. These circular velocities were then plotted against radius in Figure 6.6 along with the mean rotational velocities derived by radially binning the H II regions into groups of 40 objects and fitting gaussians to these distributions.

It is worth noting that the point at  $r = 0.93^\circ$  that is out of line with the rest lies to the outer edge of a prominent star formation ring (see Chapter 1). In all likelihood this point is being affected by some form of non-circularity due to, for example, a slight ellipticity to the ring, or non-circular motions related to spiral structure that are enhanced by the conversion to circular velocities, and is not a real increase in the circular velocity at that point.

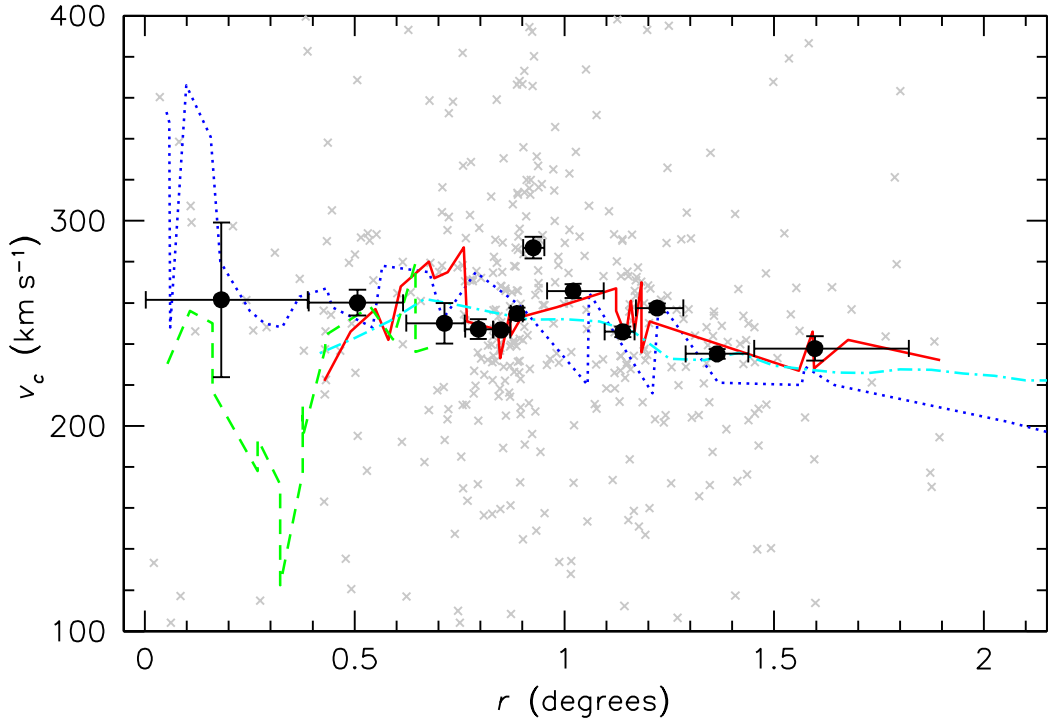


**Figure 6.6:** H II region circular velocities and the mean rotation curve. The apparent dispersion in these points is an artefact of the conversion from observed to circular velocities and not a ‘real’ dispersion. The other rotation curves are as in Figure 6.2.

Apart from this point, the resulting rotation curve, values for which are given in Table 6.2, is in extremely good agreement with the previously measured rotation curves. The general form of the rotation curve is of a steady, linear decline in velocity from  $\sim 260 \text{ km s}^{-1}$  at the centre to  $\sim 240 \text{ km s}^{-1}$  at  $1.5^\circ$  (20.55 kpc).

Having constructed rotation curves based on mean velocities assuming the disk of M31 is axisymmetric, it would be prudent to consider how realistic this assumption is. To this end we now turn our attention to the possibility of asymmetry in the disk of the galaxy.

### 6.3 Asymmetry in M31’s disk

The H I rotation curve at large radii is difficult to measure on the receding side of the disk, as velocities in this region are similar to that in the Milky Way making the two gas populations indistinguishable. Hence, the points at large radii in Carignan et al.’s H I rotation curve are measured only on the approaching side of the disk. Where data exist for both sides of the disk, we have compared them in Figure 6.7. On the whole, there is little difference between the measured rotation curves for the two different sides. However a significant difference between the two sides of Braun’s H I rotation curve is seen between  $1^\circ$  and  $1.3^\circ$ . To the eye it looks as though the rotation speed of the disk is steadily decreasing but with a ‘step’ of  $\sim 50 \text{ km s}^{-1}$  occurring at around  $1^\circ$  on the south-western side and around  $1.3^\circ$  on the north-eastern side, beyond which the two sides equalise to similar velocities. Loinard, Allen & Lequeux’s CO measurements

**Table 6.2:** Rotation curve measured from H II region circular velocities.

$\bar{r}$ (degrees)	$r_{\min}$ (degrees)	$r_{\max}$ (degrees)	$v_{\text{Rot}}$ (km s <sup>-1</sup> )	$v_{\text{err}}$ (km s <sup>-1</sup> )
0.18	0.00	0.39	261.5	37.7
0.51	0.39	0.62	260.1	6.3
0.71	0.62	0.76	250.1	9.9
0.79	0.76	0.83	247.2	4.9
0.85	0.83	0.87	246.8	1.1
0.89	0.87	0.90	254.8	2.9
0.93	0.90	0.95	286.9	5.3
1.02	0.96	1.09	265.8	3.4
1.14	1.10	1.17	245.9	2.5
1.22	1.17	1.28	257.5	2.1
1.36	1.29	1.44	235.2	2.4
1.60	1.45	1.82	237.8	5.9

do not reach far enough to detect this feature and it is not seen in Kent's H II region measurements.

When we look at our PN velocities there appears to be a difference between the two sides at radii beyond  $\sim 1^\circ$ . The upper panel of Figure 6.8 shows that the PN on the NE side of the disk reach up to the mean rotational velocity at all radii, while on the SW side of the disk PNe with  $X \gtrsim 1^\circ$  have velocities that are significantly smaller than the mean rotational velocity. To ensure that this is not simply a result of geometry, PNe that are close to the major axis, and should therefore be closest to circular velocity, have been highlighted; the trend can also be seen in these PNe. Our H II region population (lower panel of Figure 6.8) shows a similar pattern, albeit in a small number of objects as there are relatively few H II regions at these large radii. Binning up and fitting gaussians to the PNe and H II regions in the same fashion as was done previously, but for each side separately, produces the PN and H II region rotation curves shown in the upper panel of Figure 6.9 where a difference between the north-eastern and south-western sides of the disk of  $\sim 50 \text{ km s}^{-1}$  can be seen in both the PN and H II region velocities.

A possible source of variation in the mean stellar velocities comes from the asymmetric drift. As this is related to the dispersion in the stellar population, the velocity dispersion profiles for the PNe on either side of the disk are also shown in Figure 6.9. There is no discernible difference between the velocity dispersion profiles on the two sides, making variations in the asymmetric drift an unlikely source of this difference. This is of course to be expected as the difference is seen in both PNe and H II regions.

It seems quite likely that this difference is related to that seen in Braun (1991)'s H I rotation curve. From around  $1^\circ$  his H I, and our H II and PN rotation curves all show the north-eastern side of the disk to remain at the same level as at smaller radii while the south-western side displays a drop in velocity of around  $50 \text{ km s}^{-1}$ . We cannot tell if the PNe and H II regions equalise again in the way the H I rotation curve is seen to, as our PN and H II region data do not extend beyond about  $1.5^\circ$ . However, the PN

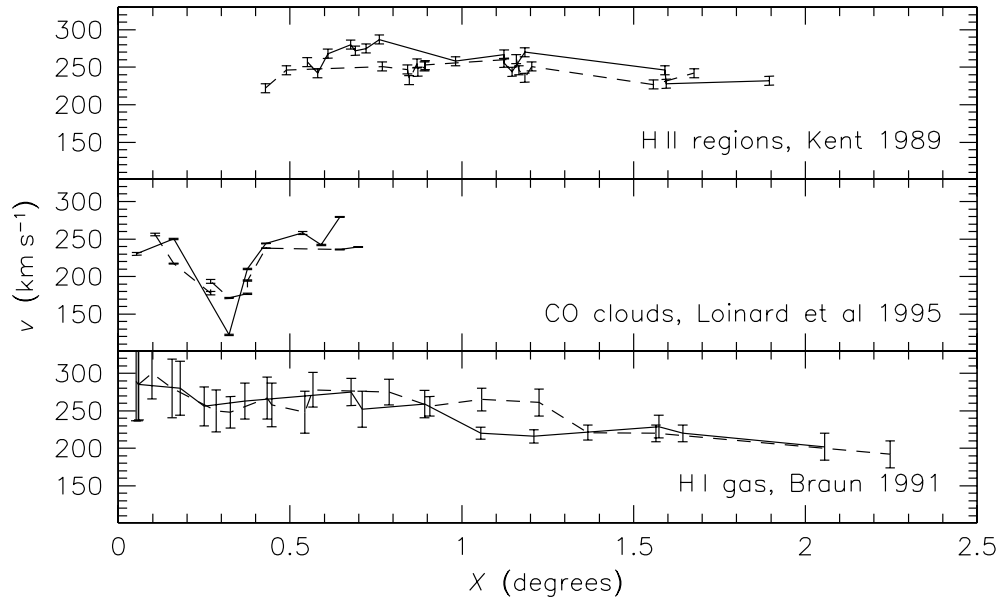


**Figure 6.7:** Comparison of rotation curves from the north-eastern (dashed lines) and south-western (solid lines) sides of M31's disk.

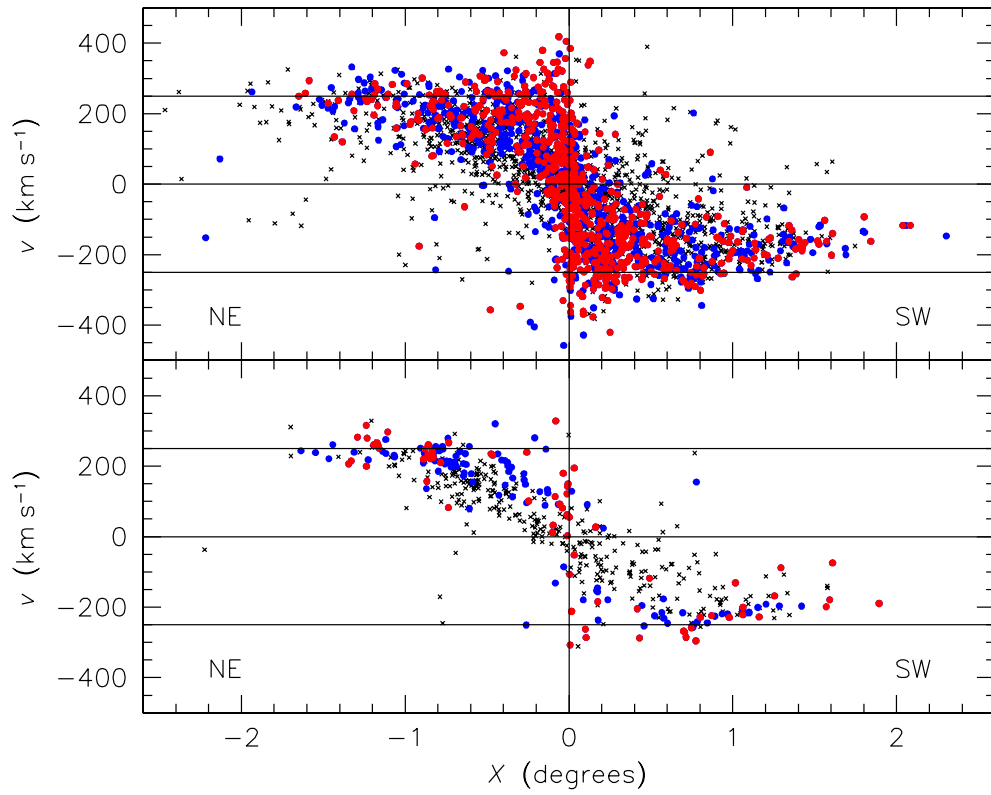


**Figure 6.8:** The upper panel shows the PN distribution and the lower panel shows the H II region distribution. Small black crosses are all objects in M31, the blue and red circles are objects close to the major axis with  $Y < 0.1^\circ$  and  $Y < 0.04^\circ$ , respectively. The lines mark the axes and provide guides at the mean rotational velocity,  $250 \text{ km s}^{-1}$  and  $-250 \text{ km s}^{-1}$ .

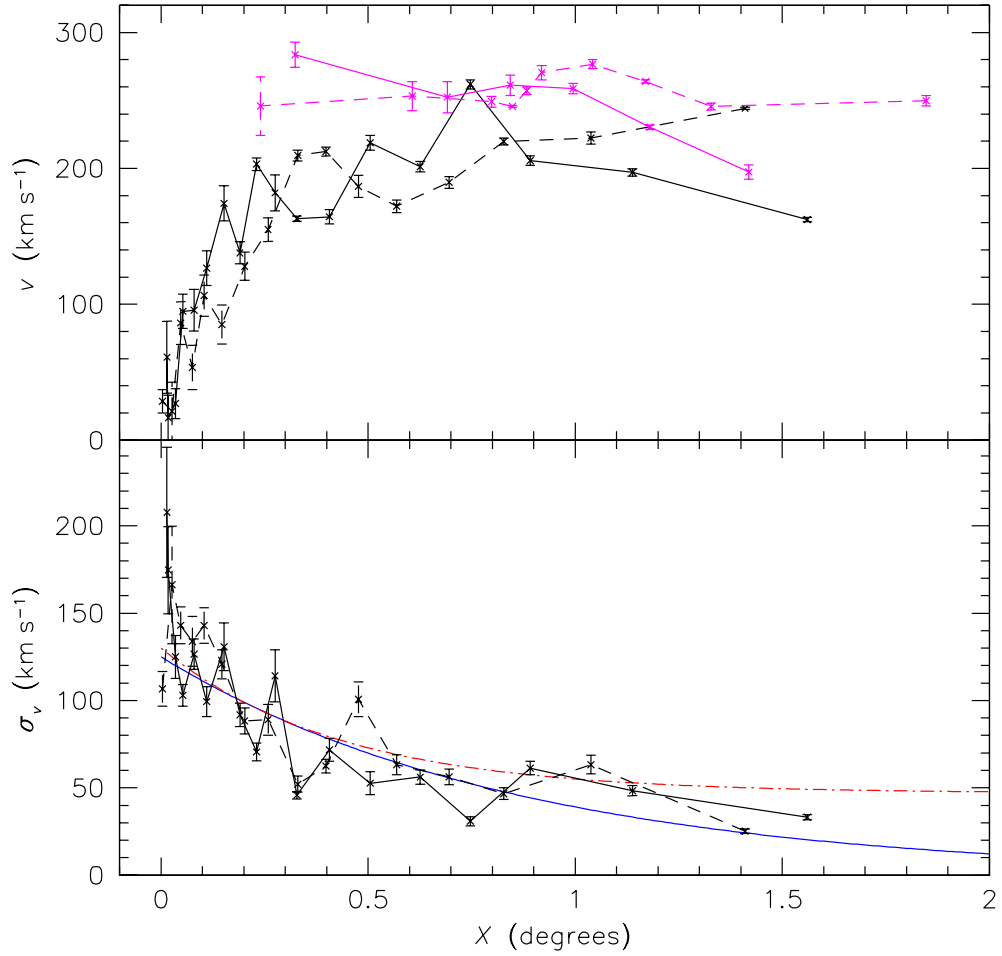


**Figure 6.9:** The upper panel shows the mean values of the binned velocities for the PNe (black lines) and H II regions (red lines) on either side on the disk. Dashed lines are used for the north-eastern side of the disk and solid lines for the south-western side. The lower panel shows the corresponding velocity dispersions for the PNe. The two curves are the standard and empirical fits to the axisymmetrically binned data in Figure 6.3.

velocities are clearly still different at this point while the H I rotation velocities have already equalised. It is therefore clear that some significant asymmetries do exist in the disk.

This difference between the mean velocities measured for the two sides will clearly contribute to the velocity dispersion when axisymmetry is assumed. This can be seen in the velocity dispersion profiles from the two sides shown in the lower panel of Figure 6.9, which lie marginally below the empirical fit of equation (6.1) at large distances. However, these data still appear to have a velocity dispersion higher than expected from the theoretical model and it appears that there is still some unpredicted addition to the velocity dispersion at large radii.

We find that the axisymmetric picture of the disk described in Sections 6.1 and 6.2 is a good first approximation. However, at the level of detail available in this new data set we can begin to explore subtle dynamical phenomena such as lopsidedness. It is therefore important to consider other deviations from a simple thin disk, the most obvious being the observed warp in the disk, which we now consider.

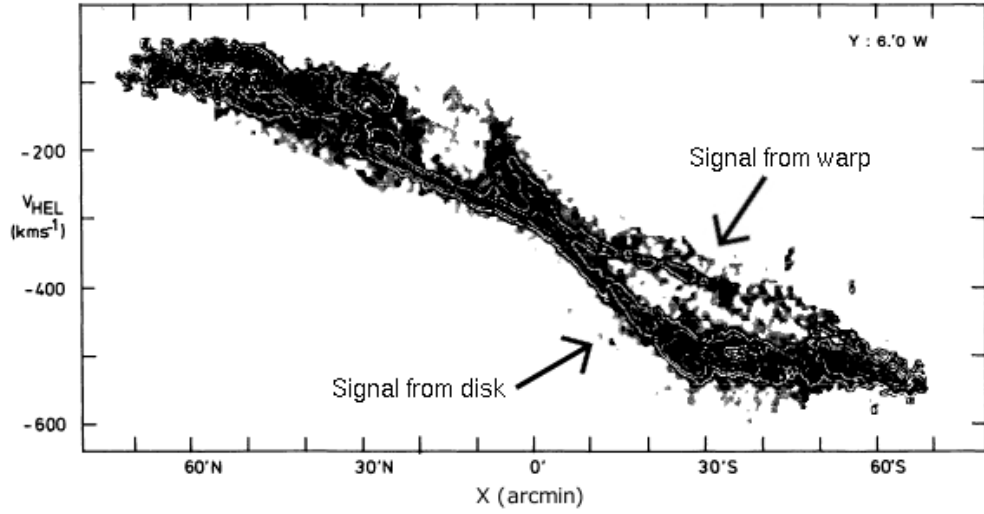


**Figure 6.10:** A section of Brinks & Shane (1984)’s Figure 8 showing the H I velocity map for a strip of data at  $Y = 0.1^\circ$  north-west of the major axis.

## 6.4 M31’s warped disk

As the simplest probe of the warp, we start by reviewing studies of the Andromeda Galaxy’s neutral hydrogen disk. These have long indicated that the disk is not a simple, thin one but is in fact distorted, bending away from the major axis at large radii (Roberts, 1966; Newton & Emerson, 1977; Cram, Roberts & Whitehurst, 1980; Brinks & Shane, 1984; Braun, 1991). The basic model produced (see also Sawa & Sofue, 1982; Brinks & Burton, 1984) has the central H I disk extending out to  $\sim 1.3^\circ$  at which point the warp starts to twist the disk towards the North in the North-East and towards the South in the South-West, whilst pushing the disk to larger inclination angles. Brinks & Burton (1984) also included a flaring scale height to the disk beyond the warp in their model. This was subsequently improved upon by Braun (1991) who was able to actually measure how the H I disk scale height varies with radius.

Images from Brinks & Shane (1984)’s H I survey are reproduced in Figures 6.10 and 6.11. These images show position-velocity maps made parallel to the major axis, the former being a detailed map for a slice at  $Y = 0.1^\circ$  ( $6.0'$ ) West, and the latter showing small versions of all the images from  $Y = 0.58^\circ$  East to  $Y = 0.58^\circ$  West. The warp exists at larger radii than the main disk; hence it is the warp layer that is visible throughout, remaining fairly constant as a shallow straight line, and the signal from the main disk that appears, and disappears again, varying in between. That the warp produces only one trace at small  $|Y|$  and crosses the minor axis at approximately  $0 \text{ km s}^{-1}$  throughout indicates that the twist angle (the angle between the major axis and the line of nodes of the warp) is small and does not vary with radius.

We have constructed a basic tilted-ring model of the warp using the model template of Christodoulou, Tohline & Steiman-Cameron (1993), taking the parameters of previous basic warp models and adjusting them until the result appeared consistent with the H I data in Figure 6.11. Shown in Figure 6.12, the warp line of nodes is twisted  $20^\circ$  in the disk plane from the major axis; and the largest ring is warped  $20^\circ$  with respect to the disk, changing the inclination angle from  $77.5^\circ$  to  $97.5^\circ$ . The warp model parameters



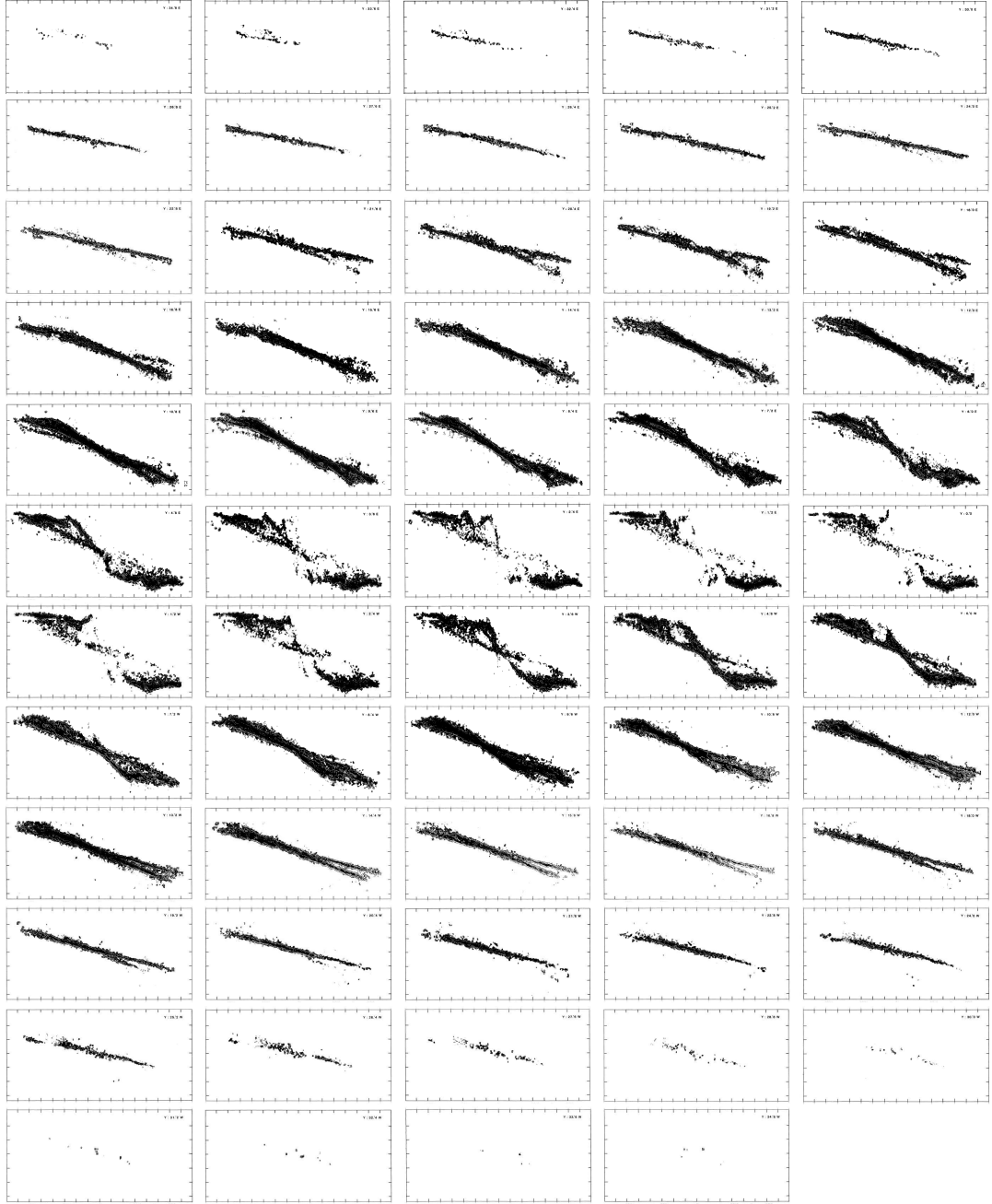


**Figure 6.11:** A compilation of Brinks & Shane (1984)'s  $X$  versus  $v_{\text{helio}}$  plots from slices parallel to the major axis, from  $Y = 0.58^\circ$  ( $34.8'$ ) East, in the top left, to  $Y = 0.58^\circ$  ( $34.8'$ ) West, in the bottom right.

**Table 6.3:** Parameters of the warp model fit by eye to the H I profiles of Brinks & Shane (1984), using the tilted rings template of Christodoulou, Tohline & Steiman-Cameron (1993).

Parameter	Value
Total number of rings	20
Ring number at which the warp begins	11
Maximum radius of the warp	2.5°
Inclination angle of the central disk	77°
Maximum rotational velocity	250 km s <sup>-1</sup>
Position angle of the warp	340°
Maximum twist angle from the projected major axis	20°
Maximum twist angle of the line of nodes	0°

are shown in full in Table 6.4. From this model, velocities for the disk and warp at any location can be predicted. This has been done for slices in  $Y$  equivalent to those of the H I data in Figure 6.11. We have also including a flaring scale height for the warp region. The resulting velocity profiles are shown in Figure 6.13 and prove to be a good representation of the H I data. However, deviations are seen at large values of  $Y$  where the warp is only seen to one side of the disk. Here the H I data and the model appear to be on opposite sides of the galaxy. Such inconsistencies, while peculiar, can hardly be unexpected. In their study of warp properties García-Ruiz, Sancisi & Kuijken (2002) found warp asymmetries to be common in their sample, while the Milky Way warp is well known to be asymmetric (Binney & Merrifield, 1998; Levine, Blitz & Heiles, 2006). However, it is beyond the scope of this thesis to explore asymmetries in M31's H I disk as the symmetric tilted ring model provides a sufficient fit to the data for comparison to stellar data.

### 6.4.1 The stellar warp

While M31's H I warp has been well examined, it was in fact in stellar number counts that this feature was first observed. Baade & Gaposchkin (1963) observed that at large radii population II stars were located, not in the disk plane, but off to opposite sides at either end of the disk. This phenomenon was not returned to until the study of Innanen et al. (1982), who showed that both the red and yellow light in M31 was anti-symmetrically warped. Their Figure 1 is reproduced in Figure 6.14, where the stellar warp is clearly visible towards the South, beginning at around 1.5°. However, the warp does not behave in the same fashion as this on the Northern side of the disk. Instead a faint trace of stars is visible coming away from the disk at a much more severe angle; this peculiar feature will be returned to in Section 6.5.

Despite this anomaly, the basic form of the the stellar warp appears to be similar to that of the H I warp, both starting at similar radii and displaying isophote twists in the same direction. This makes the most obvious course of action a straight comparison between the PN data and the H I warp model. To this end, we have overlaid the PN velocities for objects located at appropriate locations in  $Y$  over the warp model predictions in Figure 6.13. It is clear that the PNe on the whole follow the kinematics of the H I disk, albeit with a significant dispersion as would be expected from a stellar population.

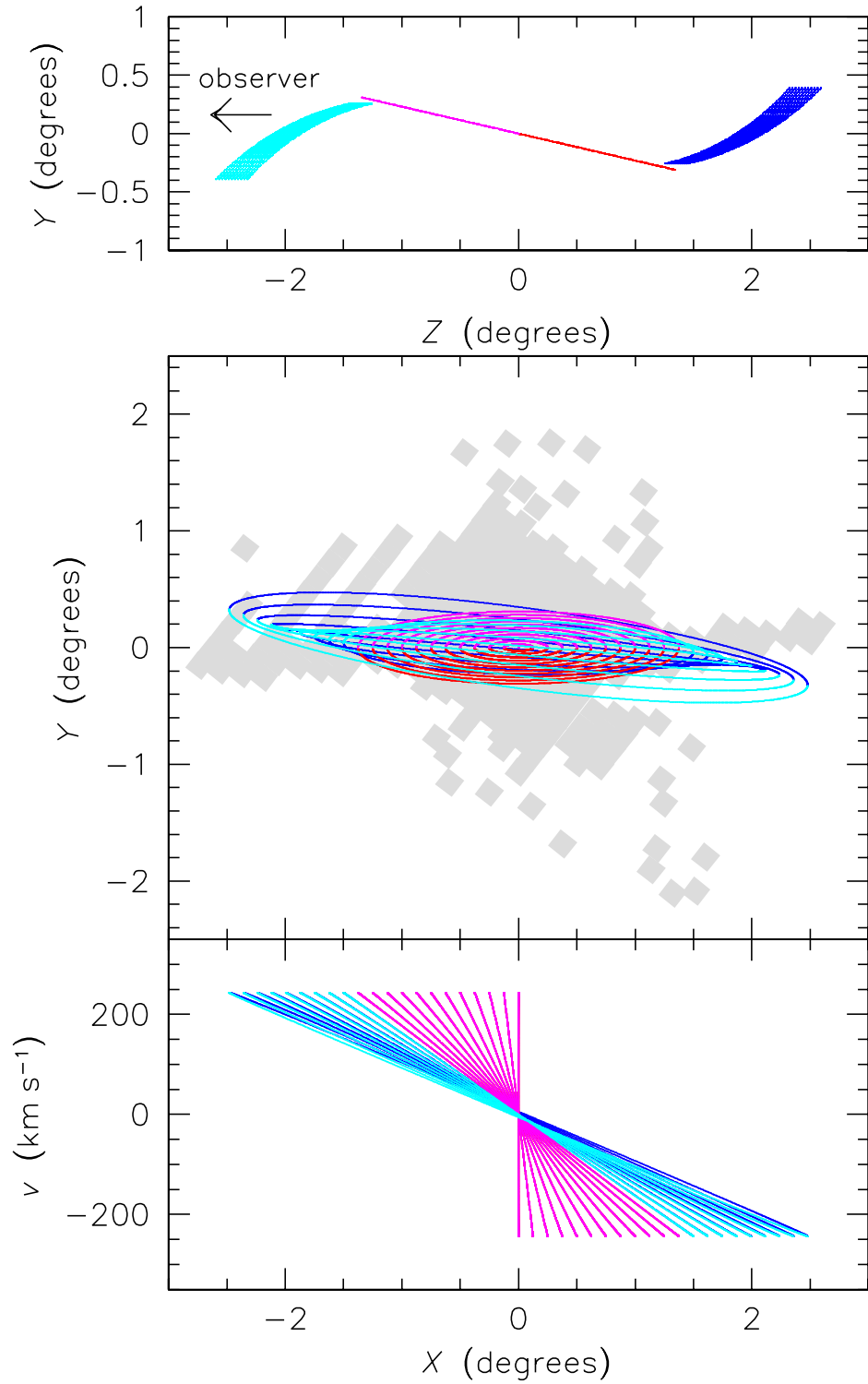


**Figure 6.12:** A tilted ring model for M31's warped disk. The model is colour coded as follows: The far and near sides of the warp are blue and cyan, respectively; the far and near sides of the main disk are red and magenta, respectively. The upper panel shows a side on view of the disk and warp. The middle panel shows the observers view of the disk and warp, with the PN.S survey area in the background. The lower panel shows velocities for each ring from material with a flat rotation curve travelling on  $250 \text{ km s}^{-1}$  circular orbits. The velocity traces from the far side of the disk and warp are largely obscured by those from the near side.

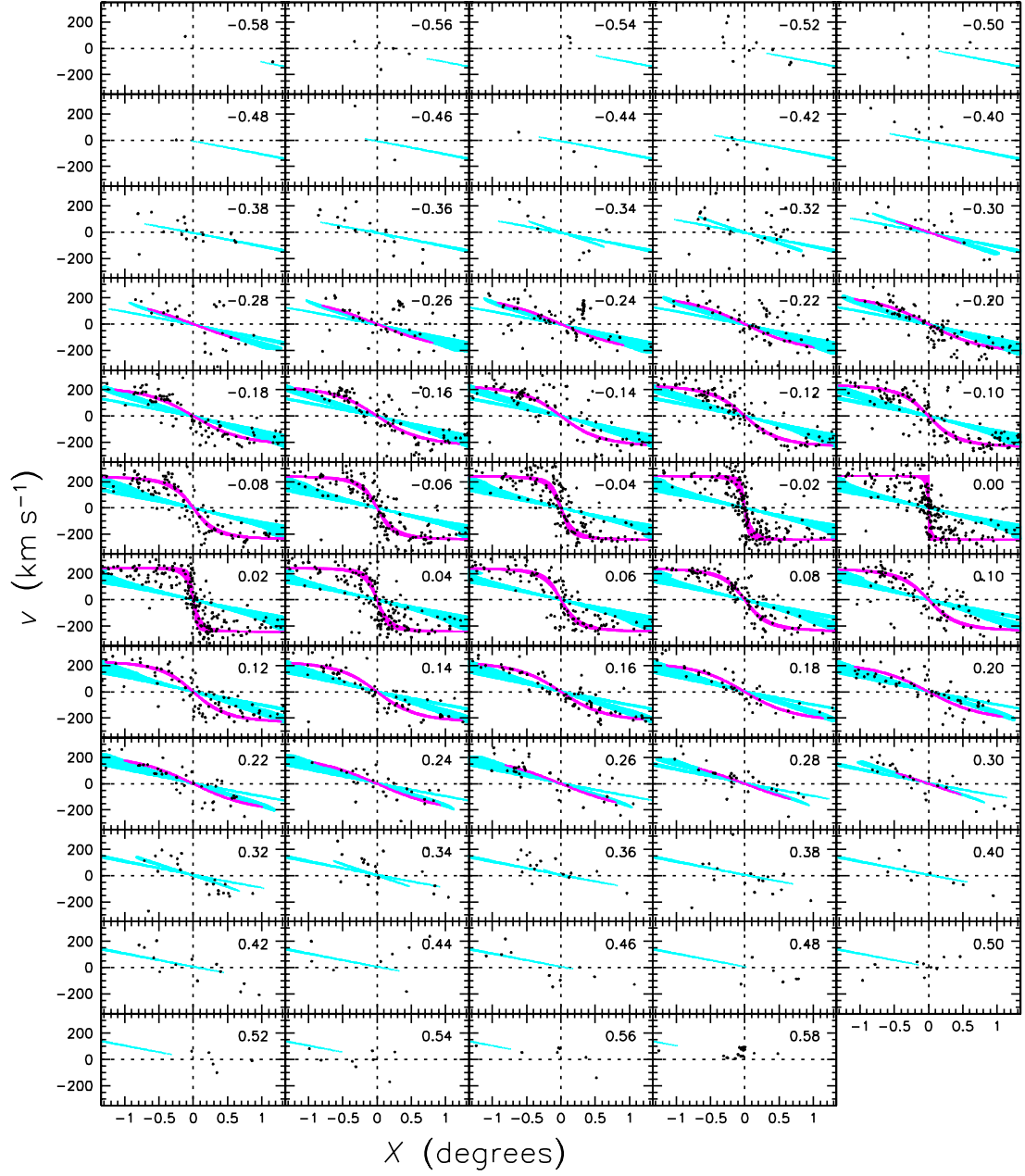


**Figure 6.13:**  $X$  versus  $v$  plots, equivalent to the H I plots of Brinks & Shane (1984) shown Figure 6.11, for the PN.S data (points) and the flaring-warping disk model of Figure 6.12. The magenta lines show the expected velocities for a thin disk of material on circular orbits with a flat rotation curve, the cyan lines are the velocities of material in the warped, increasing scale height region.

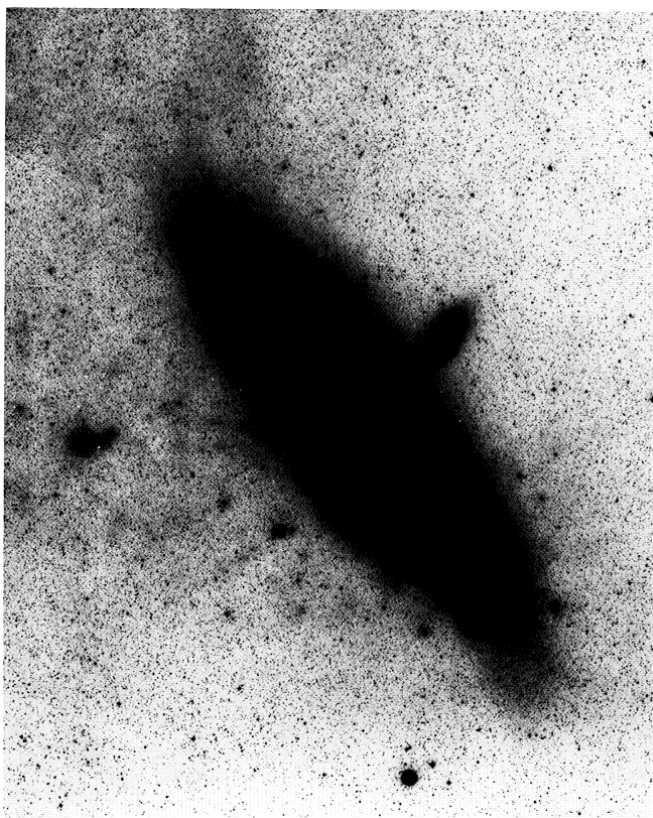


**Figure 6.14:** The stellar distribution in M31: Innanen et al. (1982)’s high contrast map of red starlight. (North is up and east to the left).

However, there is little indication of any bifurcation in the PN velocities equivalent to that from the H I warp.

In order to interpret this absence, we must consider how many PNe would be expected to exist at these large radii. Figure 6.15 shows the predicted number density of PNe in the top 4.0 mag of the PNLF as a function of distance along the major axis at locations parallel to the major axis for a standard thin exponential disk and  $R^{1/4}$  bulge – a warp is not included. From this, it is clear that the exponential decline in PN number density within the disk makes PNe at large radii relatively uncommon, and only a few PNe in our magnitude range would exist at warp radii. One must also consider that where warp layer PNe do exist, the majority will be clustered around the line of nodes where warp velocities are closest to normal disk velocities. Also the increased velocity dispersion and presence of a bulge component not visible in H I will mask their signature.

It is also worth noting at this point that as we move to larger distances from the major axis the influence of the bulge spreads to larger distances from the minor axis. By  $Y > 0.4^\circ$  the majority of PNe with  $X \lesssim 0.5^\circ$  are expected to originate from the bulge and not the disk. This is somewhat at odds with the velocity distribution of PNe that we see in Figure 6.13 with rotationally supported velocities dominating the distribution throughout, leading to the suggestion that the bulge itself must be dominated by rotation. This is consistent with the findings of Hurley-Keller et al. (2004), also based on PN velocities.

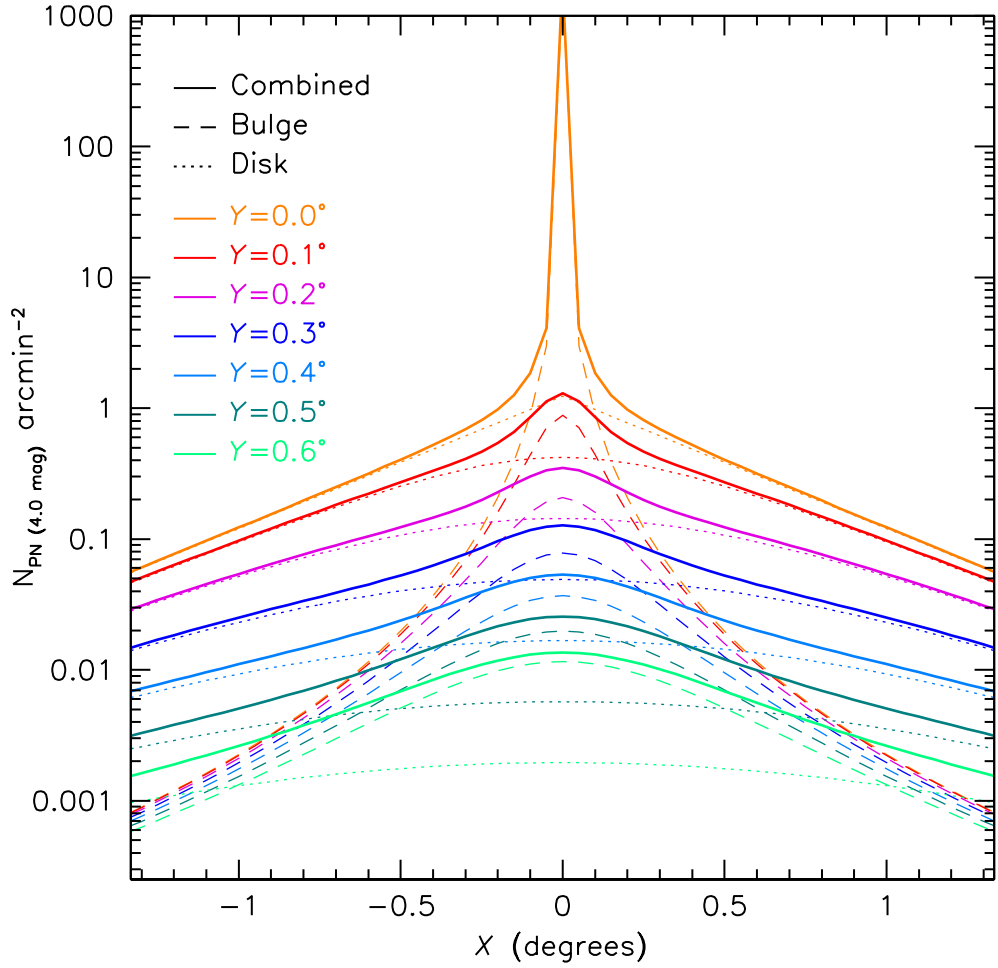


**Figure 6.15:** Expected number density of PNe in the top 4.0 mag of the PNLF for slices parallel to the major axis, as indicated. The dotted lines show the contribution from the disk and the dashed lines the contribution from the bulge at any point, with the solid line being the combined value.

## 6.5 Halo and velocity substructures

A number of substructures within the halo of M31 have been identified by Ibata et al. (2001) and Ferguson et al. (2002) in their large panoramic survey of giant stars. Ibata et al.'s RGB star distribution map has been reproduced in Figure 6.16 alongside a diagram identifying the major halo structures and showing their locations with respect to the PN.S survey fields. These features are all fairly large, with the smallest covering at least 0.2 square degrees and the largest, a stream of material  $\sim 0.5^\circ$  wide extending  $\sim 4^\circ$  in length.

These structures indicate that M31's halo is a complicated environment. Kinematic measurements are vital to a better understanding of this complex system. We have therefore covered the most significant of these regions, the Northern Spur and Southern Stream, to supplement the main disk survey.

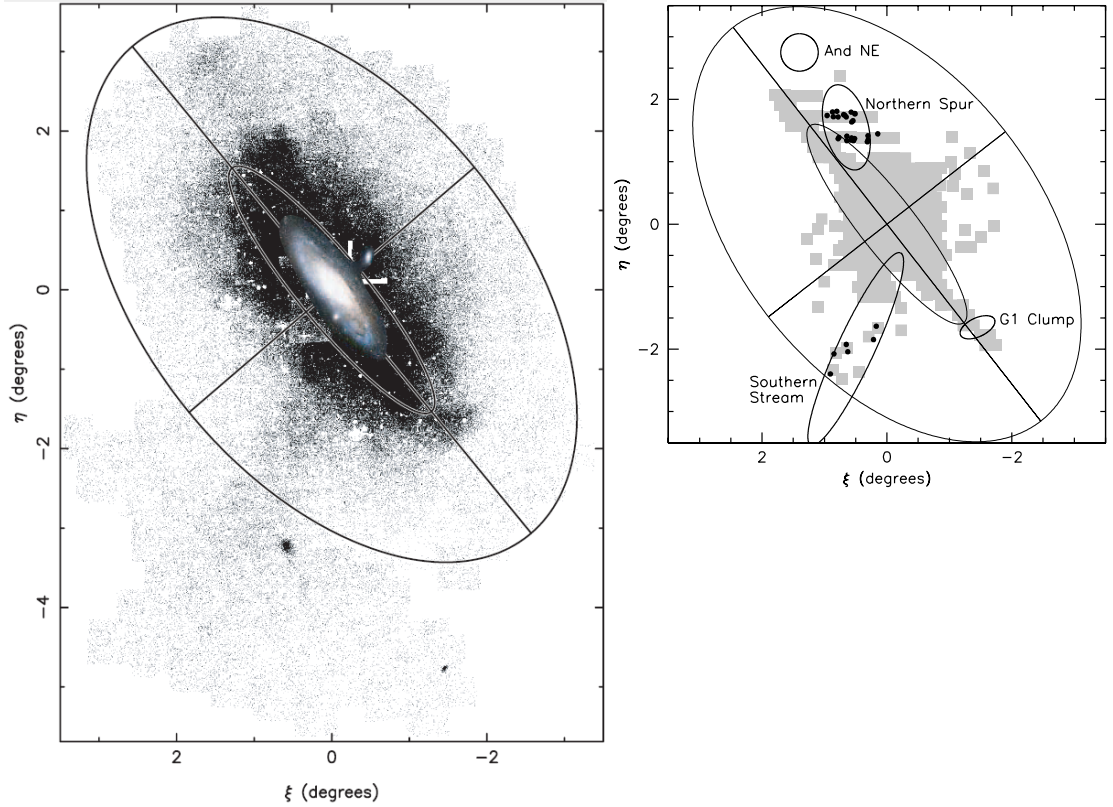


**Figure 6.16:** The left hand panel shows a map of the number density of RGB stars in in Andromeda's halo reproduced from Ibata et al. (2005), figure 1. The halo features are identified and compared to the PN.S field locations in the right hand panel; PNe in the region of the Northern Spur and Southern Stream are plotted as closed black circles.

### 6.5.1 The Northern Spur

As has been mentioned previously, the stellar distributions on the northern and southern sides of the disk are not the same. The warp is clear to the south but not to the north. Instead there is a low surface brightness feature that is just visible in Figure 6.14 and stands out in the AGB and RGB stellar distribution maps of Ferguson et al. (2002) and Ibata et al. (2005, reproduced in Figure 6.16). However, the true nature of this feature, commonly referred to as the Northern Spur, cannot be determined from stellar distributions alone. Hence, during the PN.S observing runs fields located around the Northern Spur region were specifically targeted (all the PN from this area are flagged 'NS' in the catalogue, Appendix A).

A significant overdensity of PNe was found in this region. Velocities for these PNe are plotted in Figure 6.17 both as a subset of the whole PN sample within M31 and in  $0.15^\circ$  slices in  $Y$  alongside the velocity space location of a thin, flat disk. It is clear from this that the PNe in the Northern Spur region have velocities that are consistent with a simple disk model. Therefore, the simplest conclusion that can be drawn is that the Northern Spur is part of the warp in the stellar disk. However, for this to be the case the stellar warp in M31 must be extremely severe. An alternative explanation has been put forward by Ibata et al. (2005) suggesting that the Northern Spur is simply one clump of material in an extended, clumpy disk of stars that exists at large radii.

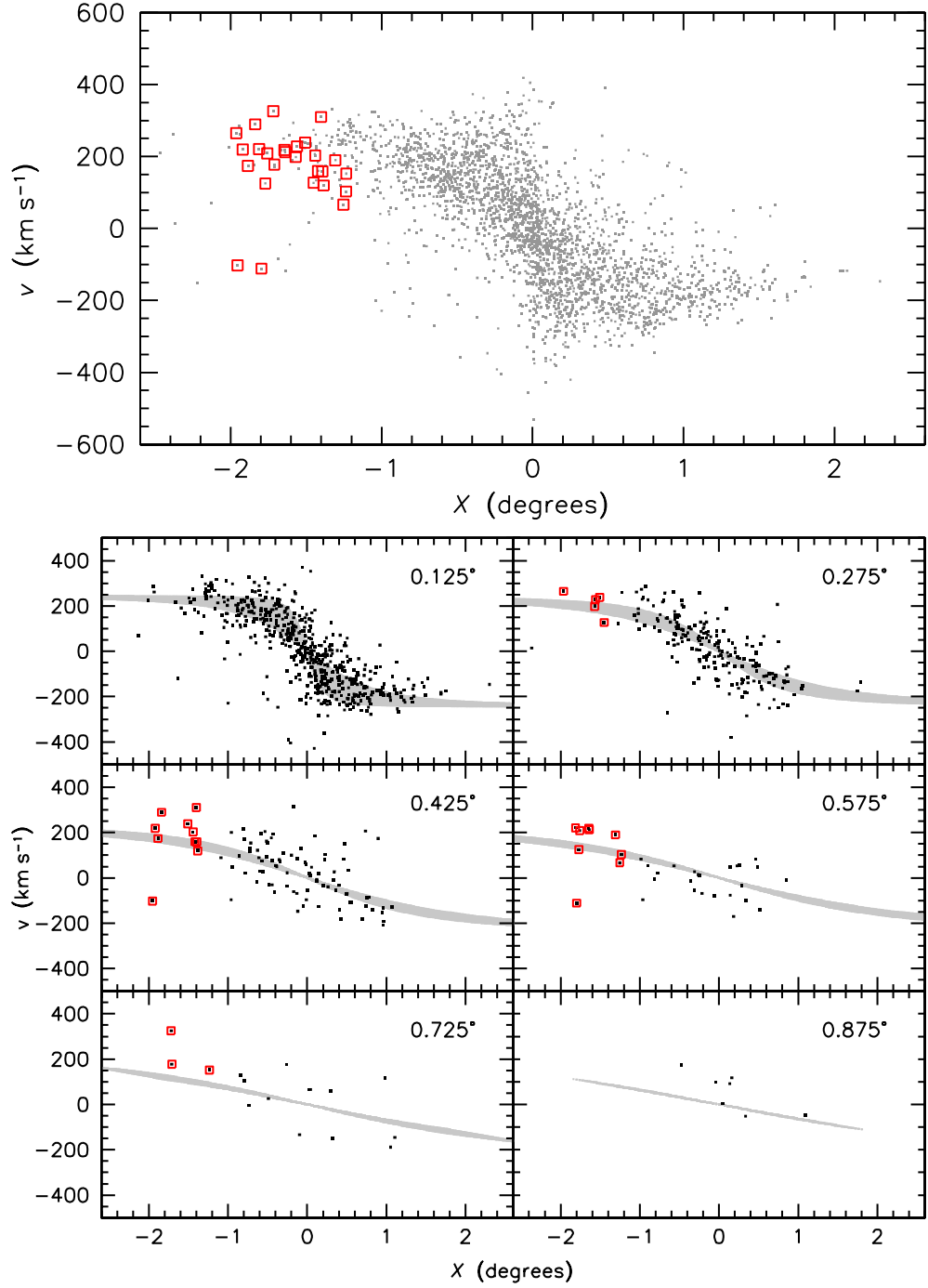


**Figure 6.17:** Velocities for M31's whole PN sample are shown in the upper panel. The lower panel shows velocities for PNe located in  $0.15^\circ$  slices centred on the  $Y$  location indicated, along with the phase space location of a thin, flat disk. PNe located in the region of the Northern Spur are highlighted by open squares.



This conclusion is based on velocity measurements of RGB stars from a number of fields around M31's disk which show rotation-like velocities at large radii all around M31. These measurements seem to be in agreement with our previous observation from Figure 6.13 that PNe at large values of  $Y$  are dominated by rotation. Distinguishing between the different interpretations of a large rotating bulge or an extended disk of stars will require further, more detailed analysis.

## 6.5.2 The Southern Stream

The Southern Stream, first recorded by Ibata et al. (2001), is an approximately linear overdensity in star counts extending out from the southern quadrant of M31 for a distance of at least  $4.4^\circ$  (60 kpc). This  $\sim 0.5^\circ$  wide structure is clearly visible in the RGB star distribution map of Ibata et al. (2005), reproduced in Figure 6.16. Since its discovery, this stream of stars has been the target of numerous observations aiming to map its structure both spatially and kinematically.

McConnachie et al. (2003) measured distances along the stream using the tip of the red giant branch as a standard candle. They found the stream to be located at approximately the same distance as M31 close to the galaxy, getting steadily further away with distance along the stream. The points measured are shown in Figure 6.18.

A number of groups have measured velocities for RGB stars in the stream region. Ibata et al. (2004) find the stream to be a dynamically cold object with a velocity dispersion of  $\sim 11 \text{ km s}^{-1}$ . The mean velocities of these stars is found to vary with a gradient along the length of the stream [ $245 \text{ km s}^{-1}$  in  $0.9^\circ$  (125 kpc)]. Guhathakurta et al. (2006b) find a velocity dispersion of  $\sim 15 \text{ km s}^{-1}$  and a mean heliocentric velocity of  $-458 \text{ km s}^{-1}$  for RGB stars in a field  $\sim 2^\circ$  (30 kpc) along the stream. Most recently Kalirai et al. (2006) have detected two velocity components within one field on the stream, both of which are cold, with a dispersion of  $\sim 16 \text{ km s}^{-1}$ . The velocity of the primary peak ( $-513 \text{ km s}^{-1}$ ) is in good agreement with the previous measurements and separated from the secondary component by  $\sim 100 \text{ km s}^{-1}$ . All these results are plotted in Figure 6.18.

We have also measured the velocities of a few PNe in this region (see Figure 6.16). Two of these have velocities that are similar to the RGB star measurements (or the predicted stream velocity) at that location, and are likely to belong to the stream. Two others have velocities offset by  $\sim 100 \text{ km s}^{-1}$  from the expected stream velocity and may be analogous to the secondary component found by Kalirai et al. (2006). The others have velocities that are closer to the systemic velocity of M31 and may be members of a normal M31 population. That we see only a small number of PNe that could be stream members is quite reasonable given the low surface brightness of this feature [ $\Sigma_V \approx 30 \pm 0.5 \text{ mag arcsec}^{-2}$ , Ibata et al. (2001)].

Given all these observations, a picture can be built up of the Southern Stream as the tidal tail of an object falling into M31 from behind on a trajectory that will take it close to the centre of M31. What is not clear, is what happens beyond this. Star counts closer into the galaxy are dominated by the disk population, and the stream's signature is drowned out at about  $1^\circ$  from the centre. Star counts in the rest of the halo show large

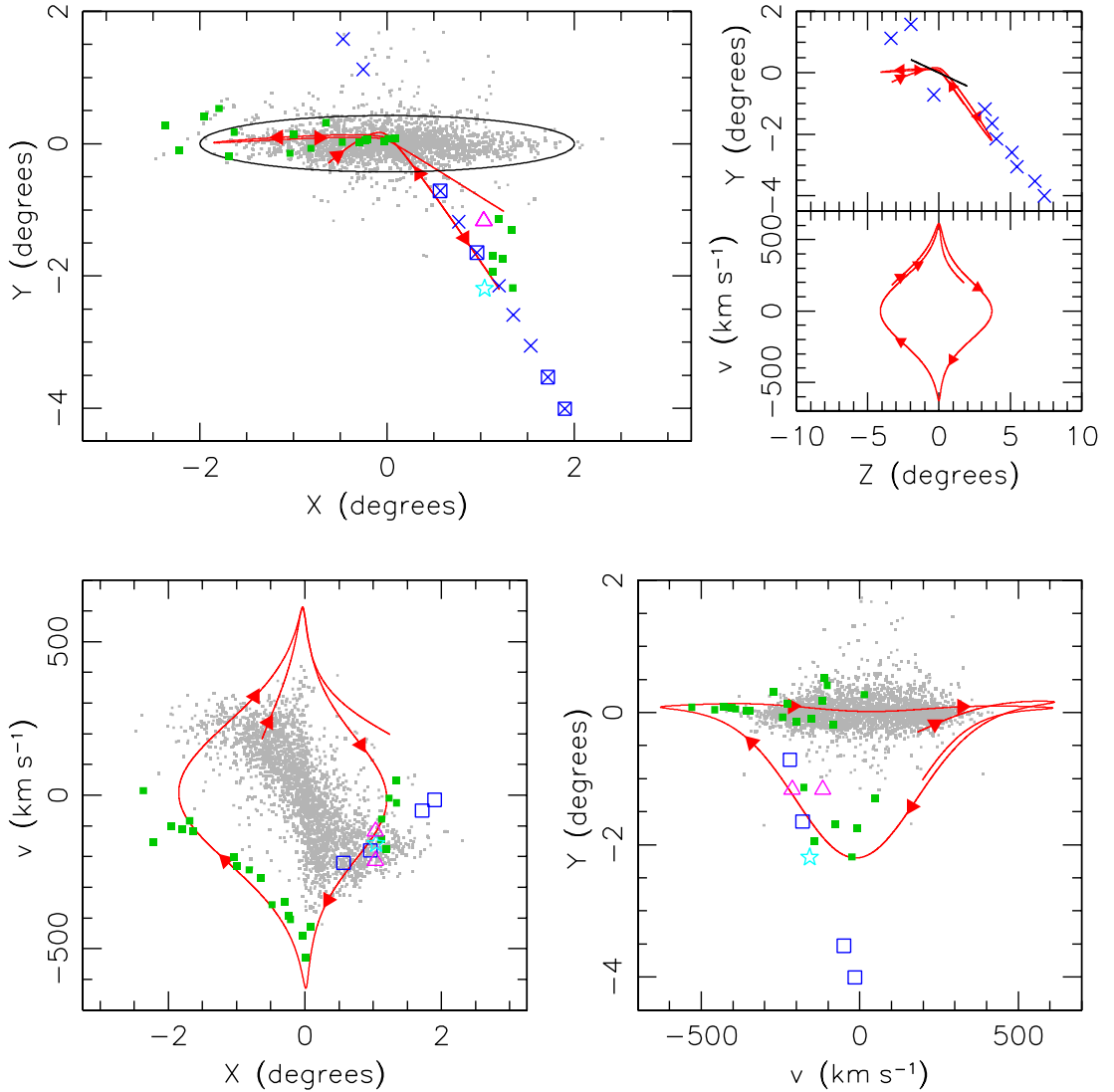


**Figure 6.18:** The Southern Stream. The PN.S data are represented by the gray points, with those objects that appear to constitute a coherent velocity substructure and those found in the region of the Southern Stream highlighted with filled green squares. In the upper left panel the projected  $2^\circ$  disk radius is drawn as an ellipse, while in the upper right panel the disk location is indicated by a black line. A number of additional points are marked on these plots: the fields with distance measurements by McConnachie et al. (2003) are shown as blue crosses; the fields with velocity measurements by Ibata et al. (2004) are marked by open blue squares; the cyan star is the field where Guhathakurta et al. (2006b) have made a velocity measurement; and the magenta triangles are the two velocities measured in a single field by Kalirai et al. (2006). The red line shows a simple orbit linking these features, the direction of the orbit is indicated by the arrows.

amounts of structure, but it is not clear if any of these are related to the stream as there is no direct link at the galaxy centre and a number of these features are disfavoured as continuations of the stream due to their colour (Ferguson et al., 2002).

At this point the PN.S catalogue presents an alternative. As the stream reaches Andromeda it has a velocity that is markedly different to that of the disk. Therefore any PNe that are associated with the stream would stand out in velocity space. In order to identify PNe with velocities unlike that of any visible structures at an object's location we have used a 'friendless' algorithm. This calculates the mean velocity,  $\bar{v}$ , and dis-

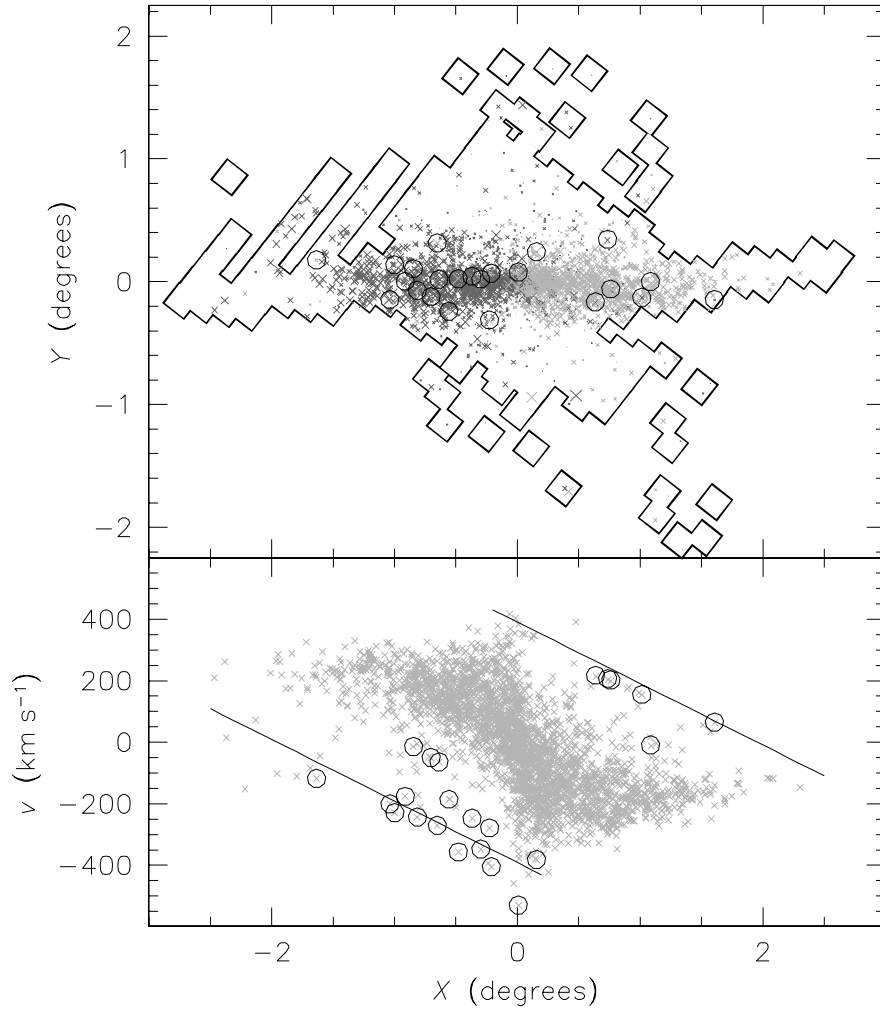


**Figure 6.19:** PNe selected as lying more than  $4\sigma$  from the mean velocity of their 30 nearest neighbours by our ‘friendless’ algorithm, highlighted by circles. The lines show the final cut to select PNe that appear to belong to the velocity substructure.

person,  $\sigma_v$ , of a PN’s  $N$  nearest neighbours. PNe with velocities more than  $n\sigma_v$  from  $\bar{v}$  are flagged as ‘friendless’. This routine seems fairly robust as the specific values of  $N$  and  $n$  chosen do not dramatically affect the overall results. Simulations have shown that only a small number of ‘false friendless’ PNe would be found in a system that contained only a disk population (Napolitano, private communication). The resulting ‘friendless’ PNe for  $N = 30$  and  $n = 4$  are shown in Figure 6.19 and it is clear that the PNe picked out by this non-parametric approach are pretty much the same as would be by eye. It is also apparent that there is a significant asymmetry between the two sides of the disk: of the 23 PNe selected, 5 lie in the  $X > 0, v > 0$  quadrant, while 15 PNe lie in the opposite quadrant ( $X < 0, v < 0$ ). A binomial test shows this lopsidedness to be inconsistent with a symmetric distribution at 95% confidence. This asymmetry effectively rules out the simplest sources of peculiar velocity objects, such as the extreme tail of a hot disk population or a relaxed halo population, for the majority of our ‘friendless’ PNe.

This selection mechanism is considerably less effective in areas where there is naturally a large scatter in PN velocities and in areas where peculiar velocity PNe are a

significant part of the general population. Now that we have established that the population is real, we can make a cut based on velocity to identify sources belonging to this velocity substructure. The cut made (indicated by the straight line in Figure 6.19) was chosen so that very few PNe lay above the equivalent line in the opposite quadrant. The selected PNe are those highlighted in Figure 6.18 and are indicated in the catalogue (Appendix A) as members of this source by the designation ‘Stream?’ . These PNe are scattered throughout the disk on the northern side with velocities decreasing steadily from  $\sim -450 \text{ km s}^{-1}$  at the centre to  $0 \text{ km s}^{-1}$  at about  $2^\circ$ . Assuming these PNe represent the tidal debris of a galaxy being stripped of material as it passes through M31, the stream itself would be completely obscured by the disk of M31.

We must now ask ourselves if it is likely, or even possible, that these PNe could belong to a continuation of the Southern Stream. Firstly, and most obviously, do the PNe lie on an orbit that connects with the visible stream? A simple, single orbit model ought to be sufficient to find out if such a situation is likely to arise.

A first constraint on possible orbits comes from the sharp angle through which the stream must turn if it is to bend into the disk. This would require a fairly radial orbit, passing close to the centre of the potential. It also requires that the potential does not have a large ‘softening’ core that would prevent such a tight turn. As we have seen previously, M31’s rotation curve is close to flat even at small radii, providing no evidence of a significant core (see also Section 6.2). We are therefore able to use a flattened singular isothermal potential

$$\Phi(R, z) = \frac{1}{2}v_c^2 \ln \left( R^2 + \frac{z^2}{q^2} \right) \quad (6.3)$$

where  $R$  and  $z$  are polar coordinates aligned with the disk plane of M31. The amplitude,  $v_c$ , is set to  $250 \text{ km s}^{-1}$ , the approximate value of the flattened rotation curve from most observational measures and the approximate upper envelope of the PN velocity distribution. For the flattening we adopt a value of  $q = 0.9$ , in line with what is found in other galaxies (e.g. Majewski et al., 2003).

A simple orbit is generated by choosing a start point in position and velocity space and integrating the orbit both forwards and backwards in time. As it is best to choose a well defined location in both position and velocity, the most obvious location to use is the position on the Southern Stream where the radial velocity is close to zero, where (as the feature is seen to be linear) one can assume that there is a turning point in the orbit. Hence locations in position and velocity space are defined as  $(X, Y, Z) \sim (1.8^\circ, -3.5^\circ, 6.0^\circ)$  and  $(v_x, v_y, v_z) \sim (0, 0, 0) \text{ km s}^{-1}$ . Generating an orbit from this point does turn the stream into the disk; in fact the turn is somewhat sharper than is required for the PN continuation. Apart from this, the orbit produces a fairly poor fit to the data, with velocities in both the RGB and PNe data badly matched. Fortunately there is some leeway in the exact positions of this start point as the stream is a broad feature and the  $Z$  direction measurements have a significant uncertainty error associated with them.

A better overall fit to the PNe is produced from an orbit start point of  $(X, Y, Z) = (1.2^\circ, -2.2^\circ, 3.7^\circ)$  and  $(v_x, v_y, v_z) = (0, 0, -12.5) \text{ km s}^{-1}$ ; the orbit generated is shown in Figure 6.18. While this demonstrates that an orbit connecting the Southern Stream

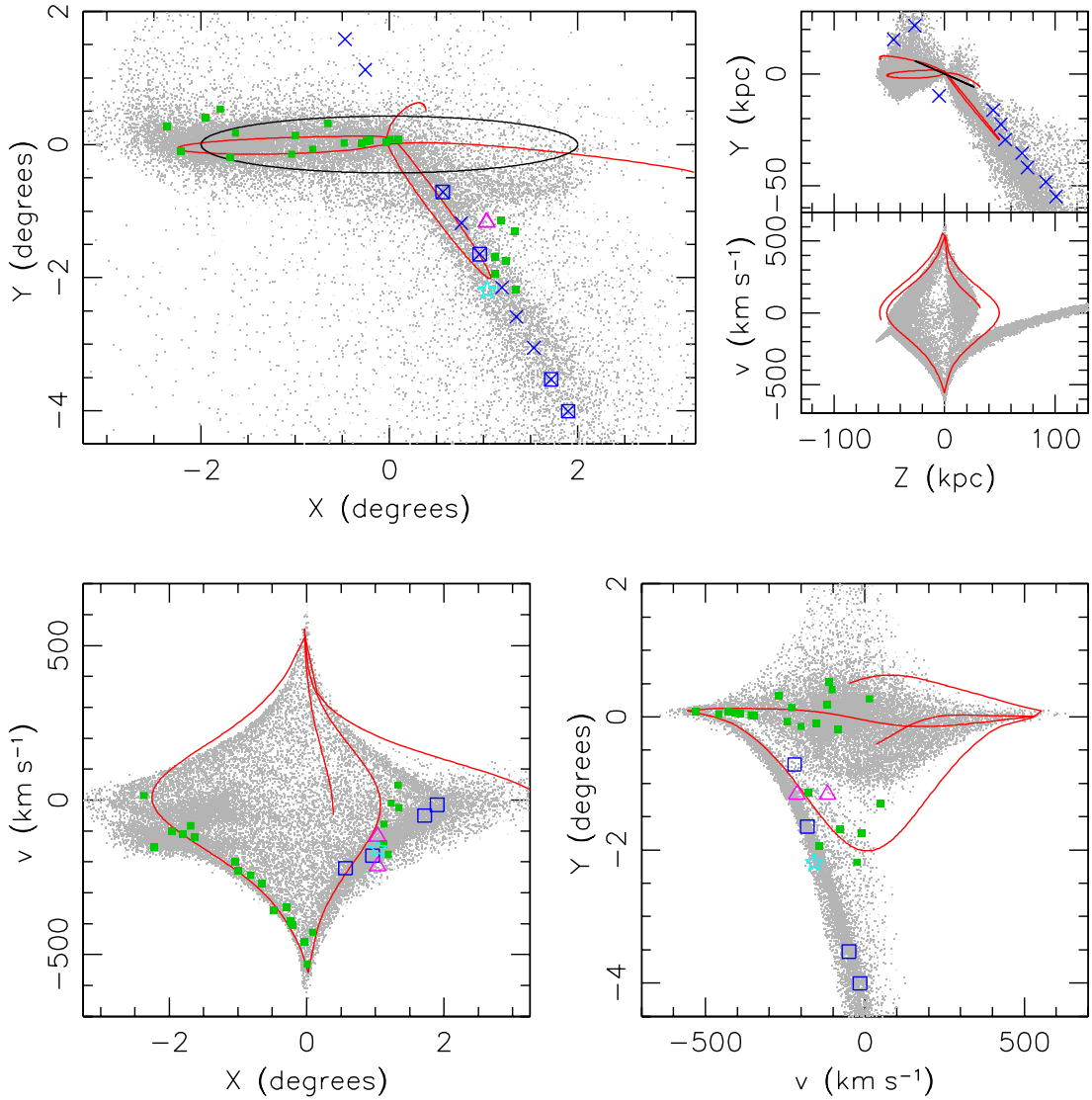


**Figure 6.20:** Fardal et al. (2006)’s N-body simulation of the tidal stripping of a dwarf galaxy passing through M31 on an orbit taking it through the Southern Stream and our PN velocity substructure. The N-body simulation data and progenitor orbit, kindly provided by Mark Fardal (private communication), are shown as gray points and the red line, respectively. The other points are the selected PNe, and RGB star measurements as in Figure 6.18.

and this PN population is possible, again it appears to be a fairly poor fit to some of the data, with the Southern Stream itself coming up somewhat too short. However, it would appear that this is not as significant a problem as it might at first seem. Fardal et al. (2006) have produced a number of N-body simulations for the Southern Stream, fitting the orbits to coincide with a number of features including our velocity substructure. As can be seen in Figure 6.20, as the progenitor reaches the turning point at the extremity of its orbit along the Southern Stream, material is thrown off to much greater distances than its own extent. Fardal et al.’s progenitor orbit is similar to that shown in Figure 6.18, and it is the material that has been stripped off the progenitor galaxy that follows the path of the Southern Stream. Fardal et al. deem this orbit to be the most plausible of all the orbits they generated for the route of the progenitor galaxy.

We are therefore able to confirm that not only is it possible to generate an orbit that

takes in both the Southern Stream and our velocity substructure, but that it is likely that the stream continuation will lie somewhere in this region, with velocities that are similar to those of the PN substructure.

The second question we must ask is: allowing that there are at most one or two PNe in the whole of the Southern Stream, why are there so many buried within the disk on the opposite side of the orbit? In fact we see seventeen PNe and three extended objects apparently associated with this structure. If we are to assume the surface brightness is similar on both sides, this would seem so many objects as to entirely rule this structure out as a continuation of the stream. However, we have no reason to assume this. The stream continuation is clearly hidden amongst the disk of M31 on the northern side of its orbit and no measurement of its surface brightness can be made. The orbit we have generated has the stream turning towards the line of sight, which would naturally increase its surface brightness, though probably not by the amount required.

A more plausible alternative is that the PNe we see are located within the highly disrupted progenitor galaxy. In Fardal et al.'s N-body simulation (Figure 6.20) we see that this is the case for their particular model and in general Fardal et al. find that it is likely that the progenitor lies beyond the next pericentre. Fardal et al. (2006) have calculated the mass of the progenitor galaxy to be of the order  $10^9 M_\odot$ . Given that M32 has a mass of  $\sim 2 \times 10^9 M_\odot$  (Mateo, 1998) and we see 46 PNe associated with it (see Chapter 4), it seems quite reasonable for the stream progenitor to have the observed number of PNe associated with it.

### 6.5.3 Possible other velocity substructures

The stream continuation PNe do not account for all the 'friendless' PNe, and rerunning the algorithm ( $N = 30$ ,  $n = 4$ ; as before) with this substructure removed finds 15 PNe with peculiar velocities, shown in Figure 6.21. Unlike the last time these are distributed fairly evenly between the two sides of the disk making the simplest explanation that they result from a normal galactic population such as the tail of the disk distribution or the bulge.

There is, however, some indication that a few of these PNe are part of a small cluster of objects that have similar velocities and originate from a relatively localised area within the disk (highlighted in red in Figure 6.21). It is possible that these PNe are located on the same stream as those discussed in the previous section, or come from another stream. Simple symmetry arguments would imply that if these PNe are located in a stream then the PNe occupying the equivalent velocity space location on the opposite side of the disk would also have to belong to stream-like objects. While this is not impossible, it seems highly unlikely, and the simplest explanation, that all these objects are members of a bulk population within M31, seems favourable.

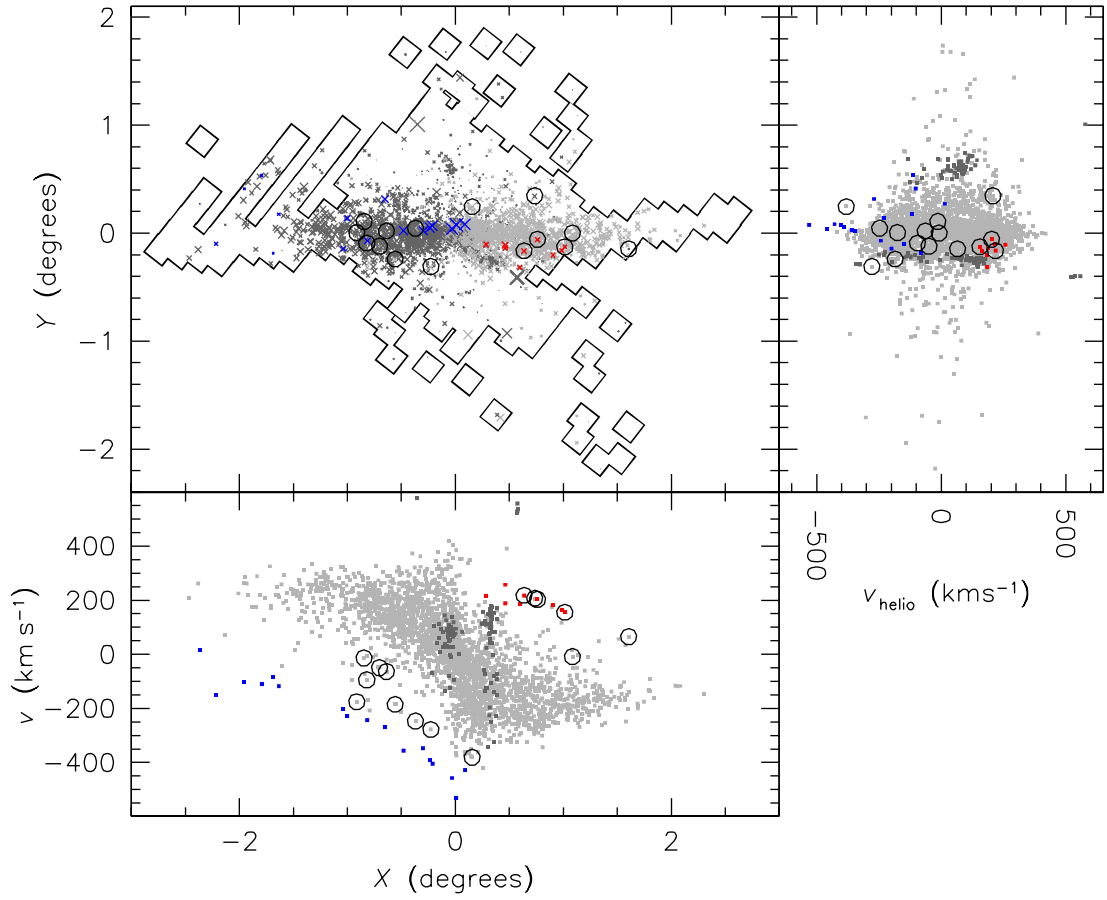


**Figure 6.21:** The open circles indicate the locations of PNe selected as lying more than  $4\sigma$  from the mean velocity of their 30 nearest neighbours by our ‘friendless’ algorithm. The stream continuation PNe are highlighted in blue and were eliminated from the sample before the algorithm was run. The PNe highlighted in red have similar velocities and originate from a relatively localised area, leading to the possibility they may be related to one another. The PNe plotted in dark gray in the velocity plots originate from other galaxies as in Figure 6.1.

# Chapter 7

## Dynamics of the Andromeda Galaxy

Having measured the basic kinematic properties of the Andromeda Galaxy in Chapter 6, we may now consider from what dynamical structures they arise.

### 7.1 A flaring disk model for M31's stellar disk

As we saw in Section 6.1, under the assumption of an axisymmetric disk, the velocity dispersion profile of M31 does not follow the expected profile of an exponentially declining thin disk, though we must keep in mind that some component of this dispersion may originate from an asymmetry in the mean velocity of the disk. This being said the simplest explanation for an elevated velocity dispersion at large radii is that M31's disk is not of constant thickness. Brinks & Burton (1984) found that the best fit to their warped disk model came when the scale height of the H I disk was allowed to increase linearly from the start of the warp. Their model for the flaring, shown schematically in Figure 7.1 without the warp, assumes that the H I scale-height is constant at  $z_{\text{in}} = 0.01^\circ$  (136 pc) out to  $R_{\text{in}}$  ( $1.33^\circ$ , 18 kpc), then increases linearly out to  $R_{\text{out}}$  ( $2.54^\circ$ , 34.5 kpc) where  $z_{\text{out}} = 0.14^\circ$  (1.9 kpc). Beyond this radius the H I became undetectable and Brinks & Burton's model stopped, but Ibata et al. (2005) have assumed the disk scale height becomes constant from this point onwards whilst analysing their RGB star observations.

If the scale-height increases in this way, then equation (6.2) implies that, for a given

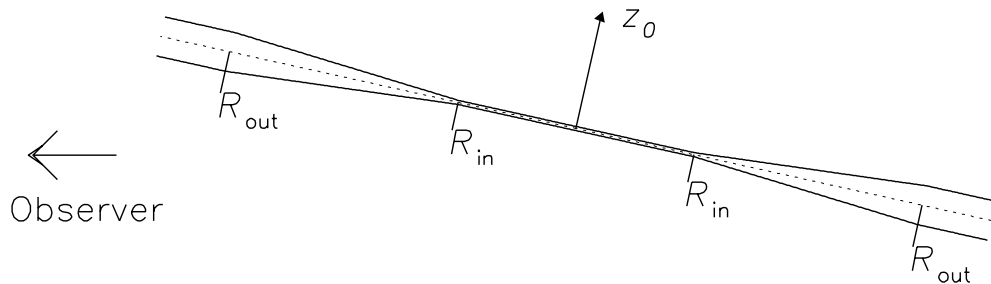


**Figure 7.1:** Schematic diagram of the flaring disk of M31. The disk scale height is constant out to a radius  $R_{\text{in}}$  it then increases linearly with radius to  $R_{\text{out}}$ , at which point it becomes constant again.



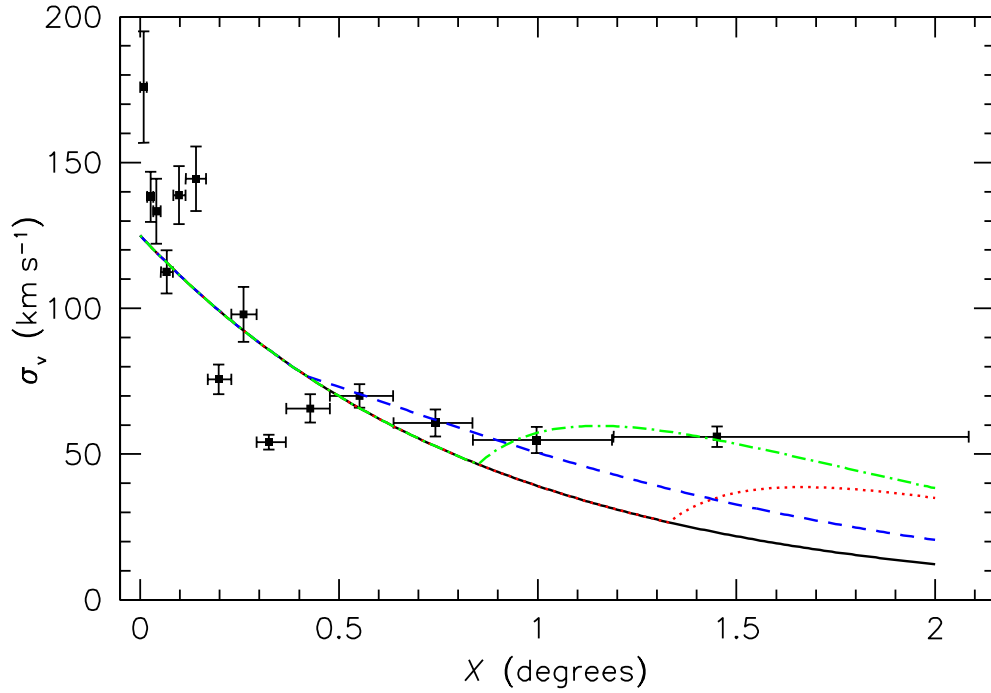


**Figure 7.2:** Velocity dispersion profile (points are the same as in Figure 6.3). The curves are for a selection of models: the solid black line shows a simple exponential decrease; the dotted red line is for a flaring disk model with parameters from Brinks & Burton (1984); the dashed blue line shows a flaring disk model with parameters from Braun (1991); and the dot-dashed green line is for a flaring disk model with parameters matched to the PN velocity dispersion profile using a  $\chi^2$  minimisation.

mass density, the vertical velocity dispersion also increases. If we insert the above prescription for the scale-height into this equation, but continue to assume that the disk density drops exponentially with radius, then we find the velocity dispersion profile shown as a red dotted line in Figure 7.2.

Braun (1991) was actually able to measure the variation of the H I disk thickness with radius and thus derive the variation in scale height. He found a somewhat more gentle flare in the scale height than was used by Brinks & Burton (1984), but starting at a much smaller radius. Updating to a newer distance to M31 his disk scale height is found to be about  $0.017^\circ$  (230 pc) at  $R_{\text{in}} = 0.42^\circ$  (5.7 kpc), flaring approximately linearly to about  $0.05^\circ$  (680 pc) at  $R_{\text{out}} = 2.1^\circ$  (28 kpc). Altering the velocity dispersion as before we find the profile shown as the blue dashed line in Figure 7.2.

These profiles are clearly a step in the right direction, though the fits to the observed profile are still not particularly good. Of course, there is no reason why the stellar disk, having been built up over an extended period and undergone secular heating since it formed, should flare in the same way as the H I distribution. Indeed, it is often assumed that the stellar scale-heights of disk galaxies remain constant with radius. However, recent analysis has shown that existing photometric data do not rule out significant variation in scale-height with radius (Narayan & Jog, 2002). Further, if a disk comprises two components of different constant scale-heights, with the “thick disk” having a longer scale-length than the “thin disk,” then one would expect a variation with radius in their combined effective scale-height similar to this simple flaring model. Whether such components should be combined or should be considered as

discrete entities is largely a matter of semantics unless one can establish some other feature that distinguishes their constituent stars. If we use the toy varying-scale-height model of Brinks & Burton (1984), but move the point at which the flaring starts to  $R_{\text{in}} = 0.85^\circ$  (11.6 kpc) while leaving all the other parameters unaltered, we obtain the green dot-dashed line in Figure 7.2, in respectable agreement with the data. Clearly, by altering the way in which the layer flares, or by varying the mass-to-light ratio of the disk with radius, we could improve the fit still further, but such detailed modelling goes beyond what is justified by the simplifying approximations of a one-dimensional sheet of stars in hydrostatic equilibrium.

## 7.2 The asymmetric drift

The presence of significant random velocities at all radii means that the support against gravitational collapse does not come entirely from circular motions even at large distances from the centre of M31. We would therefore expect the observed mean rotational streaming of the stars,  $\overline{v}_\phi$ , to lag behind the circular speed,  $v_c$ . As noted in Section 6.1, such an asymmetric drift is seen, but having measured the velocity dispersion profile we can now quantify whether the predicted velocity difference is dynamically consistent with the observations.

The relationship between  $\overline{v}_\phi$  and  $v_c$  at any radius  $R$ , can be calculated from the appropriate Jeans equation (Binney & Tremaine, 1987, equation 4-33), which we can rewrite as

$$\overline{v}_\phi = \sqrt{v_c^2 - \sigma_\phi^2 + \overline{v_R^2} + \frac{R}{\nu} \frac{\partial(\nu \overline{v_R^2})}{\partial R} + R \frac{\partial(\overline{v_R v_z})}{\partial z}}, \quad (7.1)$$

where we have adopted a cylindrical coordinate system,  $\{R, \phi, z\}$ , and measure stellar velocities  $\{v_R, v_\phi, v_z\}$  and number density  $\nu(R, z)$  in this reference frame. Formulating this equation, it has been assumed that the system is axisymmetric, symmetric about its equator and in a steady state. As we have seen in Chapter 6, the assumption of axisymmetry starts to break down at very large disk radii, but provides a reasonable first approximation. The assumption of a steady state is also affected by the observed asymmetry, as the velocity of a star would be expected to vary as it orbits the galaxy. In the above equation, this assumption eliminates a time derivative of the radial component of velocity. As this value is expected to be small and the timescale large, eliminating this should have little effect on the final result. Also, as the model assumes axisymmetry, it is appropriate to use the axisymmetrically binned data in Table 6.1 when exploiting it.

To solve this equation, we have to make some further assumptions. First, the last term in equation (7.1) arising from any tilt in the velocity ellipsoid is unobservable. However, for all plausible dynamical models it remains small and has little impact on an analysis of this kind (Gerßen, Kuijken & Merrifield, 1997). Second, we must assume something about the shape of the velocity ellipsoid of random motions. The simplest assumption is that it remains constant with position, so that we can write

$$\overline{v_R^2} = \alpha \sigma_\phi^2, \quad (7.2)$$

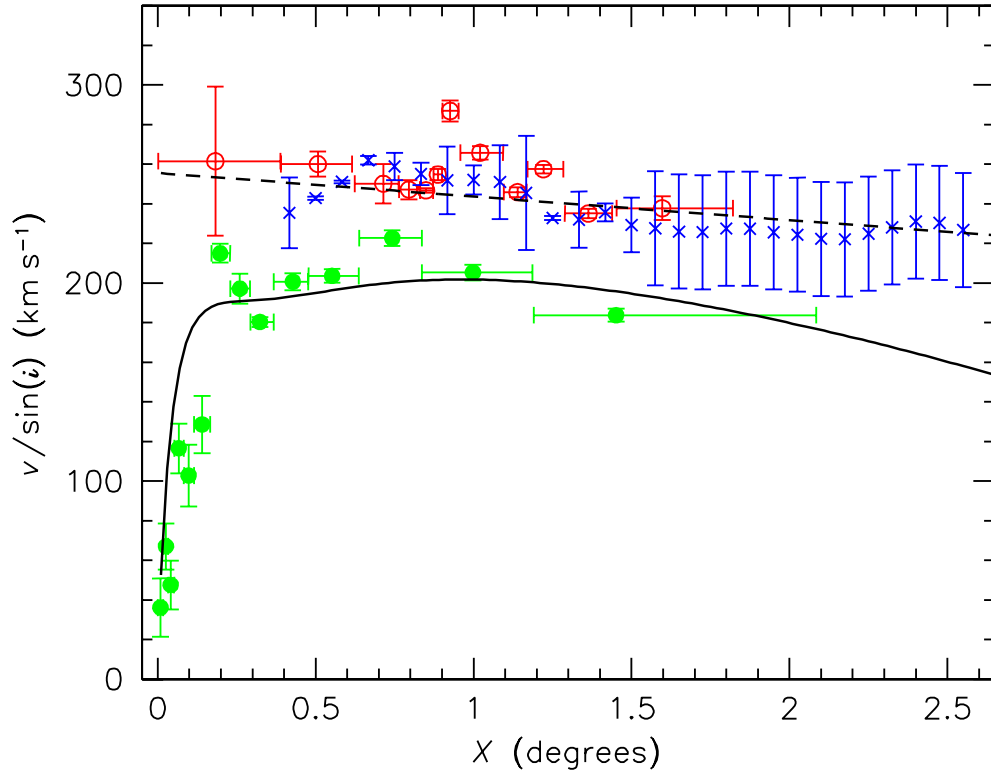


**Figure 7.3:** Predicted and observed rotational motions of PNe in M31. The filled green circles show the observed streaming of stars, as in Figure 6.2. The red open circles show the rotation curve measured from the H II regions and the blue crosses the H I rotation curve from Carignan et al. (2006). A linear fit to these two sets of points is shown by the dashed line. The solid line shows the predicted mean stellar rotational velocities obtained by correcting the linear rotation curve for geometry and asymmetric drift.

where  $\alpha$  is a constant. In the solar neighbourhood of the Milky Way,  $\alpha$  is found to be  $\sim 2$  (Binney & Merrifield, 1998), and in the absence of any other constraint we set it to this value at all radii in M31 (varying  $\alpha$  by  $\pm 0.5$  makes little difference to the final result). If we make this approximation, use the H II and H I data to obtain a simple linear approximation to the rotation curve  $v_c(R)$ , take the number counts of PNe in Section 5.2 to give the exponential disk distribution for  $\nu(R)$ , and use the smooth empirical fit to  $\sigma_\phi(R)$  of equation (6.1), then we can substitute these quantities into equation (7.1) to predict the value of  $\bar{v}_\phi$ .

To compare this value to the observed mean streaming of stars, we must make a couple of corrections to the model. The first is due to the inclination of the galaxy, but M31 is sufficiently close to edge-on that this effect is relatively minor and has already been accounted for in the PN rotation curve of Figure 6.2. The second effect is more significant: although we have selected a sample of PNe whose positions lie close to the major axis of M31, the cut at  $|Y| < 0.04^\circ$  does sample a range of azimuths, particularly at small radii. We have allowed for this effect by averaging the line-of-sight component of  $\bar{v}_\phi$  in the model over the range of azimuths admitted at each position  $X$  along the major axis.

The net result of this calculation is shown as the solid line in in Figure 7.3. At small radii, the detailed match between model and observation is not perfect, but discrep-

ancies here are not surprising since many of the PNe in this region will belong to the bulge rather than the disk as modelled here; even PNe from the disk will have their kinematics affected by the bar (see Section 6.1.1), which also has not been accounted for in this simple axisymmetric picture. At larger radii, however, the agreement is remarkably good. It should be stressed that this model has not been fitted to the data: the amplitude of the asymmetric drift between  $\overline{v}_\phi$  and  $v_c$  is entirely fixed by the Jeans equation once we have determined the other quantities in this equation as described. Note also that although we have constructed this dynamical model by assuming the velocity dispersion profile varies as a result of an increase with radius in the scale-height of M31's disk population, the absence of  $\sigma_z$  in equation (7.1) means that the agreement is not dependent on this specific model. All that is required is that the radial and tangential kinematics are coupled via equation (7.2); if  $\sigma_z$  is not coupled to these motions, then any scale-height can be accommodated. The generic agreement between model and data therefore provides a healthy consistency check on this analysis, and leaves us with a relatively simple self-consistent picture of the dynamics of M31's surprisingly warm disk.

### 7.3 Simple disk-bulge-halo fits to the rotation curve

Now that we have established that the asymmetric drift of the stellar population puts the PN rotation curve in agreement with the other rotation curve measures, we may turn our attention to a physical interpretation of the source of this motion.

The simplest thing to do at this point is to combine theoretical rotation profiles for M31's main three components – the bulge, disk and halo – and calculate the resulting curve. As this is only to give a general picture of the constituent parts of the rotation curve, we will use only very simple models for the components.

We have used a Hernquist model for the bulge (Hernquist, 1990) with a density profile of the form

$$\rho_{\text{Bulge}}(r) = \frac{\rho_b}{\frac{r}{a_b} \left(1 + \frac{r}{a_b}\right)^3} \quad (7.3)$$

where  $\rho_b$  is the characteristic density of the bulge and  $a_b$  is the scale radius of the bulge. The density profile has been integrated out to give the mass profile and the subsequent rotation curve arising from the bulge is given by

$$v_{c \text{ Bulge}}(r) = \frac{\sqrt{2\pi G \rho_b a_b^3 r}}{a_b + r} \quad (7.4)$$

In this model, the scale radius of the bulge is the radius within which half the mass of the bulge resides. This is related to the effective radius,  $R_e$ , by the relationship  $a \approx R_e/1.8153$  (Hernquist, 1990). As the effective radius of the bulge has been measured [ $0.10^\circ$ , 1.4 kpc, Pritchett & van den Bergh (1994)], we are able to calculate a value for  $a_b$  ( $0.055^\circ$ , 771 pc), leaving only  $\rho_b$  as a variable.

Moving on to the disk, we have used a simple exponential disk model where the surface density profile takes the form  $\Sigma_{\text{Disk}}(R) = \Sigma_d e^{-R/r_d}$ , where  $r_d$  is the disk scale length

**Table 7.1:**  $\chi^2$  fits of a simple bulge-disk-halo model to the H II regions rotation curve. These models are shown in Figure 7.4.

	$\rho_b$ $M_\odot \text{ pc}^{-3}$	$\Sigma_d$ $M_\odot \text{ pc}^{-2}$	$a_h$ kpc	$C_h$ $10^3 M_\odot \text{ pc}^{-1}$	$\rho_h$ $M_\odot \text{ pc}^{-3}$	$\chi^2$	Comment
(a)	18.2	570	8.90	680	0.0086	129.8	Best fit
(b)	11.2	740	9.90	500	0.0051	133.1	Maximum disk
(c)	3.5	990	-	-	-	158.6	No halo
(d)	2.0	440	0.10	640	64	133.8	Fixed bulge
(e)	7.0	370	0.60	680	1.9	133.4	Fixed bulge
(f)	12.0	720	10.00	540	0.0054	132.3	Fixed bulge
(g)	17.0	600	9.20	660	0.0078	129.9	Fixed bulge
(h)	22.0	480	8.70	780	0.010	130.6	Fixed bulge
(i)	27.0	340	7.80	900	0.015	134.2	Fixed bulge

and  $\Sigma_d$  is the central surface density. Binney & Tremaine (1987, Section 2.6) have shown such a disk to produce the rotation curve

$$v_{c \text{ Disk}}(r) = \sqrt{\frac{\pi G \Sigma_d r^2}{r_d} [I_0(r') K_0(r') - I_1(r') K_1(r')]} \quad (7.5)$$

where  $I_n$  and  $K_n$  are modified Bessel functions of the first and second kind, respectively [for these we have used function forms given in (Press et al., 1992)] and  $r' = r/2r_d$ . As  $r_d$  has been measured to be  $0.43^\circ$  (5.9 kpc) for the PN population, we are left with only  $\Sigma_d$  as a variable.

For the halo we have once again taken the simplest model available, opting for a halo density profile of the form

$$\rho_{\text{Halo}}(r) = \frac{C_h}{a_h^\gamma + r^\gamma} \quad (7.6)$$

where  $C_h = \rho_h a_h^\gamma$ ,  $\rho_h$  being the central density of the halo; and  $a_h$  is the scale radius over which the halo moves away from the central value and towards an  $r^{-\gamma}$  regime (Binney & Tremaine, 1987, p601). For simplicity we have chosen to use  $\gamma = 2$ , which tends towards a flat rotation curve. Again, this has been integrated through to give the mass profile and subsequent rotation curve

$$v_{c \text{ Halo}}(r) = \sqrt{4\pi G C_h \left[ 1 - \frac{a_h}{r} \tan^{-1} \left( \frac{r}{a_h} \right) \right]} \quad (7.7)$$

where  $C_h$  and  $a_h$  are variables to be fit.

Now that we have model rotation curves for the three major components of the galaxy we can combine them together as follows

$$v_{c \text{ Total}}(r) = \sqrt{v_{c \text{ Bulge}}^2(r) + v_{c \text{ Disk}}^2(r) + v_{c \text{ Halo}}^2(r)} \quad (7.8)$$

and fit them to a measured rotation curve. We have chosen to use our H II region circular velocities for the rotation curve.  $\chi^2$  fits to this are shown in Table 7.1 for the overall best fit, the model with the largest disk contribution, a model with no halo and

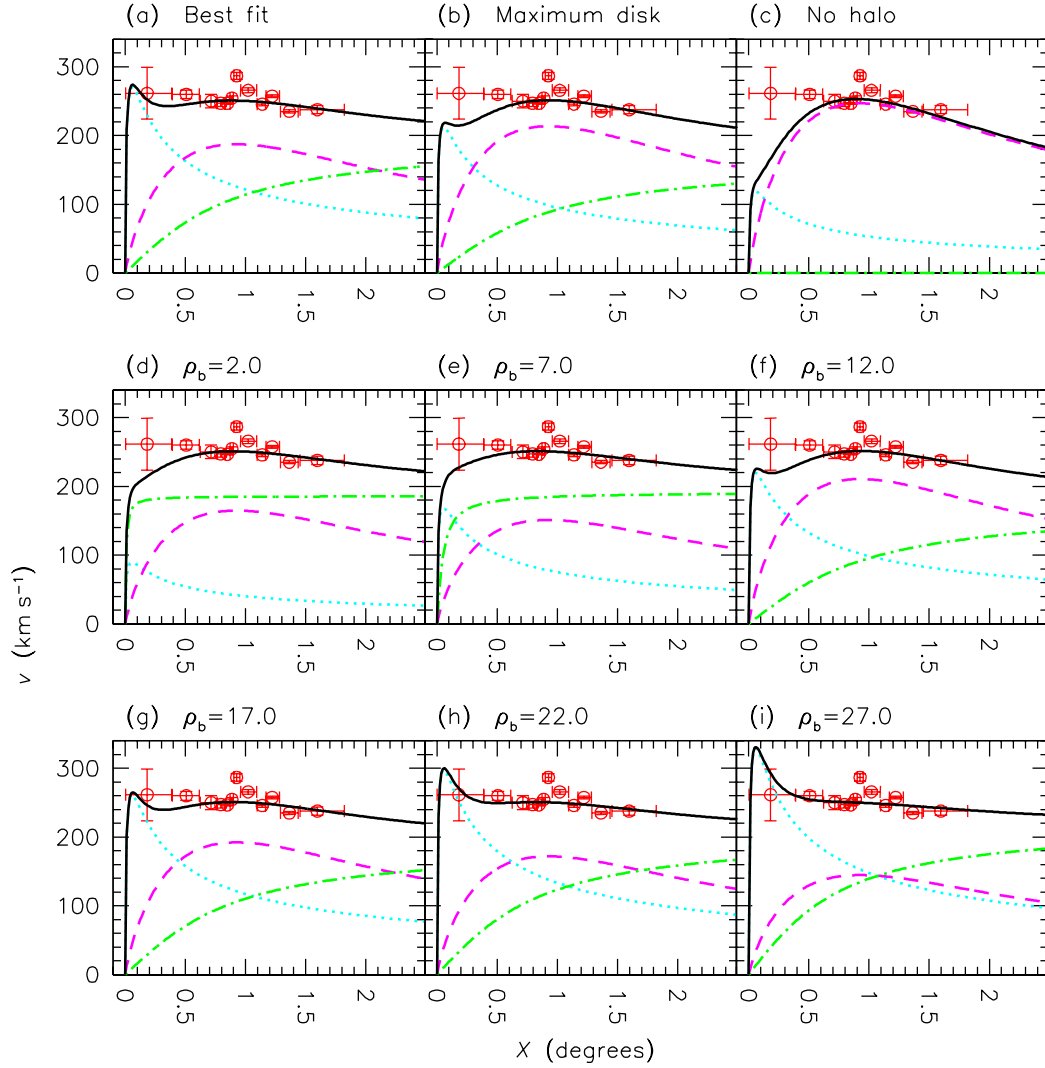


**Figure 7.4:** A range of models fit to our H II rotation curve (open red circles). The models are labelled and correspond to those listed in Table 7.1. The solid black line is the overall model fit, while the dotted cyan, dashed magenta and dot-dashed green lines are for the bulge, disk and halo components respectively. The only model that is a statistically poor fit to the data is the no halo model.

for a range of fixed bulge densities. All these models are plotted in Figure 7.4. The best fit model has fairly even contributions to the rotation curve from all three components. The other models illustrate the range of parameters that can produce an acceptable fit to the data. As  $\Delta\chi^2 = 4.7$  gives a  $1\sigma$  range from the best fit model, all the listed models are acceptable with the exception of the no halo model. These range from a model with a very low mass bulge and the majority of its mass coming from the halo, through models that are dominated by the disk component, to models that are dominated by the bulge at small radii and the halo at large radii, with only a small contribution from the disk. This degeneracy is partly due to the large error on the first data point, which does not constrain the model well. Using other rotation curves, such as the H I observations, produces different ranges of acceptable model fits as they provide better constraints at different points in the model. However, some of the other rotation curves are known to be affected by non-circular motions and none of the available data provide a clear picture of how the rotation curve behaves at small radii. This is due in part to a lack

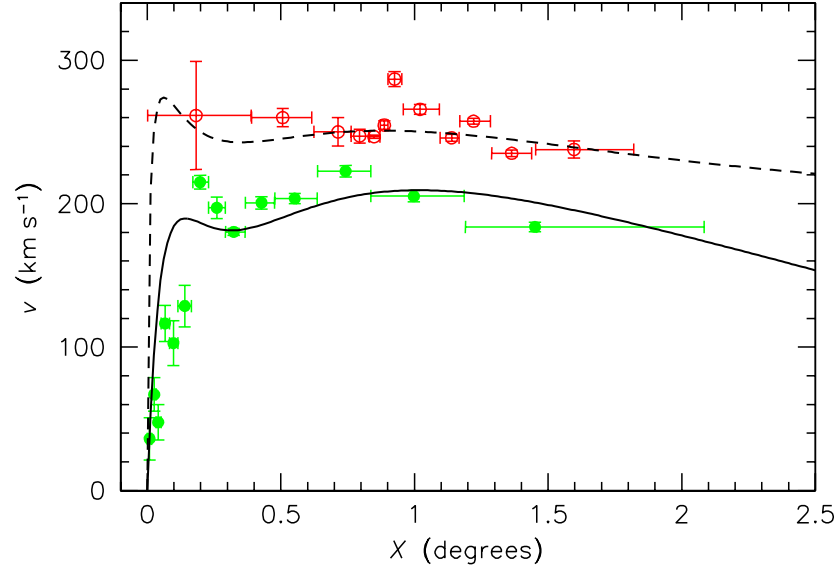


**Figure 7.5:** The best fit bulge-disk-halo model and the corresponding stellar rotation curve. The open red circles are the H II region velocities; the closed green circles are the PN rotational velocities as in Figure 6.2. The best fit to our H II regions is shown by the dashed line and the predicted mean stellar rotation velocities calculated from the asymmetric drift and geometry, as in Section 7.2, is shown as the solid line.

of H I gas and H II regions near the centre and also to non-circular motions from the bulge component.

The asymmetric drift correction (see Section 7.2) to the best fit model is shown in Figure 7.5. This provides a fair approximation to the PN rotation curve value for  $X$  greater than  $\sim 0.3^\circ$ . Again the central rotation curve is likely affected by non-circular motions from PNe in the bulge population.

These fits to the rotation curve serve to illustrate the difficulty one finds in constraining the absolute contributions from multiple components when only surface brightness, rotation and velocity dispersion profiles are available. This degeneracy is inherent in model fitting and cannot be eliminated by using more sophisticated models. We have therefore chosen to explore a non-parametric way of examining our data.

## 7.4 An analysis of the energy-angular momentum plane

In the apparent asymmetry found in Section 6.3 we have identified a large scale substructure in the kinematics of M31. We now turn our attention to the possibility of smaller scale substructures. Firstly, we should consider whether such formations are likely to exist in a galaxy's disk. The easiest way to answer this is to consider the stellar velocity distribution in the solar neighbourhood of the Milky Way.

### 7.4.1 Moving groups in the Milky Way

For many years studies of the velocities of stars in the solar neighbourhood of the Milky Way have shown substructures to exist within this distribution. When radial ( $v_R$  pointing towards the Galactic centre) and azimuthal ( $v_\theta$  pointing in the direction of Galactic rotation) velocities are examined for stars in the solar neighbourhood, clumps can be seen in the velocity field superimposed upon more global dynamical features such as the stellar velocity dispersion and asymmetric drift. Despite the stars in these velocity space clumps not being in physical proximity to one another, but spread throughout the sky, they are thought to be fundamentally linked.

The most prominent of these velocity space clumps are commonly known as the Hyades stream, as it is associated with the Hyades cluster (Eggen, 1958); the local association, or Pleiades stream, associated with the Pleiades cluster (Eggen, 1975); and the Sirius stream, or Ursa Major group, associated with the Ursa Major cluster (Eggen, 1958). These streams, or moving groups, have classically been thought to be the remnants of disrupted star clusters. Open clusters in the disk of the Galaxy can be only weakly gravitationally bound, making them susceptible to disruption during tidal encounters with objects such as molecular clouds. After break up the members of the cluster would continue to move in the direction that the cluster had been moving at the time of disruption. This leaves the individual cluster stars moving on orbits that are very similar despite no longer being gravitationally bound together.

Recent developments in instrumentation have prompted a reexamination of this phenomenon. The European Space Agency's High Precision Parallax Collecting Satellite (HIPPARCOS), which operated through the early 1990's, measured accurate 3-dimensional positions and proper motions for stars in the solar neighbourhood, allowing a large amount of new work to be done in this field (e.g. Chereul, Cr    & Bienaym   1998; 1999; Dehnen 1998; de Zeeuw et al. 1999). The most recent studies have combined the HIPPARCOS data with radial velocity surveys, producing fully-determined phase space distributions for the stars (e.g. Famaey et al., 2005).

One result of these studies has been the observation that while the  $R$  and  $\theta$  velocity components of these stars are clearly seen to be correlated, the  $z$  components are not ( $z$  points in the direction of the north Galactic pole). Dehnen (1998) examined the  $R$ ,  $\theta$  and  $z$  components of stellar velocities observed by HIPPARCOS, finding a number of stellar groups with correlated  $R$  and  $\theta$  velocities, but only a few groups where the  $z$  component was also correlated. Dehnen suggests this to be a result of phase mixing. If variations in the Galactic potential occur more rapidly in disk height than in the radial and azimuthal directions, the  $z$  component velocities will exhibit greater variations than the  $R$  and  $\theta$  components, making it unlikely that the velocities in this direction will remain correlated over a lengthy period.

A second and more unexpected result of these studies has been the finding that stars in these clusters are not all of the same age (Chereul, Cr    & Bienaym   1998; 1999). Famaey et al. (2005) have shown stars in these groups to cover a wide range of ages when compared to isochrones in the Hertzsprung-Russell diagram. This has led to the suggestion that these groups are not a result of the break up of open clusters but are instead a consequence of dynamical perturbations from spiral waves with young



stars, old stars and stellar clusters alike being perturbed into similar orbits forming ‘dynamical streams’.

What is patently clear from these studies is that the properties of stars in the solar neighbourhood do not take a simple smooth form. It is therefore reasonable to assume that the same will be true elsewhere in the Milky Way and also in external disk galaxies. We must therefore consider ways of looking for inhomogeneities in the velocity distribution of the PN population of the Andromeda Galaxy.

### 7.4.2 Searching for inhomogeneities in M31’s energy-angular momentum space

Allowing that the dynamical streams seen in the Milky Way are made up of stars that are on very similar orbits around the Galaxy, the energies and angular momenta of these stars will be similar and groups of stars can be identified from these properties. Support for this comes from Helmi & de Zeeuw (2000), who have shown through simulations that the energies and angular momenta of stars in halo streams from disrupted satellites remain correlated and provide a good tracer of the progenitor galaxies. These quantities are conserved fairly well if the galactic halo evolves only slightly, but are poorly conserved if the evolution is significant. It is therefore only possible to identify groups of stars via this technique that have formed in the late stages of a galaxy’s evolution.

It is reasonable to assume that dynamical streams similar to those seen in the Milky Way will exist in the Andromeda Galaxy. The recent observation that such features may be associated with spiral waves rather than individual, or groups of, open clusters (Famaey et al., 2005) stands in our favour as we would have little hope of finding any, let alone several, PNe associated with such low luminosity objects. One way to identify dynamical streams in M31 would be through the energies and angular momenta of the constituent stars. Unfortunately it is not possible to measure full 6-dimensional phase space locations for the PNe in Andromeda and therefore we cannot measure either the energy or angular momentum of an individual object. However, if we are to concentrate on the stellar disk and assume it to be thin, we can set both the height of a star above the plane,  $z$ , and the vertical component of a star’s velocity,  $v_z$ , to zero. We can measure the other two spatial coordinates and the line of sight velocity, which leaves us with just one undefined variable: the velocity component tangential to the observer. For a given PN we can input a range of possible values for this velocity and hence calculate a range of possible energies and angular momenta. As discussed above, if a group of PNe are on the same orbits, but at different locations on the orbit path they will all have the same energy and angular momentum. Therefore the individual PN tracks that we have generated should intersect at the energy and angular momentum of the orbit they are on. It follows that if we generate these tracks for all our PNe, any moving groups should show up as points where such loci intersect in the energy-angular momentum plane.

It should be noted at this stage that this analysis is only applicable to moving groups with velocities close to that of the galaxy disk. Hence velocity substructures, such as

the stream found in Section 6.5.2, which have orbits that are very different to M31's disk will not be picked out by this analysis. It is also worth noting that any overdensities this analysis may pick will reside within the disk and therefore would not have been found using the friendlessness algorithm in Section 6.5.2.

Energies and angular momenta are calculated from the following set of equations,

$$L = L_z = rv_\theta = -xv_y + yv_x \quad (7.9)$$

$$E = \Phi(r) + \frac{1}{2}(v_\theta^2 + v_r^2) = \Phi(r) + \frac{1}{2}(v_x^2 + v_y^2) \quad (7.10)$$

$$\Phi(r) = \frac{1}{2}v_c^2 \ln(r^2) = \frac{1}{2}v_c^2 \ln(x^2 + y^2) \quad (7.11)$$

in which  $r, \theta$  and  $x, y$  are standard spatial coordinates in the disk plane, the signs in the angular momentum equation are chosen to make the net angular momentum positive;  $v_r, v_\theta$  and  $v_y, v_x$  are the corresponding velocity components, with  $v_y$  as the observed line-of-sight velocity corrected for the disk inclination and  $v_x$  the unknown transverse value; and  $\Phi(r)$  is the gravitational potential energy – for simplicity we use a singular isothermal potential.

For the tangential velocity component,  $v_x$ , one should input a range of all the possible velocities, but in practice we must limit this to a more realistic range. Initially, we tried all velocities around the values of  $v_x$  that give  $\sqrt{v_x^2 + v_y^2} = v_c = 250 \text{ km s}^{-1}$ , but found this ultimately tended to assign a large number of PNe to velocities that were larger than  $v_c$ . While we would expect a few PNe to have velocities greater than the mean rotational velocity, this picked out far too many. We have therefore restricted the range of  $v_x$  to values lower than that which would give the PNe total velocities equal to M31's mean rotational velocity. We have chosen to use a range of  $v_c/4$  as this is approximately equal to the mean velocity dispersion we see for PNe in the disk. Using a larger range produces longer tracks which increase confusion. However the basic result remains similar, though it extends to higher energies. An example of the values obtained for a small sample of our PNe is shown in Figure 7.6. The black line shows the energies of circular orbits and the lowest possible values. The sample clearly contains a number of disk-like PNe with orbit energies that lie very close to the circular value. As the PN orbits become less disk-like, their orbit tracks move towards higher energies.

It is helpful to look at the tracks generated in a coordinate system that offers a clearer view of PNe on nearly circular orbits. This is done by using a reduced energy value defined as  $\sqrt{2[E - E_c(L)]}$ , where  $E_c(L)$  is the lowest possible energy for a star with a given angular momentum, which corresponds to a circular orbit, and is given by

$$E_c(L) = \Phi(L) + \frac{1}{2}v_c^2. \quad (7.12)$$

$$\Phi(L) = \frac{1}{2}v_c^2 \ln \left[ \left( \frac{L}{v_c} \right)^2 \right] \quad (7.13)$$

Tracks for all the PNe in M31 are shown in the upper panel of Figure 7.7, with the lower panel showing the equivalent area in the reduced energy plane. The enhanced

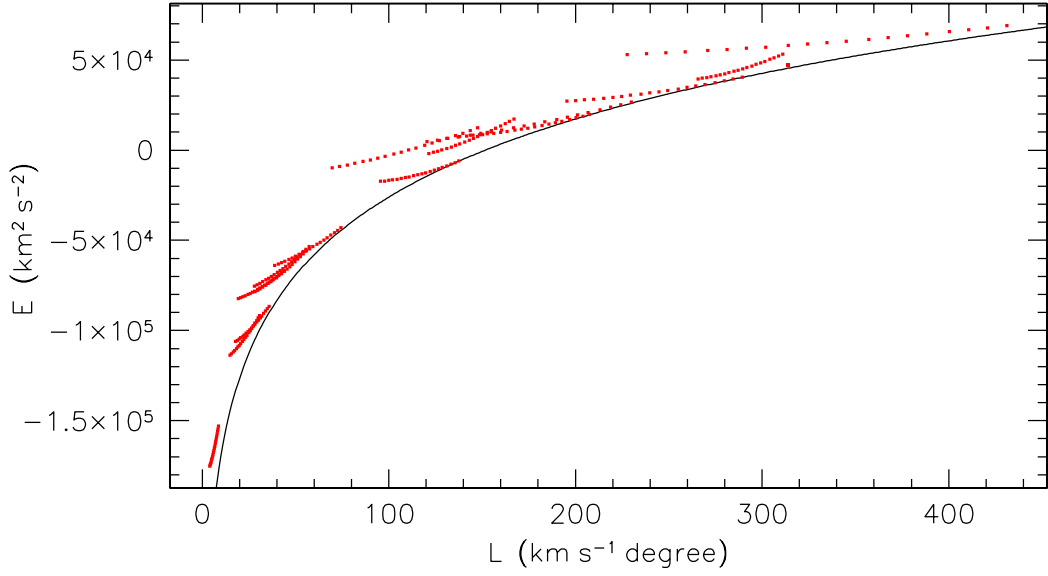


**Figure 7.6:** Projection of a selection of PNe into the energy-angular momentum plane. The PNe are shown as red dotted lines and the black line represents the lowest possible energy for an object with that angular momentum. The PN shown as a single dot at  $L \sim 310$  has a radial velocity that is faster than the nominal rotational velocity. We therefore assume this to be its actual velocity and do not add an additional component to it.

view in the lower panel is clear and it is this plane that we have chosen to examine further. The majority of the PN tracks are clustered just above the circular energy value and have angular momenta of less than  $1000 \text{ degrees km s}^{-1}$ ; the few with larger values are mostly located some distance along the minor axis and have large projected radii that are the cause of these large values. As we are interested in the disk of the galaxy and it is unlikely that any of these are members of the disk, we have chosen to limit our search area to values of angular momentum lower than this value. The remaining area can then be divided into a grid and the number of PN tracks passing through a particular location can be calculated.

The choice of grid size is important: too small and features will be spread across a number of grid-points which may cause them to be missed; too large and details will be lost. Reducing the energy to the  $\sqrt{2(E - E_c)}$  value means the two axes are comparable in size. We have therefore chosen to try out a range grid sizes:  $5 \times 5$ ,  $10 \times 10$  and  $20 \times 20 \text{ [km s}^{-1} \times \text{degrees km s}^{-1}]$ .

Figure 7.8 shows this distribution for all the PNe in M31 using a  $10 \times 10$  grid and the numbers of PNe crossing grid-points as a function of both angular momentum and the reduced energy value. There are two grid-points with 57 PN tracks crossing them, one at (200, 50), the other at (220, 50). These are marginally overdense compared to other grid-points around them, though this region generally appears to have a high density of PN tracks. As Figure 7.9 shows, we also see overdensities in approximately this region when we look at the  $5 \times 5$  [at (225, 50) and (245, 55)] and  $20 \times 20$  [at (240, 50)] grids. The overdensity is particularly visible in the  $20 \times 20$  grid. We therefore believe this overdensity to be a real one, though there is some variation in exactly which PNe are picked out by different size grids.

In order to search for other substructures in this plane, we have created an iterative

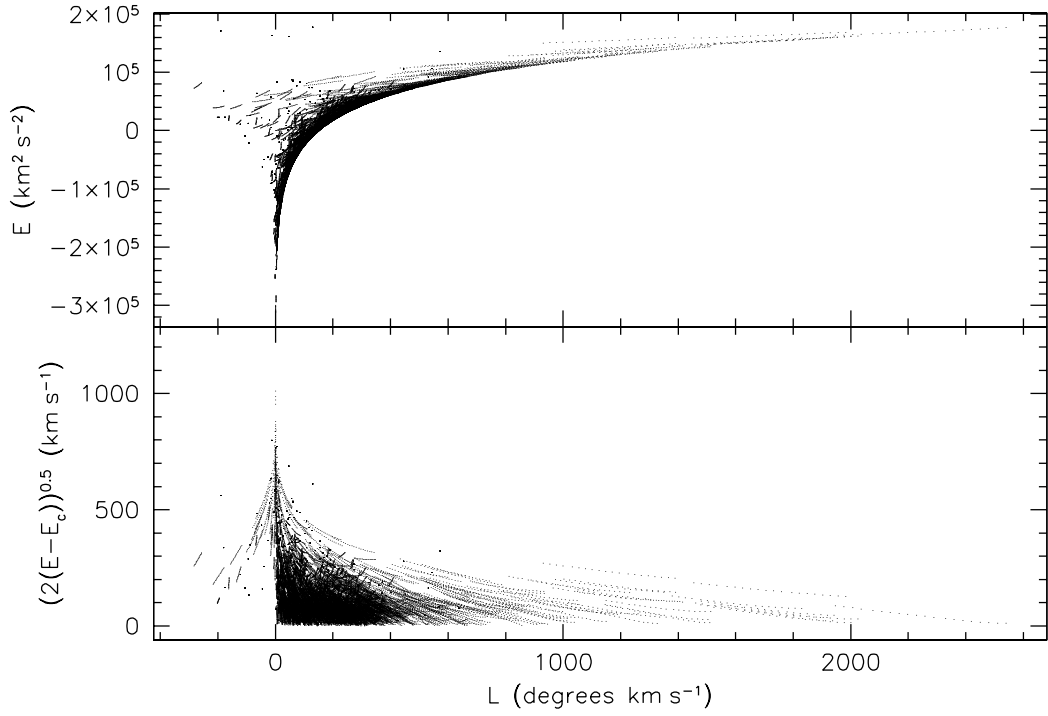


**Figure 7.7:** PN tracks in the  $(L, E)$   $\left(L, \sqrt{2(E - E_c)}\right)$  planes for all the PNe in the Andromeda Galaxy.

process that allocates PNe to grid-points in the energy-angular momentum plane. This is done by assigning all the PNe with tracks crossing the most densely packed grid-point to that point and removing them from the sample. The track generation process is then repeated and the new densest grid-point found. Again all the PNe with tracks crossing this grid-point are allocated to it. The whole process is repeated until we find only two PNe per grid-point, leaving us with a list of grid-points in the energy-angular momentum plane where subsequent overdensities were found. The resulting distributions from the three different grid sizes are shown in Figure 7.10. The overall distribution of PNe with all three grid sizes are very similar indicating that this general result is fairly independent of grid size and therefore quite robust. The majority of PNe are found to lie on a ridge with a constant, relatively low reduced energy, indicative of the dominance of near circular orbits in this disk-dominated system. There are however very few objects with energies actually at the circular value. This is easily explained as a result of the stellar asymmetric drift causing the stars to orbit with velocities that are generally smaller than  $v_c$  and hence have larger energies.

We must now consider whether or not any of these overdensities can be identified as arising from a known physical structure. In order to do this we have plotted the physical locations of the PNe from the densest two grid-points of the  $10 \times 10$  grid in Figure 7.11. We can see that the PNe from each of these grid-points lie approximately in a ring around the galaxy. The mean value of the disk radii of the PNe in grid-point (200, 50) is  $0.88^\circ$ , while for grid-point (220, 50) it is  $0.98^\circ$ . Dividing the grid-point angular momenta by these values gives  $v_\theta \sim 225 \text{ km s}^{-1}$  for both grid-points. This is somewhat higher than the mean rotation velocity of around  $200 \text{ km s}^{-1}$  we found for PNe in Chapter 6, but approximately the same as the velocity at the highest point

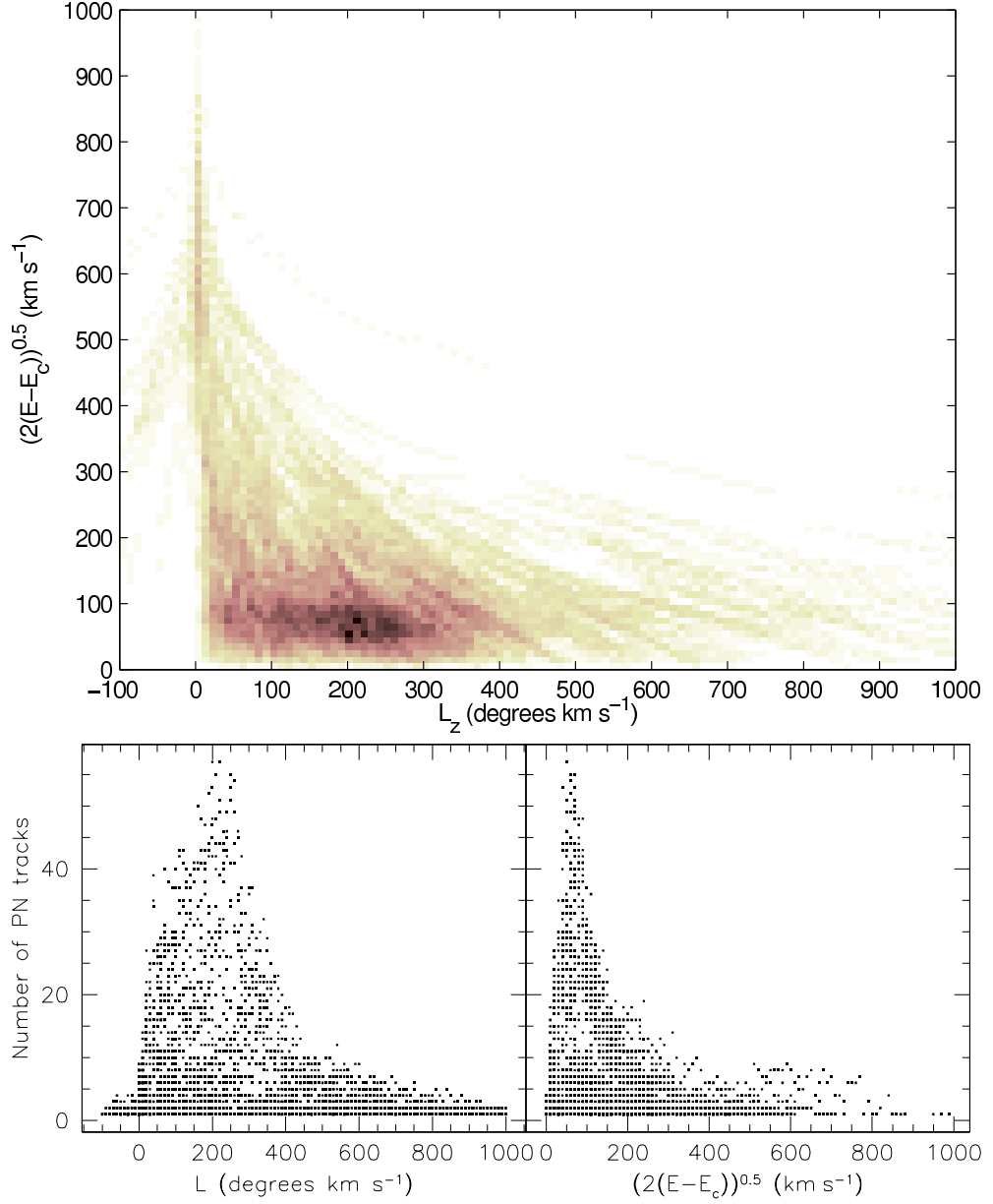


**Figure 7.8:** The upper panel shows the density of PN tracks in the  $(L, \sqrt{2(E-E_c)})$  plane. The number of tracks at a given point is related to the shade of the location, with darker shades relating to a larger numbers of PN tracks. The lower panels show the number of PN tracks crossing all the grid-boxes as a function of angular momentum (left) and the reduced energy (right).

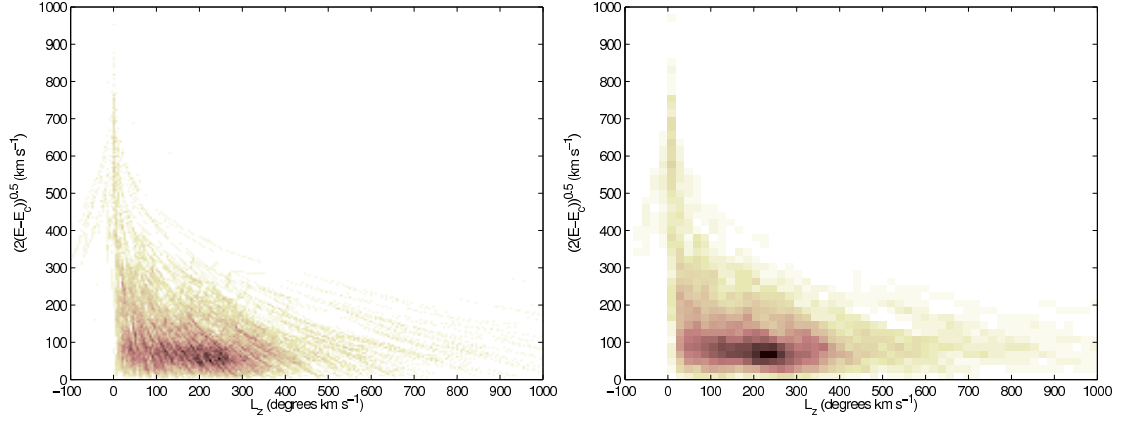


**Figure 7.9:** The density of PN tracks in the  $\left(L, \sqrt{2(E - E_c)}\right)$  plane for the  $5 \times 5$  (left) and a  $20 \times 20$  grids (right).

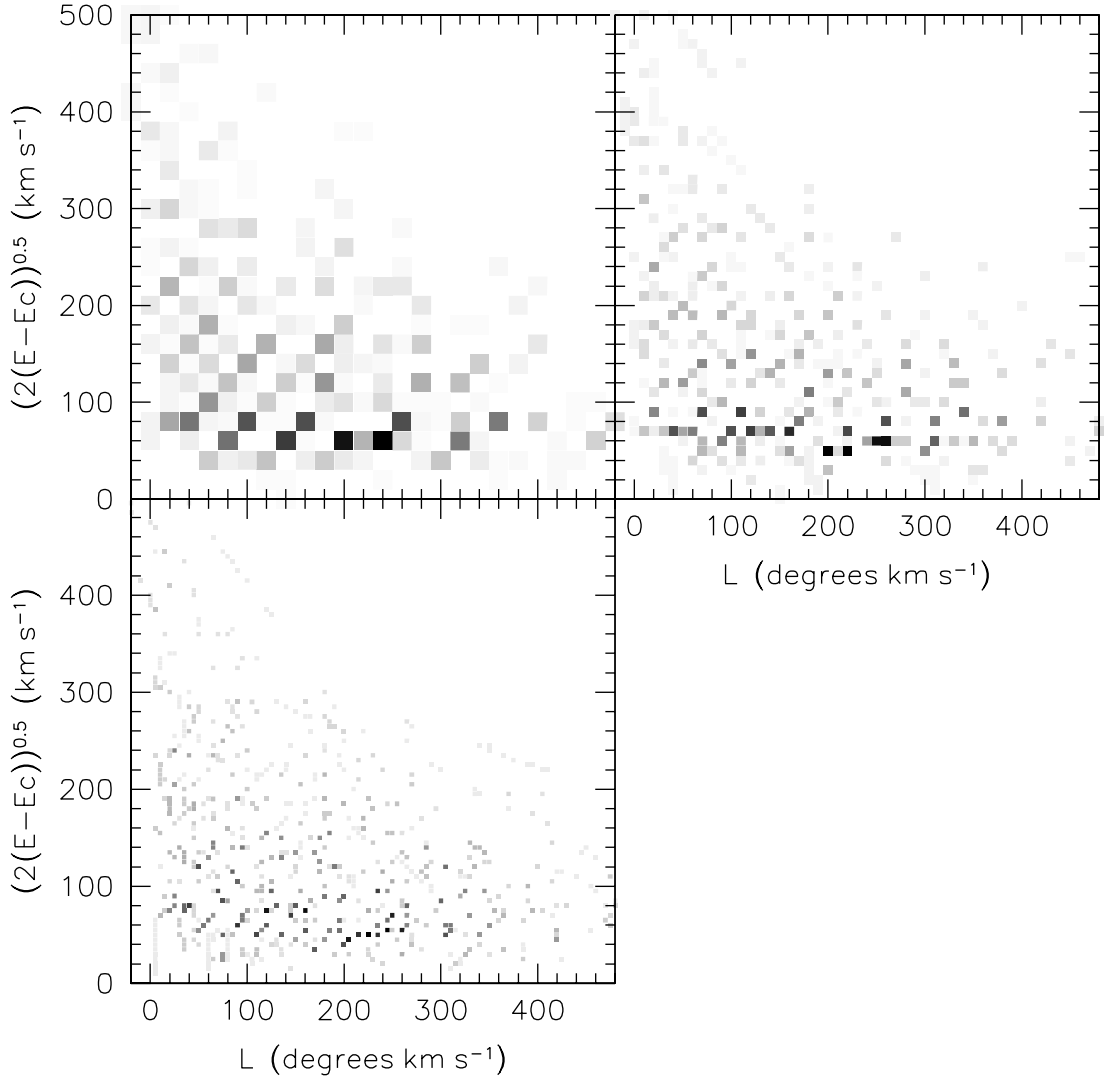


**Figure 7.10:** Locations of the grid-points with the subsequently densest concentrations of PN tracks for all the PNe in M31. Top left is for the  $20 \times 20$  grid; top right the  $10 \times 10$ ; and bottom the  $5 \times 5$  grid.

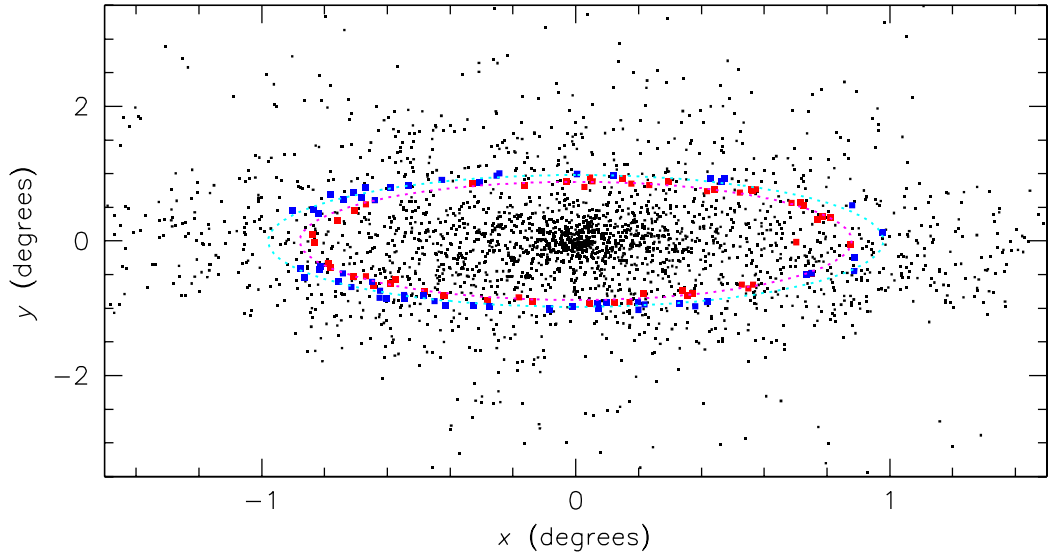


**Figure 7.11:** Physical locations of the PNe found in Figure 7.8’s highest density grid-points. The red points are PNe from the (200, 50) grid-point, and the blue points PNe from the (220, 50) grid-point. The magenta and cyan ellipses show circular rings in the disk plane with the mean radii of these two grid-points.

on the rotation curve (at  $0.74^\circ$ , see Table 6.1). The equivalent grid-points in the  $5 \times 5$  and  $20 \times 20$  grids have radii between  $1.00^\circ$  and  $1.10^\circ$ , and corresponding values of  $v_\theta$  between  $\sim 220$  and  $225 \text{ km s}^{-1}$ .

This location is approximately coincident with the ring of star formation discussed in Chapter 1, where the majority of our H II regions are located (see Figure 3.16). Both this overdensity of PNe and the slightly elevated mean rotational velocity could be explained by the misclassification of compact H II regions as PNe, which would affect this region most significantly. We must therefore look again at the PNLf and surface density of PNe to see if there is any indication of contamination from H II regions resulting in an overdensity of objects at this radius.

Firstly we may remind ourselves of the examination of the PNLf performed in Chapter 5. In this we saw no evidence for any deviation from the standard monotonic function at this, or any other radius. What we did observe was a dearth of PNe from the near side of the disk at approximately the ring radius believed to be the result of extinction from a thin ring of dust. This apparent dearth of PNe is somewhat at odds with the overdensity we have observed and we must now consider the spatial distribution of PNe once more.

In Chapter 5 we saw that the main distribution of light in the disk can be approximated to a smooth exponential decline (Figure 5.5). However, there are significant deviations from this. In order to build up a prediction for PN number counts we have taken Walterbos & Kennicutt (1987)’s V-band surface density profile and compared the two sides of the disk. Figure 7.12 shows these two profiles to be very similar, with the major features the same on either side of the disk to near the limits of the data. We have taken the mean of these values and smoothed the profile with a boxcar function. An  $r^{1/4}$  bulge with an effective radius of  $0.1^\circ$  (Irwin et al., 2005) was then subtracted off, leaving us with a disk light profile. The bulge and disk profiles can now be combined

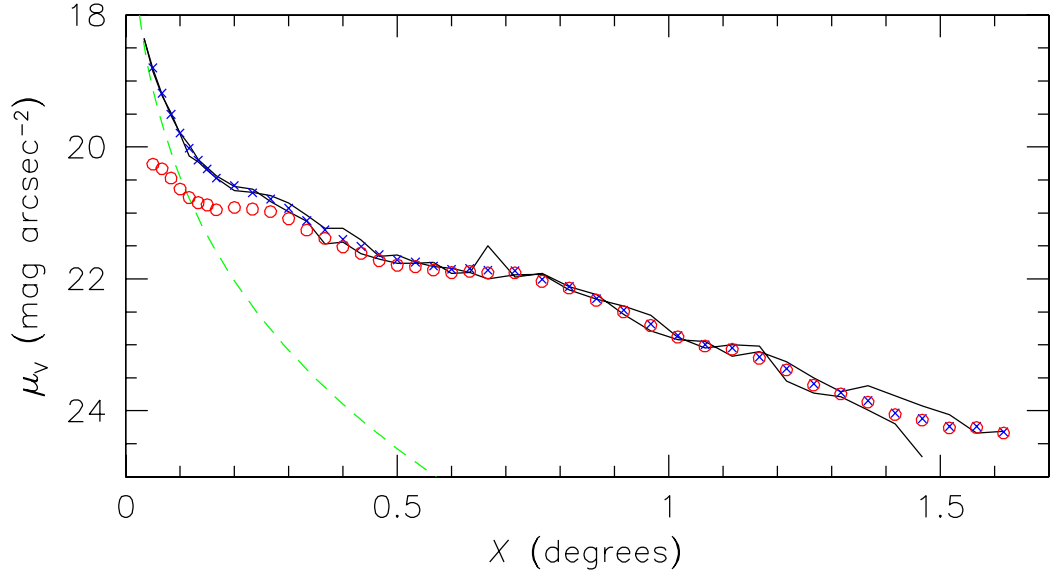


**Figure 7.12:** Surface brightness profile of V-band light in M31. The solid black lines are Walterbos & Kennicutt (1987)’s major axis V-band light profiles for the two sides of the disk; the blue crosses show a smoothed mean value for this; the green dashed line is an  $r^{1/4}$  profile for bulge; the red circles are the disk light profile with the bulge model subtracted off.

together to work out the total light, and hence number of PNe, we should see coming from rings at any given radius within M31. The resulting profile, normalised to the number of PNe we actually see in a number of rings around M31’s centre, is plotted in Figure 7.13.

The first thing we notice is that this is not the smooth, monotonic profile that we would expect from a simple, exponential disk. The bumps we see at  $\sim 0.25^\circ$  and  $\sim 0.75^\circ$  are clearly visible in the disk photometry, and are associated with ring-like spiral structures in the disk. When we look at the number of PNe per ring in this figure it is clear that while they do increase at the approximate radius of the star formation ring, they do not increase as much as expected from the surface density profile. We have also split this distribution into those PNe originating on the far and near sides of the disk. This shows a marked difference: the far side follows the photometry prediction fairly well, but the near side shows a significant dearth of PNe as we would expect from the PNLf observations discussed previously.

We must also consider the indication that the selected PNe are moving with a mean velocity that is slightly faster than is seen elsewhere. This does not necessarily indicate H II region contamination as the ring is a region of star formation and will contain a large fraction of younger stars. Younger stars in the solar neighbourhood are observed to have smaller asymmetric drifts than older stars (Binney & Merrifield, 1998, Section 10.3.1). By the time the population has aged sufficiently to produce PNe, the dispersion will have increased, but possibly not to the level of the rest of the disk, and a smaller asymmetric drift may well remain in the velocities of PNe originating from this region.

We may therefore be fairly confident that the increase in PN numbers at the radius of the star formation ring is the result of a predictable increase in stellar density. The result of this physical overdensity is an overdensity of stars with the energy and angular



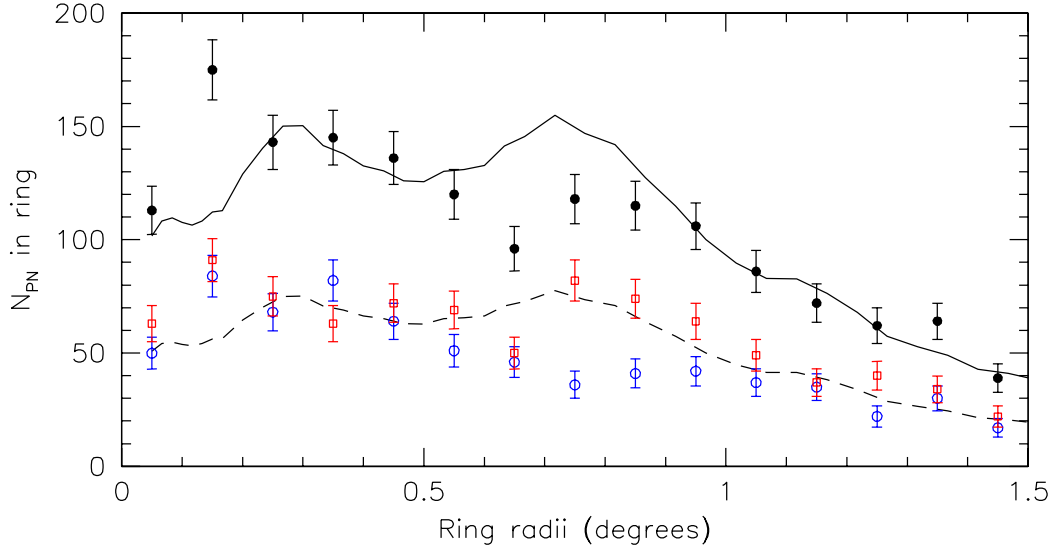


**Figure 7.13:** The number of PNe brighter than 24 mag found in rings in the disk. The solid black circles are for the complete ring, with the open red squares and open blue circles showing the number of PNe in the halves to the far and near sides of the disk, respectively. The solid and dashed lines show predictions for the number of PNe in the whole ring and half the ring, respectively, assuming the PN density follows the light profiles for the disk and bulge shown in Figure 7.12; the curves have been normalised to the PN data.

momentum associated with the star formation ring. That we have picked out this very real structure in our analysis provides a proof of concept and hope that smaller, less obvious structures may have also been picked out.

There is one major difficulty associated with this analysis. The uncertainty associated with the radial velocity measurement is relatively large ( $\sim 15 \text{ km s}^{-1}$ ). Transferring it into the energy and angular momentum plane creates significant errors associated with these, as the upper panel of Figure 7.14 illustrates. We have chosen to examine the reduced energy plane because it enhances the area closest to disk-like energies. Unfortunately, the errors associated with these reduced energies will also be enhanced. This is readily apparent in the lower panel of Figure 7.14, where as the tracks get closer to circular, the errors associated with the reduced energy values become very large. It might be better to use Halliday et al.'s fibre spectroscopy data as the measured velocity errors are smaller than for PN.S. However, this sample is not only smaller, but patchy and we would risk picking out patches in the data set rather than genuine features that would show up in a complete survey.

Even if we cannot be certain about the validity of some of the kinematic substructures that the analysis has picked out, this technique provides a new way of looking at the distribution function (DF) of M31. A galaxy's DF describes the full 6-dimensional phase space density of its stars and fully specifies the dynamics of the system. In some cases, it can be expressed in terms of the energies and angular momenta of its constituent stars, and we have therefore effectively constructed a clumpy approximation to such a two integral DF. As the DF is described in terms of the absolute numbers of stars, we have remade this function in Figure 7.15 with only PNe brighter than 24 mag so that the sample is approximately spatially complete. This shows similar features to the full sample, with a ridge of PNe at energies close to circular, indicative of a disk

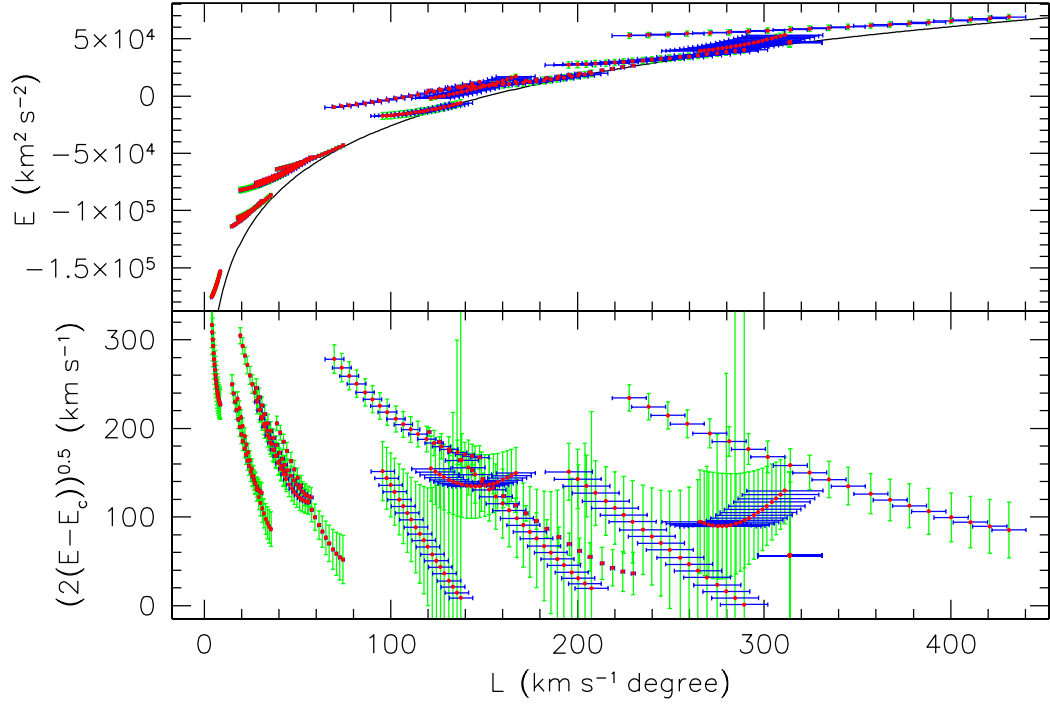


**Figure 7.14:** The upper panel is the same as Figure 7.6, but including error bars on the points. The lower panel shows the conversion to the reduced energy frame.

population dominating the distribution.

A further and more detailed exploitation of this new tool is somewhat beyond the limits of our data set and the scope of this thesis. However, this technique potentially provides a powerful new tool for studying the distribution functions of discrete kinematic tracers in disk galaxies and a way of searching for dynamical substructure in a non-parametric manner.

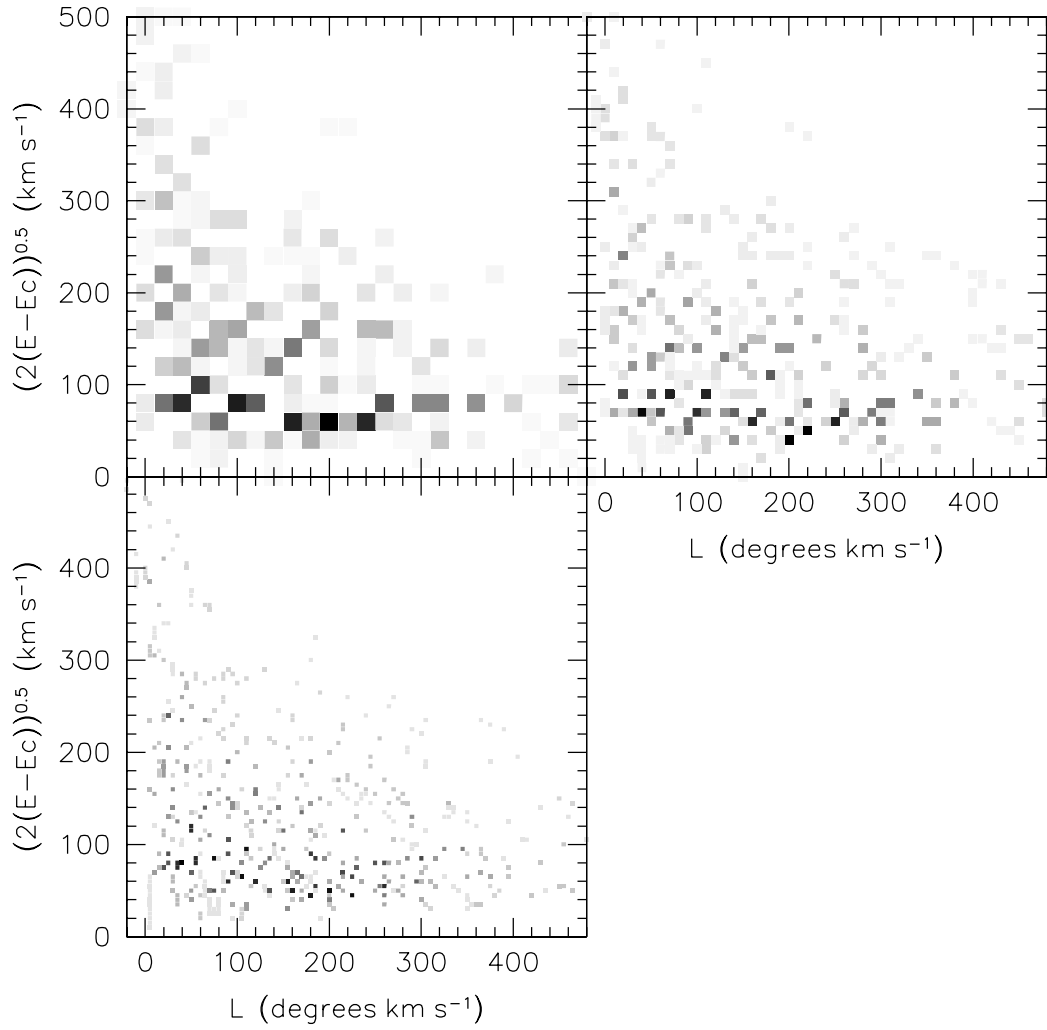


**Figure 7.15:** Approximations to the distribution function of PNe brighter than 24 mag using  $20 \times 20$  (top left),  $10 \times 10$  (top right) and  $5 \times 5$  (bottom) grids.

# Chapter 8

## Summary and future extensions

### 8.1 Summary

Using the Planetary Nebula Spectrograph (PN.S), we have surveyed a wide area over the Andromeda Galaxy. Some 3300 emission-line objects have been detected and their velocities measured. This data set provides not only an unprecedented tracer population for studying M31's properties, but, when used in conjunction with other surveys, an effective tool for testing the Planetary Nebula Spectrograph's capabilities.

Internal and external comparisons show the PN.S measurements for astrometry, photometry and velocity to be accurate to well within acceptable levels. Some small systematic effects have been found and corrected for.

Efforts have been made to create a clean sample of PNe originating from M31. Probable H II regions and background galaxies are excluded on the basis of their full widths at half maximum and, incorporating data from Massey et al. (2002)'s local group survey, their  $[\text{O III}]/(\text{H}\alpha + [\text{N II}])$  flux ratios. H II regions are found to be mainly located in rings around M31's disk at the locations of the known spiral structures.

Our survey area also took in a number of M31's satellite galaxies and some other background galaxies. PNe and H II regions in close proximity to and associated with these galaxies have been flagged in the catalogue and eliminated from the M31 sample. A significant number of PNe have been found in the two largest satellite galaxies, M32 and NGC 205. Though not enough sources for a detailed examination of their system dynamics, information has been extracted about their basic kinematic properties. A handful of source have been identified in the relatively nearby background galaxy Andromeda IV, and a couple in the 2MASS galaxy 2MASXi J0039374+420956. However, the existence of the recently-proposed disrupted satellite galaxy Andromeda VIII is brought into question by this larger data set.

We have examined the planetary nebula luminosity function across M31 and find it to be well reproduced by the usual simple functional form, with no strong evidence for spatial variations that cannot be attributed to modest amounts of obscuration. There is no indication of a variation between the disk and bulge populations as would be expected if the bright end of the luminosity function is dominated by relatively massive

stars and is therefore highly dependent on the age of the last burst of star formation, as has been suggested in recent years (Marigo et al., 2004).

We see a very good agreement between the number counts of PNe and the R-band surface photometry along both the major and minor axes. These are dominated by the disk and bulge populations, respectively, further indicating that both arise from the same, old population. With these dynamically-selected number counts of discrete objects, we can also go much deeper than the conventional photometry of M31. There is no evidence for a cut-off in its exponential disk population to beyond four scale-lengths, and there are no signs of a halo population that is distinct from the bulge out to ten effective bulge radii.

Some variation in the form of the luminosity-specific PN density is seen between the disk and bulge populations. This quantity is seen to be slightly lower for the bulge than for the disk. This result fits with observations that red ellipticals have a lower luminosity specific PN density than blue spirals, but it is the first time that this phenomenon has been observed in a single galaxy, ruling out an environmental origin.

Rotation curves for both the PNe and H II regions in M31 are presented. The H II region rotation curve is seen to be in very good agreement with rotation curves in the literature. It has a mean value of  $\sim 250 \text{ km s}^{-1}$  and shows a gentle decline from the centre outwards. The PN rotation curve is not quite so straightforward, displaying a large, almost constant, asymmetric drift at all radii. The velocity dispersion profile for the PNe is also rather unusual, initially dropping in roughly the expected fashion, but then levelling off to a near constant value of  $\sim 55 \text{ km s}^{-1}$ . These data can be self-consistently reproduced by a simple disk model which is partially supported by random motions even at large radii. If the shape of the velocity ellipsoid remains approximately constant, then M31's disk must increase in scale-height at large radii or its mass-to-light ratio must increase significantly. However, this picture is somewhat complicated by the observation of an asymmetry between the two sides of M31's major axis.

The flatness of the velocity dispersion profile has allowed us to examine the velocity dispersion as a function of magnitude. We would expect to see some variation in this if the bright and faint PNe originate from different age populations. As no variation is seen, we may again conclude that PNe of all luminosities arise from a relatively homogeneous, old stellar population.

A number of photometric substructures are known to exist in M31 and we have searched for PNe associated with the largest two. A number of PNe are found in the region of the Northern Spur, which have velocities similar to the mean rotational velocity of the galaxy. We therefore conclude that this feature is mostly likely associated with the disk, either as part of a warp or as an isolated clump of stars. The Southern Stream is very low surface brightness feature, and while a few PNe have been found in its vicinity they may belong to a normal global M31 population. A number of PNe on one side of M31's disk are identified as a velocity substructure, the simplest explanation for their origin being that they represent a continuation of the Southern Stream.

In an attempt to identify moving groups in the disk of M31 we have developed a new technique for examining discrete tracer populations. This involves projecting the PNe

into the energy-angular momentum plane and searching for overdensities in this phase space. Despite the limitations of this technique, some success has been achieved and this may provide a novel non-parametric way to look at the distribution function of stellar populations in external galaxies.

## 8.2 Future extensions

### 8.2.1 Extensions to the data set

An extension of our survey area would be relatively straightforward and a number of candidate objects found in the INT-WFC survey still require follow up spectroscopy. However, only a small number of PNe are likely to result from this and it may be more worthwhile to consider what information we could obtain from existing sources. The most obvious source is Massey et al. (2002)'s Local Group Survey, which we have used to help distinguish between PNe and H II regions. It would be worthwhile looking into a more sophisticated method for locating our sources and measuring photometry from their images. It would then be possible to add photometry for the ( $H\alpha$ +[N II]) and [S II] emission lines to many of our PNe. This would allow an extra dimension of information to be considered alongside the kinematic properties.

### 8.2.2 Other analyses

As it is only in very recent years that stellar populations have become available as kinematic tracer populations in galaxies beyond the Milky Way, there are very few 'standard' things to do with a data set such as ours, and many areas of analysis that could be explored. It may be interesting to perform a data simulation style analysis, such as that of Hurley-Keller et al. (2004), with our larger data set. It would also be interesting to add a flaring, warping disk to the model to see how this affects the requirement for a large, fast rotating bulge.

In order to examine the distribution function more fully it would be worthwhile looking into a more traditional, parametric approach, such as those employed by Widrow, Perrett & Suyu (2003) and Widrow & Dubinski (2005), but fit to our discrete, 2-dimensional dataset.

# Appendix A

## The Catalogue

### Notes for Table A.1

- <sup>a</sup> Probable H II regions (or background galaxies):  
 E – extended in the PN.S data,  
 R – Flux ratio  $R$  below cutoff value (see Figure 3.15),  
 other – excluded as a PN due to flux.
- <sup>b</sup> Sources of non-M31 objects:  
 M32 / M32? – Objects associated with and in the vicinity of M32.  
 NGC205 / NGC205? – Objects associated with and in the vicinity of NGC205.  
 AndIV – Objects associated with the galaxy Andromeda IV.  
 2MASXi – Non-M31 source in the 2MASS catalogue.  
 MLA93 – Non-M31 source listed in Meyssonnier, Lequeux & Azzopardi (1993).  
 NS – Objects in the region of the Northern Spur.  
 Stream? – Objects referred to in Section 6.5 as being a possible extension of the Southern Stream.
- <sup>c</sup> Cross-identifications from other catalogues:  
 H06 – Halliday et al. (2006);  
 HK04 – Hurley-Keller et al. (2004) (format: table\_ID);  
 C89 – Ciardullo et al. (1989);  
 MLA93 – Meyssonnier, Lequeux & Azzopardi (1993).

**Table A.1:** Emission line objects identified in the M31 survey.

ID	RA J2000.0	Dec J2000.0	$m_{5007}$	$v_{\text{helio}}$ km s <sup>-1</sup>	Note <sup>a</sup>	Host <sup>b</sup>	Date	Field Number	H06 <sup>c</sup>	HK04 <sup>c</sup>	C89 <sup>c</sup>	MLA93 <sup>c</sup>
1	0:41:01.7	42:07:58.6	25.48	-283.3	-	-	2002.10.12	1	-	-	-	-
2	0:40:35.4	42:10:32.0	22.16	-133.9	-	-	2002.10.10	2	-	-	-	-
3	0:39:35.9	42:09:39.5	25.51	268.9	-	2MASXi	2002.10.10	3	-	-	-	-
4	0:39:37.3	42:09:59.6	23.52	354.5	E	2MASXi	2002.10.10	3	-	-	-	-
5	0:39:31.6	42:11:56.6	23.28	-343.3	-	-	2002.10.10	3	-	-	-	-
6	0:38:54.0	42:09:39.3	25.36	-266.7	E	-	2002.10.10	4	-	-	-	-
7	0:37:54.3	42:14:49.3	23.37	-328.1	-	-	2002.10.10	5	-	-	-	-
8	0:43:11.6	42:07:13.0	22.31	-194.0	-	-	2002.10.12	7	PN_10_3_1	-	-	-
9	0:43:10.5	42:11:33.3	23.58	-286.1	-	-	2002.10.12	7	PN_10_3_2	-	-	-
10	0:43:09.5	42:14:24.2	24.87	-314.2	-	-	2002.10.12	7	-	-	-	-
11	0:42:49.6	42:15:03.7	24.38	107.3	E	-	2002.10.12	7	-	-	-	-
12	0:44:08.6	42:06:00.0	25.62	-202.5	-	-	2002.10.13	8	-	-	-	-
13	0:44:09.8	42:06:40.2	22.99	-108.0	-	-	2002.10.13	8	PN_10_3_7	-	-	-

Continued on next page

Table A.1 – continued from previous page

ID	RA	Dec	$m_{5007}$	$v_{\text{helio}}$	Note	Host	Date	Field	H06	C89	HK04	MLA93
14	0:43:31.0	42:09:25.7	24.20	-136.6	-	-	2002.10.13	8	-	-	-	-
15	0:43:39.8	42:13:46.3	25.07	-210.8	-	-	2002.10.13	8	-	-	-	-
16	0:43:37.6	42:06:58.6	24.65	-554.4	E	Stream?	2002.10.13	8	-	-	-	-
17	0:44:59.8	42:07:44.8	21.76	-193.6	-	-	2002.10.12	9	PN_9_3_4	-	-	1091
18	0:45:00.9	42:08:44.8	23.53	-72.2	-	-	2002.10.12	9	-	-	-	-
19	0:44:30.5	42:08:55.2	22.36	-81.9	-	-	2002.10.12	9	PN_10_3_8	-	-	1005
20	0:44:51.4	42:09:34.2	23.81	-148.4	E,R	-	2002.10.12	9	-	-	-	-
21	0:44:36.3	42:10:18.5	25.22	-22.3	-	-	2002.10.12	9	-	-	-	-
22	0:44:48.0	42:11:54.2	23.07	-79.0	-	-	2002.10.12	9	-	-	-	-
23	0:44:52.2	42:11:57.5	21.52	-35.2	-	-	2002.10.12	9	PN_9_3_2	-	-	1064
24	0:44:55.5	42:13:46.2	23.61	-209.8	-	-	2002.10.12	9	-	-	-	-
25	0:44:56.4	42:14:30.9	23.30	-121.1	-	-	2002.10.12	9	-	-	-	-
26	0:45:52.7	42:05:12.6	24.55	-22.1	-	-	2002.10.13	10	-	-	-	-
27	0:45:45.9	42:06:17.2	24.84	-142.8	-	-	2002.10.13	10	-	-	-	-
28	0:45:41.7	42:06:27.4	25.18	-81.8	-	-	2002.10.13	10	-	-	-	-
29	0:45:50.7	42:06:49.3	24.40	2.9	-	-	2002.10.13	10	-	-	-	-
30	0:45:26.6	42:08:33.8	22.89	-538.0	-	Stream?	2002.10.13	10	PN_9_3_13	-	-	-
31	0:45:31.5	42:08:38.6	21.79	-268.1	-	-	2002.10.13	10	PN_9_3_14	-	-	1161
32	0:45:53.3	42:08:50.4	22.14	-70.3	-	-	2002.10.13	10	PN_9_3_19	-	-	1208
33	0:45:29.2	42:09:00.2	24.50	-105.7	-	-	2002.10.13	10	-	-	-	-
34	0:45:43.5	42:09:24.6	22.58	-342.2	-	-	2002.10.13	10	PN_9_3_16	-	-	-
35	0:45:53.2	42:09:35.8	23.90	-82.6	E	-	2002.10.13	10	-	-	-	-
36	0:45:26.9	42:09:27.0	25.37	-179.1	-	-	2002.10.13	10	-	-	-	-
37	0:45:14.3	42:11:56.7	22.65	-141.7	-	-	2002.10.13	10	PN_9_3_9	-	-	1125
38	0:45:18.9	42:12:44.5	22.39	-174.2	-	-	2002.10.13	10	PN_9_3_10	-	-	1134
39	0:45:23.7	42:13:01.6	23.82	-204.5	-	-	2002.10.13	10	-	-	-	-
40	0:45:42.2	42:13:50.4	23.58	-109.3	E	-	2002.10.13	10	-	-	-	-
41	0:45:12.7	42:13:46.9	25.36	-47.5	-	-	2002.10.13	10	-	-	-	-
42	0:45:25.4	42:14:10.6	24.15	-150.2	-	-	2002.10.13	10	PN_9_3_11	-	-	-
43	0:46:42.9	42:06:32.5	23.96	-33.1	E	-	2002.10.12	11	-	-	-	-
44	0:46:07.4	42:06:38.0	22.79	-86.4	-	-	2002.10.12	11	-	-	-	-
45	0:46:06.2	42:07:00.9	21.45	-79.7	-	-	2002.10.12	11	PN_9_3_23	-	-	1223
46	0:46:02.1	42:07:38.7	23.55	-202.3	-	-	2002.10.12	11	-	-	-	-
47	0:46:43.0	42:07:55.3	24.39	-126.3	-	-	2002.10.12	11	-	-	-	-
48	0:46:09.6	42:08:20.7	24.95	-26.2	-	-	2002.10.12	11	-	-	-	-
49	0:46:27.4	42:08:29.7	23.26	-63.1	-	-	2002.10.12	11	-	-	-	1247
50	0:46:42.9	42:08:35.3	20.33	-41.6	-	-	2002.10.12	11	-	-	-	1269
51	0:46:15.8	42:09:20.7	22.70	-53.0	-	-	2002.10.12	11	PN_9_3_27	-	-	-
52	0:46:38.5	42:10:58.2	22.93	-39.1	-	-	2002.10.12	11	-	-	-	-
53	0:46:43.0	42:11:08.9	21.31	-45.8	E,R	-	2002.10.12	11	-	-	-	-
54	0:46:10.5	42:11:21.5	24.33	-63.3	-	-	2002.10.12	11	-	-	-	-
55	0:46:33.2	42:11:38.1	20.60	-49.5	E,R	-	2002.10.12	11	-	-	-	-
56	0:46:08.4	42:11:31.2	21.03	-72.7	R	-	2002.10.12	11	PN_9_3_20	-	-	1228
57	0:46:34.3	42:11:43.1	17.75	-51.9	R	-	2002.10.12	11	-	-	-	1253
58	0:46:41.8	42:11:48.2	24.10	-24.1	-	-	2002.10.12	11	-	-	-	-
59	0:46:41.5	42:11:57.0	22.39	-54.9	-	-	2002.10.12	11	PN_9_3_29	-	-	1265
60	0:46:10.6	42:12:43.9	20.97	-66.3	E,R	-	2002.10.12	11	-	-	-	-
61	0:46:25.6	42:12:49.9	23.56	-86.5	-	-	2002.10.12	11	-	-	-	-
62	0:46:43.3	42:13:08.1	24.26	-68.6	-	-	2002.10.12	11	-	-	-	-
63	0:46:34.5	42:13:16.3	24.29	-112.8	-	-	2002.10.12	11	-	-	-	-
64	0:46:34.9	42:11:45.0	22.08	-42.8	E,R	-	2002.10.12	11	-	-	-	-
65	0:46:22.1	42:08:38.2	22.31	-11.5	E	-	2002.10.12	11	-	-	-	-
66	0:46:29.0	42:11:45.1	22.90	-57.9	E	-	2002.10.12	11	-	-	-	-
67	0:38:37.8	41:59:36.5	24.67	-254.9	-	-	2002.10.10	16	-	-	-	-
68	0:42:42.0	41:56:56.1	23.50	-104.1	-	-	2002.10.13	17	PN_10_4_2	-	-	-
69	0:42:51.7	41:58:46.3	23.50	-233.8	-	-	2002.10.13	17	PN_10_4_1	-	-	-
70	0:43:00.5	41:58:55.7	21.17	-279.8	-	-	2002.10.13	17	PN_10_4_9	-	-	660
71	0:42:59.0	42:02:14.2	20.83	-328.5	-	-	2002.10.13	17	PN_10_4_10	-	-	651
72	0:43:48.3	41:56:40.2	23.68	-220.3	E	-	2002.10.12	18	-	-	-	-
73	0:43:48.1	41:56:41.8	23.95	-188.2	E	-	2002.10.12	18	-	-	-	-
74	0:43:07.0	41:56:54.0	24.95	-113.7	-	-	2002.10.12	18	-	-	-	-
75	0:43:39.7	41:58:02.5	23.70	-160.1	-	-	2002.10.12	18	-	-	-	-
76	0:43:46.0	41:58:21.0	24.42	-204.4	E	-	2002.10.12	18	-	-	-	-
77	0:43:32.3	41:58:42.5	20.99	-579.0	-	Stream?	2002.10.12	18	PN_10_4_11	-	-	792
78	0:43:17.2	41:59:04.6	23.25	-186.6	-	-	2002.10.12	18	-	-	-	-
79	0:43:46.2	42:01:17.1	25.36	-91.6	-	-	2002.10.12	18	-	-	-	-
80	0:43:43.6	42:01:41.2	24.52	-195.2	E	-	2002.10.12	18	-	-	-	-
81	0:43:53.5	42:02:33.4	25.71	-146.7	-	-	2002.10.12	18	-	-	-	-
82	0:44:28.8	41:56:59.2	23.57	-134.3	-	-	2002.10.12	19	PN_10_4_28	-	-	-
83	0:44:16.2	41:57:02.7	20.84	-247.3	-	-	2002.10.12	19	PN_10_4_27	-	-	957
84	0:44:34.1	41:57:15.1	23.41	-165.3	E	-	2002.10.12	19	-	-	-	-
85	0:44:44.3	41:57:50.8	24.19	-131.3	E	-	2002.10.12	19	-	-	-	-
86	0:44:40.4	41:58:39.2	24.16	-155.1	-	-	2002.10.12	19	-	-	-	-
87	0:44:10.2	41:58:50.7	21.05	-165.3	E,R	-	2002.10.12	19	-	-	-	-
88	0:44:25.7	41:59:57.1	21.47	-173.5	-	-	2002.10.12	19	PN_10_4_25	-	-	989
89	0:44:30.5	42:00:35.2	21.05	-193.6	-	-	2002.10.12	19	-	-	-	1006
90	0:44:21.8	42:01:27.9	24.43	-168.4	-	-	2002.10.12	19	-	-	-	-
91	0:44:26.0	42:02:02.1	22.06	-170.6	R	-	2002.10.12	19	PN_9_2_42	-	-	992
92	0:44:10.1	42:02:59.0	21.55	-209.7	E,R	-	2002.10.12	19	-	-	-	-
93	0:44:15.0	42:01:56.4	22.73	519.0	R	MLA93_0953	2002.10.12	19	-	-	-	953
94	0:45:25.3	41:55:37.9	25.82	-83.6	E	-	2002.10.13	20	-	-	-	-
95	0:45:20.4	41:56:01.7	26.04	-74.6	-	-	2002.10.13	20	-	-	-	-
96	0:44:50.7	41:56:09.7	24.84	-60.2	R	-	2002.10.13	20	-	-	-	-
97	0:45:32.9	41:56:27.3	25.11	-56.2	-	-	2002.10.13	20	-	-	-	-
98	0:45:24.1	41:56:29.8	25.07	-86.8	-	-	2002.10.13	20	-	-	-	-
99	0:45:35.2	41:56:36.2	24.56	-48.4	E	-	2002.10.13	20	-	-	-	-
100	0:45:19.8	41:56:33.7	25.04	-97.3	-	-	2002.10.13	20	-	-	-	-
101	0:45:17.9	41:56:49.9	21.15	-227.5	-	-	2002.10.13	20	PN_9_4_7	-	-	1133
102	0:45:24.4	41:57:10.4	24.50	-87.8	E	-	2002.10.13	20	-	-	-	-
103	0:45:16.5	41:57:31.9	24.43	-81.9	-	-	2002.10.13	20	-	-	-	-
104	0:45:01.3	41:57:36.8	24.71	-82.4	-	-	2002.10.13	20	-	-	-	-
105	0:45:31.0	41:57:51.2	25.50	-152.2	E	-	2002.10.13	20	-	-	-	-
106	0:45:34.5	41:58:11.6	23.70	-60.5	E,R	-	2002.10.13	20	-	-	-	-

Continued on next page



Table A.1 – continued from previous page

ID	RA	Dec	$m_{5007}$	$v_{\text{helio}}$	Note	Host	Date	Field	H06	C89	HK04	MLA93
107	0:45:03.4	41:58:17.1	20.99	-126.2	-	-	2002.10.13	20	PN_9_4_11	-	-	1100
108	0:45:23.2	41:58:25.2	25.46	-106.7	-	-	2002.10.13	20	-	-	-	-
109	0:45:28.0	41:59:30.0	24.30	-72.0	R	-	2002.10.13	20	-	-	-	-
110	0:45:03.0	41:59:23.2	23.34	-92.8	-	-	2002.10.13	20	-	-	-	-
111	0:44:49.2	41:59:31.1	24.80	-119.1	-	-	2002.10.13	20	-	-	-	-
112	0:45:03.5	41:59:49.8	23.73	-202.2	-	-	2002.10.13	20	PN_9_4_9	-	-	-
113	0:45:12.7	42:00:00.9	23.78	-150.6	-	-	2002.10.13	20	-	-	-	-
114	0:45:04.2	42:00:11.3	24.99	-322.6	-	-	2002.10.13	20	-	-	-	-
115	0:45:23.0	42:00:38.9	22.91	-150.8	-	-	2002.10.13	20	PN_9_4_13	-	-	-
116	0:45:32.1	42:00:44.3	25.36	-57.7	E	-	2002.10.13	20	-	-	-	-
117	0:45:10.0	42:01:44.2	22.73	-58.5	E,R	-	2002.10.13	20	-	-	-	-
118	0:44:47.5	42:01:49.8	24.48	-141.3	-	-	2002.10.13	20	-	-	-	-
119	0:45:17.7	42:02:26.7	23.53	-105.2	-	-	2002.10.13	20	PN_9_4_8	-	-	-
120	0:45:10.3	42:02:27.8	21.21	-64.3	E,R	-	2002.10.13	20	-	-	-	1109
121	0:44:53.4	42:02:34.1	20.83	-125.0	E	-	2002.10.13	20	-	-	-	1067
122	0:44:47.3	42:02:59.4	23.07	-193.1	-	-	2002.10.13	20	-	-	-	-
123	0:44:53.0	42:03:35.2	23.37	-100.8	-	-	2002.10.13	20	-	-	-	-
124	0:44:53.5	42:04:03.9	25.19	-128.0	-	-	2002.10.13	20	-	-	-	-
125	0:44:47.4	41:57:00.7	22.46	-54.6	E	-	2002.10.13	20	-	-	-	1055
126	0:44:47.3	41:56:57.7	20.92	-87.1	E,R	-	2002.10.13	20	-	-	-	1055
127	0:45:28.8	41:57:18.1	24.67	-50.5	E	-	2002.10.13	20	-	-	-	-
128	0:46:04.9	41:56:37.2	21.36	-126.6	-	-	2002.10.10	21	PN_9_4_33	-	-	1222
129	0:45:42.9	41:58:19.8	21.15	-7.9	-	-	2002.10.10	21	PN_9_4_27	-	-	1183
130	0:45:43.8	41:59:33.1	23.07	-484.7	-	-	2002.10.10	21	-	-	-	-
131	0:45:49.0	41:59:38.1	21.77	-123.5	-	-	2002.10.10	21	PN_9_4_28	-	-	1198
132	0:45:46.2	41:59:42.2	22.76	-108.1	-	-	2002.10.10	21	PN_9_4_29	-	-	-
133	0:45:52.5	42:00:10.2	23.38	-251.2	-	-	2002.10.10	21	-	-	-	-
134	0:45:38.4	42:00:24.6	22.82	-127.5	-	-	2002.10.10	21	PN_9_4_14	-	-	1175
135	0:45:52.4	42:02:12.9	22.05	-132.0	-	-	2002.10.10	21	PN_9_4_32	-	-	1206
136	0:46:18.5	42:03:07.9	22.71	-196.5	-	-	2002.10.10	21	-	-	-	1239
137	0:45:46.0	42:03:33.7	22.48	-139.4	-	-	2002.10.10	21	PN_9_3_17	-	-	1193
138	0:45:52.1	42:04:05.1	23.13	-24.0	-	-	2002.10.10	21	PN_9_3_18	-	-	-
139	0:45:44.6	41:57:27.0	21.99	-89.2	E	-	2002.10.10	21	-	-	-	-
140	0:47:09.3	41:56:12.1	21.55	-94.0	-	-	2002.10.13	22	-	-	-	1288
141	0:47:04.9	41:56:37.9	24.06	-173.2	-	-	2002.10.13	22	-	-	-	-
142	0:46:24.5	41:56:25.5	25.54	-65.3	E	-	2002.10.13	22	-	-	-	-
143	0:46:43.8	41:56:39.2	24.75	-227.8	E	-	2002.10.13	22	-	-	-	-
144	0:46:24.7	41:56:37.4	24.21	-349.9	-	-	2002.10.13	22	-	-	-	-
145	0:46:32.9	41:56:42.5	25.33	-34.7	-	-	2002.10.13	22	-	-	-	-
146	0:47:05.2	41:56:59.6	24.43	-136.0	E	-	2002.10.13	22	-	-	-	-
147	0:46:33.1	41:57:03.0	23.49	-84.1	E,R	-	2002.10.13	22	-	-	-	-
148	0:47:12.2	41:57:19.3	25.32	-76.9	-	-	2002.10.13	22	-	-	-	-
149	0:46:43.9	41:58:09.7	23.53	-127.0	-	-	2002.10.13	22	-	-	-	-
150	0:46:33.7	41:59:12.3	24.02	-74.1	E	-	2002.10.13	22	-	-	-	-
151	0:46:45.8	41:59:53.1	23.77	-508.9	-	Stream?	2002.10.13	22	-	-	-	-
152	0:46:48.9	42:00:01.5	25.03	15.7	-	-	2002.10.13	22	-	-	-	-
153	0:46:31.2	42:00:34.3	25.35	-90.8	E	-	2002.10.13	22	-	-	-	-
154	0:46:25.1	42:00:33.3	25.22	-53.3	-	-	2002.10.13	22	-	-	-	-
155	0:46:54.5	42:00:48.3	20.28	-104.4	E,R	-	2002.10.13	22	-	-	-	1279
156	0:46:44.2	42:01:57.4	25.13	-107.4	E	-	2002.10.13	22	-	-	-	-
157	0:46:53.1	42:02:48.2	21.73	-83.9	E,R	-	2002.10.13	22	-	-	-	1278
158	0:46:42.2	42:03:06.4	24.86	-57.3	-	-	2002.10.13	22	-	-	-	-
159	0:46:39.7	42:03:06.7	25.00	-78.0	E	-	2002.10.13	22	-	-	-	-
160	0:46:27.0	42:03:08.6	25.36	-67.1	-	-	2002.10.13	22	-	-	-	-
161	0:46:28.9	42:03:10.4	23.85	-148.9	-	-	2002.10.13	22	-	-	-	-
162	0:46:32.4	42:03:42.0	22.17	14.3	-	-	2002.10.13	22	PN_9_3_30	-	-	1251
163	0:46:30.2	41:59:15.7	22.78	-65.9	E	-	2002.10.13	22	-	-	-	-
164	0:46:32.3	41:59:44.7	23.49	-71.7	E	-	2002.10.13	22	-	-	-	1250
165	0:41:07.8	41:48:55.2	25.67	-296.3	-	-	2002.10.11	23	-	-	-	-
166	0:41:07.4	41:49:56.8	24.40	-294.5	-	-	2002.10.11	23	-	-	-	-
167	0:41:26.6	41:50:41.7	25.21	-364.0	-	-	2002.10.11	23	-	-	-	-
168	0:41:19.1	41:51:46.5	22.68	-282.0	-	-	2002.10.11	23	-	-	-	-
169	0:41:39.1	41:52:54.4	24.51	-322.4	-	-	2002.10.11	23	-	-	-	-
170	0:40:54.6	41:48:16.0	21.53	-377.8	-	NGC205?	2002.10.10	24	PN_11_1_1	-	-	283
171	0:40:38.0	41:48:16.6	24.77	-489.8	E	NGC205?	2002.10.10	24	-	-	-	-
172	0:40:35.0	41:49:33.7	24.63	-203.0	-	NGC205	2002.10.10	24	-	-	-	-
173	0:40:00.4	41:49:19.4	21.90	-214.6	-	NGC205	2002.10.10	25	PN_7_1_6	-	-	161
174	0:39:01.0	41:51:11.1	20.89	-209.0	-	-	2002.10.10	26	PN_7_1_2	-	-	78
175	0:42:30.7	41:47:16.0	25.57	-258.9	-	-	2002.10.11	28	-	-	-	-
176	0:42:28.6	41:48:43.2	25.30	-253.8	-	-	2002.10.11	28	-	-	-	-
177	0:42:36.1	41:49:07.9	25.35	-370.7	-	-	2002.10.11	28	-	-	-	-
178	0:42:26.1	41:51:14.0	23.48	-116.1	-	-	2002.10.11	28	-	-	-	-
179	0:42:34.1	41:54:38.1	24.16	-340.7	-	-	2002.10.11	28	-	-	-	-
180	0:43:09.9	41:45:57.9	24.83	-224.4	E	-	2002.10.11	29	-	-	-	-
181	0:43:24.6	41:46:06.0	25.50	-249.4	-	-	2002.10.11	29	-	-	-	-
182	0:43:12.5	41:47:31.5	24.87	-103.8	-	-	2002.10.11	29	-	-	-	-
183	0:43:07.2	41:48:05.9	23.62	-81.7	-	-	2002.10.11	29	-	-	-	-
184	0:43:02.9	41:48:09.3	23.57	-228.1	E,R	-	2002.10.11	29	-	-	-	-
185	0:42:59.2	41:48:40.4	23.06	-213.9	-	-	2002.10.11	29	PN_10_1_7	-	-	-
186	0:42:50.6	41:49:52.2	25.46	-113.7	-	-	2002.10.11	29	-	-	-	-
187	0:43:19.2	41:50:17.0	22.61	-205.4	-	-	2002.10.11	29	-	-	-	-
188	0:43:23.7	41:50:19.0	21.99	-194.5	-	-	2002.10.11	29	PN_10_1_8	-	-	765
189	0:42:43.1	41:50:43.9	24.39	-132.4	-	-	2002.10.11	29	-	-	-	-
190	0:43:21.9	41:51:20.8	24.80	-180.9	-	-	2002.10.11	29	-	-	-	-
191	0:43:11.3	41:51:58.7	24.44	-158.2	-	-	2002.10.11	29	-	-	-	-
192	0:43:04.5	41:52:20.8	24.32	-276.3	-	-	2002.10.11	29	-	-	-	-
193	0:42:52.7	41:52:36.0	24.65	-153.1	-	-	2002.10.11	29	-	-	-	-
194	0:42:57.1	41:53:08.1	24.02	-147.4	-	-	2002.10.11	29	-	-	-	-
195	0:43:20.8	41:53:19.0	24.11	-133.1	-	-	2002.10.11	29	-	-	-	-
196	0:43:23.5	41:53:36.3	21.71	-283.0	-	-	2002.10.11	29	PN_10_4_15	-	-	764
197	0:43:17.4	41:53:47.1	22.02	-169.3	-	-	2002.10.11	29	-	-	-	-
198	0:43:00.7	41:53:51.4	23.44	-356.4	-	-	2002.10.11	29	-	-	-	-
199	0:43:11.8	41:53:57.6	24.21	-158.2	-	-	2002.10.11	29	-	-	-	-

Continued on next page

Table A.1 – continued from previous page

ID	RA	Dec	$m_{5007}$	$v_{\text{helio}}$	Note	Host	Date	Field	H06	C89	HK04	MLA93
200	0:42:51.7	41:54:23.6	22.78	-217.5	-	-	2002.10.11	29	-	-	-	-
201	0:43:00.6	41:50:12.7	23.41	-193.8	E	-	2002.10.11	29	-	-	-	-
202	0:44:01.3	41:47:08.7	23.62	-188.3	-	-	2002.10.12	30	PN_10.1.30	-	-	-
203	0:43:41.9	41:47:09.9	24.87	-170.2	-	-	2002.10.12	30	-	-	-	-
204	0:44:11.1	41:47:22.4	25.10	-170.8	E	-	2002.10.12	30	-	-	-	-
205	0:43:56.9	41:47:20.6	24.58	-207.9	E	-	2002.10.12	30	-	-	-	-
206	0:43:58.3	41:47:28.5	22.75	-171.4	E,R	-	2002.10.12	30	-	-	-	-
207	0:43:43.5	41:47:55.7	24.85	-167.0	-	-	2002.10.12	30	-	-	-	-
208	0:43:56.8	41:48:31.3	23.32	-160.9	E,R	-	2002.10.12	30	-	-	-	-
209	0:43:58.6	41:48:39.5	24.56	-164.6	E	-	2002.10.12	30	-	-	-	-
210	0:44:01.4	41:49:09.8	21.38	-176.2	E,R	-	2002.10.12	30	-	-	-	901
211	0:43:38.7	41:49:31.5	22.88	-200.9	-	-	2002.10.12	30	PN_10.1.18	-	-	-
212	0:43:36.6	41:49:43.2	21.04	-233.9	-	-	2002.10.12	30	PN_10.1.17	-	-	809
213	0:44:03.0	41:49:55.2	22.79	-164.6	E,R	-	2002.10.12	30	-	-	-	-
214	0:43:57.1	41:50:24.4	24.81	-147.2	-	-	2002.10.12	30	-	-	-	-
215	0:43:59.9	41:50:57.2	21.46	-39.5	-	-	2002.10.12	30	PN_10.1.31	-	-	898
216	0:43:39.1	41:51:00.9	24.83	-232.4	-	-	2002.10.12	30	-	-	-	-
217	0:44:11.1	41:51:31.9	24.20	-171.6	R	-	2002.10.12	30	-	-	-	-
218	0:44:13.2	41:51:55.4	23.69	-209.0	E	-	2002.10.12	30	-	-	-	-
219	0:43:33.1	41:52:45.8	21.69	-258.7	-	-	2002.10.12	30	PN_10.4.16	-	-	799
220	0:43:53.6	41:53:23.3	24.66	-227.6	E	-	2002.10.12	30	-	-	-	-
221	0:44:12.0	41:54:11.4	22.49	-164.0	-	-	2002.10.12	30	PN_10.4.23	-	-	941
222	0:43:32.8	41:54:10.1	21.31	-335.3	-	-	2002.10.12	30	PN_10.4.13	-	-	794
223	0:43:59.6	41:54:20.2	25.45	-271.5	-	-	2002.10.12	30	-	-	-	-
224	0:43:37.5	41:54:28.3	24.02	-233.7	E	-	2002.10.12	30	-	-	-	-
225	0:44:09.8	41:54:50.0	24.42	-177.6	-	-	2002.10.12	30	-	-	-	-
226	0:43:34.3	41:45:37.7	24.26	-230.8	E	-	2002.10.12	30	-	-	-	-
227	0:43:39.3	41:54:47.6	22.76	-179.6	-	-	2002.10.12	30	-	-	-	-
228	0:44:49.5	41:47:16.8	21.06	-170.6	-	-	2002.10.10	31	-	-	-	1057
229	0:44:50.7	41:47:33.7	21.58	-120.8	-	-	2002.10.10	31	-	-	-	1061
230	0:44:48.5	41:48:17.8	20.92	-143.0	-	-	2002.10.10	31	PN_9.1.4	-	-	1056
231	0:44:39.5	41:49:13.8	25.15	-45.8	-	-	2002.10.10	31	-	-	-	-
232	0:44:24.1	41:49:18.6	21.87	-104.2	E,R	-	2002.10.10	31	-	-	-	-
233	0:44:25.3	41:49:34.5	23.61	-73.4	E,R	-	2002.10.10	31	-	-	-	-
234	0:44:52.7	41:49:44.3	21.52	-174.2	-	-	2002.10.10	31	PN_9.1.3	-	-	1065
235	0:44:36.7	41:49:53.1	21.22	-239.3	-	-	2002.10.10	31	-	-	-	1024
236	0:44:28.6	41:49:56.3	23.97	-101.8	E	-	2002.10.10	31	-	-	-	-
237	0:44:38.5	41:50:19.7	21.43	-5.0	-	-	2002.10.10	31	-	-	-	1032
238	0:44:31.4	41:50:32.1	24.78	-167.2	-	-	2002.10.10	31	-	-	-	-
239	0:44:37.6	41:50:44.0	21.79	-141.1	-	-	2002.10.10	31	PN_9.2.32	-	-	1028
240	0:44:43.2	41:50:49.2	23.89	-98.1	-	-	2002.10.10	31	-	-	-	-
241	0:44:31.1	41:51:09.0	23.86	-67.3	E,R	-	2002.10.10	31	-	-	-	-
242	0:44:29.8	41:51:46.4	24.08	-119.1	E	-	2002.10.10	31	-	-	-	-
243	0:44:38.0	41:51:53.0	22.23	-109.5	R	-	2002.10.10	31	-	-	-	1030
244	0:44:30.7	41:51:52.5	23.14	-60.7	E,R	-	2002.10.10	31	-	-	-	-
245	0:44:30.7	41:51:58.1	22.45	-90.7	E,R	-	2002.10.10	31	-	-	-	-
246	0:44:30.1	41:51:58.2	22.65	-113.2	E,R	-	2002.10.10	31	-	-	-	-
247	0:44:37.6	41:52:02.8	21.62	-80.3	E	-	2002.10.10	31	-	-	-	1027
248	0:44:26.0	41:52:07.6	24.55	-115.3	-	-	2002.10.10	31	PN_10.4.31	-	-	-
249	0:44:37.0	41:52:48.3	22.78	-98.5	E	-	2002.10.10	31	-	-	-	1026
250	0:44:33.8	41:52:51.5	24.64	-44.9	-	-	2002.10.10	31	-	-	-	-
251	0:44:36.1	41:52:54.5	24.63	-17.3	E	-	2002.10.10	31	-	-	-	-
252	0:44:54.7	41:53:05.4	23.18	17.5	-	-	2002.10.10	31	PN_9.4.6	-	-	-
253	0:44:38.5	41:53:02.3	22.24	-132.3	-	-	2002.10.10	31	PN_10.4.32	-	-	1033
254	0:44:53.6	41:53:25.3	20.74	-112.0	-	-	2002.10.10	31	PN_9.4.3	-	-	1070
255	0:44:37.9	41:53:21.3	24.03	-131.1	R	-	2002.10.10	31	-	-	-	-
256	0:44:23.3	41:53:35.8	21.38	-105.9	-	-	2002.10.10	31	PN_10.4.30	-	-	978
257	0:44:44.1	41:53:59.2	21.29	-95.5	R	-	2002.10.10	31	-	-	-	1048
258	0:44:51.8	41:54:26.2	23.10	-94.7	E,R	-	2002.10.10	31	-	-	-	-
259	0:44:56.9	41:54:29.6	21.96	-72.7	-	-	2002.10.10	31	PN_9.4.4	-	-	1084
260	0:44:56.5	41:54:57.4	23.69	-69.1	-	-	2002.10.10	31	-	-	-	-
261	0:44:52.8	41:55:01.0	24.14	-102.2	R	-	2002.10.10	31	-	-	-	-
262	0:44:59.5	41:55:12.3	24.35	-53.0	R	-	2002.10.10	31	-	-	-	-
263	0:45:02.7	41:55:34.3	23.27	-96.8	E	-	2002.10.10	31	-	-	-	1098
264	0:44:44.6	41:47:05.9	22.28	-373.1	-	-	2002.10.10	31	PN_9.1.5	-	-	1050
265	0:44:25.2	41:50:05.0	20.53	-128.3	E,R	-	2002.10.10	31	-	-	-	-
266	0:44:38.2	41:52:11.1	23.49	-134.5	-	-	2002.10.10	31	-	-	-	-
267	0:44:37.6	41:53:02.5	22.70	-98.5	E	-	2002.10.10	31	-	-	-	-
268	0:44:46.0	41:52:58.9	23.50	-105.4	E	-	2002.10.10	31	-	-	-	-
269	0:45:45.8	41:47:05.8	22.58	-104.8	-	-	2002.10.10	32	-	-	-	1191
270	0:45:36.8	41:47:20.6	22.16	-80.6	-	-	2002.10.10	32	PN_9.1.26	-	-	1166
271	0:45:24.8	41:47:31.7	21.61	-100.8	-	-	2002.10.10	32	PN_9.1.19	-	-	1146
272	0:45:33.5	41:47:41.6	23.58	-30.0	E	-	2002.10.10	32	-	-	-	-
273	0:45:11.7	41:47:39.8	20.88	-142.8	-	-	2002.10.10	32	PN_9.1.20	-	-	1116
274	0:45:12.5	41:47:45.2	21.49	-102.4	-	-	2002.10.10	32	PN_9.1.21	-	-	1120
275	0:45:18.9	41:48:06.4	23.76	-216.6	-	-	2002.10.10	32	-	-	-	-
276	0:45:29.1	41:48:22.0	22.90	-179.8	-	-	2002.10.10	32	-	-	-	-
277	0:45:10.6	41:49:26.2	23.25	-118.8	-	-	2002.10.10	32	-	-	-	-
278	0:45:45.8	41:49:44.3	20.69	-220.9	-	-	2002.10.10	32	PN_9.1.24	-	-	1192
279	0:45:39.2	41:49:55.7	23.39	-85.0	-	-	2002.10.10	32	-	-	-	-
280	0:45:17.1	41:49:53.9	21.50	-84.6	-	-	2002.10.10	32	PN_9.1.22	-	-	1129
281	0:45:10.0	41:50:09.4	23.87	-112.6	-	-	2002.10.10	32	-	-	-	-
282	0:45:37.8	41:50:42.2	23.85	-119.1	-	-	2002.10.10	32	-	-	-	-
283	0:45:41.3	41:50:57.4	23.47	-152.1	-	-	2002.10.10	32	-	-	-	-
284	0:45:10.1	41:50:54.6	24.24	-226.3	E	-	2002.10.10	32	-	-	-	-
285	0:45:37.2	41:51:06.8	21.10	-65.1	E,R	-	2002.10.10	32	-	-	-	1169
286	0:45:37.2	41:51:12.9	21.60	-64.4	E,R	-	2002.10.10	32	-	-	-	-
287	0:45:40.8	41:51:15.9	22.11	-50.9	-	-	2002.10.10	32	-	-	-	1179
288	0:45:39.4	41:51:17.5	23.86	-123.5	E	-	2002.10.10	32	-	-	-	-
289	0:45:37.8	41:51:17.4	22.62	-149.0	-	-	2002.10.10	32	-	-	-	1173
290	0:45:48.6	41:51:22.7	23.92	-120.7	-	-	2002.10.10	32	-	-	-	-
291	0:45:45.1	41:51:37.4	23.75	-113.7	-	-	2002.10.10	32	-	-	-	-
292	0:45:29.8	41:51:44.3	24.50	-95.9	E	-	2002.10.10	32	-	-	-	-

Continued on next page

Table A.1 – continued from previous page

ID	RA	Dec	$m_{5007}$	$v_{\text{helio}}$	Note	Host	Date	Field	H06	C89	HK04	MLA93
293	0:45:14.8	41:51:45.1	24.29	-54.1	-	-	2002.10.10	32	-	-	-	-
294	0:45:24.3	41:52:00.1	22.35	-70.8	-	-	2002.10.10	32	PN_9_4_17	-	-	1144
295	0:45:44.2	41:52:07.2	21.20	-93.6	E,R	-	2002.10.10	32	-	-	-	1188
296	0:45:43.9	41:52:09.8	22.18	-57.9	E,R	-	2002.10.10	32	-	-	-	-
297	0:45:21.1	41:52:07.9	22.39	-51.7	-	-	2002.10.10	32	PN_9_4_16	-	-	1136
298	0:45:42.9	41:52:34.6	21.67	-66.1	R	-	2002.10.10	32	-	-	-	1182
299	0:45:38.7	41:52:35.3	22.47	-52.8	E,R	-	2002.10.10	32	-	-	-	-
300	0:45:44.7	41:52:40.9	23.15	-62.7	-	-	2002.10.10	32	-	-	-	-
301	0:45:43.3	41:53:00.3	19.67	-74.8	E,R	-	2002.10.10	32	-	-	-	1184
302	0:45:32.5	41:52:57.4	23.97	-52.2	-	-	2002.10.10	32	-	-	-	-
303	0:45:33.0	41:53:00.5	23.67	-46.5	-	-	2002.10.10	32	-	-	-	-
304	0:45:16.7	41:53:31.3	24.40	-98.4	E	-	2002.10.10	32	-	-	-	-
305	0:45:24.3	41:53:52.1	24.02	-123.0	-	-	2002.10.10	32	-	-	-	1143
306	0:45:49.6	41:54:02.1	22.13	-133.4	-	-	2002.10.10	32	-	-	-	1200
307	0:45:37.6	41:54:24.2	22.84	-68.5	R	-	2002.10.10	32	-	-	-	1172
308	0:45:15.8	41:54:30.0	24.34	-119.2	-	-	2002.10.10	32	-	-	-	-
309	0:45:48.9	41:55:26.7	23.27	-172.4	E	-	2002.10.10	32	-	-	-	-
310	0:45:16.0	41:49:52.2	23.82	-42.2	E	-	2002.10.10	32	-	-	-	-
311	0:45:35.6	41:51:20.6	24.82	-216.1	-	-	2002.10.10	32	-	-	-	-
312	0:45:42.7	41:52:07.4	22.49	-551.8	-	Stream?	2002.10.10	32	PN_9_4_25	-	-	-
313	0:45:49.3	41:51:35.1	23.40	-404.0	-	-	2002.10.10	32	-	-	-	-
314	0:45:12.2	41:54:34.5	23.93	-45.2	-	-	2002.10.10	32	-	-	-	-
315	0:46:29.3	41:47:29.5	23.94	-178.9	-	-	2002.10.11	33	-	-	-	-
316	0:46:24.7	41:47:55.0	24.54	-96.8	-	-	2002.10.11	33	-	-	-	-
317	0:46:05.2	41:47:48.6	24.32	-156.3	E	-	2002.10.11	33	-	-	-	-
318	0:46:07.3	41:48:08.9	21.49	-133.6	-	-	2002.10.11	33	PN_9_1_39	-	-	1226
319	0:46:13.6	41:49:30.1	20.37	-130.2	-	-	2002.10.11	33	-	-	-	1235
320	0:46:19.1	41:49:42.7	22.37	-88.3	-	-	2002.10.11	33	PN_9_1_41	-	-	1241
321	0:46:01.9	41:49:47.2	20.79	-66.1	-	-	2002.10.11	33	PN_9_1_37	-	-	1220
322	0:46:19.6	41:50:30.8	22.11	-140.9	E,R	-	2002.10.11	33	-	-	-	-
323	0:46:08.1	41:51:00.0	22.35	-89.0	-	-	2002.10.11	33	PN_9_1_38	-	-	1227
324	0:46:17.6	41:51:58.3	19.19	-89.3	R	-	2002.10.11	33	-	-	-	1237
325	0:46:07.1	41:52:04.7	23.36	-19.8	-	-	2002.10.11	33	-	-	-	-
326	0:46:18.3	41:52:22.3	21.12	-125.1	-	-	2002.10.11	33	PN_9_4_40	-	-	1238
327	0:46:13.2	41:52:24.8	21.66	-95.0	E,R	-	2002.10.11	33	-	-	-	1234
328	0:45:59.8	41:52:26.1	23.91	-196.4	E	-	2002.10.11	33	-	-	-	-
329	0:46:04.5	41:52:41.9	23.41	-132.4	-	-	2002.10.11	33	-	-	-	1221
330	0:46:35.6	41:52:53.9	24.50	-137.2	-	-	2002.10.11	33	-	-	-	-
331	0:46:44.7	41:53:20.6	21.97	-270.0	-	-	2002.10.11	33	-	-	-	1272
332	0:46:12.0	41:53:34.9	24.05	-55.9	-	-	2002.10.11	33	-	-	-	-
333	0:45:59.7	41:54:24.1	23.28	-84.7	-	-	2002.10.11	33	-	-	-	-
334	0:46:00.5	41:55:09.6	24.18	-99.9	E	-	2002.10.11	33	-	-	-	-
335	0:41:57.0	41:37:03.9	24.85	-264.1	E	-	2002.10.11	34	PN_1_3_7	-	-	426
336	0:41:55.7	41:38:17.7	24.20	-209.0	-	-	2002.10.11	34	-	-	-	-
337	0:41:41.0	41:38:14.8	20.58	4.7	-	-	2002.10.11	34	-	-	-	386
338	0:42:09.9	41:38:45.0	22.07	-179.4	-	-	2002.10.11	34	-	-	-	458
339	0:42:07.1	41:38:45.2	23.88	-221.7	-	-	2002.10.11	34	-	-	-	-
340	0:42:00.1	41:39:22.5	24.65	-179.3	E	-	2002.10.11	34	-	-	-	-
341	0:41:49.7	41:43:04.7	24.75	-343.6	-	-	2002.10.11	34	-	-	-	-
342	0:42:09.7	41:43:29.7	24.75	-198.7	-	-	2002.10.11	34	-	-	-	-
343	0:41:48.3	41:43:30.4	23.93	-287.1	-	-	2002.10.11	34	PN_1_1_1_6	-	-	-
344	0:40:38.8	41:38:18.4	25.69	-310.3	-	NGC205	2002.10.10	35	-	-	-	-
345	0:41:11.6	41:38:34.5	25.46	-455.9	-	-	2002.10.10	35	-	-	-	-
346	0:41:19.6	41:41:09.9	22.85	-369.2	-	-	2002.10.10	35	PN_1_1_1_5	-	-	-
347	0:41:10.6	41:42:10.9	23.71	-265.3	-	NGC205	2002.10.10	35	-	-	-	-
348	0:40:49.5	41:38:12.2	22.65	-278.8	E	NGC205	2002.10.10	35	-	-	-	-
349	0:39:31.5	41:40:51.6	25.30	-243.1	-	-	2002.10.10	37	-	-	-	-
350	0:39:10.2	41:43:16.9	24.04	-302.5	-	-	2002.10.10	37	-	-	-	-
351	0:39:20.1	41:43:22.9	25.17	-242.6	-	-	2002.10.10	37	-	-	-	-
352	0:38:48.4	41:39:37.5	22.35	-216.9	-	-	2002.10.10	38	-	-	-	70
353	0:38:12.4	41:42:47.7	24.12	-191.0	-	-	2002.10.10	38	-	-	-	-
354	0:42:26.3	41:38:25.3	21.18	-426.8	-	-	2002.10.10	39	-	-	-	509
355	0:42:37.9	41:38:31.0	24.75	-301.6	-	-	2002.10.10	39	-	-	-	-
356	0:42:17.0	41:38:34.5	22.00	-52.8	-	-	2002.10.10	39	-	-	-	478
357	0:42:42.9	41:39:29.1	22.24	-195.8	-	-	2002.10.10	39	-	-	-	583
358	0:42:44.3	41:39:43.9	24.38	-447.6	-	-	2002.10.10	39	-	-	-	-
359	0:42:19.8	41:40:05.9	24.46	-252.1	-	-	2002.10.10	39	-	-	-	-
360	0:42:51.5	41:40:58.1	23.70	-296.1	-	-	2002.10.10	39	-	-	-	-
361	0:42:54.3	41:41:28.7	24.16	-211.2	-	-	2002.10.10	39	PN_10_1_3	-	-	-
362	0:42:27.5	41:43:01.5	24.76	-157.8	E	-	2002.10.10	39	-	-	-	-
363	0:42:38.2	41:44:45.3	25.36	-258.0	R	-	2002.10.10	39	-	-	-	-
364	0:43:10.1	41:37:20.9	24.59	-173.1	E	-	2002.10.10	40	-	-	-	-
365	0:43:23.6	41:37:33.8	24.03	-152.4	-	-	2002.10.10	40	-	-	-	-
366	0:43:38.7	41:37:51.6	23.76	-174.0	-	-	2002.10.10	40	-	-	-	-
367	0:43:10.0	41:37:51.5	24.05	-243.7	-	-	2002.10.10	40	-	-	-	-
368	0:43:49.6	41:38:07.7	22.08	-107.3	-	-	2002.10.10	40	PN_6_3_52	-	-	864
369	0:43:36.0	41:38:55.4	24.24	-102.2	-	-	2002.10.10	40	-	-	-	-
370	0:43:40.5	41:39:15.8	24.60	-222.0	-	-	2002.10.10	40	-	-	-	-
371	0:43:45.9	41:42:36.8	24.06	-135.1	-	-	2002.10.10	40	-	-	-	-
372	0:43:36.3	41:42:57.3	23.37	-124.9	-	-	2002.10.10	40	PN_10_1_15	-	-	-
373	0:43:05.9	41:42:57.5	23.86	-228.4	-	-	2002.10.10	40	-	-	-	-
374	0:43:05.7	41:43:07.1	23.01	-232.1	R	-	2002.10.10	40	-	-	-	-
375	0:43:44.1	41:43:40.1	24.36	-233.8	-	-	2002.10.10	40	-	-	-	-
376	0:43:18.2	41:43:35.6	21.70	-239.5	-	-	2002.10.10	40	PN_10_1_14	-	-	743
377	0:43:41.4	41:45:21.7	24.41	-177.1	E,R	-	2002.10.10	40	-	-	-	-
378	0:43:13.6	41:45:30.6	23.30	-111.9	-	-	2002.10.10	40	-	-	-	-
379	0:43:43.2	41:38:31.8	24.78	-204.0	-	-	2002.10.10	40	-	-	-	-
380	0:43:12.1	41:41:46.1	23.60	-152.2	-	-	2002.10.10	40	-	-	-	-
381	0:43:35.0	41:43:58.2	23.59	-294.8	-	-	2002.10.10	40	-	-	-	-
382	0:44:29.7	41:37:28.2	25.01	-246.9	-	-	2002.10.10	41	-	-	-	-
383	0:44:30.6	41:37:44.7	22.41	-57.8	-	-	2002.10.10	41	-	-	-	1008
384	0:43:56.5	41:38:09.2	22.17	-191.0	R	-	2002.10.10	41	-	-	-	886
385	0:44:14.3	41:38:22.9	24.03	-78.1	E	-	2002.10.10	41	-	-	-	-

Continued on next page

Table A.1 – continued from previous page

ID	RA	Dec	$m_{5007}$	$v_{\text{helio}}$	Note	Host	Date	Field	H06	C89	HK04	MLA93
386	0:44:25.0	41:38:30.6	21.48	-206.1	-	-	2002.10.10	41	PN_6_3_88	-	-	984
387	0:44:40.4	41:38:41.3	24.36	-312.1	-	-	2002.10.10	41	-	-	-	-
388	0:44:03.4	41:38:31.1	22.42	-161.9	-	-	2002.10.10	41	-	-	-	-
389	0:44:33.3	41:38:46.6	23.70	-8.6	-	-	2002.10.10	41	-	-	-	-
390	0:44:12.2	41:38:41.1	23.63	-191.1	-	-	2002.10.10	41	-	-	-	-
391	0:44:17.0	41:38:45.2	23.17	-150.8	-	-	2002.10.10	41	-	-	-	-
392	0:44:06.1	41:38:45.7	24.63	-106.5	-	-	2002.10.10	41	-	-	-	-
393	0:43:53.8	41:38:47.1	24.83	-125.3	-	-	2002.10.10	41	-	-	-	-
394	0:44:29.5	41:39:00.5	23.80	-99.6	-	-	2002.10.10	41	-	-	-	-
395	0:44:21.3	41:39:29.7	21.65	-140.8	-	-	2002.10.10	41	-	-	-	973
396	0:44:08.7	41:39:33.6	21.87	-257.8	-	-	2002.10.10	41	-	-	-	926
397	0:44:11.2	41:39:45.1	23.78	-211.7	-	-	2002.10.10	41	-	-	-	-
398	0:44:21.4	41:39:50.6	24.89	-186.3	-	-	2002.10.10	41	-	-	-	-
399	0:44:08.4	41:39:49.3	24.91	-47.0	-	-	2002.10.10	41	-	-	-	-
400	0:44:07.5	41:39:49.6	23.58	-173.8	-	-	2002.10.10	41	-	-	-	-
401	0:44:09.4	41:39:59.5	21.11	-126.7	-	-	2002.10.10	41	-	-	-	930
402	0:44:21.5	41:40:05.8	22.55	-224.6	-	-	2002.10.10	41	-	-	-	-
403	0:44:00.6	41:40:22.1	24.44	-170.3	-	-	2002.10.10	41	-	-	-	-
404	0:44:16.7	41:40:37.5	25.21	-45.5	-	-	2002.10.10	41	-	-	-	-
405	0:44:23.6	41:40:49.4	21.96	-14.8	-	-	2002.10.10	41	PN_10_1_37	-	-	979
406	0:44:06.3	41:41:33.5	24.11	-8.7	-	-	2002.10.10	41	-	-	-	-
407	0:44:19.6	41:41:58.9	24.58	-112.7	-	-	2002.10.10	41	-	-	-	-
408	0:44:20.1	41:42:02.8	23.45	-67.7	-	-	2002.10.10	41	-	-	-	-
409	0:44:32.9	41:42:10.4	25.16	-87.7	-	-	2002.10.10	41	-	-	-	-
410	0:43:56.7	41:42:01.3	23.39	-219.2	-	-	2002.10.10	41	-	-	-	-
411	0:44:16.3	41:42:22.6	23.30	-150.9	-	-	2002.10.10	41	PN_10_1_36	-	-	-
412	0:43:57.6	41:42:21.5	24.19	-197.4	-	-	2002.10.10	41	-	-	-	-
413	0:44:28.4	41:42:35.2	23.40	-168.5	-	-	2002.10.10	41	-	-	-	-
414	0:44:09.5	41:42:35.7	23.06	-47.0	-	-	2002.10.10	41	-	-	-	-
415	0:44:25.1	41:42:45.4	23.16	-85.6	-	-	2002.10.10	41	PN_10_1_33	-	-	-
416	0:44:24.4	41:42:50.1	24.67	-1.9	-	-	2002.10.10	41	-	-	-	-
417	0:44:13.4	41:43:12.5	23.87	14.0	-	-	2002.10.10	41	-	-	-	-
418	0:44:08.6	41:43:43.6	22.40	-72.5	-	-	2002.10.10	41	-	-	-	925
419	0:44:38.2	41:43:53.9	22.66	-168.6	-	-	2002.10.10	41	PN_10_1_38	-	-	-
420	0:43:54.9	41:43:52.0	22.47	-520.8	-	-	2002.10.10	41	PN_10_1_27	-	-	879
421	0:44:00.3	41:43:57.1	21.03	-135.6	-	-	2002.10.10	41	PN_10_1_26	-	-	900
422	0:44:31.7	41:44:12.1	24.23	-96.4	-	-	2002.10.10	41	-	-	-	-
423	0:44:25.5	41:44:18.9	25.59	-46.1	-	-	2002.10.10	41	-	-	-	-
424	0:44:02.1	41:44:16.1	22.68	-216.4	-	-	2002.10.10	41	-	-	-	-
425	0:44:12.4	41:44:19.6	21.69	-172.8	-	-	2002.10.10	41	PN_10_1_24	-	-	946
426	0:44:27.6	41:44:29.0	22.19	-156.9	-	-	2002.10.10	41	-	-	-	999
427	0:44:05.1	41:45:14.8	23.40	-174.6	-	-	2002.10.10	41	-	-	-	-
428	0:44:22.0	41:46:54.6	24.91	-62.9	-	-	2002.10.10	41	-	-	-	-
429	0:44:12.1	41:39:49.0	22.31	-665.7	-	Stream?	2002.10.10	41	PN_6_3_85	-	-	945
430	0:43:54.8	41:42:03.7	24.39	-148.6	-	-	2002.10.10	41	-	-	-	-
431	0:45:29.8	41:37:52.8	24.62	-200.3	-	-	2002.10.10	42	-	-	-	-
432	0:45:00.7	41:37:57.7	24.51	-160.2	E	-	2002.10.10	42	-	-	-	-
433	0:45:02.0	41:38:03.8	24.53	-191.3	-	-	2002.10.10	42	-	-	-	-
434	0:44:49.6	41:38:03.2	24.26	-313.0	-	-	2002.10.10	42	-	-	-	-
435	0:44:59.6	41:38:19.7	24.94	-201.5	E	-	2002.10.10	42	-	-	-	-
436	0:45:08.0	41:38:45.9	24.35	-173.5	-	-	2002.10.10	42	-	-	-	-
437	0:45:14.8	41:38:58.3	24.27	-125.3	-	-	2002.10.10	42	-	-	-	-
438	0:45:14.4	41:39:03.3	21.82	-143.6	-	-	2002.10.10	42	PN_5_3_19	-	-	1126
439	0:45:14.8	41:39:15.5	23.89	-176.9	-	-	2002.10.10	42	-	-	-	-
440	0:45:00.4	41:39:15.1	20.68	-179.6	-	-	2002.10.10	42	-	-	-	1094
441	0:45:18.1	41:39:21.9	21.78	-133.1	E,R	-	2002.10.10	42	-	-	-	-
442	0:45:12.4	41:39:20.7	20.46	-123.2	-	-	2002.10.10	42	-	-	-	1119
443	0:44:49.8	41:39:16.4	21.86	-193.7	-	-	2002.10.10	42	PN_5_3_2	-	-	1058
444	0:44:57.3	41:39:27.6	24.41	-182.2	-	-	2002.10.10	42	-	-	-	-
445	0:45:27.3	41:39:44.3	23.45	-139.8	-	-	2002.10.10	42	-	-	-	-
446	0:45:08.4	41:39:38.7	22.30	-150.1	-	-	2002.10.10	42	-	-	-	-
447	0:45:27.7	41:39:58.3	23.50	-163.0	-	-	2002.10.10	42	-	-	-	-
448	0:45:18.5	41:40:13.8	21.64	-159.9	R	-	2002.10.10	42	-	-	-	-
449	0:45:06.2	41:40:18.7	23.98	-187.0	-	-	2002.10.10	42	-	-	-	-
450	0:45:13.3	41:40:29.0	23.11	-193.7	-	-	2002.10.10	42	-	-	-	-
451	0:45:15.0	41:40:30.1	23.15	-149.4	E,R	-	2002.10.10	42	-	-	-	-
452	0:45:21.4	41:40:40.9	24.89	-209.5	-	-	2002.10.10	42	-	-	-	-
453	0:45:02.0	41:40:38.1	23.33	-154.3	E	-	2002.10.10	42	-	-	-	-
454	0:45:26.7	41:40:48.5	23.05	-219.9	-	-	2002.10.10	42	-	-	-	-
455	0:45:22.6	41:40:56.8	23.47	-148.9	E,R	-	2002.10.10	42	-	-	-	-
456	0:45:27.1	41:41:18.0	22.62	-165.4	-	-	2002.10.10	42	PN_9_1_29	-	-	1153
457	0:44:56.9	41:41:11.3	24.51	-207.1	-	-	2002.10.10	42	-	-	-	-
458	0:45:08.8	41:41:18.9	24.49	-53.2	E	-	2002.10.10	42	-	-	-	-
459	0:45:09.3	41:41:23.5	23.83	-151.4	-	-	2002.10.10	42	-	-	-	-
460	0:45:08.0	41:41:23.3	24.45	-170.5	-	-	2002.10.10	42	-	-	-	-
461	0:45:13.2	41:41:39.1	23.84	-209.3	-	-	2002.10.10	42	-	-	-	-
462	0:45:25.3	41:41:58.0	24.77	-105.9	-	-	2002.10.10	42	-	-	-	-
463	0:44:56.6	41:41:49.0	23.86	-217.9	-	-	2002.10.10	42	-	-	-	-
464	0:44:59.2	41:41:49.9	24.38	-130.2	E	-	2002.10.10	42	-	-	-	-
465	0:45:06.8	41:41:54.0	24.45	-204.3	-	-	2002.10.10	42	-	-	-	-
466	0:44:45.0	41:41:56.4	23.12	-101.8	-	-	2002.10.10	42	PN_9_1_14	-	-	-
467	0:45:18.4	41:42:15.7	23.27	-144.4	-	-	2002.10.10	42	-	-	-	-
468	0:44:46.8	41:42:05.9	24.42	-30.9	-	-	2002.10.10	42	-	-	-	-
469	0:45:10.2	41:42:26.0	21.97	-98.9	-	-	2002.10.10	42	-	-	-	1110
470	0:44:53.8	41:42:23.0	21.28	-109.2	-	-	2002.10.10	42	PN_9_1_12	-	-	1071
471	0:45:25.1	41:42:47.5	23.33	-150.5	E	-	2002.10.10	42	-	-	-	-
472	0:44:53.4	41:43:04.4	23.33	-103.9	-	-	2002.10.10	42	-	-	-	-
473	0:44:56.1	41:43:08.9	24.71	-229.3	E	-	2002.10.10	42	-	-	-	-
474	0:45:13.7	41:43:16.6	23.40	-136.4	E	-	2002.10.10	42	-	-	-	-
475	0:45:24.4	41:43:35.0	21.73	-100.3	-	-	2002.10.10	42	-	-	-	1145
476	0:45:12.1	41:43:41.5	24.89	-110.2	-	-	2002.10.10	42	-	-	-	-
477	0:45:14.9	41:43:46.6	23.06	-173.5	-	-	2002.10.10	42	-	-	-	-
478	0:44:44.5	41:44:12.7	22.80	-177.8	-	-	2002.10.10	42	-	-	-	1051

Continued on next page

Table A.1 – continued from previous page

ID	RA	Dec	$m_{5007}$	$v_{\text{helio}}$	Note	Host	Date	Field	H06	C89	HK04	MLA93
479	0:45:21.6	41:44:36.6	21.69	-175.5	-	-	2002.10.10	42	-	-	-	1140
480	0:45:28.7	41:45:15.8	23.84	-157.8	E	-	2002.10.10	42	-	-	-	-
481	0:45:11.6	41:37:16.7	22.08	-158.5	E,R	-	2002.10.10	42	-	-	-	-
482	0:45:18.6	41:40:40.2	24.12	-152.7	R	-	2002.10.10	42	-	-	-	-
483	0:45:31.4	41:45:33.3	24.22	-119.6	E	-	2002.10.10	42	-	-	-	-
484	0:45:33.6	41:38:59.4	24.77	-189.3	-	-	2002.10.11	43	-	-	-	-
485	0:46:01.0	41:39:15.0	24.72	-190.9	-	-	2002.10.11	43	-	-	-	-
486	0:46:00.6	41:39:26.3	22.96	-117.1	-	-	2002.10.11	43	PN_5_3_32	-	-	-
487	0:46:04.6	41:39:33.6	24.76	-354.8	E	-	2002.10.11	43	-	-	-	-
488	0:45:53.9	41:39:55.9	23.76	-167.2	-	-	2002.10.11	43	-	-	-	-
489	0:45:38.7	41:40:37.1	23.68	-220.9	-	-	2002.10.11	43	PN_9_1_31	-	-	-
490	0:46:07.3	41:41:10.5	24.49	-355.5	-	-	2002.10.11	43	-	-	-	-
491	0:45:50.0	41:41:19.5	24.63	-169.9	-	-	2002.10.11	43	-	-	-	-
492	0:46:15.9	41:42:01.7	23.30	-112.9	-	-	2002.10.11	43	-	-	-	-
493	0:45:42.6	41:42:05.8	25.01	-71.8	E	-	2002.10.11	43	-	-	-	-
494	0:45:43.6	41:42:35.8	22.32	-126.5	E,R	-	2002.10.11	43	-	-	-	-
495	0:45:36.7	41:42:52.1	23.26	-138.1	E,R	-	2002.10.11	43	-	-	-	-
496	0:45:41.6	41:43:06.4	22.37	-193.3	-	-	2002.10.11	43	PN_9_1_32	-	-	1181
497	0:46:15.3	41:43:22.1	23.62	-124.0	-	-	2002.10.11	43	-	-	-	-
498	0:45:56.0	41:43:16.4	20.75	-158.3	-	-	2002.10.11	43	PN_9_1_33	-	-	1214
499	0:46:17.4	41:43:28.5	22.79	-319.9	-	-	2002.10.11	43	-	-	-	-
500	0:45:42.0	41:43:27.0	24.21	-123.1	E	-	2002.10.11	43	-	-	-	-
501	0:45:42.1	41:44:27.6	22.93	-112.2	E,R	-	2002.10.11	43	-	-	-	-
502	0:45:42.3	41:44:28.9	22.47	-169.6	-	-	2002.10.11	43	PN_9_1_28	-	-	-
503	0:46:00.4	41:44:38.3	23.57	-144.5	E	-	2002.10.11	43	-	-	-	-
504	0:45:52.6	41:44:39.3	24.13	-123.7	-	-	2002.10.11	43	-	-	-	-
505	0:46:00.5	41:44:48.3	21.44	-134.7	R	-	2002.10.11	43	-	-	-	1218
506	0:45:54.3	41:44:54.0	23.13	-76.3	-	-	2002.10.11	43	-	-	-	-
507	0:45:54.0	41:45:09.3	23.98	-44.7	-	-	2002.10.11	43	-	-	-	-
508	0:45:37.0	41:45:09.6	25.25	-35.4	-	-	2002.10.11	43	-	-	-	-
509	0:41:42.8	41:27:39.6	25.38	-274.0	-	-	2002.10.11	44	-	-	-	-
510	0:41:21.5	41:28:53.9	24.14	-276.7	-	-	2002.10.11	44	-	-	-	-
511	0:41:33.3	41:29:09.5	24.82	-433.0	-	-	2002.10.11	44	-	-	-	-
512	0:41:39.1	41:29:25.4	24.76	-384.0	-	-	2002.10.11	44	-	-	-	-
513	0:41:07.3	41:30:06.7	25.48	-364.3	-	-	2002.10.11	44	-	-	-	-
514	0:41:27.2	41:33:13.2	25.36	-179.3	-	-	2002.10.11	44	-	-	-	-
515	0:41:41.7	41:34:03.1	21.51	-314.3	-	-	2002.10.11	44	-	-	-	388
516	0:41:41.7	41:35:10.1	25.37	-222.5	-	-	2002.10.11	44	-	-	-	-
517	0:41:21.4	41:29:59.5	24.59	-239.2	-	-	2002.10.11	44	-	-	-	-
518	0:41:42.5	41:35:03.3	24.48	-377.9	-	-	2002.10.11	44	-	-	-	-
519	0:40:45.3	41:28:37.8	24.62	-409.5	E	-	2002.10.11	45	-	-	-	-
520	0:40:42.6	41:29:38.7	24.03	-262.0	-	-	2002.10.11	45	PN_1_3_3	-	-	-
521	0:40:28.7	41:33:00.9	22.60	-307.3	-	NGC205	2002.10.11	45	PN_8_3_12	-	-	223
522	0:40:47.4	41:33:44.1	25.52	-405.1	-	NGC205?	2002.10.11	45	-	-	-	-
523	0:40:54.2	41:36:09.2	23.72	-433.9	-	NGC205?	2002.10.11	45	-	-	-	-
524	0:39:50.7	41:30:43.1	22.78	-260.5	-	-	2002.10.11	46	PN_8_3_2	-	-	-
525	0:39:35.8	41:32:35.2	25.48	-385.4	-	-	2002.10.11	46	-	-	-	-
526	0:39:56.6	41:35:19.1	22.69	-225.9	-	NGC205	2002.10.11	46	PN_8_3_3	-	-	-
527	0:37:59.7	41:31:29.1	25.43	-360.7	-	-	2002.10.12	48	-	-	-	-
528	0:42:21.8	41:28:27.7	21.96	-299.7	E,R	-	2002.10.10	49	-	-	-	-
529	0:42:33.5	41:29:16.7	22.52	-254.2	E	-	2002.10.10	49	-	-	-	-
530	0:42:30.2	41:29:36.3	23.24	-280.4	R	-	2002.10.10	49	-	-	-	-
531	0:42:06.8	41:29:30.6	23.59	-244.8	-	-	2002.10.10	49	-	-	-	-
532	0:42:34.2	41:30:04.4	23.37	-323.8	E,R	-	2002.10.10	49	-	-	-	-
533	0:42:34.1	41:30:08.1	23.98	-308.1	R	-	2002.10.10	49	-	-	-	-
534	0:42:30.7	41:30:24.6	23.23	-218.0	-	-	2002.10.10	49	-	-	-	-
535	0:42:33.2	41:30:35.0	23.22	-161.0	-	-	2002.10.10	49	-	-	-	-
536	0:42:12.9	41:30:34.6	24.80	-322.3	-	-	2002.10.10	49	-	-	-	-
537	0:42:22.9	41:30:44.2	24.04	-329.7	-	-	2002.10.10	49	-	-	-	-
538	0:42:26.2	41:31:01.1	22.39	-347.2	-	-	2002.10.10	49	-	-	-	-
539	0:42:31.6	41:31:13.6	25.31	-287.7	E	-	2002.10.10	49	-	-	-	-
540	0:42:22.2	41:31:24.3	24.32	-180.2	-	-	2002.10.10	49	-	-	-	-
541	0:42:12.5	41:31:24.9	25.18	-237.0	-	-	2002.10.10	49	-	-	-	-
542	0:41:59.1	41:31:49.1	24.09	-265.4	-	-	2002.10.10	49	-	-	-	-
543	0:42:12.4	41:33:06.1	22.77	-228.2	-	-	2002.10.10	49	-	-	-	-
544	0:42:06.6	41:33:16.9	24.96	-227.0	-	-	2002.10.10	49	-	-	-	-
545	0:42:23.8	41:33:35.9	24.13	-379.7	-	-	2002.10.10	49	-	-	-	-
546	0:42:21.9	41:33:44.7	21.89	-203.0	-	-	2002.10.10	49	-	-	-	488
547	0:42:03.1	41:33:53.3	22.46	-248.9	-	-	2002.10.10	49	-	-	-	439
548	0:42:12.7	41:35:20.5	22.52	-266.0	E	-	2002.10.10	49	-	-	-	-
549	0:42:38.2	41:35:30.6	24.62	-354.6	-	-	2002.10.10	49	-	-	-	-
550	0:42:12.9	41:35:22.0	22.63	-297.2	E	-	2002.10.10	49	-	-	-	-
551	0:42:09.9	41:35:39.6	22.00	-333.8	-	-	2002.10.10	49	PN_1_3_13	-	-	457
552	0:42:09.5	41:35:57.5	24.53	-231.1	-	-	2002.10.10	49	-	-	-	-
553	0:41:54.5	41:36:16.7	20.54	-139.0	-	-	2002.10.10	49	PN_1_3_8	-	-	419
554	0:42:46.5	41:28:04.8	24.07	-196.1	-	-	2002.10.09	50	-	-	-	-
555	0:43:18.7	41:28:25.6	22.78	-158.2	-	-	2002.10.09	50	-	-	-	744
556	0:43:19.7	41:28:47.6	23.91	-192.3	-	-	2002.10.09	50	-	-	-	-
557	0:43:20.5	41:29:09.2	22.51	-226.4	-	-	2002.10.09	50	-	-	-	751
558	0:43:19.8	41:29:13.1	23.65	-219.8	-	-	2002.10.09	50	-	-	-	-
559	0:43:03.0	41:29:26.1	21.55	-253.4	-	-	2002.10.09	50	-	-	-	671
560	0:43:21.6	41:29:36.7	23.30	-394.9	-	-	2002.10.09	50	-	-	-	-
561	0:43:19.0	41:29:44.1	23.52	-247.9	-	-	2002.10.09	50	-	-	-	-
562	0:42:56.4	41:29:41.7	22.11	-235.9	-	-	2002.10.09	50	PN_6_3_8	-	-	635
563	0:43:24.2	41:29:52.8	22.57	-193.2	-	-	2002.10.09	50	-	-	-	769
564	0:42:55.9	41:30:07.6	23.09	-229.6	-	-	2002.10.09	50	-	-	-	-
565	0:43:06.2	41:30:19.6	21.40	-260.5	-	-	2002.10.09	50	PN_6_3_12	-	-	682
566	0:43:23.8	41:30:26.5	24.10	-120.3	-	-	2002.10.09	50	-	-	-	-
567	0:43:11.1	41:30:25.4	22.04	-210.0	-	-	2002.10.09	50	-	-	-	704
568	0:43:14.7	41:30:33.7	22.24	-146.3	-	-	2002.10.09	50	-	-	-	723
569	0:42:59.3	41:30:29.8	20.82	-288.4	-	-	2002.10.09	50	-	-	-	654
570	0:43:21.6	41:30:41.3	23.82	-233.8	-	-	2002.10.09	50	-	-	-	-
571	0:43:13.0	41:30:42.4	23.69	-228.2	-	-	2002.10.09	50	-	-	-	-

Continued on next page

Table A.1 – continued from previous page

ID	RA	Dec	$m_{5007}$	$v_{\text{helio}}$	Note	Host	Date	Field	H06	C89	HK04	MLA93
572	0:43:08.7	41:31:07.1	24.17	-116.5	-	-	2002.10.09	50	-	-	-	-
573	0:42:50.8	41:31:19.4	24.10	-287.9	-	-	2002.10.09	50	-	-	-	-
574	0:42:42.4	41:31:54.9	20.40	-306.4	R	-	2002.10.09	50	-	-	-	579
575	0:43:16.4	41:32:59.7	20.88	-15.5	-	-	2002.10.09	50	-	-	-	729
576	0:42:52.5	41:32:55.9	24.57	-188.7	-	-	2002.10.09	50	-	-	-	-
577	0:43:12.2	41:33:16.0	22.90	-130.9	-	-	2002.10.09	50	-	-	-	-
578	0:43:15.6	41:33:47.7	23.53	-259.6	-	-	2002.10.09	50	-	-	-	-
579	0:42:58.0	41:34:37.3	23.19	-282.1	-	-	2002.10.09	50	-	-	-	-
580	0:42:53.6	41:34:45.2	22.83	-161.1	-	-	2002.10.09	50	-	-	-	-
581	0:42:53.6	41:35:16.7	23.41	-290.4	R	-	2002.10.09	50	-	-	-	-
582	0:43:14.1	41:35:27.7	21.17	-167.4	-	-	2002.10.09	50	-	-	-	721
583	0:43:12.8	41:35:29.1	22.20	-217.0	-	-	2002.10.09	50	-	-	-	714
584	0:43:23.6	41:36:11.3	22.07	-229.1	-	-	2002.10.09	50	PN_6.3.21	-	-	766
585	0:42:53.1	41:36:21.7	23.06	-134.5	E	-	2002.10.09	50	-	-	-	-
586	0:43:07.9	41:28:45.5	20.82	-713.5	-	Stream?	2002.10.09	50	-	-	-	692
587	0:43:17.5	41:29:17.2	21.66	-700.3	-	Stream?	2002.10.09	50	-	-	-	737
588	0:43:23.8	41:30:13.5	22.58	-559.7	E	-	2002.10.09	50	-	-	-	767
589	0:43:00.8	41:30:11.5	20.35	-313.5	E	-	2002.10.09	50	PN_6.3.11	-	-	661
590	0:42:56.0	41:32:42.3	24.10	-255.7	-	-	2002.10.09	50	-	-	-	-
591	0:43:42.7	41:27:23.5	24.54	-123.8	-	-	2002.10.10	51	-	-	-	-
592	0:44:11.4	41:28:20.4	24.79	-97.8	-	-	2002.10.10	51	-	-	-	-
593	0:43:33.4	41:28:33.3	23.88	-69.3	E	-	2002.10.10	51	-	-	-	-
594	0:43:42.0	41:28:39.1	22.87	-198.9	-	-	2002.10.10	51	-	-	-	838
595	0:43:35.6	41:28:46.1	24.45	-43.5	-	-	2002.10.10	51	-	-	-	-
596	0:43:50.9	41:28:52.7	23.50	-218.0	-	-	2002.10.10	51	-	-	-	-
597	0:43:38.6	41:28:51.7	22.82	-115.1	-	-	2002.10.10	51	-	-	-	-
598	0:43:36.7	41:28:51.5	24.52	-174.9	-	-	2002.10.10	51	-	-	-	-
599	0:43:39.6	41:29:18.5	21.81	-257.9	-	-	2002.10.10	51	-	-	-	828
600	0:43:32.1	41:29:44.3	24.14	-30.5	-	-	2002.10.10	51	-	-	-	-
601	0:44:11.6	41:30:06.1	24.62	-112.0	E	-	2002.10.10	51	-	-	-	-
602	0:44:13.2	41:30:09.9	21.88	-323.0	-	-	2002.10.10	51	P545	-	545	949
603	0:44:11.4	41:30:36.4	22.94	-106.6	-	-	2002.10.10	51	-	-	-	-
604	0:43:55.8	41:30:31.8	24.40	-308.3	-	-	2002.10.10	51	-	-	-	-
605	0:44:07.7	41:30:41.0	23.77	-165.6	-	-	2002.10.10	51	P538	-	538	-
606	0:43:37.4	41:30:33.2	24.82	-80.5	-	-	2002.10.10	51	-	-	-	-
607	0:43:58.2	41:30:45.7	23.44	-2.2	-	-	2002.10.10	51	P529	-	529	-
608	0:43:34.6	41:30:43.8	23.09	-83.1	-	-	2002.10.10	51	-	-	-	-
609	0:43:36.0	41:30:52.3	23.52	-85.0	-	-	2002.10.10	51	-	-	-	-
610	0:43:43.5	41:30:57.4	21.43	-122.2	-	-	2002.10.10	51	-	-	-	843
611	0:44:02.9	41:31:17.4	24.20	-91.9	-	-	2002.10.10	51	P533	-	533	-
612	0:44:08.1	41:31:19.1	22.59	-187.7	-	-	2002.10.10	51	P539	-	539	923
613	0:43:37.6	41:31:13.9	24.60	-53.8	-	-	2002.10.10	51	-	-	-	-
614	0:43:44.7	41:31:18.5	21.92	-329.8	-	-	2002.10.10	51	-	-	-	847
615	0:43:48.2	41:31:26.4	21.67	14.8	-	-	2002.10.10	51	PN_6.3.45	-	-	857
616	0:44:08.7	41:31:43.3	22.78	-124.4	E	-	2002.10.10	51	-	-	-	-
617	0:44:07.1	41:31:44.9	23.46	-120.4	-	-	2002.10.10	51	-	-	-	-
618	0:44:10.9	41:31:46.7	22.40	-64.6	-	-	2002.10.10	51	-	-	-	-
619	0:43:37.2	41:31:40.0	24.27	-77.7	-	-	2002.10.10	51	-	-	-	-
620	0:44:13.4	41:31:53.9	22.31	-26.4	-	-	2002.10.10	51	PN_6.3.68	-	-	951
621	0:44:06.4	41:32:03.2	20.93	-309.2	-	-	2002.10.10	51	-	-	-	920
622	0:44:09.1	41:32:04.7	22.97	-108.2	E,R	-	2002.10.10	51	-	-	-	-
623	0:44:11.0	41:32:06.9	23.47	-98.3	R	-	2002.10.10	51	-	-	-	-
624	0:43:37.8	41:32:01.0	22.42	-215.7	-	-	2002.10.10	51	-	-	-	820
625	0:44:07.6	41:32:12.0	24.72	-38.7	-	-	2002.10.10	51	-	-	-	-
626	0:44:09.5	41:32:14.8	22.02	12.6	-	-	2002.10.10	51	-	-	-	931
627	0:43:35.6	41:32:06.1	23.61	-104.7	-	-	2002.10.10	51	-	-	-	-
628	0:43:39.5	41:32:09.7	21.56	-200.2	-	-	2002.10.10	51	-	-	-	827
629	0:44:14.1	41:32:20.8	24.02	-194.7	-	-	2002.10.10	51	-	-	-	-
630	0:43:50.7	41:32:51.8	23.07	-119.2	-	-	2002.10.10	51	-	-	-	-
631	0:43:36.5	41:33:02.6	22.34	-203.1	-	-	2002.10.10	51	-	-	-	813
632	0:43:57.5	41:33:24.8	23.96	-54.1	-	-	2002.10.10	51	-	-	-	-
633	0:43:46.4	41:33:22.5	24.08	-135.7	-	-	2002.10.10	51	-	-	-	-
634	0:44:11.2	41:34:24.3	22.01	-97.8	-	-	2002.10.10	51	PN_6.3.70	-	-	937
635	0:44:04.6	41:34:32.4	20.90	-63.1	-	-	2002.10.10	51	-	-	-	913
636	0:43:38.2	41:34:25.4	24.95	-109.4	-	-	2002.10.10	51	-	-	-	-
637	0:44:04.5	41:34:37.5	24.51	63.8	-	-	2002.10.10	51	-	-	-	-
638	0:43:43.1	41:34:31.1	24.28	-101.1	-	-	2002.10.10	51	-	-	-	-
639	0:43:54.7	41:35:02.3	22.54	-70.6	-	-	2002.10.10	51	PN_6.3.58	-	-	877
640	0:43:39.0	41:35:01.9	23.97	-110.4	-	-	2002.10.10	51	-	-	-	-
641	0:43:40.1	41:35:04.7	21.51	-149.5	-	-	2002.10.10	51	PN_6.3.47	-	-	830
642	0:43:49.3	41:35:31.2	22.99	-133.4	-	-	2002.10.10	51	-	-	-	-
643	0:43:30.0	41:35:42.7	24.82	-195.5	E	-	2002.10.10	51	-	-	-	-
644	0:44:12.0	41:35:56.0	23.70	-98.6	-	-	2002.10.10	51	-	-	-	-
645	0:43:28.3	41:35:46.5	24.94	-142.4	E	-	2002.10.10	51	-	-	-	-
646	0:43:36.4	41:35:49.7	22.91	-37.4	-	-	2002.10.10	51	-	-	-	810
647	0:43:40.1	41:36:01.5	22.84	-80.3	-	-	2002.10.10	51	-	-	-	-
648	0:43:42.5	41:37:20.2	24.72	-92.8	E	-	2002.10.10	51	-	-	-	-
649	0:44:08.4	41:27:08.6	24.13	-158.1	-	-	2002.10.10	51	-	-	540	-
650	0:43:37.2	41:31:04.9	21.21	-655.7	-	Stream?	2002.10.10	51	PN_6.3.36	-	-	816
651	0:44:01.8	41:32:56.0	24.43	-47.6	-	-	2002.10.10	51	-	-	-	-
652	0:43:45.2	41:35:18.0	22.85	-556.1	-	-	2002.10.10	51	PN_6.3.48	-	-	850
653	0:44:25.6	41:27:03.3	24.39	-171.4	R	-	2002.10.10	52	-	-	-	-
654	0:44:17.6	41:27:27.8	25.03	-248.9	E	-	2002.10.10	52	-	-	-	-
655	0:44:27.7	41:28:01.1	24.72	-118.8	-	-	2002.10.10	52	-	-	-	-
656	0:44:32.9	41:28:06.8	23.99	-313.5	-	-	2002.10.10	52	-	-	-	-
657	0:44:20.4	41:28:04.6	24.25	-8.0	-	-	2002.10.10	52	-	-	-	-
658	0:44:20.6	41:28:22.6	24.70	-47.0	-	-	2002.10.10	52	-	-	-	-
659	0:45:00.6	41:28:36.4	20.03	-248.5	R	-	2002.10.10	52	-	-	-	1095
660	0:45:00.8	41:28:42.1	21.43	-211.0	E,R	-	2002.10.10	52	-	-	-	1096
661	0:44:44.9	41:28:41.1	22.74	-173.0	E,R	-	2002.10.10	52	-	-	-	-
662	0:44:58.9	41:28:58.2	23.23	-238.6	E	-	2002.10.10	52	-	-	-	-
663	0:44:44.4	41:28:54.9	23.18	-127.3	-	-	2002.10.10	52	-	-	-	-
664	0:44:34.7	41:29:17.0	20.84	-188.5	-	-	2002.10.10	52	PN_6.3.95	-	-	1019

Continued on next page

Table A.1 – continued from previous page

ID	RA	Dec	$m_{5007}$	$v_{\text{helio}}$	Note	Host	Date	Field	H06	C89	HK04	MLA93
665	0:44:54.7	41:29:27.5	24.50	-159.1	-	-	2002.10.10	52	-	-	-	-
666	0:44:47.7	41:29:27.4	22.57	-205.6	E	-	2002.10.10	52	-	-	-	-
667	0:44:50.0	41:29:31.1	23.67	-186.3	-	-	2002.10.10	52	-	-	-	-
668	0:44:52.0	41:29:37.2	24.19	-184.9	-	-	2002.10.10	52	-	-	-	-
669	0:44:23.3	41:29:33.0	22.59	-446.2	-	-	2002.10.10	52	-	-	-	-
670	0:44:24.5	41:29:46.8	20.68	-106.8	-	-	2002.10.10	52	P555	-	555	983
671	0:44:25.5	41:29:53.2	22.27	-145.6	-	-	2002.10.10	52	P558	-	558	990
672	0:45:01.5	41:30:18.9	22.83	-236.0	-	-	2002.10.10	52	-	-	-	-
673	0:44:24.6	41:30:27.1	24.31	-111.1	-	-	2002.10.10	52	-	-	556	-
674	0:44:47.2	41:30:42.9	24.70	-191.3	E	-	2002.10.10	52	-	-	-	-
675	0:44:29.4	41:30:41.3	24.86	-238.7	-	-	2002.10.10	52	-	-	-	-
676	0:45:01.1	41:30:56.7	22.86	-159.9	E,R	-	2002.10.10	52	-	-	-	1097
677	0:44:50.2	41:31:08.1	20.66	-113.3	-	-	2002.10.10	52	P568	-	568	1059
678	0:45:03.2	41:31:15.6	24.11	-178.6	E	-	2002.10.10	52	-	-	-	-
679	0:44:54.6	41:31:13.0	22.93	-128.5	E,R	-	2002.10.10	52	-	-	-	-
680	0:44:56.1	41:31:22.6	22.35	-155.2	E	-	2002.10.10	52	-	-	-	-
681	0:44:38.9	41:31:31.5	22.56	-149.8	-	-	2002.10.10	52	P564	-	564	1035
682	0:45:00.2	41:31:43.5	23.36	-361.2	-	-	2002.10.10	52	-	-	-	-
683	0:44:57.3	41:31:43.4	23.91	-123.7	R	-	2002.10.10	52	-	-	-	-
684	0:44:50.3	41:31:51.0	21.79	-154.4	-	-	2002.10.10	52	P569	-	569	1060
685	0:44:45.3	41:31:49.7	22.17	-181.6	-	-	2002.10.10	52	P567	-	567	1053
686	0:44:25.0	41:31:45.9	21.24	-70.1	-	-	2002.10.10	52	P557	-	557	985
687	0:44:41.7	41:32:04.2	22.06	-193.7	-	-	2002.10.10	52	P566	-	566	1039
688	0:44:24.4	41:32:04.8	23.66	-66.5	-	-	2002.10.10	52	-	-	-	-
689	0:44:34.0	41:32:21.8	24.49	-259.4	-	-	2002.10.10	52	-	-	-	-
690	0:44:59.1	41:32:34.0	21.70	-193.6	E,R	-	2002.10.10	52	-	-	-	-
691	0:44:37.9	41:32:27.5	24.87	-140.9	-	-	2002.10.10	52	-	-	-	-
692	0:45:03.7	41:32:38.6	22.85	-153.7	-	-	2002.10.10	52	PN_5_3_12	-	-	-
693	0:44:41.1	41:32:38.3	24.84	-101.2	-	-	2002.10.10	52	-	-	-	-
694	0:44:30.2	41:32:35.3	24.37	-206.8	-	-	2002.10.10	52	P561	-	561	-
695	0:44:29.8	41:32:45.2	21.56	-191.9	-	-	2002.10.10	52	P560	-	560	1004
696	0:45:00.0	41:33:00.7	24.30	-157.7	-	-	2002.10.10	52	-	-	-	-
697	0:44:23.8	41:32:52.7	23.69	-91.6	E	-	2002.10.10	52	-	-	-	-
698	0:44:39.5	41:33:09.7	23.70	-99.2	-	-	2002.10.10	52	-	-	565	-
699	0:44:26.3	41:33:14.9	20.49	-117.0	-	-	2002.10.10	52	P559	-	559	994
700	0:44:34.5	41:33:29.3	20.86	-155.4	-	-	2002.10.10	52	P563	-	563	1017
701	0:44:27.3	41:33:36.0	22.65	-154.8	-	-	2002.10.10	52	-	-	-	-
702	0:44:44.4	41:33:42.8	24.73	-108.0	E	-	2002.10.10	52	-	-	-	-
703	0:44:52.7	41:33:47.2	22.66	-146.1	E,R	-	2002.10.10	52	-	-	-	-
704	0:44:30.9	41:33:41.6	23.84	-67.3	-	-	2002.10.10	52	P562	-	-	-
705	0:44:53.9	41:34:05.4	23.38	-265.0	-	-	2002.10.10	52	-	-	-	-
706	0:44:46.2	41:34:26.5	24.11	-109.8	E	-	2002.10.10	52	-	-	-	-
707	0:44:26.4	41:34:19.7	23.14	-74.1	E	-	2002.10.10	52	-	-	-	-
708	0:44:26.2	41:34:39.2	24.39	-41.6	-	-	2002.10.10	52	-	-	-	-
709	0:44:54.0	41:35:08.7	22.46	-245.3	-	-	2002.10.10	52	PN_5_3_1	-	-	1073
710	0:44:22.5	41:35:33.6	23.96	-84.0	-	-	2002.10.10	52	-	-	-	-
711	0:44:25.4	41:35:38.2	24.28	11.1	E	-	2002.10.10	52	-	-	-	-
712	0:45:03.2	41:35:52.0	20.56	-102.5	-	-	2002.10.10	52	PN_5_3_13	-	-	1101
713	0:44:22.4	41:35:51.5	21.08	-1.5	-	-	2002.10.10	52	PN_6_3_83	-	-	976
714	0:44:50.4	41:32:09.2	23.07	-183.4	E,R	-	2002.10.10	52	-	-	-	-
715	0:45:24.9	41:28:37.3	25.12	-206.8	-	-	2002.10.11	53	-	-	-	-
716	0:45:48.3	41:29:35.3	24.34	-281.0	-	-	2002.10.11	53	-	-	-	-
717	0:45:27.0	41:30:13.4	20.94	-200.5	-	-	2002.10.11	53	PN_5_3_28	-	-	1152
718	0:45:12.3	41:30:08.8	24.86	-222.4	-	-	2002.10.11	53	-	-	-	-
719	0:45:27.0	41:32:09.4	22.48	-50.1	-	-	2002.10.11	53	PN_5_3_27	-	-	1151
720	0:45:12.9	41:32:07.4	24.79	-228.7	-	-	2002.10.11	53	-	-	-	-
721	0:45:19.2	41:32:11.6	24.81	-133.4	E	-	2002.10.11	53	-	-	-	-
722	0:45:16.1	41:33:05.2	23.49	-94.1	-	-	2002.10.11	53	-	-	-	-
723	0:45:51.5	41:33:34.2	24.86	-77.2	-	-	2002.10.11	53	-	-	-	-
724	0:45:21.1	41:33:28.4	21.41	-231.4	-	-	2002.10.11	53	-	-	-	1137
725	0:45:14.5	41:33:32.4	23.68	-145.0	E	-	2002.10.11	53	-	-	-	-
726	0:45:09.6	41:33:37.7	23.41	-104.5	-	-	2002.10.11	53	-	-	-	-
727	0:45:11.6	41:34:24.0	23.17	6.7	-	-	2002.10.11	53	-	-	-	-
728	0:45:28.1	41:34:34.5	22.85	-151.3	-	-	2002.10.11	53	PN_5_3_22	-	-	-
729	0:45:09.5	41:34:30.2	21.12	-111.8	-	-	2002.10.11	53	PN_5_3_14	-	-	1108
730	0:45:26.2	41:34:46.5	21.29	-129.1	-	-	2002.10.11	53	-	-	-	1149
731	0:45:38.0	41:34:58.8	24.99	-296.9	E	-	2002.10.11	53	-	-	-	-
732	0:45:47.4	41:35:12.8	23.94	-106.6	-	-	2002.10.11	53	-	-	-	-
733	0:45:51.1	41:35:17.9	21.15	-112.3	-	-	2002.10.11	53	-	-	-	1204
734	0:45:18.2	41:35:11.1	24.62	-200.4	-	-	2002.10.11	53	-	-	-	-
735	0:45:53.8	41:35:34.9	21.68	-92.2	-	-	2002.10.11	53	PN_5_3_30	-	-	1210
736	0:45:16.7	41:35:24.6	24.60	-160.7	-	-	2002.10.11	53	-	-	-	-
737	0:45:15.7	41:35:38.3	24.48	-170.2	-	-	2002.10.11	53	-	-	-	-
738	0:45:23.6	41:35:50.7	21.51	-137.4	-	-	2002.10.11	53	PN_5_3_25	-	-	1142
739	0:45:09.9	41:35:59.7	21.51	-93.9	E	-	2002.10.11	53	-	-	-	-
740	0:45:28.9	41:36:14.6	22.03	-83.9	-	-	2002.10.11	53	-	-	-	1155
741	0:45:14.0	41:36:14.1	21.42	-118.0	E,R	-	2002.10.11	53	-	-	-	-
742	0:45:34.5	41:33:40.7	21.82	-493.9	-	-	2002.10.11	53	-	-	-	1164
743	0:46:36.9	41:28:54.5	22.28	-246.6	-	-	2002.10.13	54	-	-	-	1260
744	0:46:07.0	41:29:25.3	24.69	-272.7	-	-	2002.10.13	54	-	-	-	-
745	0:46:10.5	41:29:48.0	25.31	-195.2	-	-	2002.10.13	54	-	-	-	-
746	0:46:18.3	41:31:09.9	20.45	-155.9	-	-	2002.10.13	54	PN_5_3_35	-	-	1240
747	0:46:02.0	41:31:40.5	22.88	-121.7	-	-	2002.10.13	54	PN_5_3_34	-	-	-
748	0:45:58.6	41:31:53.5	24.74	-203.9	-	-	2002.10.13	54	-	-	-	-
749	0:45:57.5	41:32:12.2	24.99	-211.0	E	-	2002.10.13	54	-	-	-	-
750	0:46:09.2	41:32:23.6	24.27	-78.5	-	-	2002.10.13	54	-	-	-	-
751	0:46:05.2	41:34:15.0	25.14	-273.6	E	-	2002.10.13	54	-	-	-	-
752	0:46:12.4	41:35:31.2	25.36	-163.6	-	-	2002.10.13	54	-	-	-	-
753	0:46:21.7	41:36:08.6	24.81	-211.6	-	-	2002.10.13	54	-	-	-	-
754	0:46:09.9	41:35:00.4	22.96	-155.6	E	-	2002.10.13	54	-	-	-	-
755	0:42:01.0	41:18:11.1	24.65	-272.0	E	-	2002.10.10	55	-	-	-	-
756	0:42:08.2	41:19:29.9	22.69	-420.4	-	-	2002.10.10	55	-	-	-	-
757	0:42:14.2	41:19:55.4	24.23	-458.3	-	-	2002.10.10	55	-	-	-	-

Continued on next page

Table A.1 – continued from previous page

ID	RA	Dec	$m_{5007}$	$v_{\text{helio}}$	Note	Host	Date	Field	H06	C89	HK04	MLA93
758	0:41:54.4	41:19:57.3	22.33	-335.2	-	-	2002.10.10	55	-	-	-	420
759	0:42:09.1	41:20:22.8	22.57	-395.9	E	-	2002.10.10	55	-	-	-	-
760	0:41:45.4	41:20:37.5	21.13	-304.5	-	-	2002.10.10	55	PN_1.4_13	-	-	399
761	0:42:10.3	41:20:45.8	23.24	-464.3	-	-	2002.10.10	55	PN_6.2_109	-	-	-
762	0:41:55.1	41:21:10.8	24.91	-362.7	-	-	2002.10.10	55	-	-	-	-
763	0:41:43.9	41:21:26.1	23.25	-309.9	-	-	2002.10.10	55	-	-	-	-
764	0:41:43.0	41:21:36.4	23.76	-340.9	-	-	2002.10.10	55	-	-	-	-
765	0:42:14.5	41:22:22.8	24.14	-309.9	-	-	2002.10.10	55	-	-	-	-
766	0:42:13.9	41:23:19.2	24.64	-330.6	-	-	2002.10.10	55	-	-	-	-
767	0:41:49.0	41:23:50.0	23.76	-306.1	-	-	2002.10.10	55	-	-	-	-
768	0:41:59.8	41:24:03.9	24.58	-180.1	-	-	2002.10.10	55	-	-	-	-
769	0:42:08.7	41:24:10.7	22.36	-327.2	E,R	-	2002.10.10	55	-	-	-	-
770	0:42:09.7	41:24:12.8	22.40	-328.2	R	-	2002.10.10	55	-	-	-	-
771	0:42:09.7	41:24:22.6	24.32	-329.0	-	-	2002.10.10	55	-	-	-	-
772	0:42:01.5	41:24:21.5	21.18	-241.4	-	-	2002.10.10	55	PN_1.4_19	-	-	436
773	0:41:52.1	41:24:19.0	23.82	-463.8	-	-	2002.10.10	55	-	-	-	-
774	0:42:01.9	41:24:39.6	24.97	-325.8	-	-	2002.10.10	55	-	-	-	-
775	0:41:48.7	41:25:19.4	22.89	-164.8	-	-	2002.10.10	55	-	-	-	-
776	0:41:52.3	41:25:32.6	22.55	-217.8	-	-	2002.10.10	55	PN_1.4_17	-	-	416
777	0:42:04.8	41:25:37.2	23.84	-219.5	-	-	2002.10.10	55	-	-	-	-
778	0:42:07.4	41:25:56.1	23.86	-116.0	-	-	2002.10.10	55	-	-	-	-
779	0:41:45.9	41:26:34.7	21.82	-434.9	-	-	2002.10.10	55	PN_1.4_16	-	-	401
780	0:41:28.8	41:26:48.2	22.91	-266.2	-	-	2002.10.10	55	PN_1.4_8	-	-	-
781	0:41:48.2	41:21:04.0	23.61	44.3	-	-	2002.10.10	55	-	-	-	-
782	0:40:56.7	41:19:31.4	24.17	-285.6	E	-	2002.10.11	56	-	-	-	-
783	0:41:14.6	41:19:52.9	25.69	-360.1	-	-	2002.10.11	56	-	-	-	-
784	0:41:21.6	41:20:42.4	22.47	-321.9	E,R	-	2002.10.11	56	-	-	-	351
785	0:41:09.8	41:20:45.8	23.45	-259.5	-	-	2002.10.11	56	PN_1.4_4	-	-	-
786	0:40:43.9	41:22:11.1	21.34	-289.0	-	-	2002.10.11	56	PN_1.4_3	-	-	253
787	0:41:23.4	41:23:44.0	25.33	-217.2	-	-	2002.10.11	56	-	-	-	-
788	0:40:50.4	41:23:35.4	23.72	-322.2	-	-	2002.10.11	56	PN_1.4_1	-	-	-
789	0:41:22.3	41:24:10.4	24.85	-369.0	-	-	2002.10.11	56	-	-	-	-
790	0:40:58.4	41:24:24.3	25.43	-122.1	-	-	2002.10.11	56	-	-	-	-
791	0:41:01.3	41:20:56.8	23.53	-324.8	E	-	2002.10.11	56	-	-	-	-
792	0:40:52.5	41:25:39.4	23.61	-294.4	E	-	2002.10.11	56	-	-	-	-
793	0:41:15.7	41:27:19.9	22.34	-322.9	-	-	2002.10.11	56	PN_1.4_6	-	-	330
794	0:39:53.3	41:19:57.3	25.22	-307.6	E	-	2002.10.11	57	-	-	-	-
795	0:40:26.2	41:20:27.8	20.56	-342.2	-	-	2002.10.11	57	PN_8.4_10	-	-	219
796	0:40:10.6	41:21:24.0	22.52	-206.1	-	-	2002.10.11	57	PN_8.4_9	-	-	-
797	0:39:55.5	41:23:25.4	24.22	-228.4	-	-	2002.10.11	57	-	-	-	-
798	0:39:49.2	41:24:09.6	22.19	-256.3	-	-	2002.10.11	57	PN_8.4_3	-	-	146
799	0:39:38.6	41:21:00.4	24.88	-343.0	-	-	2002.10.12	58	-	-	-	-
800	0:39:34.9	41:23:44.4	23.52	-252.4	-	-	2002.10.12	58	PN_8.4_2	-	-	-
801	0:42:56.3	41:19:13.9	22.49	-345.5	-	-	2002.10.09	60	P122	-	122	-
802	0:42:41.3	41:19:10.8	22.83	-166.1	-	-	2002.10.09	60	P105	-	105	-
803	0:42:45.5	41:19:19.9	23.03	-171.1	-	-	2002.10.09	60	P107	-	107	-
804	0:42:38.5	41:19:22.8	21.24	-293.3	-	-	2002.10.09	60	-	-	-	561
805	0:42:54.8	41:19:54.9	21.90	-48.7	-	-	2002.10.09	60	-	-	123	-
806	0:42:58.3	41:19:45.0	22.96	-227.4	-	-	2002.10.09	60	-	-	-	-
807	0:42:56.7	41:19:44.0	23.61	-193.9	-	-	2002.10.09	60	-	-	-	-
808	0:42:53.5	41:19:53.2	22.70	-218.9	-	-	2002.10.09	60	P222	-	222	-
809	0:42:57.7	41:19:52.0	23.37	-329.6	-	-	2002.10.09	60	-	-	-	-
810	0:42:45.6	41:19:59.2	22.81	-345.9	-	-	2002.10.09	60	P109	-	109	-
811	0:42:59.7	41:20:04.2	23.55	19.5	E	-	2002.10.09	60	P484	-	484	-
812	0:42:49.9	41:20:08.8	22.54	-297.1	-	-	2002.10.09	60	P113	-	113	-
813	0:42:14.3	41:19:56.7	24.29	-497.9	-	-	2002.10.09	60	-	-	-	-
814	0:42:24.3	41:20:12.3	21.89	-264.4	-	-	2002.10.09	60	-	-	-	502
815	0:42:52.9	41:20:20.5	23.65	-239.5	-	-	2002.10.09	60	P223	-	223	-
816	0:42:52.7	41:20:24.5	23.02	-202.3	-	-	2002.10.09	60	P224	-	224	-
817	0:42:17.6	41:20:34.0	22.61	-314.7	-	-	2002.10.09	60	PN_1.4_29	-	-	-
818	0:42:46.4	41:20:49.7	22.48	-203.9	-	-	2002.10.09	60	-	-	-	-
819	0:42:54.5	41:20:57.6	24.21	-340.0	-	-	2002.10.09	60	-	-	-	-
820	0:42:48.0	41:21:00.4	22.00	-161.5	-	-	2002.10.09	60	P114	-	114	598
821	0:42:34.7	41:20:59.1	22.33	-272.5	-	-	2002.10.09	60	-	-	-	547
822	0:42:52.7	41:21:04.6	22.63	-260.9	-	-	2002.10.09	60	P225	-	225	-
823	0:42:33.3	41:21:00.2	23.60	-218.1	-	-	2002.10.09	60	-	-	-	-
824	0:42:54.5	41:21:24.6	20.74	-370.4	-	-	2002.10.09	60	P116	-	116	623
825	0:42:39.0	41:21:17.8	21.81	-292.8	-	-	2002.10.09	60	-	-	-	563
826	0:42:40.2	41:21:12.6	23.77	60.7	-	-	2002.10.09	60	-	-	-	-
827	0:42:24.0	41:21:22.6	23.55	-381.3	-	-	2002.10.09	60	-	-	-	-
828	0:43:00.2	41:21:35.2	23.57	-297.7	E	-	2002.10.09	60	P485	-	485	-
829	0:42:18.3	41:21:23.8	23.51	-242.6	-	-	2002.10.09	60	-	-	-	-
830	0:42:42.9	41:21:32.5	23.68	-289.6	-	-	2002.10.09	60	-	-	-	-
831	0:42:59.4	41:21:47.5	22.09	-295.4	-	-	2002.10.09	60	P221	-	221	656
832	0:42:49.2	41:21:44.5	21.25	-440.5	E	-	2002.10.09	60	-	-	-	-
833	0:42:58.1	41:21:53.4	23.71	-336.4	-	-	2002.10.09	60	-	-	-	-
834	0:42:56.2	41:22:04.2	21.63	-29.9	-	-	2002.10.09	60	P117	-	117	633
835	0:42:58.9	41:22:14.5	21.38	-171.2	-	-	2002.10.09	60	PN_6.4_54	1.89	-	650
836	0:42:49.5	41:22:11.5	22.96	-316.0	-	-	2002.10.09	60	P227	-	227	-
837	0:42:22.0	41:22:02.8	23.82	-202.9	-	-	2002.10.09	60	-	-	-	-
838	0:42:55.2	41:22:22.8	22.96	-142.0	-	-	2002.10.09	60	-	-	-	-
839	0:42:29.7	41:22:15.8	23.77	-353.0	-	-	2002.10.09	60	-	-	-	-
840	0:42:42.6	41:22:21.9	23.44	-520.8	-	-	2002.10.09	60	-	-	-	-
841	0:42:55.6	41:22:34.6	21.69	-148.7	-	-	2002.10.09	60	-	-	-	628
842	0:42:48.7	41:22:26.9	23.61	-434.6	-	-	2002.10.09	60	-	-	-	-
843	0:42:59.6	41:22:37.3	22.35	-113.3	-	-	2002.10.09	60	-	-	-	-
844	0:42:43.4	41:22:38.3	22.48	-523.2	-	-	2002.10.09	60	-	-	-	584
845	0:42:14.7	41:22:24.4	23.95	-312.9	-	-	2002.10.09	60	-	-	-	-
846	0:42:59.4	41:22:40.6	23.65	-237.6	-	-	2002.10.09	60	-	-	-	655
847	0:42:18.4	41:22:33.3	23.42	-333.1	-	-	2002.10.09	60	-	-	-	-
848	0:42:17.3	41:22:38.7	22.63	-267.6	-	-	2002.10.09	60	PN_1.4_26	-	-	-
849	0:42:57.5	41:23:06.3	21.07	-332.1	-	-	2002.10.09	60	P232	-	232	640
850	0:42:59.6	41:23:08.7	22.80	-190.8	-	-	2002.10.09	60	P231	-	231	658

Continued on next page



Table A.1 – continued from previous page

ID	RA	Dec	$m_{5007}$	$v_{\text{helio}}$	Note	Host	Date	Field	H06	C89	HK04	MLA93
851	0:42:23.1	41:23:08.2	20.98	-339.8	-	-	2002.10.09	60	-	-	-	498
852	0:42:45.9	41:23:35.2	21.68	-228.0	-	-	2002.10.09	60	-	-	-	592
853	0:42:43.5	41:23:42.2	23.53	-152.0	-	-	2002.10.09	60	-	-	-	-
854	0:42:45.4	41:23:47.5	23.53	-304.0	-	-	2002.10.09	60	-	-	-	-
855	0:42:22.1	41:23:56.9	24.02	-341.5	-	-	2002.10.09	60	-	-	-	-
856	0:42:31.6	41:26:48.7	23.80	-315.0	-	-	2002.10.09	60	-	-	-	-
857	0:42:21.6	41:25:21.2	22.42	-296.2	-	-	2002.10.09	60	PN_1_4_24	-	-	487
858	0:42:53.1	41:25:41.2	22.65	-201.5	-	-	2002.10.09	60	-	-	-	-
859	0:42:46.6	41:25:31.2	23.05	-308.8	-	-	2002.10.09	60	-	-	-	-
860	0:42:41.2	41:24:23.5	23.04	-411.0	-	-	2002.10.09	60	-	-	-	-
861	0:42:57.6	41:24:34.1	21.66	-256.0	-	-	2002.10.09	60	-	-	233	641
862	0:42:50.1	41:25:13.3	22.70	-175.9	E	-	2002.10.09	60	-	-	-	-
863	0:42:37.7	41:25:48.7	22.73	-278.0	-	-	2002.10.09	60	-	-	-	-
864	0:42:49.4	41:25:09.2	22.37	-185.1	E,R	-	2002.10.09	60	-	-	-	602
865	0:42:58.3	41:25:11.2	22.03	-424.8	-	-	2002.10.09	60	P234	-	234	646
866	0:42:16.9	41:24:38.6	23.60	-291.7	-	-	2002.10.09	60	-	-	-	-
867	0:42:34.9	41:24:13.8	24.42	-222.6	-	-	2002.10.09	60	-	-	-	-
868	0:42:55.7	41:25:49.3	22.94	-272.6	-	-	2002.10.09	60	P479	-	479	-
869	0:42:49.2	41:25:56.1	21.43	-326.8	-	-	2002.10.09	60	-	-	-	600
870	0:42:53.7	41:25:51.3	21.29	-220.1	E,R	-	2002.10.09	60	-	-	-	620
871	0:42:33.5	41:19:53.0	24.19	-160.8	-	-	2002.10.09	60	-	-	-	-
872	0:42:35.0	41:23:06.4	23.28	-355.9	-	-	2002.10.09	60	-	-	-	-
873	0:42:46.2	41:22:52.0	23.70	-173.4	-	-	2002.10.09	60	-	-	-	-
874	0:42:42.4	41:21:41.5	24.04	-170.1	-	-	2002.10.09	60	-	-	-	-
875	0:42:56.3	41:25:05.3	23.91	-60.5	E	-	2002.10.09	60	-	-	-	-
876	0:43:08.1	41:17:42.6	23.23	-217.3	E	-	2002.10.09	61	P499	-	499	-
877	0:43:18.1	41:18:15.3	24.14	-256.1	-	-	2002.10.09	61	-	-	-	-
878	0:43:25.3	41:18:28.7	22.58	-297.0	-	-	2002.10.09	61	-	-	-	-
879	0:43:08.5	41:18:32.1	23.97	-233.9	-	-	2002.10.09	61	-	-	-	-
880	0:43:43.6	41:19:13.5	21.41	-131.1	-	-	2002.10.09	61	-	-	-	844
881	0:43:45.7	41:19:18.9	23.52	-322.5	-	-	2002.10.09	61	-	-	-	-
882	0:43:06.4	41:19:14.9	23.61	-172.2	-	-	2002.10.09	61	-	-	494	-
883	0:43:05.9	41:19:16.6	21.86	-242.4	-	-	2002.10.09	61	P130	-	130	-
884	0:43:43.2	41:19:28.5	23.93	-281.8	-	-	2002.10.09	61	-	-	-	-
885	0:43:40.9	41:19:32.6	22.80	-258.1	-	-	2002.10.09	61	-	-	-	-
886	0:43:07.3	41:19:22.8	20.97	-329.2	-	-	2002.10.09	61	P131	-	131	689
887	0:43:15.8	41:19:26.5	22.97	-88.7	-	-	2002.10.09	61	P212	-	212	-
888	0:43:44.3	41:19:37.1	23.74	-261.3	-	-	2002.10.09	61	-	-	-	-
889	0:43:34.3	41:19:35.4	22.08	-250.6	-	-	2002.10.09	61	-	-	-	803
890	0:43:17.2	41:19:33.6	22.52	-71.8	-	-	2002.10.09	61	P211	-	211	735
891	0:43:18.1	41:19:35.9	21.57	-276.9	-	-	2002.10.09	61	P210	-	210	742
892	0:43:18.0	41:19:44.1	22.94	-65.6	-	-	2002.10.09	61	P213	-	213	-
893	0:43:10.1	41:19:44.3	23.84	-301.1	-	-	2002.10.09	61	-	-	-	-
894	0:43:16.7	41:19:46.9	23.18	-115.2	-	-	2002.10.09	61	P214	-	214	-
895	0:43:10.8	41:19:54.6	21.75	-95.8	-	-	2002.10.09	61	P203	-	203	702
896	0:43:09.5	41:19:55.5	23.02	-265.9	-	-	2002.10.09	61	-	-	202	-
897	0:43:08.8	41:20:01.7	21.44	-358.0	-	-	2002.10.09	61	P133	-	133	693
898	0:43:30.5	41:20:11.4	22.96	-258.1	-	-	2002.10.09	61	-	-	-	-
899	0:43:06.2	41:20:04.4	21.70	-32.7	-	-	2002.10.09	61	P134	-	134	684
900	0:43:06.2	41:20:08.2	23.26	36.7	-	-	2002.10.09	61	-	-	-	-
901	0:43:43.2	41:20:22.1	21.46	-80.4	-	-	2002.10.09	61	-	-	-	840
902	0:43:28.4	41:20:18.5	20.98	-236.4	-	-	2002.10.09	61	PN_6_4_93	-	-	787
903	0:43:13.0	41:20:17.5	22.90	-180.1	-	-	2002.10.09	61	-	-	204	-
904	0:43:18.8	41:20:20.8	23.94	1.3	-	-	2002.10.09	61	-	-	-	-
905	0:43:24.7	41:20:25.5	22.96	-284.3	-	-	2002.10.09	61	P511	-	511	-
906	0:43:06.2	41:20:20.4	22.72	-276.4	E	-	2002.10.09	61	P205	-	205	-
907	0:43:26.6	41:20:27.3	21.00	-214.8	-	-	2002.10.09	61	P216	-	216	781
908	0:43:14.1	41:21:14.0	22.54	-300.1	-	-	2002.10.09	61	P218	-	218	-
909	0:43:12.6	41:21:18.0	20.78	-130.1	-	-	2002.10.09	61	P219	-	219	713
910	0:43:53.7	41:21:36.4	24.21	-36.7	-	-	2002.10.09	61	-	-	-	-
911	0:43:05.8	41:21:27.0	23.43	-155.9	-	-	2002.10.09	61	-	-	-	-
912	0:43:18.0	41:21:35.4	21.94	-228.6	-	-	2002.10.09	61	P217	-	217	740
913	0:43:15.2	41:21:41.4	23.44	6.4	-	-	2002.10.09	61	-	-	503	-
914	0:43:08.5	41:21:48.4	23.33	-11.7	-	-	2002.10.09	61	-	-	-	-
915	0:43:10.6	41:21:58.3	23.60	-337.1	-	-	2002.10.09	61	-	-	-	-
916	0:43:14.4	41:22:00.9	22.36	-330.6	-	-	2002.10.09	61	P242	-	242	722
917	0:43:24.5	41:22:04.8	21.90	-186.2	-	-	2002.10.09	61	-	-	-	771
918	0:43:06.8	41:22:11.7	23.33	-263.0	-	-	2002.10.09	61	-	-	-	-
919	0:43:35.4	41:22:30.4	21.55	-72.3	-	-	2002.10.09	61	P518	-	518	806
920	0:43:22.4	41:22:28.8	23.89	-204.5	-	-	2002.10.09	61	-	-	-	-
921	0:43:16.7	41:22:27.1	22.69	-24.3	-	-	2002.10.09	61	P243	-	243	731
922	0:43:24.5	41:22:33.0	23.73	70.6	-	-	2002.10.09	61	-	-	-	-
923	0:43:37.2	41:22:38.3	22.26	-255.7	-	-	2002.10.09	61	P520	-	520	817
924	0:43:25.8	41:22:41.5	23.16	-283.8	-	-	2002.10.09	61	P512	-	512	-
925	0:43:42.4	41:22:47.2	23.48	-384.3	-	-	2002.10.09	61	P523	-	523	-
926	0:43:31.0	41:22:47.9	24.12	-270.0	-	-	2002.10.09	61	-	-	-	-
927	0:43:39.3	41:22:57.9	21.93	-44.9	-	-	2002.10.09	61	P522	-	522	826
928	0:43:24.3	41:23:16.7	22.44	-62.2	-	-	2002.10.09	61	P246	-	246	768
929	0:43:37.0	41:23:21.7	24.32	-166.3	-	-	2002.10.09	61	-	-	-	-
930	0:43:09.2	41:23:13.6	23.53	-86.3	-	-	2002.10.09	61	-	-	-	-
931	0:43:40.5	41:23:30.4	22.51	-157.7	-	-	2002.10.09	61	P283	-	283	831
932	0:43:36.9	41:23:36.1	23.52	-202.0	-	-	2002.10.09	61	-	-	519	-
933	0:43:13.1	41:23:38.6	24.05	17.8	-	-	2002.10.09	61	-	-	-	-
934	0:43:24.5	41:23:44.7	22.20	36.7	-	-	2002.10.09	61	P245	-	245	772
935	0:43:45.2	41:23:55.5	24.22	-147.3	-	-	2002.10.09	61	P525	-	525	-
936	0:43:37.3	41:23:54.5	23.18	-138.9	-	-	2002.10.09	61	-	-	521	818
937	0:43:12.4	41:23:47.6	23.83	-282.3	-	-	2002.10.09	61	P501	-	501	-
938	0:43:23.4	41:23:51.9	22.12	-288.9	-	-	2002.10.09	61	P244	-	244	763
939	0:43:38.2	41:24:05.7	22.32	-229.9	-	-	2002.10.09	61	P282	-	282	823
940	0:43:13.2	41:24:22.9	21.59	-47.1	-	-	2002.10.09	61	P237	-	237	718
941	0:43:37.9	41:24:33.7	21.50	-156.1	-	-	2002.10.09	61	P281	-	281	821
942	0:43:24.2	41:24:37.8	22.05	-33.2	-	-	2002.10.09	61	P251	-	251	770
943	0:43:35.9	41:24:53.2	24.00	-138.4	-	-	2002.10.09	61	-	-	-	-

Continued on next page

Table A.1 – continued from previous page

ID	RA	Dec	$m_{5007}$	$v_{\text{helio}}$	Note	Host	Date	Field	H06	C89	HK04	MLA93
944	0:43:45.0	41:25:02.2	23.31	-49.9	-	-	2002.10.09	61	-	-	-	-
945	0:43:07.0	41:24:56.2	22.48	-109.3	-	-	2002.10.09	61	P241	-	241	688
946	0:43:33.1	41:25:28.6	23.42	-6.6	-	-	2002.10.09	61	-	-	280	-
947	0:43:12.3	41:25:26.0	23.13	-46.9	-	-	2002.10.09	61	P239	-	239	-
948	0:43:53.5	41:25:41.7	22.48	-212.6	E	-	2002.10.09	61	-	-	-	-
949	0:43:10.7	41:25:40.4	20.81	-85.3	-	-	2002.10.09	61	P240	-	240	701
950	0:43:26.0	41:25:54.4	23.69	-78.5	-	-	2002.10.09	61	P34	-	34	-
951	0:43:32.5	41:26:16.6	22.92	-154.5	-	-	2002.10.09	61	P279	-	279	-
952	0:43:39.1	41:26:29.4	22.12	-120.4	-	-	2002.10.09	61	P278	-	278	824
953	0:43:16.6	41:26:27.4	21.60	-183.8	-	-	2002.10.09	61	P252	-	252	730
954	0:43:39.2	41:26:52.9	20.35	-208.2	E,R	-	2002.10.09	61	P276	-	276	825
955	0:43:09.7	41:26:51.5	22.27	-83.7	-	-	2002.10.09	61	P254	-	254	698
956	0:43:01.2	41:20:05.8	21.57	-195.1	E	-	2002.10.09	61	P198	-	198	-
957	0:43:46.5	41:20:08.0	24.55	-400.4	-	-	2002.10.09	61	-	-	-	-
958	0:43:54.3	41:19:54.3	24.02	-285.6	-	-	2002.10.09	61	-	-	-	-
959	0:43:36.9	41:22:01.3	22.62	-181.0	E,R	-	2002.10.09	61	-	-	-	-
960	0:43:23.2	41:21:57.4	21.23	-248.1	-	-	2002.10.09	61	-	-	-	762
961	0:43:24.7	41:24:48.7	23.84	-106.4	-	-	2002.10.09	61	P250	-	250	-
962	0:43:23.1	41:24:44.0	24.19	-242.5	-	-	2002.10.09	61	-	-	-	-
963	0:43:28.0	41:24:34.9	24.29	-221.1	-	-	2002.10.09	61	-	-	-	-
964	0:43:37.4	41:24:17.6	22.83	-28.8	E	-	2002.10.09	61	-	-	-	-
965	0:43:49.7	41:22:42.3	21.48	-186.2	-	-	2002.10.09	61	-	-	-	865
966	0:43:49.7	41:22:40.1	21.90	-374.1	-	-	2002.10.09	61	-	-	-	862
967	0:43:58.6	41:19:23.4	21.38	-314.2	-	-	2002.10.09	62	-	-	-	891
968	0:44:01.7	41:19:39.2	21.91	-309.1	-	-	2002.10.09	62	-	-	-	903
969	0:43:59.4	41:19:48.6	23.55	-230.8	-	-	2002.10.09	62	-	-	-	-
970	0:44:12.3	41:20:40.3	22.75	-208.3	-	-	2002.10.09	62	-	-	-	944
971	0:44:01.1	41:21:05.5	22.33	-199.2	E	-	2002.10.09	62	-	-	-	-
972	0:44:07.6	41:21:08.6	22.68	-278.4	R	-	2002.10.09	62	-	-	-	-
973	0:44:31.4	41:21:31.8	21.39	-270.9	-	-	2002.10.09	62	PN_6.4_157	-	-	1009
974	0:44:16.9	41:21:43.5	23.34	-330.6	-	-	2002.10.09	62	-	-	-	-
975	0:43:59.3	41:21:48.7	22.40	-168.0	-	-	2002.10.09	62	-	-	-	896
976	0:44:15.9	41:22:11.0	21.95	-266.3	-	-	2002.10.09	62	-	1_110	-	956
977	0:43:56.2	41:22:14.1	20.71	-228.7	-	-	2002.10.09	62	-	-	-	885
978	0:44:31.0	41:22:26.0	23.10	-393.8	-	-	2002.10.09	62	-	-	-	-
979	0:44:27.5	41:22:29.3	22.50	-252.2	-	-	2002.10.09	62	PN_6.4_154	-	-	998
980	0:43:55.6	41:22:21.0	23.09	-271.5	-	-	2002.10.09	62	-	-	-	-
981	0:44:10.7	41:22:36.4	23.94	-72.2	-	-	2002.10.09	62	-	-	-	-
982	0:44:02.2	41:22:51.1	22.29	-278.5	-	-	2002.10.09	62	-	-	-	905
983	0:44:05.2	41:23:10.1	22.21	-227.1	-	-	2002.10.09	62	-	-	-	916
984	0:44:28.3	41:23:17.9	22.44	-385.8	-	-	2002.10.09	62	PN_6.4_153	-	-	1000
985	0:44:13.6	41:23:32.2	23.07	-1.0	-	-	2002.10.09	62	-	-	-	-
986	0:44:27.1	41:24:01.0	23.55	-143.5	-	-	2002.10.09	62	-	-	-	-
987	0:44:10.4	41:24:18.0	20.96	-227.6	-	-	2002.10.09	62	-	-	-	935
988	0:44:20.9	41:24:27.1	21.52	-208.6	-	-	2002.10.09	62	PN_6.4_151	-	-	969
989	0:44:23.7	41:24:37.7	21.97	-245.1	R	-	2002.10.09	62	-	-	-	980
990	0:43:58.2	41:24:29.6	23.46	-147.9	-	-	2002.10.09	62	-	-	528	-
991	0:44:13.4	41:25:06.1	22.14	-323.5	-	-	2002.10.09	62	-	-	-	950
992	0:44:07.4	41:25:32.4	21.19	-166.0	-	-	2002.10.09	62	P537	-	537	921
993	0:44:32.2	41:25:47.3	21.45	-134.0	-	-	2002.10.09	62	PN_6.4_152	-	-	1014
994	0:44:23.7	41:25:51.8	22.64	-305.7	-	-	2002.10.09	62	PN_6.4_147	-	-	-
995	0:44:06.1	41:26:00.4	23.28	-459.0	-	-	2002.10.09	62	-	-	535	-
996	0:43:55.0	41:26:04.6	21.93	-160.3	R	-	2002.10.09	62	P288	-	288	882
997	0:44:23.9	41:26:18.2	21.59	53.1	-	-	2002.10.09	62	-	-	-	982
998	0:44:25.6	41:26:40.5	20.28	-351.9	-	-	2002.10.09	62	PN_6.4_149	-	-	991
999	0:44:38.4	41:25:11.5	20.89	-193.9	E,R	-	2002.10.09	62	-	-	-	-
1000	0:43:55.9	41:26:33.9	21.66	-147.9	R	-	2002.10.09	62	-	-	-	-
1001	0:43:56.5	41:26:29.0	21.74	-129.9	R	-	2002.10.09	62	-	-	-	-
1002	0:45:17.3	41:19:29.0	24.55	-282.9	-	-	2002.10.11	63	-	-	-	-
1003	0:44:41.3	41:19:33.0	24.82	-224.9	-	-	2002.10.11	63	-	-	-	-
1004	0:44:56.3	41:20:25.6	21.04	-314.0	-	-	2002.10.11	63	PN_5.4_3	1_124	-	1081
1005	0:44:40.5	41:20:52.4	24.32	-239.0	-	-	2002.10.11	63	-	-	-	-
1006	0:44:48.5	41:22:54.9	23.42	-246.5	E,R	-	2002.10.11	63	-	-	-	-
1007	0:44:56.0	41:23:24.5	23.76	-259.5	-	-	2002.10.11	63	PN_5.4_2	-	-	-
1008	0:45:06.7	41:23:35.7	21.98	-208.8	-	-	2002.10.11	63	PN_5.4_5	-	-	1105
1009	0:45:28.6	41:24:03.2	24.59	-13.2	-	-	2002.10.11	63	-	-	-	-
1010	0:44:40.8	41:23:53.7	24.62	-258.4	-	-	2002.10.11	63	-	-	-	-
1011	0:45:13.5	41:24:04.7	22.35	-145.6	-	-	2002.10.11	63	-	-	-	1124
1012	0:44:55.9	41:25:01.3	24.83	-178.7	-	-	2002.10.11	63	-	-	-	-
1013	0:44:48.9	41:25:17.9	24.87	-223.3	E	-	2002.10.11	63	-	-	-	-
1014	0:45:07.4	41:25:28.7	23.85	-204.1	-	-	2002.10.11	63	PN_5.4_8	-	-	-
1015	0:45:03.0	41:25:27.6	20.68	-266.1	-	-	2002.10.11	63	PN_5.4_7	-	-	1099
1016	0:45:21.5	41:25:57.2	23.81	-221.2	-	-	2002.10.11	63	PN_5.4_9	-	-	-
1017	0:44:57.1	41:26:16.9	22.47	-178.9	-	-	2002.10.11	63	PN_5.4_1	-	-	1085
1018	0:44:45.6	41:27:37.5	23.41	-160.7	E	-	2002.10.11	63	-	-	-	-
1019	0:44:42.0	41:21:50.8	23.68	-263.2	E	-	2002.10.11	63	-	-	-	-
1020	0:44:47.4	41:25:53.4	21.90	-195.3	E,R	-	2002.10.11	63	-	-	-	-
1021	0:45:44.0	41:22:40.5	22.16	-305.9	-	-	2002.10.13	64	PN_5.4_10	-	-	1187
1022	0:45:44.8	41:24:29.6	23.25	-125.6	-	-	2002.10.13	64	PN_5.4_11	-	-	-
1023	0:46:03.2	41:24:46.6	25.27	-169.3	-	-	2002.10.13	64	-	-	-	-
1024	0:45:47.6	41:25:22.8	23.97	-218.6	-	-	2002.10.13	64	PN_5.4_12	-	-	-
1025	0:45:44.7	41:26:26.0	25.62	-185.6	-	-	2002.10.13	64	-	-	-	-
1026	0:41:36.3	41:10:05.6	24.31	-668.3	-	-	2002.10.10	65	-	-	-	-
1027	0:41:12.8	41:10:04.6	24.06	-326.0	-	-	2002.10.10	65	-	-	-	-
1028	0:41:36.3	41:10:16.8	24.40	-396.5	-	-	2002.10.10	65	-	-	-	-
1029	0:41:20.7	41:10:17.4	21.97	-301.0	-	-	2002.10.10	65	-	-	-	349
1030	0:41:45.8	41:10:36.7	22.41	-428.9	-	-	2002.10.10	65	-	-	-	402
1031	0:41:45.7	41:10:52.7	23.65	-444.4	-	-	2002.10.10	65	-	-	-	-
1032	0:41:37.6	41:11:42.4	23.09	-328.1	E	-	2002.10.10	65	-	-	-	-
1033	0:41:13.4	41:11:35.1	22.42	-407.7	-	-	2002.10.10	65	-	-	-	321
1034	0:41:37.4	41:11:44.7	22.68	-540.0	-	-	2002.10.10	65	-	-	-	-
1035	0:41:45.4	41:11:59.8	24.51	-463.4	-	-	2002.10.10	65	-	-	-	-
1036	0:41:25.5	41:11:54.6	22.63	-407.2	E,R	-	2002.10.10	65	-	-	-	-

Continued on next page

Table A.1 – continued from previous page

ID	RA	Dec	$m_{5007}$	$v_{\text{helio}}$	Note	Host	Date	Field	H06	C89	HK04	MLA93
1037	0:41:41.1	41:12:03.9	24.26	-503.6	E	-	2002.10.10	65	-	-	-	-
1038	0:41:03.1	41:11:58.3	23.31	-471.8	-	-	2002.10.10	65	PN_1.1_7	-	-	-
1039	0:41:17.5	41:12:06.7	22.20	-368.0	-	-	2002.10.10	65	-	-	-	335
1040	0:41:27.8	41:12:15.3	23.97	-325.3	-	-	2002.10.10	65	-	-	-	-
1041	0:41:16.9	41:12:12.0	22.67	-266.9	-	-	2002.10.10	65	PN_1.1_16	-	-	-
1042	0:41:28.0	41:12:22.7	25.31	-401.8	E,R	-	2002.10.10	65	-	-	-	-
1043	0:41:09.9	41:12:24.7	23.62	-333.0	-	-	2002.10.10	65	-	-	-	-
1044	0:41:33.7	41:12:56.5	20.73	-401.5	-	-	2002.10.10	65	PN_1.1_25	-	-	372
1045	0:41:26.8	41:13:01.0	23.76	-418.5	-	-	2002.10.10	65	-	-	-	-
1046	0:41:31.9	41:13:32.4	23.23	-415.4	R	-	2002.10.10	65	-	-	-	-
1047	0:41:34.0	41:13:38.3	24.58	-432.5	E,R	-	2002.10.10	65	-	-	-	-
1048	0:41:41.9	41:13:53.9	25.14	-469.9	-	-	2002.10.10	65	-	-	-	-
1049	0:41:08.7	41:13:59.1	24.50	-314.0	-	-	2002.10.10	65	-	-	-	-
1050	0:41:23.8	41:14:23.1	24.18	-283.6	-	-	2002.10.10	65	-	-	-	-
1051	0:41:23.4	41:14:28.1	20.77	-397.2	-	-	2002.10.10	65	PN_1.1_11	-	-	355
1052	0:41:37.5	41:15:10.7	22.19	-362.5	-	-	2002.10.10	65	-	-	-	378
1053	0:41:17.2	41:16:01.9	21.80	-455.0	-	-	2002.10.10	65	-	-	-	333
1054	0:41:45.3	41:16:27.8	23.58	-435.0	-	-	2002.10.10	65	-	-	-	-
1055	0:41:24.3	41:16:29.0	23.68	-325.0	-	-	2002.10.10	65	-	-	-	-
1056	0:41:42.9	41:16:36.8	21.30	-356.3	-	-	2002.10.10	65	PN_1.1_27	-	-	392
1057	0:41:38.4	41:17:01.8	22.64	-467.4	-	-	2002.10.10	65	-	-	-	-
1058	0:41:10.1	41:17:17.8	25.03	-272.2	-	-	2002.10.10	65	-	-	-	-
1059	0:41:11.8	41:17:41.3	24.68	-689.7	-	-	2002.10.10	65	-	-	-	-
1060	0:41:12.1	41:08:21.3	24.72	-349.0	E	-	2002.10.10	65	-	-	-	-
1061	0:41:14.1	41:08:21.4	24.41	-457.5	R	-	2002.10.10	65	-	-	-	-
1062	0:41:12.8	41:13:32.1	22.55	-557.2	E	-	2002.10.10	65	-	-	-	-
1063	0:40:58.9	41:09:20.8	25.89	-301.8	-	-	2002.10.11	66	-	-	-	-
1064	0:40:50.0	41:10:12.2	24.76	-446.3	-	-	2002.10.11	66	-	-	-	-
1065	0:40:13.7	41:10:09.9	23.42	-423.3	-	-	2002.10.11	66	-	-	-	-
1066	0:40:51.1	41:10:27.3	24.19	-508.4	-	-	2002.10.11	66	-	-	-	-
1067	0:40:53.3	41:10:40.5	23.52	-452.5	-	-	2002.10.11	66	-	-	-	-
1068	0:40:49.1	41:10:49.0	23.43	-432.9	-	-	2002.10.11	66	PN_1.1_3	-	-	-
1069	0:40:19.7	41:13:12.2	23.11	-341.6	-	-	2002.10.11	66	-	-	-	-
1070	0:40:54.6	41:13:34.3	25.07	-305.5	E	-	2002.10.11	66	-	-	-	-
1071	0:40:27.2	41:13:44.4	25.04	-373.6	-	-	2002.10.11	66	-	-	-	-
1072	0:40:39.0	41:14:38.9	20.92	-338.5	-	-	2002.10.11	66	PN_1.1_1	-	-	244
1073	0:40:53.3	41:16:37.9	22.20	-294.4	-	-	2002.10.11	66	PN_1.1_2	-	-	280
1074	0:40:38.1	41:16:48.0	20.88	-452.9	-	-	2002.10.11	66	-	-	-	243
1075	0:40:16.7	41:17:30.2	23.82	-348.9	-	-	2002.10.11	66	PN_1.2_9	-	-	-
1076	0:39:48.5	41:10:41.0	21.53	-449.8	-	-	2002.10.12	67	PN_8.1_8	-	-	145
1077	0:39:31.3	41:11:28.8	25.15	-491.9	-	-	2002.10.12	67	-	-	-	-
1078	0:39:40.6	41:12:30.3	25.04	-339.2	-	-	2002.10.12	67	-	-	-	-
1079	0:39:51.4	41:13:38.3	22.98	-364.2	-	-	2002.10.12	67	PN_8.1_6	-	-	-
1080	0:40:02.5	41:13:56.6	23.44	-317.1	-	-	2002.10.12	67	-	-	-	-
1081	0:39:52.3	41:15:09.9	24.67	-283.2	-	-	2002.10.12	67	-	-	-	-
1082	0:38:44.6	41:11:32.9	24.30	-448.3	-	-	2002.10.12	68	-	-	-	-
1083	0:39:08.0	41:12:25.5	23.92	-226.1	-	-	2002.10.12	68	PN_8.1_3	-	-	-
1084	0:38:43.7	41:14:11.3	22.92	-263.4	-	-	2002.10.12	68	PN_8.1_1	-	-	-
1085	0:39:11.1	41:19:06.4	25.51	-292.5	E	-	2002.10.12	68	-	-	-	-
1086	0:42:33.7	41:09:49.9	23.75	-370.3	-	-	2002.10.09	70	-	-	-	-
1087	0:42:28.3	41:09:57.5	21.18	-344.1	-	-	2002.10.09	70	P413	-	413	520
1088	0:41:57.7	41:09:43.6	22.13	-454.2	E	-	2002.10.09	70	-	-	-	-
1089	0:42:21.7	41:09:55.8	21.60	-356.9	-	-	2002.10.09	70	P395	-	395	490
1090	0:42:33.9	41:10:09.5	22.98	-480.3	-	-	2002.10.09	70	-	-	426	-
1091	0:42:32.6	41:10:15.8	20.94	-595.3	-	-	2002.10.09	70	P151	-	151	540
1092	0:42:19.3	41:10:07.9	22.87	-352.5	-	-	2002.10.09	70	P388	-	388	-
1093	0:42:31.3	41:10:30.0	22.09	-512.8	-	-	2002.10.09	70	P422	-	422	-
1094	0:41:59.9	41:10:32.7	22.91	-282.2	-	-	2002.10.09	70	-	-	-	-
1095	0:42:29.5	41:10:50.8	21.20	-160.5	-	-	2002.10.09	70	P150	-	150	527
1096	0:42:10.8	41:10:40.8	22.91	-451.9	-	-	2002.10.09	70	-	-	376	-
1097	0:42:24.7	41:10:49.6	22.99	-411.5	-	-	2002.10.09	70	P404	-	404	-
1098	0:42:35.8	41:11:02.2	21.68	-280.9	-	-	2002.10.09	70	P152	-	152	550
1099	0:42:03.9	41:10:48.2	23.31	-593.3	-	-	2002.10.09	70	-	-	-	-
1100	0:42:25.9	41:11:06.9	22.86	-366.1	-	-	2002.10.09	70	P409	-	409	-
1101	0:42:16.5	41:11:07.8	22.53	-507.7	-	-	2002.10.09	70	P385	-	385	-
1102	0:42:22.1	41:11:26.6	21.41	-594.9	E	-	2002.10.09	70	P396	-	396	493
1103	0:42:21.0	41:11:28.8	23.27	-228.6	-	-	2002.10.09	70	-	-	392	-
1104	0:42:29.0	41:11:38.0	22.34	-297.8	-	-	2002.10.09	70	P419	-	419	523
1105	0:42:06.6	41:11:33.5	21.68	-323.4	-	-	2002.10.09	70	PN_1.1_71	-	-	447
1106	0:42:16.7	41:11:43.7	23.38	-505.1	-	-	2002.10.09	70	-	-	386	-
1107	0:42:09.8	41:11:55.1	22.26	-494.8	-	-	2002.10.09	70	-	-	373	-
1108	0:42:25.4	41:12:01.3	22.83	-362.5	-	-	2002.10.09	70	P407	-	407	-
1109	0:42:25.2	41:12:02.8	22.80	-557.2	-	-	2002.10.09	70	-	-	406	-
1110	0:42:24.4	41:12:12.0	21.44	-404.8	-	-	2002.10.09	70	P149	-	149	505
1111	0:41:58.6	41:12:04.5	22.10	-525.7	-	-	2002.10.09	70	-	-	-	431
1112	0:42:25.0	41:12:17.1	22.60	-677.9	-	-	2002.10.09	70	P148	-	148	-
1113	0:41:56.7	41:12:06.4	23.48	-490.9	-	-	2002.10.09	70	-	-	-	-
1114	0:42:19.0	41:12:20.0	23.25	-337.2	-	-	2002.10.09	70	-	-	-	-
1115	0:42:25.9	41:12:31.9	21.63	-459.9	-	-	2002.10.09	70	P147	-	147	-
1116	0:42:10.3	41:12:38.0	20.58	-420.2	-	-	2002.10.09	70	P375	-	375	459
1117	0:42:23.2	41:12:37.1	23.00	-669.6	-	-	2002.10.09	70	-	-	-	-
1118	0:42:24.9	41:12:44.1	22.34	-451.0	-	-	2002.10.09	70	-	-	-	-
1119	0:42:20.4	41:12:42.0	22.82	-557.5	-	-	2002.10.09	70	P391	-	391	-
1120	0:42:15.7	41:12:43.6	22.83	-453.8	-	-	2002.10.09	70	P382	-	382	-
1121	0:42:22.7	41:12:58.8	23.03	-628.2	-	-	2002.10.09	70	-	-	-	-
1122	0:42:33.1	41:13:04.9	22.95	-455.5	-	-	2002.10.09	70	-	-	-	-
1123	0:42:33.9	41:13:08.3	22.57	-310.5	-	-	2002.10.09	70	-	-	145	-
1124	0:42:12.6	41:13:25.7	21.59	-395.6	-	-	2002.10.09	70	P378	-	378	465
1125	0:42:07.7	41:13:28.8	21.51	-424.2	-	-	2002.10.09	70	PN_1.1_65	-	-	451
1126	0:41:54.5	41:13:25.4	22.16	-459.7	-	-	2002.10.09	70	-	-	-	421
1127	0:42:06.3	41:13:23.2	23.83	-461.9	-	-	2002.10.09	70	-	-	-	-
1128	0:41:53.6	41:13:24.2	22.79	-457.1	-	-	2002.10.09	70	-	-	-	-
1129	0:42:13.8	41:13:36.9	20.36	-289.2	-	-	2002.10.09	70	P380	-	380	471

Continued on next page

Table A.1 – continued from previous page

ID	RA	Dec	$m_{5007}$	$v_{\text{helio}}$	Note	Host	Date	Field	H06	C89	HK04	MLA93
1130	0:42:23.2	41:13:37.8	22.12	-394.0	-	-	2002.10.09	70	P400	-	400	499
1131	0:42:29.7	41:13:52.5	21.57	-526.8	-	-	2002.10.09	70	P98	-	98	-
1132	0:42:29.5	41:14:05.0	20.85	-294.2	-	-	2002.10.09	70	P50	-	50	528
1133	0:42:21.0	41:13:57.6	22.89	-466.0	-	-	2002.10.09	70	-	-	-	-
1134	0:42:21.8	41:14:11.6	20.70	-461.3	-	-	2002.10.09	70	P97	-	97	491
1135	0:42:26.3	41:14:20.2	23.66	-480.5	-	-	2002.10.09	70	-	-	-	-
1136	0:42:06.2	41:14:24.3	21.31	-126.7	-	-	2002.10.09	70	-	-	-	446
1137	0:42:27.2	41:14:35.0	20.54	-352.9	-	-	2002.10.09	70	P49	-	49	516
1138	0:42:02.4	41:14:27.5	22.92	-490.0	-	-	2002.10.09	70	-	-	-	-
1139	0:42:35.3	41:14:46.8	20.40	-282.4	-	-	2002.10.09	70	P53	-	53	-
1140	0:42:24.5	41:14:39.7	22.26	-421.9	-	-	2002.10.09	70	P183	-	183	-
1141	0:42:34.7	41:14:45.5	21.69	-168.0	-	-	2002.10.09	70	-	-	52	-
1142	0:42:16.4	41:14:40.6	22.73	-234.6	-	-	2002.10.09	70	-	-	-	-
1143	0:42:11.5	41:17:42.5	23.35	-203.7	-	-	2002.10.09	70	-	-	-	-
1144	0:42:08.5	41:17:22.6	23.40	-446.6	-	-	2002.10.09	70	-	-	-	-
1145	0:42:23.7	41:17:17.6	23.09	-166.5	-	-	2002.10.09	70	-	-	-	-
1146	0:42:16.3	41:17:14.9	23.87	-317.6	-	-	2002.10.09	70	-	-	-	-
1147	0:41:56.5	41:17:04.6	24.15	-437.5	E	-	2002.10.09	70	-	-	-	-
1148	0:42:24.3	41:17:13.5	23.73	-248.4	-	-	2002.10.09	70	-	-	-	-
1149	0:42:33.2	41:16:50.3	20.61	-504.3	-	-	2002.10.09	70	P41	-	41	545
1150	0:42:27.8	41:16:31.9	20.40	-466.7	-	-	2002.10.09	70	P46	-	46	518
1151	0:42:31.0	41:16:26.1	21.19	-121.4	-	-	2002.10.09	70	P43	-	43	533
1152	0:42:11.5	41:16:12.1	21.83	-324.0	-	-	2002.10.09	70	P295	-	295	460
1153	0:42:32.5	41:15:59.4	20.58	-279.5	-	-	2002.10.09	70	P45	-	45	541
1154	0:41:52.3	41:15:43.3	21.51	-409.6	-	-	2002.10.09	70	-	-	-	415
1155	0:42:15.9	41:16:17.9	22.54	-347.4	-	-	2002.10.09	70	P293	-	293	-
1156	0:42:10.5	41:16:06.1	23.39	-280.1	-	-	2002.10.09	70	P296	-	296	-
1157	0:41:57.9	41:16:15.6	22.75	-306.3	-	-	2002.10.09	70	-	-	-	429
1158	0:42:27.8	41:16:20.3	20.76	-337.4	-	-	2002.10.09	70	P47	-	47	517
1159	0:42:21.0	41:15:58.1	23.15	-311.4	-	-	2002.10.09	70	-	-	-	-
1160	0:42:23.8	41:16:19.7	23.38	-406.1	-	-	2002.10.09	70	-	-	-	-
1161	0:42:05.2	41:16:10.3	21.20	-344.2	-	-	2002.10.09	70	PN_L1_54	-	-	445
1162	0:42:31.5	41:16:15.4	21.94	-404.2	-	-	2002.10.09	70	-	-	44	-
1163	0:42:32.8	41:16:33.6	20.43	-415.7	-	-	2002.10.09	70	P42	-	42	543
1164	0:42:20.6	41:16:13.7	23.42	-515.7	-	-	2002.10.09	70	-	-	-	-
1165	0:41:55.9	41:15:45.8	23.87	-410.1	-	-	2002.10.09	70	-	-	-	-
1166	0:42:22.4	41:16:04.9	20.85	-287.2	-	-	2002.10.09	70	P92	-	92	495
1167	0:42:15.0	41:15:57.5	22.07	-139.0	-	-	2002.10.09	70	P292	-	292	476
1168	0:42:27.5	41:16:07.8	21.55	-495.3	-	-	2002.10.09	70	-	-	100	-
1169	0:42:18.6	41:16:01.5	22.67	-377.3	-	-	2002.10.09	70	P291	-	291	-
1170	0:42:25.9	41:16:01.5	22.72	-306.1	-	-	2002.10.09	70	-	-	408	-
1171	0:42:28.3	41:15:29.8	21.15	-415.3	-	-	2002.10.09	70	P95	-	95	519
1172	0:42:12.9	41:15:42.1	23.68	-379.2	-	-	2002.10.09	70	-	-	-	-
1173	0:42:25.6	41:15:43.4	21.01	-575.7	-	-	2002.10.09	70	P93	-	93	508
1174	0:41:55.3	41:15:33.7	24.75	-413.2	-	-	2002.10.09	70	-	-	-	-
1175	0:42:22.8	41:15:32.5	21.66	-416.4	-	-	2002.10.09	70	P182	-	182	497
1176	0:42:20.1	41:15:34.7	22.61	-419.8	-	-	2002.10.09	70	P389	-	389	-
1177	0:42:27.3	41:15:34.7	22.04	-409.9	-	-	2002.10.09	70	-	-	94	-
1178	0:42:29.1	41:15:17.1	20.29	-259.9	-	-	2002.10.09	70	P48	-	48	526
1179	0:42:05.9	41:14:57.2	22.91	-737.1	-	Stream?	2002.10.09	70	-	-	-	-
1180	0:42:11.4	41:15:07.4	24.10	-360.6	-	-	2002.10.09	70	-	-	-	-
1181	0:42:34.1	41:15:05.3	21.08	-368.6	-	-	2002.10.09	70	P51	-	51	-
1182	0:42:18.6	41:14:57.1	20.86	-271.4	-	-	2002.10.09	70	P387	-	387	480
1183	0:42:27.1	41:14:55.2	21.95	-514.5	-	-	2002.10.09	70	P101	-	101	-
1184	0:42:16.3	41:16:39.9	23.45	-255.0	-	-	2002.10.09	70	-	-	-	-
1185	0:42:06.9	41:16:41.5	23.46	-174.7	-	-	2002.10.09	70	-	-	-	-
1186	0:42:20.8	41:16:54.3	21.07	-197.1	-	-	2002.10.09	70	P91	-	91	484
1187	0:42:24.0	41:11:11.0	23.36	-527.7	-	-	2002.10.09	70	-	-	403	-
1188	0:42:22.1	41:11:47.2	23.89	-571.2	E	-	2002.10.09	70	-	-	-	-
1189	0:42:05.8	41:12:08.4	23.86	-340.0	-	-	2002.10.09	70	-	-	-	-
1190	0:42:22.1	41:13:02.6	22.88	-357.6	-	-	2002.10.09	70	-	-	397	-
1191	0:42:24.9	41:14:59.6	24.04	-529.6	-	-	2002.10.09	70	-	-	-	-
1192	0:42:30.2	41:14:08.2	23.49	-309.8	-	-	2002.10.09	70	-	-	420	-
1193	0:42:33.0	41:14:35.1	23.55	-475.0	-	-	2002.10.09	70	-	-	-	546
1194	0:42:35.8	41:13:50.9	22.74	-464.7	-	-	2002.10.09	70	-	-	433	-
1195	0:42:35.2	41:15:04.0	23.84	-360.9	E	-	2002.10.09	70	-	-	-	-
1196	0:42:34.2	41:16:32.4	22.87	-306.6	-	-	2002.10.09	70	-	-	428	-
1197	0:42:27.6	41:15:02.3	23.46	-340.4	-	-	2002.10.09	70	-	-	411	-
1198	0:42:22.9	41:14:27.2	23.75	-431.6	-	-	2002.10.09	70	-	-	-	-
1199	0:42:22.7	41:16:24.3	23.76	-168.1	-	-	2002.10.09	70	-	-	-	-
1200	0:41:54.4	41:16:29.7	24.18	-469.6	E	-	2002.10.09	70	-	-	-	-
1201	0:42:28.3	41:17:37.2	23.45	-360.4	-	-	2002.10.09	70	P412	-	412	-
1202	0:42:32.0	41:17:33.4	23.55	-178.7	-	-	2002.10.09	70	P424	-	424	-
1203	0:42:35.3	41:17:29.0	22.76	-461.0	-	-	2002.10.09	70	-	-	431	-
1204	0:42:28.9	41:09:58.6	23.48	-350.6	-	-	2002.10.09	70	-	-	418	-
1205	0:42:36.0	41:14:11.4	23.50	-298.5	-	-	2002.10.09	70	-	-	-	-
1206	0:42:34.4	41:13:33.1	23.99	-453.6	-	-	2002.10.09	70	-	-	-	-
1207	0:42:32.9	41:15:59.2	21.93	-291.1	-	-	2002.10.09	70	-	-	142	-
1208	0:42:25.0	41:14:30.9	23.57	-495.9	-	-	2002.10.09	70	-	-	-	-
1209	0:42:34.2	41:16:49.5	23.98	-19.8	-	-	2002.10.09	70	-	-	427	-
1210	0:43:23.0	41:10:51.0	21.54	-351.9	-	-	2002.10.09	71	-	-	-	760
1211	0:43:25.0	41:10:35.9	23.47	-364.4	-	-	2002.10.09	71	-	-	-	-
1212	0:42:49.0	41:10:33.4	22.79	-425.1	-	-	2002.10.09	71	-	-	-	-
1213	0:43:04.3	41:10:53.1	23.24	-306.3	-	-	2002.10.09	71	-	-	-	-
1214	0:42:43.9	41:10:47.5	20.47	-260.8	-	-	2002.10.09	71	P155	-	155	586
1215	0:43:06.2	41:10:56.3	20.84	-357.8	-	-	2002.10.09	71	-	1.92	-	683
1216	0:43:19.2	41:11:24.7	23.30	-368.1	-	-	2002.10.09	71	-	-	-	-
1217	0:43:16.5	41:11:26.9	23.50	-340.8	-	-	2002.10.09	71	-	-	-	-
1218	0:43:13.9	41:11:33.7	24.01	-260.8	-	-	2002.10.09	71	-	-	-	-
1219	0:42:47.6	41:11:28.6	23.35	-293.1	-	-	2002.10.09	71	P458	-	458	-
1220	0:42:47.3	41:11:33.7	23.35	-348.2	-	-	2002.10.09	71	P456	-	456	-
1221	0:42:42.3	41:11:35.4	23.86	-167.6	-	-	2002.10.09	71	-	-	-	-
1222	0:42:47.0	41:11:50.3	23.60	-450.7	-	-	2002.10.09	71	-	-	-	-

Continued on next page

Table A.1 – continued from previous page

ID	RA	Dec	$m_{5007}$	$v_{\text{helio}}$	Note	Host	Date	Field	H06	C89	HK04	MLA93
1223	0:43:19.2	41:12:13.2	21.81	-317.2	-	-	2002.10.09	71	PN_6_1_46	-	-	747
1224	0:42:53.4	41:12:00.6	23.69	-173.7	-	-	2002.10.09	71	-	-	-	-
1225	0:42:51.9	41:12:15.4	20.56	-568.6	-	-	2002.10.09	71	-	-	-	609
1226	0:43:17.9	41:12:19.8	22.54	-307.5	-	-	2002.10.09	71	-	-	-	738
1227	0:42:45.0	41:12:11.8	21.42	-371.1	-	-	2002.10.09	71	P157	-	157	589
1228	0:43:02.9	41:12:16.1	23.90	-173.1	-	-	2002.10.09	71	-	-	-	-
1229	0:43:07.8	41:12:31.8	23.01	-243.1	-	-	2002.10.09	71	-	-	-	690
1230	0:43:12.4	41:12:44.0	21.05	-349.5	-	-	2002.10.09	71	PN_6_1_44	-	-	712
1231	0:42:40.8	41:12:27.8	23.56	-528.3	-	-	2002.10.09	71	-	-	446	-
1232	0:42:57.9	41:12:43.9	21.20	-203.1	-	-	2002.10.09	71	-	1.88	-	644
1233	0:43:11.2	41:12:40.7	24.19	-336.2	-	-	2002.10.09	71	-	-	-	-
1234	0:42:58.8	41:12:50.8	21.23	-375.6	-	-	2002.10.09	71	-	-	-	652
1235	0:42:51.0	41:12:39.6	23.65	-295.7	-	-	2002.10.09	71	-	-	-	-
1236	0:43:10.0	41:12:53.6	23.57	-225.9	-	-	2002.10.09	71	-	-	-	-
1237	0:42:51.4	41:12:54.0	23.19	-342.3	-	-	2002.10.09	71	-	-	-	-
1238	0:43:09.0	41:13:09.3	23.18	-199.1	-	-	2002.10.09	71	-	-	-	-
1239	0:42:40.6	41:13:05.1	22.57	-461.3	-	-	2002.10.09	71	-	-	-	-
1240	0:42:46.7	41:13:17.1	20.79	-424.8	-	-	2002.10.09	71	P67	-	67	593
1241	0:42:54.2	41:13:37.3	23.26	-356.8	-	-	2002.10.09	71	P475	-	475	-
1242	0:43:15.3	41:13:49.5	24.45	-253.5	E	-	2002.10.09	71	-	-	-	-
1243	0:43:09.1	41:13:51.9	22.52	-343.7	-	-	2002.10.09	71	-	-	-	-
1244	0:42:47.7	41:13:49.1	22.38	-156.0	-	-	2002.10.09	71	P163	-	163	-
1245	0:42:49.3	41:13:54.2	22.20	-235.0	-	-	2002.10.09	71	-	-	164	-
1246	0:42:42.5	41:13:57.1	22.11	-424.5	-	-	2002.10.09	71	-	-	99	-
1247	0:42:53.8	41:14:00.3	23.32	-309.7	-	-	2002.10.09	71	-	-	472	-
1248	0:42:57.0	41:14:09.2	23.37	-416.8	-	-	2002.10.09	71	P171	-	171	-
1249	0:42:42.2	41:14:10.2	21.04	-327.5	-	-	2002.10.09	71	P57	-	57	-
1250	0:42:40.8	41:14:10.6	20.94	-266.5	-	-	2002.10.09	71	P56	-	56	573
1251	0:42:41.4	41:14:08.1	22.19	-114.1	E	-	2002.10.09	71	-	-	141	-
1252	0:42:43.1	41:14:10.0	22.61	-434.7	-	-	2002.10.09	71	-	-	139	-
1253	0:42:54.3	41:14:18.1	22.93	-141.1	-	-	2002.10.09	71	P476	-	476	-
1254	0:42:46.8	41:14:21.9	20.96	-194.3	-	-	2002.10.09	71	P61	-	61	-
1255	0:42:42.2	41:14:23.6	22.51	-543.7	-	-	2002.10.09	71	-	-	174	-
1256	0:42:46.0	41:14:26.9	22.96	-535.3	-	-	2002.10.09	71	-	-	-	-
1257	0:43:00.7	41:14:43.5	20.74	-249.8	-	-	2002.10.09	71	P172	-	172	662
1258	0:43:04.6	41:14:43.4	22.95	-461.3	-	-	2002.10.09	71	P493	-	493	-
1259	0:42:56.2	41:17:33.3	22.29	-249.7	-	-	2002.10.09	71	P120	-	120	-
1260	0:42:57.4	41:17:26.4	21.00	-308.3	-	-	2002.10.09	71	P80	-	80	639
1261	0:42:53.6	41:17:35.0	21.10	-459.6	-	-	2002.10.09	71	P29	-	29	-
1262	0:42:54.8	41:18:57.0	24.02	-216.5	E	-	2002.10.09	71	-	-	-	-
1263	0:42:42.2	41:18:47.4	23.69	-462.5	-	-	2002.10.09	71	-	-	-	-
1264	0:42:49.1	41:14:43.1	22.70	-305.5	-	-	2002.10.09	71	-	-	166	-
1265	0:42:43.9	41:14:51.3	21.04	-444.8	-	-	2002.10.09	71	-	-	58	-
1266	0:42:45.2	41:15:24.3	21.04	-549.3	-	-	2002.10.09	71	-	-	21	-
1267	0:42:48.2	41:17:35.2	22.72	-495.4	-	-	2002.10.09	71	P460	-	460	-
1268	0:42:55.5	41:17:21.7	20.69	-307.8	-	-	2002.10.09	71	P30	-	30	626
1269	0:42:52.2	41:17:25.6	20.66	-232.2	-	-	2002.10.09	71	P28	-	28	-
1270	0:43:09.4	41:15:23.4	22.83	-462.0	-	-	2002.10.09	71	-	-	-	-
1271	0:42:55.3	41:17:12.7	21.60	-129.1	E	-	2002.10.09	71	-	-	478	-
1272	0:42:51.0	41:14:48.0	21.81	-344.7	-	-	2002.10.09	71	P78	-	78	-
1273	0:42:58.1	41:14:52.8	22.67	-443.9	-	-	2002.10.09	71	P173	-	173	-
1274	0:43:06.9	41:15:15.2	21.12	-394.2	E	-	2002.10.09	71	-	-	-	-
1275	0:43:19.4	41:15:04.1	23.07	-231.7	-	-	2002.10.09	71	-	-	-	-
1276	0:43:19.0	41:15:09.7	21.05	-128.3	-	-	2002.10.09	71	-	-	-	745
1277	0:42:49.4	41:14:57.4	21.92	-334.5	-	-	2002.10.09	71	-	-	63	-
1278	0:42:47.6	41:15:05.8	21.31	76.1	-	-	2002.10.09	71	-	-	60	-
1279	0:42:41.6	41:15:02.6	22.54	-343.6	-	-	2002.10.09	71	-	-	449	-
1280	0:42:54.2	41:15:05.0	23.50	-254.1	-	-	2002.10.09	71	-	-	474	-
1281	0:42:50.6	41:15:57.0	21.80	-306.1	R	-	2002.10.09	71	-	-	462	-
1282	0:42:54.6	41:15:22.5	21.96	-48.6	-	-	2002.10.09	71	P77	-	77	-
1283	0:43:02.6	41:17:00.5	22.98	-428.0	-	-	2002.10.09	71	P489	-	489	-
1284	0:42:58.4	41:17:10.6	20.40	-227.7	E	-	2002.10.09	71	P31	-	31	648
1285	0:43:18.7	41:15:39.1	22.78	-102.6	-	-	2002.10.09	71	P505	-	505	-
1286	0:42:43.5	41:16:58.2	22.41	-165.7	R	-	2002.10.09	71	-	-	81	-
1287	0:42:46.1	41:15:17.2	21.63	-213.3	-	-	2002.10.09	71	-	-	59	-
1288	0:43:16.8	41:15:14.6	21.76	-50.1	-	-	2002.10.09	71	-	-	-	733
1289	0:43:00.0	41:15:43.7	23.81	-344.9	-	-	2002.10.09	71	-	-	-	-
1290	0:42:43.1	41:15:37.8	21.75	-533.1	-	-	2002.10.09	71	-	-	20	-
1291	0:42:54.7	41:16:24.9	21.61	-121.3	-	-	2002.10.09	71	-	-	25	-
1292	0:42:40.7	41:17:25.3	22.82	-82.8	-	-	2002.10.09	71	-	-	445	-
1293	0:43:07.9	41:15:47.6	23.23	-45.8	-	-	2002.10.09	71	P497	-	497	-
1294	0:42:57.4	41:17:15.3	23.28	-522.0	-	-	2002.10.09	71	P189	-	189	-
1295	0:42:45.3	41:15:30.3	22.16	-292.9	-	-	2002.10.09	71	-	-	323	-
1296	0:42:46.3	41:15:23.7	22.32	-70.9	-	-	2002.10.09	71	-	-	-	-
1297	0:42:43.8	41:16:26.8	20.71	-279.1	-	-	2002.10.09	71	-	-	3	-
1298	0:42:55.1	41:17:02.8	23.00	-32.7	-	-	2002.10.09	71	-	-	477	-
1299	0:42:46.4	41:15:47.1	21.45	-378.9	-	-	2002.10.09	71	-	-	72	-
1300	0:42:45.0	41:16:24.9	21.28	-187.8	-	-	2002.10.09	71	-	-	-	-
1301	0:42:57.3	41:17:00.2	22.09	-343.7	-	-	2002.10.09	71	P136	-	136	-
1302	0:42:49.7	41:16:51.0	22.34	-296.0	-	-	2002.10.09	71	P330	-	330	-
1303	0:42:43.0	41:15:20.8	22.31	-245.7	-	-	2002.10.09	71	-	-	-	-
1304	0:43:09.5	41:15:53.2	20.47	-224.0	-	-	2002.10.09	71	P178	-	178	696
1305	0:42:55.9	41:16:16.7	22.23	-216.5	-	-	2002.10.09	71	P175	-	175	-
1306	0:42:43.1	41:15:33.0	22.33	-310.3	-	-	2002.10.09	71	-	-	20	-
1307	0:42:50.2	41:15:27.2	22.25	-308.2	-	-	2002.10.09	71	-	-	137	-
1308	0:42:55.5	41:16:25.4	20.95	-408.1	-	-	2002.10.09	71	P26	-	26	-
1309	0:42:46.8	41:16:10.5	21.26	-158.7	R	-	2002.10.09	71	-	-	10	-
1310	0:42:49.4	41:16:12.9	22.68	-240.0	-	-	2002.10.09	71	-	-	328	-
1311	0:42:51.4	41:15:57.2	21.99	-401.1	-	-	2002.10.09	71	P75	-	75	-
1312	0:42:47.3	41:16:29.4	21.18	-246.3	R	-	2002.10.09	71	-	-	13	-
1313	0:42:53.4	41:16:29.0	21.40	-279.9	-	-	2002.10.09	71	P24	-	24	-
1314	0:42:54.3	41:15:28.2	22.83	-185.6	-	-	2002.10.09	71	-	-	176	-
1315	0:43:08.0	41:15:37.9	22.88	-103.3	-	-	2002.10.09	71	P498	-	498	-

Continued on next page

Table A.1 – continued from previous page

ID	RA	Dec	$m_{5007}$	$v_{\text{helio}}$	Note	Host	Date	Field	H06	C89	HK04	MLA93
1316	0:43:23.0	41:15:40.5	22.08	-275.0	-	-	2002.10.09	71	-	1.99	-	759
1317	0:43:12.9	41:16:43.4	22.54	-238.4	-	-	2002.10.09	71	P502	-	502	-
1318	0:42:54.6	41:15:38.1	21.91	-120.5	-	-	2002.10.09	71	P76	-	76	-
1319	0:42:58.0	41:16:22.1	20.71	-131.5	-	-	2002.10.09	71	P27	-	27	-
1320	0:42:49.0	41:16:56.7	21.52	-127.8	-	-	2002.10.09	71	P23	-	23	-
1321	0:42:47.6	41:16:22.4	21.10	-339.5	-	-	2002.10.09	71	P12	-	12	-
1322	0:42:60.0	41:16:49.7	21.73	-308.8	-	-	2002.10.09	71	P135	-	135	-
1323	0:42:43.3	41:15:57.3	21.24	-235.4	-	-	2002.10.09	71	-	-	7	-
1324	0:42:43.9	41:16:02.5	19.96	-253.7	E	-	2002.10.09	71	P8	-	8	-
1325	0:42:44.9	41:17:00.1	22.13	-187.2	R	-	2002.10.09	71	-	-	-	-
1326	0:42:46.2	41:16:42.2	20.60	-509.4	-	-	2002.10.09	71	P1	-	1	-
1327	0:42:54.0	41:17:03.0	22.90	-237.0	-	-	2002.10.09	71	-	-	473	-
1328	0:43:02.4	41:16:50.2	21.99	-314.3	-	-	2002.10.09	71	P177	-	177	-
1329	0:42:47.0	41:16:56.0	22.41	96.0	-	-	2002.10.09	71	-	-	14	-
1330	0:42:46.5	41:17:03.4	21.55	-354.5	-	-	2002.10.09	71	-	-	15	-
1331	0:42:41.5	41:09:59.8	21.77	-610.4	-	-	2002.10.09	71	P153	-	153	577
1332	0:42:56.5	41:13:29.4	20.78	-684.0	-	-	2002.10.09	71	P167	-	167	636
1333	0:42:44.0	41:13:29.6	22.93	-356.1	-	-	2002.10.09	71	-	-	452	-
1334	0:42:41.8	41:14:28.9	23.49	-370.6	-	-	2002.10.09	71	-	-	-	-
1335	0:42:48.7	41:14:26.7	22.21	-587.8	-	-	2002.10.09	71	-	-	79	-
1336	0:42:49.0	41:15:24.6	21.01	-583.7	-	-	2002.10.09	71	P62	-	62	-
1337	0:42:52.8	41:14:16.2	20.68	-610.3	-	-	2002.10.09	71	P64	-	64	612
1338	0:43:15.7	41:18:01.1	21.55	-376.5	-	-	2002.10.09	71	P207	-	207	-
1339	0:42:42.4	41:15:54.3	21.07	-616.0	R	-	2002.10.09	71	P5	-	5	-
1340	0:42:38.0	41:16:03.4	23.34	-106.8	-	-	2002.10.09	71	-	-	-	-
1341	0:42:41.0	41:16:12.9	22.16	-600.8	-	-	2002.10.09	71	-	-	16	-
1342	0:42:56.3	41:10:25.7	24.47	-425.2	-	-	2002.10.09	71	-	-	-	-
1343	0:42:43.3	41:12:13.8	23.87	-378.3	-	-	2002.10.09	71	-	-	-	-
1344	0:42:40.1	41:14:05.6	23.57	-276.9	-	-	2002.10.09	71	-	-	-	-
1345	0:42:40.2	41:14:45.4	23.09	-348.8	-	-	2002.10.09	71	-	-	-	-
1346	0:42:43.3	41:14:41.9	24.10	-519.8	-	-	2002.10.09	71	-	-	-	-
1347	0:42:45.0	41:15:21.7	21.63	-652.8	-	-	2002.10.09	71	-	-	74	-
1348	0:42:45.7	41:14:21.4	23.20	-568.8	-	-	2002.10.09	71	-	-	-	-
1349	0:42:44.5	41:15:06.1	22.92	-150.6	-	-	2002.10.09	71	-	-	-	-
1350	0:42:46.8	41:14:57.8	23.01	-436.1	-	-	2002.10.09	71	-	-	-	-
1351	0:42:45.3	41:13:19.4	23.98	-161.9	-	-	2002.10.09	71	-	-	-	-
1352	0:42:50.6	41:15:35.3	22.89	-319.0	-	-	2002.10.09	71	-	-	463	-
1353	0:42:52.8	41:13:37.6	23.62	-180.1	E	-	2002.10.09	71	-	-	-	-
1354	0:43:17.6	41:15:25.3	23.87	-398.9	-	-	2002.10.09	71	-	-	-	-
1355	0:43:10.1	41:16:54.0	23.57	-117.7	-	-	2002.10.09	71	-	-	-	-
1356	0:43:00.3	41:16:53.9	23.59	-241.9	-	-	2002.10.09	71	-	-	486	-
1357	0:42:47.8	41:17:25.5	23.37	-386.9	-	-	2002.10.09	71	-	-	-	-
1358	0:42:43.4	41:17:14.2	23.25	-366.2	-	-	2002.10.09	71	-	-	-	-
1359	0:42:39.2	41:16:35.4	23.06	-415.8	E	-	2002.10.09	71	-	-	-	-
1360	0:42:45.9	41:17:36.5	22.69	47.9	-	-	2002.10.09	71	-	-	-	-
1361	0:42:43.8	41:18:08.8	24.10	-342.2	-	-	2002.10.09	71	-	-	-	-
1362	0:42:43.1	41:18:11.2	23.41	-146.1	-	-	2002.10.09	71	-	-	-	-
1363	0:42:46.2	41:18:41.2	23.75	-123.5	-	-	2002.10.09	71	-	-	-	-
1364	0:42:50.6	41:18:36.6	23.23	-285.6	-	-	2002.10.09	71	-	-	464	-
1365	0:44:07.5	41:10:09.5	21.94	-271.9	-	-	2002.10.09	72	PN_6.1.75	1.106	-	922
1366	0:43:35.4	41:10:36.5	22.73	-309.3	E	-	2002.10.09	72	-	-	-	-
1367	0:43:55.1	41:11:09.2	23.26	-367.6	-	-	2002.10.09	72	-	-	-	-
1368	0:43:36.3	41:11:22.0	23.77	-399.6	-	-	2002.10.09	72	-	-	-	-
1369	0:43:58.8	41:11:30.3	22.48	-244.7	-	-	2002.10.09	72	PN_6.1.72	-	-	893
1370	0:43:48.1	41:11:33.4	23.08	-292.4	R	-	2002.10.09	72	-	-	-	-
1371	0:43:43.9	41:11:36.9	23.21	-281.2	R	-	2002.10.09	72	PN_6.1.68	-	-	-
1372	0:43:53.3	41:11:59.0	22.76	-240.4	-	-	2002.10.09	72	-	-	-	-
1373	0:43:56.2	41:12:04.3	22.44	-277.5	-	-	2002.10.09	72	-	-	-	-
1374	0:44:04.6	41:12:08.8	21.66	-299.0	-	-	2002.10.09	72	-	1.104	-	914
1375	0:43:55.8	41:12:11.8	22.84	-272.0	-	-	2002.10.09	72	-	-	-	-
1376	0:44:14.8	41:12:21.4	23.59	-495.1	-	-	2002.10.09	72	-	-	-	-
1377	0:43:46.9	41:12:39.8	22.46	-302.5	R	-	2002.10.09	72	-	-	-	-
1378	0:43:49.7	41:12:44.4	22.00	-287.8	E	-	2002.10.09	72	-	-	-	863
1379	0:44:09.4	41:13:06.0	22.86	-416.4	-	-	2002.10.09	72	-	-	-	929
1380	0:44:11.9	41:13:59.9	21.50	-236.3	-	-	2002.10.09	72	PN_6.1.70	1.109	-	942
1381	0:43:37.3	41:14:30.0	21.36	-242.6	-	-	2002.10.09	72	PN_6.1.61	-	-	819
1382	0:43:43.5	41:14:53.1	22.44	-171.3	-	-	2002.10.09	72	-	-	-	842
1383	0:43:37.0	41:15:09.2	21.94	-231.0	-	-	2002.10.09	72	-	-	-	814
1384	0:44:08.8	41:15:20.2	23.75	-203.0	E	-	2002.10.09	72	PN_6.1.95	-	-	-
1385	0:44:15.1	41:15:31.4	23.57	-213.4	-	-	2002.10.09	72	-	-	-	-
1386	0:43:59.9	41:15:35.0	22.11	-251.1	-	-	2002.10.09	72	PN_6.1.74	-	-	899
1387	0:43:40.8	41:15:56.3	24.10	-91.1	-	-	2002.10.09	72	-	-	-	-
1388	0:43:33.8	41:16:11.2	23.55	-307.2	-	-	2002.10.09	72	-	-	-	-
1389	0:43:59.4	41:16:47.2	21.80	-18.0	-	-	2002.10.09	72	PN_6.1.73	-	-	897
1390	0:43:51.6	41:17:18.0	23.72	-279.5	-	-	2002.10.09	72	-	-	-	-
1391	0:43:32.6	41:17:20.7	23.11	-338.5	-	-	2002.10.09	72	-	-	-	-
1392	0:44:23.0	41:09:58.7	25.66	-211.3	-	-	2002.10.11	73	-	-	-	-
1393	0:44:59.2	41:10:28.7	24.71	-225.0	-	-	2002.10.11	73	-	-	-	-
1394	0:44:37.9	41:14:14.1	22.97	-215.1	-	-	2002.10.11	73	-	1.115	-	1031
1395	0:44:49.8	41:14:24.7	25.80	-323.4	E	-	2002.10.11	73	-	-	-	-
1396	0:44:43.8	41:14:27.8	21.17	-302.6	-	-	2002.10.11	73	PN_5.1.2	1.119	-	1047
1397	0:44:17.2	41:14:40.0	25.10	-293.7	E	-	2002.10.11	73	-	-	-	-
1398	0:45:00.4	41:15:21.9	24.59	-195.4	-	-	2002.10.11	73	-	-	-	-
1399	0:44:32.4	41:15:29.9	22.82	-167.9	-	-	2002.10.11	73	-	-	-	1016
1400	0:44:21.1	41:15:41.0	21.40	-281.6	-	-	2002.10.11	73	-	1.111	-	971
1401	0:44:53.1	41:15:58.1	22.62	-216.7	-	-	2002.10.11	73	PN_5.1.3	1.121	-	1069
1402	0:44:42.7	41:16:40.7	25.67	-252.3	E	-	2002.10.11	73	-	-	-	-
1403	0:44:28.1	41:16:43.2	23.95	-283.0	E	-	2002.10.11	73	-	-	-	-
1404	0:44:50.7	41:17:22.1	21.07	-282.7	-	-	2002.10.11	73	-	1.120	-	1062
1405	0:44:29.3	41:17:15.9	24.94	-299.8	E	-	2002.10.11	73	-	-	-	-
1406	0:44:16.3	41:17:23.4	25.28	-260.5	E	-	2002.10.11	73	-	-	-	-
1407	0:44:29.1	41:18:58.5	25.17	-279.0	-	-	2002.10.11	73	-	-	-	-
1408	0:44:47.0	41:15:28.6	21.86	-587.0	-	-	2002.10.11	73	-	-	-	1054

Continued on next page

Table A.1 – continued from previous page

ID	RA	Dec	$m_{5007}$	$v_{\text{helio}}$	Note	Host	Date	Field	H06	C89	HK04	MLA93
1409	0:45:49.0	41:11:49.5	25.15	-379.7	-	-	2002.10.12	74	-	-	-	-
1410	0:45:18.5	41:12:14.9	25.07	-382.1	-	-	2002.10.12	74	-	-	-	-
1411	0:45:42.7	41:14:24.3	24.52	-48.4	-	-	2002.10.12	74	-	-	-	-
1412	0:45:12.9	41:17:27.7	24.94	-76.6	-	-	2002.10.12	74	-	-	-	-
1413	0:46:11.6	41:10:42.9	24.87	-256.0	-	-	2002.10.12	75	-	-	-	-
1414	0:46:35.0	41:12:29.2	23.12	-228.1	-	-	2002.10.12	75	PN 5.1.11	-	-	1256
1415	0:46:31.6	41:12:57.3	24.12	-219.4	-	-	2002.10.12	75	PN 5.1.12	-	-	-
1416	0:46:06.5	41:15:09.2	25.53	-199.7	-	-	2002.10.12	75	-	-	-	-
1417	0:42:16.4	41:00:06.0	25.67	-480.2	E	-	2002.10.13	76	-	-	-	-
1418	0:42:07.6	41:00:27.2	25.07	-602.9	-	-	2002.10.13	76	-	-	-	-
1419	0:42:09.4	41:00:39.2	23.18	-483.5	-	-	2002.10.13	76	-	-	-	-
1420	0:41:55.9	41:00:41.5	23.84	-337.6	-	-	2002.10.13	76	-	-	-	-
1421	0:41:56.2	41:01:03.6	25.16	-421.5	E	-	2002.10.13	76	-	-	-	-
1422	0:41:45.6	41:01:01.2	22.66	-503.1	-	-	2002.10.13	76	-	-	-	-
1423	0:41:40.2	41:01:02.9	22.27	-496.0	-	-	2002.10.13	76	-	-	-	-
1424	0:41:49.2	41:01:13.1	24.80	-319.6	E,R	-	2002.10.13	76	-	-	-	384
1425	0:41:31.1	41:01:11.2	22.20	-434.1	-	-	2002.10.13	76	PN 2.3.24	-	-	367
1426	0:41:33.7	41:01:12.2	22.35	-547.4	-	-	2002.10.13	76	-	-	-	373
1427	0:41:53.6	41:01:20.1	23.93	-566.0	-	-	2002.10.13	76	-	-	-	-
1428	0:41:53.8	41:01:32.0	22.55	-586.8	-	-	2002.10.13	76	-	-	-	-
1429	0:41:28.2	41:01:24.3	24.40	-272.8	E	-	2002.10.13	76	-	-	-	-
1430	0:41:50.0	41:01:32.8	24.84	-309.2	-	-	2002.10.13	76	-	-	-	-
1431	0:41:28.4	41:01:29.4	21.63	-573.3	-	-	2002.10.13	76	-	-	-	364
1432	0:41:33.4	41:01:55.9	22.16	-468.6	-	-	2002.10.13	76	-	-	-	371
1433	0:42:00.5	41:02:06.4	21.74	-574.5	-	-	2002.10.13	76	PN 2.3.59	-	-	435
1434	0:41:43.7	41:02:02.8	24.51	-472.4	-	-	2002.10.13	76	-	-	-	-
1435	0:41:26.1	41:01:58.9	24.80	-491.1	E	-	2002.10.13	76	-	-	-	-
1436	0:41:44.4	41:02:11.3	21.20	-449.7	-	-	2002.10.13	76	-	-	-	396
1437	0:41:46.0	41:02:17.0	22.30	-546.6	-	-	2002.10.13	76	-	-	-	404
1438	0:41:60.0	41:02:45.9	25.31	-513.0	-	-	2002.10.13	76	-	-	-	-
1439	0:42:08.6	41:02:54.4	23.84	-544.8	-	-	2002.10.13	76	-	-	-	-
1440	0:41:34.7	41:02:45.1	25.34	-409.3	E	-	2002.10.13	76	-	-	-	-
1441	0:41:41.5	41:02:48.3	25.27	-437.1	-	-	2002.10.13	76	-	-	-	-
1442	0:42:01.3	41:03:13.6	24.84	-544.4	E	-	2002.10.13	76	-	-	-	-
1443	0:41:27.9	41:03:04.7	23.20	-487.3	-	-	2002.10.13	76	-	-	-	-
1444	0:41:46.0	41:03:12.2	20.91	-404.7	-	-	2002.10.13	76	PN 2.3.48	-	-	403
1445	0:42:03.8	41:03:18.5	23.11	-569.1	-	-	2002.10.13	76	-	-	-	-
1446	0:41:53.5	41:03:21.8	23.36	-376.0	-	-	2002.10.13	76	-	-	-	-
1447	0:42:01.7	41:03:26.3	23.05	-405.4	-	-	2002.10.13	76	-	-	-	-
1448	0:41:60.0	41:03:32.8	23.80	-404.6	E	-	2002.10.13	76	-	-	-	-
1449	0:41:38.7	41:03:27.6	23.79	-511.3	-	-	2002.10.13	76	-	-	-	-
1450	0:41:45.3	41:03:32.3	24.39	-581.4	-	-	2002.10.13	76	-	-	-	-
1451	0:42:07.0	41:03:45.1	21.76	-477.6	-	-	2002.10.13	76	-	-	-	449
1452	0:41:46.7	41:03:39.3	24.98	-410.2	-	-	2002.10.13	76	-	-	-	-
1453	0:42:09.8	41:03:49.5	24.80	-157.0	E	-	2002.10.13	76	-	-	-	-
1454	0:41:52.4	41:03:47.8	24.59	-581.2	E	-	2002.10.13	76	-	-	-	-
1455	0:41:46.2	41:03:45.9	25.40	-545.4	E	-	2002.10.13	76	-	-	-	-
1456	0:41:46.8	41:03:50.9	25.33	-452.0	E	-	2002.10.13	76	-	-	-	-
1457	0:42:08.1	41:03:58.7	24.75	-577.4	-	-	2002.10.13	76	-	-	-	-
1458	0:41:39.4	41:03:49.3	23.37	-364.8	-	-	2002.10.13	76	-	-	-	-
1459	0:41:58.1	41:03:58.0	24.23	-550.7	-	-	2002.10.13	76	-	-	-	-
1460	0:41:41.0	41:03:53.6	23.49	-167.5	-	-	2002.10.13	76	-	-	-	-
1461	0:41:50.7	41:03:57.7	23.04	-606.2	-	-	2002.10.13	76	-	-	-	-
1462	0:42:04.7	41:04:06.2	24.85	-479.8	E	-	2002.10.13	76	-	-	-	-
1463	0:42:09.3	41:04:08.7	25.16	-598.8	-	-	2002.10.13	76	-	-	-	-
1464	0:41:56.1	41:04:07.9	24.01	-476.9	-	-	2002.10.13	76	-	-	-	-
1465	0:42:04.2	41:04:11.7	23.73	-450.8	-	-	2002.10.13	76	-	-	-	-
1466	0:42:06.7	41:04:17.2	21.57	-545.7	-	-	2002.10.13	76	-	-	-	448
1467	0:41:48.7	41:04:15.0	24.88	-533.2	-	-	2002.10.13	76	-	-	-	-
1468	0:41:28.2	41:04:12.2	24.61	-548.5	E	-	2002.10.13	76	-	-	-	-
1469	0:41:38.0	41:04:17.9	23.18	-550.2	-	-	2002.10.13	76	-	-	-	-
1470	0:41:49.0	41:04:25.9	22.74	-330.4	-	-	2002.10.13	76	-	-	-	-
1471	0:42:07.1	41:04:32.3	24.85	-581.6	-	-	2002.10.13	76	-	-	-	-
1472	0:42:04.7	41:04:31.7	24.94	-496.7	-	-	2002.10.13	76	-	-	-	-
1473	0:42:06.3	41:04:32.5	24.89	-447.5	-	-	2002.10.13	76	-	-	-	-
1474	0:41:43.9	41:04:36.3	21.48	-390.3	-	-	2002.10.13	76	PN 2.3.47	-	-	394
1475	0:41:51.6	41:04:48.8	22.74	-729.1	-	-	2002.10.13	76	-	-	-	-
1476	0:41:39.1	41:04:45.4	23.10	-475.4	-	-	2002.10.13	76	PN 2.3.34	-	-	-
1477	0:41:54.0	41:05:13.4	24.77	-551.8	-	-	2002.10.13	76	-	-	-	-
1478	0:42:12.5	41:05:25.3	25.15	-500.7	E	-	2002.10.13	76	-	-	-	-
1479	0:41:47.9	41:05:26.5	25.13	-469.5	E	-	2002.10.13	76	-	-	-	-
1480	0:41:51.9	41:05:30.5	24.92	-255.7	-	-	2002.10.13	76	-	-	-	-
1481	0:42:03.4	41:05:34.8	24.50	-529.4	-	-	2002.10.13	76	-	-	-	-
1482	0:42:02.3	41:05:41.4	25.18	-500.3	E	-	2002.10.13	76	-	-	-	-
1483	0:41:50.4	41:05:37.8	24.55	-508.1	E	-	2002.10.13	76	-	-	-	-
1484	0:42:06.3	41:05:43.1	24.87	-549.2	E	-	2002.10.13	76	-	-	-	-
1485	0:41:52.1	41:05:43.8	23.45	-639.3	-	-	2002.10.13	76	-	-	-	-
1486	0:42:09.0	41:05:57.5	23.83	-630.7	-	-	2002.10.13	76	-	-	-	-
1487	0:41:55.6	41:05:53.6	25.18	-513.0	-	-	2002.10.13	76	-	-	-	-
1488	0:42:07.4	41:05:57.5	24.62	-421.3	-	-	2002.10.13	76	-	-	-	-
1489	0:41:48.1	41:05:55.9	21.75	-408.4	-	-	2002.10.13	76	-	-	-	409
1490	0:42:00.2	41:06:03.0	22.46	-351.7	-	-	2002.10.13	76	-	-	-	-
1491	0:42:07.6	41:06:12.0	24.33	-423.5	E	-	2002.10.13	76	-	-	-	-
1492	0:41:53.1	41:06:10.2	24.73	-528.2	-	-	2002.10.13	76	-	-	-	-
1493	0:41:56.7	41:06:12.5	22.13	-604.4	-	-	2002.10.13	76	-	-	-	427
1494	0:42:09.9	41:06:17.1	25.04	-423.3	-	-	2002.10.13	76	-	-	-	-
1495	0:42:05.7	41:06:19.0	22.82	-295.4	-	-	2002.10.13	76	-	-	-	-
1496	0:42:10.1	41:06:25.8	24.74	-412.0	-	-	2002.10.13	76	-	-	-	-
1497	0:41:32.1	41:06:15.5	23.99	-529.8	-	-	2002.10.13	76	-	-	-	-
1498	0:41:59.5	41:06:25.0	24.83	-482.2	E	-	2002.10.13	76	-	-	-	-
1499	0:41:38.9	41:06:19.0	24.23	-452.0	-	-	2002.10.13	76	-	-	-	-
1500	0:41:58.5	41:06:26.0	25.07	-507.5	-	-	2002.10.13	76	-	-	-	-
1501	0:42:00.9	41:06:29.8	25.04	-495.5	-	-	2002.10.13	76	-	-	-	-

Continued on next page

Table A.1 – continued from previous page

ID	RA	Dec	$m_{5007}$	$v_{\text{helio}}$	Note	Host	Date	Field	H06	C89	HK04	MLA93
1502	0:41:36.0	41:06:22.3	25.07	-374.9	-	-	2002.10.13	76	-	-	-	-
1503	0:41:33.4	41:06:26.9	24.59	-437.9	-	-	2002.10.13	76	-	-	-	-
1504	0:41:38.1	41:06:28.8	24.22	-309.4	E	-	2002.10.13	76	-	-	-	-
1505	0:42:04.1	41:06:39.1	25.40	-535.8	E	-	2002.10.13	76	-	-	-	-
1506	0:41:58.9	41:06:38.9	24.85	-567.1	-	-	2002.10.13	76	-	-	-	-
1507	0:41:49.5	41:06:36.3	24.30	-379.3	-	-	2002.10.13	76	-	-	-	-
1508	0:41:42.4	41:06:41.1	23.52	-487.6	-	-	2002.10.13	76	-	-	-	-
1509	0:41:29.4	41:06:38.5	23.31	-282.5	E	-	2002.10.13	76	PN_1.1.22	-	-	-
1510	0:42:13.4	41:06:53.4	25.22	-594.3	-	-	2002.10.13	76	-	-	-	-
1511	0:42:10.6	41:06:59.3	24.68	-571.3	-	-	2002.10.13	76	-	-	-	-
1512	0:41:41.0	41:06:55.4	21.83	-249.4	-	-	2002.10.13	76	-	-	-	387
1513	0:41:32.1	41:06:53.3	23.71	-593.5	-	-	2002.10.13	76	-	-	-	-
1514	0:41:51.8	41:07:06.9	24.86	-528.0	-	-	2002.10.13	76	-	-	-	-
1515	0:42:10.8	41:07:14.9	23.08	-212.3	-	-	2002.10.13	76	-	-	-	-
1516	0:42:00.3	41:07:13.8	25.29	-517.1	E	-	2002.10.13	76	-	-	-	-
1517	0:42:10.1	41:07:18.8	22.35	-456.6	-	-	2002.10.13	76	-	-	-	-
1518	0:42:01.5	41:07:19.5	21.62	-519.0	-	-	2002.10.13	76	-	-	-	437
1519	0:41:51.2	41:07:17.8	24.27	-536.0	-	-	2002.10.13	76	-	-	-	-
1520	0:41:39.4	41:07:18.4	23.88	-451.4	-	-	2002.10.13	76	-	-	-	-
1521	0:41:59.5	41:07:25.3	23.00	-549.8	-	-	2002.10.13	76	-	-	-	-
1522	0:42:08.4	41:07:35.5	22.24	-373.8	-	-	2002.10.13	76	-	-	-	454
1523	0:41:25.8	41:07:24.2	24.93	-468.7	-	-	2002.10.13	76	-	-	-	-
1524	0:41:50.1	41:07:33.8	21.92	-321.0	-	-	2002.10.13	76	PN_1.1.45	-	-	412
1525	0:41:32.2	41:07:30.1	23.60	-543.7	-	-	2002.10.13	76	-	-	-	-
1526	0:41:51.7	41:07:40.2	22.82	-448.7	-	-	2002.10.13	76	-	-	-	-
1527	0:42:03.5	41:07:53.0	25.40	-165.7	-	-	2002.10.13	76	-	-	-	-
1528	0:42:01.8	41:07:54.3	22.29	-555.2	-	-	2002.10.13	76	-	-	-	-
1529	0:41:28.4	41:07:46.6	24.78	-227.0	E	-	2002.10.13	76	-	-	-	-
1530	0:41:49.9	41:07:58.2	23.26	-397.6	-	-	2002.10.13	76	-	-	-	-
1531	0:42:11.0	41:08:05.3	24.05	-468.6	E	-	2002.10.13	76	P377	-	377	-
1532	0:41:50.0	41:08:00.8	25.11	-534.7	-	-	2002.10.13	76	-	-	-	-
1533	0:41:44.9	41:08:07.1	23.26	-531.9	-	-	2002.10.13	76	-	-	-	-
1534	0:41:54.7	41:08:15.2	25.04	-432.4	E	-	2002.10.13	76	-	-	-	-
1535	0:41:37.3	41:08:18.6	25.10	-458.7	-	-	2002.10.13	76	-	-	-	-
1536	0:41:29.5	41:08:21.0	25.28	-322.8	-	-	2002.10.13	76	-	-	-	-
1537	0:42:04.5	41:08:34.4	24.03	-366.7	-	-	2002.10.13	76	-	-	-	-
1538	0:41:52.3	41:08:42.8	25.19	-541.2	E	-	2002.10.13	76	-	-	-	418
1539	0:42:10.1	41:09:04.5	24.59	-593.7	-	-	2002.10.13	76	-	-	-	-
1540	0:42:04.0	41:09:13.1	24.94	-416.1	E	-	2002.10.13	76	-	-	-	-
1541	0:41:52.7	41:09:22.3	24.56	-453.8	-	-	2002.10.13	76	-	-	-	-
1542	0:42:03.2	41:09:36.4	24.36	-569.4	-	-	2002.10.13	76	-	-	-	-
1543	0:42:14.6	41:09:42.3	25.04	-381.5	E	-	2002.10.13	76	-	-	-	-
1544	0:41:59.5	41:09:38.4	25.10	-520.8	E	-	2002.10.13	76	-	-	-	-
1545	0:41:53.5	41:07:15.1	22.51	-508.1	E	-	2002.10.13	76	-	-	-	-
1546	0:41:55.7	41:09:53.8	24.69	-540.3	-	-	2002.10.13	76	-	-	-	-
1547	0:41:16.4	41:00:49.8	23.71	-520.3	-	-	2002.10.08	77	-	-	-	-
1548	0:41:10.6	41:01:02.8	23.28	-425.5	-	-	2002.10.08	77	-	-	-	-
1549	0:40:57.4	41:01:03.0	20.80	-435.0	-	-	2002.10.08	77	PN_2.3.2	-	-	290
1550	0:40:53.8	41:01:22.9	24.61	-459.3	-	-	2002.10.08	77	-	-	-	-
1551	0:40:48.1	41:02:02.3	22.92	-370.6	-	-	2002.10.08	77	PN_2.3.5	-	-	-
1552	0:40:42.5	41:02:07.5	23.89	-381.6	-	-	2002.10.08	77	-	-	-	-
1553	0:41:11.6	41:02:22.6	22.64	-375.4	-	-	2002.10.08	77	-	-	-	-
1554	0:40:46.7	41:02:21.7	24.15	-488.3	-	-	2002.10.08	77	-	-	-	-
1555	0:41:02.0	41:02:55.2	20.20	-407.8	R	-	2002.10.08	77	-	-	-	303
1556	0:40:59.3	41:02:58.0	23.85	-389.5	-	-	2002.10.08	77	-	-	-	-
1557	0:40:58.1	41:03:04.4	20.24	-421.5	R	-	2002.10.08	77	-	-	-	293
1558	0:40:55.9	41:03:08.7	20.54	-305.3	-	-	2002.10.08	77	PN_2.3.4	-	-	285
1559	0:40:58.7	41:03:29.2	21.10	-410.6	E,R	-	2002.10.08	77	-	-	-	298
1560	0:40:58.6	41:03:32.1	20.58	-412.5	E,R	-	2002.10.08	77	-	-	-	298
1561	0:41:09.2	41:03:43.5	22.27	-484.5	-	-	2002.10.08	77	PN_2.3.20	-	-	312
1562	0:41:23.1	41:04:12.6	22.90	-304.8	-	-	2002.10.08	77	PN_2.3.32	-	-	-
1563	0:40:48.5	41:04:09.6	23.79	-400.8	-	-	2002.10.08	77	-	-	-	-
1564	0:41:13.6	41:04:55.0	24.16	-396.0	-	-	2002.10.08	77	-	-	-	-
1565	0:41:22.7	41:05:00.8	22.52	-432.8	-	-	2002.10.08	77	-	-	-	-
1566	0:41:19.2	41:05:30.9	23.73	-281.1	-	-	2002.10.08	77	-	-	-	-
1567	0:41:16.7	41:05:57.1	23.35	-507.5	-	-	2002.10.08	77	-	-	-	-
1568	0:41:17.1	41:05:59.6	24.63	-328.9	-	-	2002.10.08	77	-	-	-	-
1569	0:40:46.1	41:06:38.3	22.76	-490.3	-	-	2002.10.08	77	-	-	-	-
1570	0:41:02.7	41:06:56.5	22.78	-318.8	-	-	2002.10.08	77	-	-	-	-
1571	0:41:15.1	41:07:27.0	22.34	-304.2	-	-	2002.10.08	77	PN_1.1.21	-	-	328
1572	0:41:13.9	41:07:35.7	21.66	-395.9	E,R	-	2002.10.08	77	-	-	-	-
1573	0:40:41.0	41:07:29.5	22.63	-280.2	-	-	2002.10.08	77	-	-	-	249
1574	0:40:53.3	41:07:47.4	23.96	-233.4	-	-	2002.10.08	77	-	-	-	-
1575	0:41:03.9	41:07:57.8	23.70	-182.2	-	-	2002.10.08	77	-	-	-	-
1576	0:41:19.9	41:08:21.1	21.17	-411.2	E,R	-	2002.10.08	77	-	-	-	-
1577	0:40:43.1	41:08:46.0	22.60	-327.3	R	-	2002.10.08	77	-	-	-	251
1578	0:41:09.9	41:08:02.8	23.91	-278.5	-	-	2002.10.08	77	-	-	-	-
1579	0:40:22.2	41:00:55.8	23.07	-397.2	-	-	2002.10.10	78	-	-	-	-
1580	0:40:25.8	41:01:09.2	22.74	-378.3	-	-	2002.10.10	78	PN_12.3.23	-	-	-
1581	0:40:30.0	41:01:20.4	21.70	-472.6	-	-	2002.10.10	78	PN_12.3.24	-	-	227
1582	0:40:30.1	41:03:04.2	24.82	-373.7	-	-	2002.10.10	78	-	-	-	-
1583	0:40:00.8	41:04:09.3	20.71	-318.0	-	-	2002.10.10	78	-	-	-	163
1584	0:40:26.5	41:04:19.7	24.67	-288.4	-	-	2002.10.10	78	-	-	-	-
1585	0:40:16.6	41:04:28.8	21.19	-348.2	-	-	2002.10.10	78	PN_12.3.14	-	-	193
1586	0:40:01.2	41:04:41.2	21.61	-362.3	-	-	2002.10.10	78	-	-	-	164
1587	0:39:56.9	41:05:07.7	20.95	-313.4	-	-	2002.10.10	78	PN_12.3.13	-	-	157
1588	0:39:50.2	41:05:55.4	24.09	-373.5	-	-	2002.10.10	78	-	-	-	-
1589	0:39:58.8	41:06:42.3	22.97	-440.5	-	-	2002.10.10	78	PN_8.1.9	-	-	-
1590	0:40:16.2	41:07:35.9	24.59	-348.2	-	-	2002.10.10	78	-	-	-	-
1591	0:39:42.5	41:02:21.1	21.77	-465.6	-	-	2002.10.12	79	PN_12.3.7	-	-	-
1592	0:39:19.4	41:02:23.9	25.63	-295.7	E	-	2002.10.12	79	-	-	-	-
1593	0:39:43.5	41:03:30.8	21.89	-442.8	-	-	2002.10.12	79	PN_12.3.8	-	-	132
1594	0:39:33.7	41:03:54.1	23.88	-275.8	-	-	2002.10.12	79	-	-	-	-

Continued on next page



Table A.1 – continued from previous page

ID	RA	Dec	$m_{5007}$	$v_{\text{helio}}$	Note	Host	Date	Field	H06	C89	HK04	MLA93
1595	0:39:24.5	41:04:32.7	23.47	-417.0	-	-	2002.10.12	79	PN_12_3_5	-	-	-
1596	0:39:22.6	41:06:57.3	20.71	-377.7	-	-	2002.10.12	79	PN_2_8_1_5	-	-	105
1597	0:42:55.3	40:59:45.7	22.73	-373.7	E	-	2002.10.09	81	-	-	-	-
1598	0:42:55.7	41:00:38.7	24.03	-420.9	-	-	2002.10.09	81	-	-	-	-
1599	0:42:56.9	41:00:40.8	23.66	-355.5	-	-	2002.10.09	81	-	-	-	-
1600	0:43:00.6	41:00:47.6	22.94	-359.6	-	-	2002.10.09	81	-	-	-	-
1601	0:42:50.1	41:00:56.4	23.51	-383.1	-	-	2002.10.09	81	-	-	-	606
1602	0:42:20.9	41:00:49.3	24.77	-305.3	-	-	2002.10.09	81	-	-	-	-
1603	0:42:21.2	41:00:54.0	22.33	-511.3	-	-	2002.10.09	81	-	-	-	485
1604	0:42:51.5	41:01:06.0	24.23	-510.4	-	-	2002.10.09	81	-	-	-	-
1605	0:42:32.9	41:01:21.8	23.98	-625.2	-	-	2002.10.09	81	-	-	-	-
1606	0:42:25.7	41:01:25.2	23.25	-344.7	-	-	2002.10.09	81	-	-	-	-
1607	0:42:53.0	41:01:35.1	22.89	-161.1	-	-	2002.10.09	81	-	-	-	614
1608	0:42:51.0	41:02:06.4	24.56	-150.9	-	-	2002.10.09	81	-	-	-	-
1609	0:42:18.2	41:01:59.1	23.90	-488.1	E	-	2002.10.09	81	-	-	-	-
1610	0:42:50.1	41:02:21.0	23.47	-517.3	-	-	2002.10.09	81	-	-	-	604
1611	0:42:54.7	41:02:26.0	19.65	-363.3	E,R	-	2002.10.09	81	-	-	-	625
1612	0:42:40.0	41:02:23.0	23.20	-424.9	E,R	-	2002.10.09	81	-	-	-	-
1613	0:42:18.9	41:02:33.6	23.88	-487.6	-	-	2002.10.09	81	-	-	-	-
1614	0:42:37.7	41:02:49.8	24.68	-386.5	-	-	2002.10.09	81	-	-	-	-
1615	0:42:41.9	41:03:03.9	22.56	-387.6	E	-	2002.10.09	81	-	-	-	-
1616	0:42:29.8	41:03:30.7	20.72	-458.8	-	-	2002.10.09	81	PN_2_3_68	1.76	-	529
1617	0:42:55.6	41:03:41.1	21.76	-613.2	-	-	2002.10.09	81	-	1.85	-	630
1618	0:42:29.6	41:03:38.2	22.88	-324.3	-	-	2002.10.09	81	-	-	-	-
1619	0:42:43.3	41:03:48.3	24.57	-380.8	-	-	2002.10.09	81	-	-	-	-
1620	0:42:58.2	41:03:54.4	22.83	-308.2	-	-	2002.10.09	81	-	-	-	647
1621	0:42:26.3	41:04:04.4	24.14	-433.1	-	-	2002.10.09	81	-	-	-	-
1622	0:42:37.2	41:04:19.6	21.73	-459.3	-	-	2002.10.09	81	-	1.78	-	559
1623	0:42:52.0	41:04:26.5	24.32	-324.0	-	-	2002.10.09	81	-	-	-	-
1624	0:42:26.8	41:04:31.2	23.77	-499.1	-	-	2002.10.09	81	-	-	-	-
1625	0:43:02.5	41:04:47.4	22.05	-380.3	-	-	2002.10.09	81	-	-	-	667
1626	0:42:29.2	41:04:52.5	24.09	-344.0	-	-	2002.10.09	81	-	-	-	-
1627	0:42:19.3	41:04:52.2	22.81	-423.3	-	-	2002.10.09	81	-	-	-	-
1628	0:42:28.5	41:04:57.7	24.38	-545.9	E	-	2002.10.09	81	-	-	-	-
1629	0:42:59.9	41:05:44.9	23.04	-377.5	-	-	2002.10.09	81	-	-	-	-
1630	0:42:33.9	41:05:41.1	22.92	-507.7	-	-	2002.10.09	81	-	-	-	-
1631	0:42:45.1	41:05:48.1	24.16	40.2	-	-	2002.10.09	81	-	-	-	-
1632	0:42:30.4	41:05:52.2	21.40	-578.6	-	-	2002.10.09	81	-	-	-	532
1633	0:42:53.4	41:06:01.5	23.13	-301.1	-	-	2002.10.09	81	-	-	-	618
1634	0:42:22.0	41:05:56.1	22.68	-415.9	-	-	2002.10.09	81	-	-	-	-
1635	0:42:28.5	41:06:11.3	24.41	-554.1	-	-	2002.10.09	81	-	-	-	-
1636	0:42:28.7	41:06:21.2	21.06	-223.3	-	-	2002.10.09	81	-	-	-	522
1637	0:43:01.1	41:06:42.9	22.74	-82.2	-	-	2002.10.09	81	-	-	-	-
1638	0:42:19.3	41:06:29.5	24.12	-493.6	E	-	2002.10.09	81	-	-	-	-
1639	0:42:34.6	41:06:38.9	23.98	-289.1	-	-	2002.10.09	81	-	-	-	-
1640	0:42:31.0	41:06:48.3	23.79	-544.1	-	-	2002.10.09	81	-	-	-	-
1641	0:42:56.2	41:07:05.1	23.69	-210.5	-	-	2002.10.09	81	-	-	-	-
1642	0:42:17.7	41:07:03.7	24.90	-558.2	-	-	2002.10.09	81	-	-	-	-
1643	0:42:28.9	41:07:13.0	21.44	-513.9	-	-	2002.10.09	81	PN_6_2_29	-	-	525
1644	0:42:24.3	41:07:11.6	21.25	-487.0	-	-	2002.10.09	81	-	-	-	504
1645	0:42:33.5	41:07:16.1	23.34	-463.4	-	-	2002.10.09	81	-	-	-	-
1646	0:42:42.5	41:07:23.1	24.47	-589.9	-	-	2002.10.09	81	-	-	-	-
1647	0:42:26.8	41:07:18.4	21.92	-659.8	-	-	2002.10.09	81	-	-	-	511
1648	0:42:24.6	41:07:28.5	21.47	-268.2	-	-	2002.10.09	81	PN_1_1_88	-	-	506
1649	0:42:55.3	41:07:39.7	24.05	-506.1	-	-	2002.10.09	81	-	-	-	-
1650	0:42:31.3	41:07:47.4	22.11	-307.4	-	-	2002.10.09	81	-	-	-	-
1651	0:42:20.4	41:08:00.1	20.55	-581.4	-	-	2002.10.09	81	P390	-	390	483
1652	0:42:56.5	41:08:20.2	24.47	-427.2	-	-	2002.10.09	81	-	-	-	-
1653	0:42:35.0	41:08:17.0	22.78	-485.7	-	-	2002.10.09	81	P430	-	430	-
1654	0:42:19.4	41:08:39.9	24.42	-685.6	-	-	2002.10.09	81	-	-	-	-
1655	0:42:33.9	41:09:12.6	23.78	-218.2	E	-	2002.10.09	81	-	-	-	-
1656	0:42:42.6	41:09:20.7	23.83	-451.3	-	-	2002.10.09	81	P154	-	154	-
1657	0:42:45.2	41:09:25.5	24.10	-488.1	E	-	2002.10.09	81	-	-	-	-
1658	0:42:19.3	41:09:21.7	24.15	-326.6	-	-	2002.10.09	81	-	-	-	-
1659	0:42:58.1	41:09:35.7	24.73	44.0	-	-	2002.10.09	81	-	-	-	-
1660	0:43:00.5	41:09:38.5	24.17	-619.8	E	-	2002.10.09	81	-	-	-	-
1661	0:42:30.2	41:09:29.3	23.95	-260.8	-	-	2002.10.09	81	-	-	-	-
1662	0:42:21.2	41:03:22.8	23.73	-375.1	-	-	2002.10.09	81	-	-	-	-
1663	0:42:24.3	41:05:48.8	21.32	-465.2	R	-	2002.10.09	81	-	-	-	503
1664	0:43:20.5	41:01:09.3	25.32	-253.0	-	-	2002.10.10	82	-	-	-	-
1665	0:43:06.3	41:01:48.8	25.62	-430.4	-	-	2002.10.10	82	-	-	-	-
1666	0:43:06.7	41:02:14.0	22.76	-338.0	E	-	2002.10.10	82	-	-	-	-
1667	0:43:26.9	41:02:21.6	25.00	-377.4	-	-	2002.10.10	82	-	-	-	-
1668	0:43:27.9	41:02:24.6	24.81	-373.0	-	-	2002.10.10	82	-	-	-	-
1669	0:43:19.8	41:02:34.1	21.54	-421.8	-	-	2002.10.10	82	PN_3_3_17	-	-	750
1670	0:43:17.9	41:02:53.8	24.86	-322.5	E	-	2002.10.10	82	-	-	-	-
1671	0:43:09.8	41:03:00.2	25.24	-345.0	-	-	2002.10.10	82	-	-	-	-
1672	0:43:36.7	41:03:33.3	22.75	-269.8	-	-	2002.10.10	82	PN_3_3_24	1.101	-	815
1673	0:43:39.7	41:03:35.4	25.28	-354.3	-	-	2002.10.10	82	-	-	-	-
1674	0:43:27.0	41:03:33.0	24.93	-360.6	-	-	2002.10.10	82	-	-	-	-
1675	0:43:15.2	41:04:21.5	20.67	-379.4	-	-	2002.10.10	82	PN_3_3_14	-	-	725
1676	0:43:09.5	41:04:26.9	23.54	-389.7	E	-	2002.10.10	82	-	-	-	-
1677	0:43:24.5	41:04:45.1	24.89	-344.2	-	-	2002.10.10	82	-	-	-	-
1678	0:43:09.4	41:04:53.0	21.46	-530.8	-	-	2002.10.10	82	-	-	-	697
1679	0:43:10.2	41:04:56.3	23.21	-365.6	E,R	-	2002.10.10	82	-	-	-	-
1680	0:43:11.3	41:04:59.7	20.68	-363.5	R	-	2002.10.10	82	-	-	-	705
1681	0:43:16.5	41:05:05.4	24.17	-487.7	-	-	2002.10.10	82	-	-	-	-
1682	0:43:16.0	41:05:05.5	23.58	-327.3	-	-	2002.10.10	82	-	-	-	-
1683	0:43:26.3	41:05:09.5	20.68	-327.0	E,R	-	2002.10.10	82	-	-	-	779
1684	0:43:16.4	41:05:10.0	25.05	-463.9	-	-	2002.10.10	82	-	-	-	-
1685	0:43:07.8	41:05:12.9	22.98	-203.0	-	-	2002.10.10	82	-	-	-	691
1686	0:43:20.0	41:05:25.7	23.70	-437.5	-	-	2002.10.10	82	-	-	-	-
1687	0:43:21.3	41:05:28.9	20.16	-362.2	-	-	2002.10.10	82	PN_3_3_18	-	-	756

Continued on next page

Table A.1 – continued from previous page

ID	RA	Dec	$m_{5007}$	$v_{\text{helio}}$	Note	Host	Date	Field	H06	C89	HK04	MLA93
1688	0:43:18.9	41:05:33.5	24.70	-486.9	-	-	2002.10.10	82	-	-	-	-
1689	0:43:53.3	41:06:18.4	24.01	-20.3	E	-	2002.10.10	82	-	-	-	-
1690	0:43:26.4	41:06:42.5	22.47	-330.8	-	-	2002.10.10	82	PN_6.1.64	-	-	780
1691	0:43:03.7	41:06:35.8	24.66	-180.6	-	-	2002.10.10	82	-	-	-	-
1692	0:43:24.6	41:07:16.1	22.95	-426.8	-	-	2002.10.10	82	-	-	-	-
1693	0:43:22.4	41:07:19.0	21.26	-429.0	-	-	2002.10.10	82	-	-	-	758
1694	0:43:06.4	41:07:22.6	22.05	-84.2	-	-	2002.10.10	82	-	-	-	685
1695	0:43:10.7	41:07:32.8	24.46	-378.9	-	-	2002.10.10	82	-	-	-	-
1696	0:43:27.3	41:07:49.1	24.67	-338.1	E	-	2002.10.10	82	-	-	-	-
1697	0:43:14.0	41:08:12.7	25.33	-386.5	-	-	2002.10.10	82	-	-	-	-
1698	0:43:34.3	41:09:31.9	24.69	-409.3	E	-	2002.10.10	82	-	-	-	-
1699	0:43:34.8	41:09:53.8	19.97	-348.5	E,R	-	2002.10.10	82	-	-	-	805
1700	0:43:43.6	41:01:07.1	22.36	-257.0	-	-	2002.10.10	82	-	-	-	845
1701	0:44:11.4	41:01:02.1	21.39	-349.7	-	-	2002.10.11	83	PN_3.3.28	1_108	-	939
1702	0:44:38.0	41:07:02.7	23.09	-360.8	-	-	2002.10.11	83	-	1_116	-	-
1703	0:44:33.4	41:08:00.5	23.26	-241.4	-	-	2002.10.11	83	-	-	-	-
1704	0:44:35.1	41:08:04.8	24.40	-328.5	E	-	2002.10.11	83	PN_5.2.5	-	-	-
1705	0:44:07.4	41:08:23.0	24.33	-243.8	E	-	2002.10.11	83	-	-	-	-
1706	0:45:28.3	41:04:53.9	22.93	-409.3	-	-	2002.10.11	84	-	1_128	-	-
1707	0:44:52.4	41:05:58.5	23.93	-342.5	-	-	2002.10.11	84	-	-	-	-
1708	0:44:50.9	41:07:55.4	25.12	-247.5	-	-	2002.10.11	84	-	-	-	-
1709	0:44:46.4	41:08:24.2	24.36	-192.7	-	-	2002.10.11	84	-	-	-	-
1710	0:45:42.0	41:08:23.3	24.72	-64.1	-	-	2002.10.11	85	-	-	-	-
1711	0:41:30.5	40:51:34.2	23.85	-558.2	-	-	2002.10.08	86	-	-	-	-
1712	0:41:11.5	40:51:39.8	24.91	-557.2	-	-	2002.10.08	86	-	-	-	-
1713	0:41:10.1	40:51:44.3	22.62	-458.6	-	-	2002.10.08	86	PN_2.4.19	-	-	314
1714	0:41:19.3	40:52:20.9	21.53	-394.3	-	-	2002.10.08	86	PN_2.4.27	-	-	345
1715	0:41:22.2	40:52:36.6	25.05	-531.0	-	-	2002.10.08	86	-	-	-	-
1716	0:41:41.1	40:52:47.0	22.56	-450.8	-	-	2002.10.08	86	PN_2.4.38	-	-	-
1717	0:41:26.4	40:52:46.3	23.91	-562.0	R	-	2002.10.08	86	-	-	-	-
1718	0:41:46.2	40:53:21.2	22.15	-505.6	-	-	2002.10.08	86	-	-	-	406
1719	0:41:14.8	40:53:20.5	23.58	-401.9	-	-	2002.10.08	86	-	-	-	-
1720	0:41:21.2	40:53:30.3	24.53	-419.8	-	-	2002.10.08	86	-	-	-	-
1721	0:41:18.0	40:53:36.2	21.95	-520.5	-	-	2002.10.08	86	-	-	-	340
1722	0:41:19.0	40:53:42.1	21.74	-466.0	-	-	2002.10.08	86	PN_2.4.26	-	-	343
1723	0:41:29.9	40:53:48.8	21.94	-418.5	-	-	2002.10.08	86	-	-	-	365
1724	0:41:06.8	40:53:58.1	22.54	-481.0	-	-	2002.10.08	86	-	-	-	311
1725	0:41:40.6	40:54:11.3	24.78	-467.4	-	-	2002.10.08	86	-	-	-	-
1726	0:41:32.5	40:54:27.4	21.28	-527.8	-	-	2002.10.08	86	-	-	-	370
1727	0:41:36.6	40:54:39.9	23.91	-634.8	-	-	2002.10.08	86	-	-	-	-
1728	0:41:42.4	40:55:01.1	24.77	-451.7	-	-	2002.10.08	86	-	-	-	-
1729	0:41:20.8	40:55:00.8	21.14	-540.8	-	-	2002.10.08	86	-	-	-	350
1730	0:41:16.0	40:55:17.0	23.10	-578.7	-	-	2002.10.08	86	-	-	-	-
1731	0:41:18.8	40:55:19.3	24.50	-419.9	-	-	2002.10.08	86	-	-	-	-
1732	0:41:10.1	40:55:27.4	22.31	-464.0	-	-	2002.10.08	86	-	-	-	-
1733	0:41:33.1	40:55:48.6	23.05	-542.8	-	-	2002.10.08	86	PN_2.3.39	-	-	-
1734	0:41:10.1	40:55:50.9	24.52	-477.6	-	-	2002.10.08	86	-	-	-	-
1735	0:41:03.3	40:55:53.8	20.71	-533.8	-	-	2002.10.08	86	PN_2.3.13	-	-	306
1736	0:41:15.9	40:55:58.4	25.34	-394.2	-	-	2002.10.08	86	-	-	-	-
1737	0:41:25.2	40:56:02.4	21.46	-514.6	-	-	2002.10.08	86	PN_2.3.38	-	-	359
1738	0:41:10.3	40:56:08.7	23.91	-538.5	-	-	2002.10.08	86	-	-	-	-
1739	0:41:07.0	40:56:07.8	22.74	-525.2	-	-	2002.10.08	86	-	-	-	-
1740	0:41:08.3	40:56:09.5	24.82	-366.2	-	-	2002.10.08	86	-	-	-	-
1741	0:41:14.2	40:56:35.6	25.09	-596.4	E	-	2002.10.08	86	-	-	-	-
1742	0:41:05.3	40:56:50.7	25.02	-504.4	E	-	2002.10.08	86	-	-	-	-
1743	0:41:42.0	40:57:19.0	24.18	-487.4	-	-	2002.10.08	86	-	-	-	-
1744	0:41:10.3	40:57:19.1	24.01	-514.2	-	-	2002.10.08	86	-	-	-	-
1745	0:41:27.5	40:57:36.5	24.42	-462.9	-	-	2002.10.08	86	-	-	-	-
1746	0:41:42.7	40:57:47.4	25.00	-435.5	-	-	2002.10.08	86	-	-	-	-
1747	0:41:39.1	40:57:49.8	22.01	-573.4	-	-	2002.10.08	86	-	-	-	381
1748	0:41:07.1	40:57:39.1	24.66	-505.6	-	-	2002.10.08	86	-	-	-	-
1749	0:41:31.2	40:57:59.1	23.02	-477.5	-	-	2002.10.08	86	-	-	-	-
1750	0:41:26.9	40:58:06.4	20.68	-403.2	-	-	2002.10.08	86	PN_2.3.35	-	-	362
1751	0:41:15.2	40:58:09.3	24.22	-380.1	-	-	2002.10.08	86	-	-	-	-
1752	0:41:42.8	40:58:20.6	25.08	-485.1	-	-	2002.10.08	86	-	-	-	-
1753	0:41:40.3	40:58:21.9	24.16	-527.6	-	-	2002.10.08	86	-	-	-	-
1754	0:41:45.4	40:58:36.4	22.21	-454.3	-	-	2002.10.08	86	PN_2.3.45	-	-	400
1755	0:41:12.7	40:58:27.0	20.57	-543.4	-	-	2002.10.08	86	-	-	-	320
1756	0:41:47.7	40:58:43.8	25.25	-457.0	-	-	2002.10.08	86	-	-	-	-
1757	0:41:31.9	40:58:40.3	25.26	-514.9	-	-	2002.10.08	86	-	-	-	-
1758	0:41:47.2	40:58:47.4	23.53	-381.1	-	-	2002.10.08	86	-	-	-	-
1759	0:41:44.6	40:58:53.6	24.33	-584.8	-	-	2002.10.08	86	-	-	-	-
1760	0:41:17.6	40:58:44.9	21.68	-438.2	-	-	2002.10.08	86	-	-	-	337
1761	0:41:16.2	40:58:59.0	21.03	-506.4	-	-	2002.10.08	86	-	-	-	331
1762	0:41:32.3	40:54:29.9	23.75	-510.1	-	-	2002.10.08	86	-	-	-	370
1763	0:41:17.6	40:54:33.0	23.85	-561.7	-	-	2002.10.08	86	-	-	-	-
1764	0:41:07.9	40:52:55.3	24.88	-426.5	E	-	2002.10.08	86	-	-	-	-
1765	0:41:17.8	40:57:04.6	22.04	-513.5	E	-	2002.10.08	86	-	-	-	-
1766	0:41:13.3	40:58:27.9	23.15	-421.4	-	-	2002.10.08	86	-	-	-	-
1767	0:41:06.3	41:00:23.7	25.03	-428.6	-	-	2002.10.08	86	-	-	-	-
1768	0:40:15.8	40:50:36.4	25.48	-418.2	-	-	2002.10.08	87	-	-	-	-
1769	0:40:46.0	40:51:24.9	22.93	-544.8	-	-	2002.10.08	87	-	-	-	261
1770	0:40:36.3	40:51:27.8	25.25	-453.2	-	-	2002.10.08	87	-	-	-	-
1771	0:40:32.5	40:51:28.1	24.33	-540.6	E	-	2002.10.08	87	-	-	-	-
1772	0:40:58.8	40:51:46.7	23.53	-529.5	-	-	2002.10.08	87	-	-	-	-
1773	0:40:25.8	40:51:45.8	23.70	-393.0	-	-	2002.10.08	87	PN_12.4.36	-	-	218
1774	0:40:43.4	40:52:08.4	22.75	-568.0	-	-	2002.10.08	87	PN_2.4.4	-	-	252
1775	0:40:18.5	40:52:01.3	23.69	-537.4	-	-	2002.10.08	87	PN_12.4.38	-	-	-
1776	0:40:44.8	40:52:14.7	25.52	-428.6	-	-	2002.10.08	87	-	-	-	-
1777	0:40:45.3	40:52:29.6	25.48	-541.6	-	-	2002.10.08	87	-	-	-	-
1778	0:40:56.4	40:53:54.1	22.39	-593.5	-	-	2002.10.08	87	-	-	-	286
1779	0:40:32.8	40:53:57.7	25.82	-344.8	E	-	2002.10.08	87	-	-	-	-
1780	0:40:33.4	40:54:09.7	26.42	-431.5	-	-	2002.10.08	87	-	-	-	-

Continued on next page

Table A.1 – continued from previous page

ID	RA	Dec	$m_{5007}$	$v_{\text{helio}}$	Note	Host	Date	Field	H06	C89	HK04	MLA93
1781	0:40:52.5	40:54:25.8	25.71	-546.4	-	-	2002.10.08	87	-	-	-	-
1782	0:40:15.1	40:54:25.0	25.10	-515.3	-	-	2002.10.08	87	-	-	-	-
1783	0:40:50.6	40:54:57.2	21.50	-425.1	-	-	2002.10.08	87	PN_2,3,7	-	-	272
1784	0:40:34.7	40:55:21.5	25.58	-499.8	-	-	2002.10.08	87	-	-	-	-
1785	0:40:42.9	40:55:27.3	24.47	-250.8	-	-	2002.10.08	87	-	-	-	-
1786	0:40:32.5	40:55:29.7	23.81	-423.5	E	-	2002.10.08	87	-	-	-	-
1787	0:40:41.5	40:55:34.8	24.01	-516.8	-	-	2002.10.08	87	PN_2,3,6	-	-	-
1788	0:40:33.3	40:55:58.6	24.35	-355.6	-	-	2002.10.08	87	PN_12,3,26	-	-	-
1789	0:40:18.1	40:55:57.2	25.72	-538.5	E	-	2002.10.08	87	-	-	-	-
1790	0:40:48.9	40:56:17.5	25.27	-274.1	-	-	2002.10.08	87	-	-	-	-
1791	0:40:42.3	40:56:36.9	25.38	-284.6	-	-	2002.10.08	87	-	-	-	-
1792	0:40:23.8	40:56:58.4	25.88	-470.5	-	-	2002.10.08	87	-	-	-	-
1793	0:40:50.5	40:57:23.3	25.36	-283.2	-	-	2002.10.08	87	-	-	-	-
1794	0:40:56.9	40:58:11.0	24.64	-450.5	-	-	2002.10.08	87	-	-	-	-
1795	0:40:24.7	40:58:02.9	23.33	-331.0	-	-	2002.10.08	87	PN_12,3,21	-	-	213
1796	0:40:15.6	40:58:29.7	24.87	-518.8	-	-	2002.10.08	87	PN_12,3,17	-	-	-
1797	0:40:51.1	40:58:48.1	21.95	-358.3	-	-	2002.10.08	87	-	-	-	273
1798	0:40:37.8	40:58:44.9	23.83	-567.5	-	-	2002.10.08	87	-	-	-	-
1799	0:40:40.3	40:58:48.0	24.60	-405.7	E	-	2002.10.08	87	-	-	-	-
1800	0:39:29.0	40:52:02.4	21.56	-429.7	-	-	2002.10.10	88	PN_12,4,11	-	-	111
1801	0:39:53.6	40:52:50.9	24.05	-455.4	-	-	2002.10.10	88	-	-	-	-
1802	0:39:26.5	40:53:38.1	24.45	-407.2	-	-	2002.10.10	88	PN_12,4,14	-	-	-
1803	0:39:47.8	40:54:04.8	23.14	-409.7	-	-	2002.10.10	88	-	-	-	-
1804	0:40:00.9	40:54:57.0	23.57	-448.7	-	-	2002.10.10	88	-	-	-	-
1805	0:39:31.8	40:55:40.0	24.47	-560.2	-	-	2002.10.10	88	-	-	-	-
1806	0:39:55.3	40:55:49.3	22.91	-400.7	R	-	2002.10.10	88	-	-	-	-
1807	0:39:50.7	40:55:49.4	23.17	-417.9	-	-	2002.10.10	88	PN_12,3,9	-	-	-
1808	0:39:35.1	40:55:54.0	23.62	-447.9	-	-	2002.10.10	88	PN_12,3,4	-	-	-
1809	0:39:59.7	40:57:03.3	23.35	-419.6	-	-	2002.10.10	88	-	-	-	-
1810	0:40:00.6	40:58:34.8	24.20	-477.0	-	-	2002.10.10	88	-	-	-	-
1811	0:39:47.3	40:58:48.3	24.50	-243.1	-	-	2002.10.10	88	-	-	-	-
1812	0:38:54.4	40:53:38.9	24.84	-101.9	-	-	2002.10.08	89	PN_12,4,5	-	-	-
1813	0:39:14.2	40:53:51.9	25.76	-521.9	-	-	2002.10.08	89	-	-	-	-
1814	0:39:11.1	40:56:57.9	24.24	-278.9	E	-	2002.10.08	89	PN_12,3,2	-	-	-
1815	0:38:44.4	40:58:27.3	24.99	-492.2	-	-	2002.10.08	89	-	-	-	-
1816	0:37:49.7	40:53:54.6	21.02	-318.7	-	-	2002.10.12	90	-	-	-	-
1817	0:38:27.1	40:55:12.9	25.33	-71.2	E	-	2002.10.12	90	-	-	-	-
1818	0:38:10.0	40:56:31.8	23.20	-395.6	-	-	2002.10.12	90	-	-	-	-
1819	0:38:19.4	40:57:24.0	24.09	-395.9	-	-	2002.10.12	90	-	-	-	-
1820	0:42:13.4	40:51:25.9	24.18	-381.5	R	-	2002.10.08	91	-	-	-	-
1821	0:42:00.4	40:52:05.8	23.49	-189.2	-	-	2002.10.08	91	-	-	-	-
1822	0:42:14.5	40:52:22.6	20.50	-438.4	-	-	2002.10.08	91	-	-	-	473
1823	0:42:09.7	40:52:35.7	22.07	-441.4	-	-	2002.10.08	91	PN_3,2,37	-	-	456
1824	0:42:13.2	40:52:48.3	23.20	-294.2	-	-	2002.10.08	91	-	-	-	-
1825	0:42:06.2	40:52:50.9	23.46	-330.6	-	-	2002.10.08	91	-	-	-	-
1826	0:42:01.9	40:53:22.6	21.60	-444.9	-	-	2002.10.08	91	PN_2,4,44	-	-	438
1827	0:41:55.0	40:53:26.2	23.64	-462.2	-	-	2002.10.08	91	-	-	-	-
1828	0:42:14.8	40:54:04.8	24.14	-366.5	-	-	2002.10.08	91	-	-	-	-
1829	0:41:58.0	40:55:26.5	23.48	-432.0	-	-	2002.10.08	91	-	-	-	-
1830	0:41:54.7	40:56:09.1	22.56	-439.7	-	-	2002.10.08	91	-	-	-	423
1831	0:42:09.4	40:57:11.6	22.78	-241.2	-	-	2002.10.08	91	-	-	-	-
1832	0:42:15.2	40:57:53.6	24.21	-207.3	-	-	2002.10.08	91	-	-	-	-
1833	0:42:03.4	40:57:49.8	24.71	-476.9	-	-	2002.10.08	91	-	-	-	-
1834	0:42:32.8	40:58:06.7	23.69	-420.8	-	-	2002.10.08	91	-	-	-	-
1835	0:41:56.3	40:57:57.8	23.45	-358.0	-	-	2002.10.08	91	-	-	-	-
1836	0:41:56.7	40:58:16.2	23.86	-417.5	-	-	2002.10.08	91	-	-	-	-
1837	0:42:20.9	40:58:33.4	24.62	-440.4	-	-	2002.10.08	91	-	-	-	-
1838	0:42:05.0	40:58:36.1	21.92	-467.3	-	-	2002.10.08	91	-	-	-	443
1839	0:42:15.0	40:58:45.4	20.54	-91.7	-	-	2002.10.08	91	-	-	-	474
1840	0:42:08.5	40:59:04.5	23.65	-331.9	-	-	2002.10.08	91	-	-	-	-
1841	0:42:00.0	40:59:10.8	24.66	-623.0	-	-	2002.10.08	91	-	-	-	-
1842	0:43:13.8	40:52:32.6	22.09	-389.8	-	-	2002.10.11	92	PN_3,4,13	1,93	-	720
1843	0:42:40.3	40:52:57.8	25.18	-235.3	-	M32	2002.10.11	92	-	-	-	-
1844	0:43:15.7	40:54:59.9	24.68	-637.5	-	-	2002.10.11	92	-	-	-	-
1845	0:43:20.6	40:55:32.3	22.97	-313.6	-	-	2002.10.11	92	PN_3,3,22	1,96	-	-
1846	0:43:15.3	40:57:27.1	25.45	-298.6	E	-	2002.10.11	92	-	-	-	-
1847	0:43:20.7	40:57:44.1	22.32	-523.4	-	-	2002.10.11	92	PN_3,3,21	1,97	-	754
1848	0:42:57.4	40:57:54.4	24.35	-127.2	-	-	2002.10.11	92	-	-	-	-
1849	0:43:19.0	40:58:01.9	22.50	-457.1	-	-	2002.10.11	92	-	1,95	-	746
1850	0:42:49.3	40:57:59.8	24.76	-431.4	-	-	2002.10.11	92	-	-	-	-
1851	0:43:20.8	40:58:10.6	24.99	-375.4	E	-	2002.10.11	92	-	-	-	-
1852	0:42:53.1	40:58:19.0	22.82	-330.5	-	-	2002.10.11	92	PN_3,3,4	-	-	616
1853	0:43:11.1	40:58:32.6	24.56	-354.1	-	-	2002.10.11	92	-	-	-	-
1854	0:43:01.2	40:58:33.2	23.33	-336.5	-	-	2002.10.11	92	-	-	-	-
1855	0:43:06.9	40:58:40.9	25.61	-279.5	E	-	2002.10.11	92	-	-	-	-
1856	0:42:48.0	40:58:43.8	24.50	-468.8	-	-	2002.10.11	92	-	-	-	-
1857	0:42:54.5	40:58:49.9	21.41	-283.7	-	-	2002.10.11	92	-	-	-	624
1858	0:42:43.2	40:59:11.3	25.11	-399.2	-	-	2002.10.11	92	-	-	-	-
1859	0:42:54.7	40:59:18.6	24.81	-433.7	E	-	2002.10.11	92	-	-	-	-
1860	0:42:44.9	40:59:40.8	25.07	-417.2	-	-	2002.10.11	92	-	-	-	-
1861	0:42:43.7	40:59:59.0	25.15	-185.3	-	-	2002.10.11	92	-	-	-	-
1862	0:43:24.9	41:00:15.7	25.32	-347.4	-	-	2002.10.11	92	-	-	-	-
1863	0:43:56.9	40:50:59.0	25.32	-395.7	-	-	2002.10.13	93	-	-	-	-
1864	0:43:46.2	40:52:47.4	25.31	-207.9	E	-	2002.10.13	93	-	-	-	-
1865	0:43:53.1	40:55:10.1	24.29	-378.1	-	-	2002.10.13	93	PN_3,3,26	-	-	-
1866	0:43:50.5	40:55:38.4	25.35	-326.7	E	-	2002.10.13	93	-	-	-	-
1867	0:43:48.3	40:56:54.7	25.51	-292.5	E	-	2002.10.13	93	-	-	-	-
1868	0:43:52.6	40:57:38.9	23.82	-377.8	-	-	2002.10.13	93	PN_3,3,27	-	-	-
1869	0:44:54.4	40:52:45.5	21.73	-470.6	-	-	2002.10.12	94	PN_4,4,1	1,122	-	1075
1870	0:44:58.0	40:54:15.3	23.65	-267.2	-	-	2002.10.12	94	-	-	-	-
1871	0:44:40.2	40:54:12.8	25.90	-325.1	E	-	2002.10.12	94	-	-	-	-
1872	0:45:32.8	40:53:36.8	23.90	-147.2	-	-	2002.10.11	95	PN_4,4,2	-	-	-
1873	0:46:31.2	40:50:04.1	24.17	-127.7	-	-	2002.10.11	96	-	-	-	-

Continued on next page

Table A.1 – continued from previous page

ID	RA	Dec	$m_{5007}$	$v_{\text{helio}}$	Note	Host	Date	Field	H06	C89	HK04	MLA93
1874	0:41:39.2	40:42:22.2	22.61	-326.5	-	-	2002.10.09	97	-	-	-	382
1875	0:41:37.2	40:42:39.4	24.45	-634.6	-	-	2002.10.09	97	-	-	-	-
1876	0:41:44.6	40:42:45.4	23.67	-453.9	-	-	2002.10.09	97	-	-	-	-
1877	0:42:05.1	40:43:17.2	22.54	-451.5	-	-	2002.10.09	97	-	1.72	-	444
1878	0:41:34.4	40:43:08.0	24.20	-526.4	-	-	2002.10.09	97	-	-	-	-
1879	0:41:35.5	40:43:08.7	23.76	-586.2	-	-	2002.10.09	97	-	-	-	-
1880	0:41:31.0	40:43:17.2	23.00	-242.4	-	-	2002.10.09	97	-	-	-	-
1881	0:41:26.9	40:43:16.0	21.96	-417.2	-	-	2002.10.09	97	PN_2.4.31	1.67	-	363
1882	0:41:38.7	40:43:59.7	20.62	-475.7	E,R	-	2002.10.09	97	-	-	-	-
1883	0:41:41.7	40:44:13.1	23.91	-606.3	-	-	2002.10.09	97	-	-	-	-
1884	0:41:30.2	40:44:12.5	23.89	-480.0	-	-	2002.10.09	97	-	-	-	-
1885	0:41:36.1	40:44:25.8	22.24	-474.4	-	-	2002.10.09	97	-	-	-	-
1886	0:42:05.2	40:45:18.4	23.33	-624.6	-	-	2002.10.09	97	-	-	-	-
1887	0:41:50.4	40:45:13.6	23.72	-485.5	E	-	2002.10.09	97	-	-	-	-
1888	0:42:06.5	40:45:30.3	23.58	-257.1	-	-	2002.10.09	97	-	-	-	-
1889	0:41:35.3	40:45:49.7	21.75	-503.9	-	-	2002.10.09	97	PN_2.4.30	-	-	377
1890	0:41:37.1	40:45:53.8	22.94	-499.0	-	-	2002.10.09	97	-	-	-	-
1891	0:41:51.7	40:46:18.8	23.01	-447.6	R	-	2002.10.09	97	-	-	-	-
1892	0:41:40.2	40:46:32.0	23.82	-618.5	-	-	2002.10.09	97	-	-	-	-
1893	0:41:40.0	40:46:48.2	21.46	-353.6	-	-	2002.10.09	97	PN_2.4.34	-	-	383
1894	0:41:29.4	40:46:47.1	23.61	-533.4	-	-	2002.10.09	97	-	-	-	-
1895	0:42:00.4	40:47:46.6	22.13	-447.4	R	-	2002.10.09	97	-	-	-	434
1896	0:41:44.7	40:48:11.4	22.57	-414.2	-	-	2002.10.09	97	-	-	-	398
1897	0:41:48.9	40:48:53.9	22.21	-415.9	-	-	2002.10.09	97	PN_2.4.36	-	-	410
1898	0:42:03.9	40:49:07.2	21.08	-455.1	R	-	2002.10.09	97	-	-	-	442
1899	0:41:48.5	40:49:12.3	23.75	-120.0	-	-	2002.10.09	97	-	-	-	-
1900	0:42:05.0	40:49:37.7	23.91	-463.5	R	-	2002.10.09	97	-	-	-	-
1901	0:41:42.4	40:49:36.1	21.32	-399.7	-	-	2002.10.09	97	-	-	-	391
1902	0:41:59.2	40:46:04.5	22.20	-368.8	-	-	2002.10.09	97	-	-	-	-
1903	0:41:25.4	40:42:00.5	22.30	-513.5	E,R	-	2002.10.09	98	-	-	-	-
1904	0:41:13.5	40:42:15.9	21.12	-539.3	-	-	2002.10.09	98	PN_2.1.13	1.63	-	322
1905	0:40:52.2	40:43:03.8	23.40	-497.8	-	-	2002.10.09	98	-	-	-	-
1906	0:41:11.9	40:43:25.4	21.59	-512.1	-	-	2002.10.09	98	PN_2.4.18	-	-	318
1907	0:40:55.6	40:43:19.9	23.74	-521.5	-	-	2002.10.09	98	-	-	-	-
1908	0:40:48.4	40:43:33.8	22.03	-542.5	-	-	2002.10.09	98	PN_2.4.12	-	-	268
1909	0:40:40.0	40:43:37.6	21.08	-446.0	-	-	2002.10.09	98	PN_2.4.9	-	-	247
1910	0:41:14.7	40:44:33.2	22.29	-481.5	-	-	2002.10.09	98	-	-	-	327
1911	0:41:21.5	40:44:57.1	23.59	-284.9	-	-	2002.10.09	98	-	-	-	-
1912	0:41:19.9	40:44:58.4	21.76	-453.5	-	-	2002.10.09	98	PN_2.4.32	-	-	348
1913	0:40:51.7	40:45:09.1	24.05	-412.7	-	-	2002.10.09	98	-	-	-	-
1914	0:40:44.1	40:45:14.0	21.60	-487.4	-	-	2002.10.09	98	-	-	-	-
1915	0:41:13.6	40:45:48.3	22.72	-540.8	-	-	2002.10.09	98	PN_2.4.16	-	-	323
1916	0:40:42.4	40:45:39.2	23.67	-493.9	-	-	2002.10.09	98	-	-	-	-
1917	0:40:58.6	40:45:56.9	22.89	-554.6	E,R	-	2002.10.09	98	-	-	-	-
1918	0:40:46.9	40:45:57.4	23.96	-481.7	-	-	2002.10.09	98	-	-	-	-
1919	0:40:47.3	40:46:05.7	23.76	-499.0	-	-	2002.10.09	98	-	-	-	-
1920	0:41:01.6	40:46:25.2	23.10	-563.8	-	-	2002.10.09	98	-	-	-	-
1921	0:40:54.0	40:46:40.2	21.31	-465.5	-	-	2002.10.09	98	PN_2.4.8	-	-	281
1922	0:41:14.0	40:46:53.9	20.75	-519.3	-	-	2002.10.09	98	-	-	-	324
1923	0:40:56.6	40:46:58.6	23.70	-281.7	-	-	2002.10.09	98	-	-	-	-
1924	0:41:10.7	40:47:06.0	23.94	-532.7	-	-	2002.10.09	98	-	-	-	-
1925	0:41:03.8	40:47:04.2	22.70	-485.3	E	-	2002.10.09	98	-	-	-	-
1926	0:41:18.6	40:47:23.7	22.63	-424.0	-	-	2002.10.09	98	-	-	-	341
1927	0:40:46.2	40:47:50.4	22.75	-550.6	-	-	2002.10.09	98	PN_2.4.11	-	-	262
1928	0:40:35.1	40:47:55.6	24.47	-540.4	-	-	2002.10.09	98	-	-	-	-
1929	0:40:55.7	40:48:02.8	22.77	-549.5	-	-	2002.10.09	98	-	-	-	284
1930	0:41:05.7	40:48:11.3	21.46	-269.1	-	-	2002.10.09	98	PN_2.4.15	-	-	309
1931	0:40:54.4	40:48:10.9	23.76	-533.7	-	-	2002.10.09	98	PN_2.4.2	-	-	-
1932	0:40:37.7	40:48:26.0	23.46	-553.1	-	-	2002.10.09	98	-	-	-	-
1933	0:41:10.2	40:48:40.2	23.57	-538.0	-	-	2002.10.09	98	-	-	-	-
1934	0:40:42.8	40:48:38.0	23.48	-471.8	-	-	2002.10.09	98	-	-	-	-
1935	0:41:03.8	40:48:50.5	21.75	-343.5	-	-	2002.10.09	98	PN_2.4.13	-	-	307
1936	0:41:19.2	40:48:56.3	24.19	-533.4	R	-	2002.10.09	98	-	-	-	-
1937	0:40:45.7	40:49:13.8	22.71	-576.4	-	-	2002.10.09	98	PN_2.4.6	-	-	259
1938	0:41:18.0	40:49:40.5	22.45	-633.7	-	-	2002.10.09	98	-	-	-	339
1939	0:40:37.9	40:49:43.7	24.25	-497.9	-	-	2002.10.09	98	-	-	-	-
1940	0:40:05.2	40:42:16.3	23.11	-467.5	-	-	2002.10.09	99	PN_2.2.21	-	-	-
1941	0:40:30.9	40:42:30.4	20.60	-577.0	R	-	2002.10.09	99	PN_2.2.29	-	-	231
1942	0:40:29.5	40:42:37.0	23.45	-584.9	-	-	2002.10.09	99	-	-	-	-
1943	0:39:53.3	40:42:30.2	23.75	-555.7	-	-	2002.10.09	99	-	-	-	-
1944	0:40:16.4	40:43:23.9	23.71	-462.8	-	-	2002.10.09	99	-	-	-	-
1945	0:39:54.6	40:43:46.8	22.45	-573.1	-	-	2002.10.09	99	-	-	-	153
1946	0:40:23.6	40:44:01.0	22.12	-580.7	-	-	2002.10.09	99	PN_12.4.30	-	-	211
1947	0:40:00.9	40:44:56.0	22.60	-464.0	-	-	2002.10.09	99	PN_12.4.20	-	-	-
1948	0:40:31.0	40:45:47.2	21.15	-553.1	-	-	2002.10.09	99	PN_12.4.33	-	-	230
1949	0:40:10.3	40:45:57.0	22.38	-524.9	E	-	2002.10.09	99	-	-	-	-
1950	0:39:55.1	40:45:52.4	21.44	-497.8	-	-	2002.10.09	99	PN_12.4.21	-	-	155
1951	0:40:13.1	40:46:18.9	24.03	-571.5	-	-	2002.10.09	99	-	-	-	-
1952	0:40:26.7	40:46:24.1	24.25	-392.8	-	-	2002.10.09	99	-	-	-	-
1953	0:40:21.2	40:46:40.8	24.79	-495.1	-	-	2002.10.09	99	-	-	-	-
1954	0:39:55.0	40:46:40.7	22.96	-470.6	-	-	2002.10.09	99	-	-	-	-
1955	0:40:09.5	40:46:59.7	22.38	-447.9	-	-	2002.10.09	99	-	-	-	178
1956	0:40:25.0	40:47:18.0	22.17	-414.7	-	-	2002.10.09	99	PN_12.4.31	-	-	215
1957	0:40:23.9	40:47:48.2	22.93	-506.7	-	-	2002.10.09	99	-	-	-	-
1958	0:40:00.6	40:47:53.0	22.00	-453.3	-	-	2002.10.09	99	-	-	-	162
1959	0:40:30.5	40:48:38.1	22.37	-500.9	-	-	2002.10.09	99	-	-	-	-
1960	0:40:22.2	40:48:50.1	21.31	-403.5	-	-	2002.10.09	99	PN_12.4.34	-	-	207
1961	0:40:00.3	40:48:43.0	23.45	-525.1	-	-	2002.10.09	99	-	-	-	-
1962	0:40:06.3	40:49:48.4	23.21	-341.4	-	-	2002.10.09	99	-	-	-	171
1963	0:40:31.9	40:43:11.2	22.92	-424.1	-	-	2002.10.09	99	-	-	-	-
1964	0:40:24.8	40:42:53.7	20.53	-579.8	R	-	2002.10.09	99	-	-	-	-
1965	0:39:43.5	40:42:45.6	24.04	-530.3	-	-	2002.10.10	100	-	-	-	-
1966	0:39:31.3	40:43:55.7	23.36	-461.5	E	-	2002.10.10	100	-	-	-	-

Continued on next page

Table A.1 – continued from previous page

ID	RA	Dec	$m_{5007}$	$v_{\text{helio}}$	Note	Host	Date	Field	H06	C89	HK04	MLA93
1967	0:39:26.1	40:44:27.1	21.51	-397.1	-	-	2002.10.10	100	PN_12_4_8	1.19	-	109
1968	0:39:17.2	40:45:13.4	23.65	-541.8	-	-	2002.10.10	100	PN_12_4_7	-	-	-
1969	0:39:21.5	40:45:30.4	24.72	-411.8	E	-	2002.10.10	100	-	-	-	-
1970	0:39:06.2	40:45:28.0	22.28	-438.7	-	-	2002.10.10	100	-	-	-	86
1971	0:39:49.2	40:45:56.3	24.67	-368.8	-	-	2002.10.10	100	-	-	-	-
1972	0:39:40.3	40:47:27.3	21.72	-470.5	-	-	2002.10.10	100	PN_12_4_17	-	-	125
1973	0:39:02.4	40:47:24.9	24.40	-472.2	-	-	2002.10.10	100	-	-	-	-
1974	0:39:36.0	40:48:36.0	24.19	-389.5	-	-	2002.10.10	100	-	-	-	-
1975	0:39:14.8	40:48:32.4	24.12	-359.5	E	-	2002.10.10	100	-	-	-	-
1976	0:39:31.2	40:48:42.9	20.94	-396.9	E	-	2002.10.10	100	-	-	-	113
1977	0:39:22.7	40:48:44.2	20.92	-558.0	-	-	2002.10.10	100	PN_12_4_13	-	-	106
1978	0:39:43.0	40:48:51.3	22.17	-503.4	-	-	2002.10.10	100	-	-	-	130
1979	0:39:03.5	40:48:50.9	24.63	-380.9	E	-	2002.10.10	100	-	-	-	-
1980	0:39:34.5	40:49:11.9	20.97	-415.2	-	-	2002.10.10	100	PN_12_4_15	-	-	117
1981	0:39:31.5	40:49:17.1	22.05	-420.6	-	-	2002.10.10	100	-	-	-	114
1982	0:37:21.8	40:41:42.6	22.30	-436.9	-	-	2002.10.12	101	-	-	-	-
1983	0:38:04.3	40:43:44.0	21.82	-498.9	-	-	2002.10.12	101	-	-	-	47
1984	0:38:02.6	40:45:26.0	24.79	-462.0	-	-	2002.10.12	101	-	-	-	-
1985	0:37:51.3	40:45:48.1	20.75	-516.8	-	-	2002.10.12	101	-	-	-	-
1986	0:38:51.1	40:42:04.1	24.09	-358.0	E	-	2002.10.12	102	PN_12_1_1	-	-	-
1987	0:38:49.5	40:44:25.8	22.19	-548.7	-	-	2002.10.12	102	PN_12_4_2	-	-	71
1988	0:38:48.3	40:45:32.0	23.26	-412.7	-	-	2002.10.12	102	PN_12_4_1	-	-	-
1989	0:38:35.2	40:46:31.7	25.06	-444.4	-	-	2002.10.12	102	-	-	-	-
1990	0:38:37.0	40:48:05.9	25.15	-386.7	-	-	2002.10.12	102	-	-	-	-
1991	0:38:36.3	40:49:15.9	24.89	-448.5	-	-	2002.10.12	102	-	-	-	-
1992	0:42:32.4	40:42:26.4	22.69	-364.1	-	-	2002.10.11	103	-	1.77	-	539
1993	0:42:37.2	40:42:41.0	25.25	-327.6	-	-	2002.10.11	103	-	-	-	-
1994	0:42:22.9	40:43:06.6	22.97	-513.3	-	-	2002.10.11	103	-	1.75	-	-
1995	0:42:52.1	40:43:50.1	25.06	-452.1	-	-	2002.10.11	103	-	-	-	-
1996	0:42:16.8	40:44:16.1	24.96	-352.8	-	-	2002.10.11	103	-	-	-	-
1997	0:42:29.0	40:44:39.0	22.52	-166.4	-	-	2002.10.11	103	PN_2_4_53	2.2	-	524
1998	0:42:31.9	40:45:09.8	23.68	-501.5	-	-	2002.10.11	103	-	-	-	-
1999	0:42:34.7	40:45:22.3	25.38	-378.8	-	-	2002.10.11	103	-	-	-	-
2000	0:42:50.7	40:45:28.4	21.64	-181.5	-	-	2002.10.11	103	PN_3_4_11	2.5	-	607
2001	0:42:13.3	40:45:35.8	25.37	-421.5	-	-	2002.10.11	103	-	-	-	-
2002	0:42:51.2	40:46:03.7	25.19	-270.7	-	-	2002.10.11	103	-	-	-	-
2003	0:42:15.0	40:49:11.3	24.83	-566.3	-	-	2002.10.11	103	-	-	-	-
2004	0:42:15.2	40:48:30.3	25.34	-161.9	-	-	2002.10.11	103	-	-	-	-
2005	0:43:24.5	40:45:27.3	24.64	-528.4	-	-	2002.10.12	104	-	-	-	-
2006	0:43:47.4	40:47:19.6	24.31	-459.9	-	-	2002.10.12	104	PN_3_4_20	-	-	-
2007	0:44:17.6	40:44:34.8	25.27	-310.7	E	-	2002.10.12	105	-	-	-	-
2008	0:44:20.4	40:49:04.8	23.65	-264.5	-	-	2002.10.12	105	PN_3_4_21	-	-	-
2009	0:44:35.9	40:49:42.1	24.68	-228.2	-	-	2002.10.12	105	-	-	-	-
2010	0:45:19.5	40:47:18.3	26.29	-264.3	-	-	2002.10.12	106	-	-	-	-
2011	0:45:29.5	40:49:16.7	26.09	-419.3	E	-	2002.10.12	106	-	-	-	-
2012	0:45:05.5	40:49:16.3	26.04	-262.4	E	-	2002.10.12	106	-	-	-	-
2013	0:45:27.3	40:51:05.9	26.39	-227.6	E	-	2002.10.12	106	-	-	-	-
2014	0:41:14.6	40:33:29.5	23.92	-582.0	-	-	2002.10.09	108	-	-	-	-
2015	0:41:11.7	40:34:15.0	23.58	-475.7	-	-	2002.10.09	108	PN_2_1_18	-	-	-
2016	0:41:26.7	40:34:28.4	23.00	-426.9	E	-	2002.10.09	108	-	-	-	-
2017	0:41:44.5	40:34:46.0	23.36	-458.5	-	-	2002.10.09	108	-	-	-	-
2018	0:41:22.9	40:35:41.6	22.86	-439.9	-	-	2002.10.09	108	-	-	-	-
2019	0:41:12.5	40:35:58.5	21.55	-542.8	-	-	2002.10.09	108	PN_2_1_17	1.62	-	319
2020	0:41:45.6	40:37:02.8	24.96	-385.9	E	-	2002.10.09	108	-	-	-	-
2021	0:41:30.1	40:37:16.1	24.02	-437.2	-	-	2002.10.09	108	-	-	-	-
2022	0:41:18.8	40:37:43.1	21.43	-531.0	-	-	2002.10.09	108	PN_2_1_16	-	-	342
2023	0:41:14.7	40:39:05.5	23.22	-633.7	-	-	2002.10.09	108	-	-	-	-
2024	0:41:22.9	40:39:13.3	23.66	-520.2	-	-	2002.10.09	108	-	-	-	-
2025	0:41:43.0	40:39:21.4	25.05	-379.1	-	-	2002.10.09	108	-	-	-	-
2026	0:41:13.7	40:39:18.7	23.35	-484.1	R	-	2002.10.09	108	-	-	-	-
2027	0:41:29.2	40:39:44.9	23.03	-466.5	-	-	2002.10.09	108	-	-	-	-
2028	0:41:21.9	40:39:53.7	23.03	-91.1	-	-	2002.10.09	108	-	-	-	-
2029	0:41:44.3	40:41:43.9	24.62	-462.2	-	-	2002.10.09	108	-	-	-	-
2030	0:40:33.8	40:32:46.5	19.66	-530.8	E,R	-	2002.10.09	109	PN_12_1_29	-	-	234
2031	0:40:38.1	40:32:57.1	23.99	-532.9	-	-	2002.10.09	109	-	-	-	-
2032	0:40:52.6	40:33:17.2	22.66	-573.5	-	-	2002.10.09	109	-	-	-	277
2033	0:40:33.5	40:33:29.9	23.40	-585.0	-	-	2002.10.09	109	-	-	-	-
2034	0:40:58.1	40:34:04.0	22.08	-433.6	-	-	2002.10.09	109	-	-	-	294
2035	0:40:38.7	40:34:31.3	23.34	-528.8	E,R	-	2002.10.09	109	-	-	-	-
2036	0:40:28.9	40:34:31.3	24.66	-653.2	-	-	2002.10.09	109	-	-	-	-
2037	0:40:33.5	40:34:33.3	23.56	-547.2	-	-	2002.10.09	109	-	-	-	-
2038	0:40:58.1	40:35:12.7	25.29	-501.8	-	-	2002.10.09	109	-	-	-	-
2039	0:40:34.7	40:35:41.2	20.81	-550.3	R	-	2002.10.09	109	-	-	-	235
2040	0:40:56.0	40:36:03.7	23.30	-358.0	-	-	2002.10.09	109	-	-	-	-
2041	0:40:51.8	40:36:04.3	21.95	-553.3	E,R	-	2002.10.09	109	-	-	-	-
2042	0:40:57.3	40:36:07.7	20.94	-529.0	R	-	2002.10.09	109	PN_2_1_9	1.58	-	291
2043	0:40:28.5	40:36:10.7	23.16	-571.2	-	-	2002.10.09	109	-	-	-	-
2044	0:40:41.7	40:36:21.3	23.92	-557.2	-	-	2002.10.09	109	-	-	-	-
2045	0:40:44.9	40:36:37.0	24.47	-482.6	-	-	2002.10.09	109	-	-	-	-
2046	0:40:18.7	40:36:32.4	23.09	-609.8	-	-	2002.10.09	109	-	-	-	-
2047	0:40:44.1	40:36:54.5	21.91	-368.4	-	-	2002.10.09	109	-	-	-	254
2048	0:40:47.4	40:36:56.4	24.50	-556.7	-	-	2002.10.09	109	-	-	-	-
2049	0:40:30.9	40:36:54.2	20.65	-488.9	-	-	2002.10.09	109	PN_12_1_23	1.47	-	229
2050	0:40:35.1	40:37:01.3	23.51	-557.6	R	-	2002.10.09	109	-	-	-	-
2051	0:40:49.5	40:37:13.9	22.78	-480.7	-	-	2002.10.09	109	-	-	-	270
2052	0:40:25.8	40:37:06.4	22.65	-530.7	-	-	2002.10.09	109	PN_12_1_24	-	-	-
2053	0:40:38.2	40:37:11.9	23.46	-571.4	-	-	2002.10.09	109	-	-	-	-
2054	0:40:32.8	40:37:17.9	24.50	-576.7	-	-	2002.10.09	109	-	-	-	-
2055	0:40:24.7	40:37:19.7	23.69	-372.2	-	-	2002.10.09	109	-	-	-	-
2056	0:40:39.3	40:37:32.9	21.06	-563.6	R	-	2002.10.09	109	-	-	-	245
2057	0:40:31.8	40:37:51.4	23.95	-106.6	-	-	2002.10.09	109	-	-	-	-
2058	0:40:39.5	40:38:14.2	24.38	-568.9	-	-	2002.10.09	109	-	-	-	-
2059	0:40:31.5	40:38:20.6	24.14	-433.4	-	-	2002.10.09	109	-	-	-	-

Continued on next page

Table A.1 – continued from previous page

ID	RA	Dec	$m_{5007}$	$v_{\text{helio}}$	Note	Host	Date	Field	H06	C89	HK04	MLA93
2060	0:40:42.9	40:38:31.6	24.60	-604.6	-	-	2002.10.09	109	-	-	-	-
2061	0:40:37.2	40:38:34.3	24.17	-578.8	-	-	2002.10.09	109	-	-	-	-
2062	0:40:14.6	40:38:50.4	20.95	-541.7	-	-	2002.10.09	109	PN_12.1_22	1.42	-	189
2063	0:40:16.0	40:39:04.0	23.88	-604.3	E	-	2002.10.09	109	-	-	-	-
2064	0:40:34.7	40:39:19.7	23.60	-444.6	-	-	2002.10.09	109	-	-	-	-
2065	0:40:29.3	40:39:25.8	24.63	-559.3	-	-	2002.10.09	109	-	-	-	-
2066	0:40:15.9	40:39:29.5	23.63	-599.5	-	-	2002.10.09	109	-	-	-	-
2067	0:40:26.5	40:39:37.6	23.09	-589.2	-	-	2002.10.09	109	-	-	-	-
2068	0:40:49.6	40:39:46.5	20.19	-423.0	-	-	2002.10.09	109	PN_2.1_5	1.56	-	271
2069	0:40:34.9	40:39:42.8	23.46	-537.1	-	-	2002.10.09	109	-	-	-	-
2070	0:40:27.8	40:40:54.1	24.83	-596.1	-	-	2002.10.09	109	-	-	-	-
2071	0:39:46.9	40:33:06.1	25.20	-400.1	-	-	2002.10.09	110	-	-	-	-
2072	0:39:44.8	40:33:51.6	23.36	-459.5	-	-	2002.10.09	110	PN_12.1_10	-	-	-
2073	0:39:58.2	40:34:05.4	22.61	-528.9	-	-	2002.10.09	110	PN_12.1_15	-	-	159
2074	0:40:01.2	40:34:33.0	24.02	-218.5	-	-	2002.10.09	110	-	-	-	-
2075	0:39:40.0	40:34:40.8	25.06	-506.4	-	-	2002.10.09	110	-	-	-	-
2076	0:39:55.4	40:34:49.2	24.95	-532.8	E	-	2002.10.09	110	-	-	-	-
2077	0:40:05.6	40:35:45.7	24.08	-402.1	-	-	2002.10.09	110	-	-	-	-
2078	0:39:44.0	40:35:41.8	22.86	-438.2	-	-	2002.10.09	110	PN_12.1_9	1.26	-	134
2079	0:40:01.9	40:37:28.5	20.54	-546.2	-	-	2002.10.09	110	PN_12.1_11	1.37	-	165
2080	0:39:49.5	40:37:34.4	24.75	-553.6	E	-	2002.10.09	110	-	-	-	-
2081	0:40:09.0	40:38:34.8	25.20	-520.8	-	-	2002.10.09	110	-	-	-	-
2082	0:40:06.8	40:38:44.0	21.80	-518.3	-	-	2002.10.09	110	-	-	-	172
2083	0:39:51.8	40:38:39.3	25.14	-488.5	-	-	2002.10.09	110	-	-	-	-
2084	0:40:00.5	40:39:12.7	24.60	-537.9	E	-	2002.10.09	110	-	-	-	-
2085	0:40:05.9	40:39:21.8	25.26	-350.6	-	-	2002.10.09	110	-	-	-	-
2086	0:39:29.5	40:39:13.6	25.01	-406.5	-	-	2002.10.09	110	-	-	-	-
2087	0:40:07.4	40:40:07.0	25.50	-566.8	-	-	2002.10.09	110	-	-	-	-
2088	0:39:48.9	40:40:16.5	24.65	-502.3	-	-	2002.10.09	110	-	-	-	-
2089	0:39:56.5	40:40:45.0	24.84	-434.5	-	-	2002.10.09	110	-	-	-	-
2090	0:39:44.5	40:41:18.7	25.27	-586.8	-	-	2002.10.09	110	-	-	-	-
2091	0:39:52.2	40:41:35.4	24.69	-520.3	-	-	2002.10.09	110	-	-	-	-
2092	0:39:08.8	40:34:10.5	24.63	-453.5	-	-	2002.10.12	111	-	-	-	-
2093	0:39:04.5	40:34:30.3	22.03	-503.1	-	-	2002.10.12	111	PN_12.1_2	1.8	-	82
2094	0:39:09.3	40:34:46.0	24.90	-471.2	-	-	2002.10.12	111	-	-	-	-
2095	0:39:06.6	40:35:31.7	25.25	-495.5	-	-	2002.10.12	111	-	-	-	-
2096	0:39:12.6	40:36:58.4	24.72	-483.0	-	-	2002.10.12	111	-	-	-	-
2097	0:39:09.9	40:37:08.2	24.53	-376.5	-	-	2002.10.12	111	-	-	-	-
2098	0:39:06.9	40:37:10.6	23.17	-487.7	E,R	-	2002.10.12	111	-	-	-	-
2099	0:39:09.5	40:37:13.8	24.90	-496.6	-	-	2002.10.12	111	-	-	-	-
2100	0:39:10.0	40:37:21.0	22.37	-494.8	R	-	2002.10.12	111	-	-	-	-
2101	0:39:10.2	40:37:23.0	23.30	-495.0	E	-	2002.10.12	111	-	-	-	-
2102	0:39:10.1	40:37:28.1	20.91	-501.9	E,R	-	2002.10.12	111	PN_12.1_4	-	-	93
2103	0:39:06.2	40:38:19.6	23.26	-282.1	-	-	2002.10.12	111	PN_12.1_5	-	-	87
2104	0:39:21.5	40:38:33.1	25.46	-483.5	-	-	2002.10.12	111	-	-	-	-
2105	0:38:17.7	40:34:53.6	22.32	-461.2	-	-	2002.10.13	112	-	-	-	56
2106	0:37:59.5	40:38:41.9	24.72	-472.8	-	-	2002.10.13	112	-	-	-	-
2107	0:37:53.9	40:34:19.6	23.75	-477.2	E	-	2002.10.13	112	-	-	-	-
2108	0:42:03.3	40:31:39.6	20.98	-544.9	-	-	2002.10.13	113	PN_2.1_25	1.70	-	440
2109	0:41:58.7	40:32:24.0	22.65	-291.0	-	-	2002.10.13	113	-	-	-	432
2110	0:42:20.3	40:32:31.8	25.27	-386.7	R	-	2002.10.13	113	-	-	-	-
2111	0:42:35.3	40:33:51.0	24.14	219.2	-	AndIV	2002.10.13	113	-	-	-	-
2112	0:42:21.2	40:33:50.0	21.74	-372.5	-	-	2002.10.13	113	-	1.74	-	-
2113	0:42:32.2	40:33:58.8	22.53	236.2	E	AndIV	2002.10.13	113	PN_3.2_5	3.3	-	-
2114	0:42:36.6	40:34:04.8	23.47	213.3	-	AndIV	2002.10.13	113	-	-	-	-
2115	0:42:31.7	40:34:11.1	23.13	253.9	E	AndIV	2002.10.13	113	-	3.4	-	-
2116	0:42:00.8	40:34:04.6	25.03	-456.9	-	-	2002.10.13	113	-	-	-	-
2117	0:42:32.7	40:34:17.0	25.20	248.8	-	AndIV	2002.10.13	113	-	-	-	-
2118	0:42:05.3	40:34:32.9	24.87	-288.4	-	-	2002.10.13	113	-	-	-	-
2119	0:42:30.6	40:34:47.3	24.43	285.7	E	AndIV	2002.10.13	113	PN_2.1_33	3.6	-	-
2120	0:42:34.7	40:35:52.1	24.91	-322.3	-	-	2002.10.13	113	-	-	-	-
2121	0:42:07.3	40:36:08.2	22.48	-124.0	-	-	2002.10.13	113	-	-	-	450
2122	0:42:13.1	40:37:15.4	24.26	-291.2	-	-	2002.10.13	113	-	-	-	-
2123	0:41:51.8	40:37:33.2	22.89	-521.8	E	-	2002.10.13	113	PN_2.1_23	-	-	414
2124	0:42:24.5	40:39:14.4	25.10	-345.4	E	-	2002.10.13	113	-	-	-	-
2125	0:42:10.1	40:39:32.4	23.70	-411.7	-	-	2002.10.13	113	-	-	-	-
2126	0:42:05.1	40:40:09.7	25.36	-398.5	-	-	2002.10.13	113	-	-	-	-
2127	0:42:05.6	40:31:06.5	24.23	-440.6	E	-	2002.10.13	113	-	-	-	-
2128	0:42:31.9	40:33:58.7	24.79	228.5	-	AndIV	2002.10.13	113	PN_3.2_5	-	-	-
2129	0:42:56.2	40:35:40.0	23.57	-509.7	E	-	2002.10.13	114	-	1.87	-	-
2130	0:43:33.8	40:33:15.8	25.63	-351.3	E	-	2002.10.12	115	-	-	-	-
2131	0:43:36.8	40:37:38.2	23.34	-322.0	-	-	2002.10.12	115	PN_3.1_2	1.102	-	-
2132	0:44:42.8	40:40:05.5	21.80	-379.1	-	-	2002.10.12	116	PN_4.1_1	1.118	-	1043
2133	0:46:36.6	40:34:23.1	24.28	-297.4	E	-	2002.10.11	118	-	-	-	-
2134	0:46:14.4	40:35:55.9	25.79	-674.3	-	-	2002.10.11	118	-	-	-	-
2135	0:46:44.5	40:37:17.9	25.68	424.2	E	-	2002.10.11	118	-	-	-	-
2136	0:46:45.7	40:37:47.5	25.71	-345.0	E	-	2002.10.11	118	-	-	-	-
2137	0:47:31.6	42:26:18.4	22.05	-79.4	-	-	2002.10.13	120	-	-	-	1294
2138	0:47:20.0	42:26:29.6	25.20	-34.9	-	-	2002.10.13	120	-	-	-	-
2139	0:47:12.5	42:26:56.8	24.67	-47.9	E	-	2002.10.13	120	-	-	-	-
2140	0:47:00.3	42:27:19.0	22.31	-124.4	-	-	2002.10.13	120	-	-	-	1285
2141	0:46:49.9	42:27:41.0	19.09	-81.7	E,R	-	2002.10.13	120	-	-	-	1277
2142	0:47:00.5	42:27:56.3	23.03	-80.6	-	-	2002.10.13	120	-	-	-	-
2143	0:47:15.5	42:28:40.8	23.65	-93.6	-	-	2002.10.13	120	-	-	-	-
2144	0:47:11.9	42:30:46.9	21.14	-73.2	-	-	2002.10.13	120	-	-	-	1291
2145	0:46:07.1	42:15:57.6	22.42	-39.1	E	-	2002.10.13	125	-	-	-	1225
2146	0:45:56.0	42:16:57.4	23.14	-122.2	-	-	2002.10.13	125	-	-	-	1213
2147	0:45:46.9	42:17:15.3	22.56	6.8	-	-	2002.10.13	125	-	-	-	1195
2148	0:46:02.9	42:18:49.1	24.40	-30.6	-	-	2002.10.13	125	-	-	-	-
2149	0:46:11.8	42:18:57.2	25.34	-13.2	-	-	2002.10.13	125	-	-	-	-
2150	0:46:03.2	42:18:57.1	25.52	-55.1	E	-	2002.10.13	125	-	-	-	-
2151	0:45:54.7	42:20:04.9	25.81	-17.1	-	-	2002.10.13	125	-	-	-	-
2152	0:45:48.2	42:22:22.7	25.35	-49.1	-	-	2002.10.13	125	-	-	-	-

Continued on next page

Table A.1 – continued from previous page

ID	RA	Dec	$m_{5007}$	$v_{\text{helio}}$	Note	Host	Date	Field	H06	C89	HK04	MLA93
2153	0:45:41.3	42:22:20.7	25.37	20.5	E	-	2002.10.13	125	-	-	-	-
2154	0:46:17.0	42:23:05.1	25.69	-74.5	-	-	2002.10.13	125	-	-	-	-
2155	0:46:11.5	42:23:10.7	22.67	-68.7	E	-	2002.10.13	125	-	-	-	-
2156	0:46:01.7	42:24:24.4	24.33	-188.0	-	-	2002.10.13	125	-	-	-	-
2157	0:46:47.1	42:15:19.5	21.79	-64.9	-	-	2002.10.13	126	-	-	-	1273
2158	0:46:43.7	42:15:25.2	25.22	-109.2	E	-	2002.10.13	126	-	-	-	-
2159	0:46:42.0	42:15:45.7	24.80	7.2	E	-	2002.10.13	126	-	-	-	-
2160	0:46:26.3	42:16:10.9	23.83	-5.3	-	-	2002.10.13	126	-	-	-	-
2161	0:46:32.3	42:16:17.0	24.40	-90.9	E	-	2002.10.13	126	-	-	-	-
2162	0:46:35.5	42:17:11.3	22.95	-45.0	-	-	2002.10.13	126	-	-	-	-
2163	0:46:37.6	42:17:24.5	25.56	-21.4	-	-	2002.10.13	126	-	-	-	-
2164	0:46:44.2	42:18:09.7	23.86	-75.8	-	-	2002.10.13	126	-	-	-	-
2165	0:46:51.2	42:18:30.1	25.47	-26.7	E	-	2002.10.13	126	-	-	-	-
2166	0:46:47.4	42:18:36.9	22.61	-11.6	-	-	2002.10.13	126	-	-	-	-
2167	0:47:00.6	42:18:50.5	23.78	-100.3	-	-	2002.10.13	126	-	-	-	-
2168	0:47:04.7	42:19:11.7	25.83	-54.0	-	-	2002.10.13	126	-	-	-	-
2169	0:46:43.0	42:19:26.9	25.47	-50.9	-	-	2002.10.13	126	-	-	-	-
2170	0:47:03.8	42:19:35.9	24.26	-93.8	E	-	2002.10.13	126	-	-	-	-
2171	0:46:39.9	42:19:40.3	24.05	-62.7	-	-	2002.10.13	126	-	-	-	-
2172	0:47:10.2	42:19:51.6	26.06	-102.4	E	-	2002.10.13	126	-	-	-	-
2173	0:46:46.5	42:20:29.8	25.18	-152.2	-	-	2002.10.13	126	-	-	-	-
2174	0:46:34.0	42:20:42.3	24.98	-34.9	-	-	2002.10.13	126	-	-	-	-
2175	0:46:45.7	42:20:54.9	25.33	-69.2	E	-	2002.10.13	126	-	-	-	-
2176	0:46:23.5	42:20:59.8	25.84	-65.5	-	-	2002.10.13	126	-	-	-	-
2177	0:46:50.6	42:21:16.9	25.46	23.9	-	-	2002.10.13	126	-	-	-	-
2178	0:47:10.8	42:22:42.9	25.45	-188.8	-	-	2002.10.13	126	-	-	-	-
2179	0:46:36.2	42:23:33.1	22.62	-225.7	-	-	2002.10.13	126	-	-	-	1258
2180	0:46:56.8	42:05:59.9	23.10	-53.5	-	-	2002.10.13	127	-	-	-	1281
2181	0:47:22.7	42:06:39.1	25.74	-106.1	-	-	2002.10.13	127	-	-	-	-
2182	0:47:06.4	42:07:15.3	20.75	-69.1	-	-	2002.10.13	127	-	-	-	1287
2183	0:46:59.5	42:07:48.4	22.93	-135.3	-	-	2002.10.13	127	-	-	-	1284
2184	0:47:34.6	42:08:23.1	24.02	-105.8	-	-	2002.10.13	127	-	-	-	-
2185	0:46:54.2	42:08:15.4	23.33	-184.0	-	-	2002.10.13	127	-	-	-	-
2186	0:46:54.3	42:08:28.9	25.62	-146.3	-	-	2002.10.13	127	-	-	-	-
2187	0:47:38.2	42:08:54.3	25.17	-61.7	-	-	2002.10.13	127	-	-	-	-
2188	0:47:06.1	42:08:45.3	24.54	-37.3	-	-	2002.10.13	127	-	-	-	-
2189	0:47:21.5	42:08:50.8	25.56	-136.8	-	-	2002.10.13	127	-	-	-	-
2190	0:47:13.8	42:09:11.2	25.88	-24.5	-	-	2002.10.13	127	-	-	-	-
2191	0:46:58.5	42:10:55.0	25.37	-38.9	-	-	2002.10.13	127	-	-	-	-
2192	0:47:23.6	42:11:26.2	24.97	-72.1	-	-	2002.10.13	127	-	-	-	-
2193	0:47:32.9	42:11:36.3	20.85	-173.3	-	-	2002.10.13	127	-	-	-	1295
2194	0:47:15.3	42:12:51.1	24.10	-68.4	-	-	2002.10.13	127	-	-	-	-
2195	0:46:57.8	42:13:02.7	25.46	-29.2	E	-	2002.10.13	127	-	-	-	-
2196	0:46:56.1	41:39:17.3	24.92	-478.8	E	-	2002.10.13	130	-	-	-	-
2197	0:47:01.0	41:39:58.2	23.89	-167.6	-	-	2002.10.13	130	-	-	-	-
2198	0:46:30.5	41:40:38.7	24.26	-85.8	-	-	2002.10.13	130	-	-	-	-
2199	0:47:12.1	41:40:56.7	24.99	-65.0	E	-	2002.10.13	130	-	-	-	-
2200	0:46:57.4	41:42:15.5	21.82	-138.8	-	-	2002.10.13	130	-	-	-	1282
2201	0:46:43.5	41:42:58.9	25.56	-477.0	-	-	2002.10.13	130	-	-	-	-
2202	0:47:02.6	41:43:25.5	23.58	-181.6	-	-	2002.10.13	130	-	-	-	-
2203	0:46:28.2	41:43:49.5	24.12	-516.4	-	-	2002.10.13	130	-	-	-	-
2204	0:46:29.8	41:46:42.6	25.30	-167.7	E	-	2002.10.13	130	-	-	-	-
2205	0:46:38.0	41:38:37.7	24.43	-60.2	-	-	2002.10.13	130	-	-	-	-
2206	0:46:55.2	41:47:21.9	23.57	-166.2	-	-	2002.10.13	130	-	-	-	-
2207	0:40:16.6	41:40:49.8	25.46	-208.7	-	NGC205	2002.10.11	131	-	-	-	-
2208	0:40:18.4	41:41:02.6	25.11	-232.2	E	NGC205	2002.10.11	131	-	-	-	-
2209	0:43:06.8	40:47:46.7	25.94	-466.1	-	-	2002.10.11	133	-	-	-	-
2210	0:42:40.9	40:50:27.4	25.48	-311.5	-	M32	2002.10.11	133	-	-	-	-
2211	0:43:07.2	40:50:38.4	25.70	-354.1	-	-	2002.10.11	133	-	-	-	-
2212	0:42:30.2	40:50:43.8	26.04	-225.6	-	M32	2002.10.11	133	-	-	-	-
2213	0:42:44.3	40:50:53.2	25.11	-141.6	-	M32	2002.10.11	133	-	-	-	-
2214	0:42:47.2	40:51:07.1	25.63	-142.5	-	M32	2002.10.11	133	-	-	-	-
2215	0:42:44.6	40:51:12.3	25.23	-163.0	-	M32	2002.10.11	133	-	-	-	-
2216	0:42:51.2	40:51:24.0	25.32	-133.8	E	M32	2002.10.11	133	-	-	-	-
2217	0:42:38.7	40:51:19.9	25.07	-172.4	E	M32	2002.10.11	133	-	-	-	-
2218	0:42:29.8	40:51:20.4	25.40	-448.3	-	M32?	2002.10.11	133	-	-	-	-
2219	0:42:40.2	40:51:25.8	24.94	-206.6	-	M32	2002.10.11	133	-	-	-	-
2220	0:42:36.5	40:51:28.6	24.74	-266.8	-	M32	2002.10.11	133	-	-	-	-
2221	0:42:43.8	40:51:41.6	24.97	-155.4	-	M32	2002.10.11	133	-	-	-	-
2222	0:42:39.2	40:52:01.0	26.51	-830.0	E	Stream?	2002.10.11	133	-	-	-	-
2223	0:42:39.8	40:52:09.2	25.70	-166.1	E	M32	2002.10.11	133	-	-	-	-
2224	0:42:16.5	40:52:13.5	25.57	-353.1	-	-	2002.10.11	133	-	-	-	-
2225	0:42:40.4	40:52:33.3	24.70	-164.8	-	M32	2002.10.11	133	-	-	-	-
2226	0:42:29.5	40:53:09.0	25.82	-559.4	-	M32?	2002.10.11	133	-	-	-	-
2227	0:42:17.8	40:54:09.5	25.72	-369.7	-	-	2002.10.11	133	-	-	-	-
2228	0:42:47.2	40:54:36.7	25.65	-186.9	-	M32	2002.10.11	133	-	-	-	-
2229	0:42:26.9	40:54:55.0	25.11	-535.0	-	M32?	2002.10.11	133	-	-	-	-
2230	0:42:58.5	40:55:40.2	25.67	-196.0	-	M32	2002.10.11	133	-	-	-	-
2231	0:43:01.6	40:56:08.8	25.78	-387.2	-	-	2002.10.11	133	-	-	-	-
2232	0:42:35.6	40:56:21.2	24.99	-443.0	-	M32?	2002.10.11	133	-	-	-	-
2233	0:43:00.9	40:56:54.7	25.44	-431.0	-	-	2002.10.11	133	-	-	-	-
2234	0:42:42.3	40:51:49.5	20.13	-147.3	E	M32	2002.10.11	133	-	-	-	-
2235	0:42:44.6	40:51:44.1	24.81	-229.4	-	M32	2002.10.11	133	-	-	-	-
2236	0:41:06.9	40:22:57.2	25.33	-517.2	-	-	2002.10.13	139	-	-	-	-
2237	0:40:40.0	40:23:12.2	23.38	-526.4	-	-	2002.10.13	139	-	-	-	-
2238	0:40:42.2	40:23:40.5	23.85	-360.3	-	-	2002.10.13	139	-	-	-	-
2239	0:41:17.9	40:24:18.1	24.01	-488.1	-	-	2002.10.13	139	-	-	-	-
2240	0:41:01.8	40:24:20.4	20.70	-394.5	-	-	2002.10.13	139	-	1.60	-	304
2241	0:40:44.0	40:25:08.7	21.76	-482.9	-	-	2002.10.13	139	-	1.51	-	255
2242	0:40:39.9	40:25:45.3	24.61	-126.4	-	-	2002.10.13	139	-	-	-	-
2243	0:41:24.2	40:26:36.5	25.61	-521.0	E	-	2002.10.13	139	-	-	-	-
2244	0:40:57.1	40:26:41.5	23.39	-410.2	-	-	2002.10.13	139	-	-	-	-
2245	0:40:46.4	40:26:44.2	22.75	-408.8	-	-	2002.10.13	139	-	-	-	263

Continued on next page

Table A.1 – continued from previous page

ID	RA	Dec	$m_{5007}$	$v_{\text{helio}}$	Note	Host	Date	Field	H06	C89	HK04	MLA93
2246	0:41:09.7	40:27:17.6	21.62	-512.9	-	-	2002.10.13	139	-	-	-	313
2247	0:40:40.5	40:27:09.4	24.92	-512.5	-	-	2002.10.13	139	-	-	-	-
2248	0:40:44.2	40:27:11.5	22.52	-491.5	-	-	2002.10.13	139	-	1.52	-	256
2249	0:40:37.4	40:27:14.8	24.93	-454.2	E	-	2002.10.13	139	-	-	-	-
2250	0:40:39.5	40:28:03.9	24.20	-433.8	-	-	2002.10.13	139	-	-	-	-
2251	0:41:05.8	40:28:13.5	22.77	-512.0	-	-	2002.10.13	139	-	-	-	310
2252	0:41:10.8	40:28:20.8	24.08	-225.4	-	-	2002.10.13	139	-	-	-	-
2253	0:40:47.3	40:28:25.5	22.95	-482.0	-	-	2002.10.13	139	-	1.55	-	265
2254	0:40:52.4	40:28:27.7	21.99	-573.7	-	-	2002.10.13	139	-	-	-	276
2255	0:41:04.9	40:28:42.9	25.40	-370.3	-	-	2002.10.13	139	-	-	-	-
2256	0:41:00.3	40:28:49.8	21.41	-428.0	-	-	2002.10.13	139	-	1.59	-	302
2257	0:40:43.6	40:29:01.3	24.70	-399.9	-	-	2002.10.13	139	-	-	-	-
2258	0:40:56.8	40:29:40.7	24.98	-538.3	-	-	2002.10.13	139	-	-	-	-
2259	0:41:25.1	40:30:02.0	25.73	-462.8	-	-	2002.10.13	139	-	-	-	-
2260	0:41:20.1	40:30:10.6	25.63	-306.7	-	-	2002.10.13	139	-	-	-	-
2261	0:41:10.2	40:30:34.4	25.12	-241.1	-	-	2002.10.13	139	-	-	-	-
2262	0:40:48.5	40:30:51.6	24.87	-513.2	E	-	2002.10.13	139	-	-	-	-
2263	0:41:07.7	40:31:36.2	25.48	-528.2	-	-	2002.10.13	139	-	-	-	-
2264	0:40:54.3	40:32:17.5	24.75	-479.4	-	-	2002.10.13	139	-	-	-	-
2265	0:40:48.4	40:32:19.6	24.44	-564.5	E	-	2002.10.13	139	-	-	-	-
2266	0:41:05.2	40:32:16.0	23.79	-555.6	E	-	2002.10.13	139	-	-	-	-
2267	0:40:14.2	40:23:24.0	21.79	-144.5	-	-	2002.10.13	140	-	1.41	-	188
2268	0:40:33.5	40:24:07.6	24.49	-451.4	R	-	2002.10.13	140	-	-	-	-
2269	0:40:15.2	40:24:05.3	25.08	-459.0	-	-	2002.10.13	140	-	-	-	-
2270	0:40:15.3	40:24:13.5	22.42	-475.7	-	-	2002.10.13	140	-	1.43	-	191
2271	0:39:57.1	40:24:19.8	24.80	-478.6	-	-	2002.10.13	140	-	-	-	-
2272	0:40:16.8	40:24:32.0	25.47	-414.2	-	-	2002.10.13	140	-	-	-	-
2273	0:40:33.9	40:25:00.2	25.10	-493.5	-	-	2002.10.13	140	-	-	-	-
2274	0:40:30.2	40:25:36.2	25.77	-323.7	-	-	2002.10.13	140	-	-	-	-
2275	0:40:12.4	40:25:49.3	24.44	-483.9	E	-	2002.10.13	140	-	-	-	-
2276	0:40:21.3	40:25:58.1	25.64	-520.8	E	-	2002.10.13	140	-	-	-	-
2277	0:39:57.9	40:26:12.3	23.54	-435.0	-	-	2002.10.13	140	-	-	-	-
2278	0:40:02.9	40:26:21.2	23.89	-473.1	-	-	2002.10.13	140	-	-	-	-
2279	0:40:16.9	40:27:13.0	25.80	-448.3	-	-	2002.10.13	140	-	-	-	-
2280	0:39:54.4	40:27:36.7	22.47	-528.3	E	-	2002.10.13	140	-	-	-	-
2281	0:40:08.9	40:27:50.8	24.58	-527.2	-	-	2002.10.13	140	-	-	-	-
2282	0:40:26.4	40:28:00.5	24.26	-486.3	E	-	2002.10.13	140	-	-	-	-
2283	0:40:20.8	40:28:09.0	21.38	-504.7	-	-	2002.10.13	140	-	1.45	-	204
2284	0:40:13.2	40:28:29.0	24.45	-559.5	-	-	2002.10.13	140	-	-	-	-
2285	0:40:18.0	40:28:34.1	22.92	-541.3	-	-	2002.10.13	140	-	-	-	196
2286	0:40:07.7	40:28:34.0	21.52	-453.1	-	-	2002.10.13	140	-	1.38	-	173
2287	0:40:22.9	40:28:59.6	24.83	-476.5	-	-	2002.10.13	140	-	-	-	-
2288	0:40:12.6	40:29:26.0	25.12	-556.8	-	-	2002.10.13	140	-	-	-	-
2289	0:39:53.8	40:29:34.2	21.25	-561.9	-	-	2002.10.13	140	-	-	-	150
2290	0:39:50.7	40:29:37.7	23.91	-421.4	-	-	2002.10.13	140	-	-	-	-
2291	0:40:29.8	40:30:04.8	25.18	-574.0	-	-	2002.10.13	140	-	-	-	-
2292	0:39:55.4	40:29:58.0	25.10	-527.7	E	-	2002.10.13	140	-	-	-	-
2293	0:40:16.9	40:30:10.2	25.07	-534.8	E	-	2002.10.13	140	-	-	-	-
2294	0:40:22.3	40:30:14.5	23.59	-530.8	-	-	2002.10.13	140	-	-	-	-
2295	0:40:19.3	40:30:17.0	24.74	-537.4	-	-	2002.10.13	140	-	-	-	-
2296	0:40:17.4	40:30:23.8	24.53	-512.1	-	-	2002.10.13	140	-	-	-	-
2297	0:39:49.4	40:30:21.5	24.45	-471.1	-	-	2002.10.13	140	-	-	-	-
2298	0:40:25.7	40:31:56.1	25.52	-541.2	-	-	2002.10.13	140	-	-	-	-
2299	0:39:42.1	40:22:31.0	24.63	-516.0	E	-	2002.10.13	141	-	-	-	-
2300	0:39:45.3	40:23:52.2	25.55	-501.2	-	-	2002.10.13	141	-	-	-	-
2301	0:39:34.2	40:24:01.5	25.80	-514.3	-	-	2002.10.13	141	-	-	-	-
2302	0:39:16.1	40:23:59.8	24.40	-524.9	-	-	2002.10.13	141	-	-	-	-
2303	0:39:35.6	40:24:33.8	22.80	-552.3	-	-	2002.10.13	141	-	-	-	-
2304	0:39:14.8	40:24:28.7	22.59	-317.6	-	-	2002.10.13	141	-	1.12	-	97
2305	0:39:34.8	40:25:03.1	25.14	-549.5	-	-	2002.10.13	141	-	-	-	-
2306	0:39:38.1	40:25:25.7	22.71	-437.4	-	-	2002.10.13	141	-	-	-	123
2307	0:39:16.8	40:26:15.9	21.90	-443.2	-	-	2002.10.13	141	-	-	-	100
2308	0:39:15.0	40:26:34.7	22.15	-520.8	-	-	2002.10.13	141	-	1.13	-	98
2309	0:39:11.6	40:26:41.3	20.56	-438.6	-	-	2002.10.13	141	-	-	-	96
2310	0:39:09.8	40:26:56.7	24.81	-509.6	E	-	2002.10.13	141	-	-	-	-
2311	0:39:09.9	40:27:04.2	20.22	-530.1	E,R	-	2002.10.13	141	-	-	-	92
2312	0:39:05.7	40:27:20.2	24.14	-530.1	E	-	2002.10.13	141	-	-	-	-
2313	0:39:28.2	40:27:42.2	25.18	-440.0	R	-	2002.10.13	141	-	-	-	-
2314	0:39:20.7	40:27:49.1	25.71	-472.8	-	-	2002.10.13	141	-	-	-	-
2315	0:39:37.2	40:28:42.2	25.16	-506.4	-	-	2002.10.13	141	-	-	-	-
2316	0:39:39.8	40:28:55.7	23.01	-538.0	E	-	2002.10.13	141	-	-	-	-
2317	0:39:27.3	40:29:03.8	23.45	-497.0	-	-	2002.10.13	141	-	1.20	-	-
2318	0:39:33.7	40:29:49.2	23.40	-474.9	-	-	2002.10.13	141	-	-	-	-
2319	0:39:24.6	40:30:26.0	23.67	-456.1	-	-	2002.10.13	141	-	-	-	-
2320	0:39:29.3	40:30:39.6	24.23	-521.0	-	-	2002.10.13	141	-	-	-	-
2321	0:39:43.5	40:30:48.4	21.54	-561.0	-	-	2002.10.13	141	-	-	-	133
2322	0:39:06.3	40:31:08.3	23.31	-503.1	-	-	2002.10.13	141	-	-	-	-
2323	0:38:49.2	40:23:13.8	25.49	-577.0	-	-	2002.10.13	142	-	-	-	-
2324	0:38:46.5	40:24:35.1	23.53	-562.8	-	-	2002.10.13	142	-	-	-	-
2325	0:38:17.6	40:25:08.3	24.21	-509.1	-	-	2002.10.13	142	-	-	-	-
2326	0:38:17.6	40:25:32.1	25.63	-491.5	-	-	2002.10.13	142	-	-	-	-
2327	0:38:36.9	40:27:00.2	24.01	-493.6	-	-	2002.10.13	142	-	-	-	-
2328	0:38:31.0	40:27:32.2	24.54	-358.3	-	-	2002.10.13	142	-	-	-	-
2329	0:38:49.5	40:28:30.5	25.67	-419.0	-	-	2002.10.13	142	-	-	-	-
2330	0:38:55.6	40:30:08.8	25.27	-512.5	-	-	2002.10.13	142	-	-	-	-
2331	0:38:31.0	40:30:02.8	25.63	-499.5	E	-	2002.10.13	142	-	-	-	-
2332	0:38:26.6	40:30:44.1	22.74	-462.5	-	-	2002.10.13	142	-	-	-	-
2333	0:38:46.5	40:31:26.6	25.67	-496.5	-	-	2002.10.13	142	-	-	-	-
2334	0:40:12.9	40:13:02.3	21.55	-397.1	-	-	2002.10.13	151	-	1.39	-	182
2335	0:39:44.8	40:14:09.8	24.27	-511.0	E	-	2002.10.13	151	-	-	-	-
2336	0:39:31.7	40:14:21.1	21.44	-506.7	-	-	2002.10.13	151	-	1.21	-	115
2337	0:39:34.3	40:15:11.3	26.21	-528.5	-	-	2002.10.13	151	-	-	-	-
2338	0:39:42.7	40:15:40.6	24.82	-475.8	-	-	2002.10.13	151	-	-	-	-

Continued on next page



Table A.1 – continued from previous page

ID	RA	Dec	$m_{5007}$	$v_{\text{helio}}$	Note	Host	Date	Field	H06	C89	HK04	MLA93
2339	0:39:37.8	40:16:51.3	24.42	-486.8	-	-	2002.10.13	151	-	-	-	-
2340	0:39:42.3	40:17:12.6	24.50	-439.6	-	-	2002.10.13	151	-	-	-	-
2341	0:40:06.2	40:17:28.4	25.47	-487.1	E	-	2002.10.13	151	-	-	-	-
2342	0:39:26.3	40:17:20.7	25.29	-480.0	-	-	2002.10.13	151	-	-	-	-
2343	0:40:05.9	40:17:54.9	25.54	-404.3	-	-	2002.10.13	151	-	-	-	-
2344	0:39:24.2	40:17:42.3	24.68	-553.1	-	-	2002.10.13	151	-	-	-	-
2345	0:39:36.7	40:17:51.3	21.03	-498.8	-	-	2002.10.13	151	-	1.22	-	120
2346	0:39:44.7	40:19:59.0	22.44	-467.2	-	-	2002.10.13	151	-	1.27	-	135
2347	0:39:29.1	40:20:12.6	25.15	-504.4	-	-	2002.10.13	151	-	-	-	-
2348	0:39:59.2	40:20:29.6	24.12	-413.0	-	-	2002.10.13	151	-	-	-	-
2349	0:39:44.5	40:20:30.1	23.28	-528.4	R	-	2002.10.13	151	-	-	-	-
2350	0:40:04.2	40:21:14.6	22.11	-497.1	-	-	2002.10.13	151	-	-	-	168
2351	0:39:30.1	40:21:06.1	23.65	-524.8	E,R	-	2002.10.13	151	-	-	-	-
2352	0:39:49.6	40:21:24.9	21.85	-388.1	-	-	2002.10.13	151	-	1.33	-	147
2353	0:39:34.0	40:20:10.5	22.97	-428.3	-	-	2002.10.13	151	-	-	-	-
2354	0:39:37.5	40:20:11.6	20.67	-522.9	E,R	-	2002.10.13	151	-	-	-	121
2355	0:40:02.3	40:20:02.4	24.78	-512.7	E	-	2002.10.13	151	-	-	-	-
2356	0:39:58.0	40:21:15.7	23.12	-526.0	E,R	-	2002.10.13	151	-	-	-	-
2357	0:39:06.6	40:15:00.0	20.72	-557.7	-	-	2002.10.13	152	-	1.10	-	88
2358	0:39:10.5	40:15:48.5	23.64	-407.6	-	-	2002.10.13	152	-	-	-	-
2359	0:39:23.7	40:16:13.7	26.11	-549.2	-	-	2002.10.13	152	-	-	-	-
2360	0:39:08.5	40:16:32.6	24.11	-500.3	E	-	2002.10.13	152	-	-	-	-
2361	0:38:41.3	40:16:33.6	25.45	-476.9	E	-	2002.10.13	152	-	-	-	-
2362	0:38:37.0	40:17:32.2	24.87	-815.0	E	-	2002.10.13	152	-	-	-	-
2363	0:39:03.5	40:18:00.9	25.76	-507.6	-	-	2002.10.13	152	-	-	-	-
2364	0:38:44.2	40:17:58.7	22.63	-461.3	-	-	2002.10.13	152	-	1.2	-	-
2365	0:39:17.4	40:19:00.3	25.73	-509.7	E	-	2002.10.13	152	-	-	-	-
2366	0:38:40.0	40:19:25.6	25.51	-465.3	-	-	2002.10.13	152	-	-	-	-
2367	0:38:44.1	40:19:34.8	23.50	-511.1	-	-	2002.10.13	152	-	-	-	-
2368	0:39:06.9	40:19:56.5	25.71	-536.5	E	-	2002.10.13	152	-	-	-	-
2369	0:39:06.9	40:21:58.6	25.50	-476.6	-	-	2002.10.13	152	-	-	-	-
2370	0:38:12.3	40:14:42.4	21.71	-475.0	-	-	2002.10.13	153	-	-	-	54
2371	0:38:02.3	40:15:09.5	20.84	-458.8	-	-	2002.10.13	153	-	-	-	46
2372	0:37:59.2	40:15:37.5	25.40	-506.8	-	-	2002.10.13	153	-	-	-	-
2373	0:38:07.7	40:15:49.7	21.63	-532.1	-	-	2002.10.13	153	-	-	-	50
2374	0:37:59.3	40:16:47.8	25.32	-468.8	E	-	2002.10.13	153	-	-	-	-
2375	0:38:04.4	40:17:31.9	25.69	-415.7	E	-	2002.10.13	153	-	-	-	-
2376	0:37:51.1	40:18:58.1	25.90	-518.3	-	-	2002.10.13	153	-	-	-	-
2377	0:37:55.0	40:21:28.2	24.69	-430.6	-	-	2002.10.13	153	-	-	-	-
2378	0:38:17.1	40:22:00.8	25.65	-478.0	-	-	2002.10.13	153	-	-	-	-
2379	0:38:07.0	40:22:53.4	25.99	-534.0	-	-	2002.10.13	153	-	-	-	-
2380	0:37:59.0	40:15:50.0	25.02	-530.5	R	-	2002.10.13	153	-	-	-	-
2381	0:38:07.6	40:21:34.8	24.94	-539.5	E	-	2002.10.13	153	-	-	-	-
2382	0:38:34.4	40:05:05.9	25.76	-506.0	E	-	2002.10.13	154	-	-	-	-
2383	0:38:19.8	40:06:54.0	24.64	-488.7	-	-	2002.10.13	154	-	-	-	-
2384	0:38:46.2	40:07:26.7	25.66	-485.5	-	-	2002.10.13	154	-	-	-	-
2385	0:38:40.2	40:08:02.1	25.93	-478.9	-	-	2002.10.13	154	-	-	-	-
2386	0:38:21.2	40:07:56.5	25.33	-487.7	-	-	2002.10.13	154	-	-	-	-
2387	0:38:53.5	40:08:38.6	24.10	-505.6	-	-	2002.10.13	154	-	-	-	-
2388	0:38:25.7	40:08:51.6	25.75	-562.8	-	-	2002.10.13	154	-	-	-	-
2389	0:38:32.1	40:10:00.1	23.54	-439.0	-	-	2002.10.13	154	-	-	-	-
2390	0:38:55.0	40:10:16.1	21.80	-376.4	-	-	2002.10.13	154	-	1.3	-	75
2391	0:38:29.7	40:10:07.9	24.23	-572.2	-	-	2002.10.13	154	-	-	-	-
2392	0:38:19.1	40:10:06.8	22.91	-492.6	-	-	2002.10.13	154	-	-	-	-
2393	0:38:42.8	40:11:17.7	25.34	-462.9	-	-	2002.10.13	154	-	-	-	-
2394	0:38:30.9	40:11:19.7	24.40	-426.4	-	-	2002.10.13	154	-	-	-	-
2395	0:37:44.9	39:58:34.3	22.34	-510.3	-	-	2002.10.13	156	-	-	-	40
2396	0:38:04.0	40:01:03.0	25.30	-424.9	-	-	2002.10.13	156	-	-	-	-
2397	0:39:14.7	40:03:17.4	23.38	-458.2	-	-	2002.10.13	161	-	-	-	-
2398	0:39:10.6	40:03:50.9	25.51	-446.1	-	-	2002.10.13	161	-	-	-	-
2399	0:39:31.8	40:04:58.3	24.10	-482.2	-	-	2002.10.13	161	-	-	-	-
2400	0:39:09.8	40:06:40.1	24.96	-433.0	-	-	2002.10.13	161	-	-	-	-
2401	0:39:24.5	40:07:02.6	20.80	-419.7	-	-	2002.10.13	161	-	1.18	-	107
2402	0:39:11.9	40:07:32.1	25.40	-443.5	-	-	2002.10.13	161	-	-	-	-
2403	0:39:25.1	40:09:02.7	25.89	-429.7	-	-	2002.10.13	161	-	-	-	-
2404	0:39:18.5	40:09:19.9	20.71	-366.9	-	-	2002.10.13	161	-	1.17	-	101
2405	0:39:16.7	40:09:43.6	24.80	-450.3	-	-	2002.10.13	161	-	-	-	-
2406	0:39:10.6	40:09:58.5	25.55	-511.4	E	-	2002.10.13	161	-	-	-	-
2407	0:39:08.7	40:10:26.3	25.16	-476.1	-	-	2002.10.13	161	-	-	-	-
2408	0:39:32.1	40:10:40.5	25.44	-519.4	-	-	2002.10.13	161	-	-	-	-
2409	0:39:46.2	40:11:02.7	21.26	-426.9	-	-	2002.10.13	161	-	1.30	-	142
2410	0:39:09.3	40:11:20.7	20.83	-426.8	-	-	2002.10.13	161	-	1.11	-	91
2411	0:39:44.8	40:12:05.3	21.85	-475.3	-	-	2002.10.13	161	-	1.28	-	137
2412	0:39:31.4	40:12:03.3	25.42	-476.5	E	-	2002.10.13	161	-	-	-	-
2413	0:39:38.0	40:12:21.5	25.05	-421.3	E	-	2002.10.13	161	-	-	-	-
2414	0:46:48.8	41:08:24.4	24.19	-227.0	-	-	2002.10.13	163	-	-	-	-
2415	0:47:16.7	41:10:42.5	25.15	-298.5	-	-	2002.10.13	163	-	-	-	-
2416	0:49:30.8	43:17:45.6	24.95	-294.5	-	Stream?	2003.10.01	221	-	-	-	-
2417	0:52:46.2	43:22:34.7	24.68	-1231.7	E	-	2003.10.01	224	-	-	-	-
2418	0:51:53.1	43:05:01.4	25.95	-931.9	E	-	2003.09.29	235	-	-	-	-
2419	0:45:48.8	42:54:10.6	23.57	-96.7	-	NS	2003.09.30	240	-	-	-	-
2420	0:46:19.1	42:54:24.8	24.07	2.1	E	NS	2003.09.30	240	-	-	-	-
2421	0:45:42.6	42:55:26.3	20.84	-90.3	-	NS	2003.09.30	240	-	-	-	-
2422	0:46:17.9	42:58:57.9	22.90	-100.0	-	NS	2003.09.30	240	-	-	-	-
2423	0:45:32.7	43:01:56.2	24.68	-131.8	-	NS	2003.09.30	240	-	-	-	-
2424	0:45:33.1	43:02:26.3	21.89	16.6	-	NS	2003.09.30	240	-	-	-	-
2425	0:45:52.5	43:03:40.7	22.86	-183.9	-	NS	2003.09.30	240	-	-	-	-
2426	0:47:00.7	42:58:55.3	20.61	-19.6	-	NS	2003.09.30	241	-	-	-	-
2427	0:46:26.5	43:00:43.0	20.48	-420.3	-	NS/Stream?	2003.09.30	241	-	1.6	-	-
2428	0:46:31.9	43:01:11.9	24.11	-88.1	-	NS	2003.09.30	241	-	-	-	-
2429	0:47:07.6	43:04:22.3	23.08	-89.7	-	NS	2003.09.30	241	-	-	-	-
2430	0:47:25.9	42:58:59.7	21.32	-135.1	-	NS	2003.09.30	242	-	-	-	-
2431	0:47:58.6	43:00:06.4	20.83	-44.4	-	NS	2003.09.30	242	-	-	-	-

Continued on next page

Table A.1 – continued from previous page

ID	RA	Dec	$m_{5007}$	$v_{\text{helio}}$	Note	Host	Date	Field	H06	C89	HK04	MLA93
2432	0:47:30.3	43:03:41.1	20.69	-411.0	-	NS/Stream?	2003.09.30	242	-	-	-	-
2433	0:48:46.9	42:56:43.5	23.14	-83.7	-	-	2003.09.30	243	-	-	-	-
2434	0:49:31.8	42:59:28.4	24.74	-237.4	-	-	2003.09.30	244	-	-	-	-
2435	0:50:34.3	42:56:53.8	24.72	-460.6	-	Stream?	2003.09.29	245	-	-	-	-
2436	0:51:22.2	43:02:25.5	23.30	-47.1	-	-	2003.09.29	246	-	-	-	-
2437	0:48:54.0	42:49:53.9	21.31	-47.4	-	-	2003.09.30	255	-	-	-	-
2438	0:48:47.9	42:51:35.8	20.74	-24.0	-	-	2003.09.30	255	-	-	-	-
2439	0:44:22.9	42:37:05.7	24.19	-242.4	-	NS	2003.09.30	261	-	-	-	-
2440	0:44:23.6	42:41:04.1	21.42	-119.1	-	NS	2003.09.30	261	-	-	-	-
2441	0:43:32.2	42:42:56.8	22.44	-156.5	-	NS	2003.09.30	261	-	-	-	-
2442	0:44:26.5	42:35:12.1	23.73	-206.1	-	NS	2003.09.30	261	-	-	-	-
2443	0:46:14.0	42:36:09.1	25.72	-181.9	-	NS	2003.09.30	263	-	-	-	-
2444	0:45:38.7	42:36:11.3	25.17	-189.5	-	NS	2003.09.30	263	-	-	-	-
2445	0:45:52.8	42:36:52.9	20.65	-149.1	-	NS	2003.09.30	263	-	-	-	-
2446	0:45:39.0	42:36:49.8	24.52	-150.2	-	NS	2003.09.30	263	-	-	-	-
2447	0:45:33.3	42:38:18.4	24.61	0.8	-	NS	2003.09.30	263	-	-	-	-
2448	0:45:48.8	42:38:57.3	24.21	-106.5	-	NS	2003.09.30	263	-	-	-	-
2449	0:46:13.8	42:40:28.5	20.88	-70.6	-	NS	2003.09.30	263	-	-	-	-
2450	0:47:14.9	42:35:01.1	24.50	-141.5	-	-	2003.09.30	264	-	-	-	-
2451	0:46:59.3	42:37:58.2	20.81	-80.8	-	NS	2003.09.30	264	-	-	-	-
2452	0:46:55.3	42:39:11.1	22.89	-110.5	-	NS	2003.09.30	264	-	-	-	-
2453	0:48:04.8	42:35:10.8	22.06	-59.3	-	-	2003.09.30	265	-	-	-	-
2454	0:48:03.5	42:36:37.8	21.10	-89.9	-	-	2003.09.30	265	-	-	-	-
2455	0:47:19.9	42:37:16.7	24.87	-118.6	-	-	2003.09.30	265	-	-	-	-
2456	0:47:25.2	42:39:52.0	24.11	-427.0	-	Stream?	2003.09.30	265	-	-	-	-
2457	0:47:56.3	42:40:11.3	25.28	-80.1	E	-	2003.09.30	265	-	-	-	-
2458	0:49:31.9	42:37:38.0	20.93	-132.8	-	-	2003.09.29	267	-	-	-	-
2459	0:48:03.9	42:25:39.0	22.94	-67.9	-	-	2003.09.29	275	-	-	-	-
2460	0:47:54.7	42:25:49.7	24.11	-85.2	-	-	2003.09.29	275	-	-	-	-
2461	0:48:03.5	42:27:30.3	22.03	-70.4	E,R	-	2003.09.29	275	-	-	-	-
2462	0:48:32.2	42:30:08.7	21.11	-65.3	E	-	2003.09.29	275	-	-	-	-
2463	0:48:09.8	42:31:24.9	23.07	-50.6	-	-	2003.09.29	275	-	-	-	-
2464	0:47:54.4	42:31:50.9	24.16	-15.4	-	-	2003.09.29	275	-	-	-	-
2465	0:48:45.3	42:25:58.9	24.37	-353.0	-	-	2003.09.29	276	-	-	-	-
2466	0:49:08.0	42:28:44.5	21.96	-392.3	-	Stream?	2003.09.29	276	-	-	-	-
2467	0:49:36.8	42:26:10.3	22.66	-138.1	-	-	2003.09.29	276	-	-	-	-
2468	0:42:16.5	42:15:58.9	23.25	-312.8	-	-	2003.09.30	279	-	-	-	-
2469	0:42:16.8	42:20:30.5	23.40	-203.6	-	-	2003.09.30	279	-	-	-	-
2470	0:42:14.8	42:23:58.1	21.11	-177.6	-	-	2003.09.30	279	-	-	-	-
2471	0:43:11.2	42:20:45.7	20.69	-253.9	-	-	2003.09.30	280	-	-	-	-
2472	0:44:02.3	42:17:16.6	20.69	-261.2	-	-	2003.09.30	281	-	-	-	904
2473	0:44:01.4	42:17:44.7	24.82	-108.1	-	-	2003.09.30	281	-	-	-	-
2474	0:43:45.7	42:20:13.4	23.92	-405.8	-	-	2003.09.30	281	-	-	-	-
2475	0:43:42.5	42:22:35.3	21.04	-225.8	-	-	2003.09.30	281	-	-	-	-
2476	0:44:21.5	42:24:50.0	21.16	-220.4	-	-	2003.09.30	281	-	-	-	972
2477	0:47:53.6	42:14:57.7	21.50	-50.6	-	-	2003.09.29	283	-	-	-	1308
2478	0:47:29.4	42:16:29.0	25.21	-67.0	-	-	2003.09.29	283	-	-	-	-
2479	0:47:30.8	42:16:59.0	24.11	-78.1	-	-	2003.09.29	283	-	-	-	-
2480	0:47:51.0	42:20:25.8	23.24	-88.8	-	-	2003.09.29	283	-	-	-	-
2481	0:47:51.8	42:21:09.7	24.09	-102.0	-	-	2003.09.29	283	-	-	-	-
2482	0:47:55.2	42:22:30.2	25.48	-87.7	E	-	2003.09.29	283	-	-	-	-
2483	0:48:35.5	42:16:54.5	23.73	-73.7	-	-	2003.09.29	284	-	-	-	-
2484	0:48:24.8	42:17:06.5	23.00	-266.4	-	-	2003.09.29	284	-	-	-	-
2485	0:48:13.2	42:17:36.4	24.15	-48.5	-	-	2003.09.29	284	-	-	-	-
2486	0:48:30.9	42:18:30.5	22.37	-293.8	-	-	2003.09.29	284	-	-	-	-
2487	0:42:45.0	40:25:01.6	25.40	-416.6	E	-	2003.09.29	290	-	-	-	-
2488	0:42:46.6	40:26:15.2	21.55	-434.0	-	-	2003.09.29	290	-	1.80	-	-
2489	0:42:52.1	40:29:03.9	21.13	-263.4	-	-	2003.09.29	290	-	1.84	-	-
2490	0:43:39.2	40:27:13.4	24.68	-368.5	-	-	2003.09.29	291	-	-	-	-
2491	0:43:59.1	40:30:18.6	23.98	-476.1	-	-	2003.09.29	291	-	-	-	-
2492	0:42:52.2	40:14:01.9	24.28	-324.6	-	-	2003.09.29	298	-	-	-	-
2493	0:42:44.5	40:17:31.0	21.55	-445.2	-	-	2003.09.29	298	-	1.79	-	-
2494	0:43:08.9	40:12:06.1	25.17	-425.2	-	-	2003.09.29	299	-	-	-	-
2495	0:44:25.5	40:14:36.6	22.71	-402.8	-	-	2003.09.29	300	-	1.112	-	-
2496	0:44:26.0	40:15:45.6	20.42	-324.0	-	-	2003.09.29	300	-	1.113	-	-
2497	0:45:04.1	40:12:18.4	24.84	-395.4	E	-	2003.09.29	301	-	-	-	-
2498	0:45:30.9	40:19:29.6	24.03	-228.1	-	-	2003.09.29	301	-	-	-	-
2499	0:45:03.2	40:19:19.9	25.39	81.3	-	-	2003.09.29	301	-	-	-	-
2500	0:42:50.6	40:04:48.6	22.81	-467.0	-	-	2003.10.01	308	-	1.82	-	-
2501	0:44:08.0	40:03:13.8	22.70	-413.2	-	-	2003.10.01	309	-	1.107	-	-
2502	0:44:30.3	40:07:29.5	21.78	-430.2	-	-	2003.10.01	310	-	1.114	-	-
2503	0:41:12.1	39:51:55.4	24.20	-475.1	-	-	2003.10.03	312	-	-	-	-
2504	0:41:38.2	39:55:00.1	21.35	-368.9	-	-	2003.10.03	312	-	1.69	-	-
2505	0:41:26.3	39:59:48.4	22.59	-411.7	-	-	2003.10.03	312	-	1.65	-	-
2506	0:48:26.9	39:53:06.1	23.77	-610.8	-	-	2003.09.29	316	-	-	-	-
2507	0:48:27.2	39:55:34.3	21.23	-146.9	-	-	2003.09.29	316	-	1.134	-	-
2508	0:41:40.3	39:30:57.1	23.79	-252.2	-	-	2003.10.01	320	-	-	-	-
2509	0:41:08.9	39:30:55.6	23.74	-274.5	-	-	2003.10.01	320	-	-	-	-
2510	0:43:37.6	39:38:05.4	22.65	-485.2	-	-	2003.10.01	321	-	-	-	-
2511	0:43:51.0	39:25:16.3	23.87	-260.4	-	-	2003.10.01	322	-	-	-	-
2512	0:45:58.5	39:13:25.6	22.12	-318.2	-	-	2003.10.01	323	-	-	-	-
2513	0:46:06.3	39:20:26.8	23.24	-386.4	-	-	2003.10.01	323	-	-	-	-
2514	0:47:06.9	39:11:12.5	23.44	-451.5	-	-	2003.10.01	324	-	-	-	-
2515	0:47:23.3	38:51:53.6	24.53	-333.5	-	-	2003.10.01	326	-	-	-	-
2516	0:37:36.9	40:05:25.1	24.15	-429.6	-	-	2003.09.29	332	-	-	-	-
2517	0:37:44.6	40:07:10.0	20.51	-503.3	-	-	2003.09.29	332	-	-	-	39
2518	0:37:40.0	40:08:51.5	21.80	-465.5	-	-	2003.09.29	332	-	-	-	37
2519	0:38:05.4	40:10:36.3	20.99	-466.6	-	-	2003.09.29	332	-	-	-	48
2520	0:37:26.4	40:12:57.2	25.26	-446.2	-	-	2003.09.29	332	-	-	-	-
2521	0:38:36.8	39:52:53.9	22.44	-448.8	E	-	2003.09.29	336	-	-	-	-
2522	0:38:36.5	39:52:56.7	24.10	-454.8	E	-	2003.09.29	336	-	-	-	-
2523	0:38:34.5	39:53:05.9	22.99	-557.3	-	-	2003.09.29	336	-	-	-	-
2524	0:37:10.6	39:56:51.9	22.11	-509.3	-	-	2003.09.29	337	-	-	-	-

Continued on next page

Table A.1 – continued from previous page

ID	RA	Dec	$m_{5007}$	$v_{\text{helio}}$	Note	Host	Date	Field	H06	C89	HK04	MLA93
2525	0:37:38.8	39:58:54.2	25.47	-383.5	E	-	2003.09.29	337	-	-	-	-
2526	0:36:59.8	39:58:40.4	22.62	-491.5	-	-	2003.09.29	337	-	-	-	-
2527	0:37:35.8	39:59:22.4	25.35	-448.9	-	-	2003.09.29	337	-	-	-	-
2528	0:37:32.8	40:01:06.0	22.86	-487.7	E	-	2003.09.29	337	-	-	-	-
2529	0:37:36.0	40:02:00.5	24.09	-470.6	-	-	2003.09.29	337	-	-	-	-
2530	0:36:07.0	39:58:33.9	23.20	-443.7	-	-	2003.09.29	338	-	-	-	-
2531	0:36:19.2	40:00:00.4	23.87	-484.2	-	-	2003.09.29	338	-	-	-	-
2532	0:36:33.0	40:02:18.7	24.77	-498.5	-	-	2003.09.29	338	-	-	-	-
2533	0:36:39.5	39:46:08.2	20.28	-498.6	E	-	2003.09.29	341	-	-	-	-
2534	0:37:13.9	39:48:27.0	22.75	-441.8	-	-	2003.09.29	341	-	-	-	-
2535	0:36:44.4	39:49:11.5	25.54	-471.0	-	-	2003.09.29	341	-	-	-	-
2536	0:36:56.8	39:50:29.2	23.49	-401.7	-	-	2003.09.29	341	-	-	-	-
2537	0:37:16.1	39:47:30.9	21.08	-445.6	-	-	2003.09.29	341	-	-	-	29
2538	0:36:28.8	39:35:26.4	20.25	-426.4	-	-	2003.09.29	345	-	-	-	-
2539	0:36:12.6	39:35:41.9	21.16	-426.0	-	-	2003.09.29	345	-	-	-	-
2540	0:36:09.9	39:39:31.8	25.24	-425.8	-	-	2003.09.29	345	-	-	-	-
2541	0:35:09.1	39:28:25.2	21.78	-455.5	-	-	2003.10.01	351	-	-	-	-
2542	0:37:09.3	42:38:18.9	22.10	-223.2	-	-	2003.09.29	366	-	-	-	-
2543	0:35:50.7	42:21:04.5	21.61	-272.0	-	-	2003.10.03	367	-	-	-	-
2544	0:37:28.4	42:10:57.4	23.11	-207.5	-	-	2003.10.03	368	-	-	-	-
2545	0:37:09.5	42:15:17.8	23.57	-173.5	-	-	2003.10.03	368	-	-	-	-
2546	0:34:24.2	42:05:14.6	22.06	-302.4	-	-	2003.09.29	369	-	-	-	-
2547	0:33:56.7	42:04:43.9	23.53	409.0	E	-	2003.09.29	369	-	-	-	-
2548	0:37:07.4	42:03:16.5	22.28	-325.2	-	-	2003.09.30	370	-	-	-	-
2549	0:36:27.2	42:06:21.9	21.35	-17.0	-	-	2003.09.30	370	-	-	-	13
2550	0:36:47.5	41:51:46.9	22.64	-419.2	-	-	2003.10.02	372	-	-	-	-
2551	0:33:37.9	41:47:48.5	22.92	-304.6	-	-	2003.10.03	373	-	-	-	-
2552	0:35:59.7	41:40:47.1	22.29	-195.1	-	-	2003.09.30	376	-	-	-	-
2553	0:35:33.6	41:46:58.9	23.05	-191.3	-	-	2003.09.30	376	-	-	-	-
2554	0:35:58.1	41:12:58.2	24.69	-370.7	-	-	2003.10.01	381	-	-	-	-
2555	0:33:37.6	41:12:07.5	24.23	-292.4	-	-	2003.10.01	382	-	-	-	-
2556	0:34:30.5	41:01:17.7	23.55	-312.4	-	-	2003.10.01	384	-	-	-	-
2557	0:34:25.8	41:04:42.8	23.87	664.0	E	-	2003.10.01	384	-	-	-	-
2558	0:36:34.9	40:49:40.5	25.04	-497.2	-	-	2003.10.01	385	-	-	-	-
2559	0:36:36.2	40:54:38.6	23.45	-192.7	-	-	2003.10.01	385	-	-	-	-
2560	0:35:33.4	40:55:20.7	21.99	-358.3	-	-	2003.10.03	386	-	-	-	-
2561	0:48:37.3	41:17:17.8	23.10	-116.0	-	-	2003.10.03	392	-	-	-	-
2562	0:48:41.2	41:23:28.7	23.02	-250.1	-	-	2003.10.03	392	-	-	-	-
2563	0:47:53.4	41:24:55.3	24.19	-134.8	E	-	2003.10.03	392	-	-	-	-
2564	0:48:24.8	41:08:11.3	19.83	-327.8	other	-	2003.10.01	395	-	1.133	-	-
2565	0:48:28.4	41:13:25.2	21.98	-240.4	-	-	2003.10.01	395	-	-	-	-
2566	0:49:28.3	40:59:53.9	21.26	-246.6	-	-	2003.10.01	397	-	1.135	-	-
2567	0:47:00.9	40:49:23.4	23.14	-336.9	-	-	2003.10.01	398	-	1.131	-	1286
2568	0:48:22.2	40:45:41.5	23.53	-307.5	-	-	2003.10.01	399	-	1.132	-	-
2569	0:43:20.2	42:05:05.1	25.70	-155.6	-	-	2002.10.12	7	-	-	-	-
2570	0:43:28.7	42:11:06.5	24.59	-91.9	-	-	2002.10.12	7	PN_10_3_4	-	-	-
2571	0:44:50.8	42:05:06.4	22.10	-175.1	-	-	2002.10.12	9	-	-	-	-
2572	0:44:53.5	42:04:24.7	22.50	-116.4	-	-	2002.10.12	9	-	-	-	1068
2573	0:45:27.4	42:04:42.7	23.08	-73.1	-	-	2002.10.13	10	-	-	-	-
2574	0:45:15.1	42:05:58.7	22.53	-11.5	-	-	2002.10.13	10	PN_9_3_8	-	-	1127
2575	0:45:57.2	42:07:45.7	22.11	-91.3	-	-	2002.10.13	10	PN_9_3_21	-	-	1215
2576	0:45:55.1	42:14:18.4	25.30	-95.0	-	-	2002.10.13	10	-	-	-	-
2577	0:46:20.9	42:05:04.4	25.15	-87.9	-	-	2002.10.12	11	-	-	-	-
2578	0:46:15.9	42:05:35.7	21.63	-150.0	-	-	2002.10.12	11	PN_9_3_25	-	-	1236
2579	0:46:22.3	42:13:26.8	24.83	-41.3	-	-	2002.10.12	11	-	-	-	-
2580	0:46:32.3	42:13:36.8	22.70	-48.6	E	-	2002.10.12	11	-	-	-	-
2581	0:46:15.5	42:14:57.0	24.53	180.2	E	-	2002.10.12	11	-	-	-	-
2582	0:46:43.0	42:15:16.3	22.63	-74.6	-	-	2002.10.12	11	-	-	-	1268
2583	0:42:12.6	42:03:42.6	24.40	-255.9	-	-	2002.10.13	12	PN_11_3_2	-	-	-
2584	0:43:05.8	41:59:21.5	25.31	-220.4	-	-	2002.10.13	17	-	-	-	-
2585	0:43:11.8	41:55:46.1	22.17	-46.5	-	-	2002.10.12	18	-	-	-	708
2586	0:43:52.7	41:58:10.8	22.71	-213.3	E	-	2002.10.12	18	-	-	-	-
2587	0:44:35.6	41:56:06.5	23.22	-105.8	-	-	2002.10.12	19	PN_10_4_33	-	-	-
2588	0:45:01.0	41:55:51.7	23.92	-88.2	-	-	2002.10.13	20	-	-	-	-
2589	0:45:39.9	41:55:09.4	23.11	-85.8	-	-	2002.10.10	21	-	-	-	-
2590	0:46:09.3	41:55:43.7	21.42	-54.7	-	-	2002.10.10	21	PN_9_4_35	-	-	1231
2591	0:45:42.2	41:55:45.7	21.91	-78.2	E,R	-	2002.10.10	21	-	-	-	-
2592	0:45:46.5	41:56:08.8	22.73	-153.5	-	-	2002.10.10	21	-	-	-	1194
2593	0:46:26.5	41:55:35.6	24.58	-64.4	-	-	2002.10.13	22	-	-	-	-
2594	0:40:10.4	41:49:19.1	23.57	-195.1	-	NGC205	2002.10.10	24	PN_7_1_7	-	-	-
2595	0:42:22.8	41:46:00.8	23.72	-229.5	-	-	2002.10.11	28	PN_11_1_7	-	-	-
2596	0:42:12.8	41:46:51.1	24.91	-236.7	-	-	2002.10.11	28	-	-	-	-
2597	0:42:38.8	41:50:39.5	22.30	-230.4	-	-	2002.10.11	28	-	-	-	-
2598	0:42:37.5	41:50:56.0	24.40	-339.4	-	-	2002.10.11	28	-	-	-	-
2599	0:43:29.1	41:48:48.6	23.26	-196.0	-	-	2002.10.11	29	-	-	-	-
2600	0:43:26.5	41:49:35.6	22.85	-205.7	-	-	2002.10.11	29	-	-	-	-
2601	0:43:28.5	41:51:55.6	22.10	-150.1	-	-	2002.10.11	29	PN_10_4_17	-	-	786
2602	0:42:44.7	41:46:44.5	23.93	-980.4	E	-	2002.10.11	29	-	-	-	-
2603	0:43:18.0	41:45:46.6	20.73	-235.1	-	-	2002.10.11	29	PN_10_1_11	-	-	741
2604	0:43:56.5	41:45:50.7	25.06	-126.5	-	-	2002.10.12	30	-	-	-	-
2605	0:44:06.2	41:45:59.2	22.53	-85.3	-	-	2002.10.12	30	-	-	-	-
2606	0:44:04.7	41:46:52.2	24.23	-162.7	-	-	2002.10.12	30	-	-	-	-
2607	0:44:17.0	41:51:17.5	24.33	-165.7	-	-	2002.10.12	30	-	-	-	-
2608	0:43:26.1	41:45:41.6	21.82	-266.8	-	-	2002.10.12	30	-	-	-	776
2609	0:44:05.3	41:46:06.9	24.12	-492.7	-	-	2002.10.12	30	-	-	-	-
2610	0:44:57.4	41:45:57.8	23.01	-193.4	-	-	2002.10.10	31	PN_9_1_9	-	-	1086
2611	0:45:04.0	41:46:07.0	20.84	-120.9	-	-	2002.10.10	31	PN_9_1_6	-	-	1102
2612	0:44:23.7	41:46:15.8	24.84	-167.2	-	-	2002.10.10	31	-	-	-	-
2613	0:44:32.4	41:46:37.9	21.56	-19.7	-	-	2002.10.10	31	PN_10_1_43	-	-	1015
2614	0:44:44.2	41:46:43.0	24.49	-19.0	-	-	2002.10.10	31	-	-	-	-
2615	0:45:06.2	41:51:55.5	24.07	-192.8	-	-	2002.10.10	31	-	-	-	-
2616	0:44:55.9	41:45:46.1	23.85	-88.4	-	-	2002.10.10	31	-	-	-	-
2617	0:45:01.6	41:45:46.6	22.77	-166.9	-	-	2002.10.10	31	-	-	-	-

Continued on next page

Table A.1 – continued from previous page

ID	RA	Dec	$m_{5007}$	$v_{\text{helio}}$	Note	Host	Date	Field	H06	C89	HK04	MLA93
2618	0:45:15.6	41:46:01.7	23.57	-118.7	-	-	2002.10.10	32	-	-	-	-
2619	0:45:21.8	41:46:50.5	23.19	-71.9	-	-	2002.10.10	32	-	-	-	-
2620	0:45:55.3	41:53:21.1	24.13	-25.8	-	-	2002.10.10	32	-	-	-	-
2621	0:45:53.8	41:53:32.2	21.85	-32.3	-	-	2002.10.10	32	-	-	-	1209
2622	0:46:31.8	41:46:36.9	24.50	-382.8	-	-	2002.10.11	33	-	-	-	-
2623	0:41:56.8	41:37:05.6	22.30	-188.1	-	-	2002.10.11	34	PN_1.3.7	-	-	426
2624	0:42:15.1	41:39:10.1	20.72	-342.4	-	-	2002.10.11	34	PN_1.3.14	-	-	475
2625	0:40:40.6	41:39:05.7	21.91	-243.6	-	NGC205	2002.10.10	35	PN_1.3.1	-	-	248
2626	0:40:45.8	41:43:36.5	25.16	-302.3	-	NGC205	2002.10.10	35	-	-	-	-
2627	0:40:41.2	41:45:17.2	23.78	-247.7	-	NGC205	2002.10.10	35	PN_1.1.1.3	-	-	-
2628	0:40:20.3	41:38:17.6	21.13	-238.9	-	NGC205	2002.10.10	36	PN_8.3.6	-	-	200
2629	0:40:19.9	41:38:24.6	21.31	-228.7	-	NGC205	2002.10.10	36	-	-	-	198
2630	0:40:17.9	41:38:32.9	21.24	-215.1	-	NGC205	2002.10.10	36	-	-	-	195
2631	0:40:21.2	41:38:38.8	22.64	-218.1	-	NGC205	2002.10.10	36	-	-	-	203
2632	0:40:17.5	41:38:40.5	24.13	-189.9	-	NGC205	2002.10.10	36	-	-	-	-
2633	0:40:20.4	41:38:44.0	22.41	-284.2	-	NGC205	2002.10.10	36	-	-	-	-
2634	0:40:13.5	41:38:42.1	20.65	-237.1	-	NGC205	2002.10.10	36	PN_8.3.9	-	-	184
2635	0:40:32.2	41:39:03.0	22.86	-254.7	-	NGC205	2002.10.10	36	PN_8.3.16	-	-	-
2636	0:40:28.2	41:39:16.3	22.74	-218.7	-	NGC205	2002.10.10	36	-	-	-	221
2637	0:40:25.4	41:40:06.7	22.33	-231.1	-	NGC205	2002.10.10	36	PN_7.1.11	-	-	216
2638	0:40:26.4	41:40:20.9	24.93	-283.9	-	NGC205	2002.10.10	36	-	-	-	-
2639	0:40:08.8	41:40:43.8	21.18	-238.1	-	NGC205	2002.10.10	36	PN_7.1.5	-	-	177
2640	0:40:11.1	41:40:48.1	23.81	-172.9	-	NGC205	2002.10.10	36	-	-	-	-
2641	0:40:20.9	41:41:41.9	23.47	-230.1	-	NGC205	2002.10.10	36	-	-	-	-
2642	0:40:19.2	41:41:47.5	23.77	-260.0	-	NGC205	2002.10.10	36	-	-	-	-
2643	0:40:15.0	41:42:02.4	24.02	-260.6	-	NGC205	2002.10.10	36	-	-	-	-
2644	0:40:21.5	41:42:26.1	21.57	-280.2	-	NGC205	2002.10.10	36	PN_7.1.10	-	-	205
2645	0:39:56.8	41:43:06.7	21.83	-320.0	-	NGC205	2002.10.10	36	PN_7.1.3	-	-	156
2646	0:40:03.3	41:43:59.8	22.79	-200.4	-	NGC205	2002.10.10	36	PN_7.1.4	-	-	-
2647	0:40:08.0	41:45:24.2	24.85	-282.7	-	NGC205	2002.10.10	36	-	-	-	-
2648	0:40:12.0	41:45:32.2	23.47	-165.4	-	NGC205	2002.10.10	36	-	-	-	-
2649	0:40:22.2	41:45:18.5	24.26	61.2	E	NGC205?	2002.10.10	36	-	-	-	-
2650	0:43:01.7	41:38:33.6	23.35	-242.0	-	-	2002.10.10	39	-	-	-	-
2651	0:43:04.7	41:41:30.2	24.72	-201.6	-	-	2002.10.10	39	-	-	-	-
2652	0:43:34.6	41:37:00.1	24.06	-98.5	-	-	2002.10.10	40	-	-	-	-
2653	0:43:39.1	41:37:18.9	23.91	-185.6	-	-	2002.10.10	40	-	-	-	-
2654	0:43:31.3	41:37:27.8	23.59	-194.6	-	-	2002.10.10	40	-	-	-	-
2655	0:43:52.4	41:44:55.1	23.60	-421.6	-	-	2002.10.10	40	-	-	-	-
2656	0:43:47.8	41:36:28.3	23.38	-120.9	-	-	2002.10.10	40	-	-	-	-
2657	0:43:58.7	41:36:19.2	24.79	-103.3	-	-	2002.10.10	41	-	-	-	-
2658	0:44:05.4	41:36:28.3	24.44	-116.5	-	-	2002.10.10	41	-	-	-	-
2659	0:44:12.7	41:36:42.5	24.65	-283.2	-	-	2002.10.10	41	-	-	-	-
2660	0:44:03.8	41:36:52.1	21.37	-49.5	-	-	2002.10.10	41	PN_6.3.57	-	-	911
2661	0:44:37.0	41:37:26.0	22.98	-42.7	-	-	2002.10.10	41	-	-	-	-
2662	0:44:15.7	41:37:20.3	24.90	-58.9	-	-	2002.10.10	41	-	-	-	-
2663	0:44:03.3	41:37:17.3	24.70	-110.5	-	-	2002.10.10	41	-	-	-	-
2664	0:44:24.9	41:37:39.3	22.88	-73.7	R	-	2002.10.10	41	-	-	-	-
2665	0:43:51.2	41:36:21.0	23.12	-74.4	-	-	2002.10.10	41	-	-	-	868
2666	0:44:44.2	41:44:04.7	22.79	-146.3	-	-	2002.10.10	41	-	-	-	-
2667	0:45:26.0	41:36:31.4	23.13	-200.7	-	-	2002.10.10	42	-	-	-	-
2668	0:44:51.0	41:36:29.1	23.97	-179.6	-	-	2002.10.10	42	-	-	-	-
2669	0:45:11.1	41:36:45.3	22.18	-147.7	R	-	2002.10.10	42	-	-	-	1113
2670	0:45:00.1	41:36:43.2	21.76	-114.1	-	-	2002.10.10	42	-	-	-	1093
2671	0:44:49.2	41:36:44.7	24.34	-156.6	-	-	2002.10.10	42	-	-	-	-
2672	0:44:58.8	41:36:51.6	22.45	-191.6	-	-	2002.10.10	42	-	-	-	1089
2673	0:45:12.4	41:37:09.4	20.52	-129.3	E,R	-	2002.10.10	42	-	-	-	1118
2674	0:45:11.8	41:37:12.9	20.06	-131.3	E,R	-	2002.10.10	42	-	-	-	1117
2675	0:45:12.6	41:37:16.5	20.82	-132.4	E,R	-	2002.10.10	42	-	-	-	-
2676	0:45:13.5	41:37:22.1	23.43	-149.0	E	-	2002.10.10	42	-	-	-	-
2677	0:44:58.0	41:37:17.5	23.95	-134.8	-	-	2002.10.10	42	-	-	-	-
2678	0:45:14.3	41:37:25.1	21.73	-134.6	E,R	-	2002.10.10	42	-	-	-	-
2679	0:45:32.7	41:43:42.7	23.40	-191.0	-	-	2002.10.10	42	-	-	-	-
2680	0:45:33.0	41:45:24.9	24.05	-156.1	-	-	2002.10.10	42	-	-	-	-
2681	0:45:33.6	41:44:54.0	23.52	-358.6	-	-	2002.10.10	42	-	-	-	-
2682	0:45:49.2	41:36:44.4	22.58	-146.7	-	-	2002.10.11	43	PN_5.3.33	-	-	-
2683	0:45:46.9	41:36:58.1	23.89	-117.5	-	-	2002.10.11	43	-	-	-	-
2684	0:45:52.3	41:37:08.4	24.18	-191.1	-	-	2002.10.11	43	-	-	-	-
2685	0:46:22.6	41:42:00.0	23.16	-136.2	-	-	2002.10.11	43	-	-	-	-
2686	0:41:13.6	41:27:53.5	23.68	-328.2	-	-	2002.10.11	44	-	-	-	-
2687	0:41:25.4	41:28:22.5	23.18	-291.6	-	-	2002.10.11	44	PN_1.4.7	-	-	-
2688	0:41:17.5	41:28:46.4	24.41	-436.4	-	-	2002.10.11	44	-	-	-	-
2689	0:41:01.7	41:32:22.7	24.12	-246.4	-	-	2002.10.11	44	-	-	-	-
2690	0:40:58.7	41:29:32.4	20.77	-289.0	-	-	2002.10.11	44	PN_1.3.4	-	-	297
2691	0:40:23.1	41:28:11.4	25.04	-231.1	E	-	2002.10.11	45	-	-	-	-
2692	0:40:15.8	41:28:23.1	23.90	-316.9	-	-	2002.10.11	45	PN_8.4.7	-	-	-
2693	0:40:36.2	41:36:15.2	24.20	-244.7	-	NGC205	2002.10.11	45	-	-	-	-
2694	0:38:46.2	41:28:19.6	20.60	-248.2	-	-	2002.10.12	47	PN_8.4.1	-	-	69
2695	0:38:28.4	41:28:37.0	23.79	-457.8	-	-	2002.10.12	48	-	-	-	-
2696	0:42:36.8	41:35:38.3	23.58	-260.7	-	-	2002.10.10	49	-	-	-	-
2697	0:42:56.8	41:27:26.9	22.86	-236.9	-	-	2002.10.09	50	-	-	-	-
2698	0:42:58.7	41:27:47.9	20.87	-225.4	-	-	2002.10.09	50	-	-	-	649
2699	0:42:45.0	41:27:56.2	21.88	-46.4	-	-	2002.10.09	50	-	-	-	588
2700	0:42:59.8	41:28:08.9	22.60	-223.3	-	-	2002.10.09	50	-	-	-	659
2701	0:43:26.9	41:28:36.2	24.56	-197.0	-	-	2002.10.09	50	-	-	-	-
2702	0:43:19.9	41:35:32.0	23.53	-109.4	-	-	2002.10.09	50	-	-	-	-
2703	0:43:09.9	41:27:07.5	21.93	-335.8	-	-	2002.10.09	50	PN_6.4.65	-	-	699
2704	0:43:16.1	41:27:04.1	21.31	-116.1	-	-	2002.10.09	50	P253	-	253	728
2705	0:43:35.3	41:27:20.3	23.87	-76.7	-	-	2002.10.10	51	-	-	-	-
2706	0:43:43.3	41:27:30.5	22.87	4.6	-	-	2002.10.10	51	P285	-	285	-
2707	0:43:37.8	41:27:38.2	22.95	-109.8	-	-	2002.10.10	51	P275	-	275	822
2708	0:43:33.2	41:27:49.3	22.53	-158.8	-	-	2002.10.10	51	P270	-	270	798
2709	0:43:45.5	41:28:04.4	24.15	-71.2	-	-	2002.10.10	51	-	-	-	-
2710	0:44:15.1	41:29:06.6	23.51	-92.2	-	-	2002.10.10	51	-	-	547	-

Continued on next page

Table A.1 – continued from previous page

ID	RA	Dec	$m_{5007}$	$v_{\text{helio}}$	Note	Host	Date	Field	H06	C89	HK04	MLA93
2711	0:44:17.1	41:29:48.5	22.61	-50.2	-	-	2002.10.10	51	P550	-	550	961
2712	0:44:17.9	41:30:12.1	23.33	-39.4	-	-	2002.10.10	51	-	-	552	-
2713	0:44:16.2	41:31:18.5	23.93	-95.7	-	-	2002.10.10	51	P549	-	549	-
2714	0:44:15.1	41:32:28.6	22.78	-167.0	-	-	2002.10.10	51	-	-	-	-
2715	0:44:17.1	41:33:52.4	23.55	-171.1	-	-	2002.10.10	51	-	-	-	-
2716	0:44:15.7	41:34:21.3	23.71	-132.8	-	-	2002.10.10	51	PN_6.3.81	-	-	-
2717	0:44:17.6	41:34:57.7	23.97	-58.5	-	-	2002.10.10	51	-	-	-	-
2718	0:44:18.7	41:35:31.7	22.37	-18.0	-	-	2002.10.10	51	-	-	-	-
2719	0:44:19.2	41:27:06.9	23.78	-90.5	-	-	2002.10.10	51	-	-	553	-
2720	0:44:48.8	41:27:12.9	24.37	-187.8	R	-	2002.10.10	52	-	-	-	-
2721	0:44:45.0	41:27:50.5	20.60	-183.8	R	-	2002.10.10	52	-	-	-	1052
2722	0:44:43.5	41:27:56.5	24.10	-177.1	R	-	2002.10.10	52	-	-	-	-
2723	0:44:57.5	41:28:07.1	23.71	-205.2	-	-	2002.10.10	52	-	-	-	-
2724	0:45:07.9	41:30:39.1	24.88	-176.7	E	-	2002.10.10	52	-	-	-	-
2725	0:45:07.7	41:34:23.3	23.71	-102.7	E,R	-	2002.10.10	52	-	-	-	-
2726	0:45:57.0	41:32:33.1	24.75	-116.6	-	-	2002.10.11	53	-	-	-	-
2727	0:45:56.1	41:34:21.1	25.12	-224.8	E	-	2002.10.11	53	-	-	-	-
2728	0:41:42.6	41:18:06.4	23.69	-349.1	-	-	2002.10.10	55	-	-	-	-
2729	0:41:30.9	41:18:42.3	24.74	-314.8	-	-	2002.10.10	55	-	-	-	-
2730	0:41:48.1	41:19:05.0	22.95	-385.0	E,R	-	2002.10.10	55	-	-	-	-
2731	0:41:20.9	41:18:18.7	24.95	-497.2	-	-	2002.10.11	56	-	-	-	-
2732	0:41:17.6	41:18:45.5	22.75	-404.2	-	-	2002.10.11	56	PN_1.4.9	-	-	334
2733	0:40:43.7	41:18:40.5	22.81	-373.9	-	-	2002.10.11	56	PN_1.4.2	-	-	-
2734	0:40:37.9	41:23:30.9	24.52	-435.4	-	-	2002.10.11	56	-	-	-	-
2735	0:39:25.3	41:18:45.2	23.47	-408.3	-	-	2002.10.12	58	-	-	-	-
2736	0:42:20.8	41:17:44.1	23.39	-218.4	-	-	2002.10.09	60	-	-	-	-
2737	0:42:53.4	41:18:18.1	20.80	-142.5	-	-	2002.10.09	60	P32	-	32	617
2738	0:42:55.4	41:18:15.9	22.54	-244.8	-	-	2002.10.09	60	P190	-	190	-
2739	0:42:57.0	41:18:15.2	22.98	-200.0	-	-	2002.10.09	60	P191	-	191	638
2740	0:42:41.3	41:18:22.3	23.02	-340.5	-	-	2002.10.09	60	P447	-	447	-
2741	0:42:46.8	41:18:21.6	23.30	-34.2	-	-	2002.10.09	60	-	-	-	-
2742	0:42:57.8	41:18:49.0	21.58	109.2	-	-	2002.10.09	60	P33	-	33	642
2743	0:43:00.9	41:18:43.3	21.46	-95.1	-	-	2002.10.09	60	P124	-	124	663
2744	0:42:44.0	41:18:40.0	23.39	-292.7	-	-	2002.10.09	60	-	-	-	-
2745	0:42:22.9	41:18:34.2	22.23	-838.7	-	Stream?	2002.10.09	60	-	-	-	-
2746	0:42:49.7	41:18:42.2	22.76	-176.1	-	-	2002.10.09	60	P112	-	112	-
2747	0:42:44.7	41:18:51.7	22.78	-638.9	-	-	2002.10.09	60	-	-	-	-
2748	0:42:59.0	41:18:55.7	22.24	17.1	-	-	2002.10.09	60	P180	-	180	-
2749	0:42:48.3	41:18:59.2	22.94	-280.6	-	-	2002.10.09	60	-	-	-	-
2750	0:42:40.3	41:19:07.4	21.23	-766.5	-	Stream?	2002.10.09	60	PN_6.4.16	-	-	567
2751	0:42:21.9	41:19:01.5	23.73	-297.2	-	-	2002.10.09	60	-	-	-	-
2752	0:42:30.3	41:19:12.2	23.32	-511.2	-	-	2002.10.09	60	-	-	-	-
2753	0:42:32.8	41:19:18.3	21.45	-538.6	-	-	2002.10.09	60	-	-	-	544
2754	0:43:02.8	41:19:46.8	23.43	-239.0	-	-	2002.10.09	60	-	-	197	-
2755	0:43:02.6	41:20:29.5	22.92	-251.4	-	-	2002.10.09	60	P200	-	200	-
2756	0:43:03.0	41:20:41.5	22.73	-142.5	-	-	2002.10.09	60	P201	-	201	-
2757	0:43:01.8	41:20:56.4	23.54	-268.5	-	-	2002.10.09	60	-	-	-	-
2758	0:43:04.8	41:21:44.2	22.60	-142.8	-	-	2002.10.09	60	P220	-	220	-
2759	0:43:03.7	41:23:54.9	22.50	-276.4	-	-	2002.10.09	60	-	-	-	672
2760	0:43:02.9	41:26:11.0	22.78	-87.8	-	-	2002.10.09	60	P491	-	491	-
2761	0:43:05.4	41:19:29.2	22.54	-358.1	-	-	2002.10.09	60	P132	-	132	-
2762	0:42:41.4	41:17:50.5	22.29	-564.3	-	-	2002.10.09	60	P83	-	83	-
2763	0:43:19.4	41:17:46.3	22.11	5.0	-	-	2002.10.09	61	P208	-	208	-
2764	0:43:20.9	41:17:52.0	21.23	-330.7	-	-	2002.10.09	61	P209	-	209	755
2765	0:43:41.3	41:18:11.5	22.21	-268.4	-	-	2002.10.09	61	PN_6.4.110	-	-	833
2766	0:43:05.7	41:18:14.4	22.51	-524.2	-	-	2002.10.09	61	P126	-	126	-
2767	0:43:32.7	41:18:32.8	21.28	-430.4	-	-	2002.10.09	61	-	-	-	796
2768	0:43:15.4	41:18:28.5	23.51	-580.3	-	-	2002.10.09	61	P504	-	504	-
2769	0:43:06.0	41:18:29.0	22.01	37.4	-	-	2002.10.09	61	P127	-	127	681
2770	0:43:41.5	41:18:48.5	23.55	-130.1	-	-	2002.10.09	61	-	-	-	-
2771	0:43:06.7	41:18:38.2	21.23	-75.9	-	-	2002.10.09	61	P128	-	128	687
2772	0:43:09.1	41:18:44.7	21.94	-432.0	-	-	2002.10.09	61	P129	-	129	694
2773	0:43:41.0	41:18:58.0	23.60	-157.6	-	-	2002.10.09	61	-	-	-	-
2774	0:43:13.0	41:18:50.2	22.34	-123.5	-	-	2002.10.09	61	P206	-	206	715
2775	0:43:52.4	41:21:29.0	23.15	-336.1	-	-	2002.10.09	61	-	-	-	-
2776	0:43:50.8	41:22:41.7	22.04	-42.5	-	-	2002.10.09	61	-	-	-	866
2777	0:43:03.7	41:17:38.0	22.31	-99.5	-	-	2002.10.09	61	P179	-	179	-
2778	0:43:05.2	41:17:38.5	21.81	-214.7	-	-	2002.10.09	61	P125	-	125	-
2779	0:43:07.2	41:18:37.0	23.44	6.1	-	-	2002.10.09	61	-	-	196	-
2780	0:43:54.8	41:22:05.1	21.97	-148.1	-	-	2002.10.09	61	-	-	-	883
2781	0:43:54.3	41:23:32.9	21.08	-196.4	-	-	2002.10.09	61	-	-	-	876
2782	0:44:05.7	41:18:02.6	21.79	-223.3	-	-	2002.10.09	62	-	-	-	918
2783	0:43:59.0	41:18:18.2	22.68	-359.3	-	-	2002.10.09	62	-	-	-	894
2784	0:45:16.2	41:18:14.4	23.44	-294.2	-	-	2002.10.11	63	PN_5.4.4	-	-	-
2785	0:41:35.9	41:08:39.7	23.30	-427.3	-	-	2002.10.10	65	-	-	-	-
2786	0:41:34.0	41:09:01.4	24.27	-526.9	-	-	2002.10.10	65	-	-	-	-
2787	0:41:31.1	41:09:36.2	21.32	-421.8	-	-	2002.10.10	65	PN_1.1.23	-	-	366
2788	0:41:27.0	41:09:43.8	25.03	-309.5	-	-	2002.10.10	65	-	-	-	-
2789	0:41:48.7	41:11:30.3	24.79	-461.7	R	-	2002.10.10	65	-	-	-	-
2790	0:41:47.2	41:14:29.0	23.80	-494.6	-	-	2002.10.10	65	-	-	-	-
2791	0:40:36.4	41:09:51.3	22.84	-491.0	-	-	2002.10.11	66	-	-	-	-
2792	0:40:21.8	41:10:04.7	22.86	-249.9	-	-	2002.10.11	66	PN_8.1.12	-	-	-
2793	0:39:22.2	41:13:38.0	25.40	-332.8	E	-	2002.10.12	67	-	-	-	-
2794	0:39:13.0	41:09:31.1	23.71	-379.0	-	-	2002.10.12	68	-	-	-	-
2795	0:42:22.6	41:08:33.7	22.71	-394.4	-	-	2002.10.09	70	P398	-	398	-
2796	0:42:28.8	41:08:51.1	23.35	-362.8	-	-	2002.10.09	70	P416	-	416	-
2797	0:42:23.7	41:09:24.7	22.55	-422.7	-	-	2002.10.09	70	P401	-	401	-
2798	0:42:28.5	41:09:35.8	21.29	29.0	-	-	2002.10.09	70	P414	-	414	521
2799	0:42:27.0	41:09:45.8	21.00	-547.8	-	-	2002.10.09	70	P410	-	410	514
2800	0:42:21.2	41:09:44.2	21.88	39.4	-	-	2002.10.09	70	P393	-	393	486
2801	0:42:38.2	41:09:56.5	22.44	-487.5	-	-	2002.10.09	70	P437	-	437	-
2802	0:42:38.4	41:09:60.0	22.30	-502.4	-	-	2002.10.09	70	P438	-	438	-
2803	0:42:36.4	41:10:12.3	23.93	-409.9	-	-	2002.10.09	70	-	-	-	-

Continued on next page

Table A.1 – continued from previous page

ID	RA	Dec	$m_{5007}$	$v_{\text{helio}}$	Note	Host	Date	Field	H06	C89	HK04	MLA93
2804	0:42:38.6	41:11:18.5	22.80	-396.1	-	-	2002.10.09	70	P439	-	439	-
2805	0:42:36.3	41:12:05.6	21.88	-551.9	-	-	2002.10.09	70	-	-	144	553
2806	0:42:37.0	41:12:10.2	20.93	-619.4	-	-	2002.10.09	70	P69	-	69	554
2807	0:42:36.8	41:13:11.9	23.02	-397.3	-	-	2002.10.09	70	-	-	184	-
2808	0:42:38.1	41:13:45.0	21.26	-309.4	-	-	2002.10.09	70	P140	-	140	560
2809	0:42:39.5	41:14:18.3	22.04	-252.6	-	-	2002.10.09	70	-	-	65	-
2810	0:42:38.4	41:14:35.1	21.37	-523.7	-	-	2002.10.09	70	P55	-	55	-
2811	0:42:37.1	41:14:36.2	20.53	-526.9	-	-	2002.10.09	70	P54	-	54	555
2812	0:42:39.0	41:14:57.1	22.09	-462.8	-	-	2002.10.09	70	-	-	70	-
2813	0:42:37.2	41:16:27.5	22.01	-346.2	-	-	2002.10.09	70	P37	-	37	-
2814	0:42:37.4	41:15:52.0	20.95	-188.5	-	-	2002.10.09	70	-	-	36	-
2815	0:42:38.3	41:15:34.6	21.47	-403.0	-	-	2002.10.09	70	P35	-	35	-
2816	0:42:36.1	41:16:35.4	21.40	-671.8	-	-	2002.10.09	70	-	-	40	-
2817	0:42:39.8	41:15:37.4	20.82	-520.8	R	-	2002.10.09	70	-	-	18	-
2818	0:42:37.8	41:16:44.3	21.49	-323.2	-	-	2002.10.09	70	P38	-	38	-
2819	0:42:36.5	41:16:58.3	21.75	-316.7	-	-	2002.10.09	70	P39	-	39	-
2820	0:42:23.8	41:08:31.4	21.95	-502.0	-	-	2002.10.09	70	P402	-	402	-
2821	0:42:40.4	41:11:34.1	22.99	-460.5	-	-	2002.10.09	70	P444	-	444	-
2822	0:42:40.2	41:13:25.3	22.43	-415.9	-	-	2002.10.09	70	-	-	159	-
2823	0:42:40.4	41:14:10.7	21.84	-382.0	-	-	2002.10.09	70	P56	-	181	573
2824	0:42:40.3	41:13:51.5	22.83	-226.1	-	-	2002.10.09	70	P160	-	160	-
2825	0:42:39.8	41:15:50.1	20.76	-512.5	-	-	2002.10.09	70	-	-	17	-
2826	0:42:37.5	41:14:35.7	21.59	-259.0	-	-	2002.10.09	70	-	-	71	-
2827	0:42:38.4	41:14:28.5	23.13	-302.7	-	-	2002.10.09	70	P143	-	143	-
2828	0:42:40.1	41:14:39.0	22.08	-419.8	-	-	2002.10.09	70	-	-	66	-
2829	0:42:51.5	41:08:57.4	22.15	-342.0	-	-	2002.10.09	71	-	-	-	608
2830	0:42:53.4	41:08:58.4	22.53	-419.1	-	-	2002.10.09	71	-	-	-	619
2831	0:42:43.9	41:09:01.5	22.51	-376.4	-	-	2002.10.09	71	P451	-	451	587
2832	0:43:19.9	41:09:26.3	24.51	-262.4	-	-	2002.10.09	71	-	-	-	-
2833	0:42:42.9	41:09:23.6	20.98	-356.2	-	-	2002.10.09	71	P154	-	154	581
2834	0:42:52.8	41:09:39.2	21.10	-322.4	-	-	2002.10.09	71	-	-	-	613
2835	0:43:24.5	41:09:49.9	24.08	-303.8	-	-	2002.10.09	71	-	-	-	-
2836	0:42:50.7	41:09:46.6	22.96	-452.7	-	-	2002.10.09	71	-	-	-	-
2837	0:42:42.9	41:09:47.9	22.17	-368.3	-	-	2002.10.09	71	P450	-	450	582
2838	0:43:27.0	41:10:28.5	21.18	-269.2	-	-	2002.10.09	71	PN_5_1_57	-	-	783
2839	0:43:29.0	41:14:49.5	23.35	-97.8	-	-	2002.10.09	71	-	-	-	-
2840	0:43:28.5	41:15:45.3	21.63	-366.0	-	-	2002.10.09	71	-	-	-	788
2841	0:42:49.5	41:08:24.2	21.90	-522.4	-	-	2002.10.09	71	-	-	-	603
2842	0:42:54.5	41:08:25.5	23.51	-461.0	-	-	2002.10.09	71	-	-	-	-
2843	0:44:04.9	41:09:18.5	21.87	-219.0	-	-	2002.10.09	72	-	1_105	-	915
2844	0:44:55.0	41:09:53.1	21.03	-327.6	-	-	2002.10.11	73	PN_5_1_4	1_123	-	1076
2845	0:45:05.1	41:12:52.3	22.53	-220.2	-	-	2002.10.11	73	PN_5_1_7	1_125	-	-
2846	0:45:47.7	41:09:17.6	24.09	-114.8	-	-	2002.10.12	74	PN_5_1_9	-	-	-
2847	0:45:34.2	41:09:59.9	25.40	-306.4	-	-	2002.10.12	74	-	-	-	-
2848	0:45:54.5	41:11:13.9	25.28	-266.5	-	-	2002.10.12	74	-	-	-	-
2849	0:45:56.2	41:12:14.7	23.98	-223.0	-	-	2002.10.12	74	PN_5_1_10	-	-	-
2850	0:41:49.3	41:00:09.1	24.81	-475.6	-	-	2002.10.13	76	-	-	-	-
2851	0:41:26.0	40:59:31.8	25.08	-421.8	-	-	2002.10.13	76	-	-	-	-
2852	0:41:07.4	40:59:25.1	24.37	-487.4	-	-	2002.10.08	77	-	-	-	-
2853	0:40:44.4	40:59:37.0	23.35	-442.8	-	-	2002.10.08	77	PN_2_3_10	-	-	-
2854	0:40:52.6	40:59:42.6	21.23	-308.5	-	-	2002.10.08	77	-	-	-	275
2855	0:40:57.6	41:00:02.0	22.47	-238.0	-	-	2002.10.08	77	PN_2_3_3	-	-	292
2856	0:41:16.4	41:00:27.5	23.81	-384.0	-	-	2002.10.08	77	-	-	-	-
2857	0:40:47.8	40:59:05.9	19.20	-351.8	R	-	2002.10.08	77	-	-	-	267
2858	0:40:17.2	40:59:45.9	22.27	-544.2	-	-	2002.10.10	78	PN_12_3_16	-	-	194
2859	0:40:08.1	41:00:32.4	22.43	-370.0	-	-	2002.10.10	78	-	-	-	174
2860	0:38:55.0	41:06:55.3	20.84	-418.6	-	-	2002.10.12	79	-	-	-	-
2861	0:42:45.6	40:59:21.6	21.19	-337.6	-	-	2002.10.09	81	PN_3_3_5	-	-	591
2862	0:42:58.5	40:59:34.8	21.59	-352.4	-	-	2002.10.09	81	PN_3_3_10	-	-	-
2863	0:42:21.0	40:59:39.9	23.76	-408.3	-	-	2002.10.09	81	-	-	-	-
2864	0:43:04.7	41:03:42.4	23.50	-454.4	-	-	2002.10.09	81	-	-	-	-
2865	0:43:03.6	41:05:33.4	21.86	-294.3	-	-	2002.10.09	81	-	-	-	673
2866	0:42:12.7	40:59:08.5	22.84	-502.9	-	-	2002.10.09	81	-	-	-	-
2867	0:43:10.0	40:59:32.1	24.70	-339.6	-	-	2002.10.10	82	-	-	-	-
2868	0:43:07.7	40:59:45.2	24.43	-593.3	-	-	2002.10.10	82	-	-	-	-
2869	0:43:44.5	40:59:59.4	21.38	-279.6	-	-	2002.10.10	82	PN_3_3_23	1_103	-	846
2870	0:43:09.8	41:00:01.9	24.39	-326.2	-	-	2002.10.10	82	-	-	-	-
2871	0:43:21.6	40:59:12.4	23.23	-367.1	-	-	2002.10.10	82	-	1_98	-	-
2872	0:45:38.1	40:59:19.0	23.04	-291.9	-	-	2002.10.11	85	-	1_130	-	1174
2873	0:46:00.0	40:59:42.8	23.99	-358.4	-	-	2002.10.11	85	-	-	-	-
2874	0:45:35.3	40:59:56.8	22.30	-219.0	-	-	2002.10.11	85	PN_4_3_4	1_129	-	1165
2875	0:41:41.4	40:50:05.2	22.89	-511.2	-	-	2002.10.08	86	-	-	-	-
2876	0:41:07.4	40:50:35.1	23.34	-564.7	-	-	2002.10.08	86	-	-	-	-
2877	0:41:00.3	40:53:53.8	23.13	-455.7	-	-	2002.10.08	86	-	-	-	301
2878	0:41:42.3	40:50:14.1	23.89	-51.4	-	-	2002.10.08	86	-	-	-	-
2879	0:41:46.8	40:49:58.3	23.90	-486.0	-	-	2002.10.08	86	-	-	-	-
2880	0:40:29.1	40:50:06.5	21.95	-444.2	-	-	2002.10.08	87	-	-	-	224
2881	0:40:22.1	40:50:28.9	23.04	-431.8	-	-	2002.10.08	87	-	-	-	-
2882	0:40:12.0	40:54:25.9	23.81	-557.4	-	-	2002.10.08	87	-	-	-	-
2883	0:40:10.8	40:54:38.7	21.83	-526.9	-	-	2002.10.08	87	PN_12_3_19	-	-	179
2884	0:40:14.0	40:55:16.9	24.00	-446.2	-	-	2002.10.08	87	-	-	-	-
2885	0:40:13.5	40:55:32.3	23.08	-440.5	-	-	2002.10.08	87	-	-	-	183
2886	0:40:03.1	40:50:36.5	23.75	-542.5	-	-	2002.10.10	88	PN_12_4_25	-	-	-
2887	0:39:31.2	40:51:25.7	22.18	-460.3	-	-	2002.10.10	88	PN_12_4_10	-	-	112
2888	0:39:13.1	40:50:07.5	25.23	-266.5	-	-	2002.10.08	89	PN_12_4_6	-	-	-
2889	0:37:50.1	40:50:52.1	24.47	-135.5	-	-	2002.10.12	90	-	-	-	-
2890	0:42:13.8	40:51:17.4	21.12	-388.5	E,R	-	2002.10.08	91	-	-	-	469
2891	0:42:44.7	40:50:33.0	25.63	-169.9	-	M32	2002.10.11	92	-	-	-	-
2892	0:43:25.1	40:51:03.7	21.65	-381.2	-	-	2002.10.11	92	-	-	-	774
2893	0:43:15.2	40:51:13.2	22.62	-521.4	-	-	2002.10.11	92	-	1_94	-	726
2894	0:42:41.7	40:51:31.6	22.30	-210.4	-	M32	2002.10.11	92	-	-	-	-
2895	0:42:42.2	40:51:39.8	20.78	-193.3	-	M32	2002.10.11	92	-	-	-	-
2896	0:42:44.2	40:51:44.2	24.68	-211.4	-	M32	2002.10.11	92	-	-	-	-

Continued on next page

Table A.1 – continued from previous page

ID	RA	Dec	$m_{5007}$	$v_{\text{helio}}$	Note	Host	Date	Field	H06	C89	HK04	MLA93
2897	0:42:45.7	40:51:49.7	23.22	-203.4	-	M32	2002.10.11	92	-	-	-	-
2898	0:42:44.4	40:52:33.4	23.78	-235.8	-	M32	2002.10.11	92	-	-	-	-
2899	0:43:05.3	40:53:33.9	22.00	-535.3	-	-	2002.10.11	92	-	1.91	-	678
2900	0:42:44.6	40:54:04.0	24.66	-431.8	-	M32?	2002.10.11	92	-	-	-	-
2901	0:42:48.2	40:54:13.6	21.36	-199.2	-	M32	2002.10.11	92	-	-	-	599
2902	0:42:42.9	40:54:33.5	24.52	-433.2	-	M32?	2002.10.11	92	-	-	-	-
2903	0:43:00.1	40:55:00.4	24.17	-194.6	-	M32	2002.10.11	92	-	-	-	-
2904	0:42:46.7	40:55:04.8	23.47	-380.3	-	M32?	2002.10.11	92	-	-	-	-
2905	0:43:06.2	40:55:18.2	22.66	-196.8	-	-	2002.10.11	92	-	-	-	680
2906	0:43:28.4	40:55:26.6	25.19	-370.9	-	-	2002.10.11	92	-	-	-	-
2907	0:42:37.7	40:55:25.6	25.36	-285.8	-	M32	2002.10.11	92	-	-	-	-
2908	0:42:52.7	40:55:53.2	23.51	-150.8	-	M32	2002.10.11	92	-	-	-	-
2909	0:42:58.2	40:56:54.6	23.82	-404.7	E	-	2002.10.11	92	-	-	-	-
2910	0:43:03.2	40:57:19.1	22.99	-376.6	-	-	2002.10.11	92	-	1.90	-	-
2911	0:42:59.7	40:53:46.8	25.50	-365.4	-	M32?	2002.10.11	92	-	-	-	-
2912	0:44:41.3	40:51:14.9	25.40	-217.4	-	-	2002.10.12	94	-	-	-	-
2913	0:44:30.9	40:49:49.1	25.44	-265.8	-	-	2002.10.12	94	-	-	-	-
2914	0:41:43.7	40:41:24.9	23.93	-460.0	-	-	2002.10.09	97	-	-	-	-
2915	0:42:12.4	40:49:19.4	24.67	-508.4	-	-	2002.10.09	97	-	-	-	-
2916	0:41:23.6	40:43:00.7	22.56	-606.6	-	-	2002.10.09	97	-	-	-	-
2917	0:40:44.4	40:40:30.8	21.25	-517.4	-	-	2002.10.09	98	PN_2.1.3	-	-	257
2918	0:40:52.7	40:40:36.8	24.09	-499.0	-	-	2002.10.09	98	-	-	-	-
2919	0:41:03.8	40:41:13.9	21.75	-572.7	-	-	2002.10.09	98	PN_2.1.11	1.61	-	308
2920	0:40:46.8	40:41:22.1	21.54	-586.3	-	-	2002.10.09	98	-	-	-	264
2921	0:40:57.5	40:41:39.4	23.41	-528.7	-	-	2002.10.09	98	-	-	-	-
2922	0:41:00.9	40:41:47.9	23.57	-554.7	-	-	2002.10.09	98	-	-	-	-
2923	0:40:40.7	40:40:25.4	21.14	-549.9	-	-	2002.10.09	98	-	-	-	250
2924	0:38:08.8	40:43:11.9	23.91	-442.8	-	-	2002.10.12	101	-	-	-	-
2925	0:38:24.5	40:41:35.7	24.31	-500.4	-	-	2002.10.12	102	-	-	-	-
2926	0:42:34.9	40:42:05.0	23.55	-468.2	-	-	2002.10.11	103	-	-	-	-
2927	0:42:23.3	40:46:29.0	22.40	-189.7	-	-	2002.10.11	103	-	2.1	-	500
2928	0:42:21.4	40:46:43.5	24.24	-431.3	-	-	2002.10.11	103	-	-	-	-
2929	0:42:40.6	40:47:33.8	22.89	-137.7	-	M32	2002.10.11	103	-	-	-	-
2930	0:42:36.8	40:48:04.7	24.38	-177.1	-	M32	2002.10.11	103	-	-	-	-
2931	0:42:53.0	40:49:00.0	21.50	-226.3	-	M32	2002.10.11	103	PN_3.4.3	2.6	-	615
2932	0:42:46.3	40:49:02.2	24.42	-633.7	-	M32?	2002.10.11	103	-	-	-	-
2933	0:42:40.7	40:49:12.8	24.52	-155.8	-	M32	2002.10.11	103	-	-	-	-
2934	0:42:27.1	40:49:09.8	25.10	-399.6	-	M32?	2002.10.11	103	-	-	-	-
2935	0:42:41.0	40:49:40.2	25.09	-389.4	-	M32?	2002.10.11	103	-	-	-	-
2936	0:42:27.0	40:49:41.2	22.02	-458.9	-	M32?	2002.10.11	103	PN_2.4.54	-	-	515
2937	0:42:23.5	40:50:49.2	25.41	-537.8	-	M32?	2002.10.11	103	-	-	-	-
2938	0:42:26.0	40:50:57.9	24.99	-469.5	E	M32?	2002.10.11	103	-	-	-	-
2939	0:40:23.1	40:31:15.9	24.02	-534.8	-	-	2002.10.09	109	-	-	-	-
2940	0:40:42.4	40:31:38.0	23.35	-535.5	-	-	2002.10.09	109	-	-	-	-
2941	0:39:49.9	40:31:29.2	24.22	-563.0	-	-	2002.10.09	110	-	-	-	-
2942	0:39:54.0	40:31:56.8	21.57	-461.5	-	-	2002.10.09	110	PN_12.1.16	1.35	-	152
2943	0:40:08.0	40:32:12.1	20.58	-327.8	-	-	2002.10.09	110	PN_12.1.17	-	-	175
2944	0:40:09.0	40:32:25.6	23.54	-294.2	-	-	2002.10.09	110	-	-	-	-
2945	0:39:25.4	40:38:25.4	22.46	-483.6	-	-	2002.10.09	110	PN_12.1.7	-	-	108
2946	0:38:38.8	40:32:04.4	24.22	-524.8	-	-	2002.10.12	111	-	-	-	-
2947	0:45:06.8	40:32:10.6	23.15	-268.9	-	-	2002.10.12	116	PN_4.1.2	-	-	-
2948	0:45:07.1	40:39:33.5	22.57	-291.9	-	-	2002.10.12	116	PN_4.1.3	1.127	-	-
2949	0:47:16.8	42:23:42.8	25.40	-71.4	-	-	2002.10.13	120	-	-	-	-
2950	0:46:55.5	42:24:02.0	20.40	-135.6	-	-	2002.10.13	120	-	-	-	1280
2951	0:47:34.9	42:22:57.3	21.84	-174.7	-	-	2002.10.13	120	-	-	-	1297
2952	0:46:21.2	42:16:56.0	23.37	-67.1	-	-	2002.10.13	125	-	-	-	-
2953	0:40:00.6	40:22:16.3	23.10	-531.0	E	-	2002.10.13	140	-	-	-	-
2954	0:39:53.3	40:22:17.8	24.84	-537.3	-	-	2002.10.13	140	-	-	-	-
2955	0:39:51.5	40:22:38.3	24.45	-492.2	-	-	2002.10.13	140	-	-	-	-
2956	0:39:49.9	40:22:51.4	23.35	-473.9	-	-	2002.10.13	140	-	-	-	-
2957	0:39:50.9	40:22:53.2	24.16	-528.8	-	-	2002.10.13	140	-	-	-	-
2958	0:40:10.0	40:23:17.8	24.29	-500.7	-	-	2002.10.13	140	-	-	-	-
2959	0:39:03.7	40:21:58.0	25.16	-495.0	-	-	2002.10.13	141	-	-	-	-
2960	0:39:16.3	40:22:13.7	21.20	-540.1	-	-	2002.10.13	141	-	1.16	-	99
2961	0:39:36.1	40:22:34.0	20.74	-513.1	-	-	2002.10.13	141	-	-	-	119
2962	0:39:25.9	40:22:40.0	23.09	-498.2	-	-	2002.10.13	141	-	-	-	-
2963	0:39:42.8	40:22:49.1	22.18	-499.1	-	-	2002.10.13	141	-	1.25	-	131
2964	0:39:02.5	40:22:50.5	21.17	-518.2	-	-	2002.10.13	141	-	1.5	-	79
2965	0:38:59.4	40:25:29.2	23.44	-479.7	-	-	2002.10.13	141	-	-	-	-
2966	0:38:55.5	40:23:56.5	24.71	-452.9	-	-	2002.10.13	141	-	-	-	-
2967	0:39:44.7	40:21:60.0	23.60	-439.2	-	-	2002.10.13	141	-	-	-	-
2968	0:39:46.9	40:12:56.5	23.06	-529.9	-	-	2002.10.13	151	-	-	-	-
2969	0:39:45.8	40:13:03.1	23.25	-485.1	-	-	2002.10.13	151	-	-	-	-
2970	0:39:40.4	40:13:24.8	21.89	-468.4	-	-	2002.10.13	151	-	1.24	-	127
2971	0:39:22.3	40:21:30.4	24.85	-552.6	-	-	2002.10.13	151	-	-	-	-
2972	0:39:15.9	40:12:39.2	21.96	-483.5	-	-	2002.10.13	152	-	1.15	-	-
2973	0:39:10.9	40:12:52.1	25.18	-518.5	E	-	2002.10.13	152	-	-	-	-
2974	0:38:49.9	40:13:07.1	25.09	-505.0	E	-	2002.10.13	152	-	-	-	-
2975	0:38:34.1	40:15:56.5	22.03	-519.0	-	-	2002.10.13	152	-	-	-	65
2976	0:38:32.3	40:20:29.8	24.80	-524.4	-	-	2002.10.13	152	-	-	-	-
2977	0:38:20.1	40:12:58.7	22.86	-471.5	-	-	2002.10.13	153	-	-	-	-
2978	0:38:08.4	40:07:19.0	22.50	-474.6	-	-	2002.10.13	154	-	-	-	52
2979	0:38:57.3	40:10:34.0	23.95	-470.8	-	-	2002.10.13	154	-	-	-	-
2980	0:38:13.0	39:54:09.6	24.97	-244.0	-	-	2002.10.13	156	-	-	-	-
2981	0:38:06.8	39:56:07.4	22.27	-460.4	-	-	2002.10.13	156	-	-	-	-
2982	0:38:03.6	39:58:01.5	24.98	-477.8	-	-	2002.10.13	156	-	-	-	-
2983	0:38:17.5	39:58:26.6	23.22	-455.8	-	-	2002.10.13	156	-	-	-	-
2984	0:38:12.4	39:59:42.6	24.44	-426.8	-	-	2002.10.13	156	-	-	-	-
2985	0:37:55.0	40:00:13.4	21.40	-411.6	-	-	2002.10.13	156	-	-	-	43
2986	0:37:38.2	40:01:53.2	24.73	-507.8	E	-	2002.10.13	156	-	-	-	-
2987	0:38:00.1	40:02:06.0	23.94	-479.2	-	-	2002.10.13	156	-	-	-	-
2988	0:52:00.0	43:03:23.5	21.98	-98.5	-	-	2003.09.29	235	-	-	-	-
2989	0:35:60.0	40:50:33.2	21.57	-454.8	-	-	2003.10.01	385	-	-	-	-

Continued on next page

Table A.1 – continued from previous page

ID	RA	Dec	$m_{5007}$	$v_{\text{helio}}$	Note	Host	Date	Field	H06	C89	HK04	MLA93
2990	0:43:53.8	41:57:43.8	20.50	-189.3	E,R	-	2002.10.12	18	-	-	-	874
2991	0:43:51.0	41:58:24.6	22.51	-52.0	-	-	2002.10.12	18	PN_10_4_19	-	-	-
2992	0:43:54.2	42:02:39.5	22.92	-217.5	-	-	2002.10.12	18	PN_10_4_20	-	-	-
2993	0:45:27.7	41:55:41.2	21.51	-149.2	-	-	2002.10.13	20	PN_9_4_18	-	-	1154
2994	0:44:58.7	41:55:37.3	20.15	-93.7	R	-	2002.10.13	20	-	-	-	1088
2995	0:45:29.1	41:55:48.3	21.17	-229.3	-	-	2002.10.13	20	PN_9_4_19	-	-	1157
2996	0:44:52.0	41:55:51.9	24.61	-173.9	-	-	2002.10.13	20	-	-	-	-
2997	0:45:29.4	41:55:20.4	23.79	-74.8	-	-	2002.10.13	20	-	-	-	-
2998	0:46:26.1	41:55:37.9	22.03	-128.8	-	-	2002.10.13	22	PN_9_4_41	-	-	1246
2999	0:43:23.3	41:46:21.7	22.68	-212.0	-	-	2002.10.11	29	-	-	-	-
3000	0:42:58.9	41:46:36.1	21.83	-231.2	E	-	2002.10.11	29	-	-	-	-
3001	0:44:18.3	41:51:38.4	24.78	-48.0	E	-	2002.10.12	30	-	-	-	-
3002	0:44:29.3	41:45:41.6	23.68	-131.2	-	-	2002.10.10	31	-	-	-	-
3003	0:42:52.0	41:36:42.3	20.68	-136.6	-	-	2002.10.10	39	-	-	-	611
3004	0:42:56.3	41:37:38.2	22.60	-274.8	-	-	2002.10.10	39	PN_2_3_7	-	-	631
3005	0:43:11.1	41:36:36.8	22.14	-244.5	-	-	2002.10.10	40	-	-	-	703
3006	0:43:20.8	41:36:58.9	23.90	-81.2	-	-	2002.10.10	40	-	-	-	-
3007	0:44:41.7	41:43:02.3	24.56	-165.4	-	-	2002.10.10	41	-	-	-	-
3008	0:45:40.8	41:36:54.9	24.90	-60.0	-	-	2002.10.11	43	-	-	-	-
3009	0:41:05.3	41:27:56.8	25.25	-299.0	-	-	2002.10.11	44	-	-	-	-
3010	0:41:54.7	41:27:46.4	25.28	-282.1	-	-	2002.10.10	49	-	-	-	-
3011	0:42:38.6	41:31:51.0	21.52	-272.5	E,R	-	2002.10.10	49	-	-	-	562
3012	0:42:36.5	41:33:10.9	21.61	-261.7	R	-	2002.10.10	49	-	-	-	552
3013	0:42:39.7	41:35:39.1	23.88	-304.3	-	-	2002.10.10	49	-	-	-	-
3014	0:42:40.5	41:35:48.6	21.62	-245.8	-	-	2002.10.10	49	-	-	-	572
3015	0:43:16.2	41:28:23.2	23.92	-245.9	-	-	2002.10.09	50	-	-	-	-
3016	0:44:09.6	41:27:12.2	21.42	-133.0	-	-	2002.10.10	51	P541	-	541	932
3017	0:43:57.2	41:27:16.7	23.31	-187.0	-	-	2002.10.10	51	-	-	527	-
3018	0:43:44.8	41:27:13.8	23.43	-177.4	-	-	2002.10.10	51	P284	-	284	-
3019	0:43:58.7	41:27:19.3	22.13	-129.4	-	-	2002.10.10	51	P530	-	530	892
3020	0:44:02.6	41:28:03.8	21.60	-50.5	-	-	2002.10.10	51	P532	-	532	907
3021	0:44:06.8	41:28:06.1	22.61	-75.7	-	-	2002.10.10	51	P536	-	536	-
3022	0:43:41.6	41:28:02.0	22.14	-196.0	-	-	2002.10.10	51	P274	-	274	836
3023	0:44:37.5	41:27:09.7	20.99	-100.2	-	-	2002.10.10	52	-	-	-	1029
3024	0:45:13.1	41:28:21.7	24.86	-97.5	-	-	2002.10.11	53	-	-	-	-
3025	0:42:14.7	41:21:06.1	24.11	-146.1	-	-	2002.10.10	55	-	-	-	-
3026	0:42:12.6	41:26:17.6	22.49	-323.0	-	-	2002.10.10	55	PN_1_4_23	-	-	464
3027	0:38:54.2	41:20:05.0	24.84	-484.5	E	-	2002.10.12	58	-	-	-	-
3028	0:42:18.4	41:17:43.3	25.68	-411.9	-	-	2002.10.09	60	-	-	-	-
3029	0:42:44.6	41:18:14.3	23.41	-69.6	-	-	2002.10.09	60	-	-	453	-
3030	0:43:03.9	41:21:25.6	22.32	-321.9	-	-	2002.10.09	60	P492	-	492	674
3031	0:43:01.2	41:26:20.4	24.00	-140.4	-	-	2002.10.09	60	P487	-	487	-
3032	0:43:06.4	41:17:50.9	23.28	-289.3	-	-	2002.10.09	61	P495	-	495	-
3033	0:43:43.5	41:18:57.8	23.78	-231.3	-	-	2002.10.09	61	-	-	-	-
3034	0:43:25.4	41:19:07.4	23.34	-372.5	-	-	2002.10.09	61	-	-	-	-
3035	0:41:08.8	41:08:44.8	23.89	-288.9	-	-	2002.10.10	65	-	-	-	-
3036	0:41:14.7	41:09:23.9	20.95	-437.1	E,R	-	2002.10.10	65	-	-	-	326
3037	0:41:47.0	41:10:18.9	22.63	-353.7	-	-	2002.10.10	65	-	-	-	-
3038	0:41:49.7	41:11:21.6	22.31	-364.1	-	-	2002.10.10	65	PN_1_1_28	-	-	-
3039	0:41:50.2	41:12:35.8	24.15	-345.4	-	-	2002.10.10	65	-	-	-	-
3040	0:41:49.3	41:13:37.7	23.85	-476.0	-	-	2002.10.10	65	-	-	-	-
3041	0:40:54.3	41:08:39.2	21.44	-435.9	-	-	2002.10.11	66	-	-	-	282
3042	0:42:35.6	41:09:02.5	23.72	-514.7	-	-	2002.10.09	70	-	-	-	-
3043	0:42:38.7	41:14:10.5	22.78	-410.8	-	-	2002.10.09	70	-	-	440	-
3044	0:43:28.2	41:14:52.2	23.41	-331.9	-	-	2002.10.09	71	-	-	-	-
3045	0:42:02.3	40:59:38.6	23.55	-508.0	-	-	2002.10.13	76	-	-	-	-
3046	0:41:34.3	40:59:44.8	21.26	-486.8	-	-	2002.10.13	76	-	-	-	375
3047	0:41:31.9	40:59:47.8	24.43	-445.9	-	-	2002.10.13	76	-	-	-	-
3048	0:42:06.7	41:00:06.9	23.02	-241.3	-	-	2002.10.13	76	-	-	-	-
3049	0:41:48.5	41:00:01.2	24.85	-430.6	-	-	2002.10.13	76	-	-	-	-
3050	0:42:00.1	41:00:06.8	24.03	-501.1	E	-	2002.10.13	76	-	-	-	-
3051	0:42:03.1	41:00:10.7	23.86	-491.8	-	-	2002.10.13	76	-	-	-	-
3052	0:41:37.1	41:00:05.0	22.77	-489.4	-	-	2002.10.13	76	-	-	-	-
3053	0:41:42.2	41:00:11.8	23.26	-476.2	-	-	2002.10.13	76	-	-	-	-
3054	0:41:32.2	41:00:12.0	21.83	-530.8	-	-	2002.10.13	76	PN_2_3_25	-	-	369
3055	0:41:46.9	41:00:21.2	22.54	-531.4	-	-	2002.10.13	76	-	-	-	-
3056	0:41:51.8	41:00:33.0	25.06	-465.1	-	-	2002.10.13	76	-	-	-	-
3057	0:41:46.2	41:00:34.7	21.17	-501.3	-	-	2002.10.13	76	PN_2_3_41	-	-	405
3058	0:42:12.9	41:02:11.3	24.40	-239.9	-	-	2002.10.13	76	-	-	-	-
3059	0:42:15.0	41:02:15.7	23.72	-487.4	-	-	2002.10.13	76	-	-	-	-
3060	0:42:15.6	41:03:38.6	22.24	-450.0	-	-	2002.10.13	76	-	-	-	-
3061	0:41:24.1	41:04:53.6	23.26	-552.1	E	-	2002.10.13	76	-	-	-	357
3062	0:41:26.8	41:05:33.7	21.52	-540.9	-	-	2002.10.13	76	-	-	-	361
3063	0:41:27.1	41:06:11.2	23.70	-439.8	-	-	2002.10.13	76	-	-	-	-
3064	0:42:14.0	41:07:22.2	22.81	-491.8	-	-	2002.10.13	76	-	-	-	-
3065	0:42:12.1	41:07:26.7	21.21	-545.9	-	-	2002.10.13	76	PN_1_1_80	-	-	463
3066	0:41:25.2	41:08:05.1	23.91	-366.7	-	-	2002.10.13	76	-	-	-	-
3067	0:42:14.9	41:08:56.8	24.50	-361.2	-	-	2002.10.13	76	-	-	-	-
3068	0:41:24.0	41:03:03.7	23.21	-402.3	-	-	2002.10.13	76	-	-	-	-
3069	0:42:16.1	41:06:51.1	23.01	-473.7	-	-	2002.10.13	76	-	-	-	-
3070	0:42:21.8	41:00:13.5	22.62	-440.2	R	-	2002.10.09	81	-	-	-	489
3071	0:43:06.6	40:59:51.2	25.29	-402.4	-	-	2002.10.10	82	-	-	-	-
3072	0:43:12.9	41:00:25.1	24.03	-294.2	-	-	2002.10.10	82	-	-	-	-
3073	0:43:52.3	41:07:25.1	23.20	-315.2	-	-	2002.10.10	82	-	-	-	-
3074	0:41:48.2	40:53:31.8	24.44	-484.2	-	-	2002.10.08	86	-	-	-	-
3075	0:41:02.4	40:58:46.3	24.29	-369.9	-	-	2002.10.08	86	-	-	-	-
3076	0:40:57.3	40:50:39.1	24.46	-521.3	-	-	2002.10.08	87	-	-	-	-
3077	0:40:41.4	40:51:04.0	23.56	-524.8	R	-	2002.10.08	87	-	-	-	-
3078	0:40:18.9	40:50:21.6	23.98	-520.3	E	-	2002.10.08	87	-	-	-	-
3079	0:41:22.7	40:44:02.2	24.09	-534.7	-	-	2002.10.09	97	-	-	-	-
3080	0:40:35.5	40:45:17.0	23.07	-482.6	-	-	2002.10.09	98	PN_12_4_41	-	-	-
3081	0:40:06.7	40:31:56.6	24.80	-540.7	-	-	2002.10.09	110	-	-	-	-
3082	0:46:43.1	40:38:37.6	25.27	164.0	E	-	2002.10.11	118	-	-	-	-

Continued on next page



Table A.1 – continued from previous page

ID	RA	Dec	$m_{5007}$	$v_{\text{helio}}$	Note	Host	Date	Field	H06	C89	HK04	MLA93
3083	0:38:49.2	40:12:41.6	24.01	-498.1	-	-	2002.10.13	152	-	-	-	-
3084	0:38:56.6	40:10:13.9	22.08	-451.1	-	-	2002.10.13	154	-	-	-	77
3085	0:38:07.1	40:08:29.2	24.57	-483.4	-	-	2002.10.13	154	-	-	-	-
3086	0:38:07.2	40:08:51.0	25.68	-497.6	-	-	2002.10.13	154	-	-	-	-
3087	0:40:24.9	41:55:42.7	25.95	-133.2	-	-	2002.10.10	14	-	-	-	-
3088	0:44:24.0	41:55:26.8	24.42	-136.7	-	-	2002.10.12	19	PN_10.4.29	-	-	-
3089	0:44:01.0	41:55:27.7	24.39	-163.0	-	-	2002.10.12	19	-	-	-	-
3090	0:44:10.8	41:56:29.7	23.56	-81.9	-	-	2002.10.12	19	PN_10.4.21	-	-	-
3091	0:44:51.1	41:55:23.8	24.28	-106.6	-	-	2002.10.13	20	-	-	-	-
3092	0:44:25.0	41:46:07.5	24.46	-127.8	-	-	2002.10.10	31	-	-	-	-
3093	0:46:00.3	41:45:46.8	22.39	-93.1	-	-	2002.10.11	33	PN_9.1.36	-	-	1217
3094	0:46:13.8	41:46:52.0	24.62	-27.9	-	-	2002.10.11	33	-	-	-	-
3095	0:46:40.3	41:45:45.9	23.12	-123.2	-	-	2002.10.11	33	PN_9.1.47	-	-	-
3096	0:40:30.4	41:38:02.1	25.64	-220.2	-	NGC205	2002.10.10	36	-	-	-	-
3097	0:40:02.7	41:42:13.8	24.05	-238.9	-	NGC205	2002.10.10	36	-	-	-	-
3098	0:40:20.5	41:42:55.7	25.06	-220.9	-	NGC205	2002.10.10	36	-	-	-	-
3099	0:43:52.2	41:39:29.1	24.20	-74.4	-	-	2002.10.10	40	-	-	-	-
3100	0:39:51.2	41:27:07.5	24.15	-479.0	-	-	2002.10.11	46	PN_8.4.6	-	-	-
3101	0:42:59.0	41:27:28.0	23.69	-198.5	-	-	2002.10.09	50	-	-	-	-
3102	0:43:08.5	41:28:13.6	23.07	-443.8	-	-	2002.10.09	50	-	-	-	-
3103	0:43:26.1	41:29:37.5	21.62	-55.2	-	-	2002.10.09	50	PN_6.3.28	-	-	777
3104	0:43:27.8	41:29:57.0	22.34	-72.6	-	-	2002.10.09	50	-	-	-	-
3105	0:43:28.3	41:29:57.7	23.00	-290.1	-	-	2002.10.09	50	-	-	-	-
3106	0:43:26.3	41:31:45.3	22.66	-196.0	-	-	2002.10.09	50	-	-	-	778
3107	0:44:17.0	41:30:09.6	24.56	-208.2	-	-	2002.10.10	51	-	-	-	-
3108	0:44:17.6	41:33:42.3	21.96	-147.4	-	-	2002.10.10	51	P551	-	551	963
3109	0:44:18.5	41:32:01.8	24.96	-162.6	R	-	2002.10.10	51	-	-	-	-
3110	0:42:07.1	41:19:03.9	24.57	-165.2	-	-	2002.10.10	55	-	-	-	-
3111	0:41:48.2	41:19:21.7	23.89	-399.4	E,R	-	2002.10.10	55	-	-	-	-
3112	0:41:24.0	41:20:48.2	24.63	-371.3	-	-	2002.10.10	55	-	-	-	-
3113	0:42:54.3	41:17:59.1	22.86	-147.6	-	-	2002.10.09	60	-	-	-	-
3114	0:42:30.8	41:17:54.5	23.34	-344.5	-	-	2002.10.09	60	P421	-	421	-
3115	0:42:52.1	41:18:09.0	23.34	-454.2	-	-	2002.10.09	60	-	-	-	-
3116	0:42:46.1	41:18:26.0	22.76	-207.1	-	-	2002.10.09	60	P455	-	455	-
3117	0:42:35.8	41:18:24.8	23.65	-247.3	-	-	2002.10.09	60	P432	-	432	-
3118	0:42:45.5	41:18:45.5	22.80	-342.9	-	-	2002.10.09	60	-	-	-	-
3119	0:42:46.0	41:18:47.3	23.79	-104.3	-	-	2002.10.09	60	-	-	-	-
3120	0:42:47.7	41:18:52.5	22.63	12.2	-	-	2002.10.09	60	-	-	-	-
3121	0:43:04.4	41:20:09.4	22.71	-231.6	-	-	2002.10.09	60	P199	-	199	-
3122	0:43:03.5	41:24:35.4	23.37	-72.8	-	-	2002.10.09	60	P235	-	235	-
3123	0:42:51.5	41:18:41.1	23.88	-348.2	-	-	2002.10.09	60	-	-	-	-
3124	0:44:10.8	41:18:14.1	22.62	-170.1	-	-	2002.10.09	62	-	-	-	-
3125	0:44:39.7	41:25:41.3	21.53	-146.8	-	-	2002.10.09	62	-	-	-	1036
3126	0:44:42.0	41:26:58.2	22.46	-182.4	E,R	-	2002.10.09	62	-	-	-	-
3127	0:44:47.0	41:18:00.7	23.64	-196.2	-	-	2002.10.11	63	-	-	-	-
3128	0:44:41.3	41:18:12.8	24.09	-267.2	-	-	2002.10.11	63	-	-	-	-
3129	0:41:45.4	41:08:46.2	24.83	-284.5	E	-	2002.10.10	65	-	-	-	-
3130	0:41:40.8	41:09:40.0	23.84	-400.7	-	-	2002.10.10	65	-	-	-	-
3131	0:41:46.7	41:18:48.8	21.51	-329.3	E,R	-	2002.10.10	65	-	-	-	-
3132	0:40:11.6	41:10:24.9	24.31	-448.5	-	-	2002.10.11	66	-	-	-	-
3133	0:41:54.2	41:08:23.3	23.73	-345.1	-	-	2002.10.09	70	-	-	-	-
3134	0:42:09.9	41:08:47.7	24.00	-281.7	R	-	2002.10.09	70	-	-	-	-
3135	0:42:10.2	41:08:51.4	22.80	-493.6	-	-	2002.10.09	70	P374	-	374	-
3136	0:42:34.5	41:09:16.3	22.77	-500.0	-	-	2002.10.09	70	PN_1.1.95	-	429	-
3137	0:42:02.1	41:09:11.3	23.10	-529.8	-	-	2002.10.09	70	-	-	-	-
3138	0:42:00.1	41:09:16.8	22.24	-433.4	-	-	2002.10.09	70	-	-	-	433
3139	0:42:05.5	41:09:30.6	23.93	-507.1	-	-	2002.10.09	70	-	-	-	-
3140	0:41:53.7	41:09:46.0	23.29	-489.6	-	-	2002.10.09	70	-	-	-	-
3141	0:42:13.1	41:09:54.1	23.61	-389.7	-	-	2002.10.09	70	P379	-	379	-
3142	0:41:52.3	41:09:53.1	23.93	-390.6	-	-	2002.10.09	70	-	-	-	-
3143	0:41:59.1	41:09:59.4	23.53	-391.2	-	-	2002.10.09	70	-	-	-	-
3144	0:42:05.7	41:10:04.4	23.56	-531.3	-	-	2002.10.09	70	-	-	-	-
3145	0:42:08.2	41:10:07.5	23.01	-606.7	-	-	2002.10.09	70	-	-	372	-
3146	0:42:38.1	41:16:53.8	22.19	-401.6	-	-	2002.10.09	70	-	-	87	-
3147	0:41:58.0	41:08:10.0	21.15	-483.9	-	-	2002.10.09	70	-	-	-	430
3148	0:42:37.6	41:13:38.9	23.08	-365.8	-	-	2002.10.09	70	-	-	436	-
3149	0:42:36.5	41:13:37.0	23.77	-136.3	-	-	2002.10.09	70	-	-	-	-
3150	0:42:39.9	41:17:04.3	22.63	-249.8	-	-	2002.10.09	70	P82	-	82	-
3151	0:43:27.9	41:08:55.9	24.92	-346.5	-	-	2002.10.09	71	-	-	-	-
3152	0:43:24.9	41:09:56.8	22.11	-361.6	-	-	2002.10.09	71	-	-	-	773
3153	0:43:02.0	41:08:32.8	24.85	-380.3	-	-	2002.10.09	71	-	-	-	-
3154	0:43:39.7	41:08:55.8	21.51	-344.5	-	-	2002.10.09	72	-	-	-	829
3155	0:44:03.5	41:09:16.9	23.64	-374.5	-	-	2002.10.09	72	-	-	-	-
3156	0:43:40.0	41:09:17.9	23.72	-412.8	-	-	2002.10.09	72	-	-	-	-
3157	0:43:43.2	41:09:31.5	21.63	-356.7	-	-	2002.10.09	72	PN_6.1.66	-	-	841
3158	0:43:34.9	41:09:52.5	19.86	-334.1	E,R	-	2002.10.09	72	-	-	-	804
3159	0:44:16.2	41:18:57.4	23.61	-244.6	E	-	2002.10.09	72	-	-	-	-
3160	0:40:36.9	41:01:05.3	21.32	-393.6	-	-	2002.10.08	77	-	-	-	242
3161	0:40:35.7	41:01:13.2	22.86	-408.3	E,R	-	2002.10.08	77	-	-	-	-
3162	0:40:36.2	41:01:18.8	21.98	-425.8	E,R	-	2002.10.08	77	-	-	-	239
3163	0:42:55.3	40:59:33.5	22.45	-315.3	-	-	2002.10.09	81	-	-	-	627
3164	0:42:55.4	40:59:42.9	23.52	-389.9	E	-	2002.10.09	81	-	-	-	-
3165	0:42:31.1	40:59:56.7	24.36	-492.3	-	-	2002.10.09	81	-	-	-	-
3166	0:44:40.3	41:06:27.9	24.30	-292.1	E	-	2002.10.11	83	-	-	-	-
3167	0:44:42.2	41:08:01.7	20.98	-241.7	-	-	2002.10.11	83	PN_5.1.5	1.117	-	1041
3168	0:41:51.7	40:57:43.2	23.80	-418.8	-	-	2002.10.08	86	-	-	-	-
3169	0:40:11.2	40:54:55.2	23.79	-431.6	-	-	2002.10.08	87	PN_12.3.20	-	-	-
3170	0:40:09.9	40:57:25.3	24.08	-345.5	-	-	2002.10.08	87	-	-	-	-
3171	0:38:35.5	40:55:54.1	24.29	-431.9	-	-	2002.10.08	89	-	-	-	-
3172	0:42:32.1	40:52:26.6	23.64	-377.7	E	M32?	2002.10.08	91	-	-	-	-
3173	0:42:18.8	40:52:47.8	24.28	-417.4	-	-	2002.10.08	91	-	-	-	-
3174	0:42:35.9	40:53:00.7	20.91	-207.7	-	M32	2002.10.08	91	-	-	-	551
3175	0:42:31.1	40:53:04.7	21.27	-414.5	-	M32?	2002.10.08	91	PN_3.2.38	-	-	535

Continued on next page

Table A.1 – continued from previous page

ID	RA	Dec	$m_{5007}$	$v_{\text{helio}}$	Note	Host	Date	Field	H06	C89	HK04	MLA93
3176	0:42:20.7	40:54:47.9	24.36	-258.3	-	-	2002.10.08	91	-	-	-	-
3177	0:42:15.2	40:55:32.2	20.86	-507.1	-	-	2002.10.08	91	PN <sub>2,3,64</sub>	-	-	477
3178	0:42:21.6	40:56:15.4	23.29	-382.1	-	-	2002.10.08	91	-	-	-	-
3179	0:42:19.1	40:57:08.8	21.87	-283.2	-	-	2002.10.08	91	PN <sub>2,3,66</sub>	1.73	-	482
3180	0:42:38.8	40:58:42.0	23.73	-342.5	-	-	2002.10.08	91	-	-	-	-
3181	0:42:38.7	40:51:35.5	24.32	-167.3	-	M32	2002.10.11	92	-	-	-	-
3182	0:42:41.0	40:51:34.6	24.01	-131.3	-	M32	2002.10.11	92	-	-	-	-
3183	0:41:47.0	40:40:49.8	23.02	-438.0	-	-	2002.10.09	97	-	-	-	-
3184	0:41:51.6	40:41:05.6	23.94	-215.0	E	-	2002.10.09	97	-	-	-	-
3185	0:41:28.8	40:41:37.0	23.50	-528.5	-	-	2002.10.09	97	-	-	-	-
3186	0:41:56.1	40:41:47.6	22.89	-317.5	E	-	2002.10.09	97	-	-	-	-
3187	0:42:12.0	40:49:08.5	21.04	-403.6	-	-	2002.10.09	97	PN <sub>3,2,28</sub>	-	-	461
3188	0:41:54.9	40:40:22.7	22.47	-484.0	E	-	2002.10.09	97	PN <sub>2,1,22</sub>	-	-	425
3189	0:41:11.4	40:41:24.4	22.95	-570.9	-	-	2002.10.09	98	-	-	-	-
3190	0:40:45.3	40:41:30.2	20.79	-548.4	-	-	2002.10.09	98	-	1.53	-	258
3191	0:40:34.5	40:46:39.1	23.35	-467.5	-	-	2002.10.09	98	-	-	-	-
3192	0:40:31.5	40:41:23.0	22.84	-594.5	E,R	-	2002.10.09	99	-	-	-	-
3193	0:40:07.2	40:41:35.7	23.32	-565.8	E	-	2002.10.09	99	-	-	-	-
3194	0:40:11.4	40:41:46.6	23.14	-567.7	E,R	-	2002.10.09	99	-	-	-	-
3195	0:39:58.4	40:41:59.2	22.24	-513.2	-	-	2002.10.09	99	-	-	-	160
3196	0:39:49.0	40:42:39.9	23.23	-154.0	R	-	2002.10.09	99	PN <sub>2,2,17</sub>	1.32	-	-
3197	0:39:16.5	40:41:05.7	22.31	-477.1	E	-	2002.10.10	100	-	-	-	-
3198	0:39:05.3	40:41:46.0	22.35	-377.9	-	-	2002.10.10	100	PN <sub>12,1,6</sub>	1.9	-	84
3199	0:42:18.6	40:40:40.8	24.89	-390.1	-	-	2002.10.11	103	-	-	-	-
3200	0:41:26.5	40:32:45.8	22.00	-403.6	-	-	2002.10.09	108	PN <sub>2,1,15</sub>	1.66	-	360
3201	0:40:13.6	40:31:05.4	24.23	-491.6	-	-	2002.10.09	109	-	-	-	-
3202	0:40:39.8	40:32:15.7	23.78	-532.4	-	-	2002.10.09	109	-	-	-	-
3203	0:40:14.1	40:34:30.5	23.19	-536.1	-	-	2002.10.09	109	-	-	-	-
3204	0:40:13.7	40:35:42.2	22.03	-562.8	-	-	2002.10.09	109	PN <sub>12,1,21</sub>	-	-	185
3205	0:40:13.1	40:36:25.2	21.89	-569.9	-	-	2002.10.09	109	-	-	-	181
3206	0:40:14.5	40:39:33.1	24.27	-422.1	-	-	2002.10.09	109	-	-	-	-
3207	0:40:45.4	40:31:10.6	21.40	-522.1	-	-	2002.10.09	109	-	-	-	260
3208	0:40:00.4	40:23:11.2	25.04	-153.6	-	-	2002.10.13	140	-	-	-	-
3209	0:38:44.8	40:13:07.0	25.61	-397.0	E	-	2002.10.13	152	-	-	-	-
3210	0:37:51.6	40:03:56.9	25.45	-470.0	-	-	2002.10.13	156	-	-	-	-
3211	0:50:57.5	42:53:59.3	25.24	-345.6	E	Stream?	2003.09.29	245	-	-	-	-
3212	0:43:27.2	42:04:45.5	23.30	-178.6	-	-	2002.10.12	7	PN <sub>10,3,6</sub>	-	-	-
3213	0:43:05.2	41:55:52.0	20.97	-280.8	-	-	2002.10.13	17	PN <sub>10,4,6</sub>	-	-	676
3214	0:40:17.4	41:45:59.0	22.90	-227.6	-	NGC205	2002.10.10	24	PN <sub>7,1,9</sub>	-	-	-
3215	0:44:19.3	41:46:09.1	21.73	-85.3	-	-	2002.10.12	30	PN <sub>10,1,32</sub>	-	-	965
3216	0:43:51.4	41:46:08.5	24.49	-148.1	-	-	2002.10.12	30	-	-	-	-
3217	0:43:54.9	41:45:39.5	22.52	-245.1	-	-	2002.10.12	30	PN <sub>10,1,16</sub>	-	-	881
3218	0:45:55.8	41:46:22.7	23.82	-181.5	-	-	2002.10.10	32	-	-	-	-
3219	0:45:30.6	41:46:39.3	21.71	-111.5	E	-	2002.10.10	32	-	-	-	1158
3220	0:40:36.2	41:42:02.5	22.42	-269.7	-	NGC205	2002.10.10	35	PN <sub>11,1,2</sub>	-	-	241
3221	0:40:32.6	41:41:00.0	24.64	-216.2	-	NGC205	2002.10.10	35	-	-	-	-
3222	0:40:24.7	41:37:28.0	21.55	-224.1	-	NGC205	2002.10.10	36	-	-	-	214
3223	0:40:14.5	41:37:42.3	21.00	-232.5	-	NGC205	2002.10.10	36	PN <sub>8,3,10</sub>	-	-	187
3224	0:44:41.0	41:37:06.5	23.41	-197.9	-	-	2002.10.10	41	PN <sub>5,3,3</sub>	-	-	-
3225	0:45:12.5	41:37:17.7	20.78	-114.9	E,R	-	2002.10.10	42	-	-	-	-
3226	0:45:31.8	41:37:26.6	24.73	-207.9	-	-	2002.10.10	42	-	-	-	-
3227	0:45:06.1	41:36:16.3	21.19	-131.1	R	-	2002.10.10	42	PN <sub>5,3,16</sub>	-	-	1104
3228	0:41:26.9	41:27:52.6	24.86	-330.5	-	-	2002.10.11	44	-	-	-	-
3229	0:41:27.4	41:18:11.7	23.81	-330.1	-	-	2002.10.10	55	-	-	-	-
3230	0:42:40.3	41:19:04.0	22.52	-185.9	-	-	2002.10.09	60	PN <sub>6,4,16</sub>	-	-	567
3231	0:41:50.6	41:09:14.8	24.53	-494.2	-	-	2002.10.10	65	-	-	-	-
3232	0:39:23.5	41:09:38.8	22.76	-157.1	-	-	2002.10.12	67	PN <sub>8,1,4</sub>	-	-	-
3233	0:43:27.2	41:09:50.4	23.66	-346.4	-	-	2002.10.09	71	-	-	-	-
3234	0:45:05.3	41:09:38.3	22.30	-287.9	-	-	2002.10.11	73	PN <sub>5,1,6</sub>	1.126	-	1103
3235	0:42:41.0	40:59:10.9	22.94	-366.1	E,R	-	2002.10.09	81	-	-	-	-
3236	0:41:23.3	40:50:52.5	21.20	-544.8	-	-	2002.10.08	86	PN <sub>2,4,23</sub>	-	-	354
3237	0:42:39.3	40:52:10.7	23.41	-149.1	-	M32	2002.10.08	91	-	-	-	-
3238	0:42:54.0	40:49:54.2	24.01	-167.0	-	M32	2002.10.11	92	-	-	-	-
3239	0:42:57.0	40:51:01.8	23.34	-160.1	-	M32	2002.10.11	92	-	2.7	-	-
3240	0:43:28.4	40:51:19.7	23.09	-489.2	-	-	2002.10.11	92	-	1.100	-	-
3241	0:42:56.0	40:51:12.6	22.21	-652.7	-	M32?	2002.10.11	92	-	1.86	-	634
3242	0:42:49.9	40:51:10.6	22.61	-505.3	-	M32?	2002.10.11	92	PN <sub>3,4,1</sub>	1.81	-	605
3243	0:42:40.0	40:49:41.3	22.03	-156.6	-	M32	2002.10.11	92	-	2.3	-	568
3244	0:41:24.3	40:41:31.5	23.16	-600.3	-	-	2002.10.09	97	-	-	-	-
3245	0:43:02.0	40:49:30.5	20.89	-160.0	-	M32	2002.10.11	103	PN <sub>3,4,12</sub>	2.8	-	665
3246	0:39:45.4	40:31:42.6	20.83	-533.2	-	-	2002.10.09	110	PN <sub>12,1,8</sub>	1.29	-	140
3247	0:40:47.7	41:37:29.5	24.69	-387.1	-	NGC205?	2002.10.10	35	-	-	-	-
3248	0:41:52.6	41:27:50.1	25.10	-332.8	-	-	2002.10.11	44	-	-	-	-
3249	0:42:40.5	41:27:31.7	23.60	-370.5	-	-	2002.10.10	49	-	-	-	-
3250	0:44:15.6	41:27:15.4	21.70	-176.0	-	-	2002.10.10	51	P548	-	548	954
3251	0:43:53.0	41:27:57.1	22.69	-252.7	-	-	2002.10.10	51	-	-	287	-
3252	0:43:49.6	41:27:57.6	22.23	-1.4	-	-	2002.10.10	51	P286	-	286	861
3253	0:41:46.8	41:18:47.8	21.68	-358.8	E,R	-	2002.10.10	55	-	-	-	-
3254	0:41:48.1	41:18:59.5	22.84	-367.3	E,R	-	2002.10.10	55	-	-	-	-
3255	0:40:58.5	41:09:07.2	22.53	-354.1	-	-	2002.10.10	65	PN <sub>1,1,16</sub>	-	-	295
3256	0:42:14.4	41:36:46.0	25.08	-248.8	-	-	2002.10.11	34	-	-	-	-
3257	0:40:35.7	41:41:39.9	24.62	-273.2	-	NGC205	2002.10.10	35	-	-	-	-
3258	0:43:27.5	41:37:33.3	23.22	-98.2	-	-	2002.10.10	40	-	-	-	784
3259	0:43:02.3	41:27:42.0	23.75	-207.5	-	-	2002.10.09	50	-	-	-	-
3260	0:43:02.3	41:28:15.7	23.25	-182.4	-	-	2002.10.09	50	-	-	-	-
3261	0:42:40.3	41:18:43.4	23.17	-360.5	-	-	2002.10.09	60	P103	-	103	-
3262	0:43:52.3	41:18:50.8	22.61	-69.7	-	-	2002.10.09	61	-	-	-	872
3263	0:41:49.8	41:09:48.8	23.03	-326.3	-	-	2002.10.10	65	-	-	-	-
3264	0:40:33.9	41:08:34.8	21.71	-593.5	-	-	2002.10.11	66	PN <sub>8,1,16</sub>	-	-	233
3265	0:42:15.3	40:59:27.8	24.55	-115.2	-	-	2002.10.13	76	-	-	-	-
3266	0:40:59.3	40:50:03.0	24.19	-499.0	-	-	2002.10.08	86	-	-	-	-
3267	0:42:48.4	40:50:09.4	25.04	-175.6	-	M32	2002.10.11	92	-	-	-	-
3268	0:46:23.3	41:47:10.2	22.54	-131.0	-	-	2002.10.11	43	-	-	-	-

Continued on next page

Table A.1 – continued from previous page

ID	RA	Dec	$m_{5007}$	$v_{\text{helio}}$	Note	Host	Date	Field	H06	C89	HK04	MLA93
3269	0:42:11.5	41:37:34.3	24.42	-278.5	-	-	2002.10.10	39	-	-	-	-
3270	0:42:39.6	41:18:32.8	22.77	-279.2	-	-	2002.10.09	70	P102	-	102	-
3271	0:43:05.4	41:18:33.2	22.63	-546.2	-	-	2002.10.09	61	P195	-	195	-
3272	0:43:02.6	41:08:43.2	21.94	-288.0	-	-	2002.10.09	81	PN_5_1_40	-	-	668
3273	0:42:23.1	40:50:23.4	22.74	-382.0	-	M32?	2002.10.11	103	-	-	-	-
3274	0:42:39.9	40:51:19.0	24.23	-180.0	-	M32	2002.10.11	92	-	-	-	-
3275	0:42:39.4	40:51:23.9	23.80	-132.3	-	M32	2002.10.11	92	-	-	-	-
3276	0:42:39.6	40:52:40.4	20.94	-250.8	-	M32	2002.10.11	92	-	-	-	565
3277	0:42:40.4	40:52:44.0	21.26	-196.9	-	M32	2002.10.11	92	-	-	-	570
3278	0:42:41.4	40:52:32.3	23.86	-265.1	-	M32	2002.10.11	92	-	-	-	-
3279	0:44:18.4	41:46:34.1	24.81	-119.1	-	-	2002.10.12	30	-	-	-	-
3280	0:40:14.5	41:37:12.3	25.17	-214.5	-	NGC205	2002.10.10	36	-	-	-	-
3281	0:41:49.4	41:28:13.9	21.11	-359.4	-	-	2002.10.11	44	-	-	-	411
3282	0:42:37.9	41:28:16.4	23.46	-54.4	-	-	2002.10.10	49	-	-	-	-
3283	0:41:49.7	40:59:27.8	23.68	-489.1	-	-	2002.10.13	76	-	-	-	-
3284	0:42:13.5	40:59:42.7	21.54	-609.6	-	-	2002.10.13	76	-	-	-	467
3285	0:41:50.7	40:59:43.4	23.86	-426.1	-	-	2002.10.13	76	-	-	-	-
3286	0:41:51.6	41:00:04.4	24.75	-446.7	-	-	2002.10.13	76	-	-	-	-
3287	0:40:35.2	40:50:07.7	23.39	-504.5	-	-	2002.10.08	87	PN_12_4_40	-	-	238
3288	0:45:55.0	41:55:58.4	22.28	-91.9	-	-	2002.10.10	32	-	-	-	1211
3289	0:43:26.9	41:28:20.6	20.96	-135.7	-	-	2002.10.10	51	-	-	-	782
3290	0:42:38.6	41:18:54.4	24.43	-308.6	-	-	2002.10.09	70	-	-	-	-
3291	0:42:13.8	41:08:58.4	23.52	-315.2	-	-	2002.10.13	76	P381	-	381	-
3292	0:42:15.8	41:09:30.5	23.80	-463.5	-	-	2002.10.13	76	-	-	383	-
3293	0:40:13.2	41:46:11.7	24.88	-282.1	-	NGC205	2002.10.11	131	-	-	-	-
3294	0:40:08.2	41:45:46.5	24.28	-442.4	-	NGC205?	2002.10.11	131	-	-	-	-
3295	0:39:59.4	41:46:17.2	24.66	-183.6	-	NGC205	2002.10.11	131	-	-	-	-
3296	0:44:16.2	41:18:53.5	21.38	-159.8	-	-	2002.10.11	73	-	-	-	958
3297	0:42:37.4	41:09:09.9	23.85	-370.2	-	-	2002.10.09	81	-	-	435	-
3298	0:42:13.7	40:50:29.2	22.35	-386.0	E	-	2002.10.11	103	PN_3_2_29	-	-	468
3299	0:39:50.1	40:40:40.8	22.80	-432.2	-	-	2002.10.09	110	PN_12_1_13	-	-	148
3300	0:42:40.2	40:51:02.7	21.06	-158.9	-	M32	2002.10.08	91	PN_3_4_7	2_4	-	569

# Bibliography

Acker A., Marcout J., Ochsenbein F., Stenholm B., Tytenda R., 1992. *Strasbourg - ESO catalogue of galactic planetary nebulae. Part 1; Part 2*, Garching: European Southern Observatory, 1992.

Arp H., 1964. ApJ, 139, 1045. *Spiral Structure in M31*.

Athanassoula E., Beaton R. L., 2006. *arXiv:astro-ph/0605090. Unravelling the mystery of the M31 bar*.

Baade W., Arp H., 1964. ApJ, 139, 1027. *Positions of Emission Nebulae in M31*.

Baade W., Gaposchkin C. H. P., 1963. *Evolution of stars and galaxies.*, Cambridge, Harvard University Press, 1963.

Baade W., 1955. AJ, 60, 151. *Planetary nebulae in M 31*.

Beaton R. L., Majewski S. R., Guhathakurta P., Skrutskie M. F., Cutri R. M., Good J., Patterson R. J., Athanassoula E., Bureau M., 2006. *arXiv:astro-ph/0605239. Unveiling the Boxy Bulge and Bar of the Andromeda Spiral Galaxy*.

Bender R., Paquet A., Nieto J.-L., 1991. A&A, 246, 349. *Internal stellar kinematics of three dwarf ellipticals in the Local Group*.

Bertin E., Arnouts S., 1996. A&AS, 117, 393. *SExtractor: Software for source extraction*.

Binney J., Merrifield M., 1998. *Galactic astronomy*, Princeton, NJ : Princeton University Press, 1998.

Binney J., Tremaine S., 1987. *Galactic dynamics*, Princeton, NJ, Princeton University Press, 1987.

Braun R., Corbelli E., Walterbos R. A. M., Thilker D., 2002. *ASTRON Newsletter*, 17, 3. *Gas and Dark Matter in the Outskirts of M31*.

Braun R., 1991. ApJ, 372, 54. *The distribution and kinematics of neutral gas in M31*.

Brinks E., Burton W. B., 1984. A&A, 141, 195. *A high resolution hydrogen line survey of Messier 31. II - The warped flaring hydrogen layer*.

- Brinks E., Shane W. W., 1984. *A&AS*, 55, 179. *A high resolution hydrogen line survey of Messier 31. I Observations and data reduction.*
- Buzzoni A., Arnaboldi M., Corradi R. L. M., 2006. *MNRAS*, 368, 877. *Planetary nebulae as tracers of galaxy stellar populations.*
- Cardelli J. A., Clayton G. C., Mathis J. S., 1989. *ApJ*, 345, 245. *The relationship between infrared, optical, and ultraviolet extinction.*
- Carignan C., Chemin L., Huchtmeier W. K., Lockman F. J., 2006. *ApJ*, 641, L109. *The Extended H I Rotation Curve and Mass Distribution of M31.*
- Carroll B. W., Ostlie D. A., 1996. *An introduction to modern astrophysics*, Reading, MA: Addison-Wesley, —c1996.
- Carter D., Sadler E. M., 1990. *MNRAS*, 245, 12P. *Kinematics of the dwarf spheroidal galaxy NGC 205.*
- Chereul E., Cr     M., Bienaym   O., 1998. *A&A*, 340, 384. *The distribution of nearby stars in phase space mapped by HIPPARCOS. II. Inhomogeneities among A-F type stars.*
- Christodoulou D. M., Tohline J. E., Steiman-Cameron T. Y., 1993. *ApJ*, 416, 74. *Kinematical Modeling of WARPS in the H I Disks of Galaxies.*
- Ciardullo R., Jacoby G. H., Ford H. C., Neill J. D., 1989. *ApJ*, 339, 53. *Planetary nebulae as standard candles. II - The calibration in M31 and its companions.*
- Ciardullo R., Feldmeier J. J., Jacoby G. H., Kuzio de Naray R., Laychak M. B., Durrell P. R., 2002a. *ApJ*, 577, 31. *Planetary Nebulae as Standard Candles. XII. Connecting the Population I and Population II Distance Scales.*
- Ciardullo R., Feldmeier J. J., Krelove K., Jacoby G. H., Gronwall C., 2002b. *ApJ*, 566, 784. *A Measurement of the Contamination in [O III]  $\lambda$ 5007 Surveys of Intra-cluster Stars and the Surface Density of  $z=3.13$  Ly $\alpha$  Galaxies.*
- Ciardullo R., Durrell P. R., Laychak M. B., Herrmann K. A., Moody K., Jacoby G. H., Feldmeier J. J., 2004. *ApJ*, 614, 167. *The Planetary Nebula System of M33.*
- Corradi R. L. M., Magrini L., Greimel R., Irwin M., Leisy P., Lennon D. J., Mampaso A., Perinotto M., Pollacco D. L., Walsh J. R., Walton N. A., Zijlstra A. A., 2005. *A&A*, 431, 555. *The Local Group Census: planetary nebulae in the spheroidal galaxies NGC 147, NGC 185 and NGC 205.*
- Cox A. N., 2000. *Allen's astrophysical quantities, 4th edition*, Publisher: New York: AIP Press; Springer, 2000. Edited by Arthur N. Cox. ISBN: 0387987460.
- Cram T. R., Roberts M. S., Whitehurst R. N., 1980. *A&AS*, 40, 215. *A complete, high-sensitivity 21-cm hydrogen line survey of M31.*
- Crane P. C., Dickel J. R., Cowan J. J., 1992. *ApJ*, 390, L9. *Detection of an unresolved nuclear radio source in M31.*

- de Jong J. T. A., Widrow L. M., Cseresnjcs P., Kuijken K., Crotts A. P. S., Bergier A., Baltz E. A., Gyuk G., Sackett P. D., Uglesich R. R., Sutherland W. J., 2006. *A&A*, 446, 855. *MACHOs in M 31? Absence of evidence but not evidence of absence.*
- de Vaucouleurs G., de Vaucouleurs A., Corwin H. G., Buta R. J., Paturel G., Fouque P., 1991. *Third Reference Catalogue of Bright Galaxies*, Springer-Verlag Berlin Heidelberg New York.
- de Vaucouleurs G., 1958. *ApJ*, 128, 465. *Photoelectric photometry of the Andromeda nebula in the UBV system.*
- de Zeeuw P. T., Hoogerwerf R., de Bruijne J. H. J., Brown A. G. A., Blaauw A., 1999. *AJ*, 117, 354. *A HIPPARCOS Census of the Nearby OB Associations.*
- Dehnen W., Binney J. J., 1998. *MNRAS*, 298, 387. *Local stellar kinematics from HIPPARCOS data.*
- Dehnen W., 1998. *AJ*, 115, 2384. *The Distribution of Nearby Stars in Velocity Space Inferred from HIPPARCOS Data.*
- Devereux N. A., Price R., Wells L. A., Duric N., 1994. *AJ*, 108, 1667. *Two views of the Andromeda Galaxy H-alpha and far infrared.*
- Douglas N. G., Taylor K., 1999. *MNRAS*, 307, 190. *Galaxy kinematics from counter-dispersed imaging.*
- Douglas N. G., Arnaboldi M., Freeman K. C., Kuijken K., Merrifield M. R., Romanowsky A. J., Taylor K., Capaccioli M., Axelrod T., Gilmozzi R., Hart J., Bloxham G., Jones D., 2002. *PASP*, 114, 1234. *The Planetary Nebula Spectrograph: The Green Light for Galaxy Kinematics.*
- Eggen O. J., Lynden-Bell D., Sandage A. R., 1962. *ApJ*, 136, 748. *Evidence from the motions of old stars that the Galaxy collapsed.*
- Eggen O. J., 1958. *MNRAS*, 118, 65. *Stellar groups. I. The Hyades and Sirius groups.*
- Eggen O. J., 1975. *PASP*, 87, 37. *Structure and age of the local association (Pleiades group).*
- Famaey B., Jorissen A., Luri X., Mayor M., Udry S., Dejonghe H., Turon C., 2005. *A&A*, 430, 165. *Local kinematics of K and M giants from CORAVEL/Hipparcos/Tycho-2 data. Revisiting the concept of superclusters.*
- Fardal M. A., Babul A., Geehan J. J., Guhathakurta P., 2006. *MNRAS*, 366, 1012. *Investigating the Andromeda stream - II. Orbital fits and properties of the progenitor.*
- Fehrenbach C., 1947. *Annales d'Astrophysique*, 10, 306. *Recherches sur la mesure des vitesses radiales au Prisme objectif. II: La méthode des longueurs du spectre. La méthode de retournement. Le Prisme à champ normal.*

- Fehrenbach C., 1948. *Annales d'Astrophysique*, 11, 35. *Recherches sur la mesure des vitesses radiales au prisme objectif. III. Résultats obtenus avec le prisme à champ normal.*
- Ferguson A. M. N., Irwin M. J., Ibata R. A., Lewis G. F., Tanvir N. R., 2002. *AJ*, 124, 1452. *Evidence for Stellar Substructure in the Halo and Outer Disk of M31.*
- Ferguson A. M. N., Gallagher J. S., Wyse R. F. G., 2000. *AJ*, 120, 821. *On the Nature of Andromeda IV.*
- Ford H. C., Jacoby G. H., 1978a. *ApJ*, 219, 437. *Planetary nebulae in local group galaxies. V - The Andromeda Galaxy.*
- Ford H. C., Jacoby G. H., 1978b. *ApJS*, 38, 351. *Planetary nebulae in local-group galaxies. VIII. A catalog of planetary nebulae in the Andromeda galaxy.*
- García-Ruiz I., Sancisi R., Kuijken K., 2002. *A&A*, 394, 769. *Neutral hydrogen and optical observations of edge-on galaxies: Hunting for warps.*
- Geha M., Guhathakurta P., Rich R. M., Cooper M. C., 2006. *AJ*, 131, 332. *Local Group Dwarf Elliptical Galaxies. I. Mapping the Dynamics of NGC 205 Beyond the Tidal Radius.*
- Gerssen J., Kuijken K., Merrifield M. R., 1997. *MNRAS*, 288, 618. *The shape of the velocity ellipsoid in NGC 488.*
- Górny S. K., Stasińska G., 1995. *A&A*, 303, 893. *On the status of planetary nebulae with WR-type nuclei.*
- Guhathakurta P., Ostheimer J. C., Gilbert K. M., Rich R. M., Majewski S. R., Kalirai J. S., Reitzel D. B., Cooper M. C., Patterson R. J., 2006a. *arXiv:astro-ph/0605172*. *Discovery of an Extended Halo of Metal-poor Stars in the Andromeda Spiral Galaxy.*
- Guhathakurta P., Rich R. M., Reitzel D. B., Cooper M. C., Gilbert K. M., Majewski S. R., Ostheimer J. C., Geha M. C., Johnston K. V., Patterson R. J., 2006b. *AJ*, 131, 2497. *Dynamics and Stellar Content of the Giant Southern Stream in M31. I. Keck Spectroscopy of Red Giant Stars.*
- Halliday C., Carter D., Bridges T. J., Jackson Z. C., Wilkinson M. I., Quinn D. P., Evans N. W., Douglas N. G., Merrett H. R., Merrifield M. R., Romanowsky A. J., Kuijken K., Irwin M. J., 2006. *MNRAS*, 369, 97. *Planetary nebula velocities in the disc and bulge of M31.*
- Helmi A., de Zeeuw P. T., 2000. *MNRAS*, 319, 657. *Mapping the substructure in the Galactic halo with the next generation of astrometric satellites.*
- Hernquist L., 1990. *ApJ*, 356, 359. *An analytical model for spherical galaxies and bulges.*
- Hubble E. P., 1925. *The Observatory*, 48, 139. *Cepheids in spiral nebulae.*

- Huchra J. P., Brodie J. P., Kent S. M., 1991. *ApJ*, 370, 495. *Extragalactic globular clusters. II - The M31 globular cluster system.*
- Huchra J. P., Vogeley M. S., Geller M. J., 1999. *ApJS*, 121, 287. *The CFA Redshift Survey: Data for the South Galactic CAP.*
- Hui X., Ford H. C., Ciardullo R., Jacoby G. H., 1993. *ApJ*, 414, 463. *The planetary nebula system and dynamics of NGC 5128. I - Planetary nebulae as standard candles.*
- Hurley-Keller D., Morrison H. L., Harding P., Jacoby G. H., 2004. *ApJ*, 616, 804. *Planetary Nebula Kinematics in M31.*
- Hyung S., Aller L. H., Han S.-R., Kim Y.-K., Han W., Choi Y., 2000. *Journal of Korean Astronomical Society*, 33, 97. *Abundances of Planetary Nebulae in M31 and M32.*
- Ibata R., Irwin M., Lewis G., Ferguson A. M. N., Tanvir N., 2001. *Nature*, 412, 49. *A giant stream of metal-rich stars in the halo of the galaxy M31.*
- Ibata R., Chapman S., Ferguson A. M. N., Irwin M., Lewis G., McConnachie A., 2004. *MNRAS*, 351, 117. *Taking measure of the Andromeda halo: a kinematic analysis of the giant stream surrounding M31.*
- Ibata R., Chapman S., Ferguson A. M. N., Lewis G., Irwin M., Tanvir N., 2005. *ApJ*, 634, 287. *On the Accretion Origin of a Vast Extended Stellar Disk around the Andromeda Galaxy.*
- Innanen K. A., Kamper K. W., van den Bergh S., Papp K. A., 1982. *ApJ*, 254, 515. *The optical warp of M31.*
- Irwin M. J., Ferguson A. M. N., Ibata R. A., Lewis G. F., Tanvir N. R., 2005. *ApJ*, 628, L105. *A Minor-Axis Surface Brightness Profile for M31.*
- Jacoby G. H., Ciardullo R., 1999. *ApJ*, 515, 169. *Chemical Abundances of Planetary Nebulae in the Bulge and Disk of M31.*
- Jacoby G. H., De Marco O., 2002. *AJ*, 123, 269. *A Survey for Very Faint Planetary Nebulae in the SMC. I. Identification, Confirmation, and Preliminary Analysis.*
- Jacoby G. H., Ford H. C., 1986. *ApJ*, 304, 490. *Chemical abundances of planetary nebulae in M31.*
- Jacoby G. H., 1980. *ApJS*, 42, 1. *The luminosity function for planetary nebulae and the number of planetary nebulae in local group galaxies.*
- Jacoby G. H., 1989. *ApJ*, 339, 39. *Planetary nebulae as standard candles. I - Evolutionary models.*
- Kalirai J. S., Guhathakurta P., Gilbert K. M., Reitzel D. B., Majewski S. R., Rich R. M., Cooper M. C., 2006. *ApJ*, 641, 268. *Kinematics and Metallicity of M31 Red Giants: The Giant Southern Stream and Discovery of a Second Cold Component at  $R=20$  kpc.*



- Kauffmann G., White S. D. M., Guiderdoni B., 1993. MNRAS, 264, 201. *The Formation and Evolution of Galaxies Within Merging Dark Matter Haloes.*
- Kent S. M., 1989. PASP, 101, 489. *A comparison of optical and H I rotation curves in M 31.*
- Kormendy J., Bender R., 1999. ApJ, 522, 772. *The Double Nucleus and Central Black Hole of M31.*
- Larson R. B., 1969. MNRAS, 145, 405. *A model for the formation of a spherical galaxy.*
- Lauer T. R., Faber S. M., Groth E. J., Shaya E. J., Campbell B., Code A., Currie D. G., Baum W. A., Ewald S. P., Hester J. J., Holtzman J. A., Kristian J., Light R. M., Ligyndy C. R., O'Neil E. J., Westphal J. A., 1993. AJ, 106, 1436. *Planetary camera observations of the double nucleus of M31.*
- Lawrie D. G., Ford H. C., 1982. ApJ, 256, 120. *Planetary nebulae in local group galaxies. IX - Velocity modulated photographs of the center of M31.*
- Lawrie D. G., 1978. *Ph.D. Thesis. The radial velocity dispersion of planetary nebulae in the nuclear bulge of M31.*
- Levine E. S., Blitz L., Heiles C., 2006. ApJ, 643, 881. *The Vertical Structure of the Outer Milky Way H I Disk.*
- Lindblad B., 1956. *Stockholms Observatoriums Annaler*, 2. *On a barred spiral structure in the Andromeda nebula.*
- Loinard L., Allen R. J., Lequeux J., 1995. A&A, 301, 68. *An unbiased survey for CO emission in the inner disk of the Andromeda galaxy.*
- Magrini L., Corradi R. L. M., Mampaso A., Perinotto M., 2000. A&A, 355, 713. *A search for planetary nebulae in M33.*
- Majewski S. R., Skrutskie M. F., Weinberg M. D., Ostheimer J. C., 2003. ApJ, 599, 1082. *A Two Micron All Sky Survey View of the Sagittarius Dwarf Galaxy. I. Morphology of the Sagittarius Core and Tidal Arms.*
- Marigo P., Girardi L., Weiss A., Groenewegen M. A. T., Chiosi C., 2004. A&A, 423, 995. *Evolution of planetary nebulae. II. Population effects on the bright cut-off of the PNLF.*
- Massey P., Hodge P. W., Holmes S., Jacoby J., King N. L., Olsen K., Smith C., Saha A., 2002. *Bulletin of the American Astronomical Society*, 34, 1272. *A Survey of the Local Group Galaxies Currently Forming Stars.*
- Mateo M. L., 1998. ARA&A, 36, 435. *Dwarf Galaxies of the Local Group.*
- McConnachie A. W., Irwin M. J., Ibata R. A., Ferguson A. M. N., Lewis G. F., Tanvir N., 2003. MNRAS, 343, 1335. *The three-dimensional structure of the giant stellar stream in Andromeda.*

- McConnachie A. W., Irwin M. J., Ferguson A. M. N., Ibata R. A., Lewis G. F., Tanvir N., 2005. MNRAS, 356, 979. *Distances and metallicities for 17 Local Group galaxies.*
- McElroy D. B., 1983. ApJ, 270, 485. *Dynamics of the stellar component of the bulge of M31.*
- McGaugh S. S., de Blok W. J. G., 1998. ApJ, 499, 41. *Testing the Dark Matter Hypothesis with Low Surface Brightness Galaxies and Other Evidence.*
- Méndez R. H., Riffeser A., Kudritzki R.-P., Matthias M., Freeman K. C., Arnaboldi M., Capaccioli M., Gerhard O. E., 2001. ApJ, 563, 135. *Detection, Photometry, and Slitless Radial Velocities of 535 Planetary Nebulae in the Flattened Elliptical Galaxy NGC 4697.*
- Merrett H. R., Kuijken K., Merrifield M. R., Romanowsky A. J., Douglas N. G., Napolitano N. R., Arnaboldi M., Capaccioli M., Freeman K. C., Gerhard O., Evans N. W., Wilkinson M. I., Halliday C., Bridges T. J., Carter D., 2003. MNRAS, 346, L62. *Tracing the star stream through M31 using planetary nebula kinematics.*
- Merrett H. R., Merrifield M. R., Douglas N. G., Kuijken K., Romanowsky A. J., Napolitano N. R., Arnaboldi M., Capaccioli M., Freeman K. C., Gerhard O., Coccato L., Carter D., Evans N. W., Wilkinson M. I., Halliday C., Bridges T. J., 2006a. MNRAS, 369, 120. *A deep kinematic survey of planetary nebulae in the Andromeda galaxy using the Planetary Nebula Spectrograph.*
- Merrett H. R., Merrifield M. R., Kuijken K., Romanowsky A. J., Douglas N. G., Napolitano N. R., Arnaboldi M., Capaccioli M., Freeman K. C., Gerhard O., Carter D., Evans N. W., Wilkinson M. I., Halliday C., Bridges T. J., 2006b. *Mapping the stellar dynamics of M31*, In: *Planetary Nebulae Beyond the Milky Way, Proceedings of the ESO Workshop held at Garching, Germany, 19-21 May, 2004.*, 281, eds Stanghellini L., Walsh J. R., Douglas N. G.
- Meyssonnier N., Lequeux J., Azzopardi M., 1993. A&AS, 102, 251. *An Objective-Prism Survey of Emission Line Objects in M31.*
- Monet D. G., Levine S. E., Canzian B., Ables H. D., Bird A. R., Dahn C. C., Guetter H. H., Harris H. C., Henden A. A., Leggett S. K., Levison H. F., Luginbuhl C. B., Martini J., Monet A. K. B., Munn J. A., Pier J. R., Rhodes A. R., Riepe B., Sell S., Stone R. C., Vrba F. J., Walker R. L., Westerhout G., Brucato R. J., Reid I. N., Schoening W., Hartley M., Read M. A., Tritton S. B., 2003. AJ, 125, 984. *The USNO-B Catalog.*
- Morrison H. L., Harding P., Hurley-Keller D., Jacoby G., 2003. ApJ, 596, L183. *Andromeda VIII: A New Tidally Distorted Satellite of M31.*
- Narayan C. A., Jog C. J., 2002. A&A, 390, L35. *Origin of radially increasing stellar scaleheight in a galactic disk.*
- Newton K., Emerson D. T., 1977. MNRAS, 181, 573. *Neutral hydrogen in the outer regions of M31.*

- Nieten C., Neininger N., Guélin M., Ungerechts H., Lucas R., Berkhuijsen E. M., Beck R., Wielebinski R., 2005. *arXiv:astro-ph/0512563. Molecular gas in the Andromeda galaxy.*
- Nolthenius R. A., Ford H. C., 1984. BAAS, 16, 456. *The Distribution and Dynamics of Planetary Nebulae in the Outer Regions of M31.*
- Nolthenius R., Ford H., 1986. ApJ, 305, 600. *The mass and halo dispersion profile of M32.*
- Nolthenius R. A., 1984. *Ph.D. Thesis. The distribution and dynamics of planetary nebulae in M32 and the Andromeda Galaxy.*
- Oke J. B., Gunn J. E., 1983. ApJ, 266, 713. *Secondary standard stars for absolute spectrophotometry.*
- Oke J. B., 1974. ApJS, 27, 21. *Absolute Spectral Energy Distributions for White Dwarfs.*
- Oke J. B., 1990. AJ, 99, 1621. *Faint spectrophotometric standard stars.*
- Pease E. G., 1918. *Proceedings of the National Academy of Science*, 4, 21. *The Rotation and Radial Velocity of the Central Part of the Andromeda nebula.*
- Peimbert M., 1990. *Revista Mexicana de Astronomía y Astrofísica*, 20, 119. *Total number of planetary nebulae in different galaxies and the PN distance scale.*
- Press W. H., Teukolsky S. A., Vetterling W. T., Flannery B. P., 1992. *Numerical recipes in C. The art of scientific computing*, Cambridge: University Press, —c1992, 2nd ed.
- Pritchett C. J., van den Bergh S., 1994. AJ, 107, 1730. *Faint surface photometry of the halo of M31.*
- Reitzel D. B., Guhathakurta P., 2002. AJ, 124, 234. *Metallicity and Kinematics of M31's Outer Stellar Halo from a Keck Spectroscopic Survey.*
- Richer M. G., Stasińska G., McCall M. L., 1999. A&AS, 135, 203. *Planetary nebulae in M 32 and the bulge of M 31: Line intensities and oxygen abundances.*
- Roberts M. S., 1966. ApJ, 144, 639. *A High-Resolution 21-CM Hydrogen-Line Survey of the Andromeda Nebula.*
- Salucci P., 2001. MNRAS, 320, L1. *The constant-density region of the dark haloes of spiral galaxies.*
- Sambhus N., Gerhard O., Méndez R. H., 2006. AJ, 131, 837. *Kinematic Evidence for Different Planetary Nebula Populations in the Elliptical Galaxy NGC 4697.*
- Sawa T., Sofue Y., 1982. PASJ, 34, 189. *Neutral Hydrogen in M31 - Part Three - the Warping of HI Disk.*

- Schlegel D. J., Finkbeiner D. P., Davis M., 1998. *ApJ*, 500, 525. *Maps of Dust Infrared Emission for Use in Estimation of Reddening and Cosmic Microwave Background Radiation Foregrounds.*
- Sevenster M. N., Chapman J. M., Habing H. J., Killeen N. E. B., Lindqvist M., 1997. *A&AS*, 122, 79. *The ATCA/VLA OH 1612 MHz survey. I. Observations of the galactic bulge Region.*
- Simien F., Prugniel P., 2002. *A&A*, 384, 371. *Kinematical data on early-type galaxies. VI.*
- Slipher V. M., 1914. *Lowell Observatory Bulletin*, 1, 66. *The detection of nebular rotation.*
- Sofue Y., Rubin V., 2001. *ARA&A*, 39, 137. *Rotation Curves of Spiral Galaxies.*
- Springel V., White S. D. M., Jenkins A., Frenk C. S., Yoshida N., Gao L., Navarro J., Thacker R., Croton D., Helly J., Peacock J. A., Cole S., Thomas P., Couchman H., Evrard A., Colberg J., Pearce F., 2005. *Nature*, 435, 629. *Simulations of the formation, evolution and clustering of galaxies and quasars.*
- Stark A. A., 1977. *ApJ*, 213, 368. *Triaxial Models of the Bulge of M31.*
- van der Kruit P. C., Searle L., 1982. *A&A*, 110, 61. *Surface photometry of edge-on spiral galaxies. III - Properties of the three-dimensional distribution of light and mass in disks of spiral galaxies.*
- van Dokkum P. G., 2001. *PASP*, 113, 1420. *Cosmic-Ray Rejection by Laplacian Edge Detection.*
- Walterbos R. A. M., Kennicutt R. C., 1987. *A&AS*, 69, 311. *Multi-color photographic surface photometry of the Andromeda galaxy.*
- Walterbos R. A. M., Kennicutt R. C., 1988. *A&A*, 198, 61. *An optical study of stars and dust in the Andromeda galaxy.*
- White S. D. M., Rees M. J., 1978. *MNRAS*, 183, 341. *Core condensation in heavy halos - A two-stage theory for galaxy formation and clustering.*
- White S. D. M., 1978. *MNRAS*, 184, 185. *Simulations of merging galaxies.*
- White S. D. M., 1979. *MNRAS*, 189, 831. *Further simulations of merging galaxies.*
- Widrow L. M., Dubinski J., 2005. *ApJ*, 631, 838. *Equilibrium Disk-Bulge-Halo Models for the Milky Way and Andromeda Galaxies.*
- Widrow L. M., Perrett K. M., Suyu S. H., 2003. *ApJ*, 588, 311. *Disk-Bulge-Halo Models for the Andromeda Galaxy.*